UNIVERSITY of BRADFORD Library

University of Bradford eThesis

This thesis is hosted in Bradford Scholars – The University of Bradford Open Access repository. Visit the repository for full metadata or to contact the repository team

© University of Bradford. This work is licenced for reuse under a Creative Commons Licence.

SHEAR AND NORMAL STRESSES IN UNIAXIAL COMPACTION

The uniaxial densification of powders was investigated and the relationships of shear stress, compaction stress and volume reduction related to the surface topography and strength of compacts.

A thesis presented by

ABDELKARIM MOHAMED ABDELKARIM

for the degree of

DOCTOR OF PHILOSOPHY

of the

UNIVERSITY OF BRADFORD

University of Bradford,
POSTGRADUATE SCHOOL OF STUDIES IN POWDER TECHNOLOGY
DEPARTMENT OF CHEMICAL ENGINEERING.

September 1982.

Erratum

Throughout this thesis the word dentritic should read dendritic

ABSTRACT

Three different groups of materials were chosen to investigate the uniaxial compaction of particulate solids. Dentritic and cubic sodium chloride were chosen as plastically deforming, dicalcium phosphate and sugar as fragmentary and styrocell, homopolymer and copolymer as non-compactable materials.

The uniaxial compaction of the materials was continuously followed by measurement of the applied force, the force transmitted radially to the die wall and the upper punch displacement. The data obtained was presented in the form of Mohr circles, stress pathways (shear-mean compaction stress planes) and a three dimensional representation in mean compaction stress, shear stress and volume change.

The yield loci evaluated from Mohr circles and shear-mean compaction stress relationships of compactable and non-compactable materials were found to be similar in shape. The unloading stress profiles were however more informative. All unloading shear-mean compaction stress curves of the compactable materials cross the mean compaction stress axis to give negative values of shear stress and reach a minimum value of τ_{min}, which was material and compaction pressure dependent. The unloading curves of non-compactable materials gave approximately zero shear. The parameters evaluated from the characteristic stress profiles were correlated to the tensile strength and hardness of compacts.

Mathematical expressions have been proposed for the shear-mean compaction stress relationships of the materials investigated.

The materials were characterised before and after compaction in terms of specific surface area, porosity and mechanical strength of compacts with compaction pressure.

ACKNOWLEDGEMENT

I would like to express my thanks to my supervisor, Dr. N.G. Stanley-Wood for his helpful guidance and encouragement during the course of this work.

Acknowledgement is also due to Dr. J.C. Williams and Mr. A.H. Birks for the helpful discussions we have had.

I would also like to thank the Sudan Government and the Institution of Chemical Engineers for the financial support.

Finally, my special thanks to all my friends, for their advice and support and to my wife and my son for their forebearance throughout the period of my research.

CONTENTS

LIST OF FIGURES

CHAPTER 1

CHAPTER 1

CHAPTER 1

Compaction of Particulate Solids

1.1 Introduction

When a compressive force of sufficient magnitude is applied to a powder confined within a mould, a coherent mass of particles with some degree of porosity and strength can usually be produced. Adjacent particles are pressed together so that at the interfacial areas of contact, surface forces can have sufficient influence to produce a stable structure. The extent of interfacial contact area or bonding is exemplified by the mechanical strength of the compacted material. The strength of a compact will thus depend on physico-chemical properties of the material being compressed and the nature of the compaction stress/force.

Scientific literature on die compaction dates back to the early nineteenth century when Wollaston (1828) described the compaction process to produce pure platinum billets. Since then several hundreds of papers have been published on the process, mechanism and instrumentation of compaction. Contradictory nomenclature, such as consolidation, compression and compaction are terms used by many workers, which can lead to confusion in the description of the physics of compaction.

In the field of soil mechanics the term consolidation is defined as the expulsion of water from interparticle spaces when soil is compressed under steady pressure. The steady pressure can be achieved from the weight imposed by a structure or the magnitude of an earth

fill (Capper and Cassie 1963).

Jenike (1961) in his work on Gravity Flow of Bulk Solids in which he investigated the behaviour of different types of particulate and granular material, stated that a solid material may be consolidated by vibration, pounding, hydrostatic pressure and pressures which are different in magnitude but whose deviator components are insufficient to cause shear. Train and Lewis (1962) used the term consolidation in two different ways. The first way was when the whole process of compaction from the stages of particle packing, re-arrangement and particle-particle bonding was described. The second way was when bonding was described. In a recent work Marshall (1977) described the physics of compaction as the compression and consolidation of a two phase system. He defined consolidation as an increase in mechanical strength and compression as an increase in bulk density. Heistand and co-workers (1977) used the term consolidation to mean the mechanism of particle re-arrangement. In this work the term compaction will incorporate the mechanisms of particle packing, re-arranagement and particle-particle bonding. The general terms compression and compressive forces will be taken to mean the application of a force to an assembly of particles, while densification will be used to describe the volume reduction of an assembly of particles..

The process of compaction of powders in a rigid die is a fabrication technique consisting of three main stages. In the first stage the powder is fed into the die, next

the powder mass is compacted into a coherent body and finally the compact is ejected from the die. Initially before the application of force, there is only point contact between particles within the die. On application of a compressive force to the powder, forces will be transmitted through these interparticulate contacts. The bulk volume will be decreased initially due to closer repacking of particles and then possibly be followed by elastic and plastic deformation and/or brittle fracture. The compaction stage in the fabrication of a coherent body has been the subject of a great number of studies. Many authors have attempted to elucidate the mechanism of compaction by monitoring the force transmission through the particle-particle contacts and the measurable properties of the powder such as density, volume change and porosity or voidage during and after compaction.

1.1.1 Force Transmission

Whilst fluids transmit the force applied at any point throughout its entire mass, powders or particulate solids resist differential movement between particles when subjected to a compressive force. The fact that the force applied to a column of powder is not transmitted isostatically was observed by Philips (1910), who noted that a downward force applied to the top of a column of sand a few diameters high was not transmitted to the bottom. Shaxby and Evans (1923) demonstrated that the decay of applied pressure at increasing depth in a non-

cohesive particulate material contained within a cylindrical tube was exponential.

In die compaction a uniaxially applied force can be considered to consist of an axial force, F_A, which is externally applied, a radial force, F_R, exerted upon the die wall, a frictional force, F_D, between the material and die wall and the force transmitted to the lower punch, F_L, (fig.1.1).

Many workers have proposed mathematical relationships between the applied and transmitted forces. Unckel (1945) developed an expression to describe the relation between the applied force, F_A, and the force transmitted to the bottom of the die, F_L, in which he considered the effect of friction between the material and container wall.

$$\ln(F_A/F_L) = 4\mu\eta L/D \qquad (1.1)$$

where μ ≡ coefficient of friction at the container wall

η ≡ the ratio of radial to axial stress in the compact

L ≡ thickness of the compact

D ≡ diameter of the compact

A similar relationship was also found by Spencer, Gilmore and Wiley (1950), who measured F_A and F_L during the compaction of Saran powders and granulated polystyrene . Nelson and co-workers (1954), while investigating the compaction behaviour of sulphathiazole granules, found that the magnitude of the force transmitted to the lower punch, F_L, was dependent upon the presence or absence of

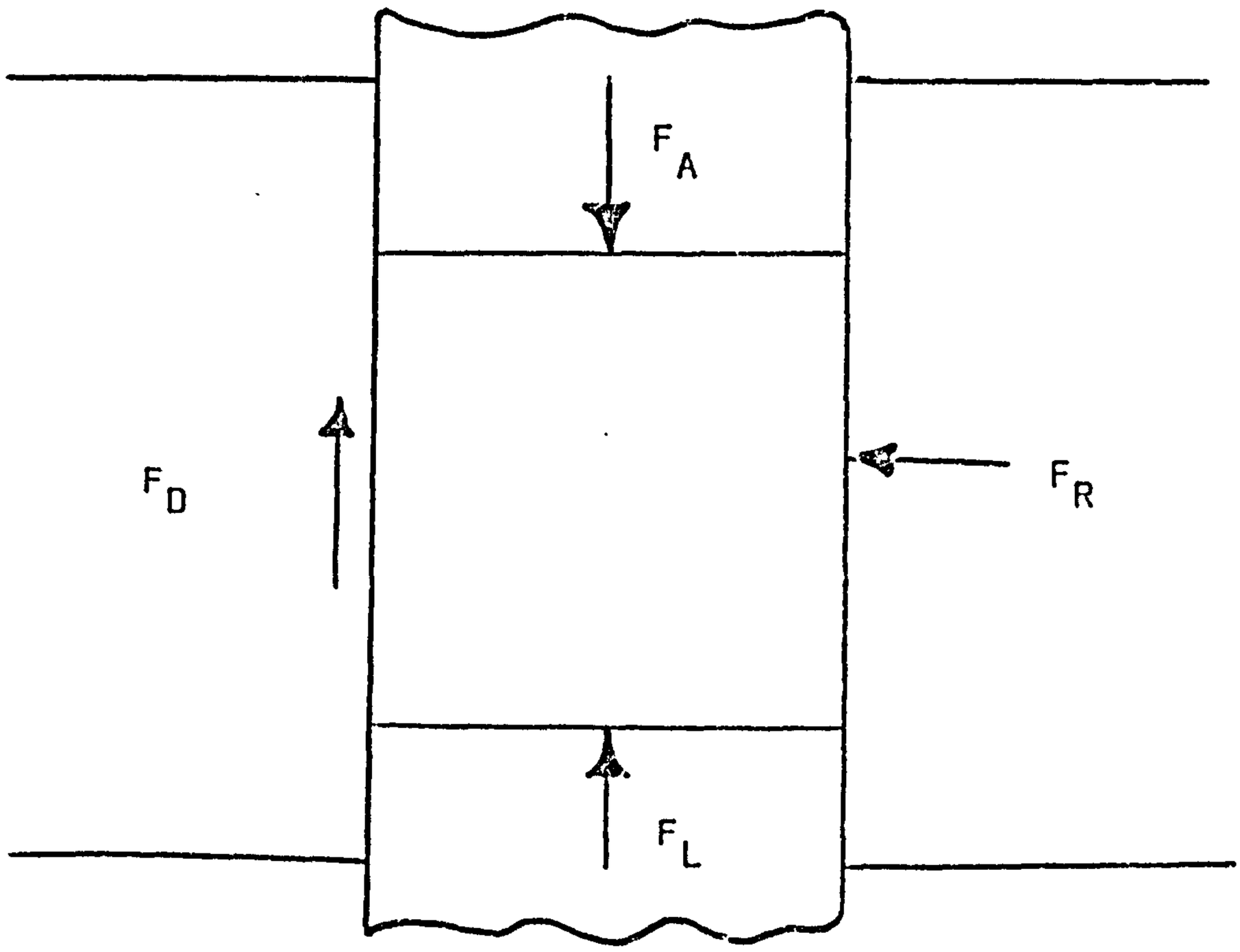

Figure 1.1 FORCES OPERATING ON A POWDER UNDER COMPRESSION.

lubricants and whether a lubricant was applied to the die wall or incorporated in the material. From the forces measured, Nelson and co-workers calculated the pressure applied, P_A and the pressure on the lower punch P_L, and evaluated the pressure ratio of P_L/P_A, which is known as the 'R' value, as a measure of the efficiency of lubricants. Shotton and Ganderton (1960) reported that the ratio of P_L/P_A was constant for sodium chloride compacts. The 'R' value was confirmed by de Blaey and Polderman (1970) to be dependent upon the material and die geometry.

The fact that a fraction of the applied compressional force is transmitted axially to the die wall was reported by Unckel (1945). Train and Hersey (1960) while investigating the compaction behaviour of metal granules and metal plugs found that the axial die wall reaction was proportional to the product of the contact area between material and die wall and the shear strength of the material. The mathematical derivation proposed agreed well with the experimental results obtained.

Long (1960) investigated the compaction behaviour of potassium bromide, lithium carbonate, the soft material indium, aluminium, copper and sodium chloride. He showed that the fraction of the force transmitted radially to the die wall was a function of the Poisson Ratio of the materials. Similar work was carried out on non-metallic powders by Higuchi et al (1965) and Ridgway and co-workers (1969), who explained that the magnitude of the radial force was dependent on the hardness of the material. The use of the radial pressure cycles, which are graphical

plots of the relationship of applied pressure to the radial pressure, was also adopted by CÂarles and Leigh (1974), Obiorah and Shotton (1976), Marshall (1977) and Ibrahim (1979).

Ho and Hersey (1980) used the Force-displacement technique of de Blaey and Polderman (1971) to calculate the compaction energy of sodium chloride and paracetamol granules prepared by different granulation methods. The net energy input into the system which was obtained from the difference between the area under the initial force displacement curve and the second force displacement curve was shown to be linearly related to the tensile strength of compacts.

From the above survey it can be shown that the measurement of the applied and transmitted forces has been widely used to examine the mechanical behaviour of powders under compaction.

In the field of soil mechanics, ceramics and flow of bulk powders, the parameter of stress rather than force is normally used to study the mechanism of compaction. This approach was used in this investigation.

1.1.2 Stress

Many attempts have been made to produce a theoretical assessment to explain the relationship between the applied and transmitted force and the mechanical properties of the material. The relationships found between these parameters are always qualitative, because it is not the

force alone that determines the behaviour of a material under load but rather the magnitude of the force acting on each unit of cross section. The term stress is used to define the quotient of load to cross sectional area.

The stress on a solid can be described in two ways, either as an engineering stress, which is the force applied divided by the original area before application of force or as the true stress, which is the force applied divided by the instantaneous area over which the force acts.

If a force is normal to a plane, then the resulting stress is called normal stress (Figure 1.2a). If the force is parallel to the plane, the stress is called shear stress (Figure 1.2b). A force at an arbitrary angle can be resolved into normal and shear components of stress (Figure 1.2c). The normal component of the stress is usually designated by Sigma (σ) and the tangential stress or shear stress designated by tau(τ). The above symbols will be used throughout this thesis to describe normal and shear stresses.

The stress at any point in a powder bed can be represented by three principal stresses σ_1, σ_2 and σ_3 parallel to the XZY directions. The three principal stresses are the major; intermediate and minor principal stresses. In uniaxial compaction it is assumed that the stress does not change in the Z direction, so that σ_1 and σ_3 can be presented in X,Y co-ordinates.

A very convenient method of representing the stress, at a point, was derived by Mohr (1900) and is termed the

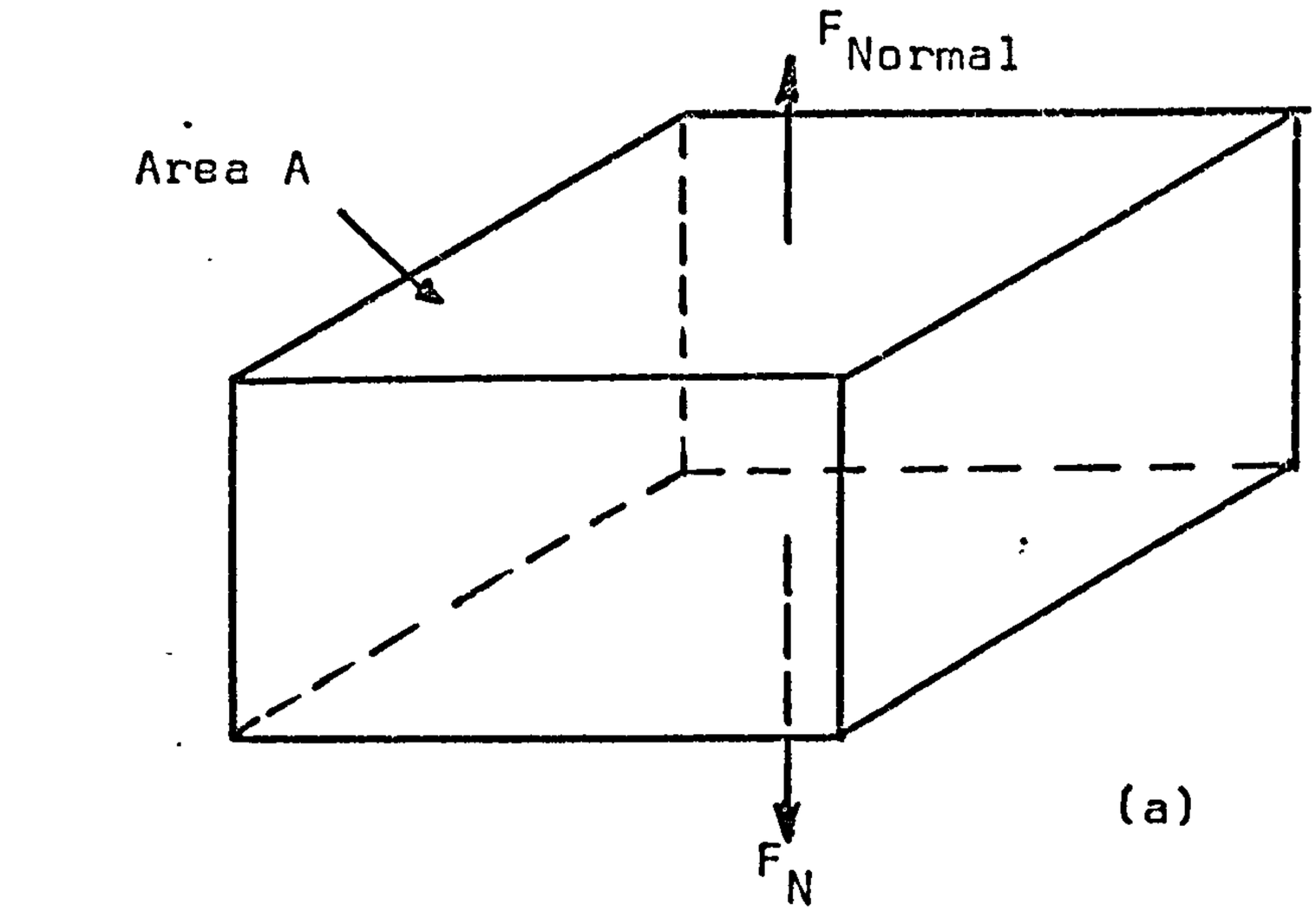
F Normal
Area A
F N
(a)
Normal Stress

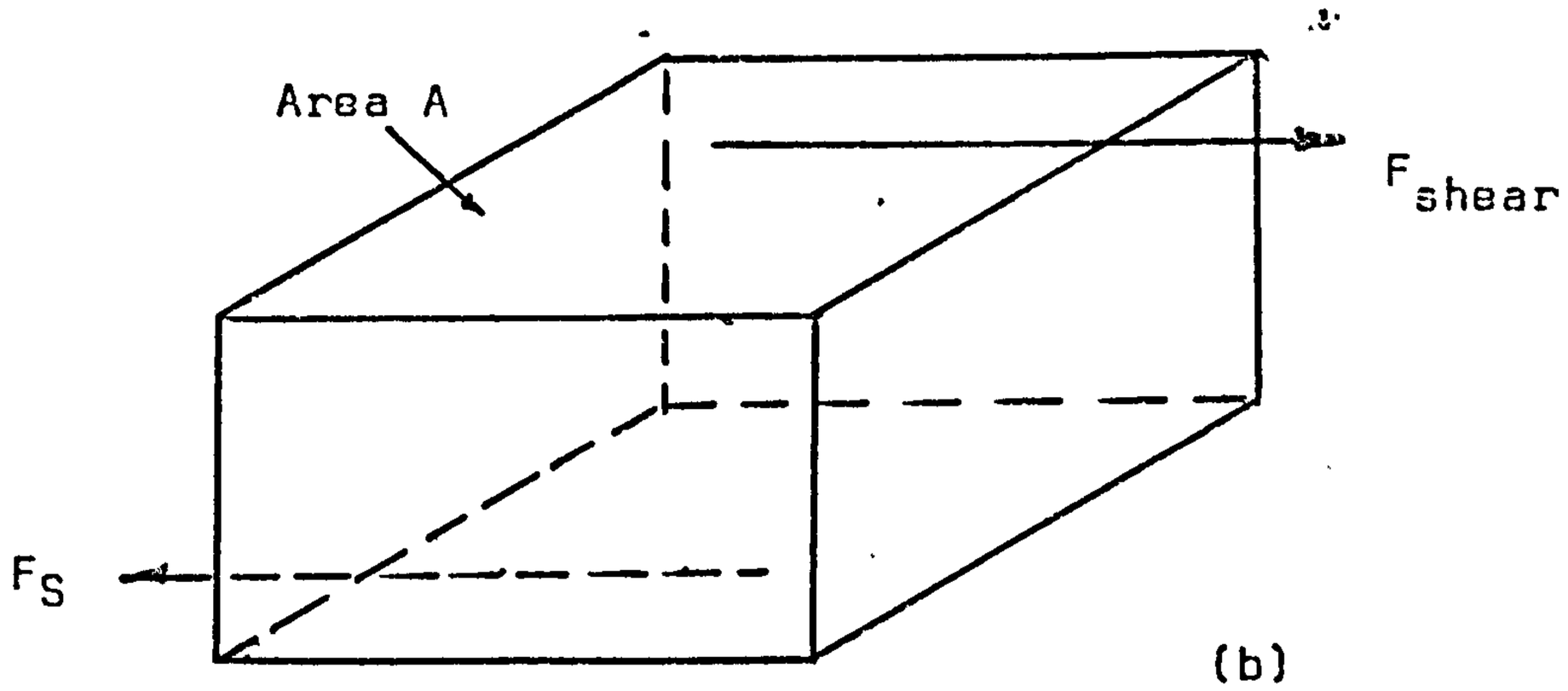
Area A
F shear
F S
(b)
shear stress

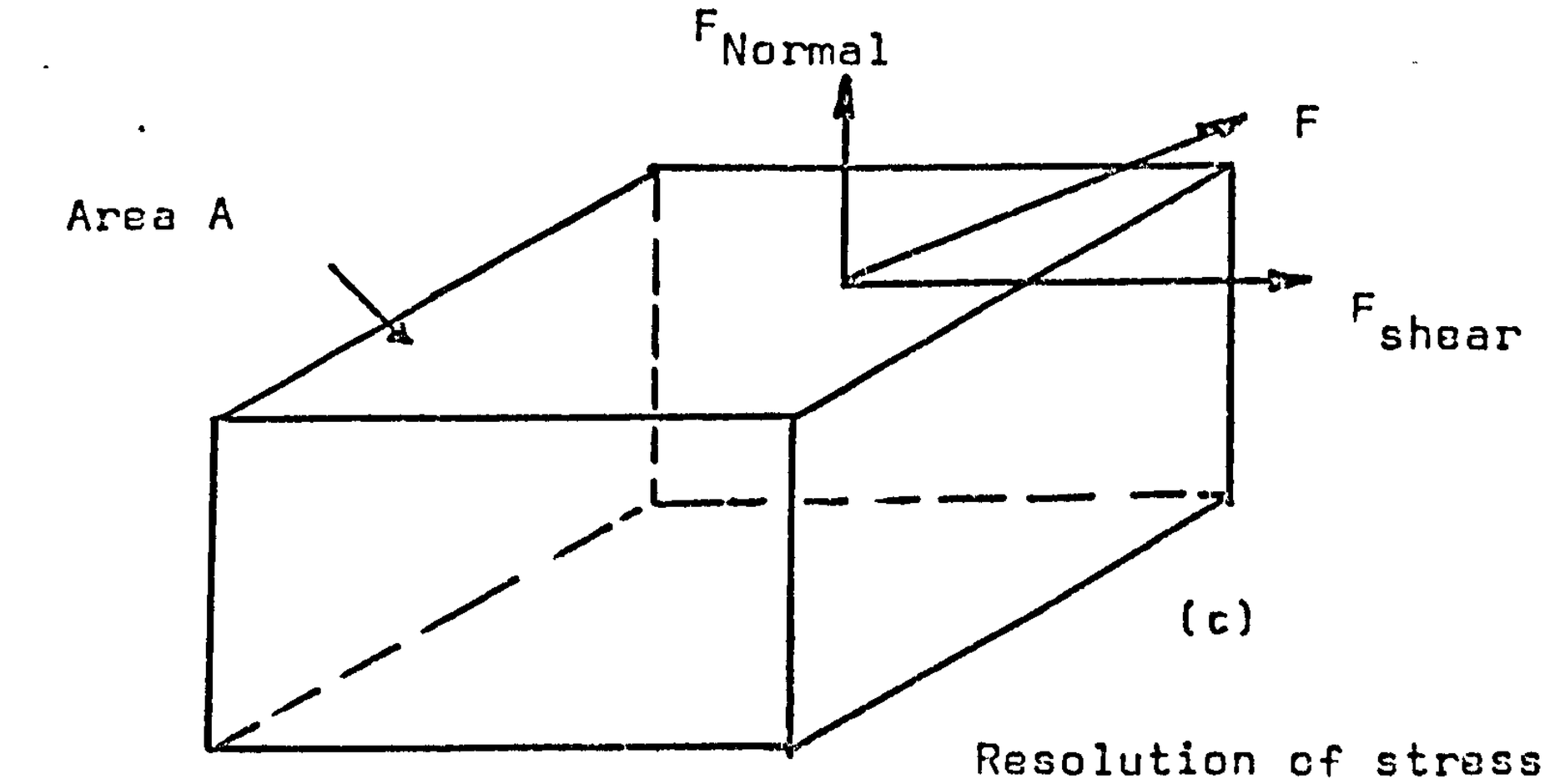
F Normal
F
Area A
F shear
(c)
Resolution of stress into two components.

Figure 1.2

Mohr stress circle (Figure 1.3). The principal stresses σ_1 and σ_3 produce normal and shearing stresses on any inclined plane such as AC, making an angle of α with the plane of σ_1. σ and τ are presented as follows.

$$\sigma = \left(\frac{\sigma_1+\sigma_3}{2}\right) + \left(\frac{\sigma_1-\sigma_3}{2}\right)\cos 2\alpha \quad (1.2)$$

$$\tau = \left(\frac{\sigma_1-\sigma_3}{2}\right)\sin 2\alpha \quad (1.3)$$

mathematical derivations are given in (Lessells 1954).

1.1.3 Stress distribution in a ccmpact

Rakowski (1935) was one of the first to investigate the density variation in metal powders. He inserted thin layers of metal foil and graphite in the powder before compaction and used the change in distance between layers as an indication of density variation in different regions. Unckel (1945) while compressing iron powders identified, by cutting the compacts into small cubes, a low density zone in the centre of the compact which was directly under the top punch. The existance of non-uniform density distribution was also reported by Seelig and Wulff (1946), who attributed this non-uniform phenomenon to die wall friction and showed that lubrication could modified the density distribution within a compact. Kamm, Steinberg and Wulff (1947) confirmed the work of Seelig and Wulff by the insertion of lead grids into powder beds before compaction and subsequently identified the deformation of the grids by X-radiographic techniques after compaction.

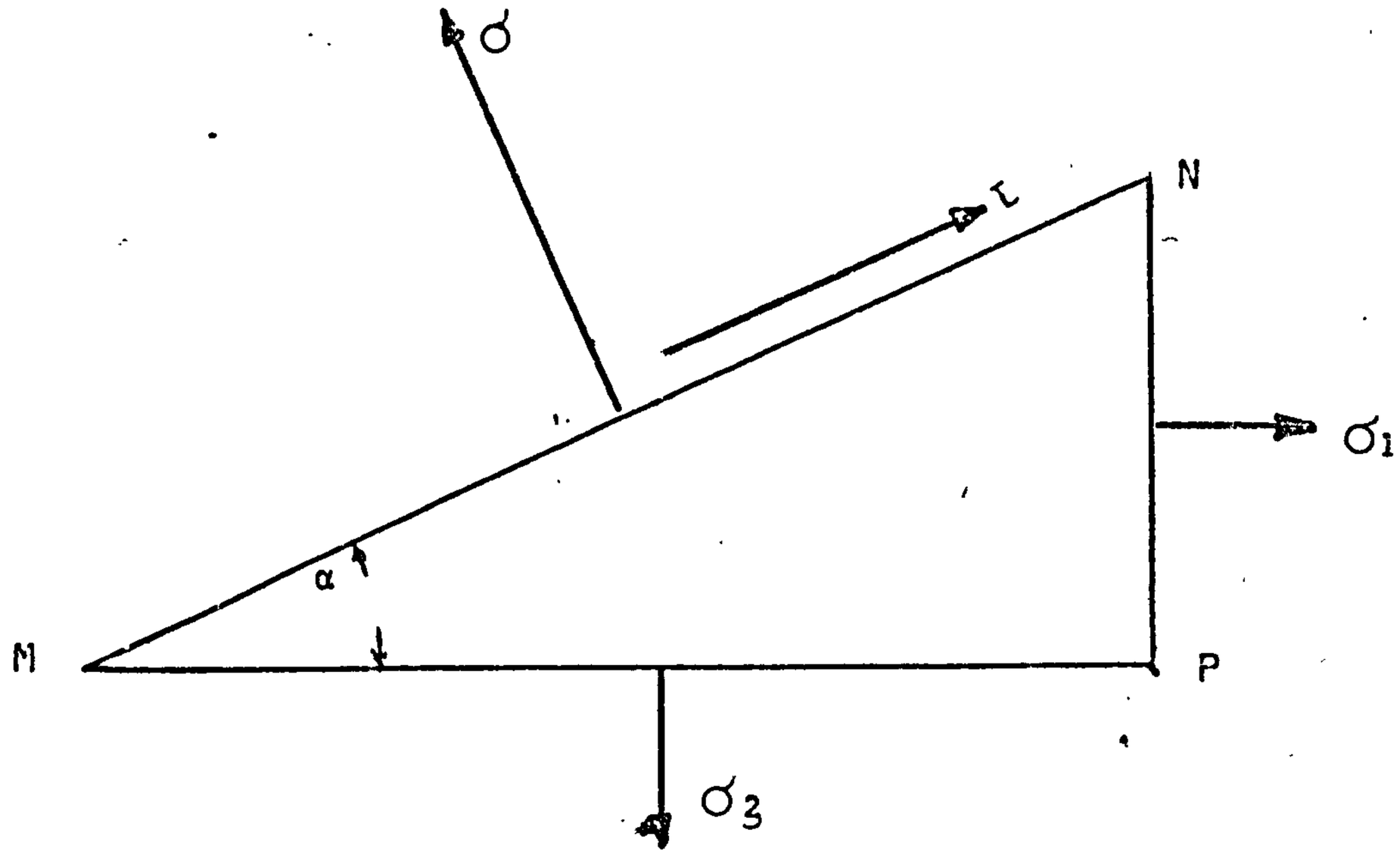

σ_1, σ_3 ≡ Principal stresses

σ ≡ Normal stress on plane MN

τ ≡ Shearing stress on plane MN

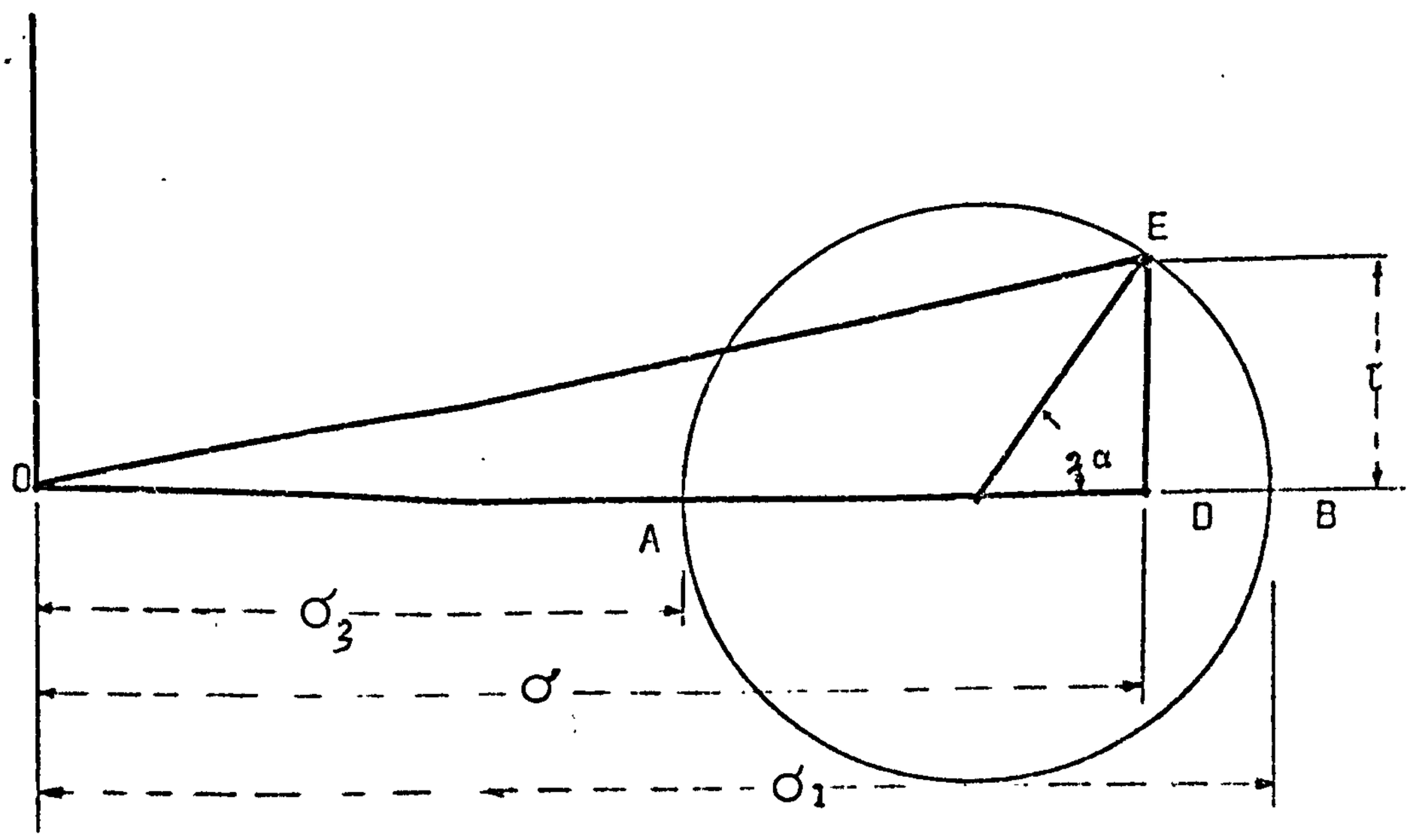

Figure 1.3 Representation of stress by Mohr's Circle

Train (1956) adopted a technique similar to that used by Rakowski (1935) by compressing different coloured identifiable layers of magnesium carbonate particles and used the distortion of the coloured layers as an indication of density variation. A different technique was used by Kuczynski and Zaplatynskyj (1956) who investigated the density distribution in compacts of Nickel powder. Thin compacts (height to diameter ratio 0.2) were produced at different compaction pressures and a set of density -hardness calibration curves were constructed. To find the density distribution within the compacts, they sectioned the compacts and measured the hardness of the specimens as a function of position. The hardness values were then translated into densities to give the density distribution within the compacts (fig. 1.4).

The above methods measured a physical property of the system that changed during the application of pressure. The first effort to measure the stress distribution directly during compaction was made by Duwez and Zwell (1949). They constructed a die with a small piston in the die wall. The piston was connected to strain gauges to measure the normal die wall reaction during compaction. The pressure distribution on the die wall was obtained by successive tests in which the relative position of piston along the die wall was altered by changing the length of the lower punch. The die wall reaction was found to increase linearly from the bottom to the top of the compact. The

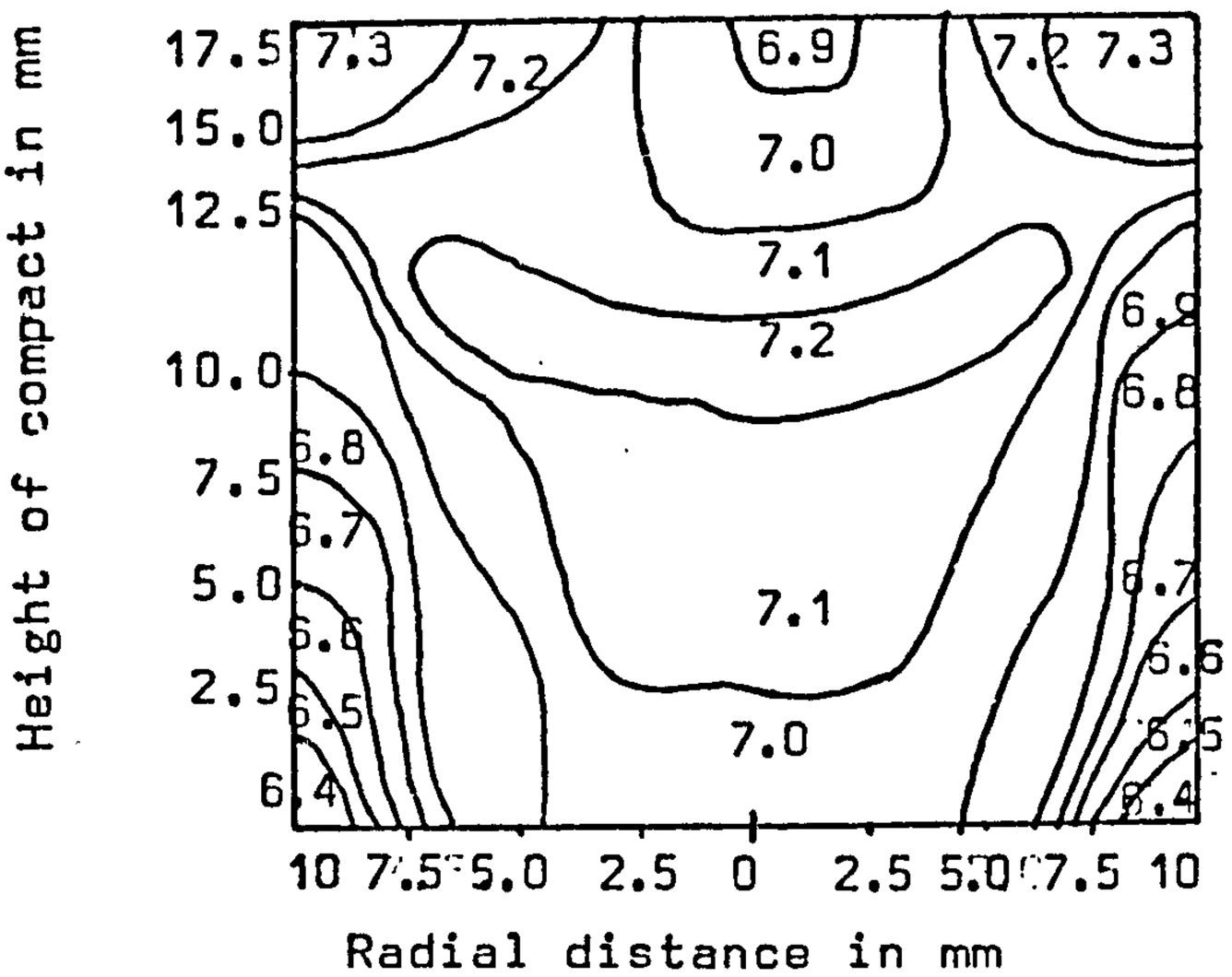

Figure 1.4 Distribution of densities in a green nickel compact pressed at 46 p.s.i. (after Kuczynski and Zaplatynskyj)

magnitude of the die wall pressure was affected by the hardness of the materials. Soft powders transmitted higher die wall pressures than the hard powders. Train(1957) directly monitored the stress distribution during the compaction of magnesium carbonate by placing manganin wire resistance gauges at uniformly spaced points in the powder bed. He found that the pressure reaction within compacts measured by this method closely agreed withthe density variations determined by an accurate sectioning of the compacts on a lathe (fig 1.5). The above observation confirmed the presence of non-uniform density distribution in compacts. A simple explanation for this phenomenon was given by Train (1957), who assumed that the relatively high shearing forces at the die wall adjacent to the moving punch developed high density wedges of material. The forces developed in the compact at equilibrium conditions, as proposed by Train are given in (Fig.1.7). The axial force F_A is supported by the punch in direction a, and by the powder mass in direction b. The radial force component is supported in direction c by the die wall and by the powder mass in direction d. The resultant forces acting on the powder mass are represented by e and because of axial symmetry in the compact the pressure front may be considered as a conical surface, with focal point B. This pressure concentration gives rise to the higher density values at point B. Area G which is adjacent to the moving punch and near the die wall is subjected to high shearing forces and will therefore be highly densified. The central area, A, will be protected from

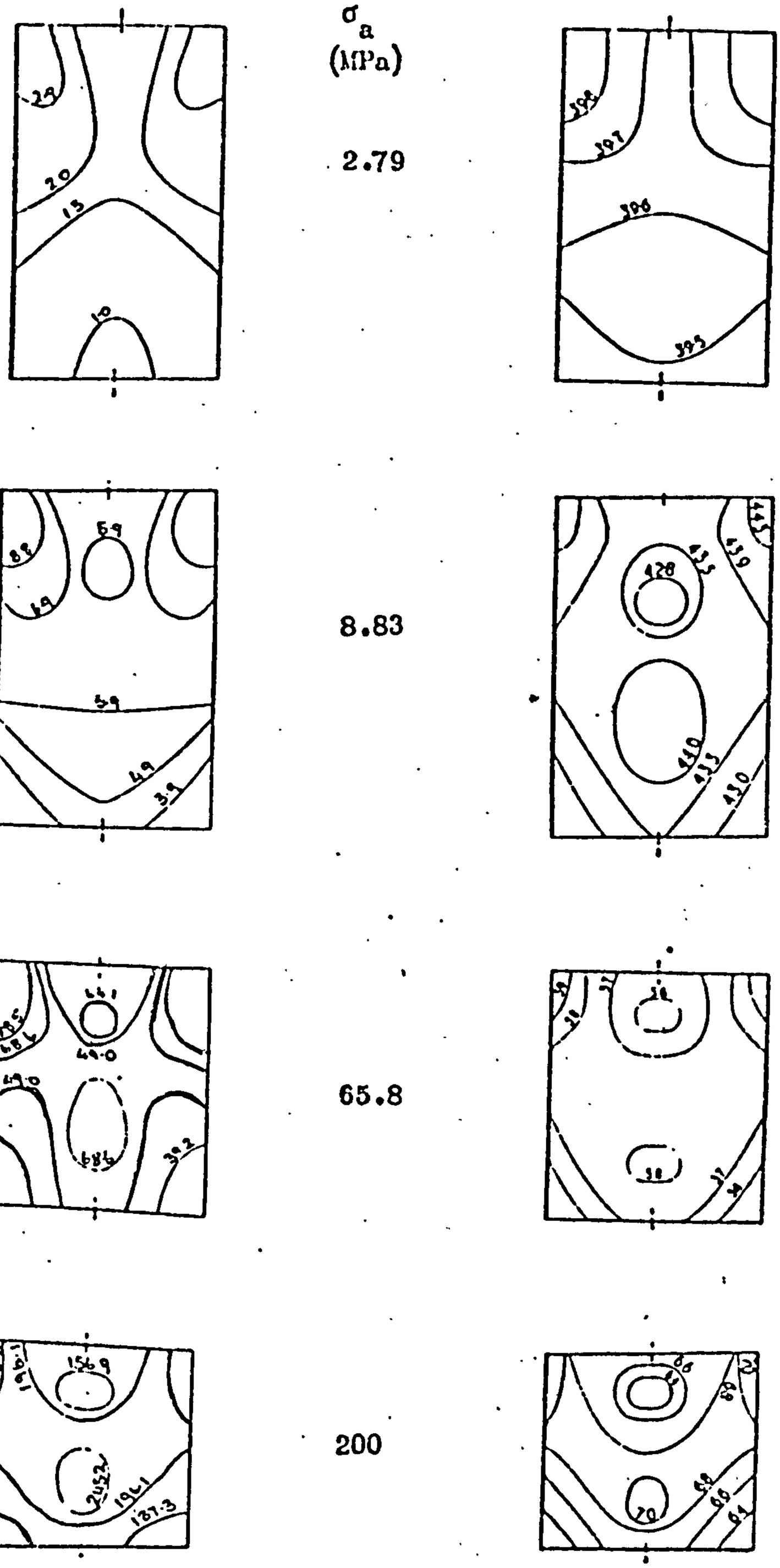

Figure 1.5
Relationship between observed pressure distribution and density distribution in compacts (after Train (120)).

normal axial pressures by the bridging effect of the high density regions. Area, C, adjacent to the stationary punch will not move relative to the die wall, so shearing forces will be absent. The density of this point will be low because densification depends only on transmitted axial forces.

Macleod and Marshall (1977), used an autoradiographic technique to investigate the density distribution in uranium dioxide compacts under varying conditions of feed size, L/D ratio, applied force and lubricating conditions. They showed that in all conditions the maximum density occurred at the circumference of the compact adjacent to the moving punch. The minimum density occurred at the circumference adjacent to the stationary punch. It was also noticed that while the mean density decreased with increasing distance from the moving punch, a high density region existed at the compact axis near the stationary punch which was often denser than the material directly between it and the moving punch (fig 1.6). The density distribution found in uranium dioxide compacts confirmed the discontinuity in the peripheral density pattern of Unckel (1945) and Train (1957). The density pattern found by Macleod and Marshall (1977) with various L/D ratios had several features in common. Each compact exhibited two high density zones, one consisted of an inner axial region and the second an outer peripheral region separated by an annulus of lower density. The distance from the stationary punch to the region of discontinuity in the peripheral density zone was dependant on the conditions of the die wall lubrication and compact

Figure 1.6

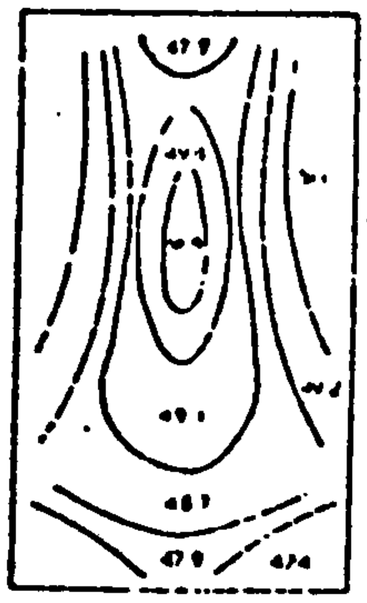

P_A = 70·91 MN m^{-2}
H/D = 1 688

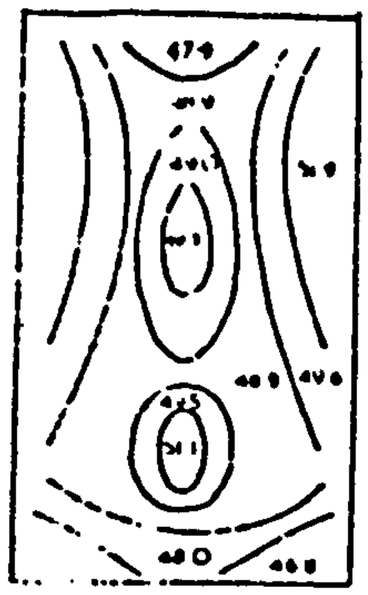

P_A = 157 37 MN m^{-2}
H/D = 1 675

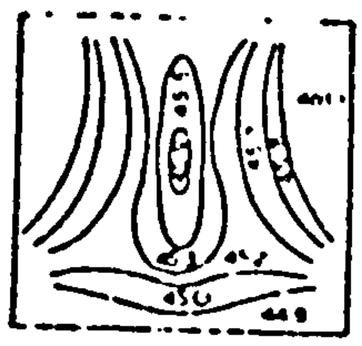

P_A = 79·38 MN m^{-2}
H/D = 0 910

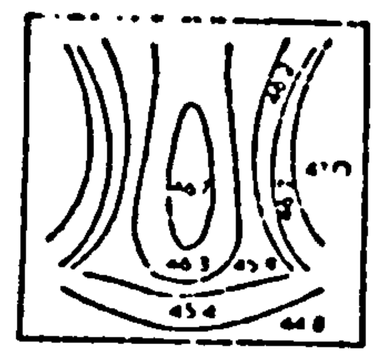

P_A = 75 83 MN m^{-2}
H/D = 0 963

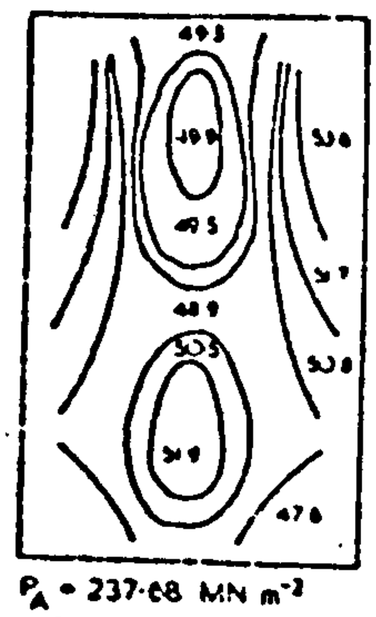

P_A = 237·68 MN m^{-2}
H/D = 1 623

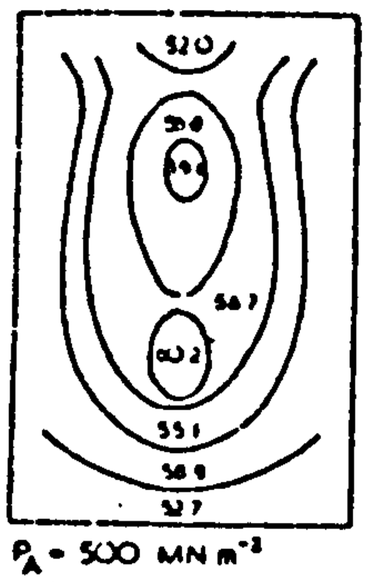

P_A = 500 MN m^{-2}
H/D = 1 489

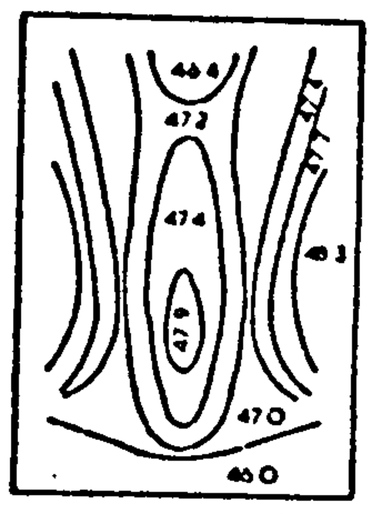

P_A = 79·38 MN m^{-2}
H/D = 1·397

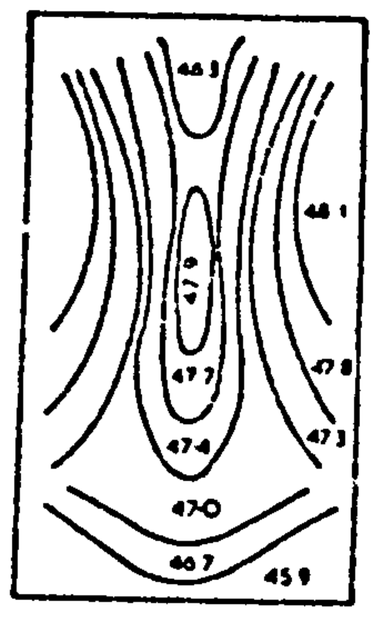

P_A = 79 30 MN m^{-2}
H/D = 1·246

Compacts produced with die wall lubrication

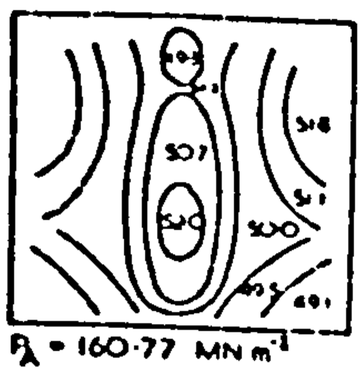

P_A = 160·77 MN m^{-2}
H/D = 0 924

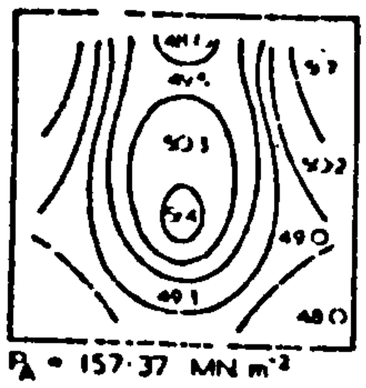

P_A = 157·37 MN m^{-2}
H/D = 0 908

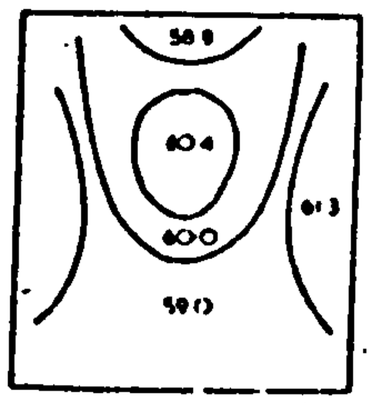

P_A = 401·82 MN m^{-2}
H/D = 1 128

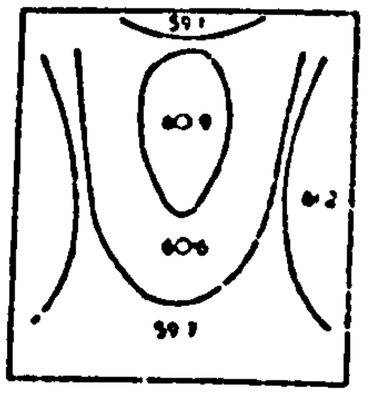

P_A = 398 33 MN m^{-2}
H/D = 1·126

Compacts produced with internal lubrication

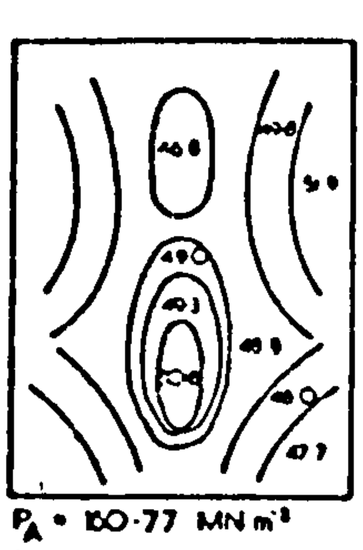

P_A = 150·77 MN m^{-2}
H/D = 1·341

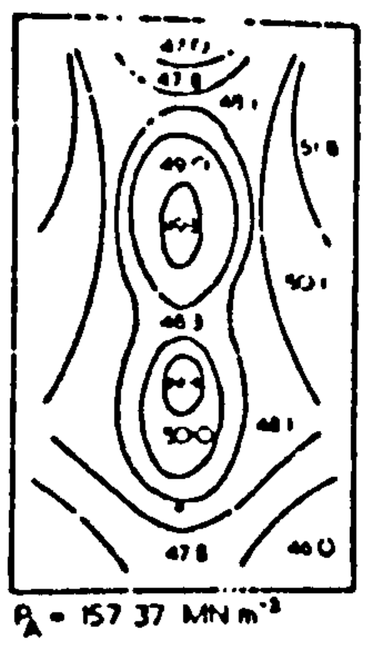

P_A = 157 37 MN m^{-2}
H/D = 1 695

Compacts produced without die lubrication

Density distribution patterns for uranium dioxide compacts of varying H/D ratio (after Macleod and Marshall (77))

H/D ratio, but independent of applied pressure (fig.1.6). This was explained by limitation of material movement at the die wall.

The simple explanation proposed by Train (1957), of the development of the density pattern does not fully explain the more complicated results obtained by Macleod (1977). The alternate sequence proposed by Macleod is presented in (fig.1.8). In the earliest stages of compaction, the conditions are described by the pressure bulb concept of Boussinesq (1876) (fig 1.8 a). As the material adjacent to the upper punch begins to move along the die wall, it di_lates and moves away from the die wall. Densification occurs when the frictional forces developed exceed the shear strength of the material. This process is repeated in successive elements to the limits of the material movement. The material movement in turn is governed by the compaction pressure and the resistance produced by the densification of material at the axis of the compact (fig 1.8 b). Material at the centre of the compact is driven downwards into less compacted material, and exhibits a hemispherical pressure front (fig 1.8 c).

When the reaction force from the lower punch exceeds the radial reaction force from the die wall, material from the centre begins to move outwards, (fig.18.d). The changes in direction of the powder movement induces high shearing forces, contributing to the formation of a high density area centered on this point (fig 1.8 e). The low density regions observed on the compact axis adjacent to the moving punch and around the die wall

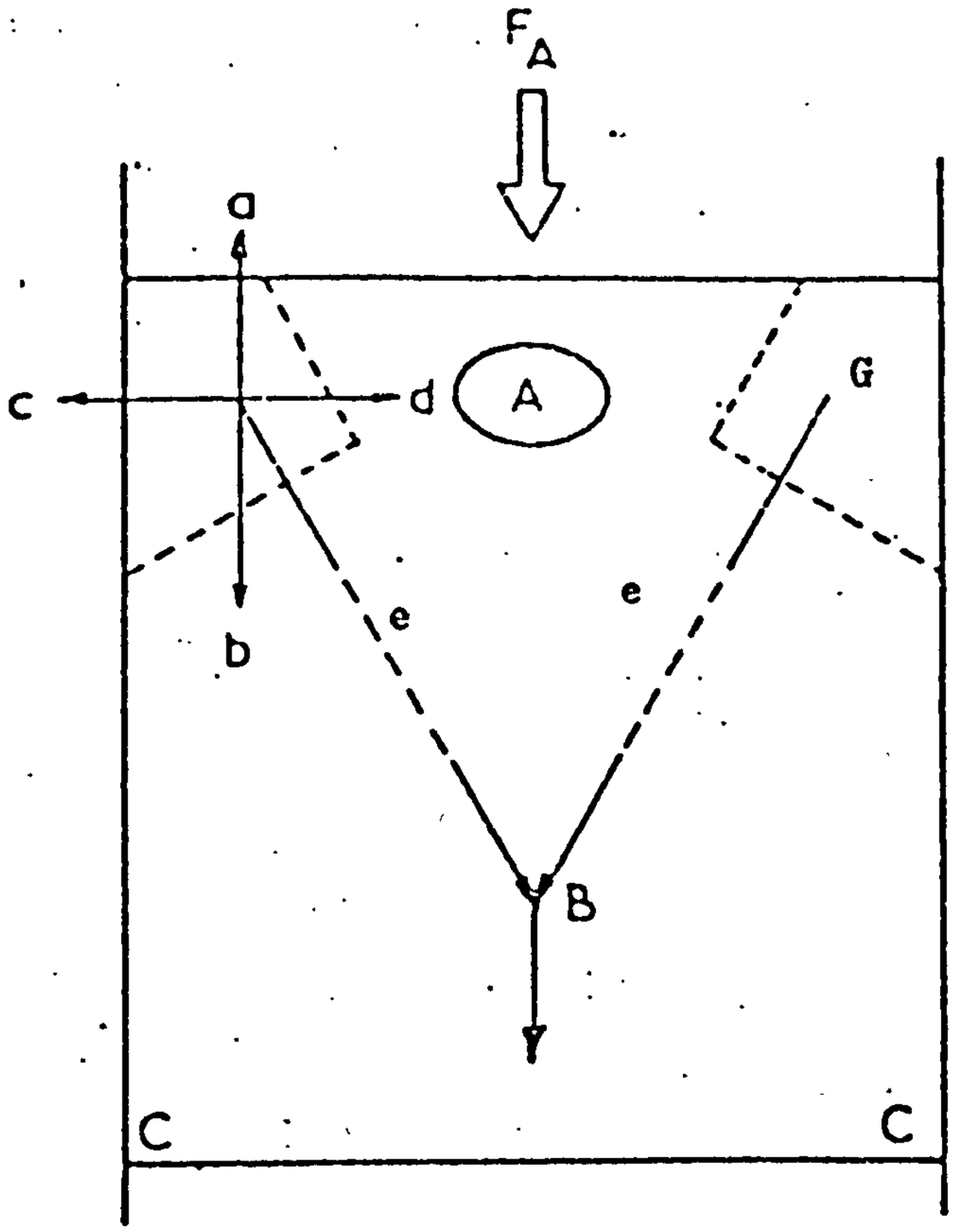

Figure 1.7 : Development of pressure pattern (after Train (120)).

Figure 1.8

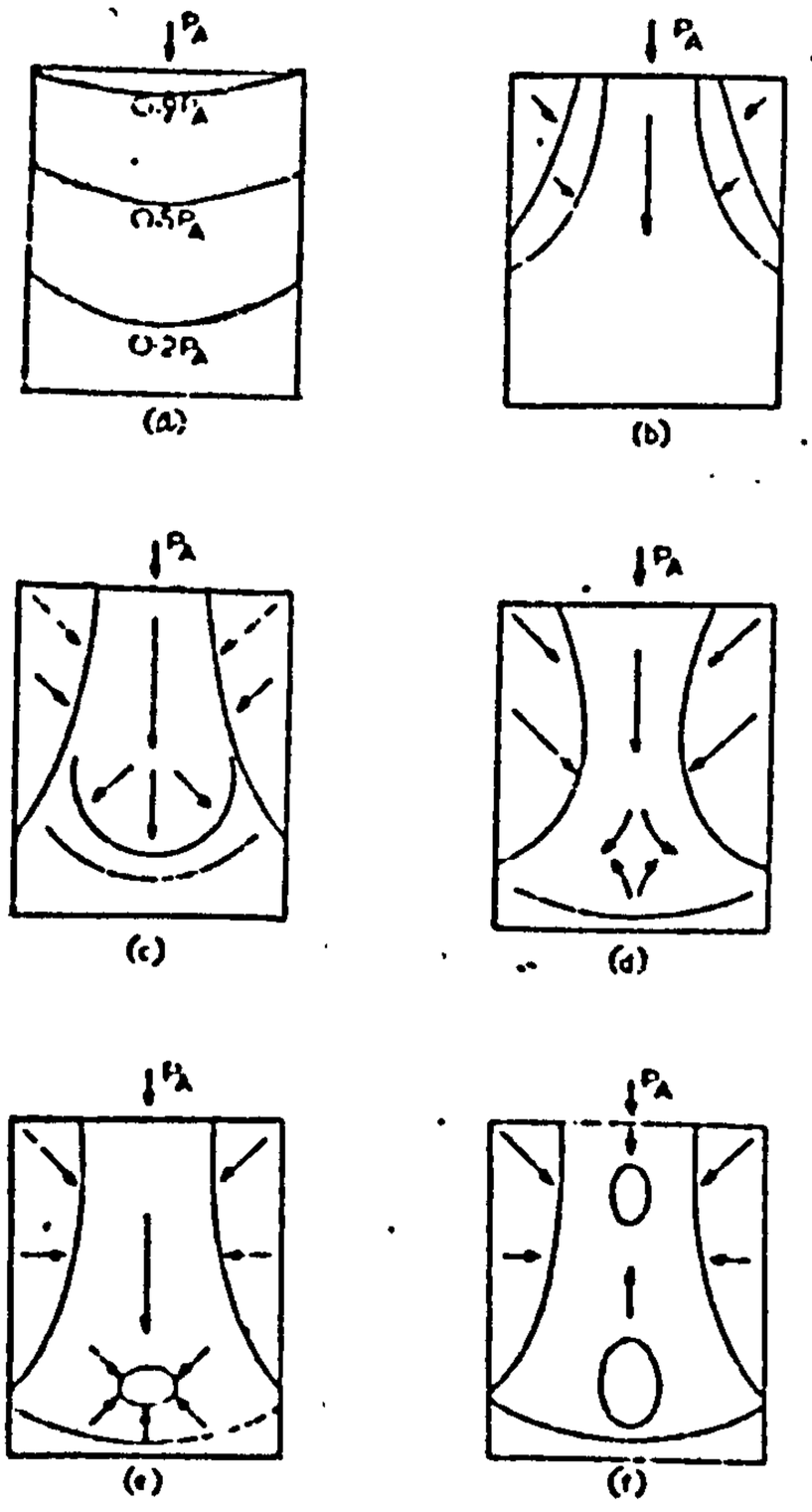

Development of pressure pattern (after Macleod and Marshall (77)).

adjacent to the stationary punch correspond to areas where negligible powder movement has occurred and shear forces are minimal. The formation of the secondary high density region in the axial zone may be explained by the assumption that the axial reaction from the primary high density zone exceeds the radial pressure at any point above it which then causes an outward material movement and densification. This mechanism being similar to that causing the primary high density zone. (Fig.1.8 f).

The above explains the complexity of the behaviour of powders under pressure, and the interdependency of stress-strain relationships in compaction.

1.1.4 Effect of particle properties on compaction processes

The effect of material characteristics and particle geometry on compaction has been reported by many authors who have discussed the process of compaction in terms of the mechanisms involved in the densification process.

The effect of particle hardness on the compaction of ceramic powders was studied by Cooper and Eaton (1961) who compacted alumina, silica, magnesia and calcite powders of the same particle size fraction in a 0.535 inch diameter die to pressures from 0-88,500 psi. They showed that the compaction behaviour of the four powders depended on their hardness, the harder materials were more difficult to compact. Huffine and Bonilla (1962) investigated the pressure-volume relationships of non-metallic crystalline powders, Sodium chloride, sucrose and quartz, and

demonstrated that the volume change accompanying a given pressure increase was greater the smaller the particles. They argued that the pressure needed for complete rearrangement or slippage of particles before the beginning of particle deformation is higher for small particles than for large particles. The effect of initial particle size on the tensile strength of compacts was reported by Shotton and Ganderton (1961) who showed that with decrease of particle size of sodium chloride powder an increase in tensile strength of compacts occurred. Beddow (1968) investigated the pressure transfer characteristics of different shaped copper powders and showed that the spherical powders transmitted the compaction pressure more effectively than the non spherical powders. The effect of particle size and shape on the initial part of the compaction process was also studied by Kostelnik (1968) who compacted iron and copper powders under low pressure ranges of 0-5 psi. He concluded that the volume pressure curves were markedly affected by particle shape. Ridgway and co-workers (1969) confirmed the effect of crystal hardness on the compaction process by measuring the radial pressure at the die wall using a photoelastic technique during compaction of pharmaceutical powders. Seven crystalline pharmaceutical materials, namely aspirin, urea, hexamine, salicylamide, potassium chloride, sodium chloride and sucrose with known crystal hardness (Ridgway, Shotton and Glasby 1969) were used.

They concluded that the pressure on the die wall increased as the hardness value decreased. Hersey and Rees (1971) reported that the volume change during the compaction was independent of particle size when crystalline Lactose and spray-dried Lactose were compacted at 49 MN/m^2 while sodium chloride showed size dependancy. York (1978) studied the effect of particle size and shape on the mechanisms of compaction for α-lactose monohydrate, chloroquine diphosphate, stearic acid and calcium carbonate powders and concluded that the degree of particle slippage and rearrangement during compression increased as the particle size of the powder decreased. The degree of slippage was more extensive for irregular shaped powders than for spherical powders.

The above work thus shows the importance of powder characteristics such as size distribution, shape and surface conditions on the compaction process (Hausner 1981).

1.1.5 The effect of compaction on surface topography

The comparison of various types of gas adsorption isotherms can be used to characterise compacted materials (Section 1.4.3). Carman and Raal (1951), used the adsorption of difluordichlormethene (CF_2Cl_2) at a temperature of 240K to investigate the porosity in compacts of silica and carbon black. They found a change in the shape of isotherms from a Type II, BDDT characterisation, for the loose powder to a Type IV for compacted powder. A pore and void size analysis of

the compacts indicated that the pore and void size distribution became more uniform when the compaction pressure increased. Higuchi and co-workers (1952-1954), investigated the effect of compaction on the specific surface area and porosity of sulphadiazine, aspirin, lactose and sulphathiazole granules. The surface areas of compacts were found to initially increase to a maximum with increase of compaction pressure and then decrease significantly with further increase in the compaction pressure. The explanation given was that the granules of the compacted material fragmented and then rebonded at higher pressures (fig 1.9). A different behaviour was observed by Matsumaru (1958-59), who investigated the specific surface area, calculated from water vapour adsorption isotherms, of aluminium silicate compacts. He found that the surface area decreased continuously as the compaction pressure increased. He also reported a change in the shape of the water vapour adsorption isotherm from a Type II, which is characteristic of non-porous uncompacted materials to a Type IV which is characteristic of porous materials. Pore size analysis, from the adsorption isotherms, showed the consecutive elimination of larger pore sizes as the compaction pressure increased. Bockstiegel (1966-1967), used a microscopic linear analysis method to investigate the interparticle and intraparticle porosity and pore/void size distribution in metal powder compacts. He showed that as compaction pressure increased

large interparticle voids in a compact disappeared first and then in the order of magnitude. The largest interparticle voids disappeared at the lowest compaction pressure and the smaller interparticle voids at the highest pressure.

The effect of compaction pressure on the surface area of tablets prepared from granulated phenacetin, paracetamol and magnesium carbonate was studied by Armstrong and Griffith (1970) and Armstrong and Haines-Nutt (1972). They showed that the specific surface area of magnesium carbonate first increased and then decreased as compaction pressure increased. This work on granules was in agreement with the work of Higuchi. A second increase in surface area was also noticed at high compaction pressures. The reason given for the second increase was assumed to be the effect of elastic recovery of the material (fig 1.10). Hardman and Lilley (1973), investigating the mechanisms of compaction of three different materials, namely sodium chloride, sucrose and coal, observed changes in specific surface determined by low temperature adsorption of nitrogen and carbon dioxide and in the pore size distributions determined by high pressure mercury penetration. It was found that the specific surface area of sodium chloride, continuously decreased with increasing compaction pressure, while sucrose and coal showed an increase of surface area with increase in compaction pressure. The decrease of the sodium chloride surface area with increase in compaction

Text cut off in original

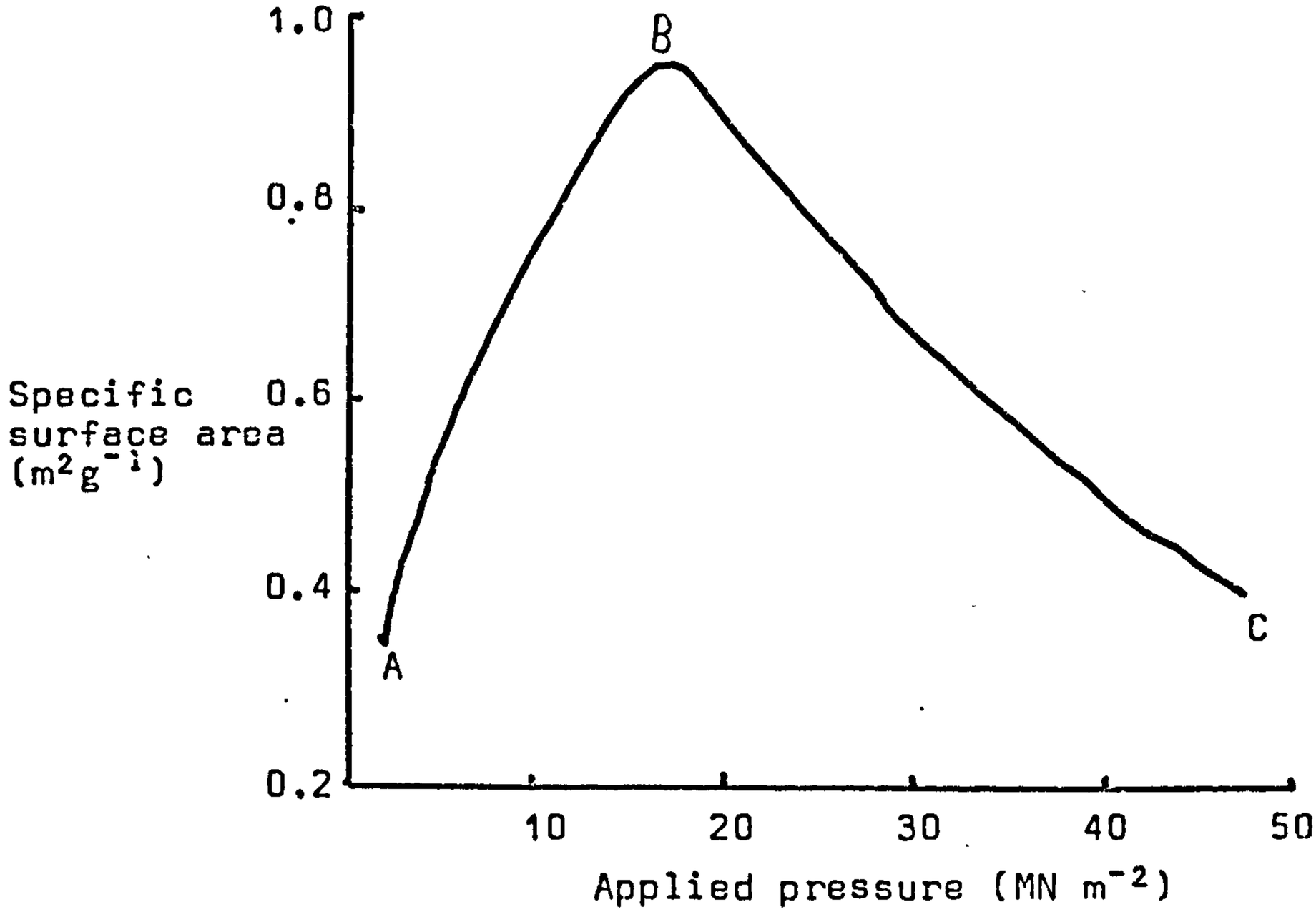

Figure 1.9 Relationship between Applied Pressure and Specific Surface Area (after HIGUCHI)

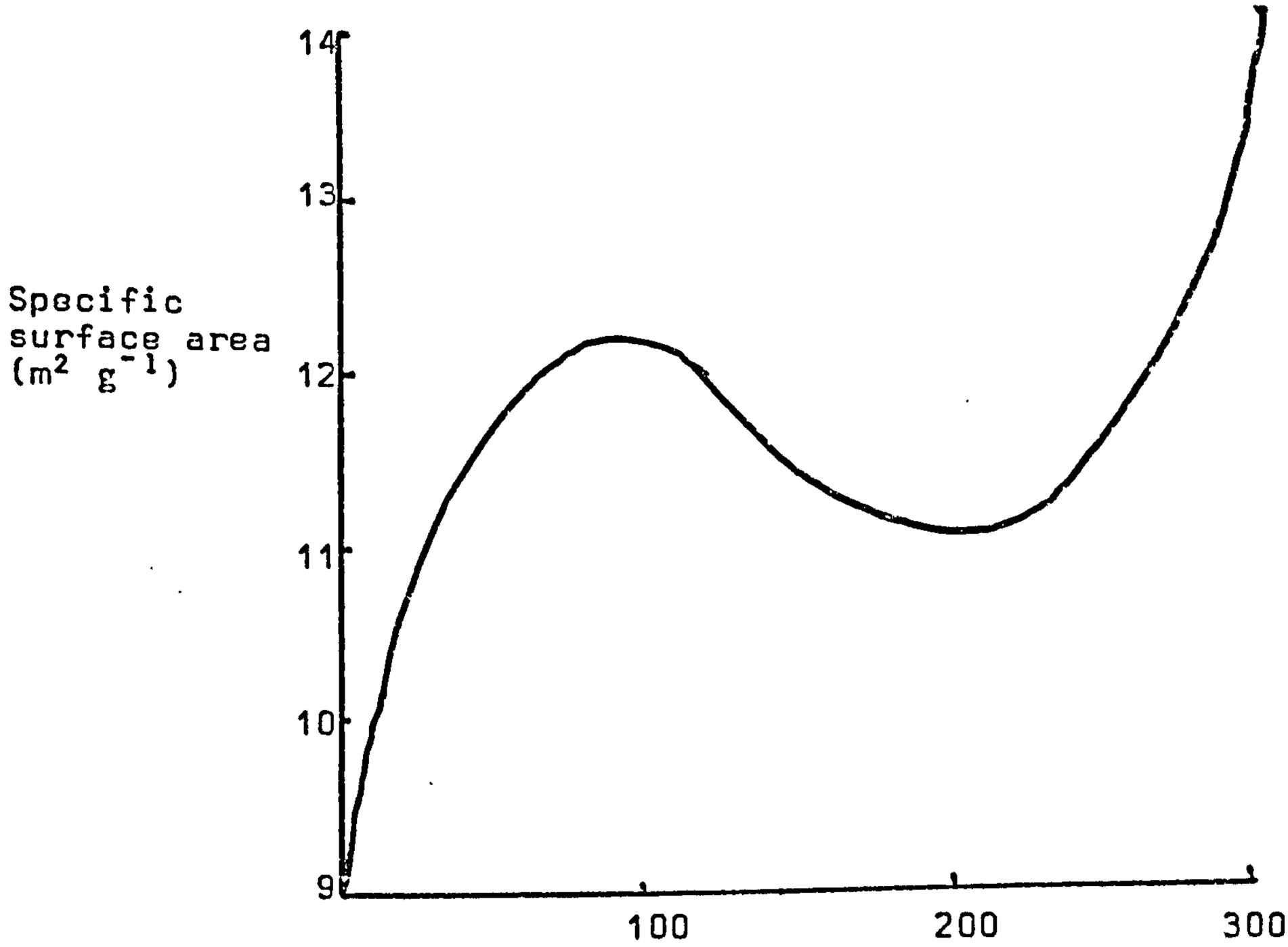

Figure 1.10 Effect of Consolidation on Specific Surface Area of Magnesium Carbonate (after ARMSTRONG et al)

pressure was explained in terms of the plastic deformation of the particles. The contact area, which can be taken as half the difference between the surface area measured before and after compaction was however found to increase with compaction pressure. The increase of surface area in sucrose and coal was attributed to the fragmentation of the material under pressure. Avery and Ramsay (1973) studied the effect of compaction on the surface area and pore structure of silica and zirconia powders. A marked decrease in surface areas was found by increasing the compaction pressure. A change in the shape of adsorption isotherms occurred from a type II BDDT isotherm for uncompacted powders, to a Type IV isotherm for compacted powders. At very high pressures both materials gave Type I isotherms which is indicative that no capillary condensation of the adsorbate takes place on or in the compacted particles. A similar study to that of Avery and Ramsay was carried out by Gregg and Langford (1977) on six powders chosen to cover a variety of particle shapes. The shapes chosen were spherical particles (alumina and silica), plate-like particles (mica and illite), aggregates of plates (Kaolin) and trough-like particles (Halloysite). Low temperature nitrogen adsorption isotherms were obtained for all the powdersbefore and after compaction. The variation of porosity and surface area evaluated from these irregular shaped powders at different compaction pressures was attributed to both the shape and hardness of the particles.

The change of surface area in compacts prepared from microcrystalline cellulose has been investigated by Sixsmith (1977). It was shown that at low compaction pressures a slight decrease in surface area from the uncompacted cellulose was followed by an increase in surface area at higher compaction pressures. The interparticle pore size distribution within the compacts calculated from adsorption isotherms showed no change in pore size distribution, but the pore size distribution obtained from mercury penetration showed a decrease in the size of the pores with increase in compaction pressure.

Stanley-Wood (1975) studied the effect of compaction on the surface area and pore size distribution of magnesium oxide and showed that the surface area initially decreased and then increased at higher compaction pressures. The increase in surface area was attributed to fracture of the particles. Stanley-wood and Johanson (1977) also studied the effect of compaction on the surface topography of three different powders. They concluded that the knowledge of the surface areas of uncompacted and compacted powders and the calculation of pore size distribution of compacts yielded useful information about the mechanism of compaction. They used the relationship between contact area and compaction pressure to show whether bonding was achieved by particle rearrangement or plastic deformation.

Stanley-Wood and Shubair (1979) compacted granules of dicalcium phosphate, a fragmenting material, with different concentrations of starch mucilage as binder

and determined the surface areas and porosities of the granulated powder before and after compaction. They proposed a method to calculate the degree of fragmentation from the knowledge of surface area and crushing force of the compacts.

1.2 Stress-Strain Relationship

The application of force to a solid can cause deformation, which depends on the nature and magnitude of the applied force. Tensile force causes an extension while compressive force causes a shortening of a solid specimen. If the force is of sufficient magnitude, permanent or plastic deformation of the body may have occurred on removal of the force. When the force is insufficient to cause permanent deformation the body may recover its original shape on removal of the force. This type of deformation is called elastic deformation.

1.2.1 Strain

Strain is a measurement of the deformation of the body. Three types of strain are recognised.

Linear or engineering strain relates the total change in length to the original length (fig.1.11).

$$e = \int_{L_0}^{L_1} \frac{dL}{L_0} = \frac{L_1 - L_0}{L_0} \qquad (1.4)$$

where $L_0 \equiv$ original length

$L_1 \equiv$ the length after deformation.

Natural or true strain is the incremental change in length divided by the instantaneous length, $d\xi = dL/L$, and the total true strain resulting from a change in length from L_0 to L_1 is given by:-

$$\xi = \int_{L_0}^{L_1} \frac{dL_1}{L_1} = \ln \frac{L_1}{L_0} \qquad (1.5)$$

Figure 1.11

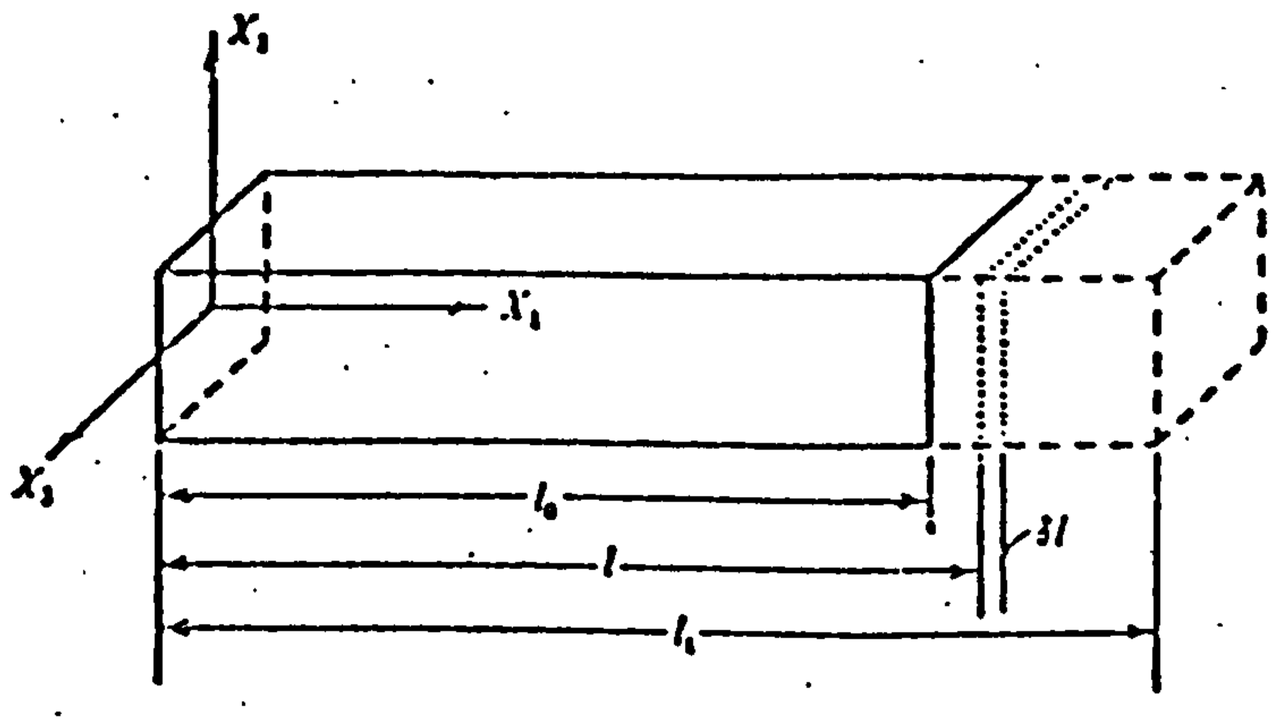

Uniaxial normal strain

Figure 1.12

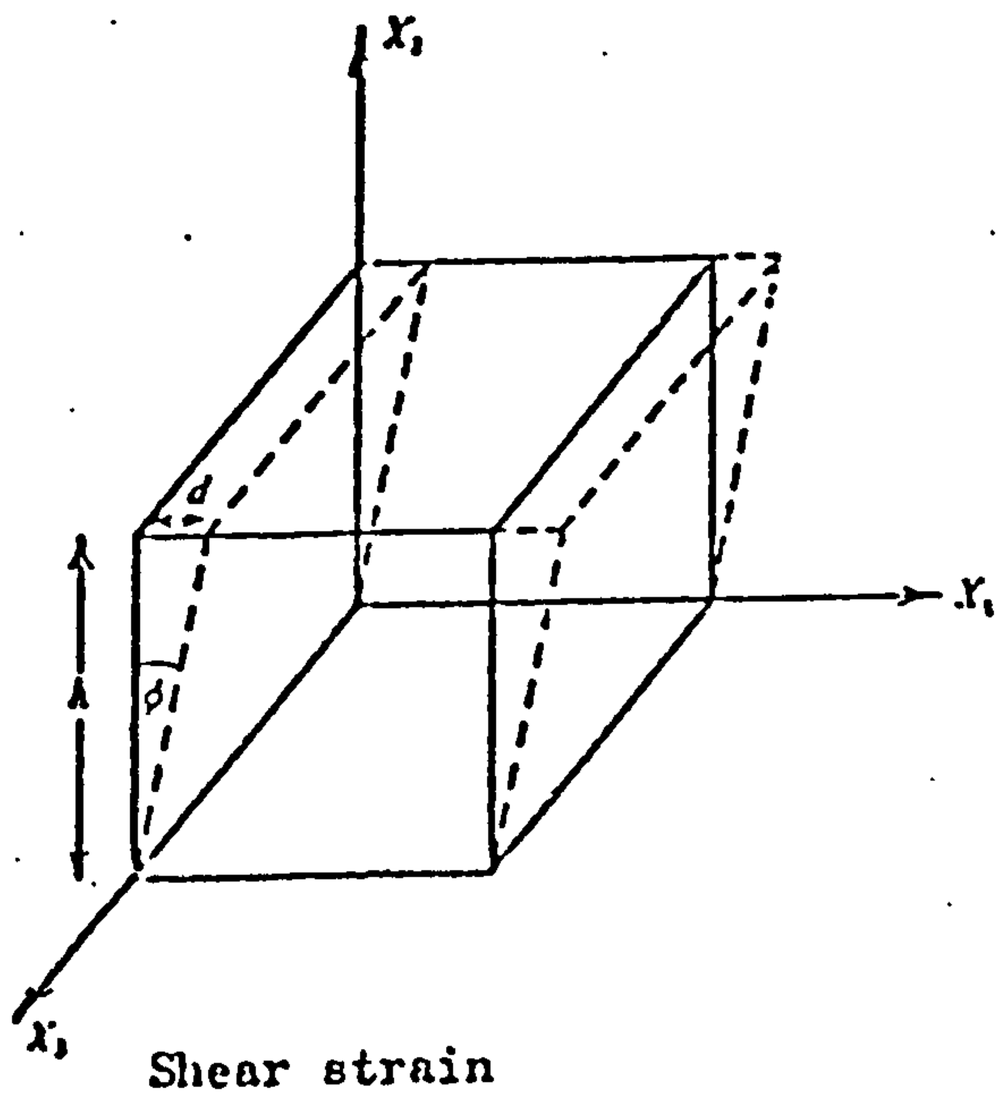

Shear strain

Shear strain occurs when parallel planes are moved relative to one another, keeping the separation between the planes constant. An example of shear strain occurs in the distortion of a rectangular block into a parallelopiped (fig.1.12).

1.2.2 Stress-Strain relationship

The simple description of stress and strain may regard these parameters as being independent of each other, stress may then be treated as a problem of statics while strain may be treated as a problem of geometry. In reality however these two parameters are intimately interrelated since strains are created when stress is applied to a body. The elastic part of this relationship is defined by Hookes law. Since there are two basically different types of stresses and strains, that of normal stress and strain and shear stress and strain, two different relationships exists:-

$$\delta = E\xi \qquad (1.6)$$

and

$$\tau = G\nu \qquad (1.7)$$

The constant E is the elastic or Young's modulus and G is the shear modulus or modulus of rigidity.

When an elastic body is stretched, it deforms in accordance with Hooke's Law and contracts laterally. This lateral strain is a fraction of longitudinal extension and is known as Poisson's Ratio. Various relations may exist between the material moduli and Poisson's ratio (Polakowski 1966):-

$$K = \frac{E}{3(1-3\nu)} \qquad G = \frac{E}{2(1+\nu)} \text{ or } E = \frac{3G}{1+G/3K} \qquad (1.8)$$

where K ≡ the bulk modulus.

The stress-strain relationship is of great importance in the characterisation of engineering materials to predict the behaviour of materials during deformation. According to the type of deformation, the relationship is termed elastic (fig 1.13 a), when the stress-strain curve is linear, and plastic when the material deforms beyond the initial elastic limit (fig. 1.13 b) Assumptions can be made in which the material is considered to be either a perfect elastic or rigid plastic material (fig 1.13 c), in order to simplify the mathematical interpretation of data.

The elastic range of solids is limited by either the occurrance of fracture in some cases and/or by permanent deformation in others. Whether a body will behave elastically or plastically is based on knowledge of the yield strength (or yield stress) obtained from a simple tension or compaction test (fig. 1.14). Yield stress can be defined as that stress at which deformation changes from elastic to plastic. It was necessary at times to relate the stress components to the yield stress in such a way as to determine whether plastic yielding will or will not occur under certain combined stresses. From such observations the theory of yield criterion has been developed.

1.2.3 Criterion of Yielding for plastic metarials

One of the theories of yield criteria is the maximum shear theory of Tresca (1865), which states that plastic

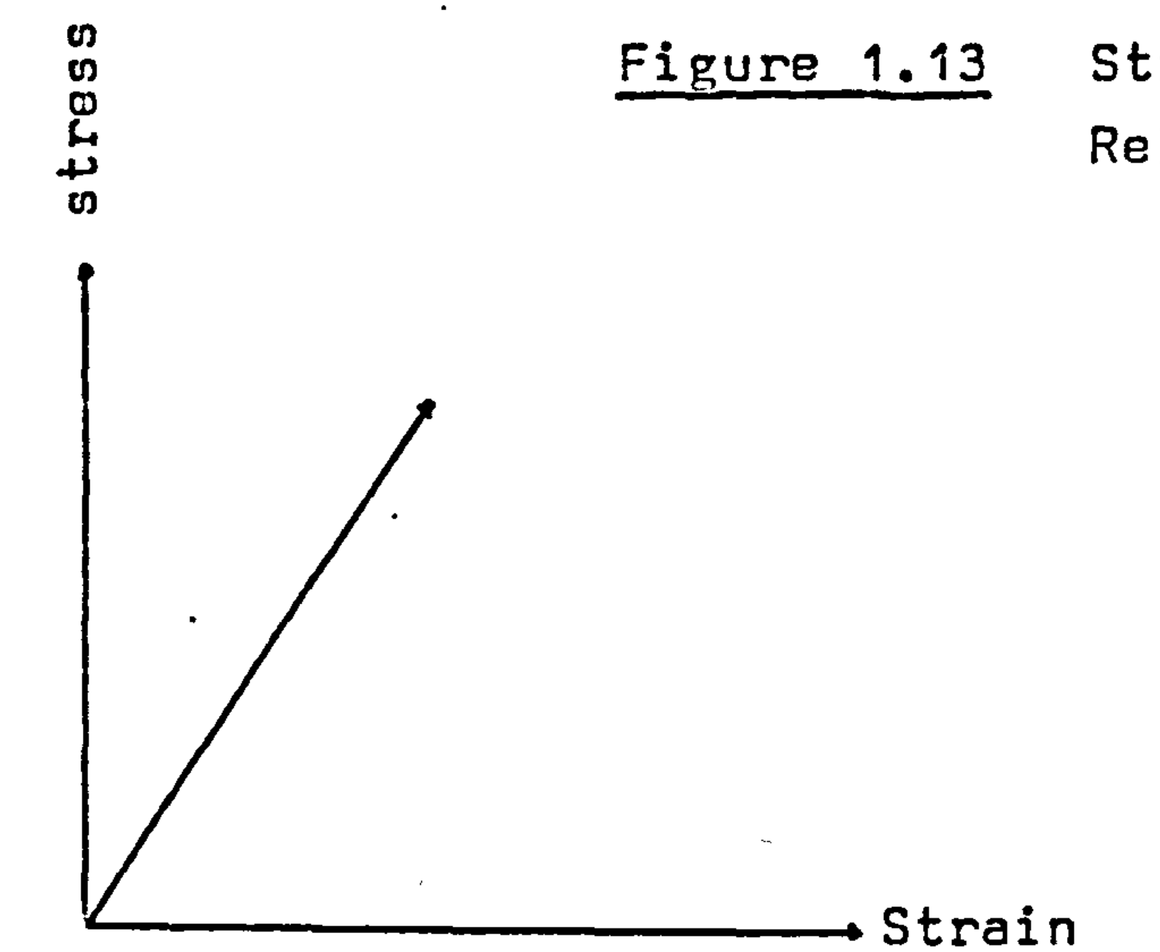

(a) Elastic

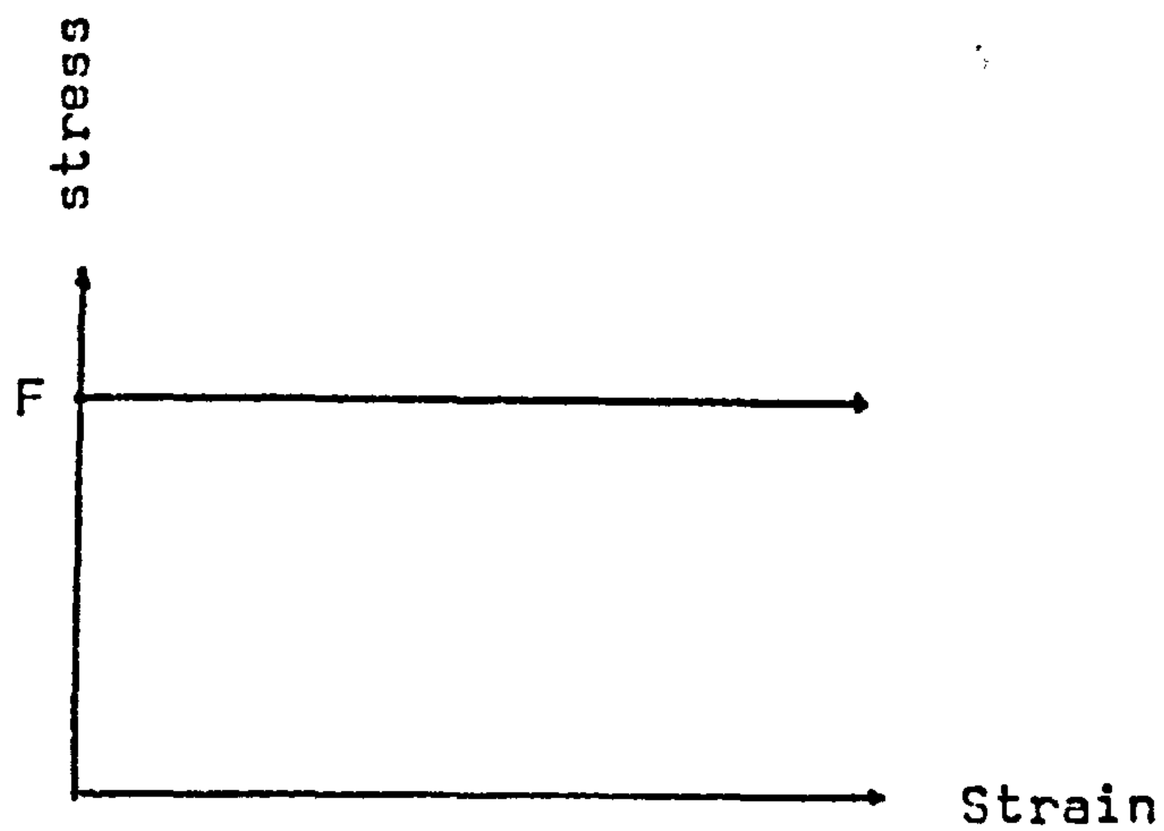

(c) Rigid plastic

Figure 1.13 Stress strain Relationship

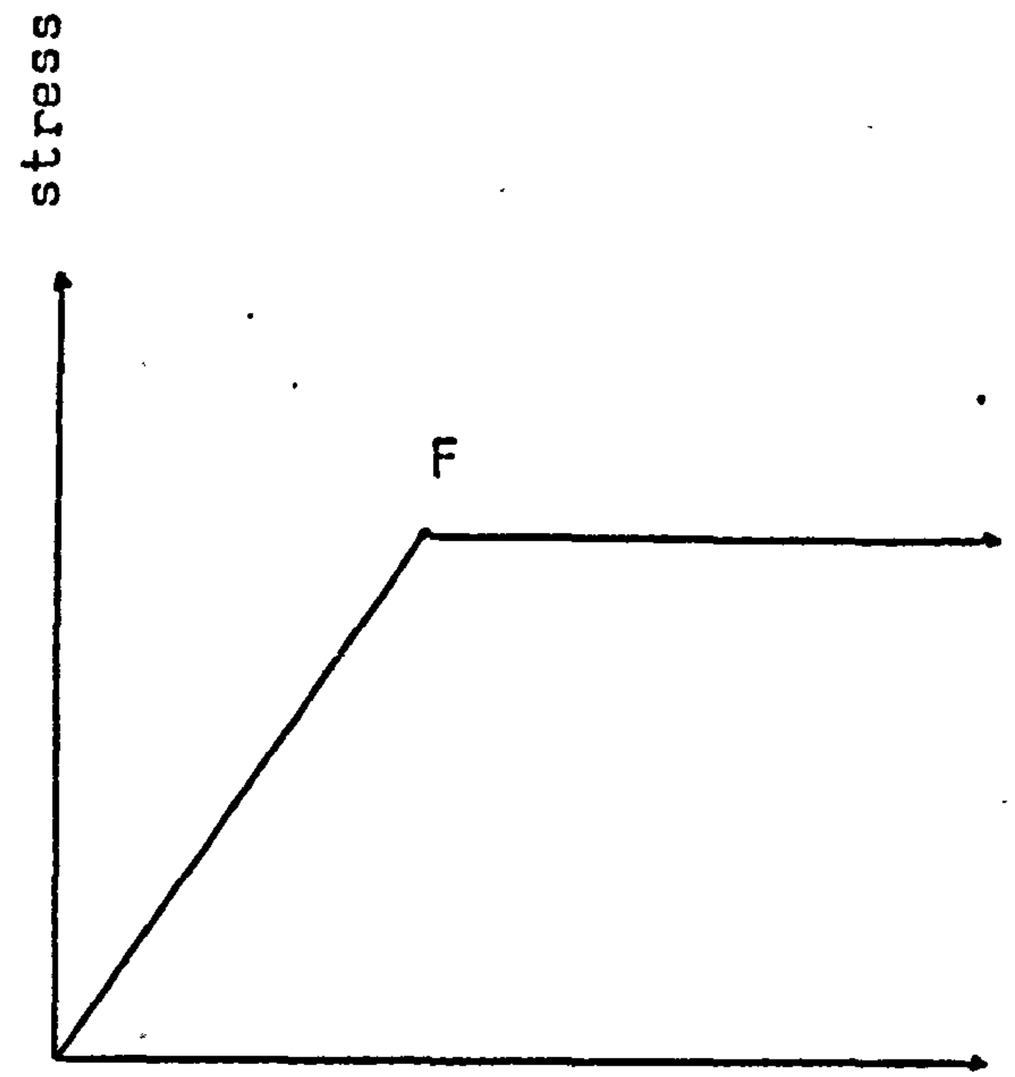

(b) Elastic plastic

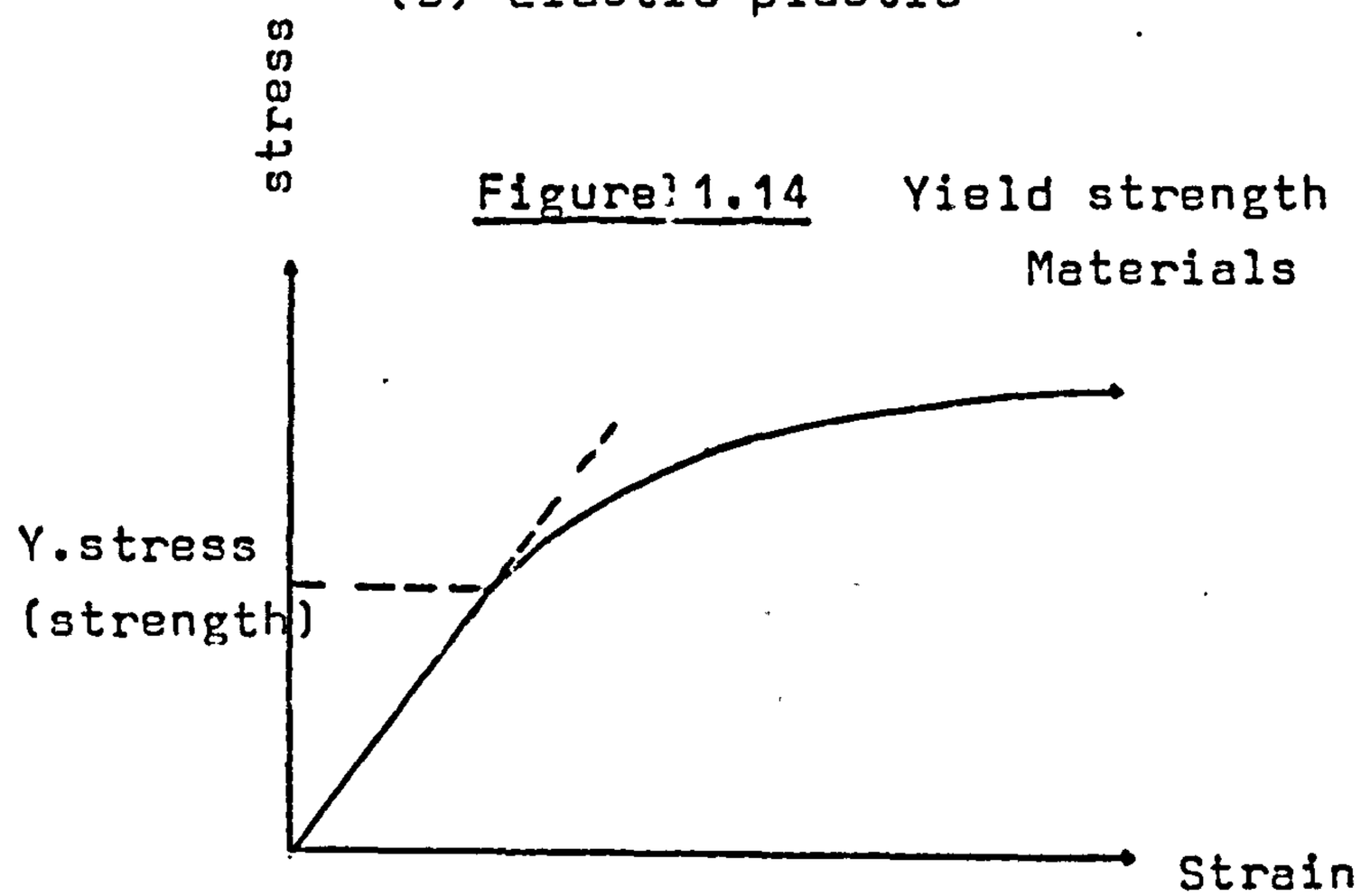

Figure 1.14 Yield strength Materials

deformation begins when a shear stress anywhere in a body reached the same value obtained from a simple tension or compression test at the yield point. If the principal stresses on a body are $\delta_1 > \delta_2 > \delta_3$, then Trescas relationship can be expressed mathematically as:-

$$F = \delta_1 - \delta_3 - 2K = 0 \qquad (1.9)$$

where K is the critical value or maximum shear stress for yield to occur and F, is the yield fraction.

An alternative yield function which has found common use in the representation of yield criteria is that of von Mises, which can be expressed as:-

$$F = (\delta_1-\delta_2)^2 + (\delta_2-\delta_3)^2 + (\delta_3-\delta_1)^2 - 2Y^2 = 0 \quad (1.10)$$

where Y is the von Mises yield stress.

The von Mises yield surface can be regarded as a circular envelope with the line $\delta_1 = \delta_2 = \delta_3$ as its axes (fig 1.15a) while Trescas yield surface (fig 1.15b) can be regarded as a hexagonal envelope around the hydrostatical stress line when $\delta_1 = \delta_2 = \delta_3$. Combinations of stress components that lie within the circular or hexagonal prism surface produce only elastic deformation. Stress component which lie outside these envlopes impart yield stresses to the material.

1.2.4 Coulomb yield criterion

In the field of soil mechanics the early work on stress distribution and compaction was based on the assumption of perfect elastic solids by Coulomb (1776), Rankine (1857) and Terzaghi (1943) while some recent workers

like Sokolovski (1960) and De Joslin de Jong (1959) adopted the assumption of perfect plastic for their investigations.

Coulomb (1776) proposed that a mass of material or solid would break by rigid body sliding along a rupture plane when the stresses on the mass were such that a critical relationship was reached between the direct stress σ and the shearing stress τ acting on that plane. Coulomb suggested that both cohesion and friction must be overcome during slippage along the rupture surface. The Coulomb yield criterion states that failure occurs when the shear stress on any plane in a material reaches a critical value which is linearly dependent on the normal stress on that plana. This can be expressed mathematically as:-

$$\tau_f = C + \sigma_f \tan \phi \qquad (1.11)$$

where $\tau \equiv$ shear at failure

$\sigma_f \equiv$ normal stress at failure

$\phi \equiv$ angle of internal friction

$C \equiv$ cohesion due to bond forces between particles

Equation 1.11 can be presented graphically in σ, τ plane as in fig 1.16 and in principal stress space as in fig 1.17 where the shear stress at failure increases with increasing normal stress (Shield 1955).

Jenike and Shield (1959) used the concept of a rigid plastic body, as suggested by Coulomb, to study the flow properties of powders. They showed that the flow of powders is governed by a limiting stress function,

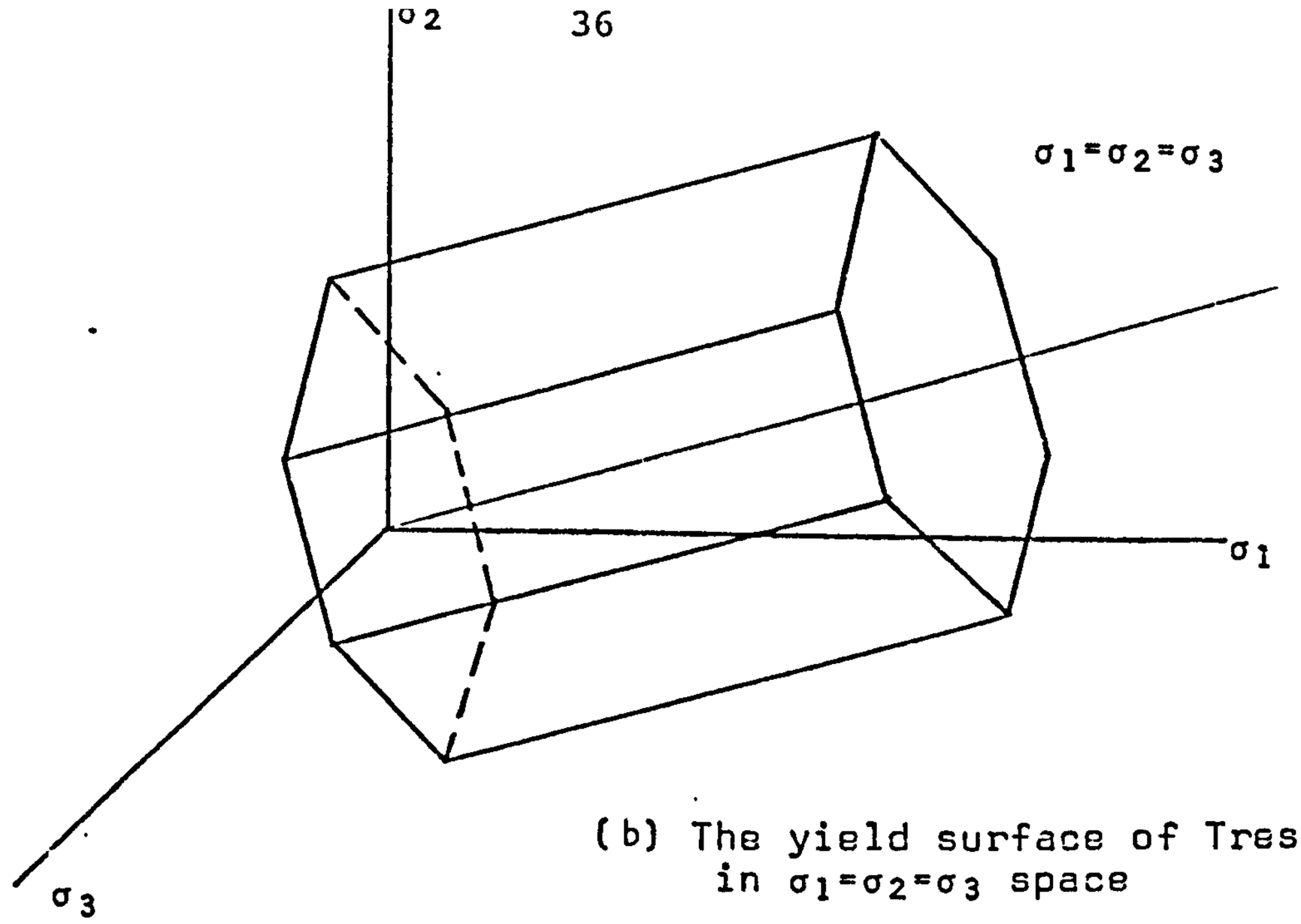

(b) The yield surface of Tresca in $\sigma_1=\sigma_2=\sigma_3$ space

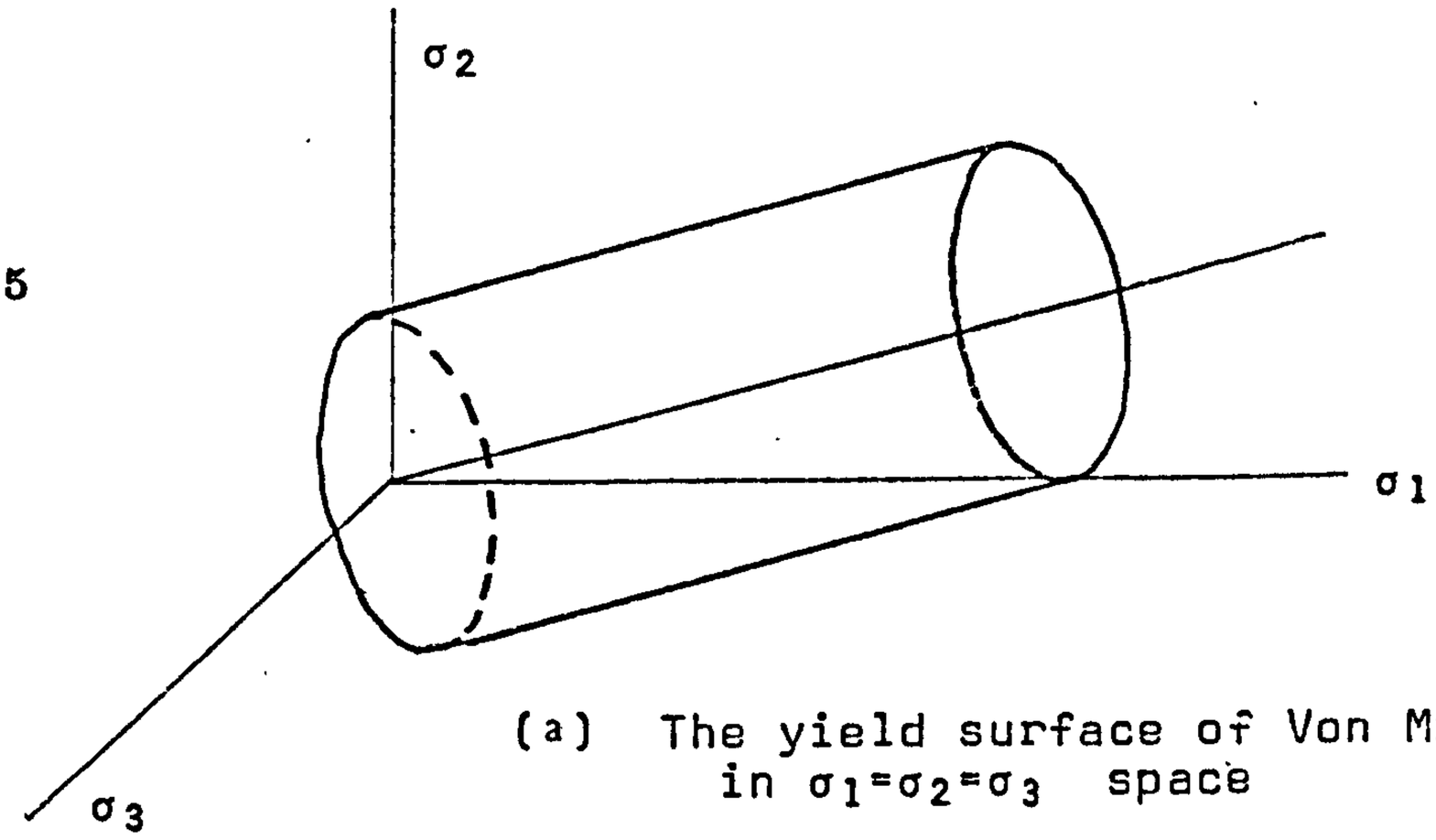

Figurel . 15

(a) The yield surface of Von Mises in $\sigma_1=\sigma_2=\sigma_3$ space

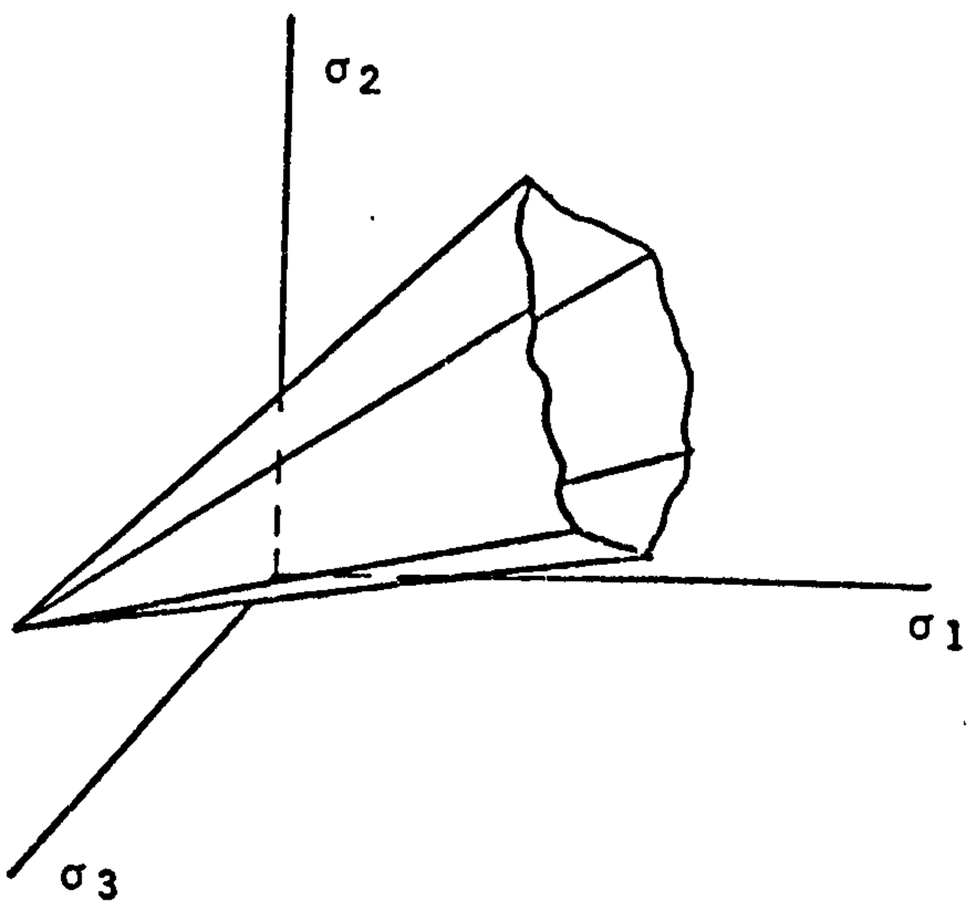

Fig. 1.17 Coulomb yield criterion in principal stress space

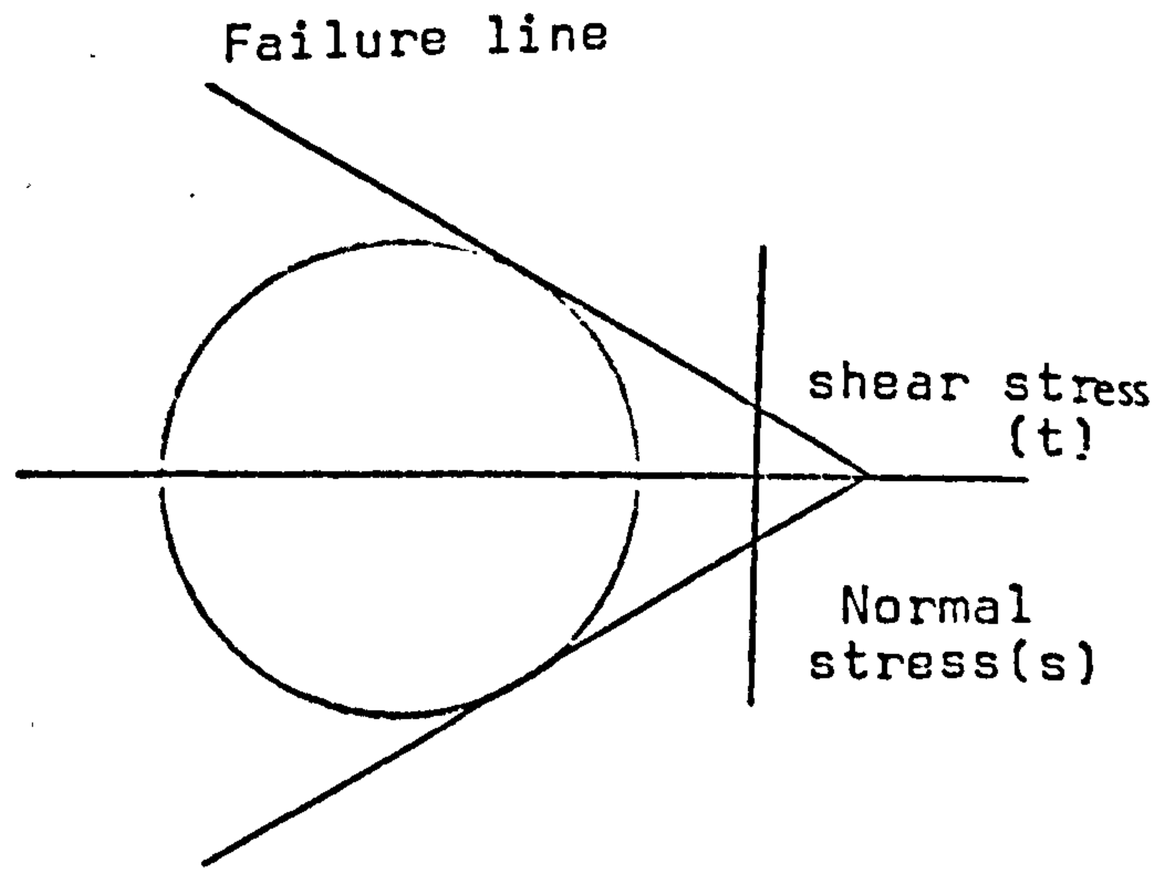

Fig.1.16 Mohr-Coulomb yield criterion

which can be expressed in a normal stress (δ) and shear stress (τ) two dimensional system of co-ordinates which produces a yield locus. The solid will fail or flow when stresses reach this yield locus or from a combination of stresses as depicted by a Mohr circle tangential to this yield locus.

The Mohr-Coulomb criterion has been used in soil mechanics to predict the failure of soils (Bishop 1971). The term failure as used by workers in the field of solid compaction does not imply the fracture of the material but the criterium in which particulate material will begin to move without a volume change. This Mohr-Coulomb criterion is based on the idealization that particulate materials behave elastically up to a certain state of stress, where after, yielding of the particulate material can occur and the shear stress required to promote this yielding or slippage is considered to be a linear function of cohesion and the pressure normal to the slip surface. Recent work by Sokolovski (1960) and De Josselin de Jong (1959) has made use of Mohr-Coulomb theory of perfectly plastic solids but in reality the observed shear-normal stress curve of granular material is generally that shown in (fig 1.18), which shows a wide divergence between observed and assumed behaviour of granular materials. Schwartz and Weinstein (1965), who investigated the compaction behaviour of ceramic particles, uranium dioxide, treated the powder as an aggregate mass of

individual particles interacting with each other through the mechanism of interparticulate friction. The Coulomb yield criterion was used to describe the compaction behaviour of the particulate assembly and to deduce the die wall force and stress distributions within the compacted powder.

Tresca and von Mises in their concepts assumed that the yield surface of metals would extend indefinitely along the space axes, where $\delta_1=\delta_2=\delta_3$.

Schwartz and Weinstein (1965) stated that, in a compressible mass of granular material, a considerable amount of flow will occur on hydrostatic loading and the yield surface is required to intersect its axis. Drucker, Gibson and Henkel (1957) while investigating the compaction process of work-hardening plastic materials, suggested the closure of the yield surface with a spherical base cutting the axis of equal stresses, while Jenike and Shield (1959) and Schwartz and Weinstein (1965) suggested the closure of the yield surface with either a flat or a pyramidal base respectively. Suh (1969) criticised the use of the Mohr-Coulomb yield criterion because it predicted that the yield locus was a straight line with constant slope, which was not shown by the work of Jenike et al (1960) and Schwartz and Holland (1969).

1.3 Stress Volume Relationship

Roscoe (1953), to determine the failure or yielding of consolidated soils, developed a shear cell which could measure the volume change when soils were subjected to shear and normal stresses. Experimental evidence accumulated to show that the loading pathways with clays had a coincidental surface as an envelope in a three dimensional shear stress, normal stress and volume space relationship. Loosely packed steel balls, which were regarded as normally consolidated, underwent a volume contraction when sheared while densely packed steel balls, regarded as overconsolidated material, underwent a volume expansion when sheared. The final point reached for these stress pathways lay on a unique line termed the critical state line. Wroth and Bassett(1965) subsequently used the concept of the critical state line to divide consolidated samples into two distinct categories; those that showed a volume expansion and those that showed a volume contraction when sheared.

1.3.1 Hvorslev Surface

Rendulic (1936) was however the first to relate the change in volume of sheared material with the effective stress state. He showed experimentally that for a given clay in equilibrium, under a known effective stress and specific volume, the specific volume changed after the application of a principal stress increment. The change in specific volume was dependent

upon the principal stress increments.

Hvorslev (1937) critisized the Coulomb equation which related the normal stress σ and shear stress τ to the yielding of material because the equation neglected the effect of volume change of a mass of soil when subjected to shear. He proposed an equation which related the shear stress, τ, at failure to the normal stress, σ, and the void ratio, e, of a particulate solid. The condition of failure of soils occurred when a combination of the shear and normal stresses reached a specific value which could be regarded as a surface known as the Hvorslev surface, in three dimensional space, whose co-ordinates are τ, δ and e (fig 1.19.)

1.3.2 Critical state

The critical state concept was introduced by Roscoe, Schofield and Wroth (1958). The concept states that an isotropic soil sample in a shear test, eventually reaches a critical state in which unlimited shear distortion could be applied without further changes of any of three parameters τ, σ and e. They plotted the ultimate values of the three parameters in three dimensional space and showed that they lay on a unique critical state line (C.S.L.) or Critical Void ratio (C.V.R.) (fig. 1.20). When the critical state line was projected onto σ, τ plane a straight line passing through the origin resulted. This line joins the end points of the family of Jenike yield loci.

Wroth and Bassett (1965), extended the work of Roscoe et al and showed experimentally that the critical state line and the line representing the ultimate tensile strength

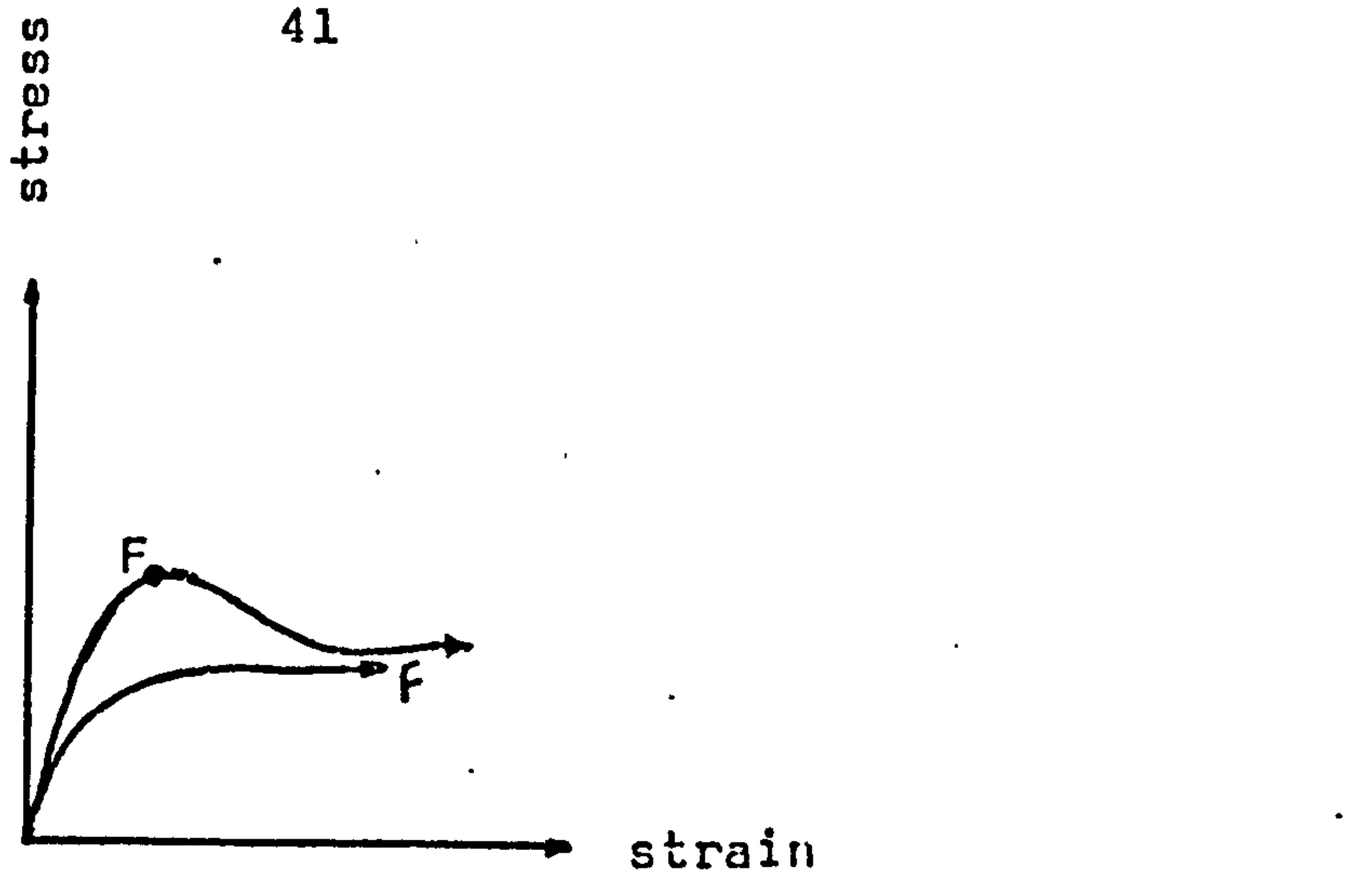

Figure 1.18 Stress strain behaviour of sails

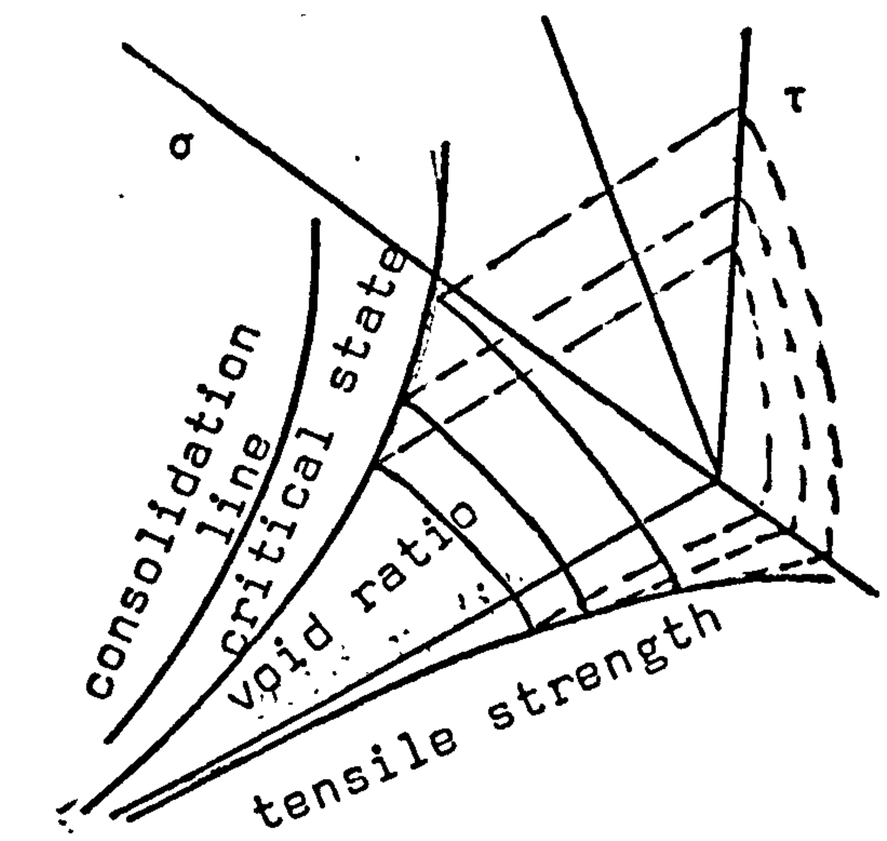

Figure 1.19 Hvorslev surface

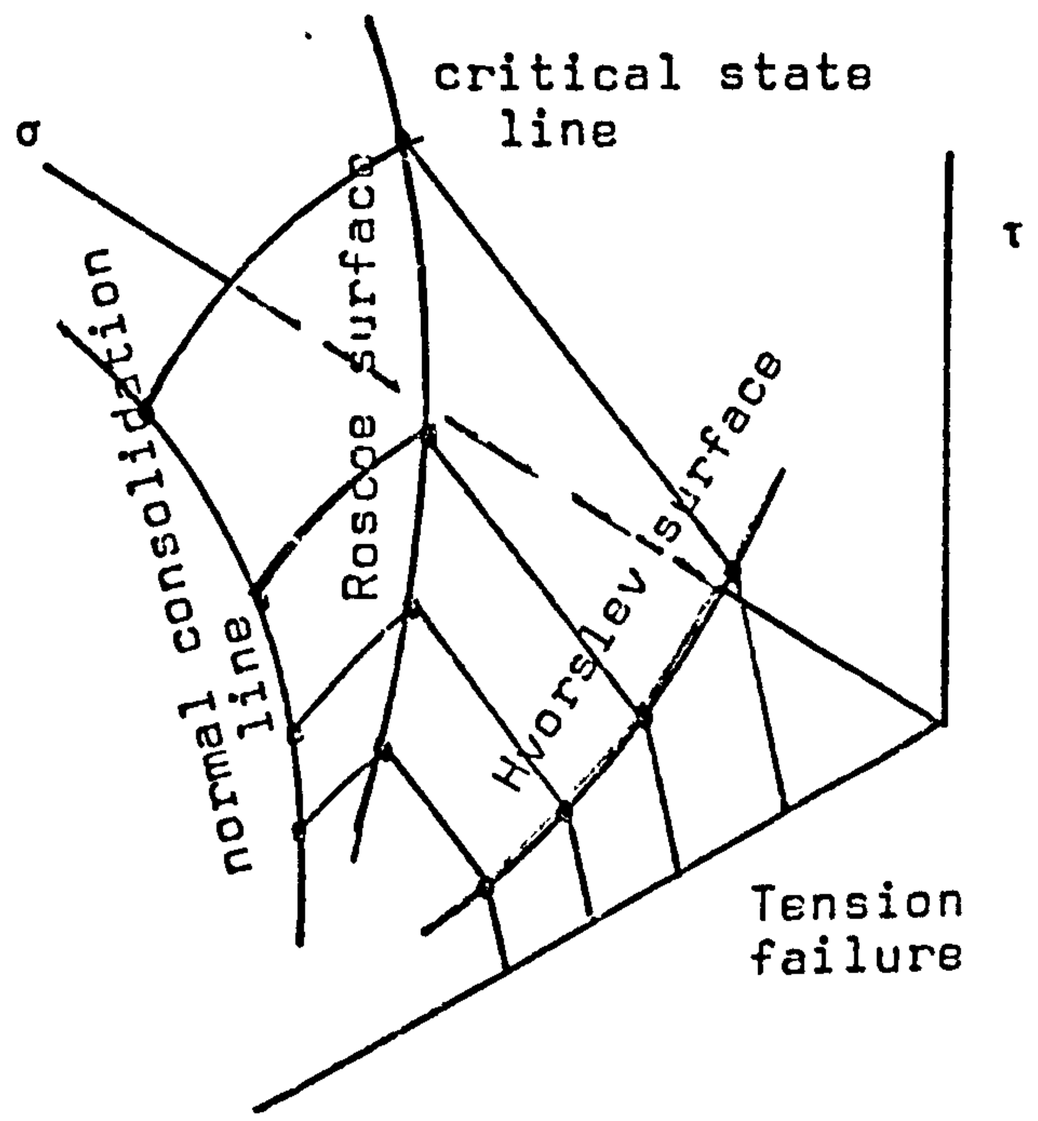

Figure 1.20 Combined Hvorslev and Roscoe surface

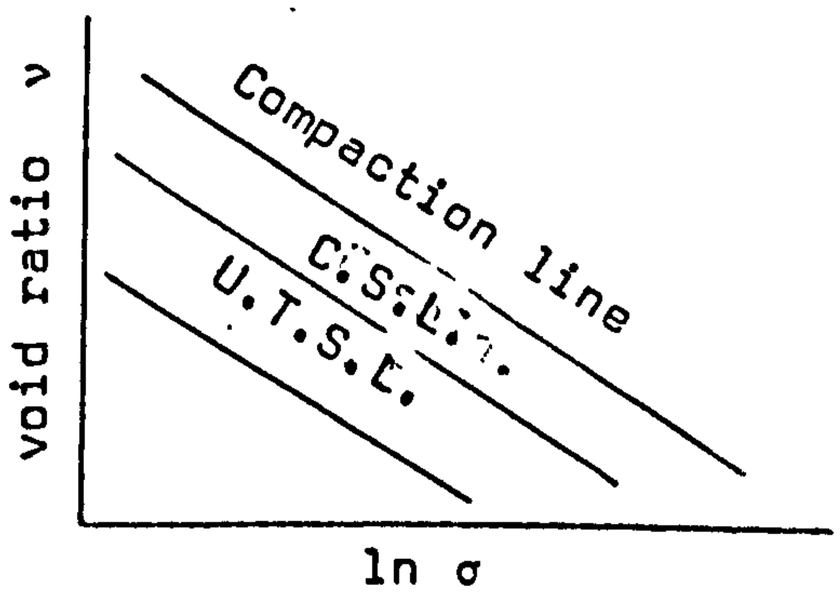

Figure 1.21 Presentation of compaction parameters in v-lnσ space (after Wroth and Bassett)

with void ratio plotted on e - ln σ_n axes, give straight lines parallel to the isostatic normal consolidation line (fig 1.21).

1.4 Particulate Solids

A powder is usually considered to be an assembly of particles of not greater than a 1000 μm in size. In any particulate material the solid particles can vary in size and shape, with gas or liquid between the interstices of the particle assembly.

When particulate solids are to be characterised it is reasonable to consider the particle properties under two main headings.

(a) Properties associated with a single particle.

(b) Properties related to powder mass or assembly of particles - the bulk properties.

1.4.1 Atomic characterisation of particles

A large number of materials consist of aggregates of crystals. The physical and chemical properties of these aggregates are related to the physical and chemical properties of the crystal units making up the aggregate. An individual particle may be characterised with respect to its crystal structure, size, shape and type of physico-chemical bond.

A crystal is usually arranged in space in a regular pattern termed a space lattice. The nature and type of the solid materials can be divided into four groups according to the nature and type of interatomic attractions.

(a) Ionic Solids.

These solids are composed of atoms or groups of atoms that either lack electrons or have a

surplus of electrons required for electroneutrality. Elements such as sodium and calcium, with one and two electrons in their valence shells, easily release these outer electrons and become positively charged ions. Likewise, chlorine and oxygen atoms readily add to their outer shells electrons to achieve stable electronic configuration and thus become negatively charged ions. The principal bonding forces arise from neighbouring ions of unlike charges.

(b) Covalent Solids

The crystal structure consists of atoms bonded together by covalent forces. This type of bonding arises from the sharing of electrons between two adjacent atoms.

(c) Metallic Solids

Metals haveaspecific crystalline array of atoms which helps to determine their mechanical, electrical and thermal properties. Van Vlack (1961), explained the nature of bonding between metallic atoms in terms of valence electrons of these solids moving more freely within the structure. These free electrons form what is described as an electron cloud. Bonding forces arise between positive ions and the negative electron cloud.

(d) Molecular Solids

These solids are bonded by means of weaker, secondary bonds called van der Waals forces.

1.4.2 <u>Characterisation by size and shape of particle</u>

The characterisation by size of an individual

particle which has a regular spherical or cubical shape can be readily achieved by the measurement of a unique dimension. For irregular shaped particles there is however, no unique dimension because the dimension of length can be oriented in numerous directions within the irregular shaped particle. The size of an irregular particle is usually measured by assigning to the irregular particle the diameter of a sphere which has an equivalent measured property. The irregular particle size measured is then termed the equivalent sphere diameter. The particle size measured however is dependent upon the technique used.

Different techniques and instruments available to characterise amd measure the parameters of size of irregular shaped particles have been presented in detail by Stanley-Wood (1977,a,b,c) and Allen (1981) together with other parameters such as the shape and surface area of particles. The techniques used to characterise and measure the irregular shaped particles used in this investigation are those of sieving and sedimentation.

(a) Sieving

The passage of an irregular shaped particle through a go-nogo aperature-sieve is one of the simplest, most widely used techniques of particle size characterisation. The aperature size in a sieve is often referred to as a mesh size which is the number of woven wires making up the aperatures in the sieve per linear inch. The British Standard sieve size, d_t, is the minimum square aperature through which a particle can pass, BS 410 (1962). Sieve

analysis covers the approximate size range 20μm to 125 mm using standard woven wire sieves (BS 410 Part:1 and Part:2). Micromesh sieves extend the particle size range down to size of 5 μm (Daecher et al 1958), while punched plate sieves extend the upper particle size range to about 203 mm. (BS 410 Part:3). Different methods of wet and dry sieving techniques are detailed by Allen (1968,1975,1981).

(b) Sedimentation

The Andreasen Pipette Method

The particle size distribution of a powder can be determined by the examination and measurement of the settling velocities of particles in a suspension of the powder. The general principle of the sedimentation method is based on the relationship between the concentration gradient and particle size distribution of particles settling from an initially homogeneous suspension. The initial concentration can be determined by:-

$$C_{(h,o)} = \frac{M_s}{V_s + V_f} \qquad (1.12)$$

where $C_{(h,o)}$ = concentration at depth, h, time, t = 0

M_s = mass of solid in suspension

V_s = volume of solid

V_f = volume of fluid

In a small horizontal element in the suspension at a depth, h, the particles leaving the element are balanced by the particles entering it from above. When the largest particles, initially present at the surface of the suspension leave the element, there are no similar particles entering to replace these particles. Hence the concentration within the element falls and becomes equal to the concentration of particles smaller than D in the suspended phase, where D is the size of the particle which falls with a velocity h/t. The concentration of the suspension at time, t, and depth, h, may be expressed as:

$$C_{(h,t)} = \frac{M_s'}{V_s' + V_f} = \int_{Dmin}^{D} F(D)\, d\,D \quad ...(1.13)$$

where $F(D)$ ≡ the relative weight frequency in the size range dD

M_s' ≡ the mass of solids in a volume of fluid V_f at time t and depth h

V_s' ≡ the volume of solids in V_f, at t and h

Equation (1.12) can be written as:-

$$C_{(h,o)} = \frac{M_s}{V_s + V_f} = \int_{Dmin}^{Dmax} F(D)\, dD \quad (1.14)$$

notations as in equations (1.12) and (1.13)

Assuming that the difference between V_s' and V_s is negligible compared with V_f and relating the concentration at time, t, to the initial concentration.

$$\frac{C_{(h,t)}}{C_{(h,o)}} = \frac{M_s'}{M_s} = \frac{\int_{Dmin}^{D} F(D)\, dD}{\int_{Dmin}^{Dmax} F(D)\, dD} \qquad \text{equation (1.14)}$$

If a graph of $100C_{(h,t)}/C_{(h,o)}$ is plotted against D, the resulting curve shows the cumulative percentage undersize by weight of the sedimentation system. Using the Andreasen method (1939), a point on the characteristic curve can be plotted whenever a sample is removed from the suspension. The equivalent sphere diameter of the particle is calculated from Stokes equation (eqn. 1.15) in accord with British Standard (3406:Part 2: 1936).

$$D = \sqrt{\frac{18.\eta.h}{(\rho_s - \rho_f)g.t}} \qquad \text{Equation (1.15)}$$

where $D \equiv$ particle (Stoke's) diameter (cm)

$\eta \equiv$ liquid viscosity(gm/ sec)

$h \equiv$ distance from the liquid surface to the monitoring zone (cm)

$\rho_s \equiv$ solid density (g/cm^3)

$\rho_f \equiv$ fluid density (g/cm^3)

$g \equiv$ gravity acceleration constant (m/sec^2)

$t \equiv$ time in seconds

1.4.3 Surface Topography

To determine the surface area of solids, various adsorption techniques can be used. Nitrogen is the most commonly used adsorbate (BS. 4359:Part 1:1969), although other gases can be used, (McClellan and Harnsberger, 1967), in special cases for measuring low surface areas.

When gas molecules come in contact with a solid surface, some of the gas molecules become physically attracted or adsorbed onto the solid. The degree of physical adsorption is dependant upon the equilibrium pressure and temperature of the adsorbate in the system.

Various equations have been proposed to evaluate monolayer coverage of the adsorbate onto the solid surface and thentocalculate the specific surface area of solids from the adsorption isotherm. Langmuir (1917) was the first to give a theoretical derivation to describe the relationship between the amount of gas adsorbed onto a solid and the equilibrium pressure of the gas at constant temperature. He assumed that the adsorption process is limited to the formation of a monomolecular layer of gas on the solid surface and expressed the volume adsorbed as:

$$Va = \frac{Vm \cdot bP}{1+bP} \qquad (1.16)$$

where Va ≡ volume adsorbed at equilibrium pressure

Vm ≡ monomolecular volume

b ≡ adsorption constant

P ≡ equilibrium adsorption pressure

From Langmuir equation (equation 1.16) it can be seen that:

(i) At low pressures or at small adsorption, the term bP can be neglected in comparison with unity, therefore

$$Va = Vm\ bP$$

the amount of gas adsorbed then becomes directly proportional to the equilibrium adsorption pressure.

(ii) At high pressures, high adsorption occurs and unity is small compared with the bP term hence V = Vm and adsorption approaches saturation. Equation (1.16) can be expressed linearly as:-

$$\frac{P}{Va} = \frac{1}{Vm\ b} + \frac{P}{Vm} \qquad (1.17)$$

A plot of the term $\frac{P}{Va}$ against P yields the monolayer capacity Vm from the slope of the curve and this can be used to calculate the solid surface area from:-

$$Sw = \frac{NAm\ Vm}{M_v\ W} \qquad (1.18)$$

where Sw ≡ specific surface area of solid (m^2/g)

N ≡ Avogadro number (6.023×10^{23} molecules/g mol)

Am ≡ area occupied by one adsorbate molecule

Vm ≡ monolayer capacity

M_v ≡ gram molecular volume (22410 ml)

W ≡ weight of the sample

Brunauer, Emmett and Teller (1935) criticised Langmuir's equation and showed that gas molecule and vapours can be adsorbed onto other molecules which have already been adsorbed forming multi-molecular adsorption layers. Brunauer, Deming, Deming and Teller (1940) classified gas adsorption isotherms into five types to cover the majority of isotherms observed to date (fig 1.22). Type I isotherm represents the Langmuir or monolayer adsorption isotherm. Type II and Type III

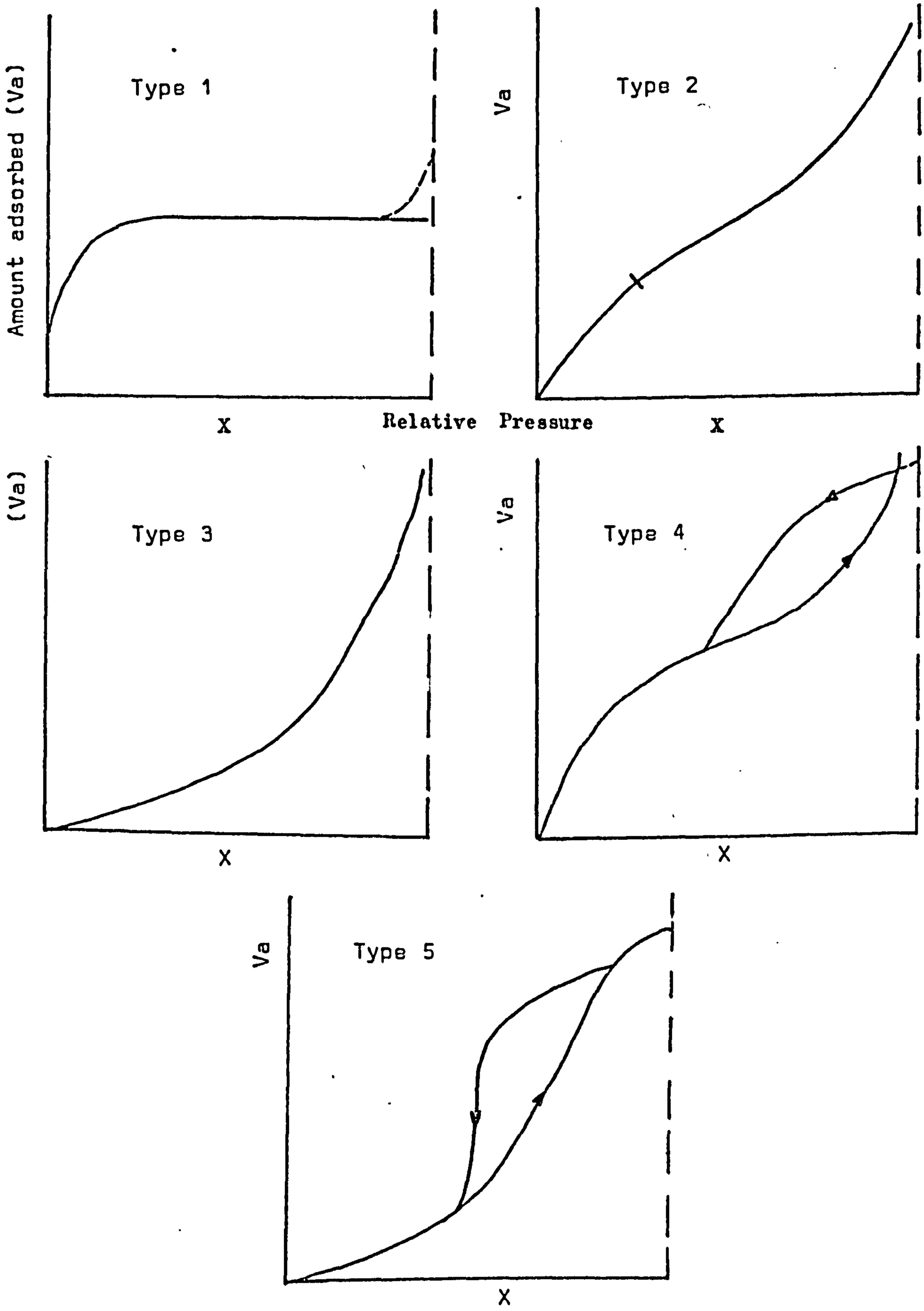

Figure 1.22 Types of adsorption isotherms.

isotherms represent mono-and multilayer adsorption while Type IV and Type V isotherms represent mono- and multilayer adsorption plus capillary condensation.

The equation developed by Brunauer, Emmett and Teller (BET) can be written as:-

$$Va = \frac{Vm\ CP}{(P_o - P)(1+(C-1)P/P_o)} \qquad (1.19)$$

where Va ≡ volume of gas adsorbed

C ≡ an adsorption constant

P ≡ experimental pressure

P_o ≡ saturated vapour pressure of the adsorbate

Vm ≡ monomolecular volume

The BET equation can be written linearly as:-

$$\frac{P}{P_o - P} \cdot \frac{1}{Va} = \frac{1}{VmC} + \frac{C-1}{VmC} \cdot \frac{P}{P_o} \qquad (1.20)$$

The linear form of the BET equation assumes that the adsorption coefficient, C, is constant over all pressures. In practise there are no adsorption isotherms in which the adsorption coefficient remains constant for all values of equilibrium pressure from zero to saturation pressure. In the majority of isotherms the adsorption constant can be regarded as constant within relative pressure (P/P_o) range of 0.05 to 0.35. The adsorption constant can be derived from:-

$$C_{BET} = \exp. \frac{(E_1 - EL)}{RT} \qquad (1.21)$$

where E_1 ≡ energy of adsorption of the vapour onto a bare surface

E_L ≡ energy of condensation of vapour

R ≡ universal gas constant

T ≡ absolute temperature

It was noted by Brunauer and Emmett (1937) that between the low pressure region of a Type II isotherm, which is concave with respect to the pressure axis, and the high pressure region, which is convex with respect to the pressure axis, there is a linear portion. The beginning of this linear portion was termed point B. Adsorption at point B corresponds to the assumed completion of the monolayer of the adsorbed gas molecules. The monolayer completion is usually between relative pressures of 0.05 to 0.15 which is within the limits of the BET equation. Although point B method can be used to evaluate the surface area of powders, comparison of the surface area of a powder obtained from this method will not always be in agreement with surface area obtained independently. Brunauer et al then proposed the evaluation of the monolayer value Vm from equation (1.20). When the BET function $\left(\frac{P}{(P_o-P)Va)}\right)$ is plotted versus the relative pressure (P/P_o) the monolayer volume (Vm) can be obtained from the slope and intercept, where slope (S):-

$$S = \frac{C-1}{VmC} \qquad (1.22)$$

and intercept (I):-

$$I = \frac{1}{VmC} \qquad (1.23)$$

The monolayer volume (Vm) then becomes:-

$$Vm = \frac{1}{S+I}$$

the adsorption coefficient (C) may also be calculated:-

$$C = 1 + \frac{S}{I} \qquad (1.24)$$

To calculate the specific surface area from the monomolecular volume, the area occupied by one adsorbate molecule must be known. The specific surface area of the solid can then be calculated from equation (1.18). When the cross sectional area of nitrogen is taken as $16.2 \times 10^{-20} m^2$ equation (1.18) can be simplified to:-

$$Sw = \frac{4.35\ Vm}{W} \qquad (1.25)$$

Hüttig (1948) proposed an equation which from the adsorption isotherm values extends the range of linearity from 0.35 to 0.7 relative pressure. He assumed that the evaporation of the gas molecules from the ith layer is entirely unimpeded by the pressure of molecules adsorbed in the (i+1) layer. The linear form of Hüttig's equation is:-

$$\frac{P}{Va}\left(1 + \frac{P}{P_o}\right) = \frac{1}{VmC} + \frac{P}{Vm} \qquad (1.26)$$

notations as in equation (1.19).

Although nitrogen is the most widely used gas for the measurement of the surface area, it can not easily be used for samples which have a relatively small surface area ($<1\ m^2/g$). Different adsorbates can be used

for low surface areas measurements. Beebe, Beckwith and Honig (1945) proposed the use of Krypton as an adsorbate at liquid nitrogen temperature. A serious difficulty in the use of Krypton for low surface area measurement is the uncertainty in the choice of the appropriate value to be taken as the saturation vapour pressure (P_o) and also the area of an adsorbed molecule of Krypton (Am). Various values of both parameters have been reported in the literature (Jaycock 1977). A comprehensive review of theoretical and experimental problems associated with Krypton adsorption is given by Jaycock (1977).

1.4.4 Pore-void size Distribution

(a) Gas Adsorption

Analysis of the adsorption isotherm can yield not only surface area but information concerning the internal structure such as porosity, pore size distribution and contact area of compressed and uncompressed powders. Dubinin (1967) proposed the following classification of pore size within solids:-

Micropores	Pore radii < 1.5 nm
Mesopores	Pore radii 1.5 - 100 nm
Macropores	Pore radii > 100 nm

The meso and macropore size distribution in a porous material can be evaluated from the adsorption isotherm on the assumption that capillary condensation occurs at high relative pressures. Capillary condensation cannot occur within microporous material although the micro porosity and micropore size distribution can be measured from adsorption isotherms. Capillary Pore size

can be calculated from equation (1.27) - the Kelvin equation:-

$$\ln \frac{P}{P_o} = \frac{2\gamma V_a}{r_K RT} \cdot \cos\theta \qquad (1.27)$$

where $P \equiv$ experimental pressure

$P_o \equiv$ saturated vapour pressure

$r_K \equiv$ Kelvin radius

$R \equiv$ Universal gas constant

$T \equiv$ absolute temperature

$V_a \equiv$ volume of gas adsorbed

$\gamma \equiv$ surface tension of the adsorbate

$\theta \equiv$ angle of contact between adsorbate and adsorbent

From the Kelvin equation (equation 1.27) the value of r_K corresponding to any given point on the adsorption isotherm can be calculated. At specific relative pressure $(P/P_o)_i$ and a known adsorbed volume (V_i), assuming that the initial amount adsorbed on the walls of pores is negligible . The volume V_i can then be equated to the volume of adsorbate within all the pores which have radii $\leq r_{ki}$. A graph of V_i against r_K can give the pore size distribution of the porous material. In reality however before capillary condensation occurs in any pore there is a build up of adsorbed molecules on the walls of the pores. Because of these adsorbed layers on the pore walls, the calculated Kelvin radius (r_K) is an underestimation of real pore radius (r_p). In order therefore to determine the pore size distribution, the relationship between the actual

pore size, the Kelvin pore size and the adsorbed layer thickness (t) for cylinderical pores has to be ascertained. This is usually expressed for open ended cylindrical pores as:-

$$r_p = r_K + t \qquad (1.28)$$

For solids with parallel sided plate shaped pores the relationship becomes:-

$$d_p = r_K + 2t \qquad (1.29)$$

Oulton (1948) assumed a constant monolayer adsorption on the walls of pores over the whole adsorption process and related the film thickness to the volume adsorbed at a given pressure by:-

$$t = \bar{\zeta}\left(\frac{V}{V_m}\right) \qquad (1.30)$$

where $\bar{\zeta}$ ≡ is the average thickness of one layer of molecules

V_m ≡ is the monolayer capacity of a non-porous reference solid

Lippens et al (1964) calculated the volume of $\bar{\zeta}$ for nitrogen, assuming hexagonal close-packing, as 0.354 from:-

$$\bar{\zeta} = \frac{M\ V_s}{N\ Am} \qquad (1.31)$$

where M ≡ molecular weight of the gas

V_s ≡ specific volume

N ≡ Avogadro number

Am ≡ area occupied by one molecule.

Wheeler (1955) suggested that the adsorption at low relative pressures on the walls of fine pores is probably greater than on an open surface and therefore proposed the use of Halsey's equation (1948) (equation 1.32) for analysis of the adsorption isotherm in the determination of pore sizes and pore size distribution in porous materials

$$t^3 \ln \frac{P_o}{P} = 5\bar{\zeta}^3 \qquad (1.32)$$

Barrett Joyner and Halenda, BJH, (1951) developed Wheeler's concept by the introduction of a correction factor for multilayer wall film thickness to give a more accurate measurement of pore size. The BJH pore size distribution model is calculated from:-

$$\Delta Vp = Rn(\Delta Vc - C\ \Delta t \Sigma Sp) \qquad (1.33)$$

where $\Delta Vp \equiv$ actual volume of pores emptied in the desorption step

$Rn \equiv rp/(\bar{r}+t^2)$ where rp is the pore radius

$\bar{r}$ is mean capillary condensate radius

t is the decrease in multilayer thickness

$\Sigma Sp \equiv$ the sum of the surface area which is

$Sp = 2\Delta V/rp$ for cylindrical pores

$C \equiv$ correction factor

Cranston and Inkley (1957) further modified the BJH method to give a more precise measure of pore size by the application of a correction factor to each of the pore sizes calculated from the Kelvin equation. They stated that their method may be applied either to the

adsorption or desorption branch of the isotherm. Critical review of pore size distribution methods and techniques can be found in Allen (1981) and Stanley-Wood (1982)

(b) The Va-t method

The Va-t method is usually applicable for analysis of the adsorption isotherm to determine micro and meso pore size distribution. Lippens et al (1964) and de Boer et al (1965) extended the work of Schull et al (1948) and developed a relationship between the nitrogen adsorbed volume on non-porous solid or adsorbents and the thickness of the adsorbed layer (t) at specific relative pressures. The equation proposed to relate the adsorbed layer thickness, t, to the adsorbed volume, Va, on non-porous solids of known specific surface area (Sw) was:-

$$t = \frac{M\ V_s}{M_v} \cdot \frac{Va}{Sw} \qquad (1.34)$$

$$= 1.547\ \frac{Va}{Sw} \cdot 10^4 nm$$

When the area occupied by a nitrogen molecule on a non-porous solid is assumed to be as $16.2 \times 10^{-20} m^2$, then Sw becomes equivalent to 4.35 Vm m^2/g (equation 1.25) and the statistical thickness (t) can be expressed as:-

$$t = 0.354\ \frac{Va}{Vm}\ nm \qquad (1.35)$$

From the adsorption isotherm at known Va values and thus known t values the appropriate relative pressure

can be evaluated. A plot of the multilayer film thickness, t, at specific relative pressure produces a t curve for non porous material. The t-curve can be described by two alternate equations. One is the Anderson equation (1946) which can be expressed as:-

$$V = \frac{Vm\ C\ K_B\ X}{(1-K_BX)\{1+(C-1)K_BX\}} \qquad (1.36)$$

where $K_B = 76$, $C = 53$ and $X = P/P_o$, and secondly the Harkin and Jura equation (1943-1944) which is:-

$$\log x = 0.034 - \frac{13.99}{t^2} \qquad (1.37)$$

With porous materials the adsorption isotherm can be compared with the t-curve from non porous materials - The Va-t plot. A linear relation would indicate a non porous material. A downward deviation from linearity would indicate microporosity and an upward deviation indicates meso porosity. Tangent of the Va-t curve obtained from micro porous material can be analysed to give pore size distribution (Brunauer 1968).

(c) Mercury porosimetry

A high pressure mercury intrusion technique can be used for the determination of pore size distribution of porous materials and/or the void size distribution in compacts. The intrusion technique is based on the principles of solid-liquid interaction and capillarity. When a liquid which does not wet the solid and has a contact angle greater than 90^o is placed in contact with a porous solid or compacted powder, penetration into

the pore is dependent upon the shape and size of the pores together with the applied pressure. For liquids which have a contact angle of less than 90^{o}, liquid can enter into pores without any external force. With liquids which have a contact angle greater than 90^{o} a positive pressure is needed to force liquid into pores. Washburn (1921) was the first to suggest the use of mercury as a penetration liquid, because mercury is non wetting and has a contact angle greater than 90^{o}. The pressure required to force mercury into a cylindrical capillary or pore can be calculated form combination of the equations of Young (1855) and Laplace (1806).

$$\Delta P = \frac{-2\gamma\cos\theta}{r} \qquad (1.38)$$

where $\gamma \equiv$ the surface tension of mercury

$\theta \equiv$ the angle of contact

$r \equiv$ pore radius

The surface area of a solid may also be obtained from the pore size distribution data. The surface volume relationship being:-

$$S_{Hg} = 2\pi rL \qquad (1.39)$$

$$V = \pi r^{2}L \qquad (1.40)$$

from which $S_{Hg} = 2V/r$.

Experimental data from this technique was first investigated by Henderson, Ridgeway and Ross (1940) in the pressure range 30 to 900 PSI. Ritter and Drake (1940) and Drake (1948)extended the pressure range to 10000 PSI and 60000 PSI respectively. Experimental

data obtained in the form of (P) against volume intruded (V) is converted to pore radius using equation (1.38). It is then possible to plot the cumulative pore size distribution by volume and differentiation of the curve yields the relative pore size distribution by volume.

1.5 Bulk Properties of Particulate Solids

An understanding of factors affecting the packing and flow of powders is essential in many chemical industries. A wide variety of bulk solids are difficult to characterize because in addition to the primary properties associated with size, shape, particle density or surface topography of the irregular assembly of particles in a powder, there are secondary properties which are not directly associated with the particles such as the moisture content, fragibility, strength and previous compaction history together with ambient temperature, which also contributes to the behaviour of the bulk solid.

When particles are collected together as an assembly of particles the powder properties can be categorised under three interrelated groups :

(i) Properties of the individual components (Section 1.4).

(ii) The properties of the gas or fluid filling the interstices between the particles. (Section 1.4.4 a and c.)

(iii) Interaction of the components of the assembly.

This interaction can be described by defining the different mechanisms taking place within the assembly of particles.

1.5.1 Packing

Packing can be regarded as the orientation in space of different components of an assembly. A powder can be considered to be a two phase system,

which comprises a solid and a fluid. Different fractional solid content of a packed mass can be obtained by movement of the particles confined in a mould or die by application of a suitable force on the particles. Since the property of powder bulk density can change by rearrangement of the particles, it is essential to investigate the manner and the factors governing the packing process and change of bulk density. The density changes that can occur within a bulk powder are dependent upon the degree and magnitude of forces applied and the amount of fines in the bulk powder assembly. Extensive amounts of work exists in the scientific literature on the packing of spherical granules. Graton and Fraser (1935) used gravitational methods to examine the packing of monosized spherical particles. They found a decrease in porosity with increasing coordination number and attributed the different packing geometries of equal dimensioned spheres to the fractional solids content of packed spheres. A more practical method was considered by McGeary (1961) to obtain a more efficient packing of spheres by placing monosized sphere particles in a container and subjecting the container to vibration to achieve a specific porosity. He then added smaller sized spheres and again vibrated the system to a lower porosity. The ease of densification by this technique is attributed to the filling of the voids created by the larger particles with smaller

particles. Ayer and Soppet (1965-1966) extended the work of McGeary and proposed a mathematical relationship for the packing efficiency of spherical particles in a container:

$$Pe = 0.635 - 0.216e^{-0.313D/d_1} \qquad (1.41)$$

where $D \equiv$ diameter of container

$d_1 \equiv$ mean particle diameter

$0.635 \equiv$ the limiting value of the packing fraction for a single component system

From equation (1.41) the void fraction V_f of the system becomes unity minus the packing fraction.

$$V_f = 1-(0.635-0.216e^{-0.313D/d_1}) \qquad (1.42)$$

$$= 0.365+0.216e^{-0.313D/d_1}$$

When a second smaller sized component was added within the previous voids, the following relationship was obtained

$$Pe = 0.635 - 0.737e^{-0.201d_1/d_2} \qquad (1.43)$$

where $d_1/d_2 \equiv$ the ratio of the largest to smallest particle size in the system.

The packing efficiency of real powders is difficult to calculate by the relationship in equation (1.43), because of the continuous size distribution. Eastwood et al (1960) and Bernal (1964) used equations based on statistical methods to predict the porosity of packed beds.

1.5.2 Co-ordination number

The degree of packing can be specified by the number of nearest neighbours of an individual particle in an assembly, this is usually defined as the co-ordination number. Smith (1929) packed equi-sized steel shots into a die and surrounded the packed mass with acetic acid. Corrosion created everywhere except at the points of contact then gave evidence of the co-ordination between individual steel shot. Bernal and Mason (1966) used a similar approach, by soaking packings of ball bearings in paint. Benett and Brown (1940) used starch coated irregular glass lumps stained with iodine. All these workers found a sharp increase in the co-ordination number as the fractional solids content increased. Avery and Ramsay (1973) examining the accessible surface of contacting of zicronia and silica particles, found an approximate linear relationship between the surface area determined by low temperature nitrogen adsorption (S_{BET}) and co-ordination number (n). With both materials a decrease in surface area produced an increase in the co-ordination number of the packed particles. Ramsay and Avery also showed a relationship between the porosity of a compact and the co-ordination number for uniform spheres.

1.5.3 Adhesion and Cohesion

Adhesion is the ability of one surface to stick to another. Theoretically it is possible to place

two perfectly flat and clean surfaces in contact and by pressure reweld the solid into a continuous whole. Practically, however, this is impossible because of the microscopic irregularities, surface adsorbed films and cracks and fissures extending below the surface of real materials. Adhesion can be defined as the force of static friction between two bodies, or the effect of this force. In the compaction of particulate solids, adhesion between solids manifests itself indirectly by such effects as friction.

Cohesion is the tendancy of parts of a body of like composition to hold together, as a result of intermolecular attractive forces. The strength of cohesion may be affected by the following factors:

(i) The chemical nature of the particles and hence the strength of the field of force of each surface

(ii) The presence or absence of contaminants on the surface of the particles

(iii) The distance between the two surfaces

(iv) The surface configuration of the particles

1.5.4 Density

The relationship of particle mass divided by particle volume is an important parameter in the description of a powder. In a powder mass which consists of individual particles the volume can be subdivided into:-

Volume of particulate solids or true volume (V_t)

Volume of open pores within the particle (V_o)

Volume of closed pores within the particle (V_c)

Volume of voids between the particles (V_r)

The four separate volumes (fig 1.23 a,b) can be combined to give three measurable quantities.

(i) The particle solid volume

$$V_s = V_t + V_c \qquad (1.44)$$

(ii) The apparent particle volume

$$V_{ap} = V_t + V_c + V_o \qquad (1.45)$$

(iii) The bulk volume

$$V_b = V_t + V_c + V_o + V_r \qquad (1.46)$$

From the different measurable volumes different densities can be defined:-

(a) Particle solid density

Particle density is usually determined by the measurement of the fluid displaced ~~from~~ by a known weight of material after evacuation of environmental gases in or around the particle. If the fluid used is liquid and the solid insoluble, the method of boiling the specimen can be used as described in BS 1902 (1952). When the fluid is a gas, a non-adsorbable inert gas such as helium is commonly used because of its small molecular size which enables penetration into open pores and non-adsorbancy onto solid surface at room temperature.

$$\rho_p = M/V_s \qquad (1.47)$$

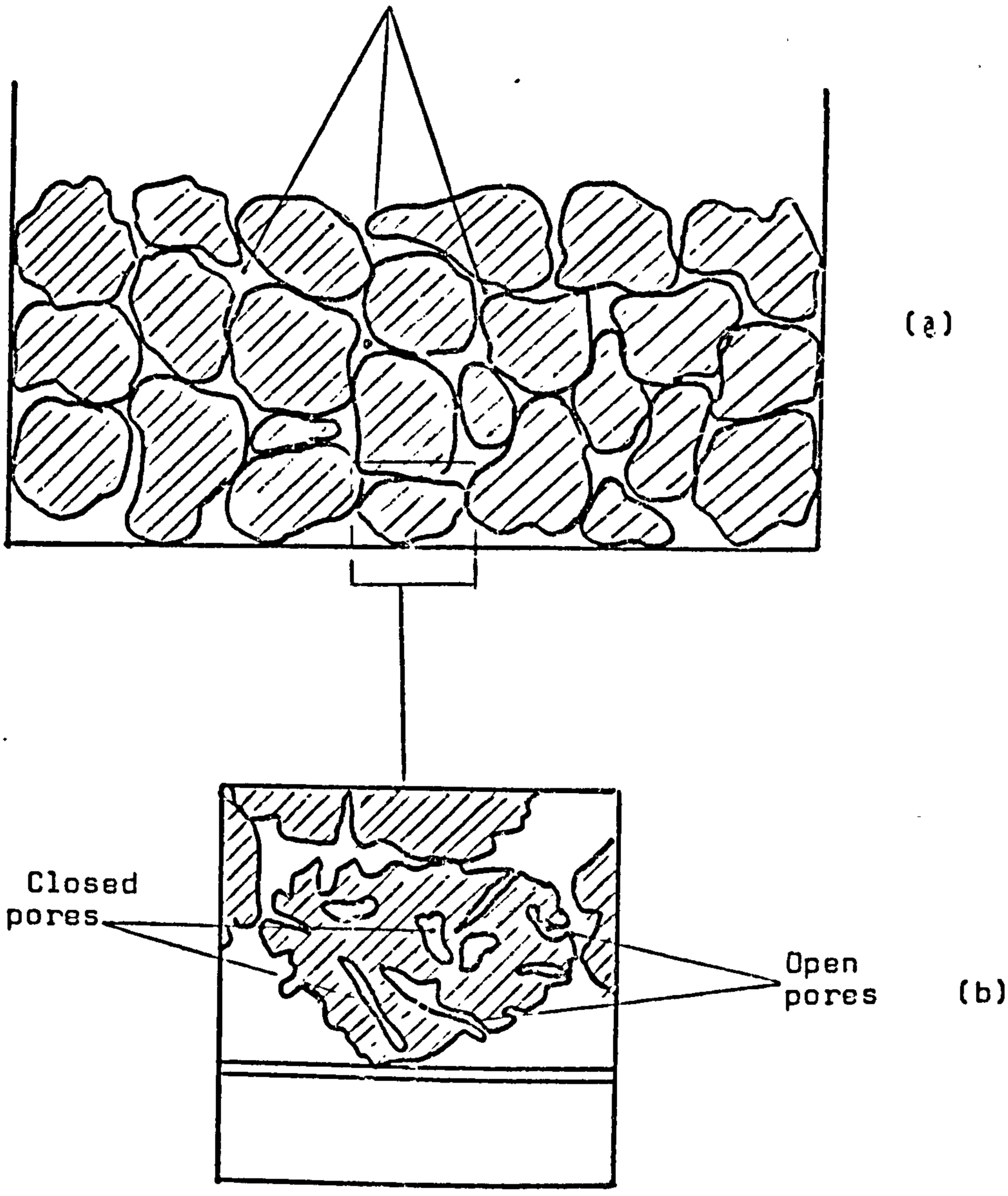

Figure 1.23 Voidage within a Powder Bed (a) Interparticulate Voidage (b) Intraparticulate Voidage.

where M ≡ mass of solid

(b) Particle bulk density

The density of a particle is defined as the mass of the assembly of particles- a powder - divided by the unit volume of solids

$$\rho_{ap} = M/V_{ap} \qquad (1.48)$$

(c) Bulk density

Bulk density of a solid material is defined as:-

$$\rho_b = \frac{M}{(V_t + V_o + V_c + V_v)} \qquad (1.49)$$

The bulk density of a given powder bed of a particulate solid is difficult to measure, because the slightest disturbance of the powder bed, the magnitude of the container or the method of container filling can result in a change of powder volume and thus a change in bulk density because of the variation of the interparticulate space.

(d) Relative density

It is usually defined as the bulk density at a known compaction pressure divided by the true density. In some cases however confusion arises because some workers have not understood the differences between true density, particle density and bulk density of a powder

$$\rho_{rel} = \frac{\rho_b}{\rho_t} \qquad (1.50)$$

(e) <u>True density</u>

The true density of a specimen can be obtained by an Xray pyknometry technique (Smakula and Kalnajas 1955) which measured the volume of a solid without the enclosure of any intercrystalline pores within the solid.

$$\rho_t = M/V_t \qquad (1.51)$$

1.6 Mechanical Strength of Compacts

It is generally accepted that compact formation by pressure occurs because of forces acting at the areas of true interparticle contact. It might be expected that all powdered materials could form strong compacts when subjected to adequate compressive pressures. Experimental evidence shows however that some materials even with a high degree of compression will form soft and crumbly compacts which can not even be ejected from the die, while others yield laminated compacts.

Stress relaxation is believed to explain some problems in the compaction process. Powder under compression in a cylindrical die is confined in a radial direction until ejection from the die. Train (1956) and Long (1960) attributed the lamination of the compacts to stress distribution and strain relief. Train argued that during ejection, the frictional effects and stress induced by the die wall can hold the strained condition in the compacted material until the edge of the die is reached. An spontaneous expansion then takes place in two directions (fig 1.24).

Long explained that failure of compacts could occur because of the stress concentration and direction of relaxation during ejection (fig. 1.25). He assumed that during decompression the compacted body will expand. The axial expression will be resisted at the

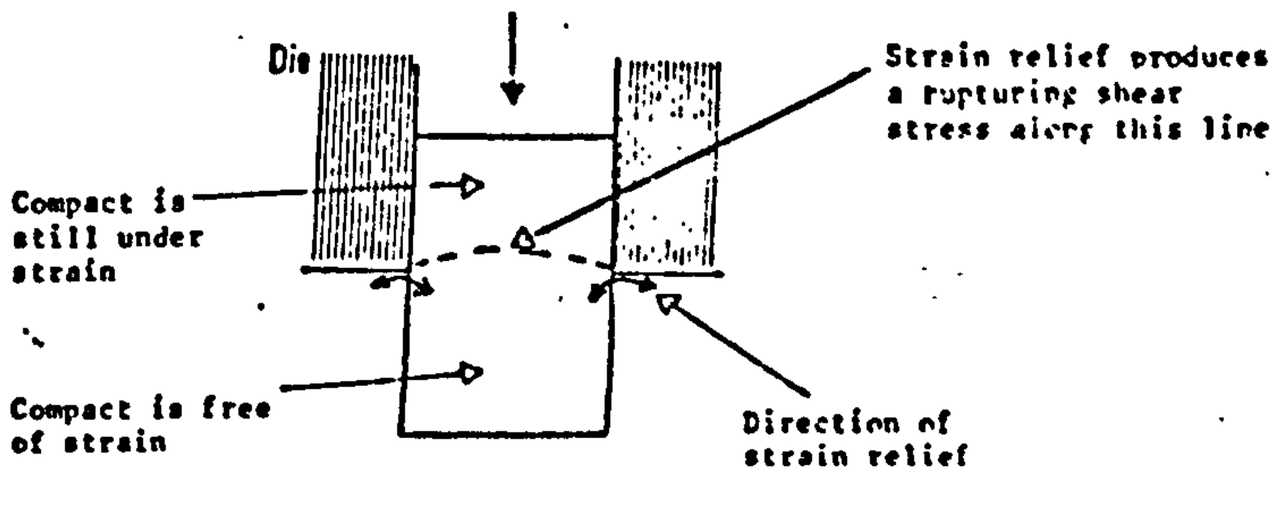

Ejection of an unlubricated compact. After Train

Figure 1.24

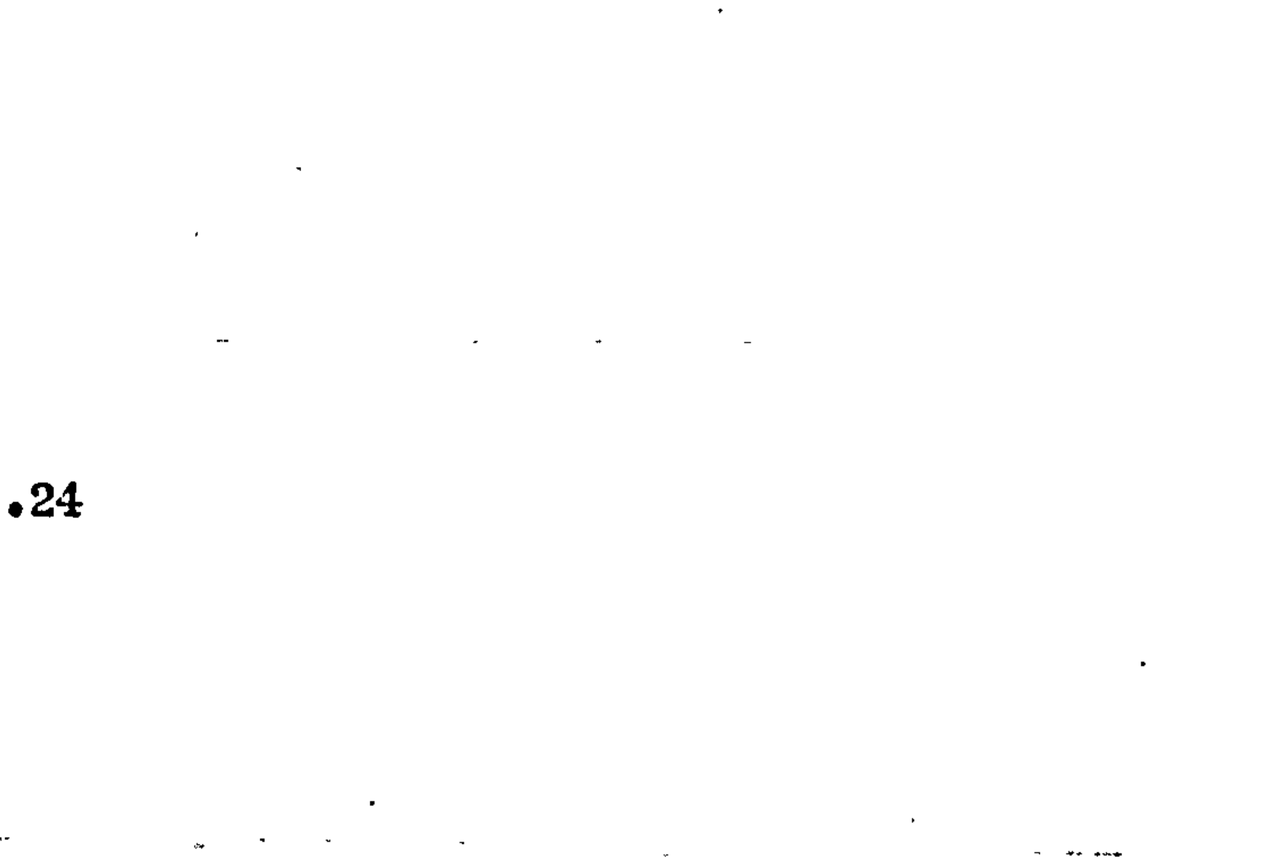

Stages in production of Laminar cracks by radial pressure (After Long).
A Compact within the die
B Compact almost clear of die.

Figure 1.25

die wall due to both the frictional effects and the physical restraint of the die material. Consequently a stress concentration along the plane (fig. 1.25a) can occur which may then become a plane of failure. Any crack starting from the edge of the compact near the die wall will follow the same contour of stress concentration shown in figure 1.25b. This is a common occurrance in practice and called capping.

Recent work by Heistand and co-workers (1977) showed that shear deformation occurred during the process of decompression and was responsible for the fracture of some materials such as phenacetin, methenamine and acetaminophen compacts. Other materials however (erythromycin) withstood the decompression stresses but laminated upon ejection due to the large stress concentrations at the edge of the die. They concluded that failure to fracture and compact formation appeared to be related to the ability of the material to undergo stress relief by plastic deformation.

1.6.1 Hardness testing

The term hardness is generally understood to imply the resistance offered to penetration of an object into the surface of a solid and is thus generally denoted by an indentation hardness number. Hardness testing methods may be grouped into static and dynamic indentation tests.

An indentation test is termed static when a ball, cone or pyramid is forced into a solid surface and the

load per unit area of indentation is taken as the measure of hardness.

Dynamic tests are performed by application of a load which is continuously increasing. In the field of metallurgy this type of hardness is especially used at elevated temperature, because the test time is short and any errors due to temperature change are assumed to be minimum. Commonly used hardness testing methods are:-

(a) Brinell

The first published data on indentation hardness of metals was Brinell (1910). In the Brinell test (B.S. 240:1962) the hardness of a solid is obtained from the dimension of the impression made by a known sized steel ball when pressed into the solid under a known load.

$$H_B = P/A \qquad (1.52)$$

where $A \equiv \pi dh = \frac{\pi D}{2}(D - \sqrt{D^2-d^2})$

$P \equiv$ load on ball in kilograms

$A \equiv$ spherical area of indentation

$D \equiv$ diameter of the ball in millimeters

$d \equiv$ diameter of the impression in millimeters

$h \equiv$ depth of the impression in millimeters

$H_B \equiv$ Brinell indentation hardness number

(b) Meyer

Meyer(1908) critisized the use of spherical area of indentation which had been used by Brinell and

suggested the use of a circular projected area. Meyer hardness number, H_M, is defined as:-

$$H_M = 4P/\pi d^2 \qquad (1.53)$$

Meyer also expressed the hardness of material by a power relationship between the load and the diameter of impression:-

$$P = a\, d^n \qquad (1.54)$$

where P ≡ load in kilograms

d ≡ diameter of impression in mm

n ≡ material constant

a ≡ material constant for a given load

(c) Vickers Method:-

Vickers (B.S.427:1961) hardness number (H_V) is defined as the load divided by the pyramid area of the impression:

$$H_V = \frac{2P\sin(136/2)}{d^2} \qquad (1.55)$$

where P ≡ load in kg.

136^o ≡ the angle between two opposite faces of the diamond pyramid

d ≡ average length of the two diagonals of the impression in mm

(d) Rockwell

The Rockwell test (B.S. 891:1940) is different from the other tests, because this test is based solely on the depth of indentation. The hardness of material

is measured by using an initial minor load followed by a major load. The difference in depths between the impressions for the minor and major loads is the Rockwell hardness number, R_c.

(e) Shore test

The method is also known as the Rebound or Scleroscope test. The Shore method (1910) is based on the loss of potential energy, when a weight is dropped vertically onto a surface and rebounds. The hardness of the surface is the difference between height of fall and the height of rebound.

1.6.2 Application of hardness testing to compacts

The first reported use of indentation testing in pharmaceutical compacts was from Spengler and Kaelin (1945) where the depth of penetration (Brinell hardness number) from different tablets was related to the hardness of compacts. The greater the depth of penetration the softer the compact. Filleborn(1948) attempted to correlate the hardness of sulphanilamide and sulphadiazine tablets to other properties of the compacts and showed a non-linear increase in disintegration time with increasing hardness.

Vickers hardness number method was used by Nutter Smith (1949) to study the hardness of pharmaceutical compacts such as boric acid, sulphanilamide, aspirin, potassium bromide and apenicillin lozenge. He found that for all materials there was no simple relationship between hardness and disintegration time. He related

the scatter observed during the hardness number measurements to the non-homogenity of compacts and suggested the use of the Rockwell hardness number on tablets to minimise the effect of surface irregularities.

Seth and Munzel (1960) critisized the use of heavy metallurgical-testers for the determination of hardness of pharmaceutical compacts and used a microhardness tester based on the Rockwell principle. The advantage of their micro-tester was the use of lower minor and major loads which enabled the measurement of more than indentation on the tablet face. Ridgway, Glasby and Rosser (1969) modified the measurement of the size of the diamond indentation by using a microscope fitted with a movable carrier to measure the enlarged diamond shaped surface indentation. The relationship between the Vickers surface hardness and compaction pressure for compacts of potassium chloride, hexamine and urea showed a slight decrease in hardness with increasing compaction pressure. Sodium chloride and aspirin compacts showed however an increase in hardness with increase in compaction pressure.

A more advanced type of ball tester was used by Ridgway, Aulton and Rosser (1970). The advantage of this new indentation tester was that it minimised experimental errors and enabled the effect of elasticity to be calculated by observing recovery on load removal. The hardness of aspirin tablets compacted at different compaction pressures, measured by this elastic-plastic hardness tester, showed that the average tablet hardness increased with increasing compaction pressure. The

average hardness also increased linearly with decrease in the initial particle size of the compacted material. When the variation of the hardness across the compact face was examined, it was found that the compacts were harder in the centre than at the periphery. This was an unexpected result since the work of Train (1956) had shown an area of high density at the periphery and lower density in the centre of the compact. Aulton, Tebby and White (1974) used the same basic concept as Ridgway et al (1970), but allowed a displacement transducer to follow the vertical displacement of the ball indentor. They also reported that the hardness at the periphery of the compacts was less than at the centre of the compacts, similar to the work of Ridgway et al. An elastic quotient-which is the height of relaxation divided by the total indentation depth, was lower for aspirin and other direct compactable materials than for poor tabletting materials such as paracetamol. Recent work by Aulton and Tebby (1976) used a ratio of penetration time as a parameter to discriminate between good and poor tabletting materials.

Brose van Groenou (1978) criticised the indentation test on the grounds that such tests were discontinuous and proposed the use of a diamond to produce a scratch on the surface of ceramic compacts. He showed that the relationship between hardness and density was identical with that between hardness and compaction pressure. Stanley-Wood and Abdel-Karim (1982) studied the relationship between the hardness and compaction

pressure of sodium chloride compacted at different compaction pressures and found that both the Brinell hardness (H_B) and Vickers hardness (H_V) increased with increasing compaction pressure.

Nutter Smith (1949) was the first to use a Shore Scleroscope method to measure the hardness on a range of pharmaceutical compacts, but found that only one formulation (a penicillin lozenge) was hard enough to give acceptable results. Heistand, Bane and Strezelinski (1971), used an impact-rebound method in which a steel sphere on a pendulum strikes the face of rigidly held compact. The energy consumed during the impact divided by the volume of the indentation provided an estimate of the mean deformation pressure while a measurement of the depth of the indentation provide an estimate of the hardness of the compacted material.

1.6.3 Diametral compression tests

Tensile testing of materials has always been of great importance in design engineering because it is the simplest and most accurate way to predict the behaviour of metallic materials.

All metallic materials have a tensile strength beyond which breakage or fracture will occur. A metal rod can simply be held between two jaws and loaded in tension. Measurement of the applied force and deformation of the test sample gives, from the stress-strain relationship, the tensile strength of the

metallic material. With brittle non-metallic materials such as ceramics, concrete or any other polycrystalline compacts, the tensile strength of such materials can be obtained from a diametral compression or Brazilian test which was originally derived for concrete by Carneiro (1943).

When a circular specimen is compressed along a longitudinal diameter, pure tensile failure occurs in a direction at right angles to the applied force. Frocht (1948) related this type of failure to the geometry of the test material and explained that although the force applied is compressive the stress within the compact is distributed in such a way that the compact fractures or fails in tension. The maximum tensile stress along the loaded diameter can be expressed as:-

$$\sigma_t = \frac{2P}{\pi Dt} \qquad (1.56)$$

where P applied load

D compact diameter

t compact thickness

One of the first diametral crushing testers for pharmaceutical tablets was the Monsanto hardness tester (1936). The use and availability of different commercial testers has been reviewed by Ridgway (1970).

Rudnick, Hunter and Holden (1963) showed that a compact subjected to diametral compression could fail in one of three ways.

(i) Compression and/or shear failure in which the compact fractures into several irregular fragments.

(ii) Normal tensile failure in which the compact splits into two halves along the loaded diameter.

(iii) Triple cleft in which the tablet splits symetrically about the loaded diameter into three pieces.

Fell and Newton (1970) measured the tensile strength of lactose tablets by diametral compression and found that the tensile strength was reproducible only when compacts failed in tension or normal tensile failure. They also reported that the tensile strength was characteristic of the material and test condition.

The effect of powder characteristics, such as particle size, shape and surface, on the strength of compacts was investigated by several workers. York and Pilpel (1973) found that the crushing strength of compacts, which consisted of a mixture of fatty acid and lactose,decreased with increase in the melting point of individual constituents of the compact. The effect of particle shape was also reported by Shotton and Obiorah (1973) who showed that the crushing strength of sodium chloride tablets prepared from dentritic crystals was always higher than those prepared from the cubic form of sodium chloride.

Rees and Hersey and Cole (1970) observed an increase in compact strength of up to 14% by increasing the rate of platten movement used in the test method. Recent work by Rees and Rue (1978) suggested that the effect of rate of loading on the observed compact strength may be dependent on other properties of the material such as plasticity

and fragmentation.

To ensure maximum reproducibility and comparison of results, the rate of movement of the platten should be constant and defined.

1.6.4 Toughness testing

Rees and Rue (1977) studied the behaviour of different compacted materials during a diametral compression test. By subjecting compacts to loads less than their breaking load and measurement of the platten displacement during loading and unloading the non-recoverable deformation of the compacts can be measured. Using the same technique from the platten displacement during diametral compression test the authors (1978), calculated the work needed to fail the compact, which was claimed to be a measurement of toughness of the compact. The methods used to ascertain the tensile strength of compacts and the advantage of this toughness technique have been reviewed by Rue (1981).

1.6.5 Time dependancy of strength test

Changes in the mechanical and physical properties of compacts can occur due to the ageing of compacts. Rees and Shotton (1970) observed a doubling of the tensile strength of sodium chloride tablets in the first hour immediately after ejection from a die. This increase in strength was attributed to the continuing deformation of particles leading to stress release and increase in interparticle bonding. York and Bailey (1977) measured the dimensional changes of compacts after ejection

from a die and found that compacts produced from methyl cellulose powders showed high axial and radial expansion while sodium chloride and spray dried lactose compacts showed little change. Chowhan and co-workers (1978-1980) investigated the effect of the percentage of moisture in compacted and non compacted powders and found that the compact hardness increased linearlywith the amount of moisture loss after compression.

CHAPTER 2

CHAPTER 2

Characterisation of Powders

2.1 Materials

Three different groups of powders were chosen in this investigation to evaluate the relationship between shear stress and compaction stress in the stress range 15-248 MPa. One group formed coherent bodies mainly by plastic deformation. In the second group densification by fragmentation predominated and the third group did not form coherent compacts in the stress range investigated.

2.1.1 Plastically deforming powders

Sodium chloride was chosen because of its availability and well established plastic deformation behaviour. Two different grades of sodium chloride were used. The first grade was a dentritic shaped product from I.C.I., Imperial Chemical Industries Ltd., Cheshire, England. The second was a vacuum dried cubic sodium chloride supplied by British Salt Ltd., Middlewich, Cheshire.

2.1.2 Fragmenting materials

Dicalcium phosphate and sugar were chosen to represent this group of materials. The brittleness of dicalcium phosphate has been reported by Khan and Rhodes (1973) and DeBoer and Bolhuis (1978), while Hardman and Lilley (1973) showed that densification of sucrose occurs by a fragmentation mechanism.

The dicalcium phosphate dihydrate, $Ca_2(H_2PO_4)_2$ was a white powder, supplied by Albright and Wilson Ltd,

Worcestershire. The granulated sugar was supplied by Tate and Lyle, London House, High Street, Croydon.

2.1.3 Non-compactable powders

Three plastic polymers were used: two grades of spherical low density polypropylene polymer (Homopolymer and co-polymer) as supplied by I.C.I Plastic Division, Welwyn Garden City, Hertfordshire and polystyrene (Styrocell) as supplied by Shell Chemicals (UK) Ltd.,

2.2 Characterisation of Materials

2.2.1 Sieve size

Sieving in accord with the British Standard BS 1796(1976) was used to characterise the coarse powders. The powders were first mechanically sieved for twenty minutes then hand sieved. Sieve fractions of selected sizes were used in the majority of the compaction tests, to minimise possible errors in reproducibility of results arising from segregation.

2.2.2 Size analysis by sedimentation method

Size distribution analyses was carried out on finer powders used in this investigation. Sedimentation using the Andreasen's technique was used to measure the size distribution of dicalcium phosphate powder.

It is of great importance in all sedimentation analyses to ensure that particles are completely dispersed and are not influenced by the proximity of other particles. In order to achieve this, 2 grams of the powder were spatulated with a small amount of 0.1% calgon(sodium hexametaphosphate) to form a thick

paste. This paste was then diluted by adding more dispersing liquid to a known volume. The suspension was then placed in an ultrasonic bath for about 30 seconds. A drop of the suspension was examined under a microscope to check on the absence of flocculation.

(a) Andreasen apparatus

In the Andreasen pipette method the concentration changes occurring within a settling suspension are followed by the withdrawal of definite volumes from the suspension at known intervals of time.

The Andreasen equipment consisted of a height graduated sedimentation vessel (0 to 20 cm) with a volume of 500 to 600 cm^3 when filled to the 20 cm mark. The stem of the pipette was fused to a ground glass socket which fitted the neck of the sedimentation vessel. Above the socket was a two-way tap which allowed the sample removed from the vessel to be eventually stored in a 10 cm^3 container.

(b) Andreasen technique

The prepared suspension was washed into the sedimentation vessel and the level made up to the top mark. The stopper with the pipette was thenreplaced and the suspension agitated by inverting the apparatus many times, Immediately after the agitation the apparatus was placed on the bench and two samples withdrawn from the suspension, the samples were taken by gently sucking a volume of 10 cm^3 of the suspension into the sample container from which they were transferred to a pre-weighed

container. About 5 cm^3 of fill liquid, without dispersing agent, was drawn into the pipette after every sample removal to wash the sample container from any possible settling of particles and added to the sample removed. The removal of the samples was continued at suitable times recording the time and height of the suspension level in the vessel.

The concentration of solids in the samples may be determined by simply drying and weighing. The equation yielding the percentage undersize D of equation (1.15) can then be expressed as follows:-

$$P = 100 \frac{M_t}{V} \cdot \frac{V_s}{M_s} \qquad (2.1)$$

where M_t ≡ the weight of powder in the removed sample

V ≡ the volume of the removed sample

M_s/V_s ≡ the solid concentration in the initial homogeneous suspension.

2.2.3 Density measurement

The powder volumes were determined using an air pyknometer (Model 930, Beckman Ltd., Fife). The instrument consisted of two cylinders interconnected via a differential pressure gauge. One cylinder was for the sample and the other for a reference. The sample was placed in the measuring cylinder and the system sealed from atmosphere. Two pistons, one in each cylinder, were screwed slowly into the cylinders. As the piston in the reference cylinder

reached a stop, the distance which the sample piston had moved to maintain a pressure balance between the two cylinders was measured. The volume of the sample was obtained directly from the digital counter connected to the sample piston. The powder particle densities were then calculated from the mass and volume of the sample.

2.2.4 Surface area measurement

The specific surface area of the powders was obtained from nitrogen adsorption isotherms. Calculations were carried out according to the BET(1.20) and Huttig equations (1.26).

The equipment used was a glass apparatus similar to that described in the British Standard (1969) (fig 2.1). It differs from the British Standard equipment in that the mercury manometer used to measure the equilibrium pressure of the adsorbate was extended to measure pressures in excess of atmospheric pressure. The apparatus consisted of three major parts. The gas burette, mercury manometer and a reservoir.

The gas burette, B, was a series of glass bulbs accurately calibrated in terms of volume at standard temperature and pressure (S.T.P.). A mercury manometer, M, consisted of a glass tube behind which was a mirrored scale. One end of the manometer was connected to the gas burette and the other to the vacuum system. A reservoir, R, supplied mercury to the burette and the manometer. The

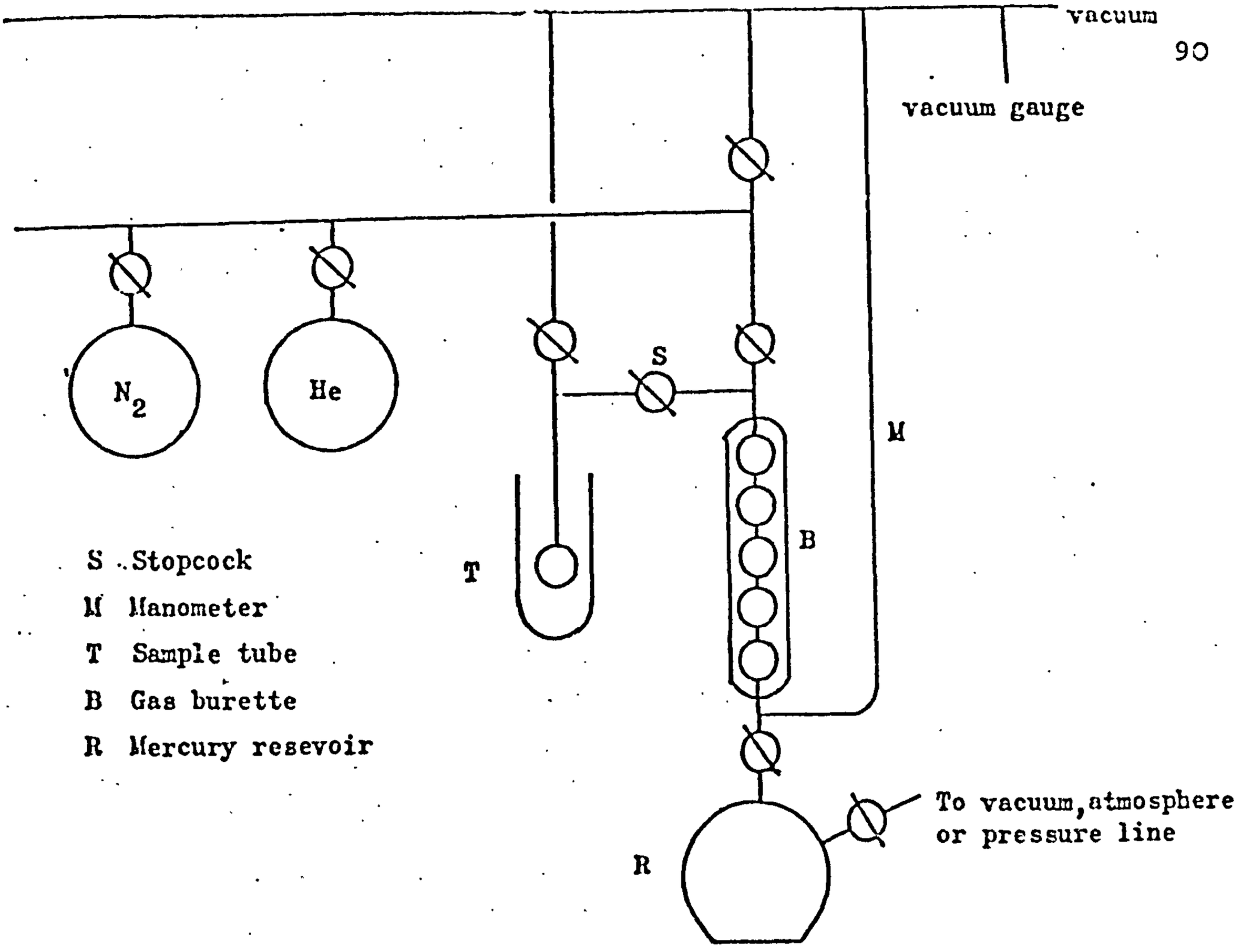

S Stopcock
M Manometer
T Sample tube
B Gas burette
R Mercury resevoir

Figure 2.1 : Schematic diagram of gas adsorption apparatus.

Figure 2. 2

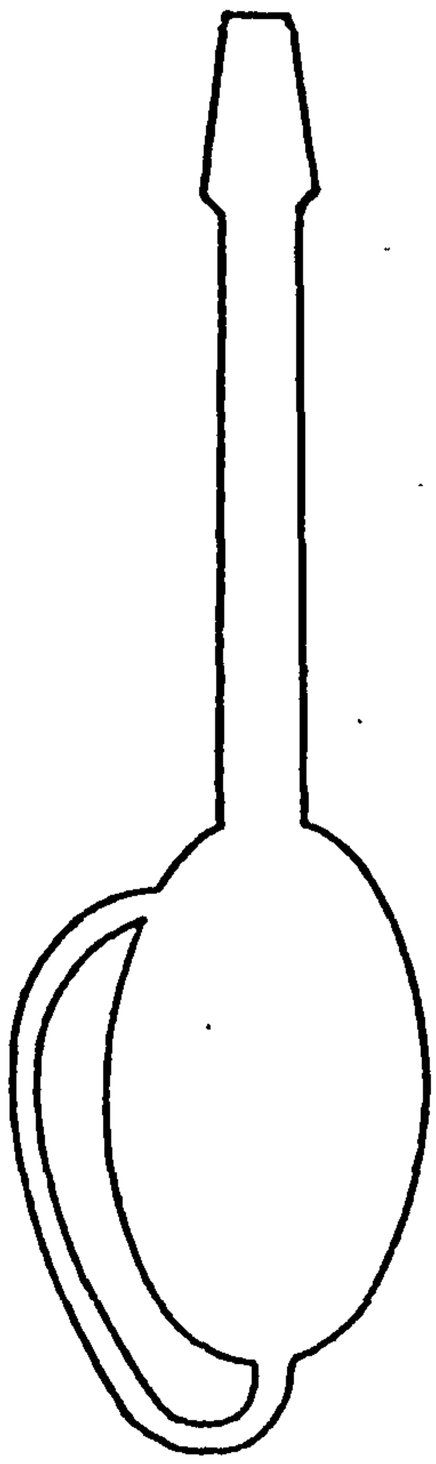

Sample tube for use with powders.

Figure 2. 3

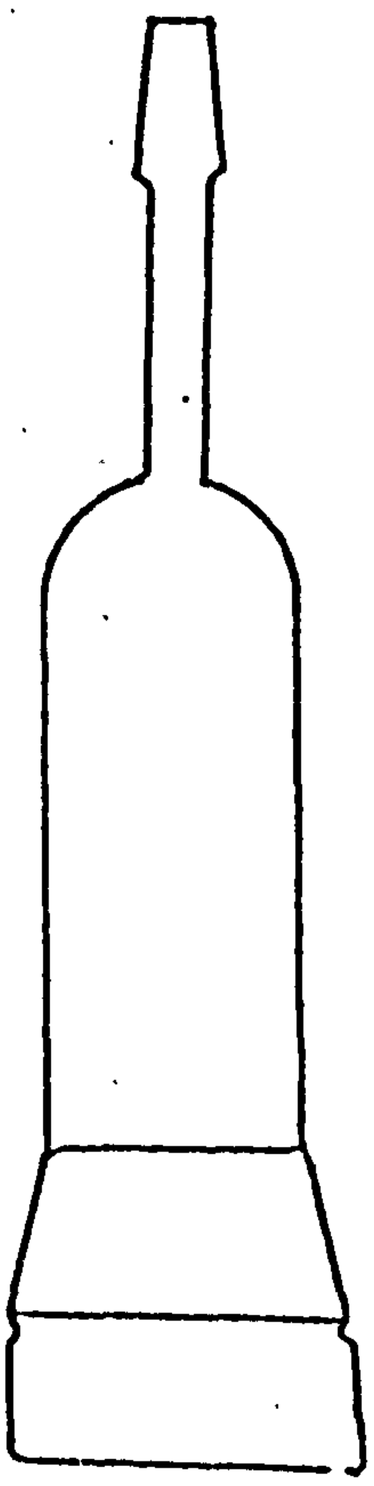

Sample tube for use with compacts.

reservoir could be connected to vacuum, to atmosphere or to compressed air to provide pressure above atmospheric. These connections provided an accurate method of controlling the mercury flow into the system. A sample tube containing the material to be tested was connected to the gas burette via a stopcock, S, The sample tube used was of special design (fig 2.2). The tube from the neck to the bottom of the sample tube served as a bypass to minimise entrainment of powder into the vacuum system due to entrapped air leaving the powder during degassing.

An accurately weighed sample of the powder was placed in the sample tube. The sample tube was then connected to the vacuum system for degassing.

Dicalcium phosphate powder was degassed at room temperature and pressure of 10^{-3} torr for 20 hours.

During adsorption measurements the sample tube was immersed in liquid nitrogen at atmospheric pressure and a temperature 77K. The level of the liquid nitrogen was kept constant. Since it was impossible to pre-calculate the volume of the sample tube not occupied by the powder, a dead space calibration had to be performed with each sample. The dead space was calculated prior to the nitrogen adsorption with a non-adsorbable gas, helium, at liquid nitrogen temperature. the dead space was measured by admitting the known volume of helium into the gas burette, with the stopcock to the

sample closed, the amount of helium admitted was calculated from the manometer pressure and the volume of the bulbs of the burette. The helium was then expanded into the sample tube by opening stopcock S. After equilibrium the amount of helium remaining in the burette was calculated from a second reading of pressure and volume. The difference between the two readings gave the volume of the space within the sample tube not occupied by the powder sample. The dead space volume at S.T.P. was divided by the second equilibrium helium pressure to give a dead space factor (D.S.F.). Standardized dead space volumes at other equilibrium pressures were obtained by multiplication of the D.S.F. by the ultimate equilibrium pressure.

$$D.S.F. = \frac{\frac{P_1V_1}{T} - \frac{P_2V_2}{T}}{P_2} \cdot \frac{273.2}{P_o} \qquad (2.2)$$

where P_1 ≡ initial gas pressure (Torr)

P_2 ≡ equilibrium gas pressure (Torr)

P_0 ≡ atmospheric pressure

V_1 ≡ volume of the burette bulb at which the initial pressure was measured

V_2 ≡ volume of the burette bulb at which the equilibrium pressure was measured

T ≡ absolute burette temperature

The adsorbate used throughout this investigation was a research grade XX nitrogen gas supplied by B.O.C., Deer Park, Wembley.

Before an adsorption measurement was carried out the system was evacuated from helium gas, Nitrogen was introduced into the gas burette and the mercury level adjusted to the mark of an appropriate glass bulb. The pressure on the manometer was recorded and the amount of gas admitted was calculated from the known volume and pressure.

$$V_{adm} = \frac{P_1 V_1}{T} \cdot \frac{273.2}{P_o} \qquad (2.3)$$

where $V_{adm} \equiv$ volume of gas admitted to the system at S.T.P.

$P_1 \equiv$ initial pressure of the gas

$P_o \equiv$ atmospheric pressure

$V_1 \equiv$ volume of the burette bulb chosen

$T \equiv$ absolute burette temperature

The gas was then expanded into the sample tube and time allowed for equilibrium. Part of the admitted gas was adsorbed onto the sample and the remaining part occupied the space in the burette and the dead space in the sample bulb. The amount of gas adsorbed onto the sample was obtained by subtracting the amount of gas which remained in the burette and dead space from the amount of gas admitted.

$$V_{ads} = V_{adm} - \left(\frac{P^2 V_2}{T} \cdot \frac{T_o}{P_o} + (DSF. P_2) \right) \qquad (2.4)$$

where $V_{ads} \equiv$ volume of gas adsorbed onto the powder (other symbols are the same notations as equation 2.1).

To obtain additional points on the adsorption isotherm, the mercury was raised to the next bulb and adjusted to the new volume fiducial mark. The equilibrium pressure was recorded and from knowledge of the calibrated volume and dead space factor, the volume adsorbed onto the powder in the sample tube, V_{ads}, was calculated.

After the last possible reading was taken from the initial nitrogen filling, tap S was closed and more nitrogen admitted to the system. The calculations are carried out cumulatively in steps in the same manner and the values of volume adsorbed at known relative pressures in the range of 0.05 to 0.35 and 0.05 to 0.7 were used to calculate the adsorption isotherm from which the specific surface area can be determined from either the BET or Huttig equations.

A computer program called NITROPLOT (appendix 5) was written to calculate the volume of gas adsorbed onto the sample and the specific surface area from the observed data. Graphs of the BET function against relative pressure- the adsorption isotherm - were plotted by the same program.

CHAPTER 3

CHAPTER 3

3.0 Compaction

3.1. Introduction

The objective of this investigation as already mentioned was to study the effect of uniaxial compression on a wide variety of particulate solids. The direct measurement of different parameters during a compaction process produced a considerable amount of data, which for accuracy and ease of analyses was recorded onto tape by the use of a cassette data logger (Digitronix Super 8, Digitronix Ltd, Milton Keynes). An instrumented (Piezo-electric transducers, Kistler Instrumente:, Zurich, Switzerland) die and punch assembly similar to that developed by Marshall (1970) was used for the continuous measurement of the applied force, transmitted forces and the upper punch displacement.

3.2 Compaction apparatus and instrumentation

A specially designed punch and die assembly (figure 3.1) which consisted essentially of a stainless steel die (20 mm) and upper and lower punches hardened after fabrication, was manufactured by A.B. Hobleys Limited, Bradford. The force exerted by the upper punch, F_A, was measured by a piezo electric transducer, A, (Kistler type 906) placed centrally on the punch head.

The die rested on top of a piezo-electric force

Figure 3 • 1

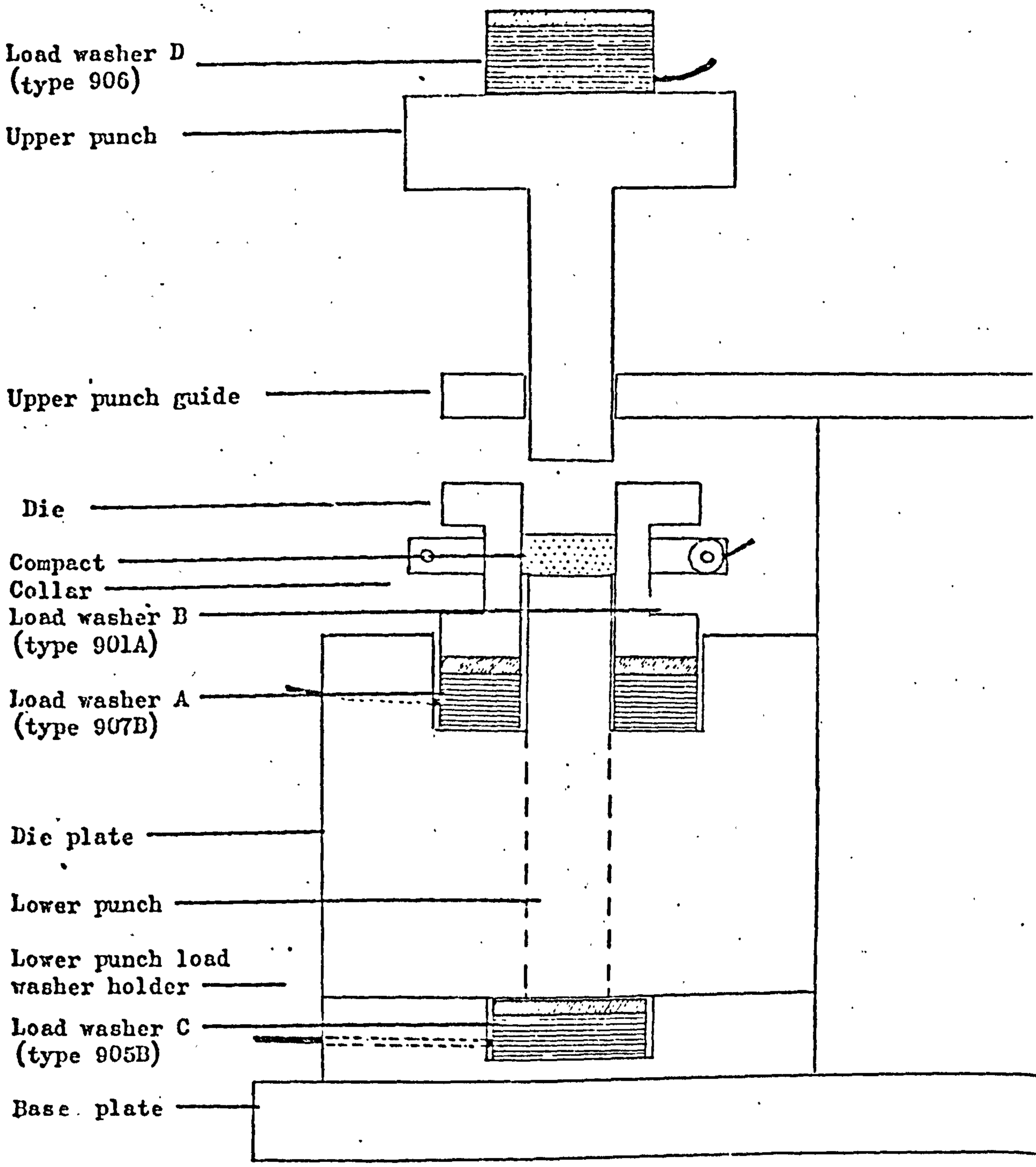

The compaction apparatus (diagrammatic).

transducer, C, (Kistler type 907B) placed within the die support body and measured the axial force, F_D, on the die. Around the circumference of the die a horizontally split collar was clamped. The collar was clamped so that the lower edge of the collar was at the same height as the upper surface of the lower punch (fig 3.2).Into this collar a load washer B (Kistler type 901A), was fastened which measured the forces transmitted radially, F_R, to the die wall.

The stationary lower punch was mounted directly on a load washer D (Kistler type 905B), which measured the force, F_L, transmitted axially through the powder from the upper punch.

The relative punch position during the compaction cycle was monitered by means of a Linear Variable Differential Transformer (L.V.D.T.) (type D401-01, Electro-Mechanisms Ltd, Slough). The L.V.D.T. was mounted onto the die plate while the sensor rod was coupled to a brass collar clamped securely to the broad head of the upper punch (fig. 3.3). A stabilised voltage supply (Farnell Instruments Ltd, Wetherby) supplied the L.V.D.T. input of 24V and the L.V.D.T. output was fed directly to the amplifier Readout Interface (figure 3.4).

Each force transducer was connected to a calibrated charge amplifier (Kistler types S68,5001, Kistler Electronics, Zurich, Switzerland, and Vibrometer type TA-3/C, Vibrometer S.A. Manchester). These charge amplifiers converted the electrostatic signals

Figure 3 • 2

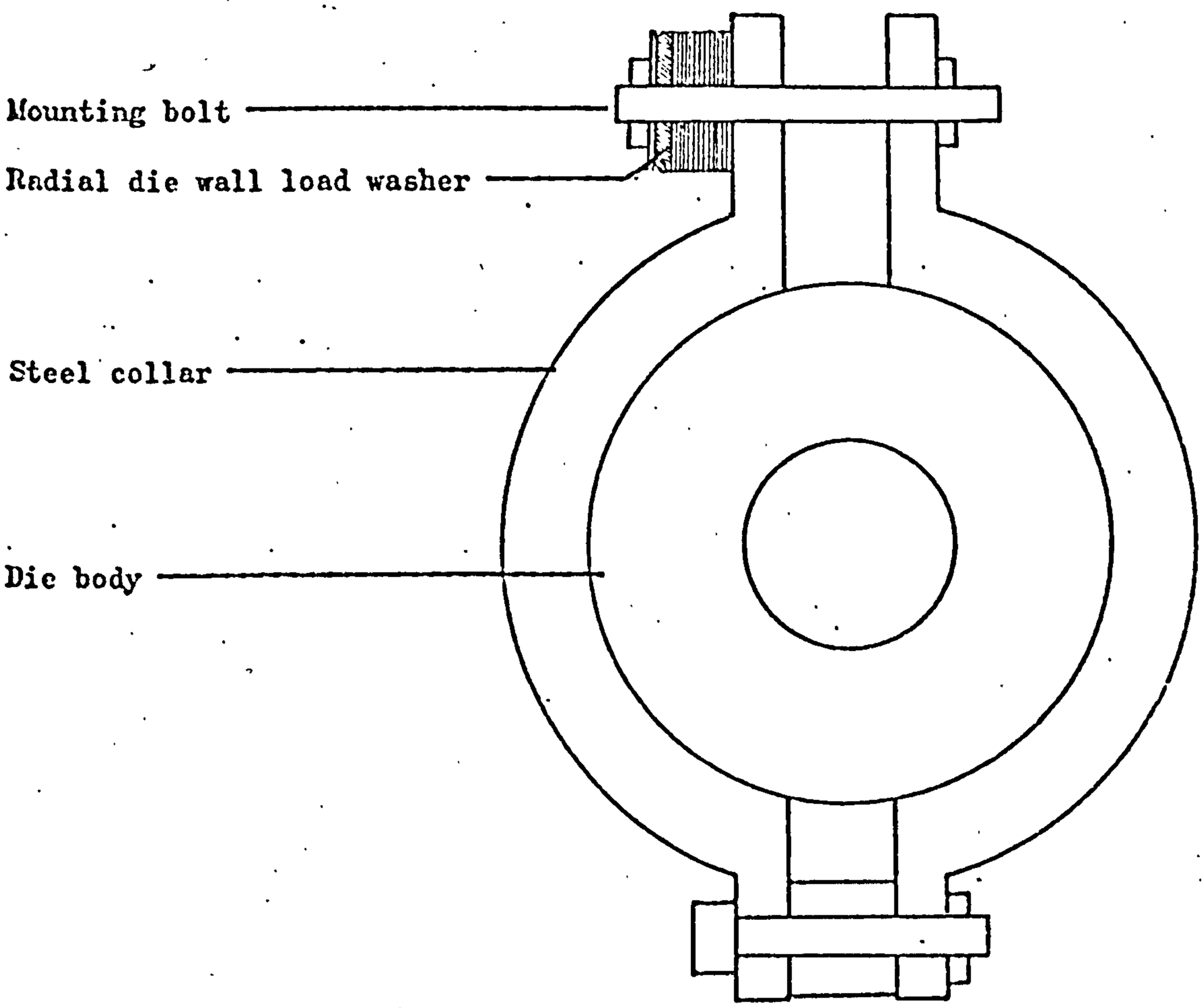

Arrangement of the radial die wall load washer and collar.

Figure 3.3

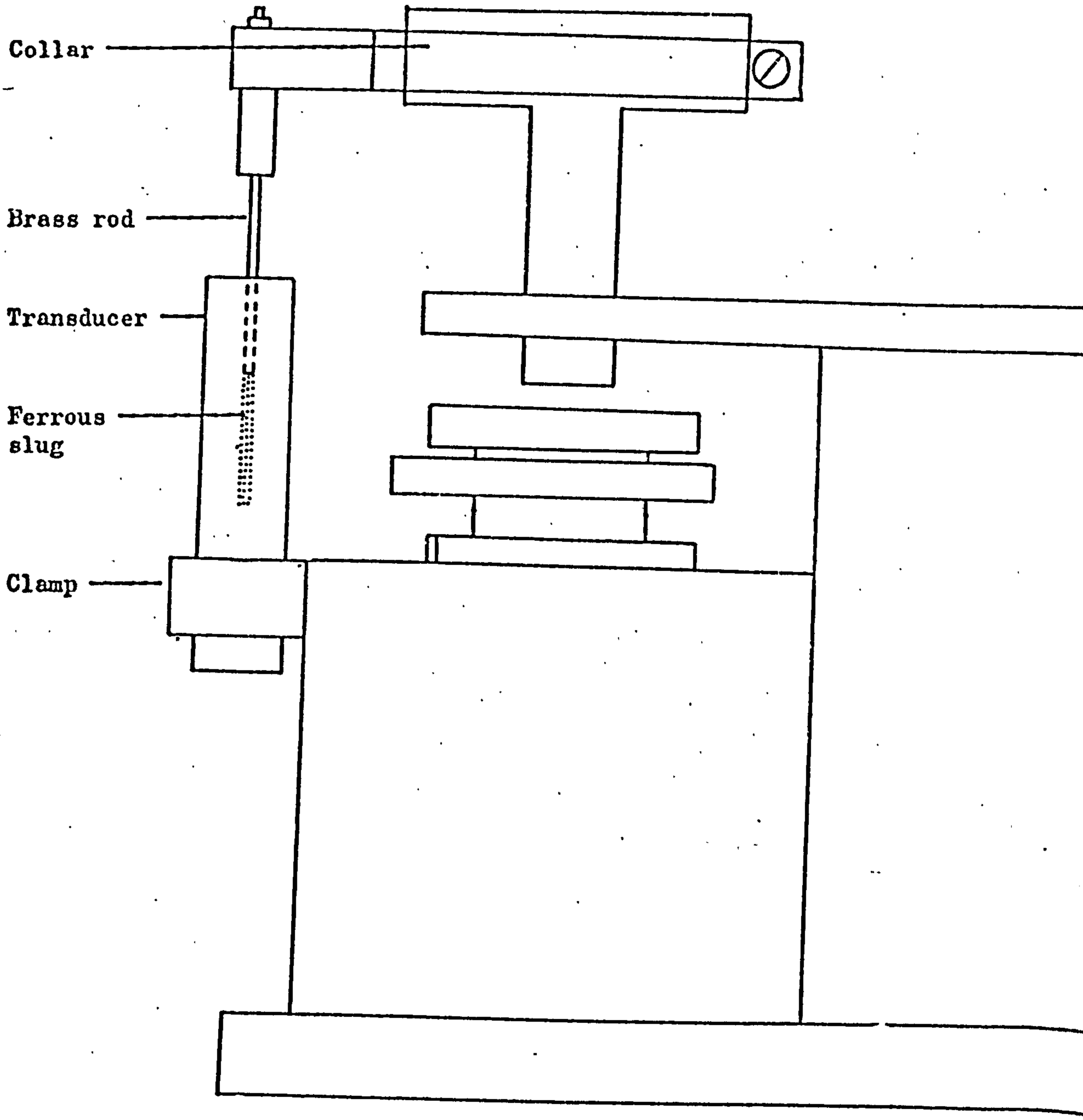

Mounting of the L.V.D.T. (diagrammatic).

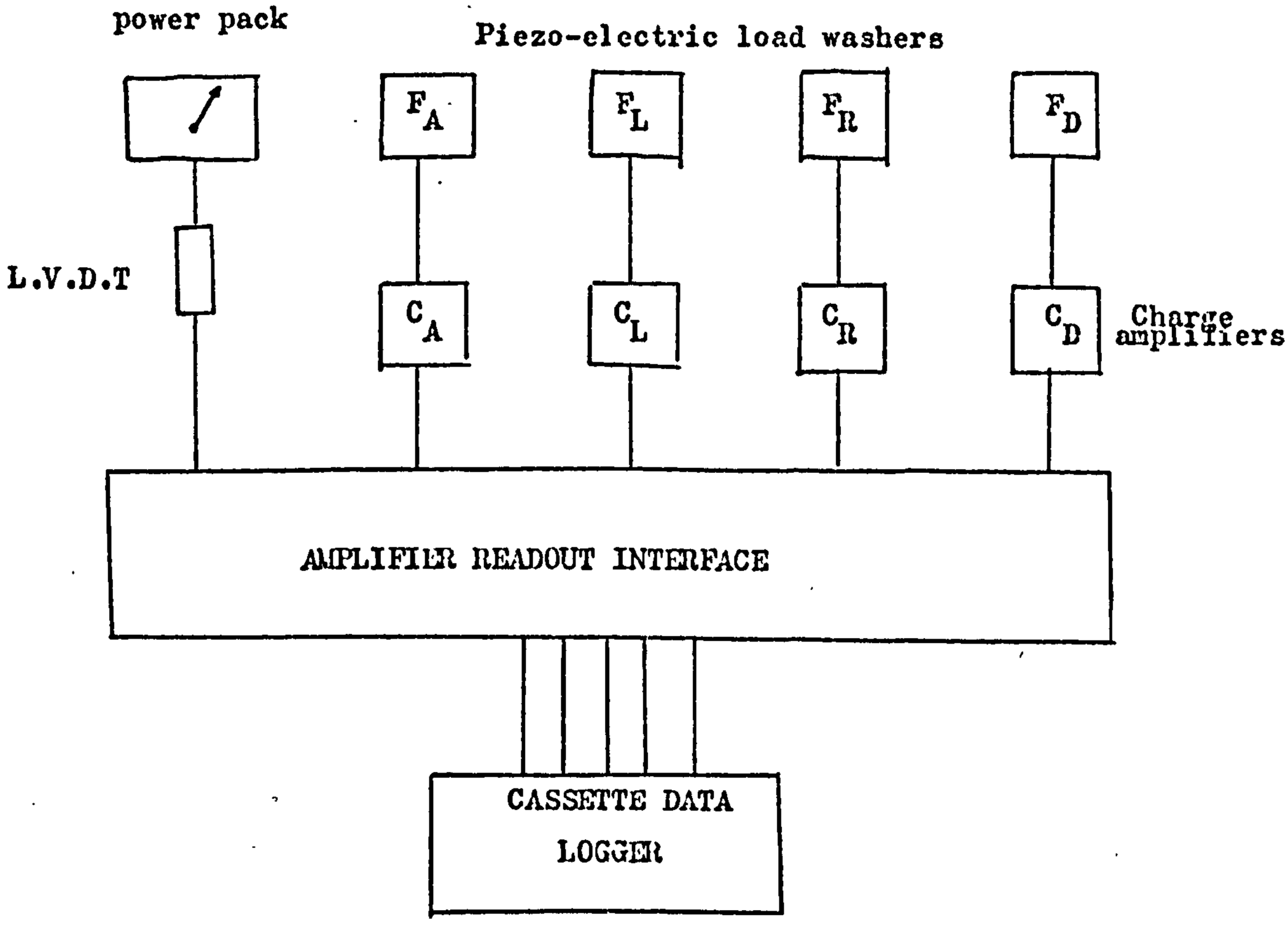

Figure 3 . 4 Block diagram of the measuring and recording system

produced by the force transducers into d.c. voltages directly proportional to the force. The output from the amplifiers were connected to the recording device through an Amplifier Readout Interface (see fig 3.4). A detailed description of the cassette data acquisition system and the relevant associated apparatus can be found in the work of A. Ibrahim (1979).

The punch and die assembly was used between the platens of a hydraulically operated Denison T42.23 Tensile Testing Machine (Denison and Sons Ltd., Leeds).

3.3 Calibration of Instrumented Punch and Die Assembly

3.3.1 Upper Punch force transducer

The upper punch force transducer was calibrated by applying known loads to the transducer by means of a Denison tensile test machine. The responses of the force transducer were displayed on the data logger and the applied load-response of different loads are presented in fig.3.5 and table 3.1.

3.3.2 Lower Punch force transducer

The lower punch force transducer was calibrated with reference to the upper punch transducer. A brass spacer was placed between the upper and lower punches to protect the punch faces. The force was then applied to the upper punch force transducer and the responses of both transducers recorded simultaneously by the data logger as an increasing load of 100 kN was applied. The computer printout was used to plot the lower punch response curve (fig 3.6, table 3.2) from which a linear relationship was obtained.

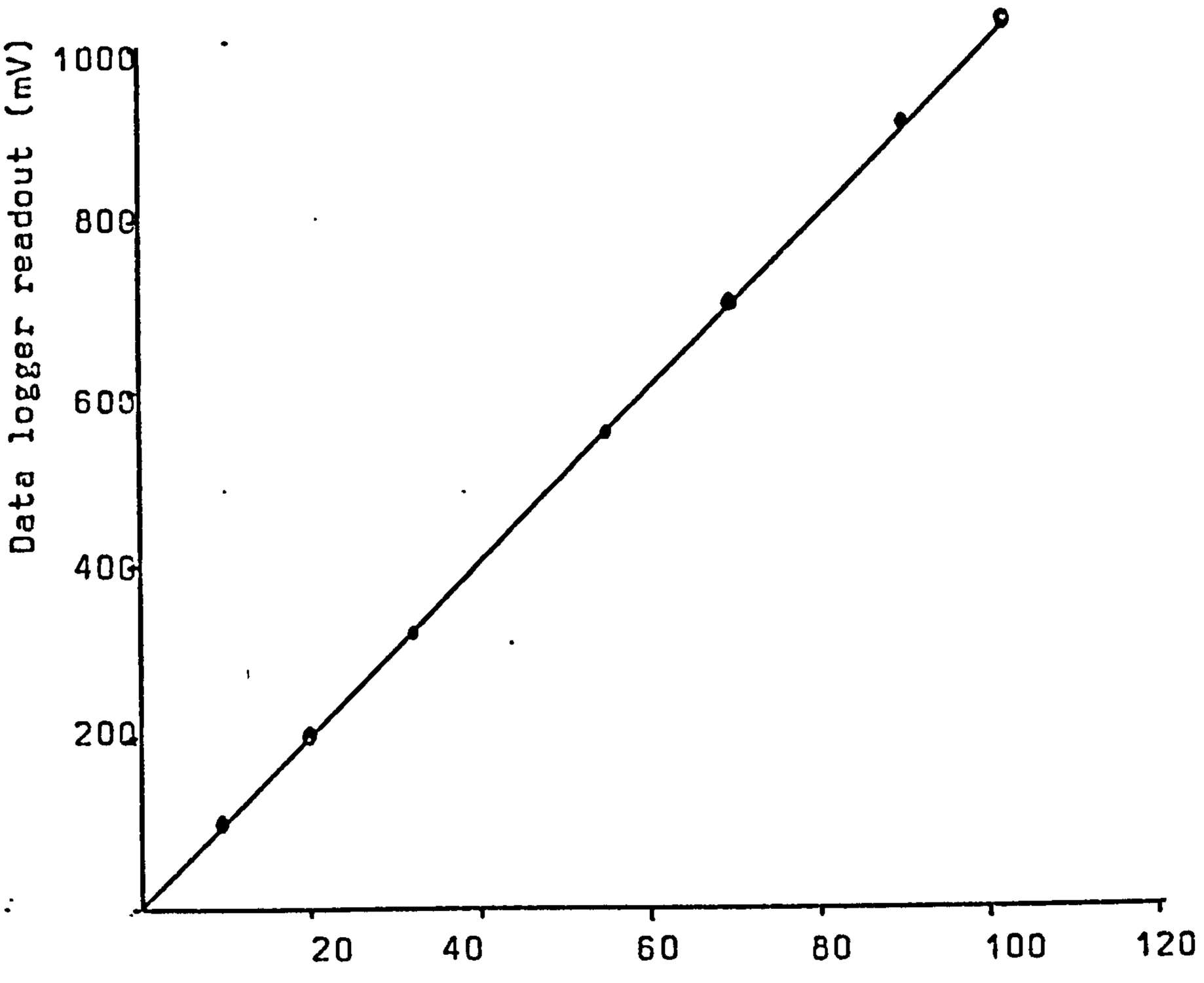

Figure 3.5 Calibration curve of the upper punch force transducer

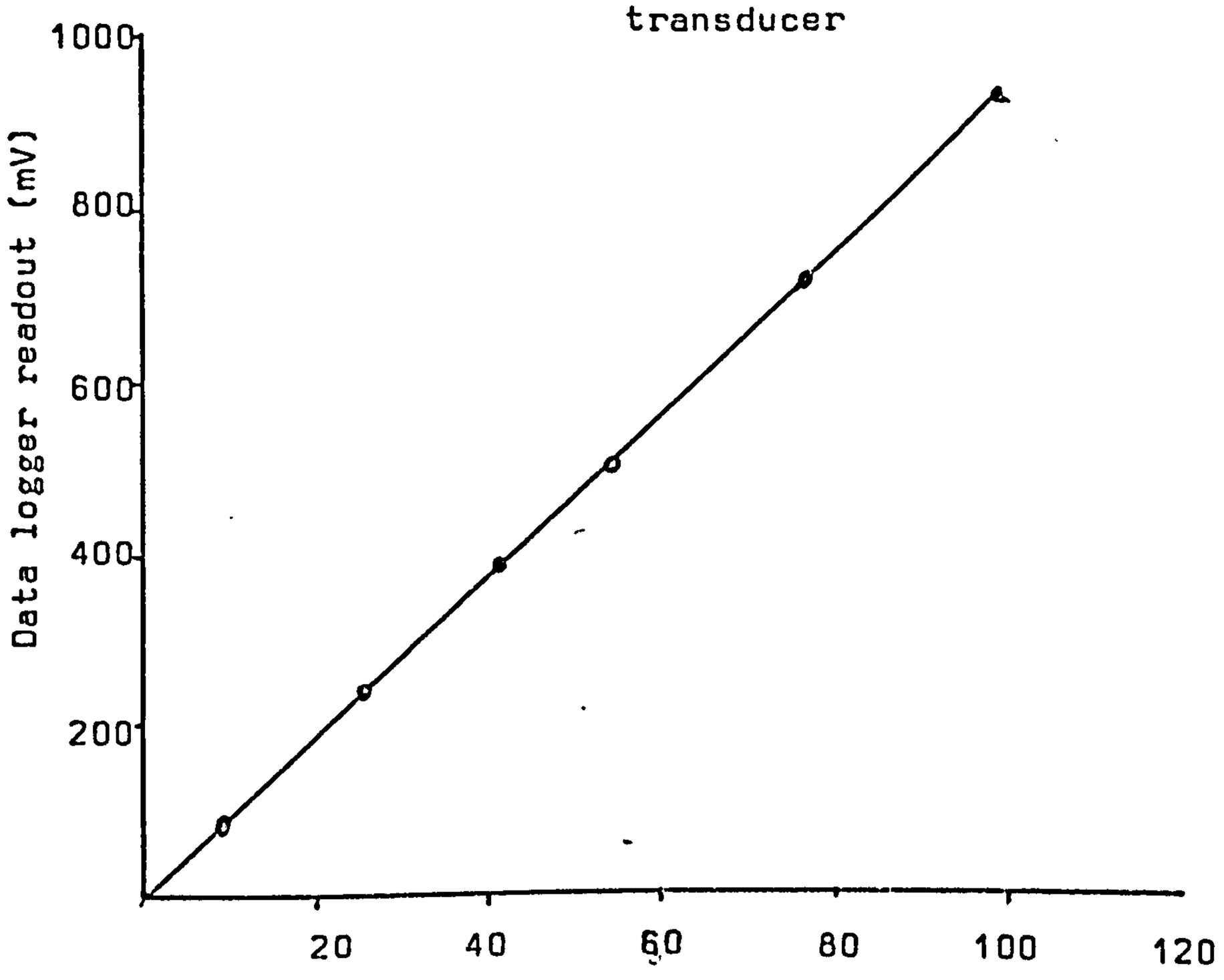

Figure 3.6 Calibration curve of the lower punch force transducer

Table 3.1 Calibration of data logger output (mV) for the upper punch force transducer against force from Denison's press.

Applied force (kN)	Data logger output (mV)
9.95	100
14.25	145
20.05	205
32.0	320
40.75	410
48.1	483
55	550
58	580
61	615
70.0	700
81.5	815
85.0	854
90.0	910
102	1025

Table 3.2 Calibration of the lower punch force transducer against absolute force from the output of the upper punch force transducer.

F_A Transducer reading (mV)	Force equivalent to F_A transducer reading (kN)	F_L Transducer reading (mV)
15	1.495	10
93	9.272	83
150	14.954	138
255	25.423	236
302	30.108	281
413	41.175	385
543	54.135	507
666	66.398	622
766	76.367	714
914	91.122	855
990	98.699	924

3.3.3 Axial die wall force transducer

The force transmitted axially to the die body was measured by a force transducer placed in the die plate. The F_D transducer was calibrated using the previously calibrated upper punch force transducer. The upper punch was withdrawn, and a flat piece of metal placed on top of the die on to which the upper punch force transducer was placed. A load of 30 kN was applied and the response of both transducers recorded. The computer printout was used to plot the axial die wall force transducer response curve (fig 3.7, table 3.3).

3.3.4 Radial die wall force transducer

The radial die wall force transducer was calibrated in a similar way to that suggested in the literature. Windheuser et al (1963), Ridgway (1966), Sixsmith (1975) and Harris (1981). These workers transmitted the applied force from the top punch to the die wall by compacting a rubber plug or rubber powder. Rubber was used because it behaved as a liquid under compression and it was assumed that the force applied to the upper punch is transmitted radially to the die wall. A rubber powder sieved through a 250 μm sieve was used for the calibration.

A constant volume of die fill, equal in weight to twice the density of the rubber, was compacted to 50 kN for 15 minutes to minimise the settling effects.

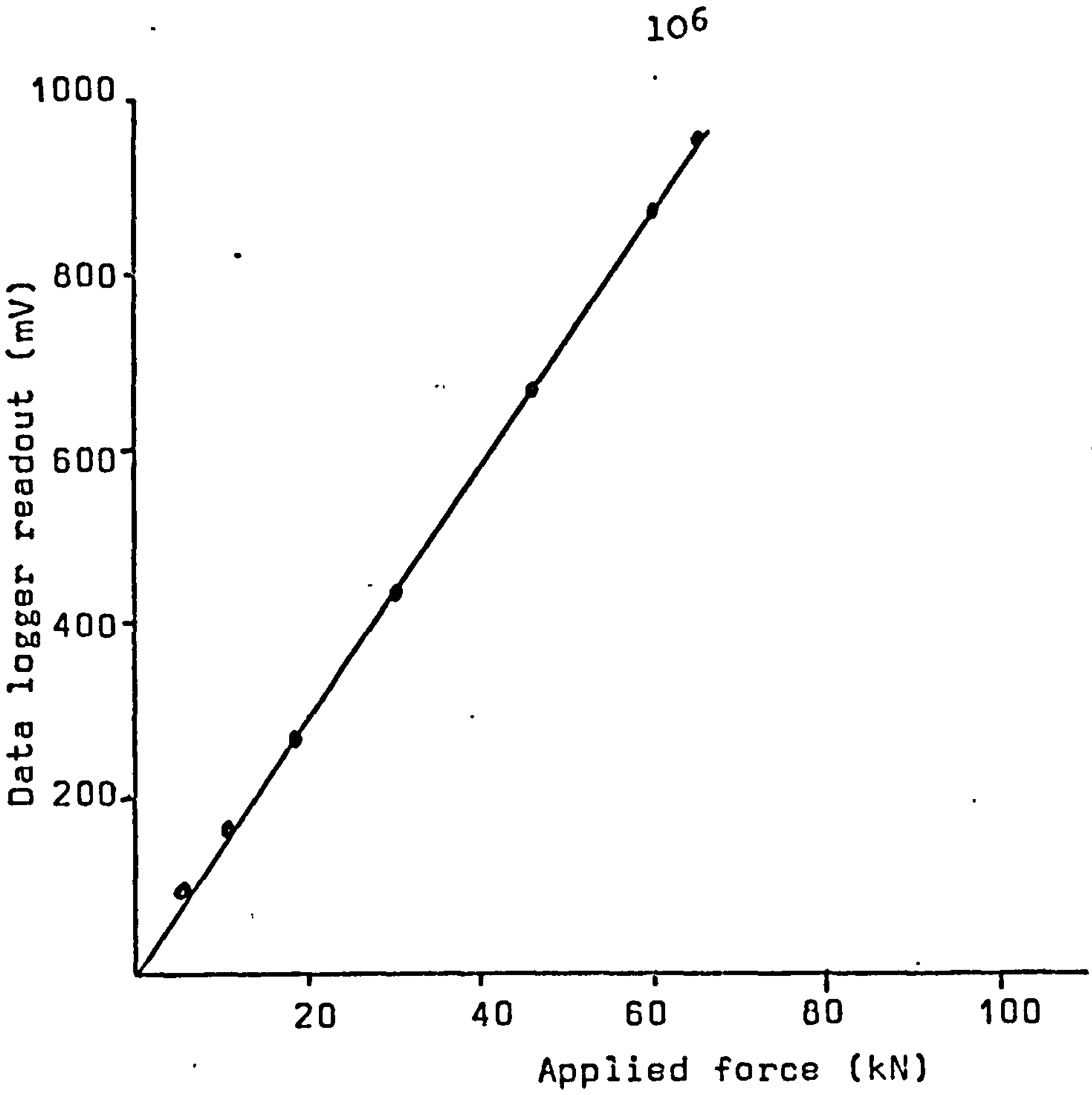

Figure 3.7 Calibration curve of axial die wall force transducer

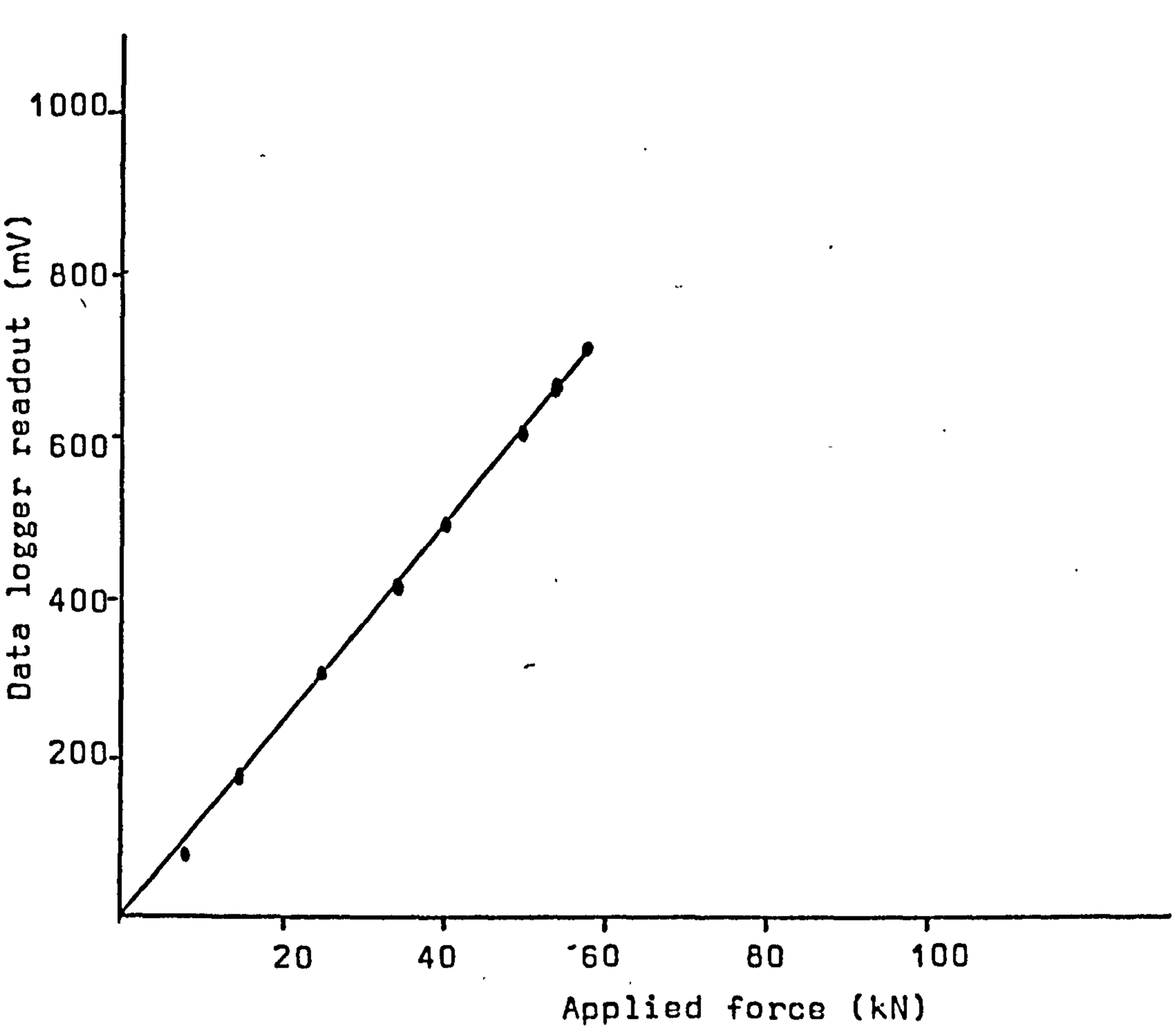

Figure 3.8 Calibration curve of radial die wall force transducer.

Table 3.3 Calibration of the axial die wall force transducer against absolute force from the upper punch force transducer

F_A Transducer reading (mV)	Force equivalent to F_A transducer reading (kN)	F_D Transducer reading (mV)
54	5.384	97
104	10.368	166
183	18.244	269
250	24.924	359
301	30.009	431
373	37.187	538
422	42.072	611
460	45.860	668
517	51.543	752
596	59.419	873
614	61.214	900
650	64.803	954

Table 3.4 Calibration of the radial die wall force transducer against absolute force from the upper punch force transducer.

F_A Transducer reading (mV)	Force equivalent to F_A transducer reading (kN)	F_R Transducer reading (mV)
76	7.577	77
150	14.954	175
200	19.939	240
250	24.924	277
300	29.909	342
350	34.894	413
410	40.876	491
500	49.848	601
540	53.836	651
580	57.824	709

A calibration compaction to determine the response of the radial transducer was then carried out and the response of the upper punch and radial die wall force transducers recorded by the data logger. The data from the computer printout showed a linear relationship between the logger readout (mV) and force at the die wall (kN) (fig 3.8, table 3.4).

3.3.5 Upper Punch displacement transducer

The output of the L.V.D.T. was adjusted by a potentiometer in the amplifier readout Interface, A.R.I, so that when the surface of the upper punch was in direct physical contact with the lower punch, the reading on the data logger display was zero mV. This arrangement was adopted to give a constant reference base line for a quick check of any zero drifts of the displacement transducer.

Several metal spacers of accurately determined height between 0 and 15 mm, were placed between the two punches and the response displayed on the data logger. The response between the data logger readout (mV) and upper punch displacement (m) was found to be a linear relationship (fig 3.9 Table 3.5).

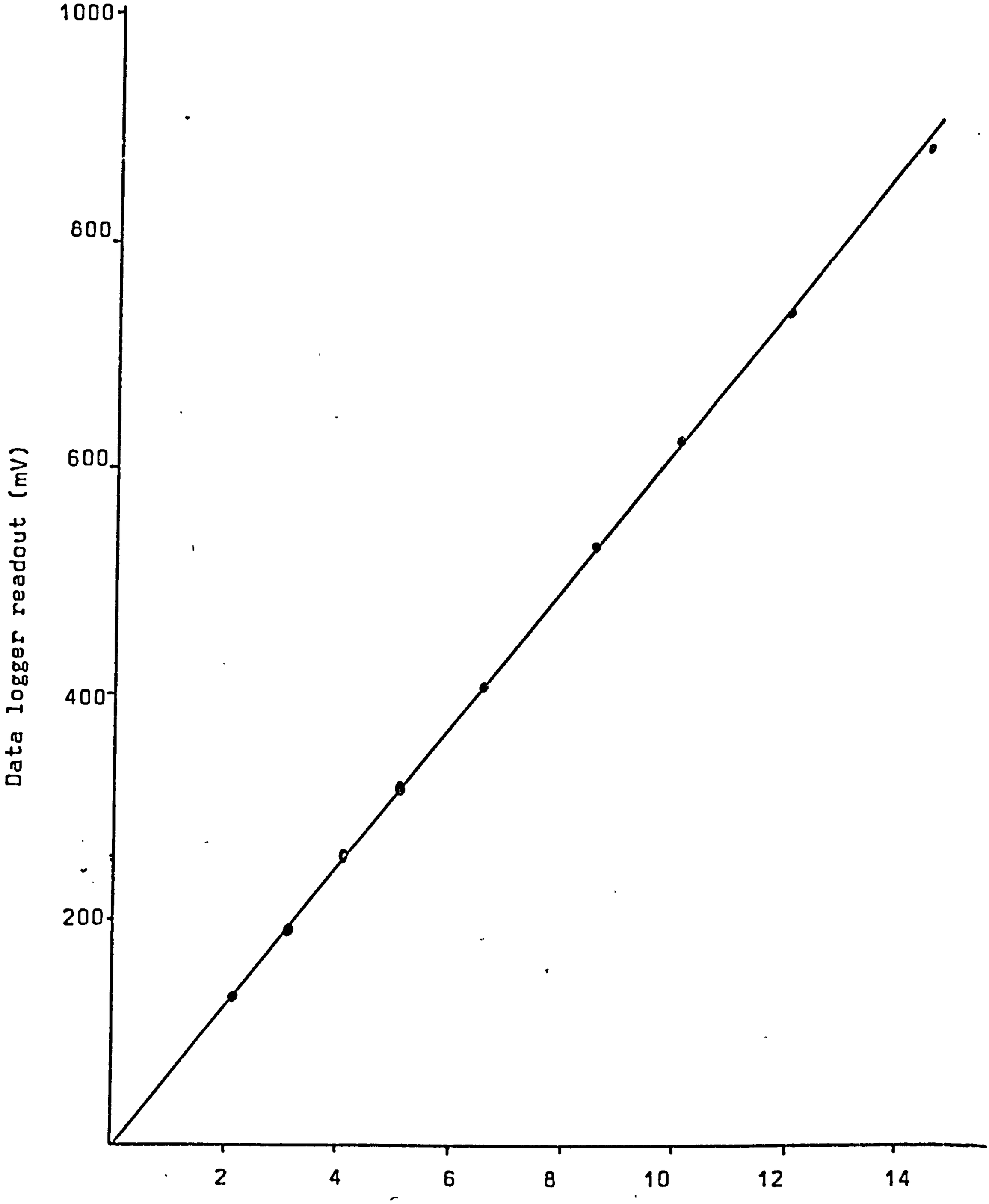

Figure 3.9 Calibration curve of the upper punch displacement transducer.

Table 3.5 Calibration of the data logger output (mV) for the upper punch displacement transducer against spacer thickness (mm)

Spacer thickness (mm)	Data logger output (mV)
2.1	130
3.1	190
4.05	255
5.05	315
6.50	405
8.50	530
10.00	625
11.95	740
14.45	888
15.45	930

3.4 Compaction Procedure

The punch faces and the internal walls of the die were repolished every time a compaction material was changed. Polishing was carried out by means of a small motor driven felt polishing pad, impregnated with a fine diamond polishing paste (Microfin 1-G-m, Universal Diamond Ltd., London).

Before a compaction was carried out, the internal walls of the die and the faces of the punches were cleaned and lubricated by a 2% w/v solution of stearic acid, in a mixture of equal volumes of acetone and carbon tetrachloride. Three to five minutes were allowed for drying before die filling.

The measurement equipment and data recorders, were switched on for at least 15 minutes to stabilise. The head of the cassette data logger was cleaned, (Ampex 220 Demagnetizer/Cleaner, Ampex Corporation, U.S. Patent No.3,647,990), and the zero calibration of the L.V.D.T. checked with the two punches in contact prior to each experimental run.

A pre-weighed amount of the material to be compacted, equal to twice the density of the powder was introduced by hand into the die. The die filling was carried out carefully by holding the sample container in contact with die bore to ensure the maximum reproducibility of the initial bulk density.

The upper punch was then positioned and the force transducer placed centrally on the punch head. All transducers were checked for zero settings before compaction. The force applied to the upper punch was observed from the scale on the press while the display facility on the data logger was used to observe the radial force transmission. Data on compaction and relaxation was recorded for all compacts. The rate of compaction was controlled from Denisons Press setting. The exact rate was calculated from the recorded Data logger data which scanned each transducer and the L.V.D.T. at 80 m.sec. intervals.

3.5 Ejection of the compacts

To eject the compact, the upper and lower punch together with the holder of the lower punch force transducer were removed. The die was then inverted and replaced in the die plate. A hard plastic spacer which had a sliding fit in the die was placed on top of the compact and pressure exerted by the upper punch to remove the compact. The ejected compacts were stored in screw-cap jars until needed.

CHAPTER 4

CHAPTER 4

4.0. Computer Analysis of Uniaxial Compaction Recorded Data

4.1 Data files

The data tape, recorded as described in chapter 3 on rewinding was inserted into a cassette replay unit (Monolog Serial ASCII logger/Replay unit. Digitronix Ltd., Milton Keynes) to produce a "print out" in 64 character per line format (table 4.1).

This raw data was then reformated to produce a format compatible with the analytic program, REFORM, for subsequent calculations. Program REFORM was written in algol 68 (table 4.2).

The reformated data file (table 4.3) consisted of the parameters from the instrumented punch and die assembly. The parameters recorded were all in millivolts where the term Va is the applied load, V_l , V_r and V_d are the force transmitted to the lower punch, the force transmitted radially to the die wall and the force transmitted axially to the die wall respectively. Vu is the millivoltage from the linear transducer.

4.2 Parameter files

The parameter file created contained the calibration constants of the punch and die assembly and the material constants (table 4.4). The first number in the first four lines was the calibration coefficient in mV/kN for F_A, F_L, F_R and F_D

Table 4.1

Dentritic sodium chloride (203 MPa)

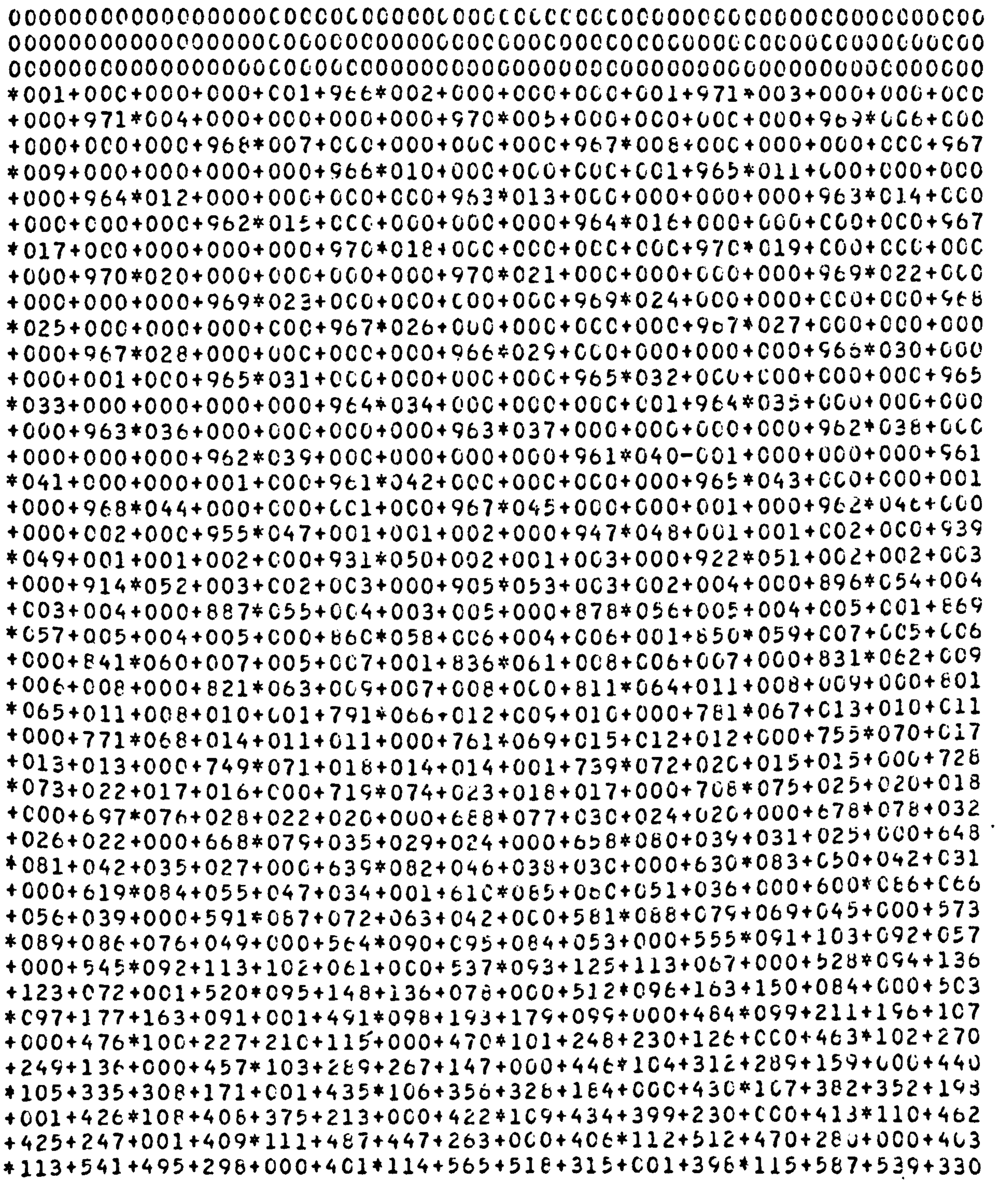

Table 4.1 continued

```
+000+392*116+605+555+342+000+391*117+620+569+352+001+390*118+635
+582+362+000+389*119+644+591+369+001+389*120+644+592+372+000+388
*121+641+592+372+000+385*122+636+589+371+001+385*123+629+587+369
+001+386*124+619+583+367+001+386*125+609+579+364+001+387*126+599
+576+362+001+388*127+590+572+359+001+385*128+581+569+357+000+386
*129+571+565+355+001+387*130+562+562+353+000+387*131+553+558+350
+001+384*132+544+554+348+001+385*133+535+550+346+001+386*134+526
+546+344+001+387*135+518+542+342+000+385*136+509+537+340+001+385
*137+502+532+338+001+387*138+494+527+336+001+388*139+486+521+333
+001+384*140+478+515+331+001+385*141+471+509+328+000+387*142+462
+501+325+001+388*143+450+490+321+001+384*144+435+475+316+000+385
*145+419+460+311+000+386*146+405+444+306+001+388*147+390+428+301
+001+385*148+376+414+296+001+386*149+363+399+292+000+387*150+350
+385+287+001+388*151+338+371+283+001+387*152+326+359+279+001+387
*153+314+345+275+000+388*154+302+333+271+001+389*155+291+321+267
+000+389*156+278+307+263+001+387*157+266+294+259+001+388*158+253
+280+254+000+389*159+242+268+251+000+390*160+230+255+246+001+387
*161+220+243+243+001+389*162+209+232+239+001+390*163+199+221+235
+000+391*164+190+210+232+001+388*165+181+200+226+000+389*166+172
+190+225+001+390*167+164+181+222+001+391*168+156+171+219+001+387
*169+148+162+216+001+389*170+141+154+213+001+389*171+134+145+210
+001+390*172+127+137+207+000+391*173+120+130+204+001+388*174+114
+123+202+001+388*175+108+115+199+000+389*176+102+109+197+000+390
*177+097+102+194+001+391*178+092+096+192+001+389*179+087+090+189
+000+388*180+082+084+187+001+389*181+077+079+185+001+390*182+072
+074+183+000+390*183+068+069+181+001+391*184+064+065+179+000+388
*185+059+061+177+001+388*186+055+056+175+001+389*187+052+053+174
+000+390*188+049+049+172+000+391*189+045+046+170+000+389*190+043
+043+169+001+389*191+040+040+167+000+389*192+037+037+166+001+391
*193+034+035+164+000+390*194+032+032+163+001+388*195+029+029+161
+000+389*196+026+027+160+001+390*197+024+025+159+000+391*198+022
+022+157+001+388*199+020+020+156+001+389*200+017+018+155+001+390
*201+015+016+153+000+390*202+013+014+152+000+390*203+011+012+151
+000+388*204+009+010+150+000+389*205+007+008+148+001+390*206+005
+007+147+000+391*207+004+005+146+000+388*208+003+004+144+001+389
*209+001+003+143+000+391*210+001+002+142+000+392*211+000+002+140
+001+389*212+000+001+140+000+390*213+000+001+140+000+391+214-001
+001+139+000+392*215-001+001+138+001+389*216-001+001+138+000+390
000000000000000000000000000000000000000000000000000000000000000
000000000000000000000000000000000000000000000000000000000000000
000000000000000000000000000000000000000000000000000000000000000
1
```

Table 4.2

(REFORM)

```
'BEGIN'
[1:24] 'CHAR' BUFF ;
'PROC' READCH = ('REF' 'CHAR' C)'VOID' :
'BEGIN'
    READ(C) ;
    'IF' C = " "
    'THEN' NEWLINE(STANDIN) ;
           READ(C) ;
           'IF' C = "0"
           'THEN' SETCHARNUMBER(STANDIN,4) ;
                  'BYTES' END ; READ(END) ;
                  'IF' END = BYTESPACK("C000")
                  'THEN' PRINT(("*-2 0 0 0 0 0 ")) ;
                         NEWLINE(STANDOUT) ;
                         'WHILE' READ(C) ; C = "0" 'DO' NEWLINE
     (STANDIN) 'OD'  'FI' ;
                  SETCHARNUMBER(STANDIN,2)
           'FI'
    'FI'
'END' ;
#                                                                    #
'PROC' GETSET = 'VOID' :
'BEGIN'
'CHAR' C ; 'BOOL' GOOD := 'TRUE' ;
'WHILE' READCH(C) ; C /= "*" 'DO' 'SKIP' 'OD' ;
BUFF[1] := C ;
   'FOR' I 'FROM' 2 'TO' 24
   'WHILE' GOOD
   'DO'
      READCH(C) ;
      'IF' C = "*"
      'THEN' OUTERR(I) ;
             BACKSPACE(STANDIN) ;
             GETSET ;
                GOOD := 'FALSE'
      'ELSE' BUFF[I] := C
      'FI'
   'OD'
'END' ;
#                                                                    #
'PROC' OUTERR=('INT' I)'VOID' :
'BEGIN'
   PUTF(ERRORS,($"INVALID DATA SET :- ",N(I)AL$,BUFF[1:I]))
'END' ;
'PROC' VALID = 'BOOL' :
```

Table 4.2 continued

```
'BEGIN'
'BOOL' V := 'TRUE' ;
'INT' C ;
'FOR' I'TO' 24 'DO'
          C := 'ABS'(BUFF[I]) ;
          'IF' (C < 48 'OR' C > 57)
           'AND' 'NOT' (     C=42
                        'OR' C = 43
                        'OR' C = 45
                         'OR' C = 20)
         'THEN' V := 'FALSE'
         'FI'
          'OD' ;
V
'END' ;
'PROC' OUTLINE = 'VOID' :
'BEGIN'
'FOR' J 'BY' 4 'TO' 23
'DO'
   'IF' BUFF[J] ="/" 'THEN' BUFF[J] := "1" 'FI'
'OD' ;
'IF' VALID 'THEN' PRINTF(($4A)4A)4A)4A)4A)4A)$,BUFF))
           'ELSE'  OUTERR(24)
           'FI' ;
NEWLINE(STANDOUT)
'END' ;
'PROC' EOF = ('REF''FILE'F)'BOOL' :
('GOTO' END OF FILE) ;
#                                                                    #
#    OPEN FILES                                                      #
CLOSE(STANDOUT) ;
CLOSE(STANDIN) ;
'FILE' ERRORS ;
OPEN(STANDIN,"RAWDATA",STAND IN CHANNEL) ;
ON LOGICAL FILE END(STANDIN,EOF) ;
ESTABLISH(STANDOUT,"OKDATA",TEXT FILE CHANNEL,5000,5000,30) ;
ESTABLISH(ERRORS,"ERRORS",TEXT FILE CHANNEL,50,60,50) ;
# NOW POINT TO START OF DATA #
'CHAR' CH ;
'WHILE' READ(CH) ; CH /= "*" 'DO' 'SKIP' 'OD' ;
BACKSPACE(STANDIN) ;
'DO'
GETSET ;
OUTLINE
'OD' ;
END OF FILE : PRINT(("*-2 0 0 0 0 0")) ; NEWLINE(STANDOUT)
'END'
```

Table 4.3

Dentritic sodium chloride (203 MPa)

	V_a	V_l	V_r	V_d	V_u
*001	+000	+000	+000	+001	+966
*002	+000	+000	+000	+001	+971
*003	+000	+000	+000	+000	+971
*004	+000	+000	+000	+000	+970
*005	+000	+000	+000	+000	+969
*006	+000	+000	+000	+000	+968
*007	+000	+000	+000	+000	+967
*008	+000	+000	+000	+000	+967
*009	+000	+000	+000	+000	+966
*010	+000	+000	+000	+001	+965
*011	+000	+000	+000	+000	+964
*012	+000	+000	+000	+000	+963
*013	+000	+000	+000	+000	+963
*014	+000	+000	+000	+000	+962
*015	+000	+000	+000	+000	+964
*016	+000	+000	+000	+000	+967
*017	+000	+000	+000	+000	+970
*018	+000	+000	+000	+000	+970
*019	+000	+000	+000	+000	+970
*020	+000	+000	+000	+000	+970
*021	+000	+000	+000	+000	+969
*022	+000	+000	+000	+000	+969
*023	+000	+000	+000	+000	+969
*024	+000	+000	+000	+000	+968
*025	+000	+000	+000	+000	+967
*026	+000	+000	+000	+000	+967
*027	+000	+000	+000	+000	+967
*028	+000	+000	+000	+000	+966
*029	+000	+000	+000	+000	+966
*030	+000	+000	+001	+000	+965
*031	+000	+000	+000	+000	+965
*032	+000	+000	+000	+000	+965
*033	+000	+000	+000	+000	+964
*034	+000	+000	+000	+001	+964
*035	+000	+000	+000	+000	+963
*036	+000	+000	+000	+000	+963
*037	+000	+000	+000	+000	+962
*038	+000	+000	+000	+000	+962
*039	+000	+000	+000	+000	+961
*040	-001	+000	+000	+000	+961
*041	+000	+000	+001	+000	+961
*042	+000	+000	+000	+000	+965
*043	+000	+000	+001	+000	+968
*044	+000	+000	+001	+000	+967
*045	+000	+000	+001	+000	+962
*046	+000	+000	+002	+000	+955
*047	+001	+001	+002	+000	+947
*048	+001	+001	+002	+000	+939
*049	+001	+001	+002	+000	+931
*050	+002	+001	+003	+000	+922
*051	+002	+002	+003	+000	+914
*052	+003	+002	+003	+000	+905
*053	+003	+002	+004	+000	+896
*054	+004	+003	+004	+000	+887
*055	+004	+003	+005	+000	+878
*056	+005	+004	+005	+001	+869
*057	+005	+004	+005	+000	+860
*058	+006	+004	+006	+001	+850
*059	+007	+005	+006	+000	+841
*060	+007	+005	+007	+001	+836
*061	+008	+006	+007	+000	+831
*062	+009	+006	+008	+000	+821
*063	+009	+007	+008	+000	+811
*064	+011	+008	+009	+000	+801
*065	+011	+008	+010	+001	+791
*066	+012	+009	+010	+000	+781
*067	+013	+010	+011	+000	+771
*068	+014	+011	+011	+000	+761
*069	+015	+012	+012	+000	+755
*070	+017	+013	+013	+000	+749
*071	+018	+014	+014	+001	+739
*072	+020	+015	+015	+000	+728
*073	+022	+017	+016	+000	+719
*074	+023	+018	+017	+000	+708
*075	+025	+020	+018	+000	+697
*076	+028	+022	+020	+000	+688
*077	+030	+024	+020	+000	+678
*078	+032	+026	+022	+000	+668
*079	+035	+029	+024	+000	+658
*080	+039	+031	+025	+000	+648
*081	+042	+035	+027	+000	+639
*082	+046	+038	+030	+000	+630
*083	+050	+042	+031	+000	+619
*084	+055	+047	+034	+001	+610
*085	+060	+051	+036	+000	+600
*086	+066	+056	+039	+000	+591
*087	+072	+063	+042	+000	+581
*088	+079	+069	+045	+000	+573
*089	+086	+076	+049	+000	+564
*090	+095	+084	+053	+000	+555
*091	+103	+092	+057	+000	+545
*092	+113	+102	+061	+000	+537
*093	+125	+113	+067	+000	+528
*094	+136	+123	+072	+001	+520
*095	+148	+136	+078	+000	+512
*096	+163	+150	+084	+000	+503
*097	+177	+163	+091	+001	+491
*098	+193	+179	+099	+000	+484
*099	+211	+196	+107	+000	+476
*100	+227	+210	+115	+000	+470
*101	+248	+230	+126	+000	+463

Table 4.3 continued

```
*102 +270 +249 +136 +000 +457
*103 +289 +267 +147 +000 +446
*104 +312 +289 +159 +000 +440
*105 +335 +308 +171 +001 +435
*106 +356 +328 +184 +000 +430
*107 +382 +352 +198 +001 +426
*108 +408 +375 +213 +000 +422
*109 +434 +399 +230 +000 +413
*110 +462 +425 +247 +001 +409
*111 +487 +447 +263 +000 +406
*112 +512 +470 +280 +000 +403
*113 +541 +495 +298 +000 +401
*114 +565 +518 +315 +001 +398
*115 +587 +539 +330 +000 +392
*116 +605 +555 +342 +000 +391
*117 +620 +569 +352 +001 +390
*118 +635 +582 +362 +000 +389
*119 +644 +591 +369 +001 +389
*120 +644 +592 +372 +000 +388
*121 +641 +592 +372 +000 +385
*122 +636 +589 +371 +001 +385
*123 +629 +587 +369 +001 +386
*124 +619 +583 +367 +001 +386
*125 +609 +579 +364 +001 +387
*126 +599 +576 +362 +001 +388
*127 +590 +572 +359 +001 +385
*128 +581 +569 +357 +000 +386
*129 +571 +565 +355 +001 +387
*130 +562 +562 +353 +000 +387
*131 +553 +558 +350 +001 +384
*132 +544 +554 +348 +001 +385
*133 +535 +550 +346 +001 +386
*134 +526 +546 +344 +001 +387
*135 +518 +542 +342 +000 +385
*136 +509 +537 +340 +001 +385
*137 +502 +532 +338 +001 +387
*138 +494 +527 +336 +001 +388
*139 +486 +521 +333 +001 +384
*140 +478 +515 +331 +001 +385
*141 +471 +509 +328 +000 +387
*142 +462 +501 +325 +001 +388
*143 +450 +490 +321 +001 +384
*144 +435 +475 +316 +000 +385
*145 +419 +460 +311 +000 +386
*146 +405 +444 +306 +001 +388
*147 +390 +428 +301 +001 +385
*148 +376 +414 +296 +001 +386
*149 +363 +399 +292 +000 +387
*150 +350 +385 +287 +001 +388
*151 +338 +371 +283 +001 +387
*152 +326 +359 +279 +001 +387
*153 +314 +345 +275 +000 +388
*154 +302 +333 +271 +001 +389
*155 +291 +321 +267 +000 +389
*156 +278 +307 +263 +001 +387
*157 +266 +294 +259 +001 +388
*158 +253 +280 +254 +000 +389
*159 +242 +268 +251 +000 +390
*160 +230 +255 +246 +001 +387
*161 +220 +243 +243 +001 +389
*162 +209 +232 +239 +001 +390
*163 +199 +221 +235 +000 +391
*164 +190 +210 +232 +001 +388
*165 +181 +200 +228 +000 +389
*166 +172 +190 +225 +001 +390
*167 +164 +181 +222 +001 +391
*168 +156 +171 +219 +001 +387
*169 +148 +162 +216 +001 +389
*170 +141 +154 +213 +001 +389
*171 +134 +145 +210 +001 +390
*172 +127 +137 +207 +000 +391
*173 +120 +130 +204 +001 +388
*174 +114 +123 +202 +001 +388
*175 +108 +115 +199 +000 +389
*176 +102 +109 +197 +000 +390
*177 +097 +102 +194 +001 +391
*178 +092 +096 +192 +001 +389
*179 +087 +090 +189 +000 +388
*180 +082 +084 +187 +001 +389
*181 +077 +079 +185 +001 +390
*182 +072 +074 +183 +000 +390
*183 +068 +069 +181 +001 +391
*184 +064 +065 +179 +000 +388
*185 +059 +061 +177 +001 +388
*186 +055 +056 +175 +001 +389
*187 +052 +053 +174 +000 +390
*188 +049 +049 +172 +000 +391
*189 +045 +046 +170 +000 +388
*190 +043 +043 +169 +001 +389
*191 +040 +040 +167 +000 +389
*192 +037 +037 +166 +001 +391
*193 +034 +035 +164 +000 +390
*194 +032 +032 +163 +001 +388
*195 +029 +029 +161 +000 +389
*196 +026 +027 +160 +001 +390
*197 +024 +025 +159 +000 +391
*198 +022 +022 +157 +001 +388
*199 +020 +020 +156 +001 +389
*200 +017 +018 +155 +001 +390
*201 +015 +016 +153 +000 +390
*202 +013 +014 +152 +000 +390
*203 +011 +012 +151 +000 +388
*204 +009 +010 +150 +000 +389
*205 +007 +008 +148 +001 +390
*206 +005 +007 +147 +000 +391
*207 +004 +005 +146 +000 +388
*208 +003 +004 +144 +001 +389
*209 +001 +003 +143 +000 +391
*210 +001 +002 +142 +000 +392
*211 +000 +002 +140 +001 +389
*212 +000 +001 +140 +000 +390
*213 +000 +001 +140 +000 +391
*214 -001 +001 +139 +000 +392
*215 -001 +001 +138 +001 +389
*216 -001 +001 +138 +000 +390
*217 -001 +001 +138 +000 +391
*218 -001 +001 +138 +000 +392
*-2   0   0   0   0   0
```

Table 4.4

PARAMETER FILE

(D- sodium chloride)

10.030457 0.0

9.3318848 0.0

12.533626 0.0

14.429558 0.0

0.00001657 0.0

0.00435

0.000316

2175

respectively. The second number in the first four lines was the correction factor for the original zero settings. The fifth line was the calibration coefficient in mV/m for the displacement transducer together with the zero correction factor. The fifth line was the weight of the powder (Kg), the sixth line - the cross sectional area of the die (m^2) and the final line the density of powder (kg/m^3).

4.3 Calculations of forces and punch displacement.

In this investigation only the Va, V_r and Vu values were used for the calculation of the applied force F_A(kN), the radial force F_R(kN) and the upper punch displacement Hu(m). These calculations were obtained from the program, PROG Q2 (App. 5.). A typical computer printout from PROG Q2 is shown in table 4.5.

4.4 Calculation of Stress and Strain

The data file from PROG Q2 termed RDATA1 (table 4.5) contained parameters F_A, F_R, Hu and the numbers 99.99, 0.0, 0.0 at the end of the file to indicate the end of a compaction cycle, was used in a program called KARIM (Table 4.6). Program KARIM calculated eight parameters from the above data. The parameters were i-mean compaction stress (σ) ii- mean deviatoric stress (τ), iii - strain (ε) iv - volume (V), v - $\ln^{(\sigma)}$, vi - axial stress (σ_A), vii - radial stress (σ_R) and viii - the stress ratio (σ_R/σ_A).

The mean compaction stress was equivalent to $\frac{\sigma_A+\sigma_R}{2}$ and the mean deviatoric stress $\frac{\sigma_A-\sigma_R}{2}$.

Table 4.5

Dentritic sodium chloride (203 MPa)

FA	FR	HU			
.1994	.1596	.0153	8.5739	3.8297	.0092
.1994	.1596	.0150	9.4712	4.1488	.0090
.2991	.1596	.0148	10.2687	4.4680	.0089
.2991	.2394	.0147	11.2657	4.7871	.0088
.3988	.2394	.0145	12.4620	5.2658	.0086
.3988	.3191	.0144	13.5587	5.6648	.0085
.4985	.3191	.0142	14.7551	6.1435	.0083
.4985	.3191	.0141	16.2505	6.6222	.0082
.5982	.3989	.0140	17.6463	7.1807	.0080
.6979	.3989	.0139	19.2414	7.8190	.0079
.6979	.4787	.0137	21.0359	8.4572	.0078
.7976	.4787	.0136	22.6311	9.0955	.0077
.8973	.5585	.0134	24.7247	9.9732	.0075
.8973	.5585	.0133	26.9180	10.7710	.0074
1.0967	.6383	.0131	26.8122	11.6487	.0073
1.0967	.7181	.0129	31.1053	12.6061	.0072
1.1964	.7181	.0128	33.3983	13.5635	.0071
1.2961	.7979	.0126	35.4919	14.6007	.0071
1.3957	.7979	.0125	38.0840	15.7177	.0070
1.4954	.8776	.0124	40.6761	16.9145	.0069
1.6948	.9574	.0122	43.2682	18.2708	.0068
1.7945	1.0372	.0121	46.0597	19.6272	.0067
1.9939	1.1170	.0119	48.5521	20.9038	.0067
2.1933	1.1968	.0117	51.0445	22.2601	.0066
2.2930	1.2766	.0116	53.9357	23.6963	.0066
2.4924	1.3564	.0114	56.3284	25.0526	.0065
2.7915	1.5159	.0112	58.5218	26.2494	.0065
2.9909	1.5159	.0111	60.3163	27.2068	.0065
3.1903	1.6755	.0109	61.8117	28.0047	.0065
3.4894	1.8351	.0107	63.3072	28.8025	.0064
3.0882	1.9148	.0106	64.2045	29.3610	.0064
4.1872	2.0744	.0104	64.2045	29.6004	.0064
4.5860	2.3138	.0103	63.9054	29.6004	.0064
4.9848	2.3936	.0101	63.4069	29.5206	.0064
5.4833	2.6329	.0099	62.7090	29.3610	.0064
5.9818	2.7925	.0098	61.7120	29.2014	.0064
6.5800	3.0318	.0096	60.7151	28.9621	.0064
7.1781	3.2712	.0095	59.7181	28.8025	.0064
7.8760	3.5106	.0093	58.8208	28.5632	.0064
			57.9236	28.4036	.0064
			56.9266	28.2440	.0064
			56.0294	28.0845	.0064
			55.1321	27.8451	.0064
			54.2348	27.6855	.0064
			53.3375	27.5260	.0064
			52.4403	27.3664	.0064
			51.6427	27.2068	.0064
			50.7454	27.0472	.0064
			50.0476	26.8877	.0064
			49.2500	26.7281	.0064

Table 4.5 continued

48.4524	26.4687	.0064	4.4863	13.4837	.0064
47.6549	26.3292	.0064	4.2869	13.4039	.0065
46.9570	26.0898	.0064	3.9879	13.2444	.0065
46.0597	25.8505	.0064	3.6888	13.1646	.0065
44.8634	25.5313	.0064	3.3897	13.0050	.0064
43.3679	25.1324	.0064	3.1903	12.9252	.0064
41.7728	24.7335	.0064	2.8912	12.7657	.0065
40.3770	24.3345	.0064	2.5921	12.6859	.0065
38.8816	23.9356	.0064	2.3927	12.6061	.0065
37.4858	23.5367	.0064	2.1933	12.4465	.0064
36.1898	23.2175	.0064	1.9939	12.3667	.0065
34.8937	22.8186	.0064	1.6948	12.2869	.0065
33.6974	22.4995	.0064	1.4954	12.1274	.0065
32.5010	22.1803	.0064	1.2961	12.0476	.0064
31.3047	21.8612	.0064	1.0967	11.9678	.0064
30.1083	21.5421	.0064	.8973	11.8880	.0065
29.0116	21.2229	.0064	.6979	11.7284	.0065
27.7156	20.9038	.0064	.4985	11.6487	.0065
26.5192	20.5846	.0064	.3988	11.5689	.0064
25.2232	20.1857	.0064	.2991	11.4093	.0064
24.1265	19.9463	.0064	99.99,0.0,0.0		
22.9302	19.5474	.0064			
21.9332	19.3081	.0065			
20.8365	18.9889	.0065			
19.8396	18.6698	.0065			
18.9423	18.4304	.0064			
18.0450	18.1113	.0065			
17.1478	17.8719	.0065			
16.3502	17.6326	.0064			
15.5526	17.3932	.0064			
14.7551	17.1539	.0065			
14.0572	16.9145	.0065			
13.3593	16.6751	.0065			
12.6614	16.4358	.0064			
11.9636	16.1964	.0064			
11.3654	16.0369	.0064			
10.7672	15.7975	.0065			
10.1690	15.6379	.0065			
9.6705	15.3986	.0065			
9.1721	15.2390	.0064			
8.6736	14.9996	.0064			
8.1751	14.8401	.0065			
7.6766	14.6805	.0065			
7.1781	14.5209	.0065			
6.7794	14.3614	.0064			
6.3806	14.2018	.0064			
5.8821	14.0422	.0064			
5.4833	13.8827	.0065			
5.1842	13.8029	.0065			
4.8851	13.6433	.0065			

Table 4.6

```
PROGRAM KARIM USES TABLE AS INPUT DATA
AND CALCULATES EIGHT DIFFERENT PARAMETERS.
SYMBOLES USED ARE:
A          AXIAL FORCE(FA)
B          RADIAL FORCE(FR)
C          UPPER PUNCH DISPLACEMENT(HL)
X          AXIAL STRESS
Y          RADIAL STRESS
AX         MEAN COMPACTION STRESS
AY         MEAN DEVIATORIC STRESS
AC         COMPACT STRAIN
Y/X        STRESS RATIO
      PROGRAM KARIM
      DIMENSION C(2000),Z(2000),AX1(2000)
      I=1
      N=0
10    READ*,A,B,C(I)
       IF(A.EQ.99.99)GOTO 5
      N=N+1
      X=A/(0.000316*1000)
      Y=B/(0.06283*C(I)*1000)
      AX=(X+Y)/2.0
      Z(I)=0.000316*1000000*C(I)
      AY=(X-Y)/2.0
     IF(I.EQ.1) DV=0.0
     IF(I.GT.1) DV=Z(I-1)-Z(I)
      AC=(C(1)-C(I))/C(I)
      AX1(I)=ALOG(AX)
      AB=Y/X
      IF(I.EQ.1) DAX1=0.0000000001
      IF(I.GT.1) DAX1=AX1(I)-AX1(I-1)
      IF(DAX1.EQ.0.0) GOTO 12
      DVA=DV/DAX1
      GOTO 13
12     DVA=0.0000000001
13    WRITE(2,6)AX,AY,AC,Z(I),AX1(I),X,Y,AB
      I=I+1
      GOTO 10
 5    WRITE(2,8)N
      STOP
 6    FORMAT(5(2X,F11.3,3(2X,F11.3)))
 8    FORMAT(2X,I5)
      END
```

Table 4.7 Compaction data for dentritic sodium chloride (203 MPa)

σ (MPa)	τ (MPa)	ε	V ($mx10^{-6}$)	ln σ	σ_A (MPa)	σ_R (MPa)	σ_R/σ_A
.399	.232	0.000	4.635	-.920	.631	.166	.263
.400	.231	.020	4.740	-.916	.631	.169	.268
.559	.387	.034	4.677	-.581	.947	.172	.181
.603	.344	.041	4.645	-.506	.947	.259	.274
.762	.500	.055	4.582	-.271	1.262	.263	.208
.807	.455	.062	4.550	-.214	1.262	.353	.279
.968	.610	.077	4.487	-.033	1.578	.358	.227
.969	.609	.085	4.456	-.032	1.578	.360	.228
1.173	.720	.093	4.424	.160	1.893	.453	.240
1.333	.876	.101	4.392	.287	2.209	.457	.207
1.382	.826	.117	4.329	.324	2.209	.556	.252
1.542	.982	.125	4.298	.433	2.524	.560	.222
1.751	1.088	.142	4.234	.560	2.840	.663	.234
1.754	1.086	.150	4.203	.562	2.840	.668	.235
2.123	1.348	.166	4.140	.753	3.471	.776	.223
2.178	1.292	.186	4.076	.779	3.471	.886	.255
2.339	1.447	.195	4.045	.850	3.766	.893	.236
2.555	1.547	.214	3.982	.938	4.102	1.008	.246
2.716	1.700	.224	3.950	.999	4.417	1.016	.230
2.929	1.803	.234	3.918	1.075	4.732	1.126	.238
3.306	2.057	.254	3.855	1.196	5.363	1.249	.233
3.522	2.157	.264	3.824	1.259	5.679	1.364	.240
3.902	2.408	.286	3.760	1.361	6.310	1.494	.237
4.284	2.656	.308	3.697	1.455	6.941	1.628	.235
4.504	2.752	.319	3.666	1.505	7.256	1.752	.241
4.891	2.997	.342	3.602	1.587	7.887	1.894	.240
5.494	3.340	.366	3.539	1.704	8.834	2.154	.244
5.819	3.646	.378	3.508	1.761	9.465	2.174	.230

Table 4.7 continued

6.271	3.825	.404	3.444	1.836	10.096	2.447	.242
6.886	4.156	.430	3.381	1.929	11.042	2.730	.247
7.590	4.715	.443	3.350	2.027	12.304	2.875	.234
8.213	5.038	.471	3.286	2.106	13.251	3.175	.240
9.044	5.469	.485	3.255	2.202	14.513	3.575	.246
9.773	6.001	.515	3.192	2.280	15.775	3.772	.239
10.793	6.560	.545	3.128	2.379	17.352	4.233	.244
11.732	7.197	.561	3.097	2.462	18.930	4.535	.240
12.925	7.898	.594	3.034	2.559	20.823	5.026	.241
14.098	8.618	.611	3.002	2.646	22.716	5.480	.241
15.466	9.458	.645	2.939	2.739	24.924	6.008	.241
16.879	10.254	.663	2.907	2.826	27.133	6.625	.244
18.655	11.318	.700	2.844	2.926	29.972	7.337	.245
20.243	12.253	.719	2.812	3.008	32.496	7.990	.246
22.155	13.496	.739	2.781	3.098	35.651	8.658	.243
24.591	14.846	.779	2.718	3.202	39.437	9.745	.247
26.757	16.150	.800	2.686	3.287	42.907	10.607	.247
29.237	17.456	.843	2.623	3.375	46.693	11.781	.252
32.140	19.286	.866	2.591	3.470	51.426	12.853	.250
35.064	20.778	.913	2.528	3.557	55.843	14.286	.256
38.322	22.569	.937	2.496	3.646	60.891	15.753	.259
41.913	24.656	.962	2.465	3.736	66.569	17.257	.259
45.209	26.408	.987	2.433	3.811	71.617	18.800	.263
49.704	28.539	1.040	2.370	3.906	78.243	21.164	.270
54.175	31.009	1.068	2.338	3.992	85.184	23.166	.272
58.268	32.890	1.096	2.307	4.065	91.178	25.397	.279
63.150	35.284	1.125	2.275	4.146	98.434	27.866	.283
68.048	37.643	1.155	2.244	4.220	105.691	30.405	.288
72.523	39.793	1.155	2.244	4.284	112.316	32.730	.291
78.128	42.391	1.186	2.212	4.358	120.519	35.737	.297
83.869	44.853	1.217	2.180	4.429	128.722	39.016	.303
89.845	47.080	1.250	2.149	4.498	136.925	42.764	.312
96.192	49.567	1.284	2.117	4.566	145.759	46.625	.320
101.652	51.994	1.284	2.117	4.622	153.646	49.657	.323
107.607	53.926	1.318	2.086	4.678	161.533	53.680	.332

Table 4.7 continued

113.913	56.769	1.318	2.086	4.735	170.683	57.144	.335
119.799	58.455	1.354	2.054	4.786	178.254	61.344	.344
124.735	60.461	1.354	2.054	4.826	185.196	64.275	.347
128.747	62.128	1.354	2.054	4.858	190.874	66.619	.349
132.090	63.517	1.354	2.054	4.883	195.607	68.573	.351
135.984	64.356	1.391	2.022	4.913	200.339	71.628	.358
138.098	65.081	1.391	2.022	4.928	203.179	73.017	.359
138.396	64.783	1.391	2.022	4.930	203.179	73.612	.362
137.922	64.310	1.391	2.022	4.927	202.232	73.612	.364
137.034	63.620	1.391	2.022	4.920	200.655	73.414	.366
135.732	62.715	1.391	2.022	4.911	198.446	73.017	.368
133.956	61.336	1.391	2.022	4.898	195.291	72.620	.372
132.081	60.056	1.391	2.022	4.883	192.136	72.025	.375
130.305	58.677	1.391	2.022	4.870	188.981	71.628	.379
128.587	57.554	1.391	2.022	4.857	186.142	71.033	.382
126.969	56.333	1.391	2.022	4.844	183.303	70.636	.385
125.193	54.954	1.391	2.022	4.830	180.147	70.239	.390
123.575	53.733	1.391	2.022	4.817	177.308	69.842	.394
121.858	52.611	1.391	2.022	4.803	174.469	69.247	.397
120.240	51.389	1.391	2.022	4.789	171.629	68.850	.401
118.622	50.168	1.391	2.022	4.776	168.790	68.454	.406
117.003	48.947	1.391	2.022	4.762	165.950	68.057	.410
115.543	47.883	1.391	2.022	4.750	163.426	67.660	.414
113.925	46.662	1.391	2.022	4.736	160.587	67.263	.419
112.622	45.756	1.391	2.022	4.724	158.378	66.866	.422
111.162	44.693	1.391	2.022	4.711	155.854	66.469	.426
109.602	43.728	1.391	2.022	4.697	153.330	65.874	.430
108.142	42.665	1.391	2.022	4.683	150.807	65.477	.434
106.740	41.858	1.391	2.022	4.670	148.598	64.882	.437
105.023	40.736	1.391	2.022	4.654	145.759	64.287	.441
102.733	39.240	1.391	2.022	4.632	141.973	63.493	.447
99.871	37.370	1.391	2.022	4.604	137.240	62.501	.455
96.851	35.342	1.391	2.022	4.573	132.192	61.509	.465
94.146	33.629	1.391	2.022	4.545	127.775	60.517	.474
91.284	31.759	1.391	2.022	4.514	123.043	59.525	.484

Table 4.7 continued

88.579	30.047	1.391	2.022	4.484	118.626	58.533	.493
86.132	28.393	1.391	2.022	4.456	114.525	57.739	.504
83.585	26.838	1.391	2.022	4.426	110.423	56.747	.514
81.295	25.342	1.391	2.022	4.398	106.637	55.953	.525
79.005	23.846	1.391	2.022	4.370	102.851	55.160	.536
76.716	22.350	1.391	2.022	4.340	99.066	54.366	.549
74.426	20.854	1.391	2.022	4.310	95.279	53.572	.562
72.294	19.515	1.391	2.022	4.281	91.809	52.779	.575
69.846	17.861	1.391	2.022	4.246	87.708	51.985	.593
67.556	16.365	1.391	2.022	4.213	83.922	51.191	.610
65.010	14.811	1.391	2.022	4.175	79.820	50.199	.629
62.977	13.373	1.391	2.022	4.143	76.350	49.604	.650
60.588	11.976	1.391	2.022	4.104	72.564	48.612	.670
58.343	11.065	1.354	2.054	4.066	69.409	47.278	.681
56.217	9.721	1.354	2.054	4.029	65.938	46.496	.705
54.249	8.534	1.354	2.054	3.994	62.784	45.715	.728
52.889	7.055	1.391	2.022	3.968	59.944	45.834	.765
50.726	6.378	1.354	2.054	3.926	57.104	44.348	.777
49.013	5.252	1.354	2.054	3.892	54.265	43.761	.806
47.796	3.946	1.391	2.022	3.867	51.741	43.850	.847
46.236	2.981	1.391	2.022	3.834	49.217	43.255	.879
44.348	2.345	1.354	2.054	3.792	46.693	42.003	.900
42.951	1.534	1.354	2.054	3.760	44.485	41.417	.931
41.554	.723	1.354	2.054	3.727	42.276	40.831	.966
40.471	-.403	1.391	2.022	3.701	40.068	40.874	1.020
39.069	-1.209	1.391	2.022	3.665	37.859	40.278	1.064
37.924	-1.958	1.391	2.022	3.636	35.966	39.882	1.109
36.378	-2.304	1.354	2.054	3.594	34.073	38.682	1.135
35.236	-3.055	1.354	2.054	3.562	32.180	38.291	1.190
34.154	-3.551	1.354	2.054	3.531	30.603	37.705	1.232
33.462	-4.436	1.391	2.022	3.510	29.026	37.897	1.306
32.375	-4.927	1.391	2.022	3.477	27.448	37.302	1.359
31.104	-5.234	1.354	2.054	3.437	25.871	36.338	1.405
30.120	-5.827	1.354	2.054	3.405	24.293	35.947	1.480
29.136	-6.420	1.354	2.054	3.372	22.716	35.556	1.565

Table 4.7 continued

28.584	-7.131	1.391	2.022	3.353	21.454	35.715	1.665
27.755	-7.563	1.391	2.022	3.323	20.192	35.318	1.749
26.768	-8.153	1.391	2.022	3.287	18.614	34.921	1.876
25.673	-8.321	1.354	2.054	3.245	17.352	33.993	1.959
25.102	-8.696	1.354	2.054	3.223	16.406	33.798	2.060
24.433	-8.974	1.354	2.054	3.196	15.459	33.407	2.161
23.865	-9.668	1.391	2.022	3.172	14.197	33.532	2.362
23.194	-9.627	1.354	2.054	3.144	13.566	32.821	2.419
22.525	-9.905	1.354	2.054	3.115	12.620	32.430	2.570
21.954	-10.281	1.354	2.054	3.089	11.673	32.235	2.761
21.534	-10.807	1.391	2.022	3.070	10.727	32.342	3.015
21.120	-11.024	1.391	2.022	3.050	10.096	32.143	3.184
20.204	-11.054	1.354	2.054	3.006	9.149	31.258	3.416
19.633	-11.430	1.354	2.054	2.977	8.203	31.063	3.767
19.220	-11.648	1.354	2.054	2.956	7.572	30.867	4.077
18.947	-12.006	1.391	2.022	2.942	6.941	30.953	4.460
18.296	-11.986	1.354	2.054	2.907	6.310	30.281	4.799
17.725	-12.361	1.354	2.054	2.875	5.363	30.086	5.610
17.214	-12.481	1.354	2.054	2.846	4.732	29.695	6.275
17.031	-12.930	1.391	2.022	2.835	4.102	29.961	7.305
16.616	-13.146	1.391	2.022	2.810	3.471	29.762	8.576
15.974	-13.135	1.354	2.054	2.771	2.840	29.109	10.251
15.463	-13.255	1.354	2.054	2.738	2.209	28.718	13.003
15.050	-13.473	1.354	2.054	2.711	1.578	28.523	18.031
15.016	-13.754	1.391	2.022	2.709	1.262	28.770	22.797
14.660	-13.713	1.391	2.022	2.685	.947	28.373	29.977

A typical computer printout is shown in table 4.7.

4.5 Presentation of data

The graphical presentation of data from table 4.7 was carried out by a program called GRAPH4 (App. 5). A parameter file was created to contain the information needed by the program to produce four graphs for each compaction relaxation cycle.

CHAPTER 5

CHAPTER 5

5. Compact Characterisation

5.1 Density of Compacts

The compact density is defined as the weight of the compact divided by the compact volume. The volumes of the compacts (V_{comp}) were determined 24 hours after ejection from the die, by measuring the compact thickness and diameter with a micrometer screw to an accuracy of 0.001 cm.

5.2 Surface Area of Compacts

5.2.1 Nitrogen adsorption

The surface area of dicalcium phosphate dihydrate compacts was evaluated by the BET equation (1.20) following the technique described in section 2.2.4. The only difference in the nitrogen adsorption apparatus was a sample bulb (fig 2.3) specially designed to contain compacts. The compact sample bulb consisted of an open ended glass container which was closed with a ground-glass stopper smeared with Apiezon T, high vacuum grease (Apiezon Products Ltd, London) to produce a gas tight seal.

The dicalcium phosphate compacts were degassed for a minimum of 24 hours at a temperature of $50^{o}C$.

5.2.2 Krypton adsorption

It was found impossible to determine the surface area of sodium chloride compacts by low temperature nitrogen adsorption because the compacts had a very low surface area. Krypton adsorption (Beebe et al 1945) was used to determine the low surface area of sodium

chloride compacts. With low surface area powders or ccmpacts the magnitude of the error in the dead space factor used with the nitrogen method is unsuitable because the amount of gas in the dead-space volume is proportional to the absolute vapour pressure of the adsorbate. A gas with a low saturation vapour pressure such as Krypton is preferable for low surface area powders (Allen 1981).

In Krypton adsorption the mercury manometer usually used with nitrogen gas cannot be used because the saturated vapour pressure of Krypton has a value of the order of 2 Torr. The low temperature nitrogen adsorption apparatus was then modified for use with Krypton by the introduction of a pressure transducer into a specially designed Krypton adsorption section (fig 5.1). A high vacuum Pirani gauge (Pirani vacuum gauge Model 9, Edwards High Vacuum Ltd, Manor Royal, Crawley, Sussex) was used to measure gas pressure as low as 0.001 Torr. The electrical signals from the Pirani gauge were recorded on a calibrated pen recorder to accurately observe the equilibrium adsorption pressures between sodium chloride and adsorbate.

5.2.3 Calibration of Krypton apparatus

The three range pressure gauge (Pirani vacuum Gauge model 9) enable an expanded pressure range from 0.001 to 5 Torr to be used to determine the Krypton adsorption equilibrium pressures. A pen recorder, to produce a permanent record of pressures was calibrated

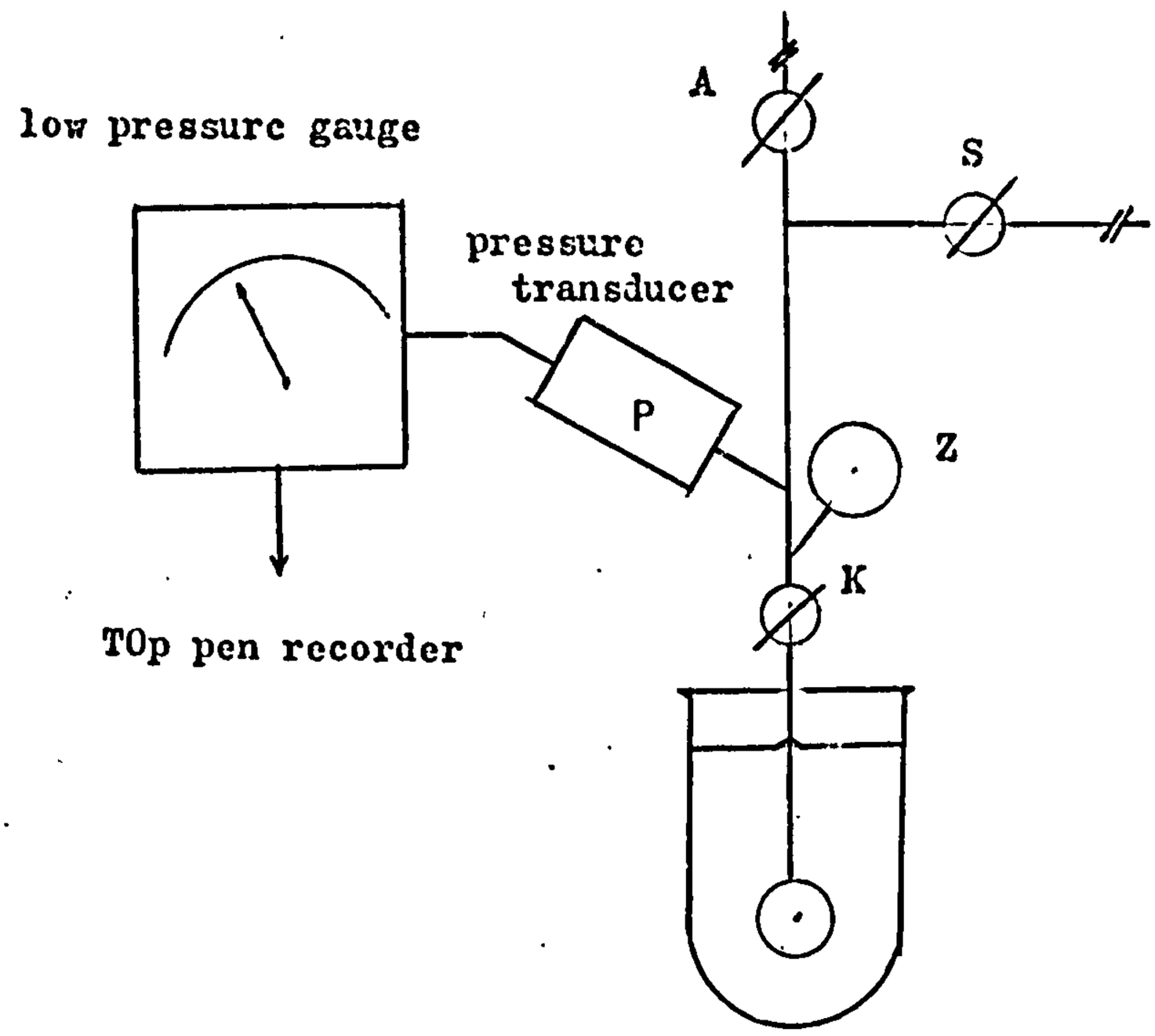

Figure 5.1 Krypton adsorption section

by the introduction of a small amount of helium gas into the burette (fig. 2.1) by the closure of tap S. Tap A and tap K were also closed and helium introduced to the Krypton adsorption section through tap S. The Pirani gauge pressure scale and recorder chart readings at selected pressures were used to plot two separate calibration curves for the pressure ranges between 0.001 to 0.1 and between 0.1 to 5 Torr respectively. Because the Pirani gauge was calibrated by the manufacturers with dry air, the true Krypton pressure was obtained from a dry air Krypton conversion chart.

To calculate the volume of the Krypton adsorption glass section, a known quantity of helium was introduced into the nitrogen calibrated burette section. The manometer pressure of the gas was recorded. Tap S was then opened and helium allowed to expand into the Krypton adsorption section with taps A and K closed. The volume of the Krypton adsorption section was calculated from the equation:

$$Vn = \frac{P_1V_1 - P_2V_2}{P_2} \qquad (5.1)$$

where Vn ≡ volume of tubing at S.T.P.

P_1 ≡ initial gas pressure (Torr)

P_2 ≡ equilibrium gas pressure after expansion (Torr)

V_1 ≡ volume of the burette bulb at which the initial pressure was measured, at S.T.P.

V_2 ≡ volume of the burette bulb at which equilibrium pressure was measured, at S.T.P.

The surface area of compacts was calculated from the BET equation (1.20) assuming that the Krypton vapour pressure, P_o was 2.51 Torr and the Krypton molecular adsorption cross-sectional area, Am, was 0.195 nm^2 (Meihuizen and Cromelin 1937).

5.3 Porosity and voidage by nitrogen adsorption

The meso-and macropore size distribution of the materials was calculated using the mathematical model of Barrett Joyner and Halenda. A full nitrogen adsorption isotherm was determined and then analysed by the selection of 40 known relative pressure values together with the corresponding volume adsorbed at these known relative pressures. This data was then fed into a program called BJHPORE (appendix 5). The computer program calculated the radii according to the Kelvin equation (eqn. 1.27), the actual pore radius, which took into account the multilayer adsorption thickness onthe walls of the pores and pore size distribution by surface and volume (section 1.4.4a).

The micropore size distribution was calculated using Brunauers MP method (section 1.4.4b). Relative pressures and the statistical thickness of the adsorbed nitrogen layer obtained from the t-curve published by Lippens and co-workers (1961) together with the unit volume of nitrogen adsorbed,

obtained from the experimental adsorption isotherm, at the same relative pressures were used. These values were then input into a program called VATCURVE (appendix 5) to determine the meso and micropore distribution of the sample.

5.4 Porosity and Voidage by Mercury Penetration

The determination of the pore size and pore size distribution by mercury pressure intrusion was determined using a Micrometrics mercury porosimeter model 905-1 (Coulter Electronics Ltd., Dunstable, Bedfordshire). The apparatus (fig 5.2) measured mercury pressures in the range 0 to 50 000 PSI (0-345 MPa). The sample cell (fig 5.3), which was constructed from glass, consisted of two pieces. The sample container (a) and a cap (b) which contained a precision bored tube. A mechanical/electrical probe could travel down the calibrated precision bored tube to give eventually the volume of mercury intruded into the porous material at known pressure.

A weighed sample could be sealed into the sample holder by closure of the lightly greased ground glass surfaces of the cap with the body of the sample chamber. The closed sample cell with compact or powder was then inserted in the pressure chamber and subjected to vacuum. All materials were degassed at reduced pressures (<20 µm of mercury) for at least 24 hours.

After the degassing, the vacuum was disconnected and mercury introduced to fill the sample holder. Excess

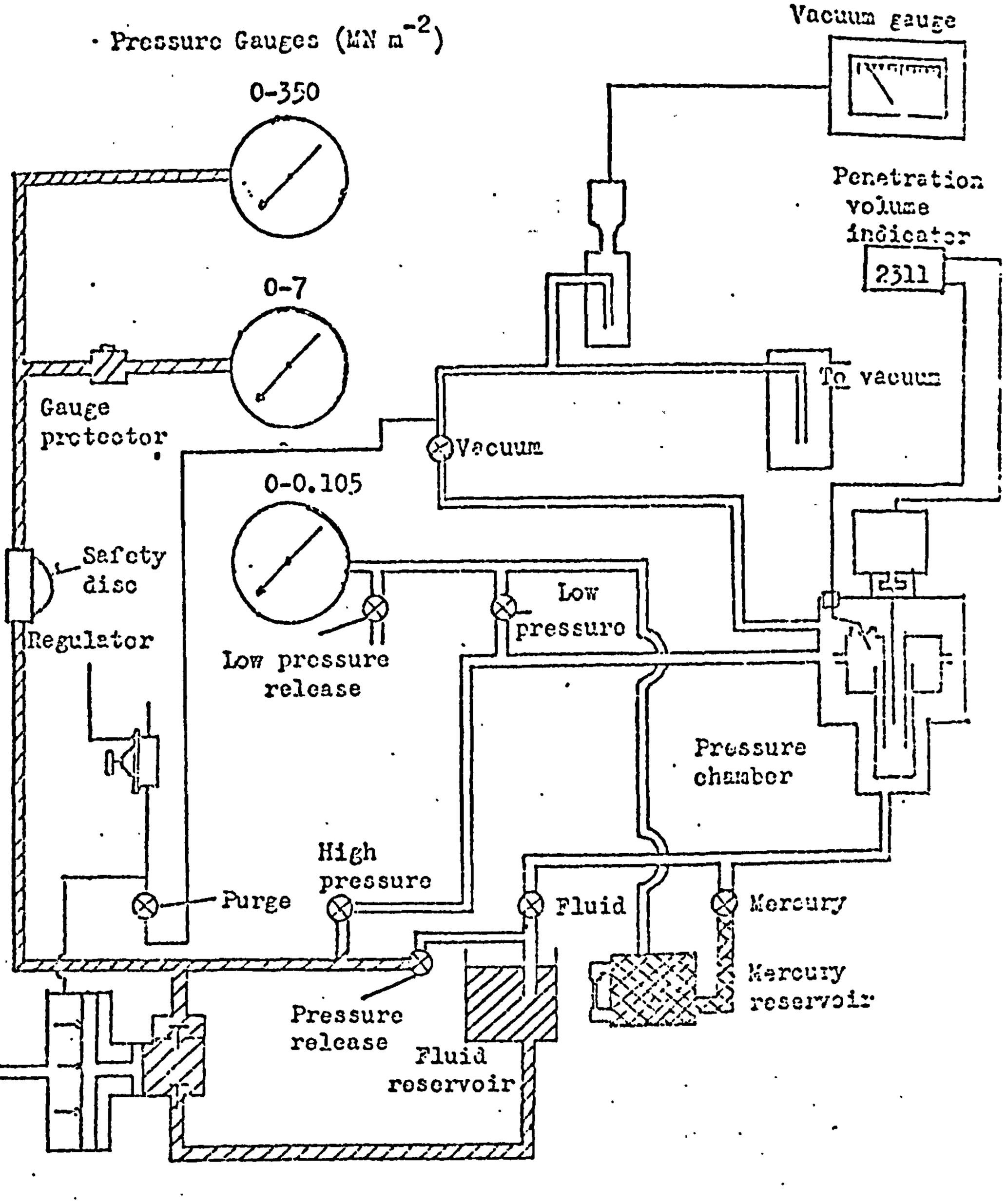

Figure 5.2 Schematic Diagram of the Mercury Penetration Porosimeter

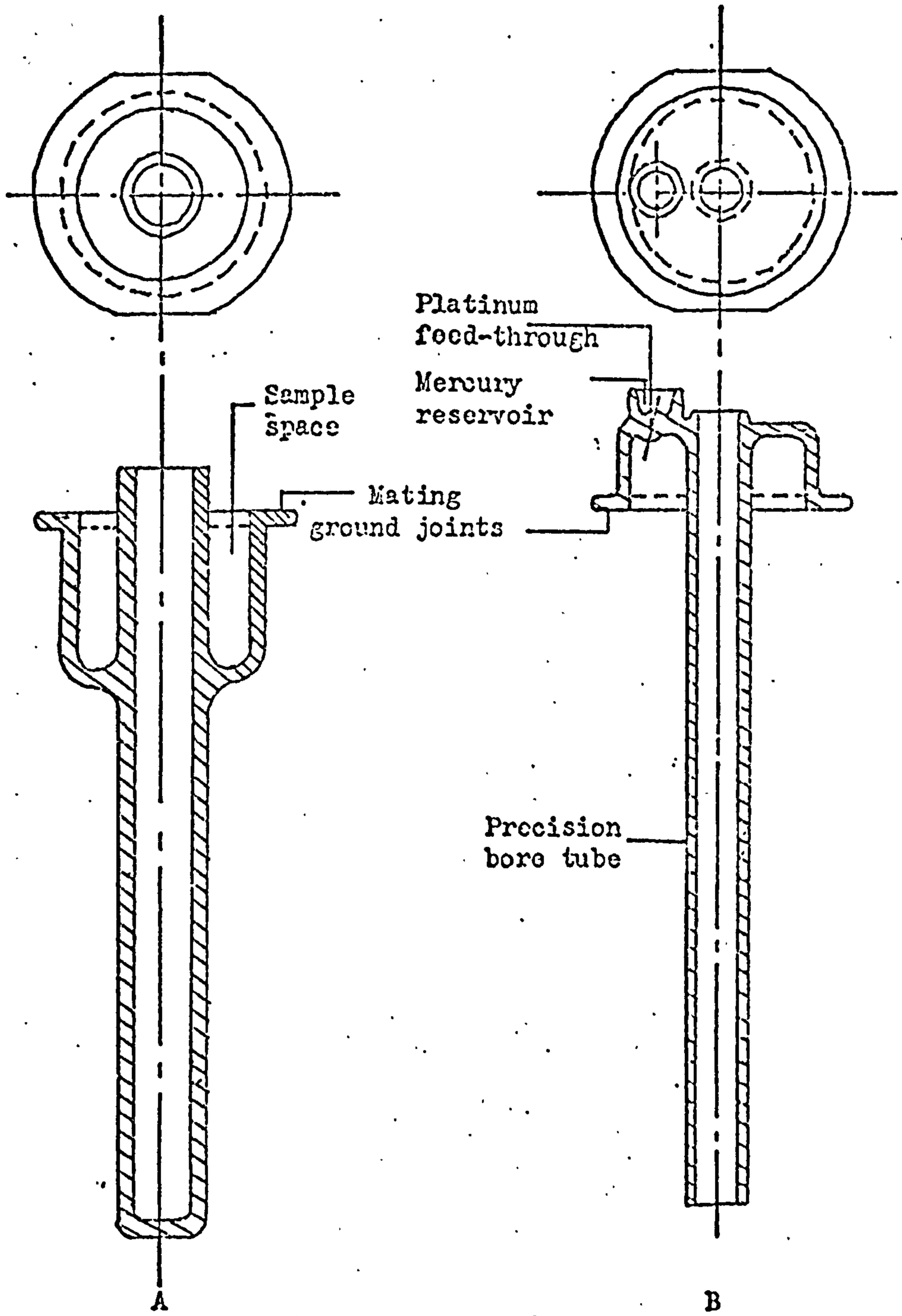

Figure 5.3 Sample Cell for Mercury Penetration Porosimeter

mercury was drained off and the pressure raised to a starting pressure of 0.5 PSI. Pressure was increased in small increments to atmospheric pressure recording both the pressure and penetration volume. Pressures above atmospheric were achieved by filling the pressure chamber around the sample cell with hydraulic fluid and readings continued in the sub-atmospheric pressure method.

All experimental data were obtained in form of pressure (P_{Hg}) against the volume of mercury intruded (V_{Hg}). The mathematical manipulation of data was carried out by a computer program called HGPORES developed by Raotare (1972). The program HGPORES (appendix 5) calculated the pore radius, volume, surface and differential pore size distribution (section 1.4.4c).

5.5 Mechanical Strength of Compacts

Mechanical strength is an important property of compacted material because it can measure the toughness, hardness and strength of compacts to withstand handling or any other subsequent processing. It has also been used to assess the behaviour of the particulate solids under compaction. Cole, Rees and Hersey (1975) related the tensile strength of compacts to the amount of bonding which occurred during compaction, while Stanley-Wood and Shubair (1979) used the logarithmic relationship between surface area and crushing strength of dicalcium phosphate (DCP) compacts to evaluate the surface area generated by fragmentation.

To ascertain the fracture strength of compacts used in this investigation at least four compacts from each powder and compaction pressure were subjected to a diametral crushing test and to a hardness test.

5.5.1 Diametral fracture test

Because of reported variations in the strength of compacts due to age and storing conditions (Rees and Shotton, 1970), four compacts prepared at each compaction pressure were stored in screw-cap jars for at least 48 hours. The measured compact was placed diametrically between the upper and lower platens of a Denison Press (Model T.42,U, Denison Ltd., Leeds). The upper punch moved at a constant strain rate of 0.4 inch/min to increase the applied force on the circumference of the compact. The fracture force, f_c, was recorded when the compact failed. Only the fracture force which split the compacts into two halves were used for the calculation of mean tensile strength σ_t (B.S. 1881:Part 4, 1970).

5.5.2 Hardness tests

Hardness testing was carried out by a Metallurgical hardness testing machine (Vickers Armstrongs, Engineers, Ltd., Crayford, Kent, England). Two indentations were made on each half of the compact and the mean indentation diameter calculated for each type of indentor.

(a) Vickers Hardness Test

Vickers hardness test was performed in accord with British Standard BS 427 Part 1(1961). The mean diameter

of the indentation was found from the two diagonals measured by the microscope attached to the testing machine and a 5 Kg load used. The hardness of compact H_v was calculated from 4 indentations.

(b) Brinell Hardness Test

The Brinell hardness number, Hg, was found as described in British Standard BS 240: Part I(1962). The diameter of the ball was 1 mm and the load to cause indentation was 5 kg.

(c) Meyer hardness test

The Meyer hardness test, H_M, was tested by the same ball indentor used for the Brinel Hardness Test but different compaction loads applied for the measurement of the Meyers Power Relation (1.54). Successive indentations were made at a single spot beginning with the lowest load.

CHAPTER 6

Notations and Legend for Figures in Chapter 6

Mohr Circles

τ = shear stress (MPa)

σ = compaction stress (MPa)

Stress Pathways

$(\sigma_A + \sigma_R)/2$ = mean compaction stress (MPa)

$(\sigma_A - \sigma_R)/2$ = mean deviatoric stress (MPa)

V = volume of compact ($m^3 \times 10^{-6}$)

$\frac{V_o - V_i}{V_i}$ = compact strain

Three Dimensional Figures

○ compaction line on σ, τ, V axis

◒ relaxation (unloading) line on σ, τ, V axis

◐ projection of compaction line on σ, V axis

× projectionof unloading line on σ, V axis

CHAPTER 6

Results

6.1 Characterisation of Powders

The results presented in this section include microscopical investigations, particle size measurements and the powder density of different materials used.

6.1.1 Microscopical investigation

The photomicrographs from light microscopy (Olympus BHB, Olympus, Japan) taken of the uncompacted materials are presented in appendix 3 Figure A.1 - A.5.

6.1.2 Particle size measurements

Sieve fractions of 250-300 and 425-500 micrometre. were used for sodium chloride and sugar respectively. This size range will be used for the production of all the compacts unless stated otherwise.

The particle size distribution of dicalcium phosphate powder was determined by the technique described in section 1.4.2 and the results are presented in Figure 6.1 and Table 6.1. The median particle size of the powder, taken from the 50% under size value, was found to be 12.85 μm.

6.1.3 Density of powders

The density of uncompacted powders measured with an air comparison pyknometer (section 1.5.4) are shown in Tables 6.2-6.6. The literature density values of two grades of polypropylene ((a) Homopolymer

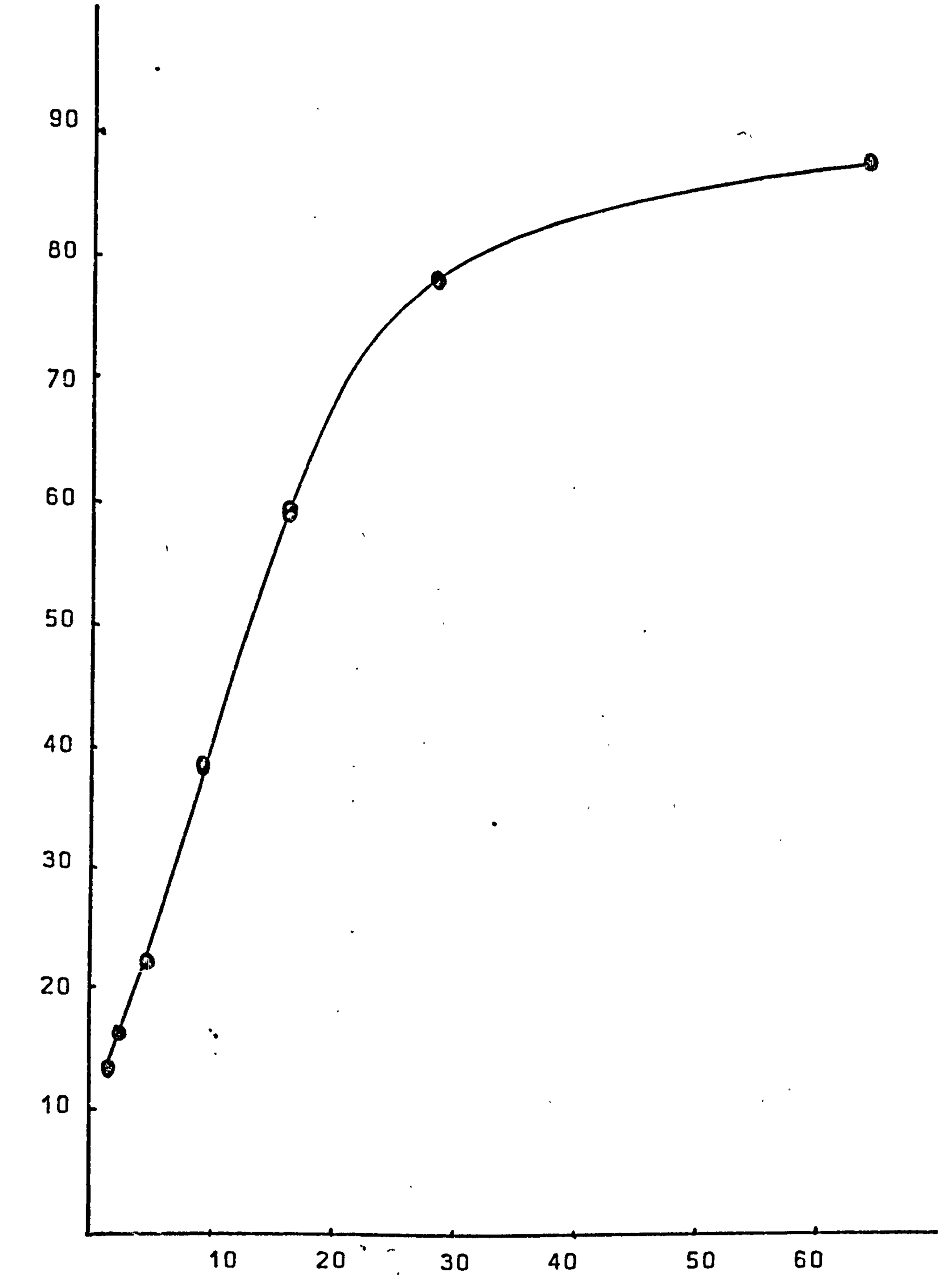

Figure 6.1 Particle size distribution of uncompacted dicalcium phosphate powder.

NO	Height of fall h	Weight of beakers	Time t	Weight of beakers and sediment	Weight of sediment	Weight of Powder	Particle size d_{st}	Percentage undersize
	(cm)	(g)	(min)	(g)	(g)	(g)	(μm)	(%)
1	-	1.2694	0	1.3155	0.0461	0.0348	-	100.0
2	-	1.2607	0	1.3062	0.0455	0.0343	-	100.0
3	20.0	1.2546	1	0.0416	0.0416	0.0303	63.82	87.7
4	19.57	1.2576	5	1.2958	0.0382	0.0269	28.23	77.85
5	19.14	1.2588	15	1.2905	0.0317	0.0204	16.12	59.04
6	18.71	1.2622	45	1.2868	0.0246	0.0133	9.2	38.5
7	18.28	1.2664	150	1.2854	0.019	0.0077	4.98	22.28
8	17.85	1.2602	450	1.2771	0.0169	0.0056	2.84	16.20
9	17.43	1.2512	1380	1.2673	0.058	0.0045	1.6	13.02

Table 6.1 Size distribution data for Dicalcium phosphate powder by Andreasons technique

and (b) copolymer)* were 0.922 and 0.905 kg/m^3 respectively.

* (a) Ibrahim Ph.D Thesis (1979)

(b) Shell Chemicals U.K. Ltd., Manchester M31 4AJ.

Table 6.2 Density of D-sodium chloride

(250 - 300 μm)

weight (g)	volume (cm^3)	density (g/cm^3)	Mean density (g/cm^3)
29.5264	13.6	2.171	2.175
26.8175	12.3	2.18	
22.7842	10.475	2.175	
31.2580	14.375	2.174	

Table 6.3 Density of C-sodium chloride

(250 - 300 μm)

weight (g)	volume (cm^3)	density (g/cm^3)	Mean density (g/cm^3)
28.8793	13.45	2.147	2.14
31.2704	14.64	2.136	
24.4569	11.44	2.137	
27.9275	13.05	2.140	

Table 6.4 Density of Dicalcium phosphate

Weight (g)	Volume (cm^3)	Density (g/cm^3)	Mean density (g/cm^3)
26.7426	11.14	2.401	2.4
29.1825	12.10	2.412	
23.2570	9.72	2.393	
28.3112	11.79	2.400	

Table 6.5 Density of Sugar

(425 - 500) µm

Weight (g)	Volume (cm^3)	Density (g/cm^3)	Mean density (g/cm^3)
30.6057	19.50	1.569	1.57
33.6016	21.40	1.570	
21.4833	13.64	1.575	
27.4957	17.55	1.567	

Table 6.6 Density of styrocell

Weight grams	Volume	Density	Mean density
20.9188	19.75	1.059	
19.9120	18.76	1.061	1.06
23.8571	22.5	1.06	

6.2 Compaction.

At least five compacts were produced at each compaction pressure, using a standard compaction procedure (section 3.1). The compaction data is graphically presented as:-

(a) Mohr's Circles

(b) Stress pathways in $\tau:\sigma$;$\sigma:\varepsilon$;$V:\sigma$ and $V:\ln\sigma$ space

(c) Three dimensional $\tau:\sigma:V$ space

The compaction data from plastically deforming materials (dentritic and cubic sodium chloride) are shown in Figures 6.2 to 6.19 and 6.20 to 6.35 respectively. The compaction data from fragmenting materials (dicalcium phosphate and sugar) are shown in Figures 6.36 to 6.55 and 6.56 to 6.72 respectively. The graphical data for non-compacting materials (styrocell, homopolymer and copolymer) are shown in Figures 6.73 to 6.91.

The solid lines in the three dimensional graphs represent the stress pathway in $\tau:\sigma:V$ space while the dashed lines represent the values below zero. The dashed lines on $\sigma:V$ space are the projection of the three dimensional pathways.

Tabulated data for compaction is presented in appendix 2 (Tables A1- A8) as an example of data for each material used in this section.

Figure 6.2 Mohr circles constructed for D-sodium chloride compacted at 36 MPa

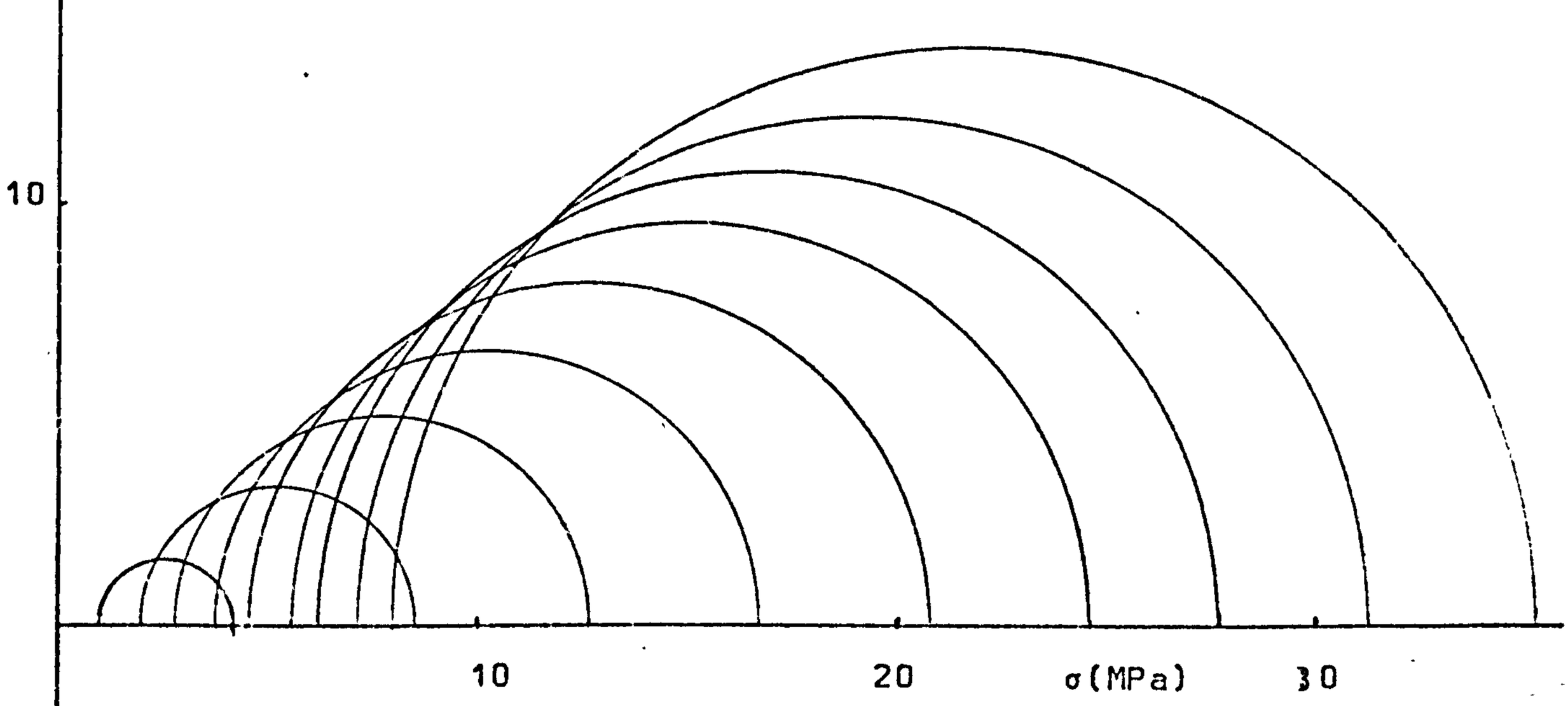

Figure 6.3 Mohr circles constructed for D-sodium chloride compacted at 87 MPa

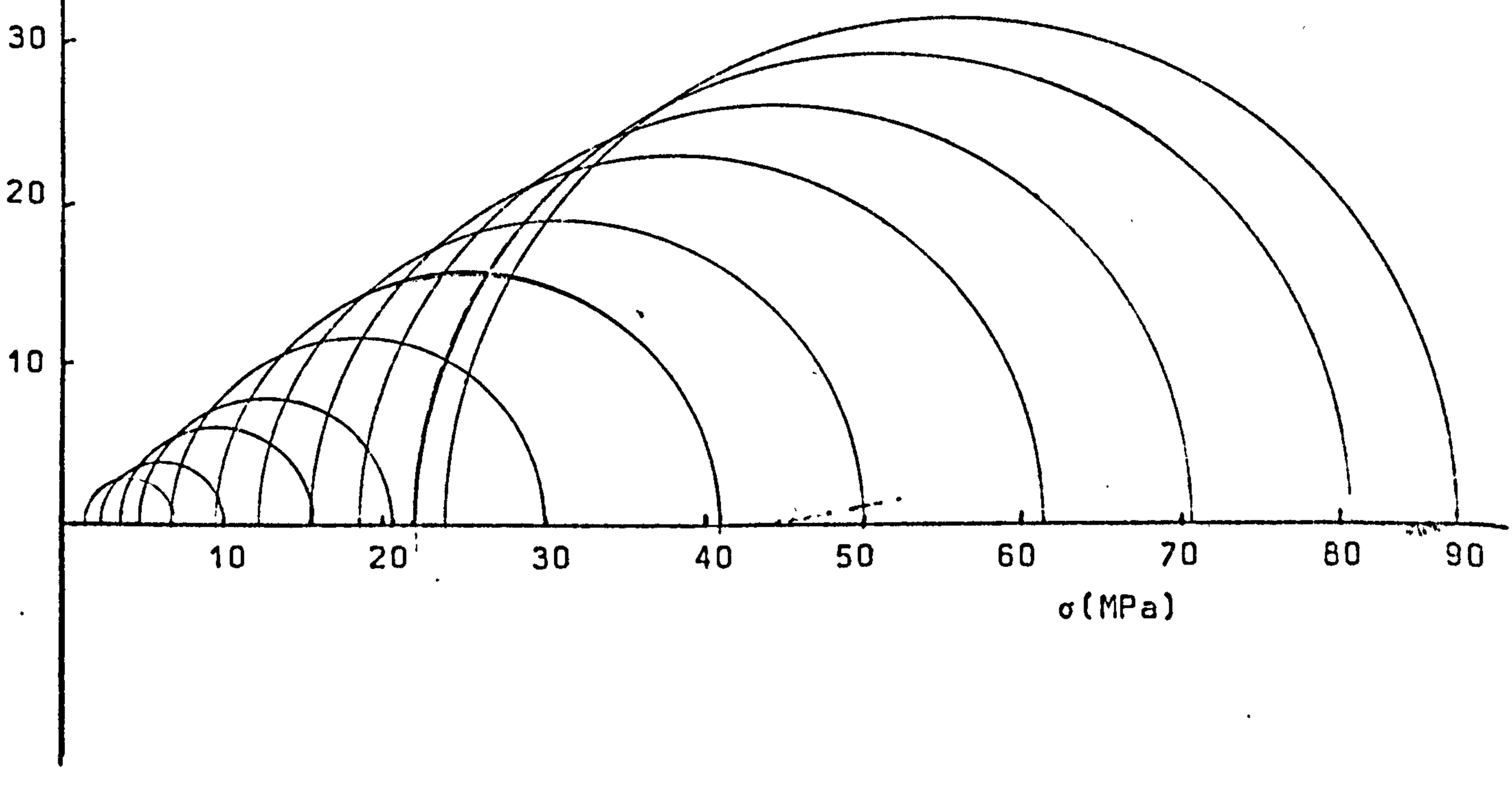

Figure 6.4 Mohr circles constructed for D-sodium chloride compacted at 203 MPa

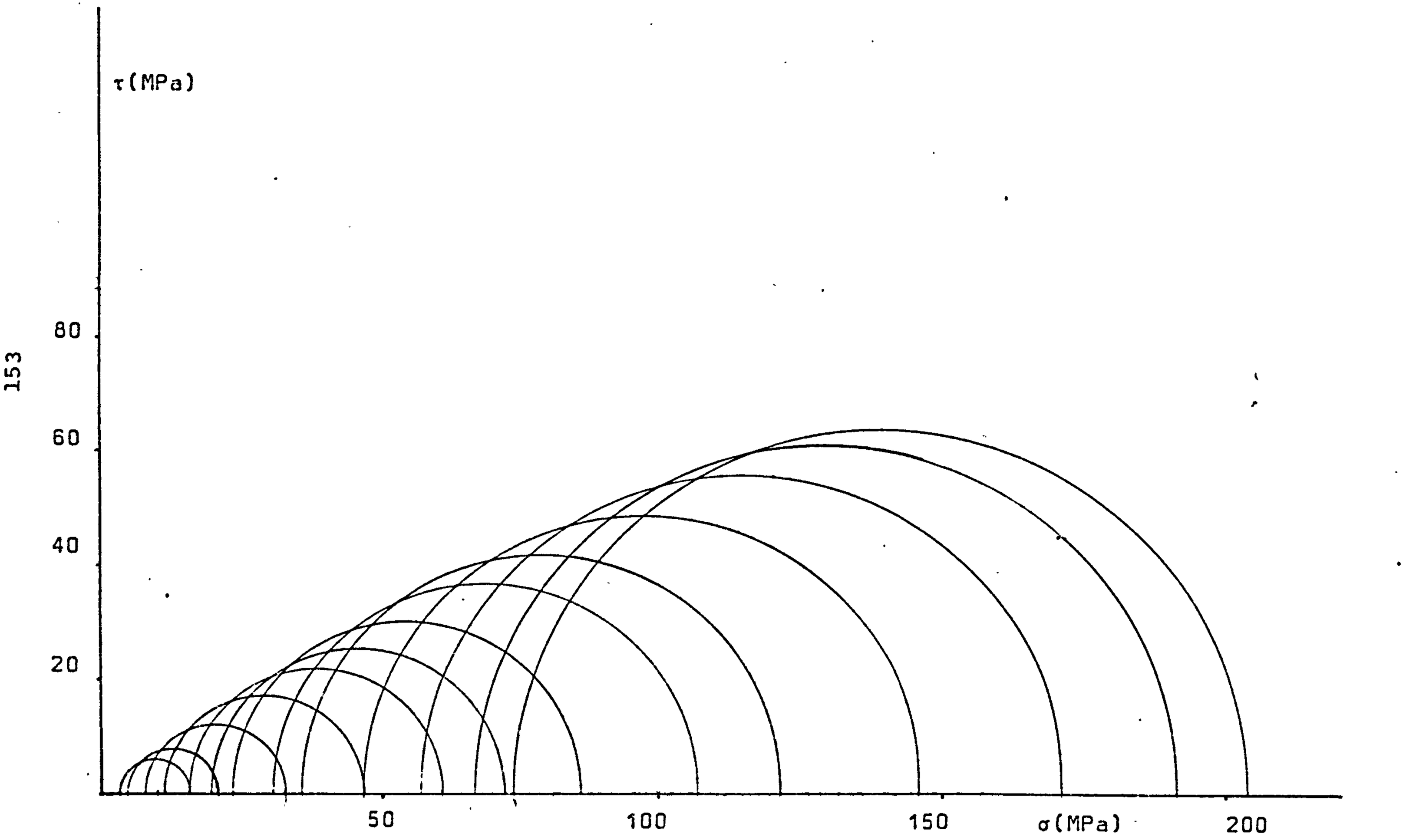

Figure 6.5 Mohr circles constructed for D-sodium chloride compacted at 246 MPa

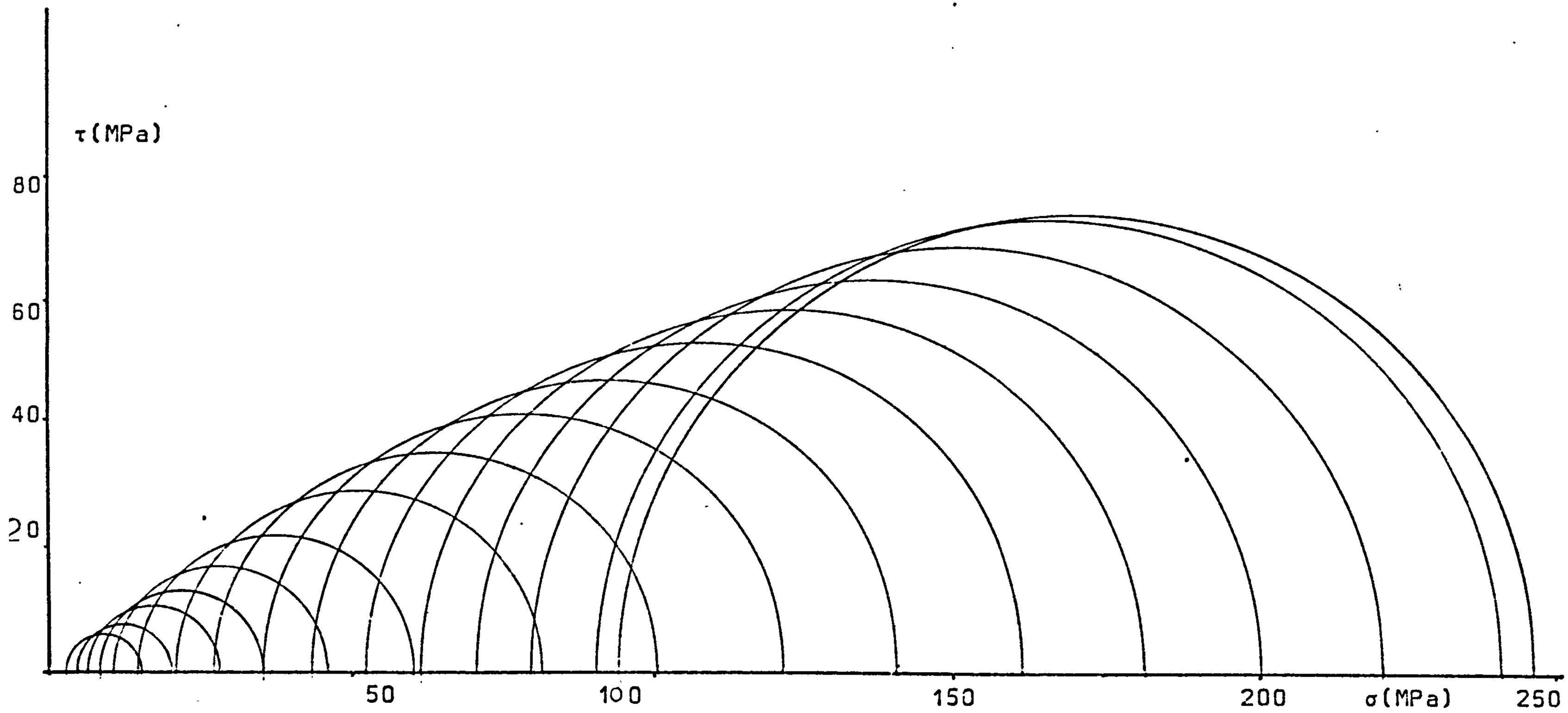

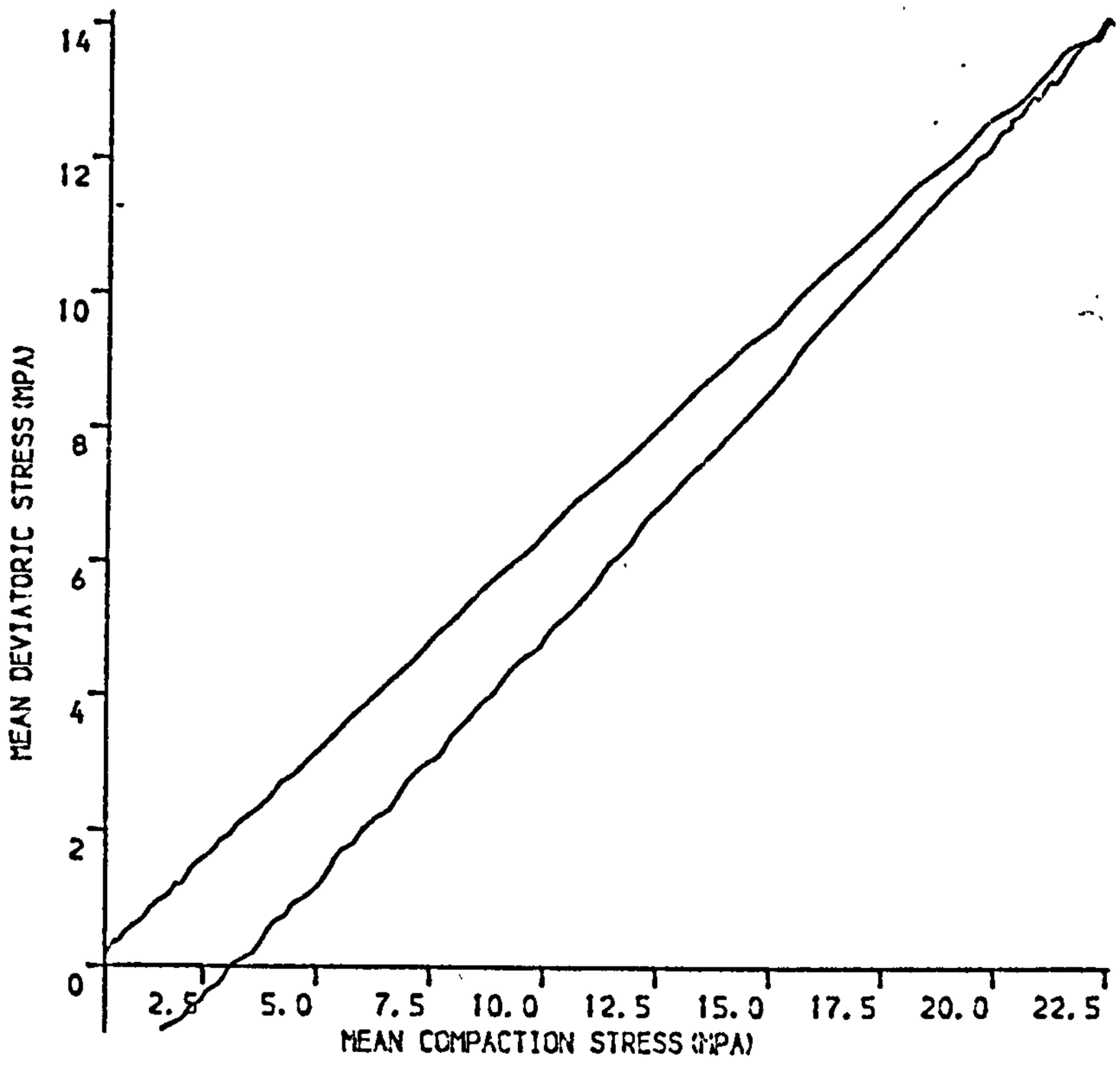

(A)

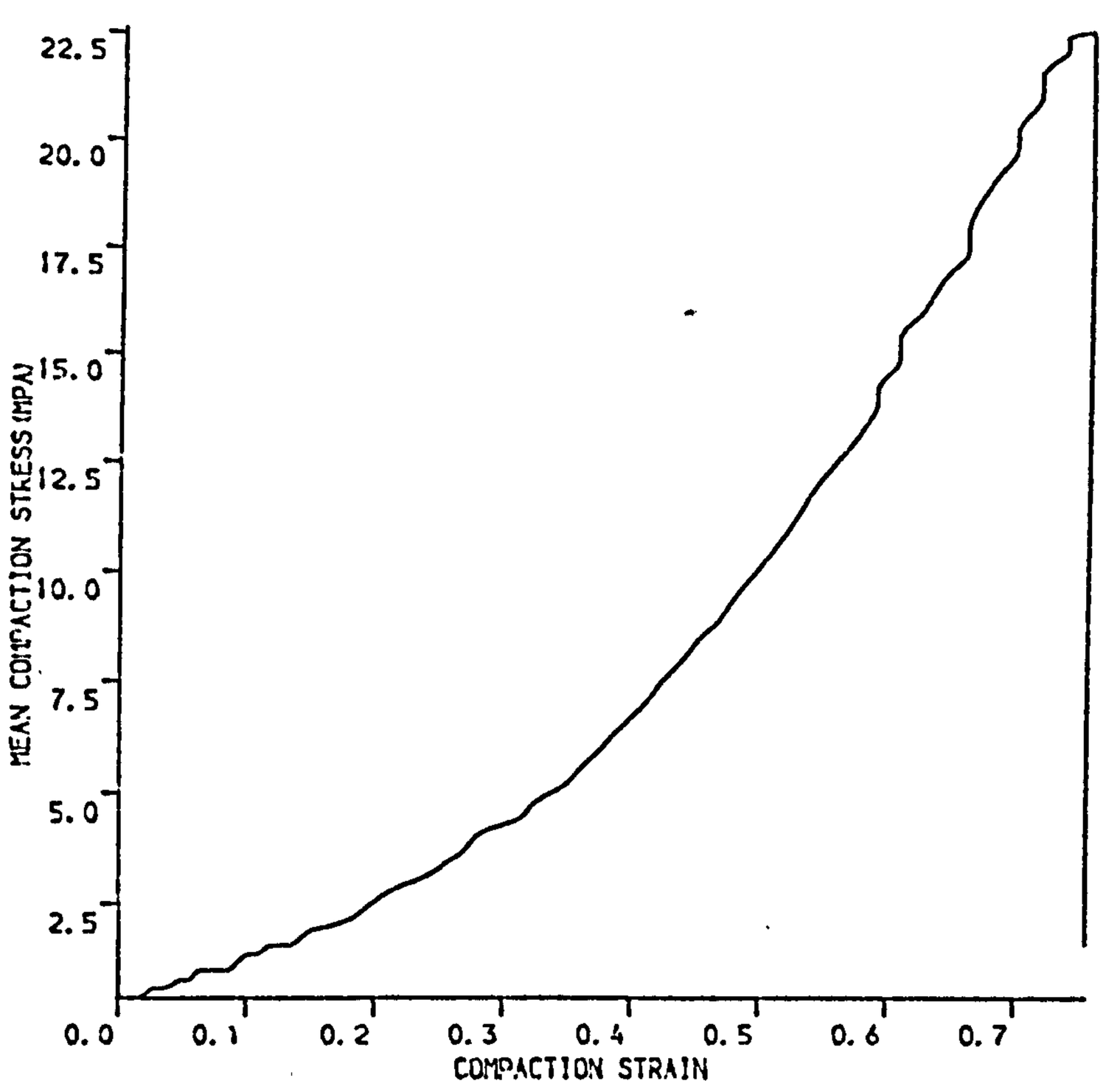

(B)

Figure 6.6 D-SODIUM CHLORIDE COMPACTED UNIAXIALLY AT 36MPA
(A) SHEAR STRESS VERSUS COMPACTION STRESS
(B) COMPACTION STRESS VERSUS NATURAL STRAIN

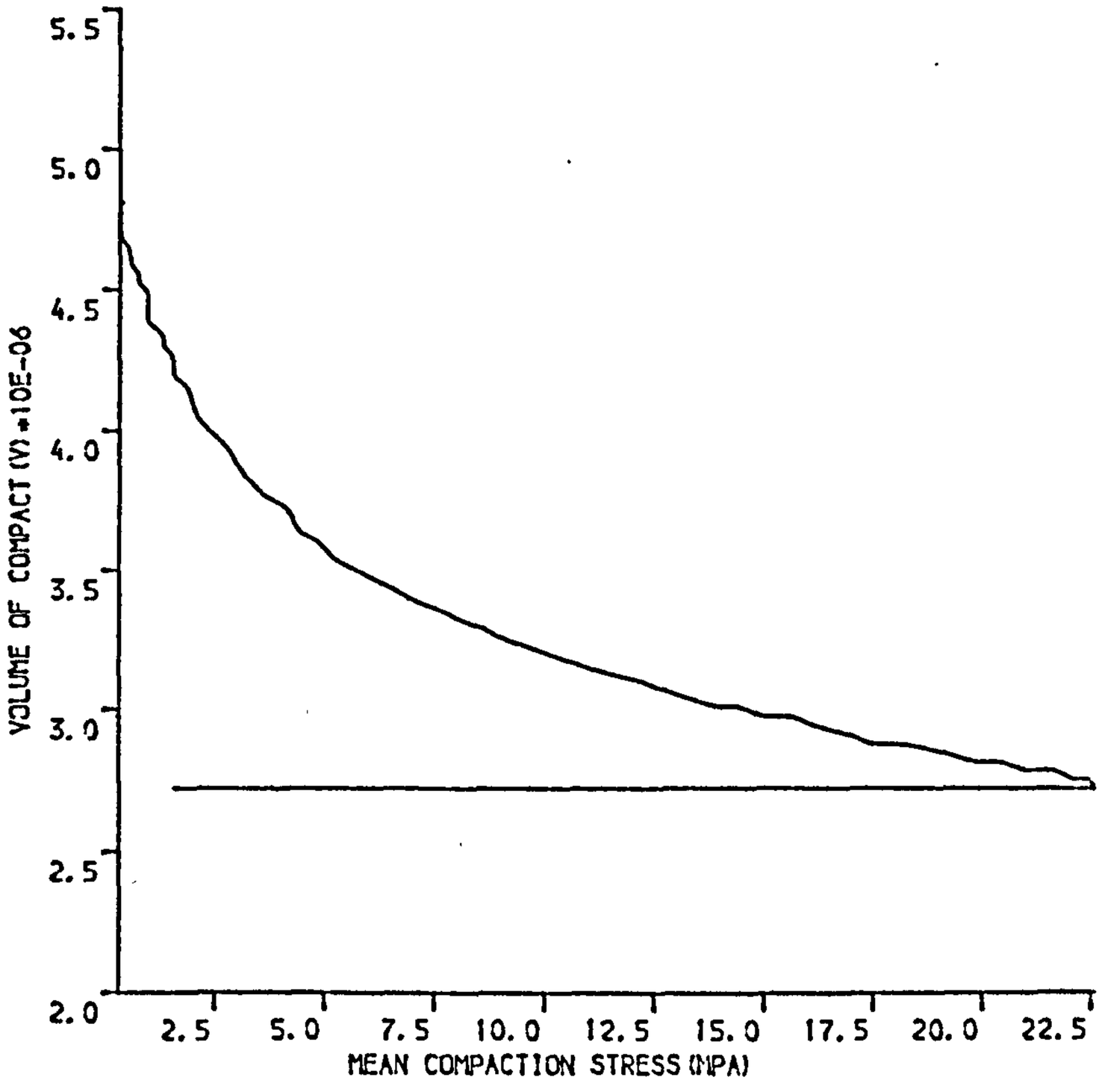

(A)

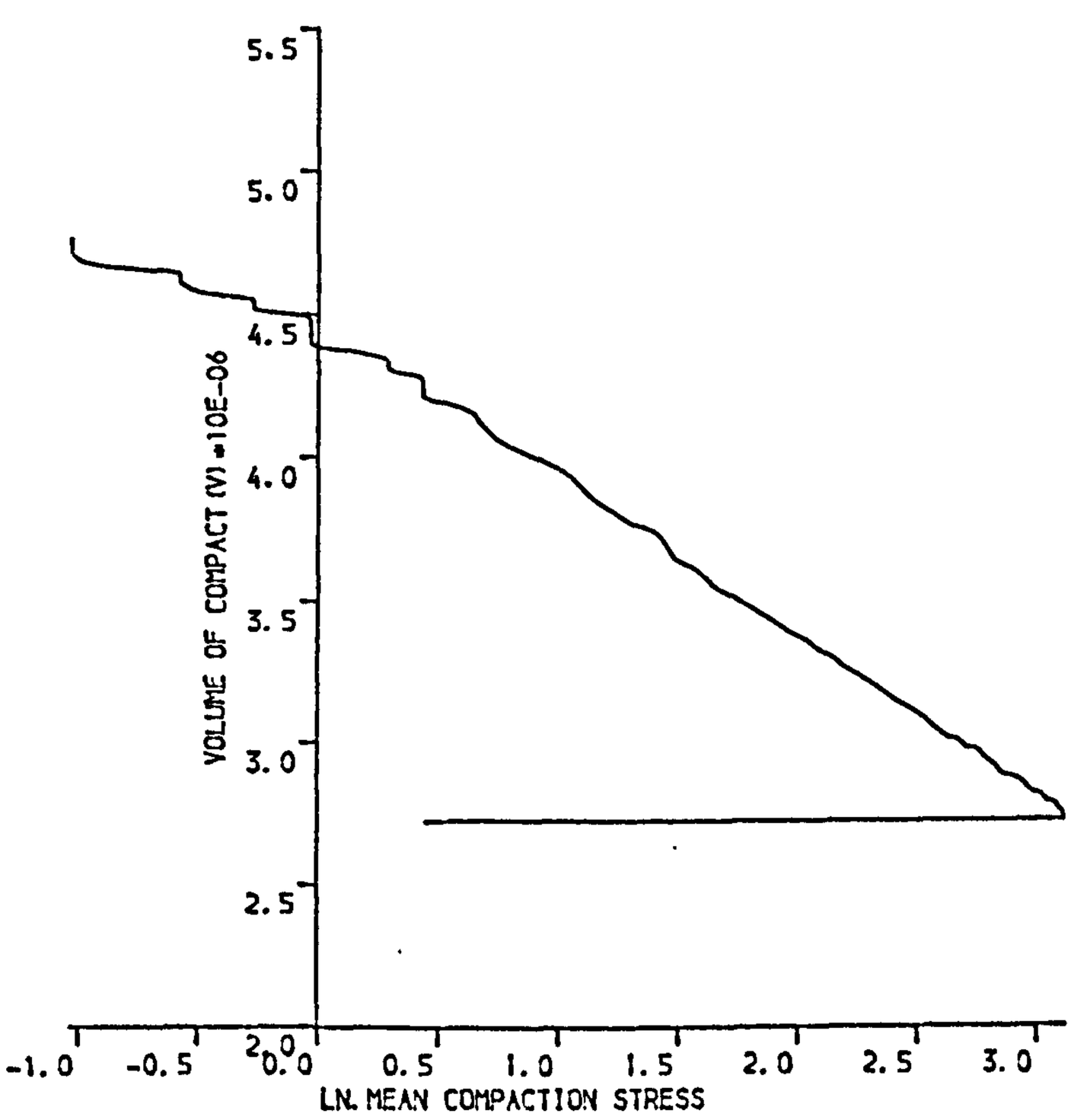

(B)

Figure 6.7 D-SODIUM CHLORIDE UNIAXIALLY COMPACTED AT 36MPA
(A) COMPACT VOLUME VERSUS MEAN COMPACTION STRESS
(B) COMPACT VOLUME VERSUS NATURAL LOGARITHMIC COMPACTION STRESS

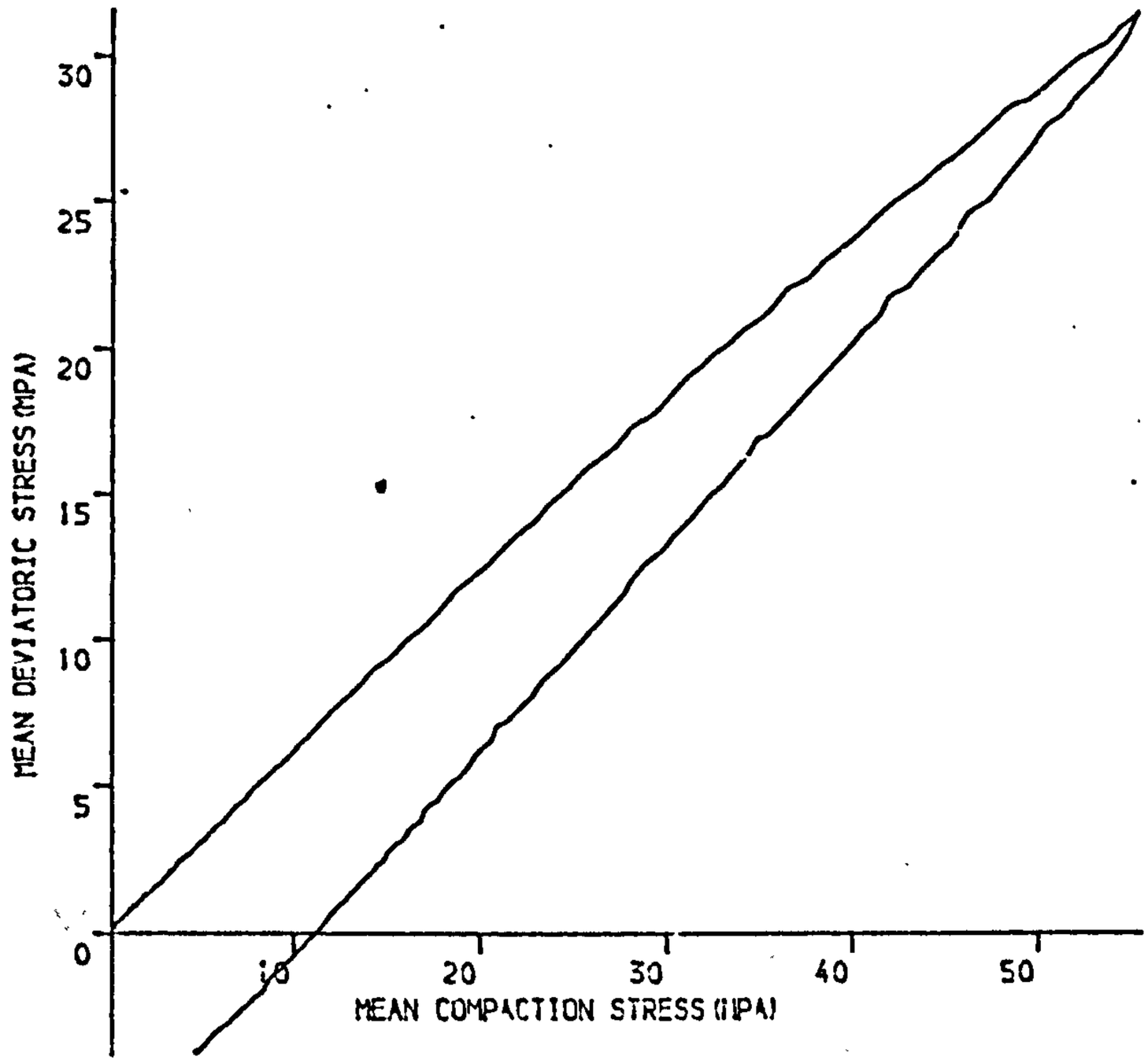

(A)

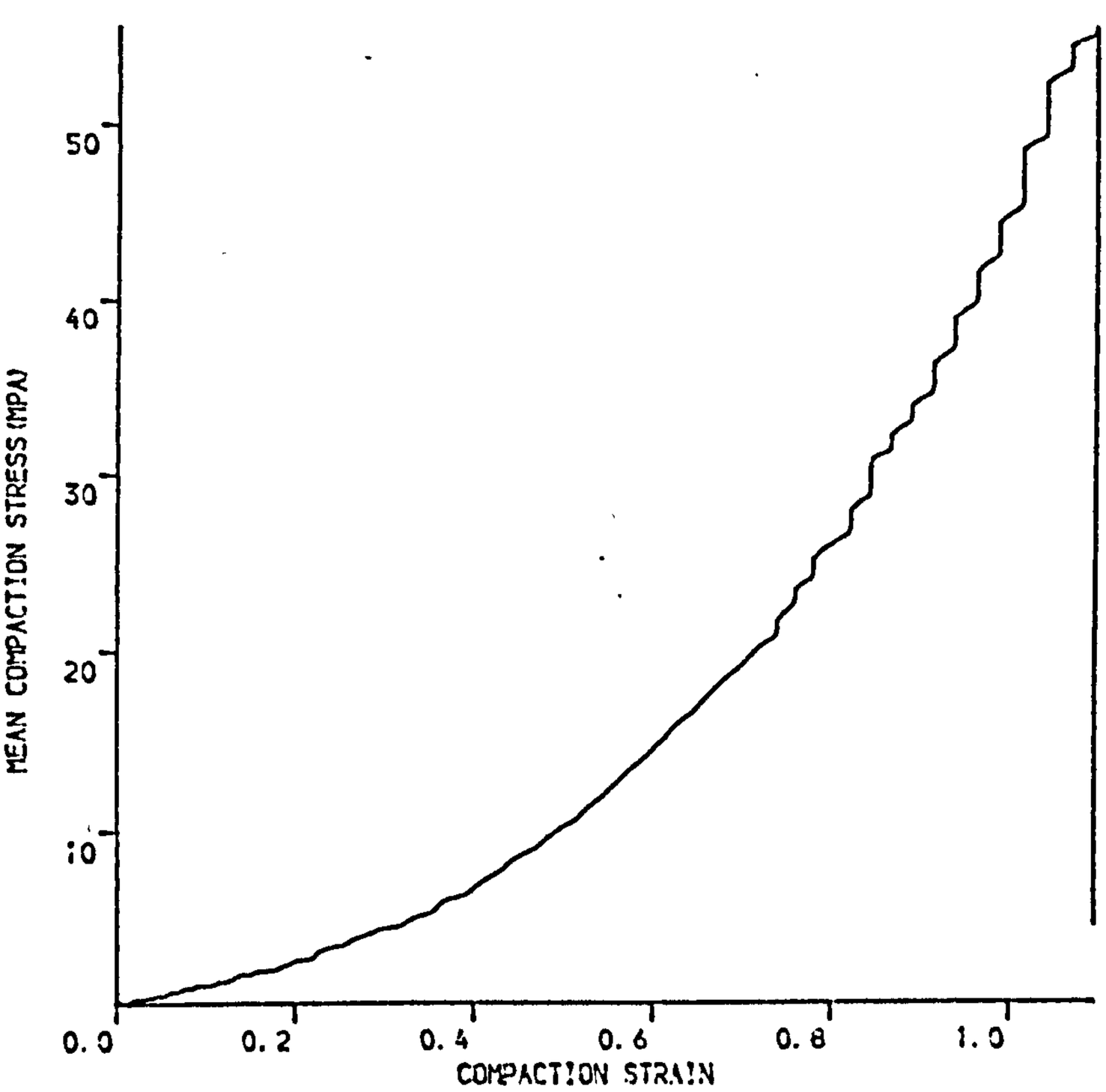

(B)

Figure 6.8 D-SODIUM CHLORIDE COMPACTED UNIAXIALLY AT 87MPA
(A) SHEAR STRESS VERSUS COMPACTION STRESS
(B) COMPACTION STRESS VERSUS NATURAL STRAIN

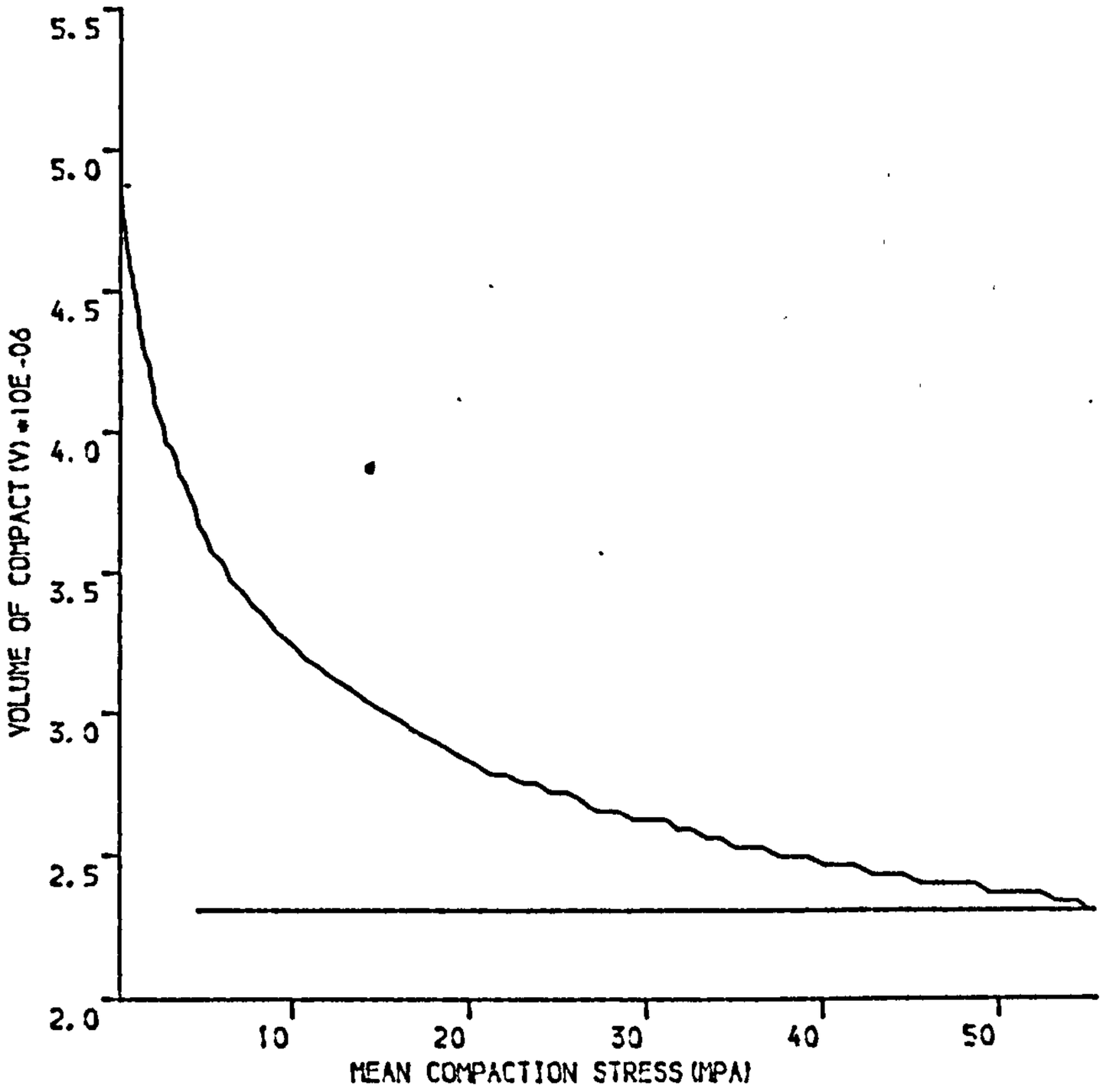

(A)

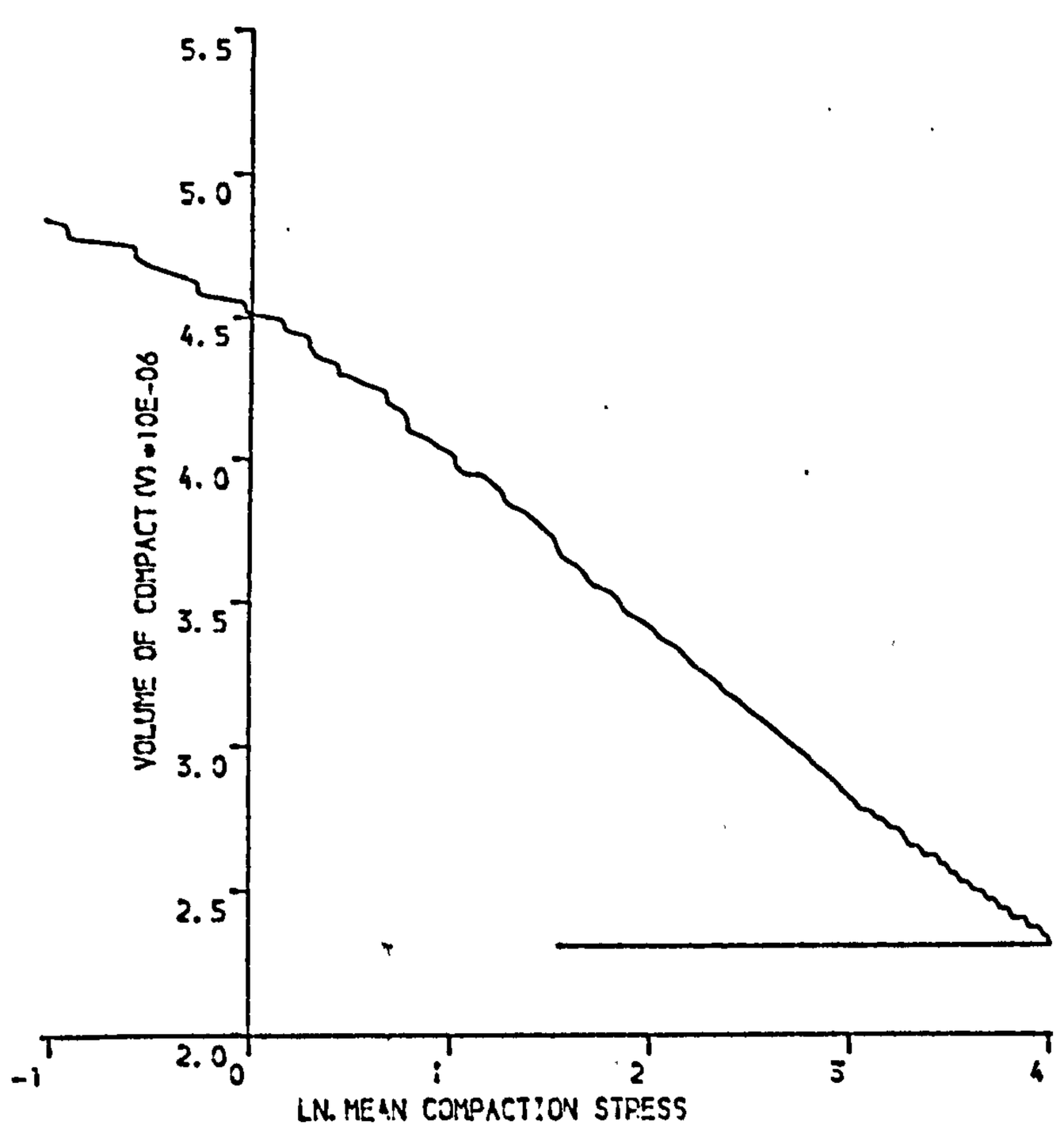

(B)

Figure 6.9 D-SODIUM CHLORIDE UNIAXIALLY COMPACTED AT 87MPA
(A) COMPACT VOLUME VERSUS MEAN COMPACTION STRESS
(B) COMPACT VOLUME VERSUS NATURAL LOGARITHMIC COMPACTION STRESS

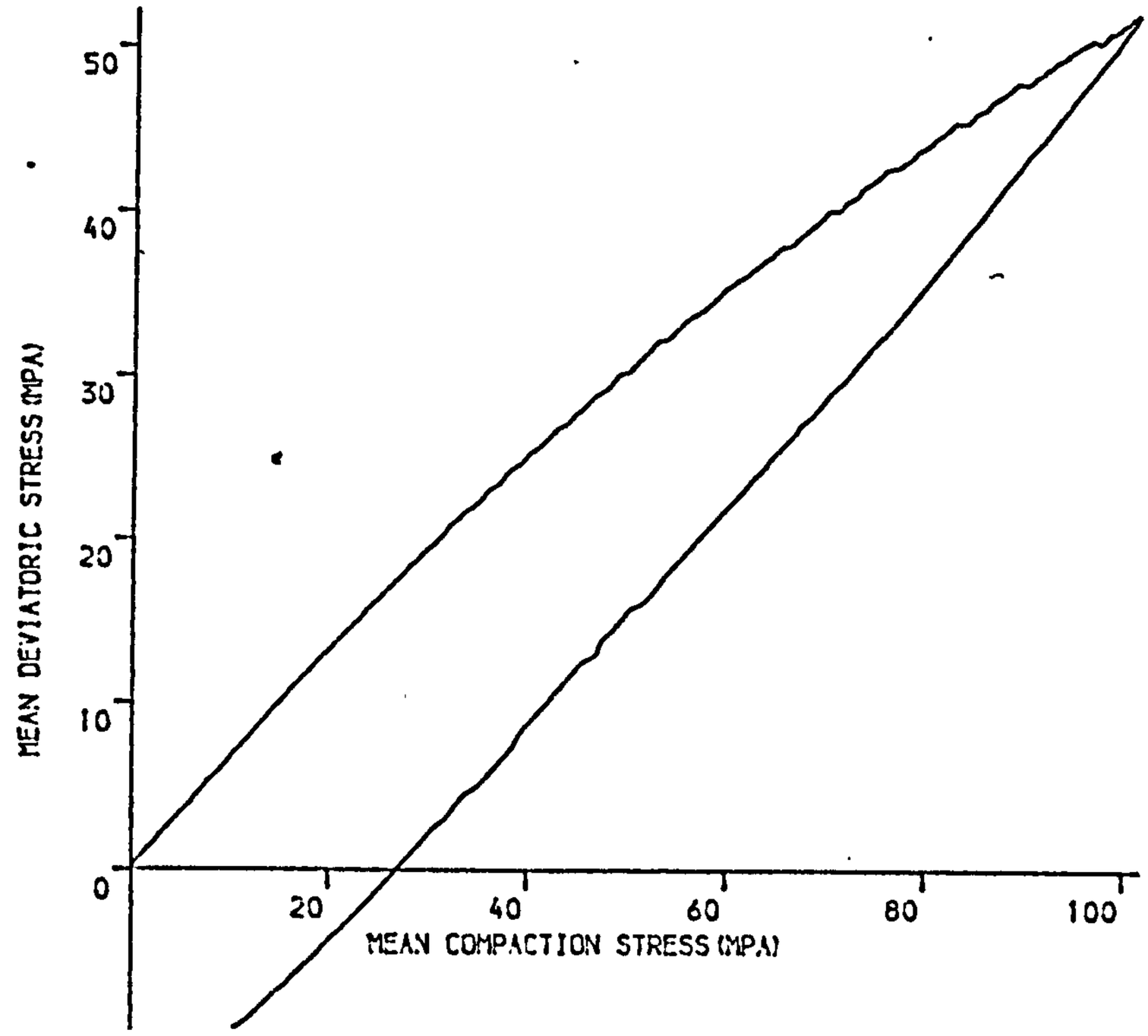

(A)

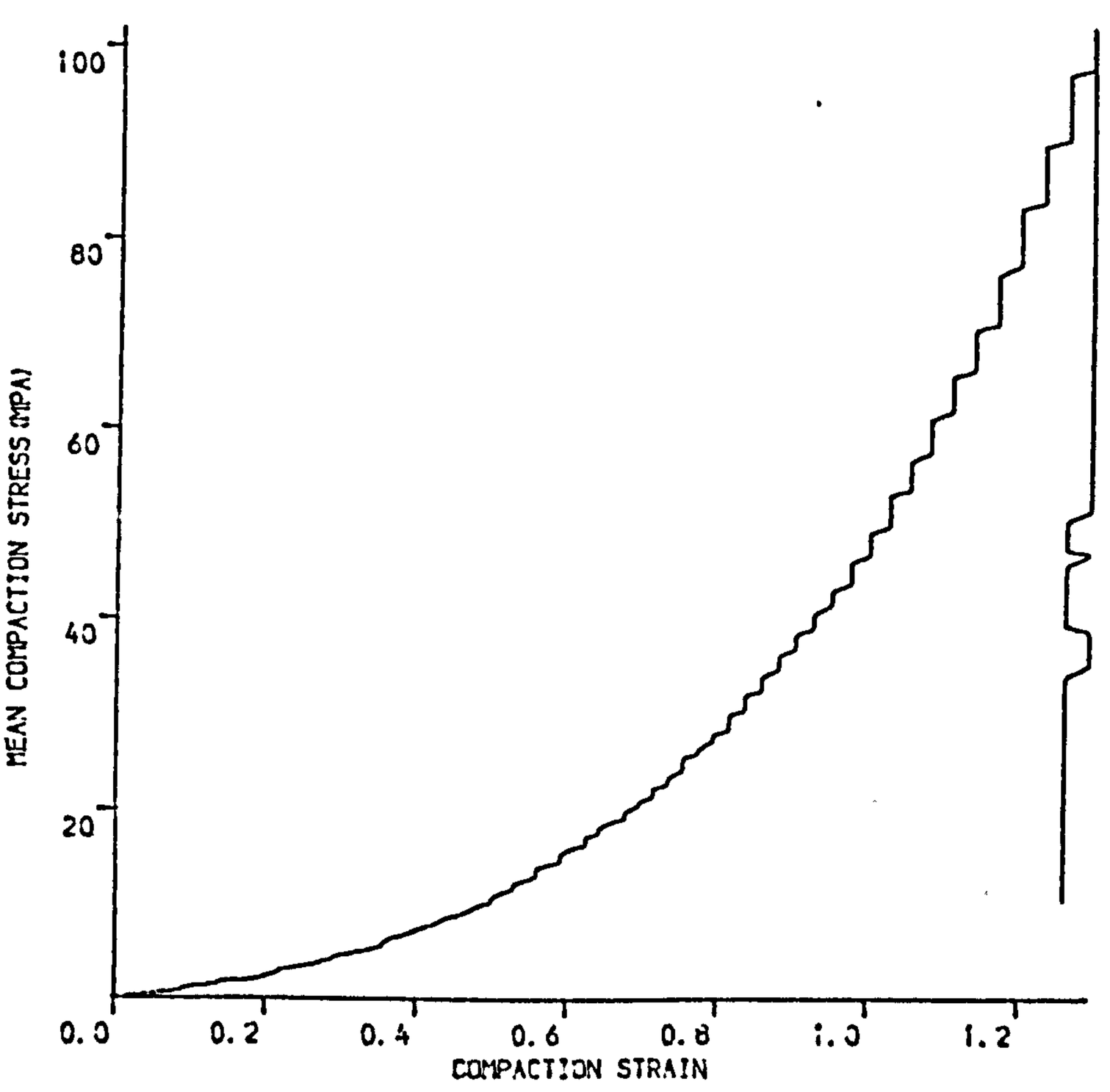

(B)

Figure 6.10 D-SODIUM CHLORIDE COMPACTED UNIAXIALLY AT 153MPA

(A) SHEAR STRESS VERSUS COMPACTION STRESS

(B) COMPACTION STRESS VERSUS NATURAL STRAIN

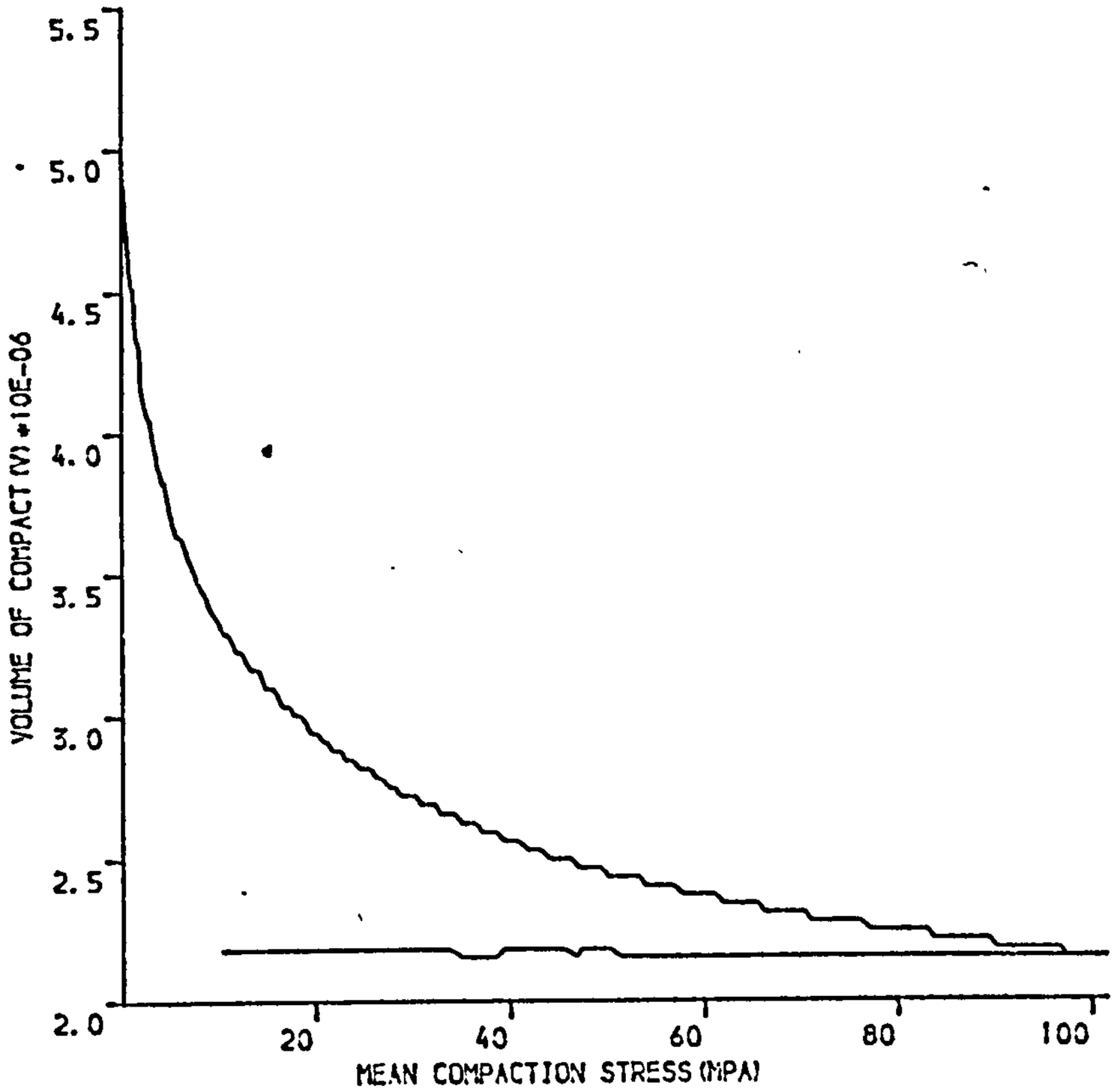

(A)

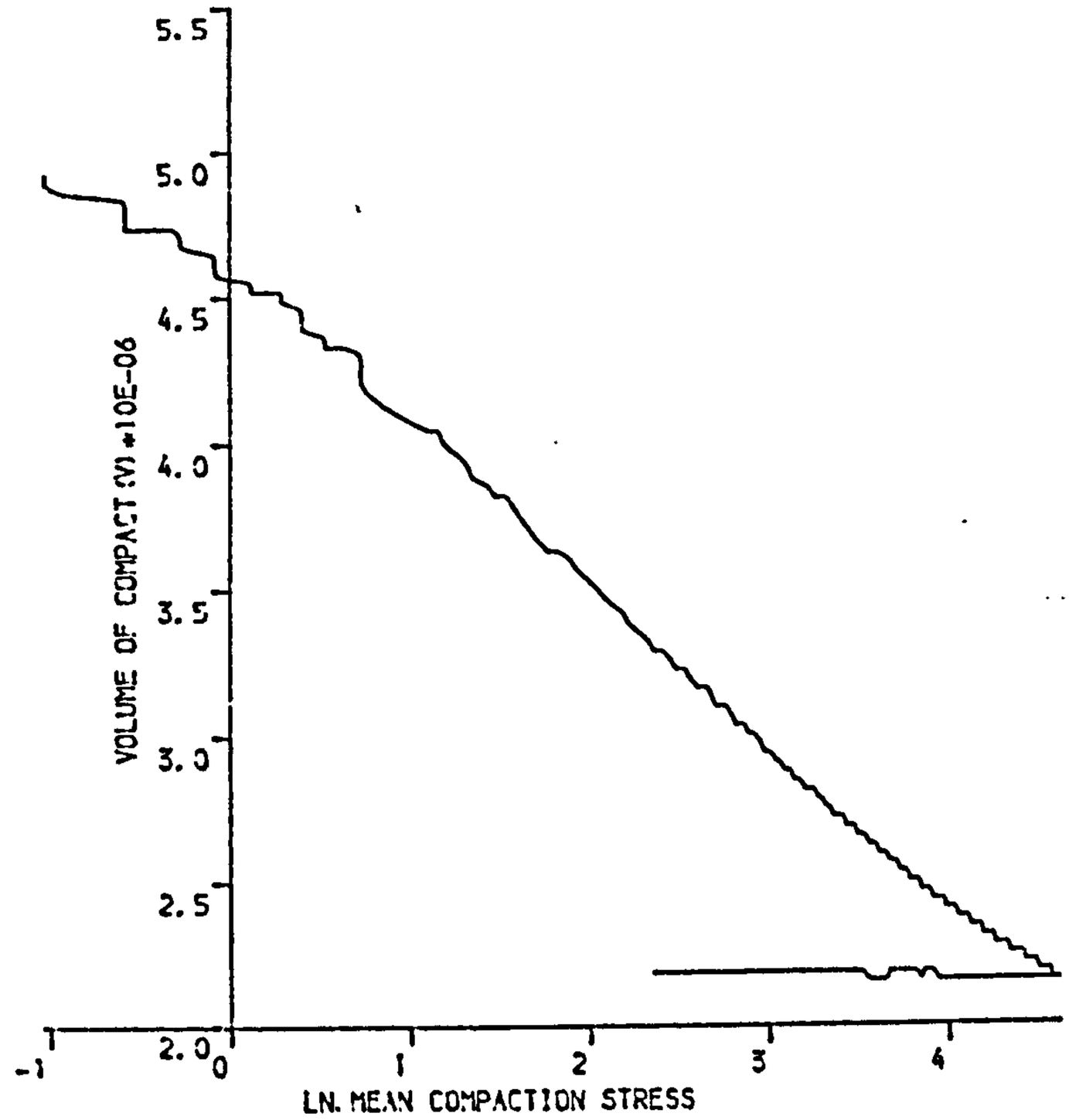

(B)

Figure 6.11 D-SODIUM CHLORIDE UNIAXIALLY COMPACTED AT 153MPA

(A) COMPACT VOLUME VERSUS MEAN COMPACTION STRESS

(B) COMPACT VOLUME VERSUS NATURAL LOGARITHMIC COMPACTION STRESS

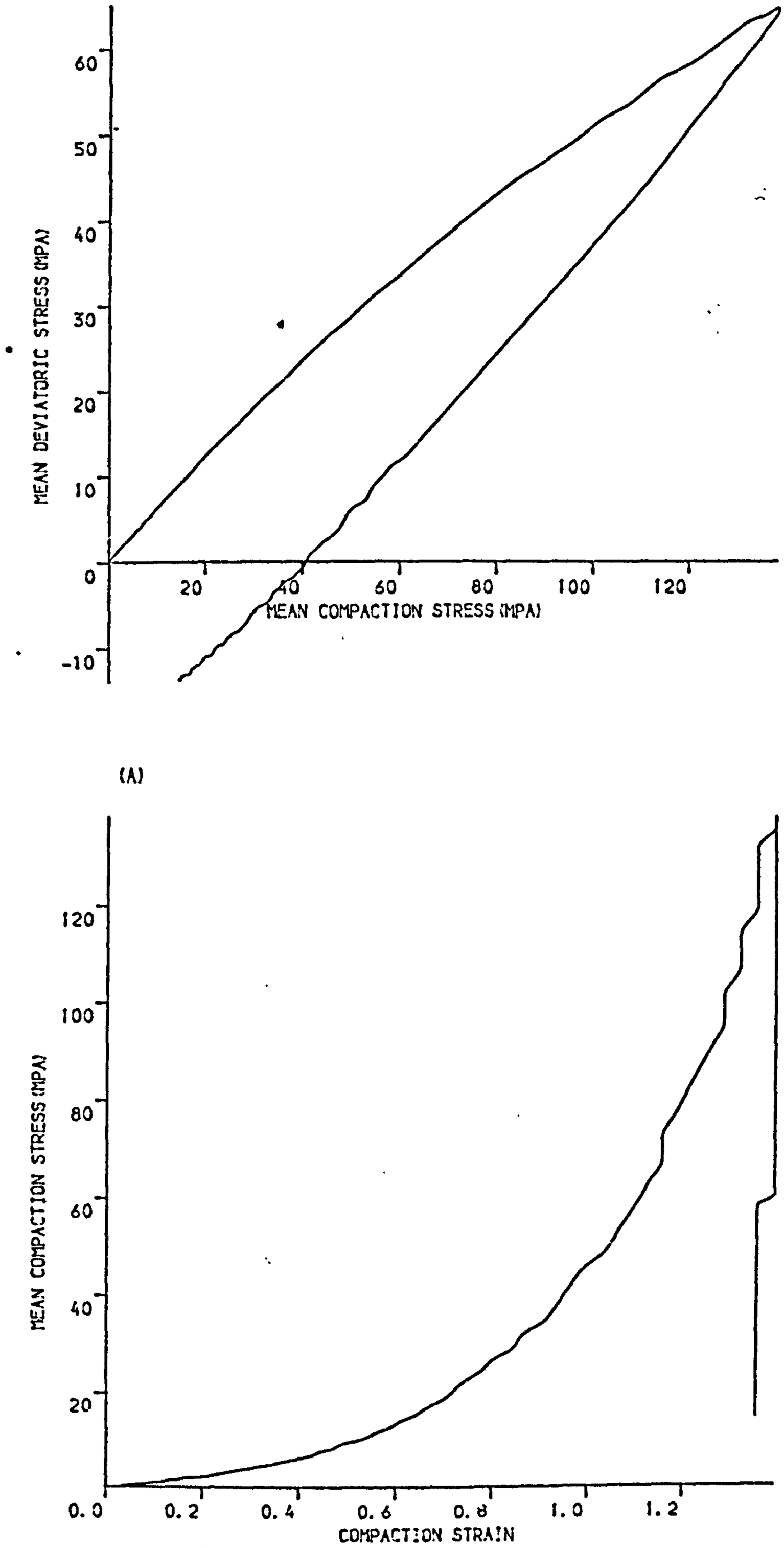

Figure 6.12 D-SODIUM CHLORIDE COMPACTED UNIAXIALLY AT 203MPA
(A) SHEAR STRESS VERSUS COMPACTION STRESS
(B) COMPACTION STRESS VERSUS NATURAL STRAIN

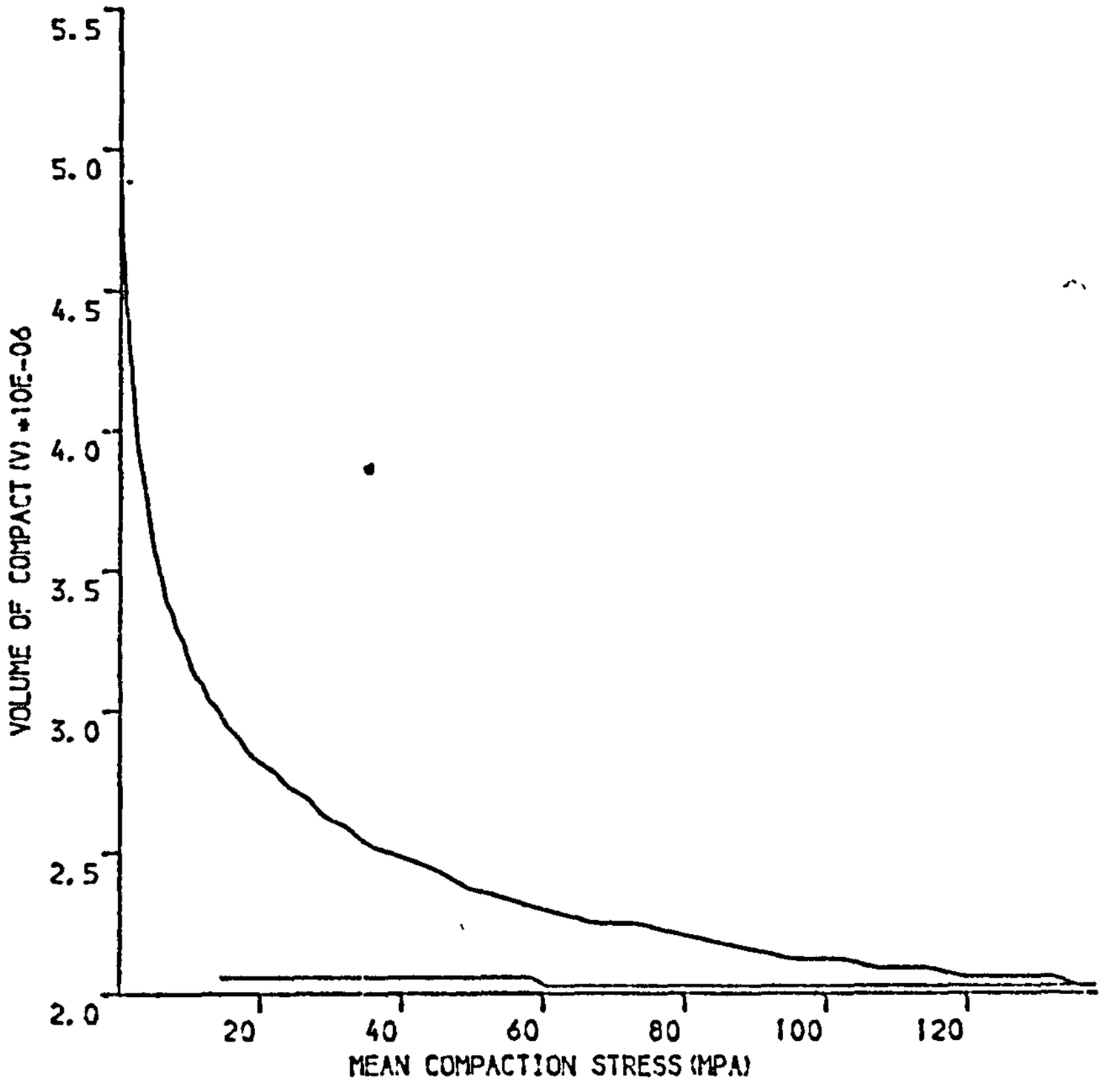

(A)

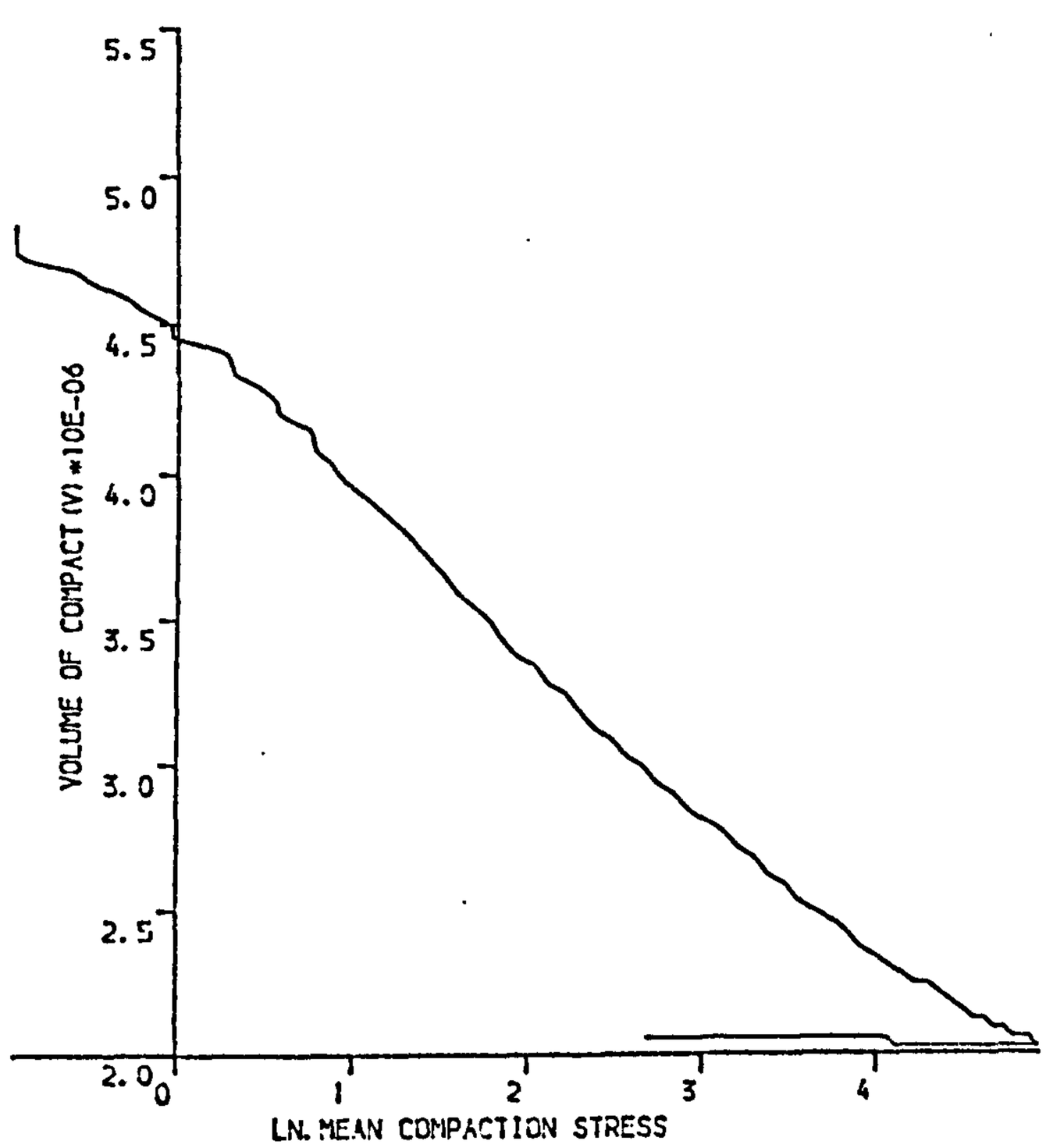

(B)

Figure 6.13 D-SODIUM CHLORIDE UNIAXIALLY COMPACTED AT 203MPA
(A) COMPACT VOLUME VERSUS MEAN COMPACTION STRESS
(B) COMPACT VOLUME VERSUS NATURAL LOGARITHMIC COMPACTION STRESS

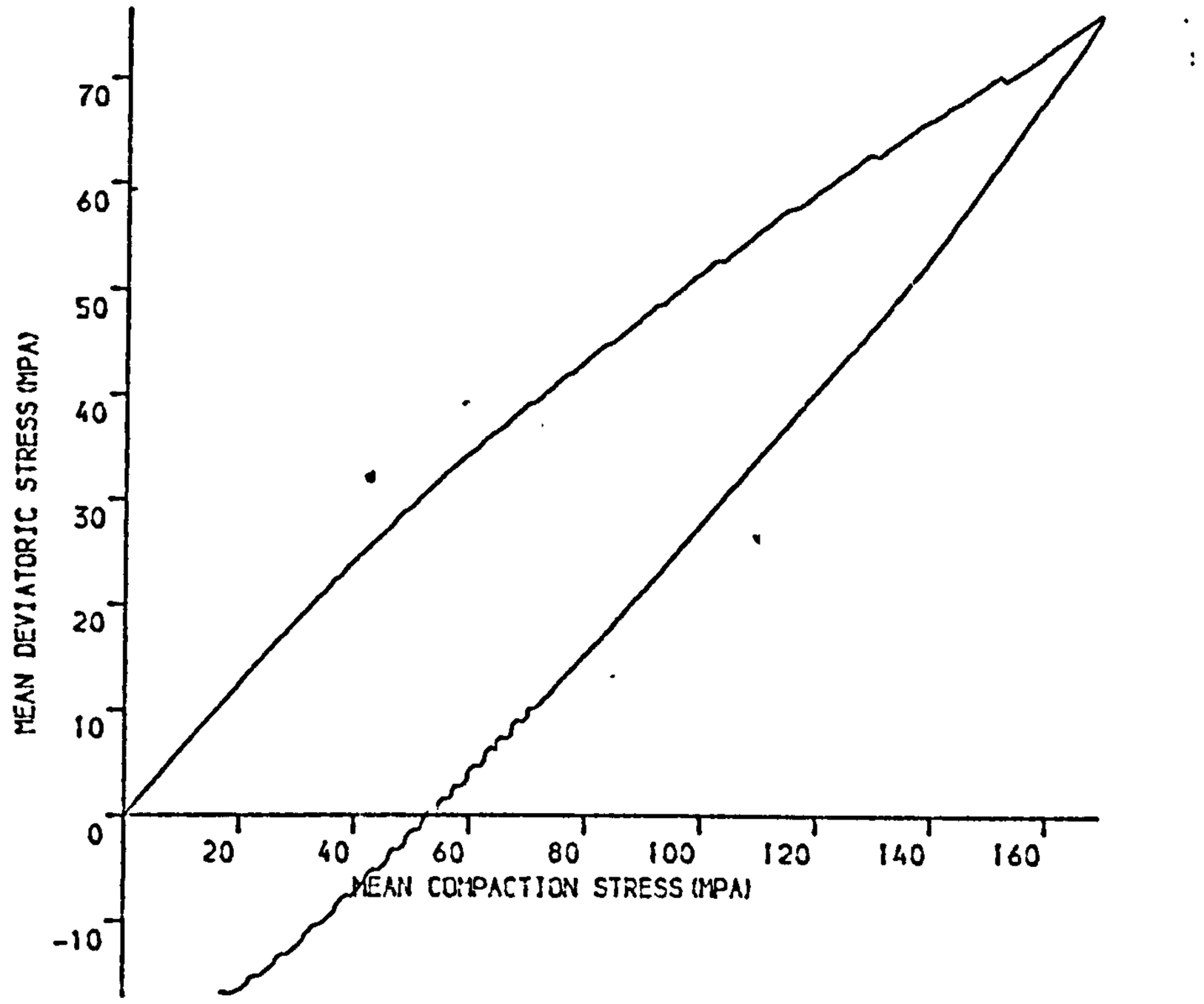

(A)

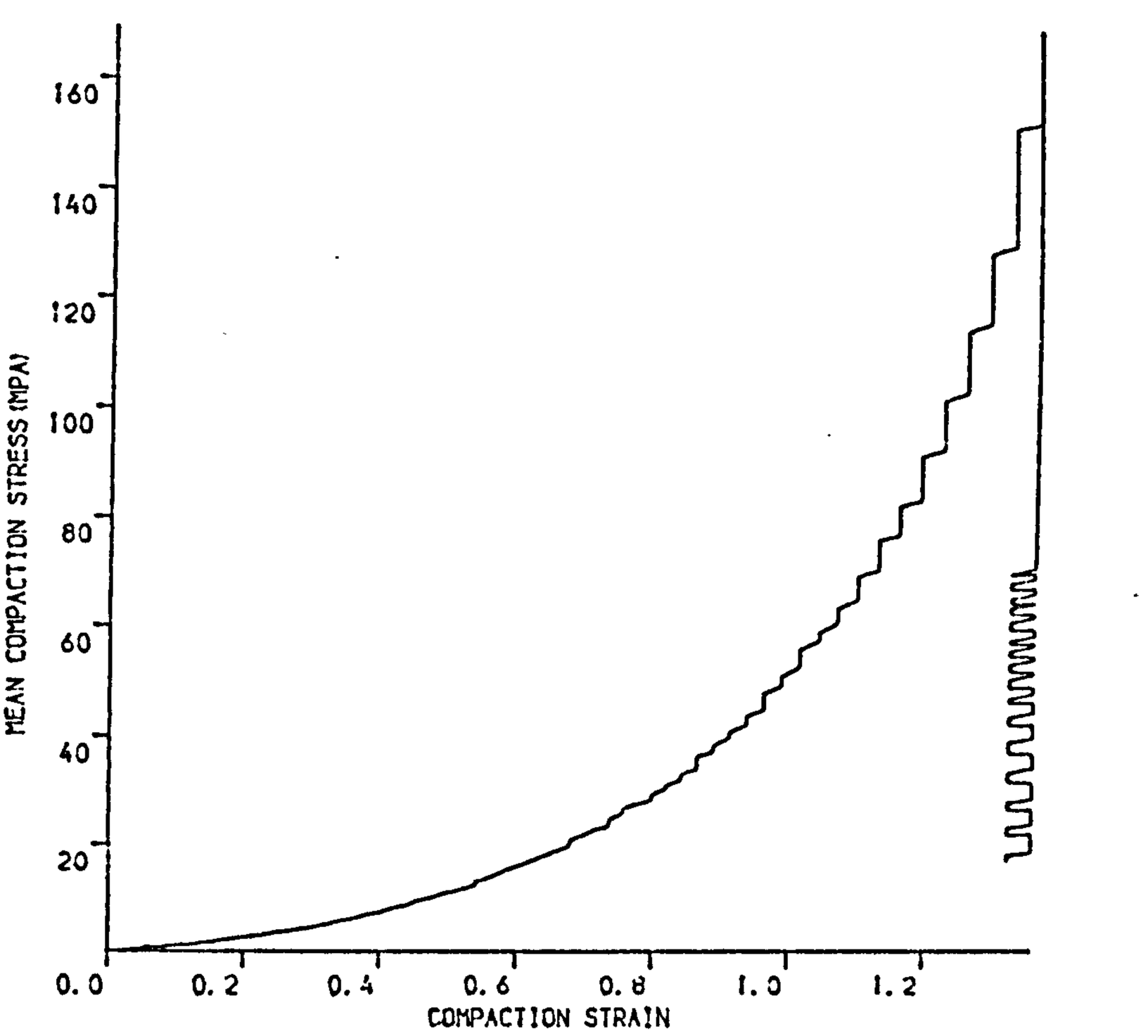

(B)

Figure 6.14 D-SODIUM CHLORIDE COMPACTED UNIAXIALLY AT 246MPA
(A) SHEAR STRESS VERSUS COMPACTION STRESS
(B) COMPACTION STRESS VERSUS NATURAL STRAIN

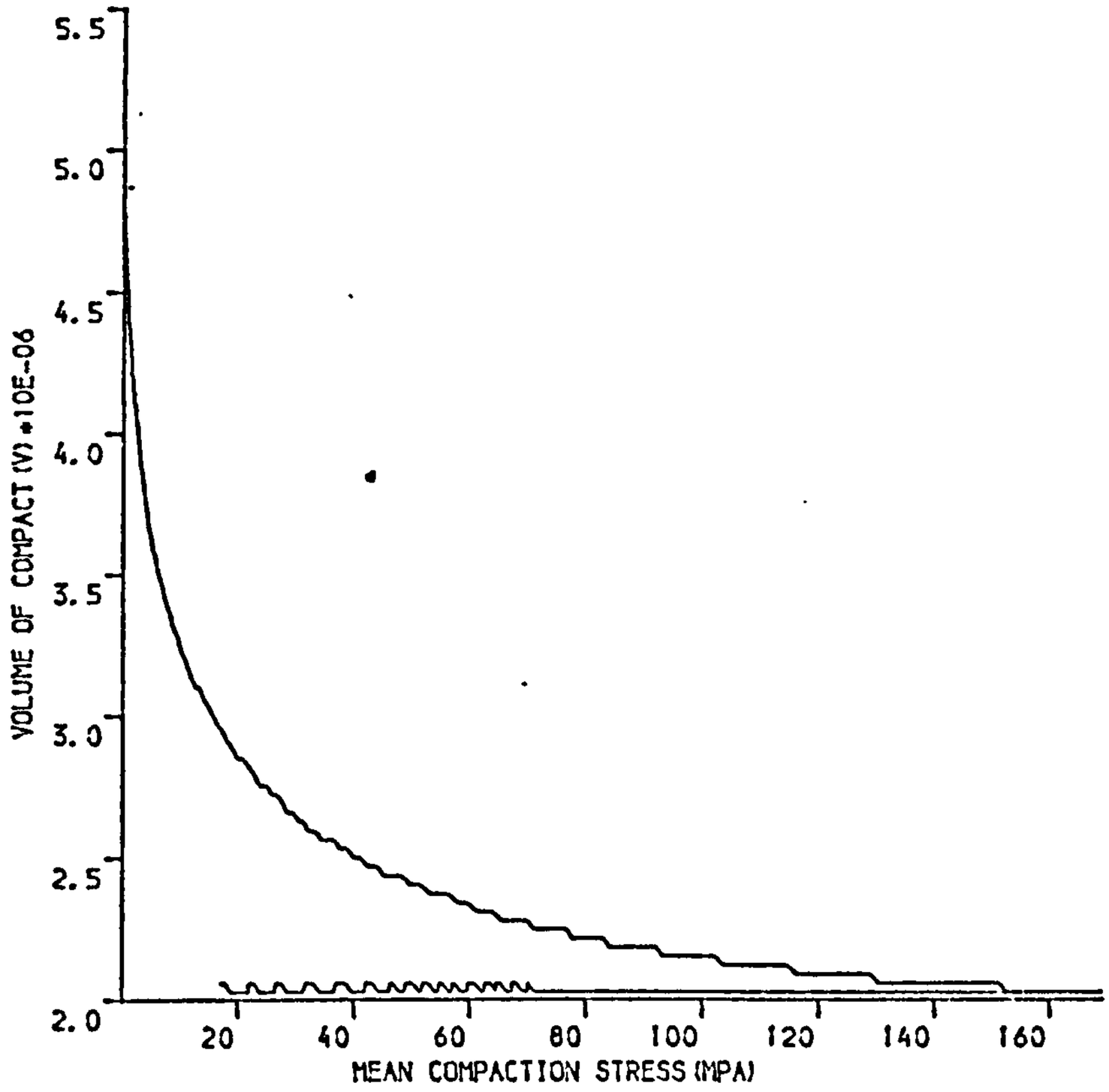

(A)

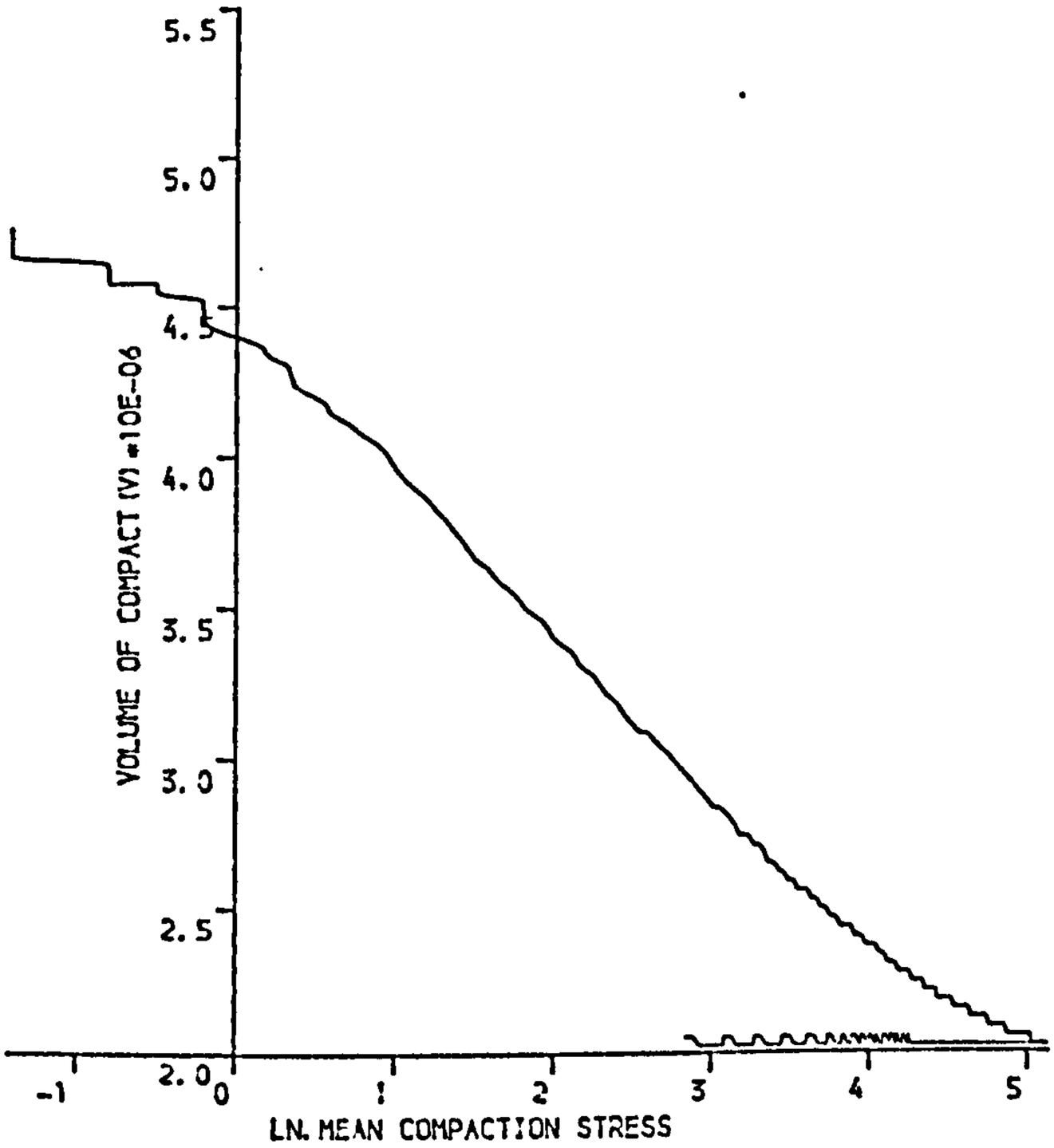

(B)

Figure6.15 D-SODIUM CHLORIDE UNIAXIALLY COMPACTED AT 246MPA
(A) COMPACT VOLUME VERSUS MEAN COMPACTION STRESS
(B) COMPACT VOLUME VERSUS NATURAL LOGARITHMIC COMPACTION STRESS

Figure 6.16 3-D representation of D-sodium chloride compacted at 36 MPa

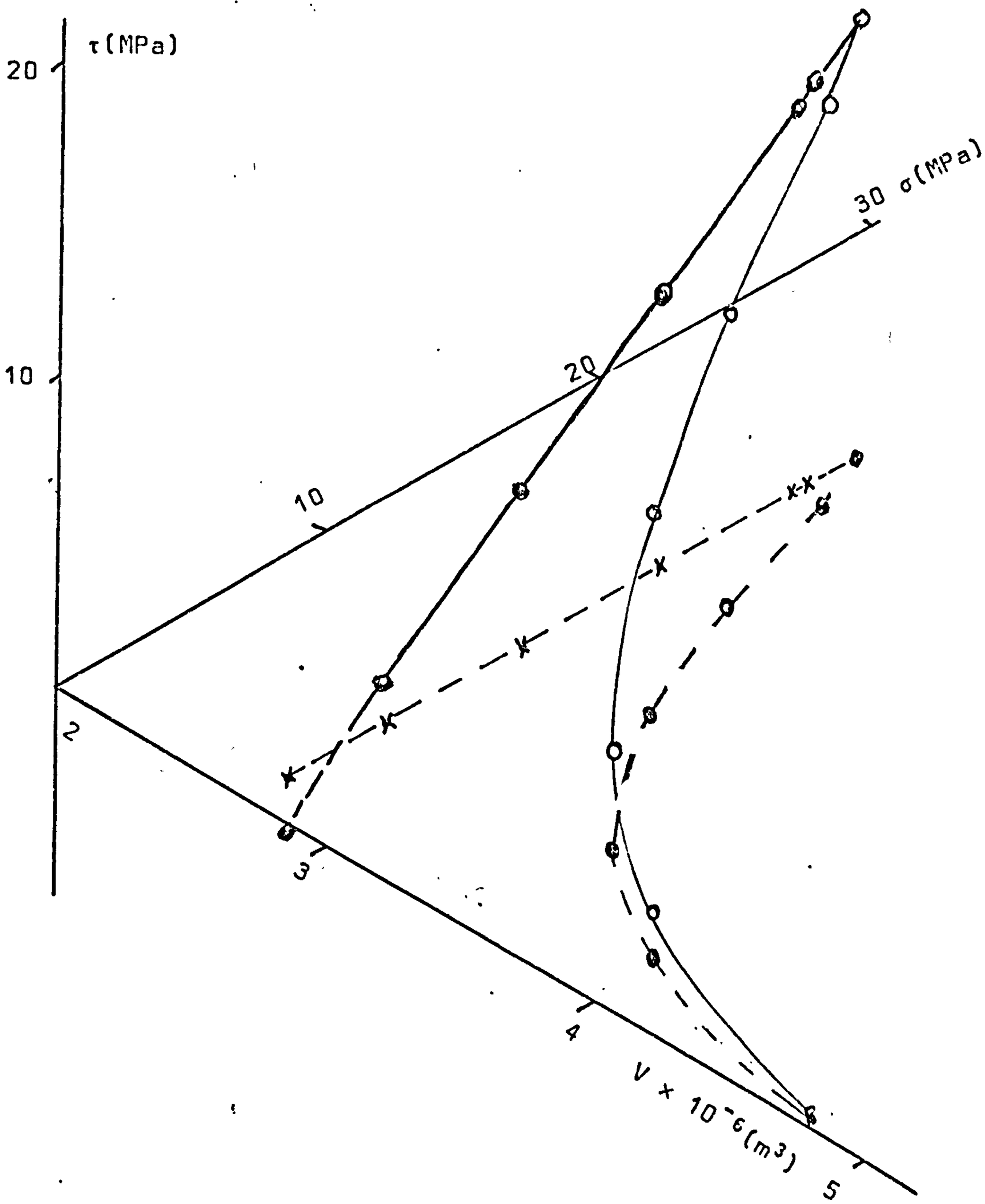

Figure 6.17 3-D representation of D-sodium chloride compacted at 87 MPa

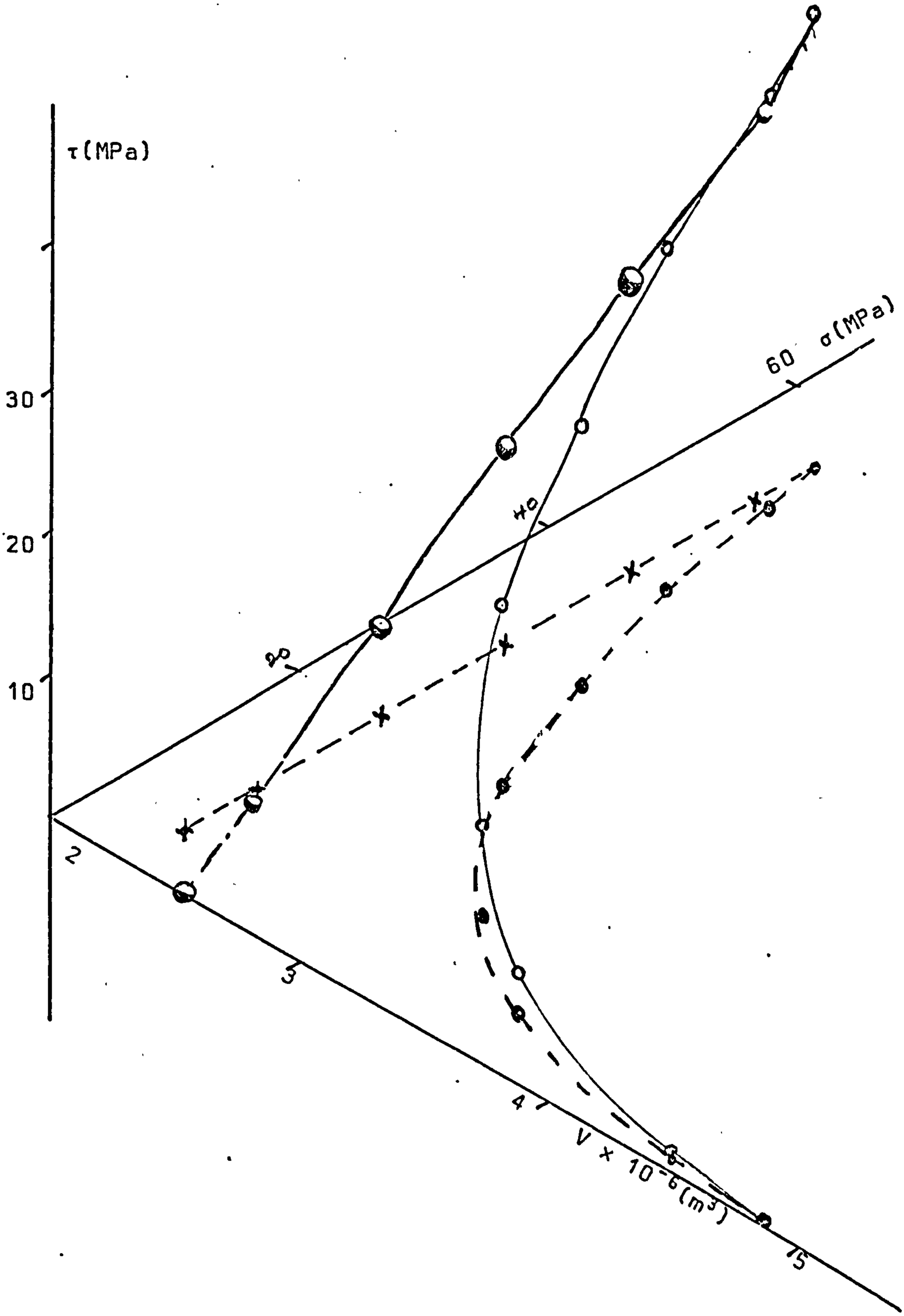

Figure 6.18 3-D representation of D-sodium chloride at 203 MPa

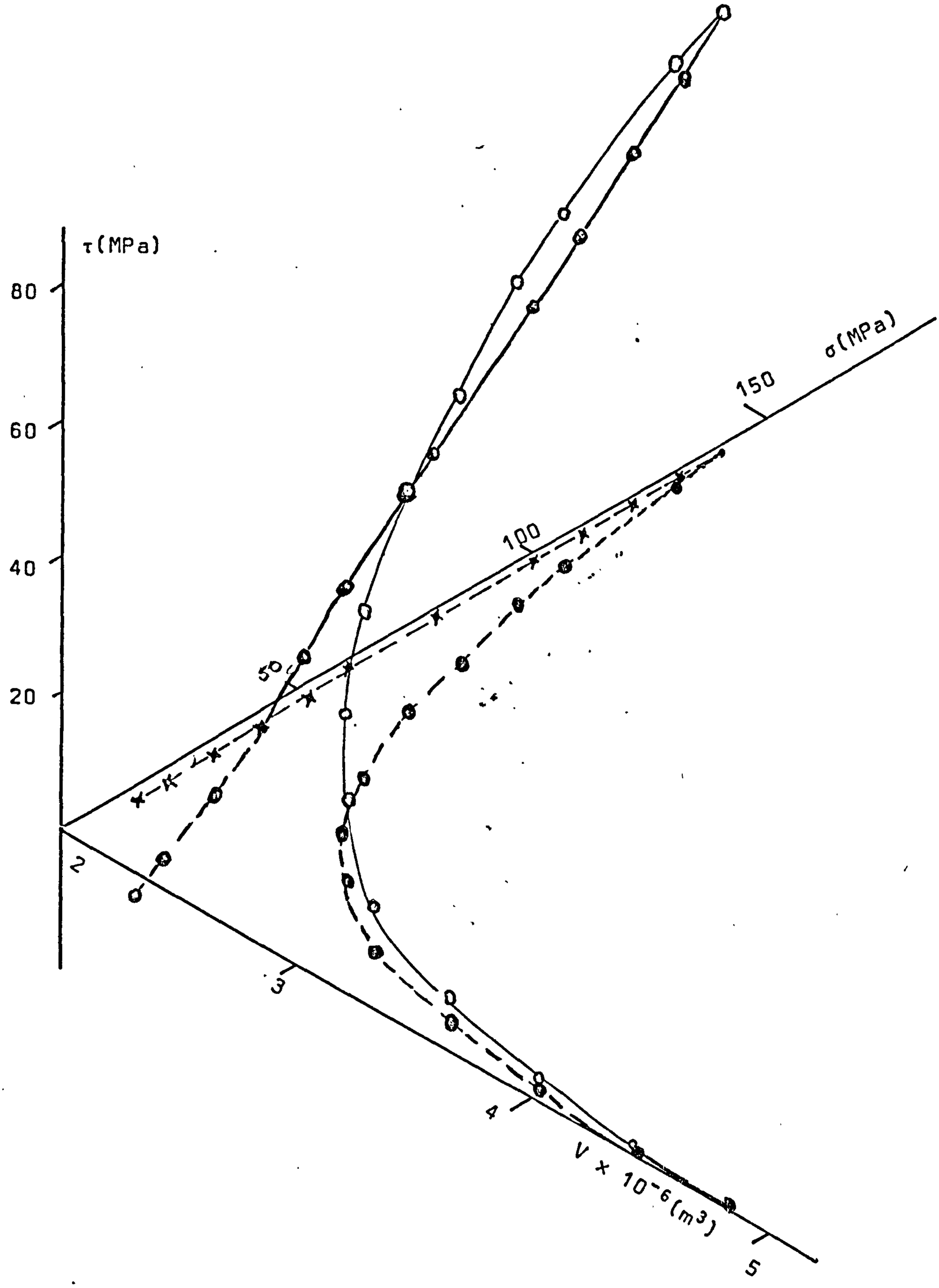

Figure 6.19 3-D representation of D-sodium chloride compacted at 246 MPa

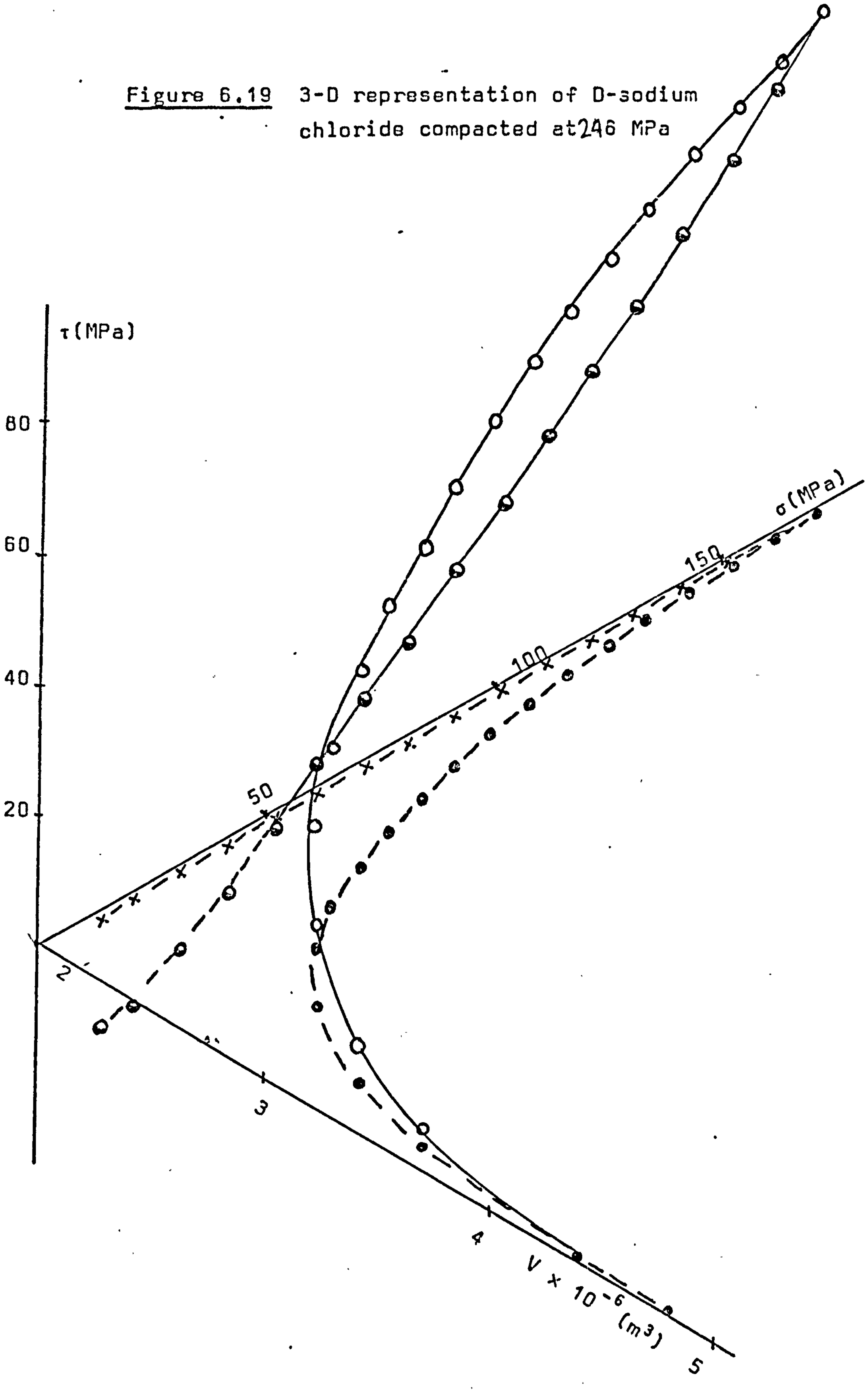

Figure 6.20 Mohr circles constructed for c- sodium chloride compacted at 54 MPa

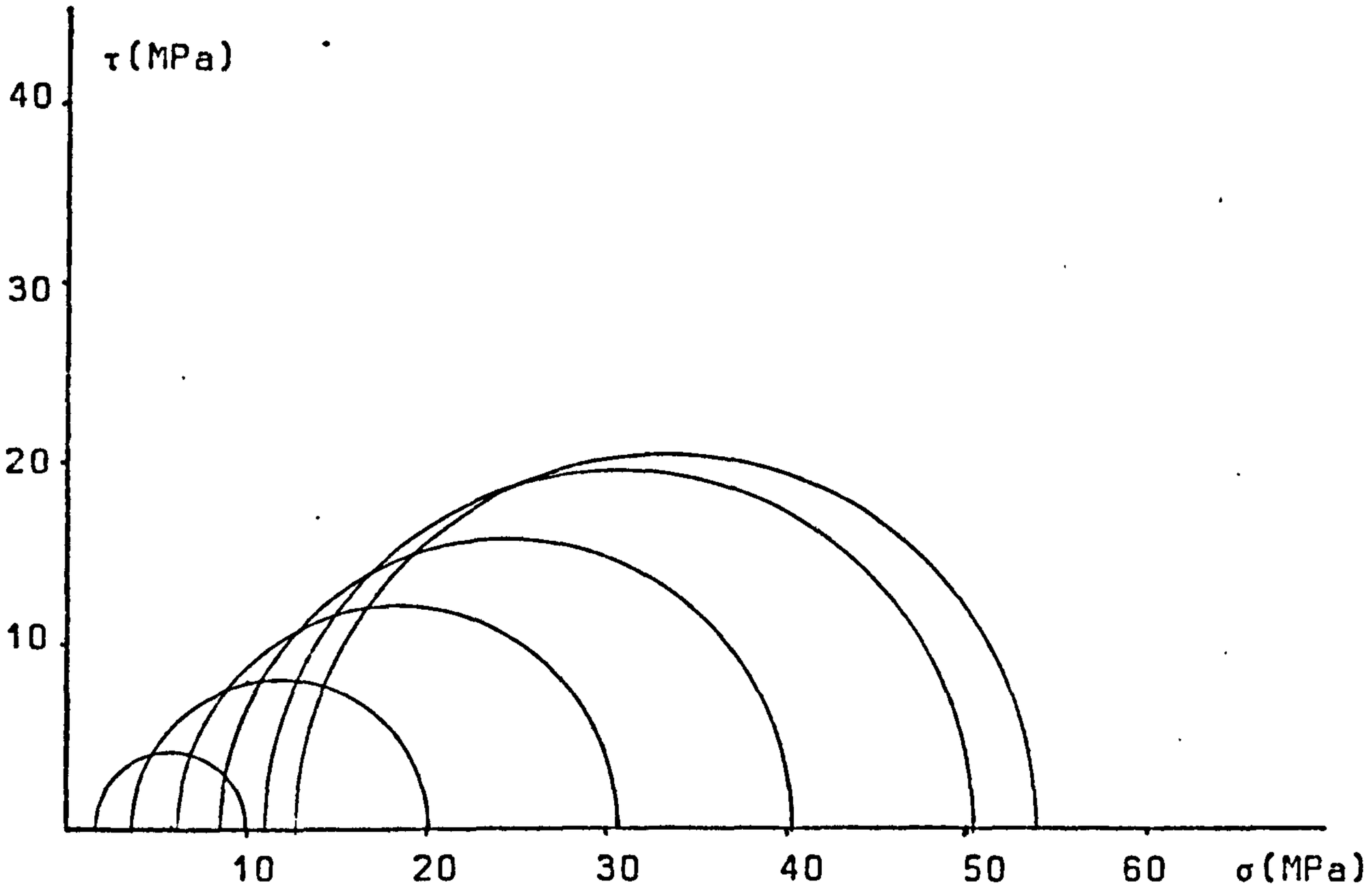

Figure 6.21 Mohr circles constructed for c-sodium chloride compacted at 77 MPa

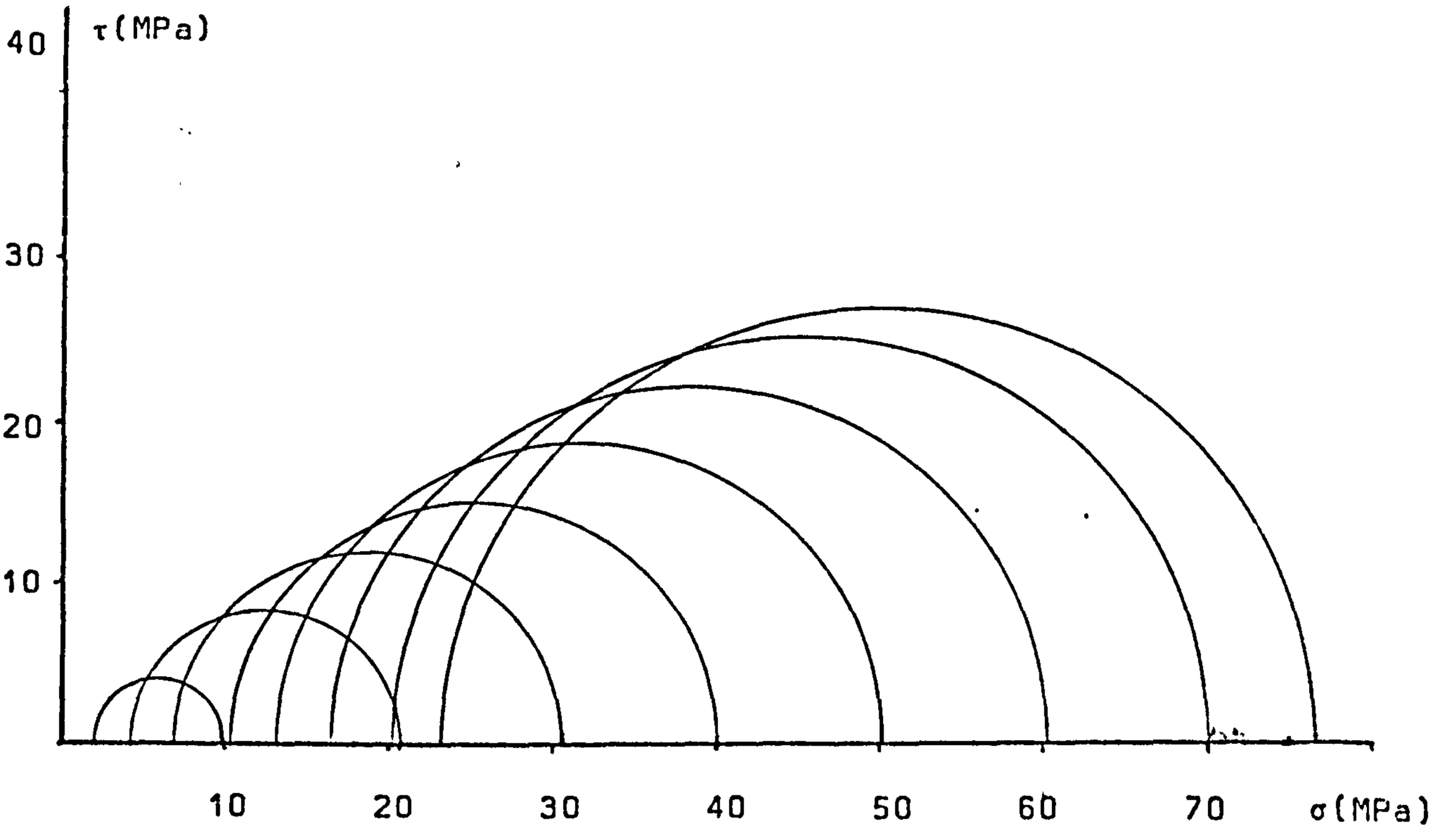

Figure 6.22 Mohr circles constructed for c-sodium chloride compacted at 125 MPa

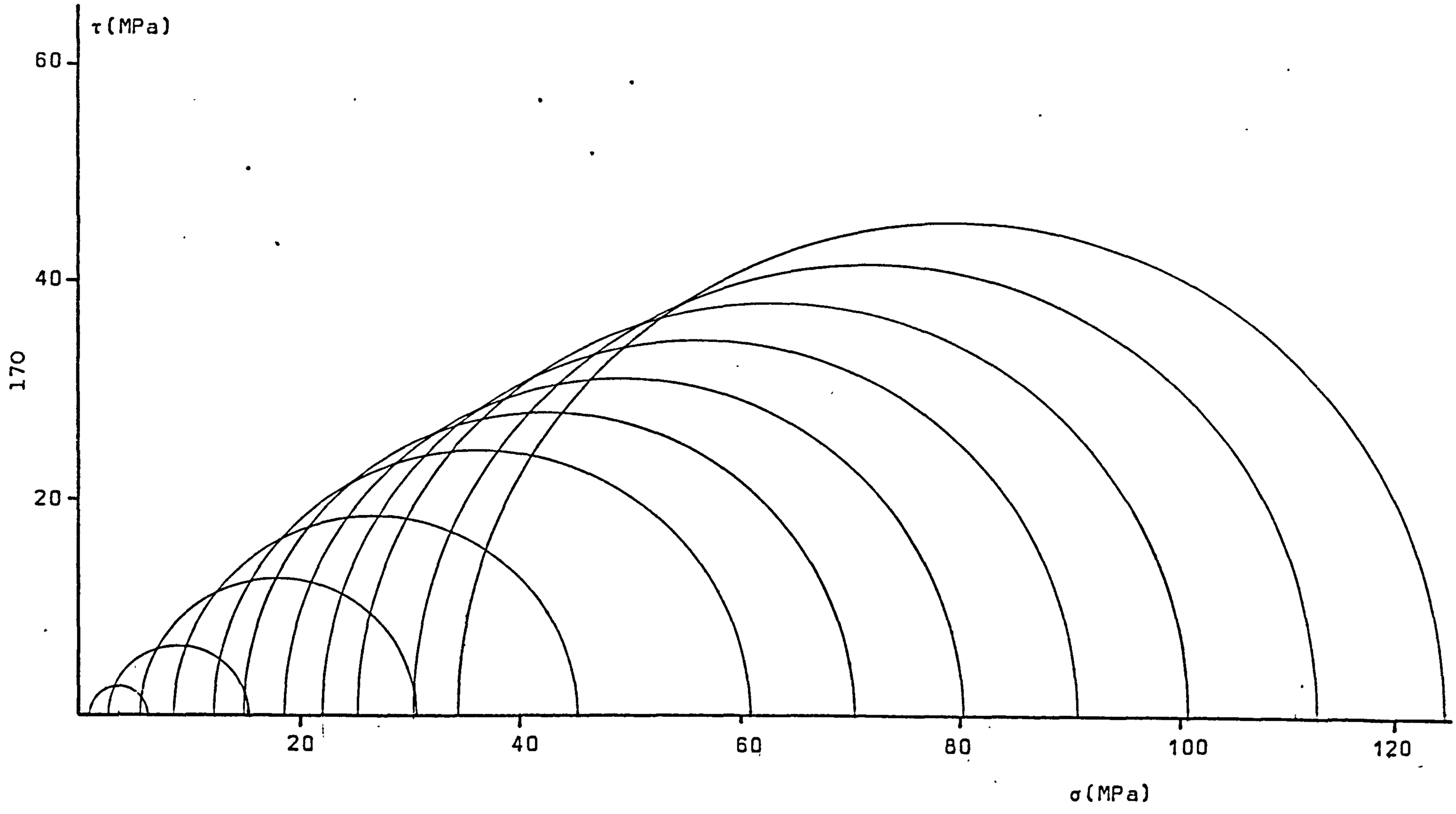

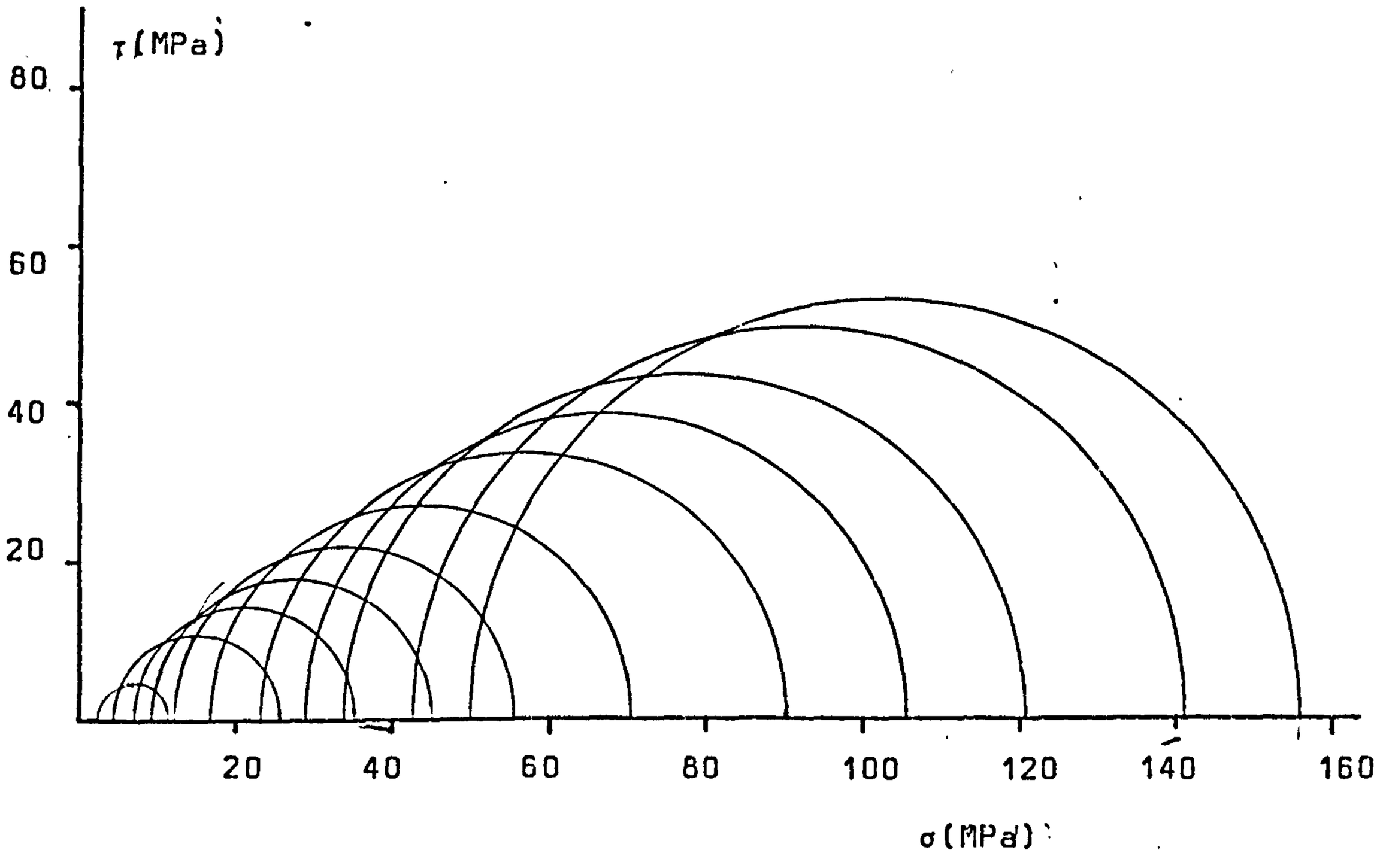

Figure 6.23 Mohr circles constructed for c-sodium chloride compacted at 155 MPa

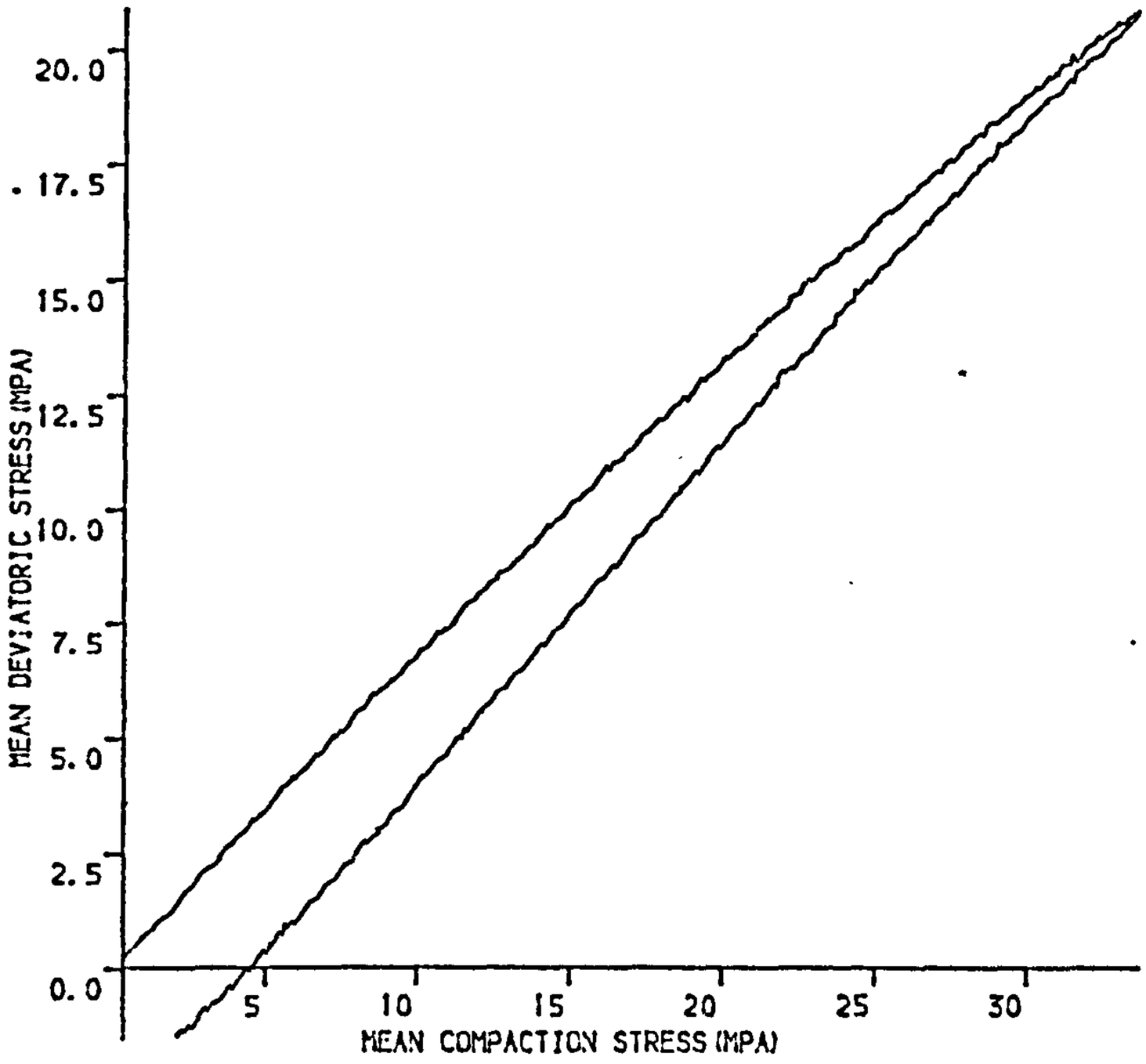

(A)

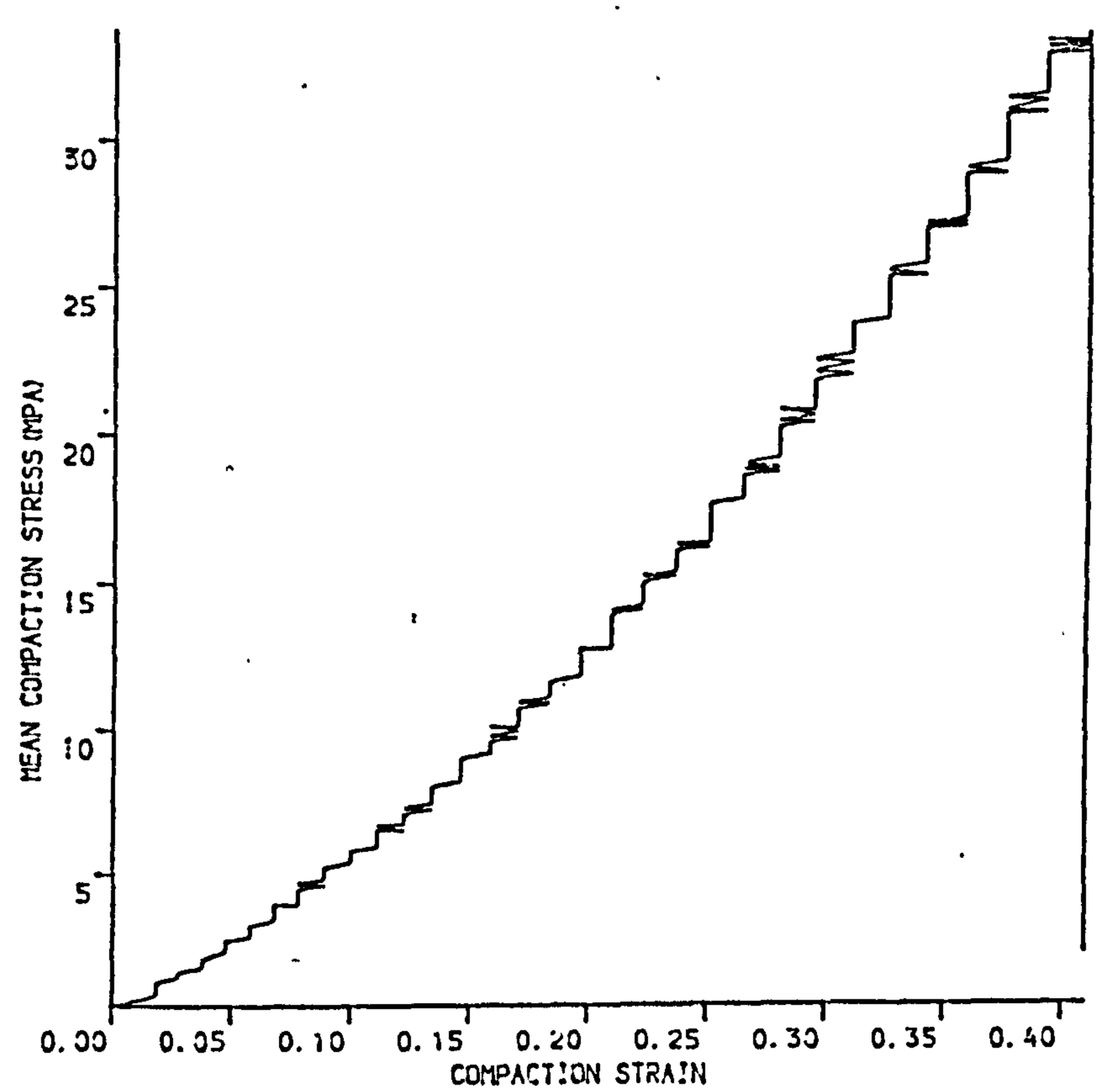

(B)

Figure 6.24 C-SODIUM CHLORIDE COMPACTED UNIAXIALLY AT 54MPA

(A) SHEAR STRESS VERSUS COMPACTION STRESS

(B) COMPACTION STRESS VERSUS NATURAL STRAIN

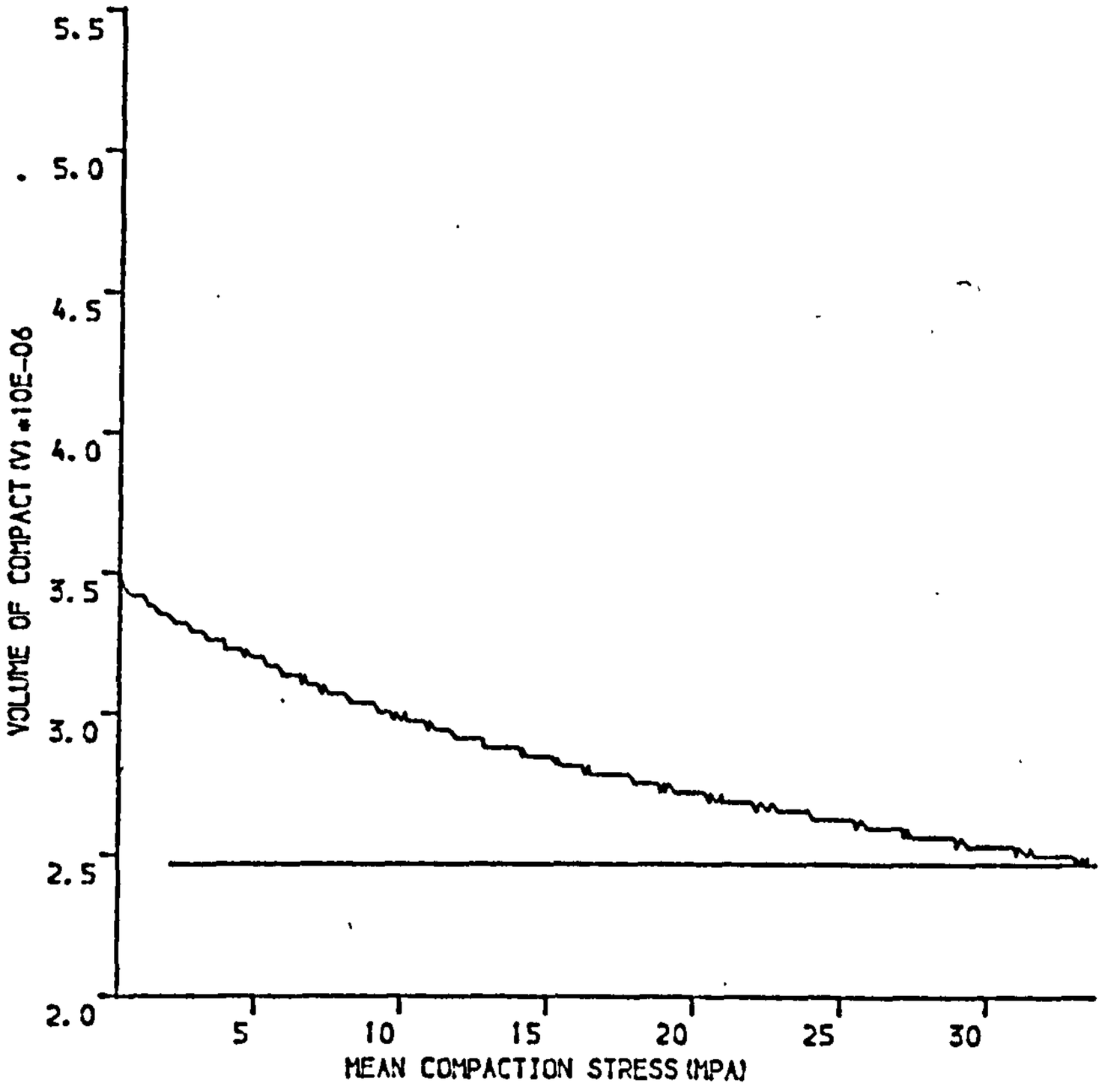

(A)

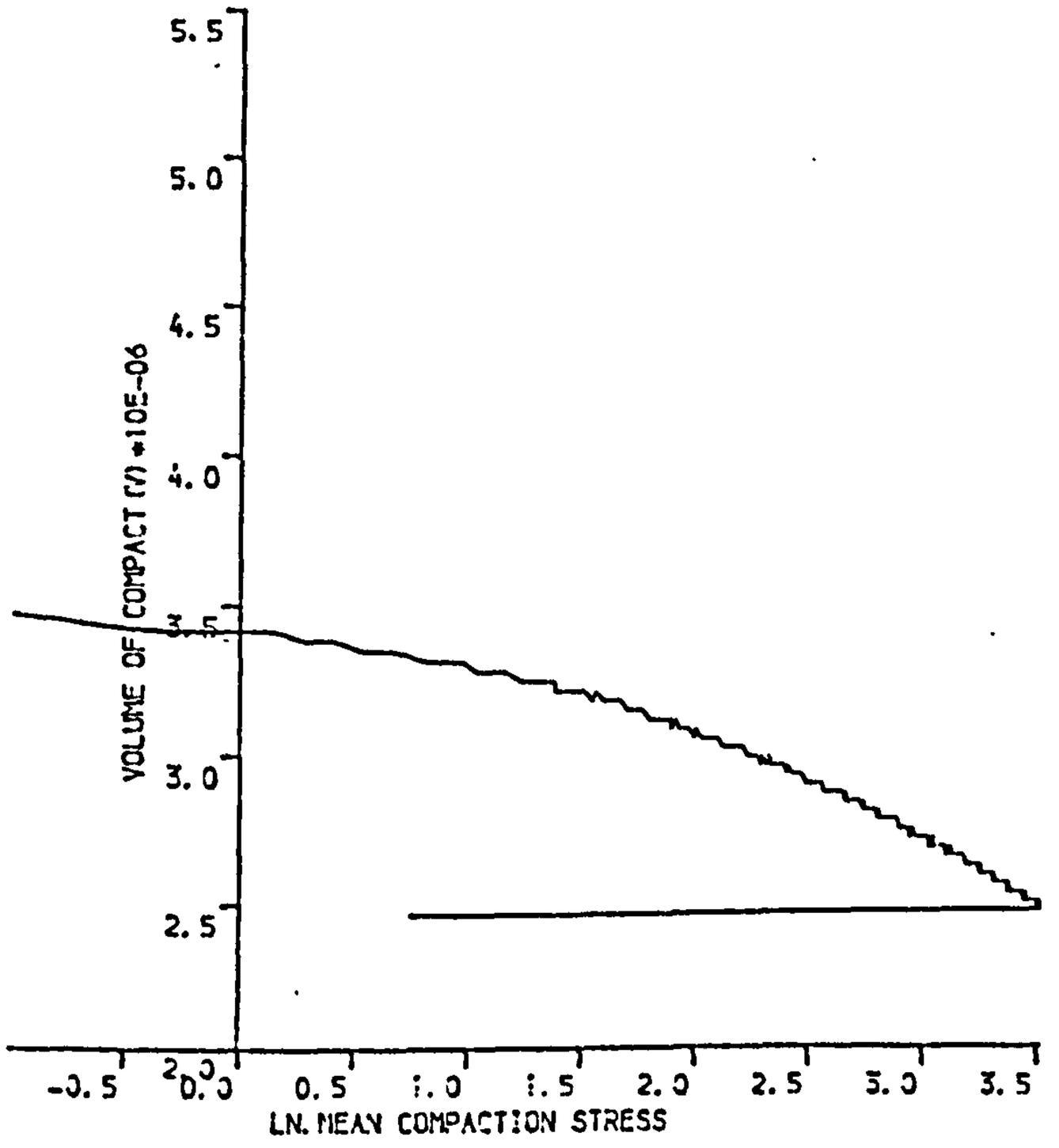

(B)

Figure 6.25 C-SODIUM CHLORIDE UNIAXIALLY COMPACTED AT 54MPA

(A) COMPACT VOLUME VERSUS MEAN COMPACTION STRESS

(B) COMPACT VOLUME VERSUS NATURAL LOGARITHMIC COMPACTION STRESS

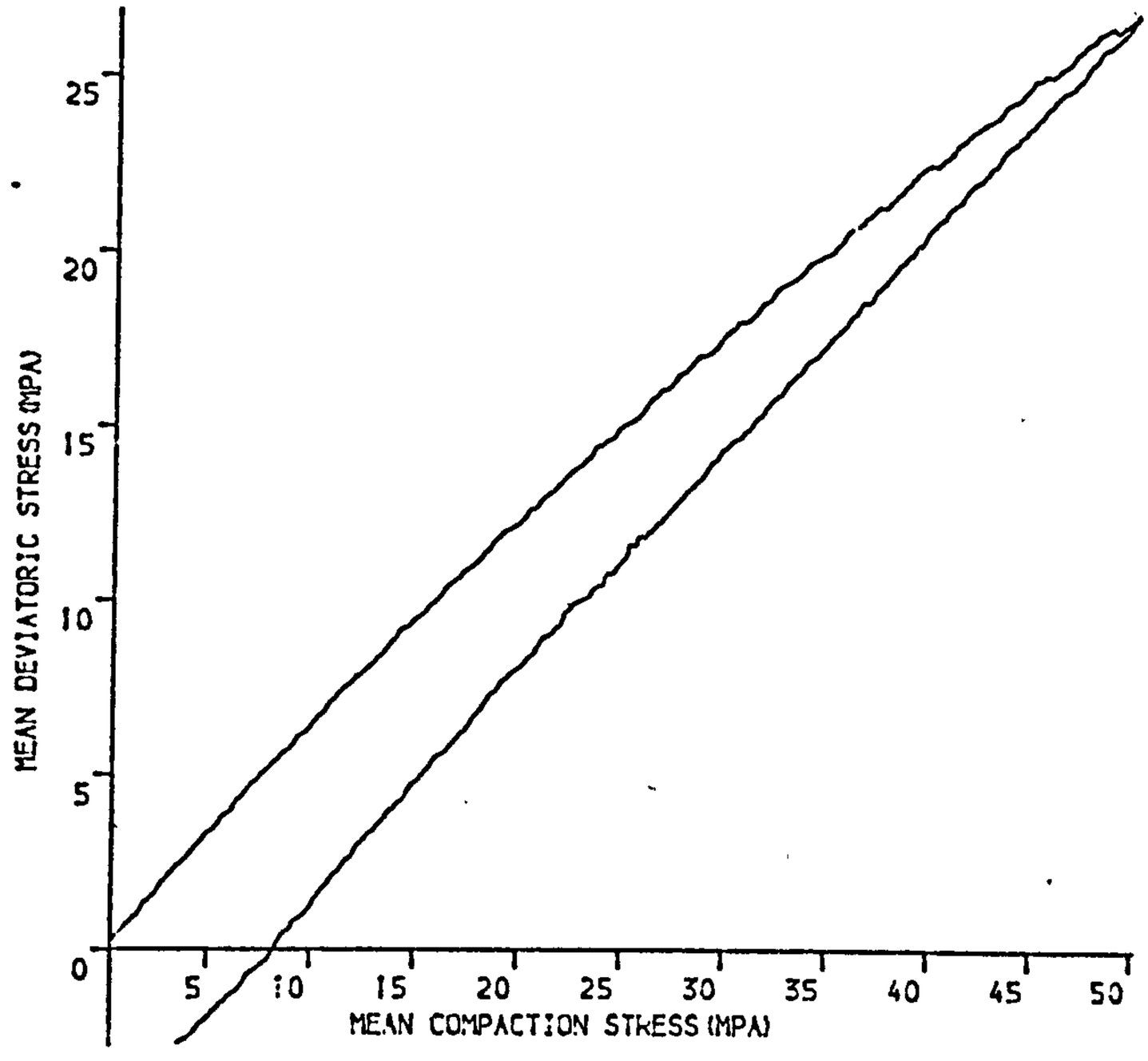

(A)

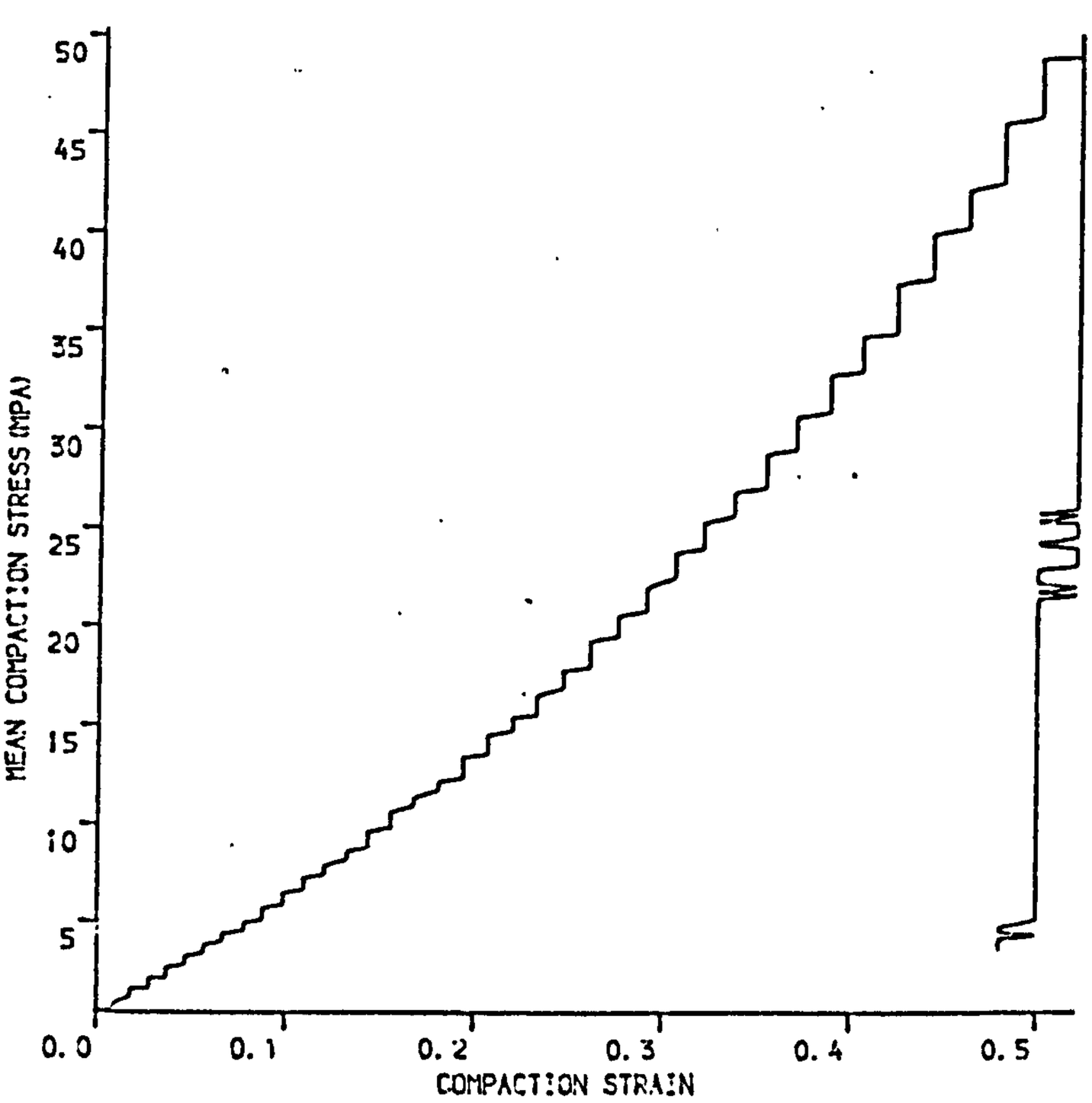

(B)

Figure 6.26 C-SODIUM CHLORIDE COMPACTED UNIAXIALLY AT 77MPA

(A) SHEAR STRESS VERSUS COMPACTION STRESS

(B) COMPACTION STRESS VERSUS NATURAL STRAIN

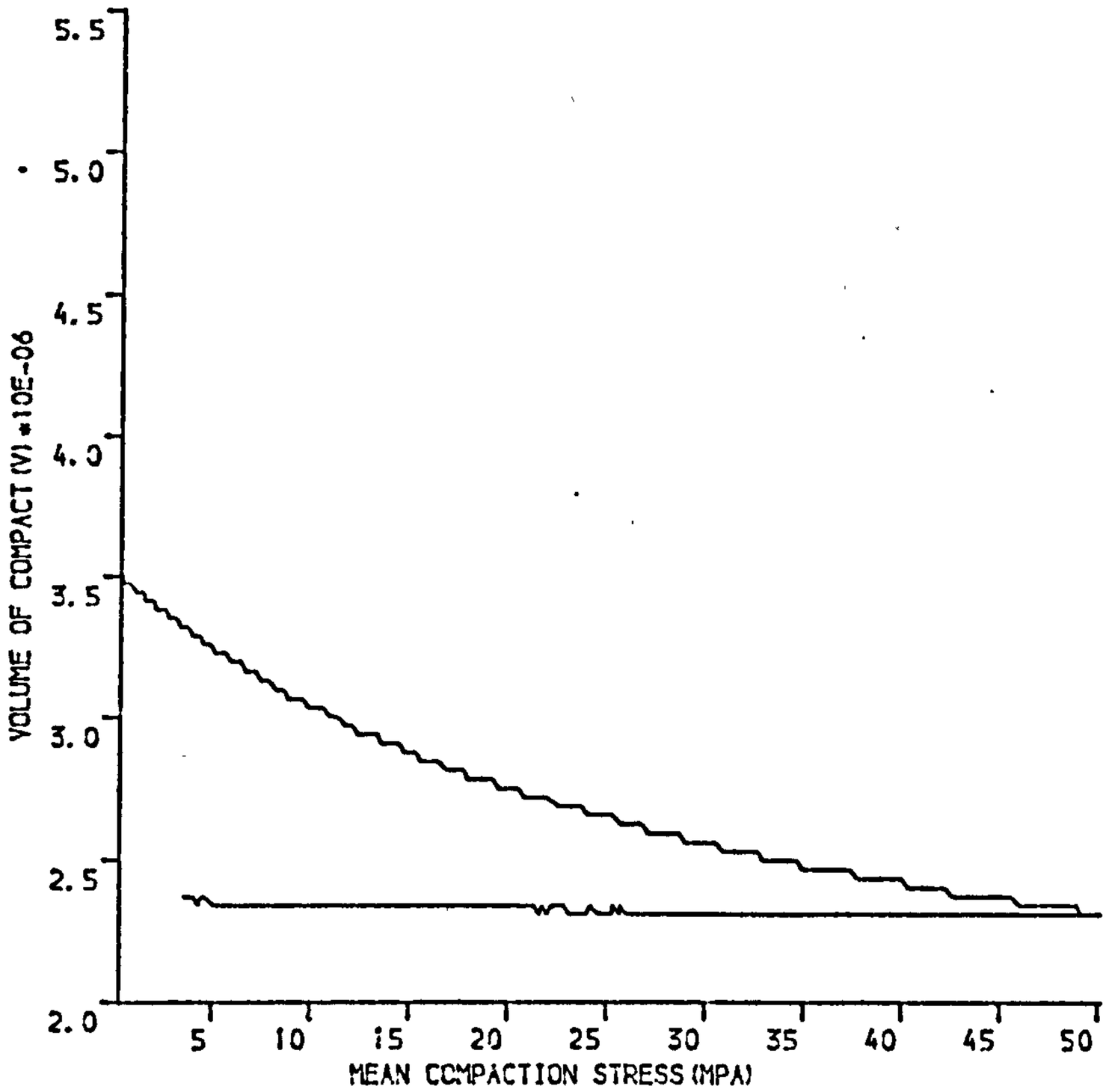

(A)

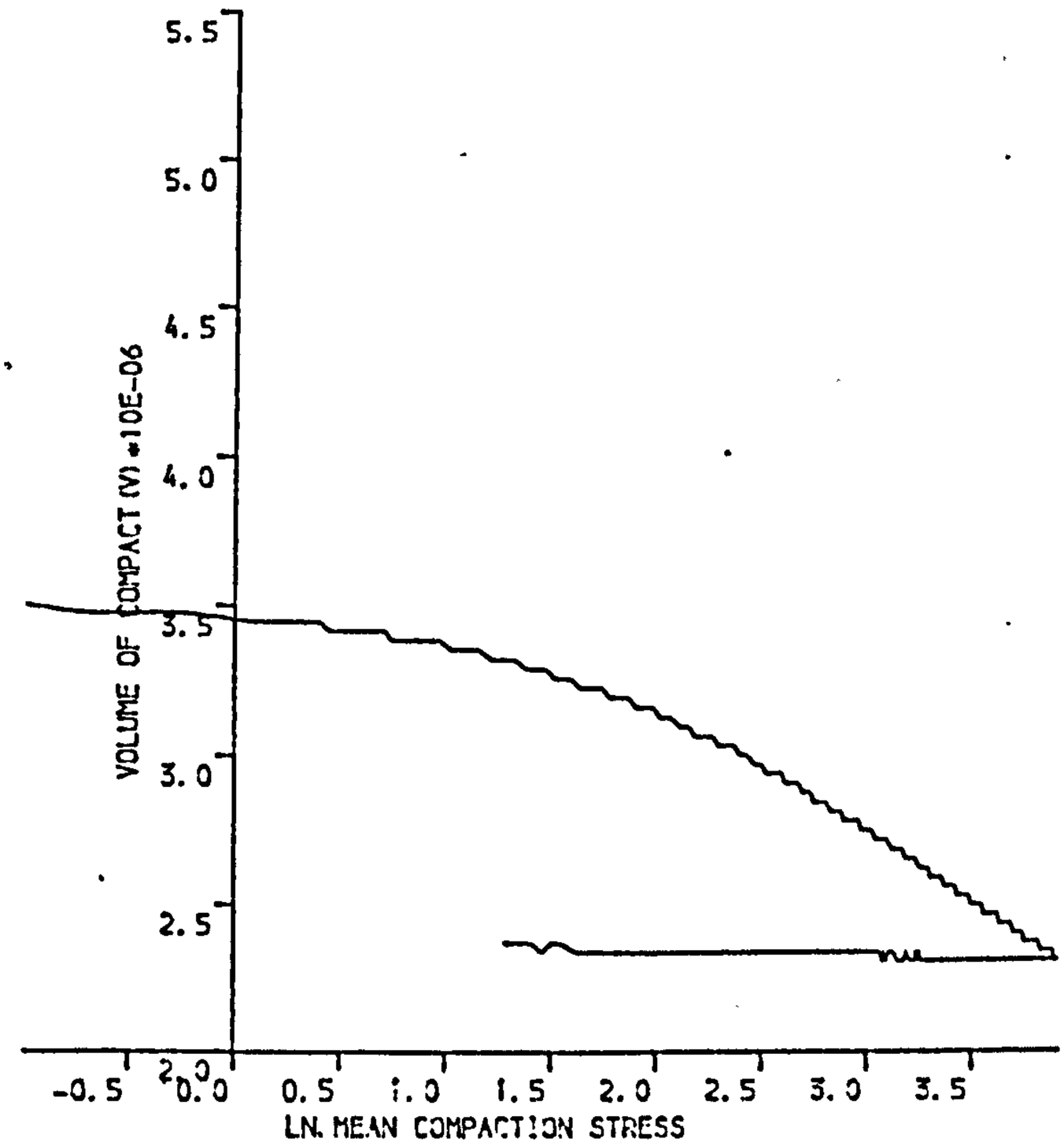

(B)

Figure 6.27 C-SODIUM CHLORIDE UNIAXIALLY COMPACTED AT 77MPA

(A) COMPACT VOLUME VERSUS MEAN COMPACTION STRESS

(B) COMPACT VOLUME VERSUS NATURAL LOGARITHMIC COMPACTION STRESS

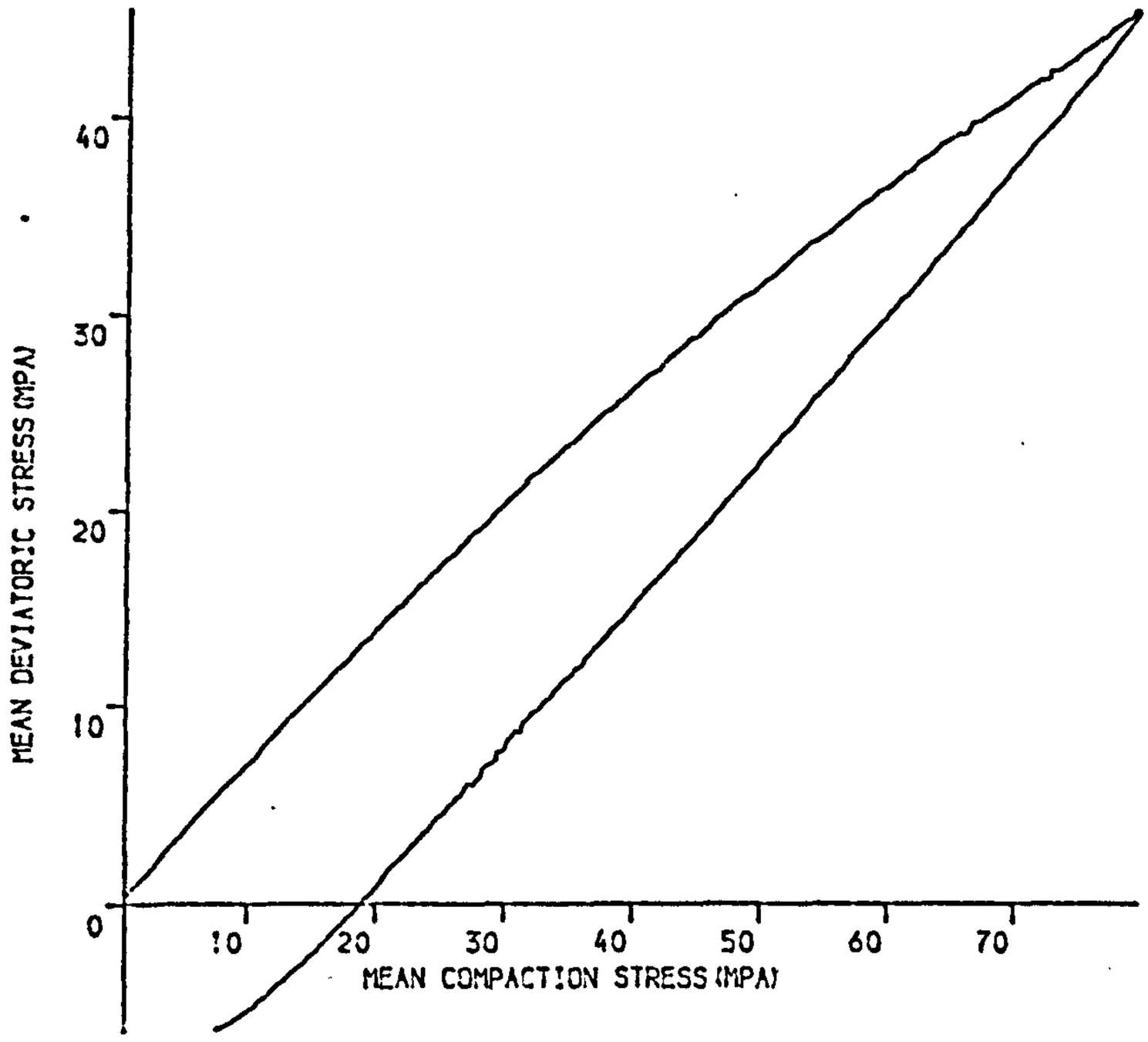

(A)

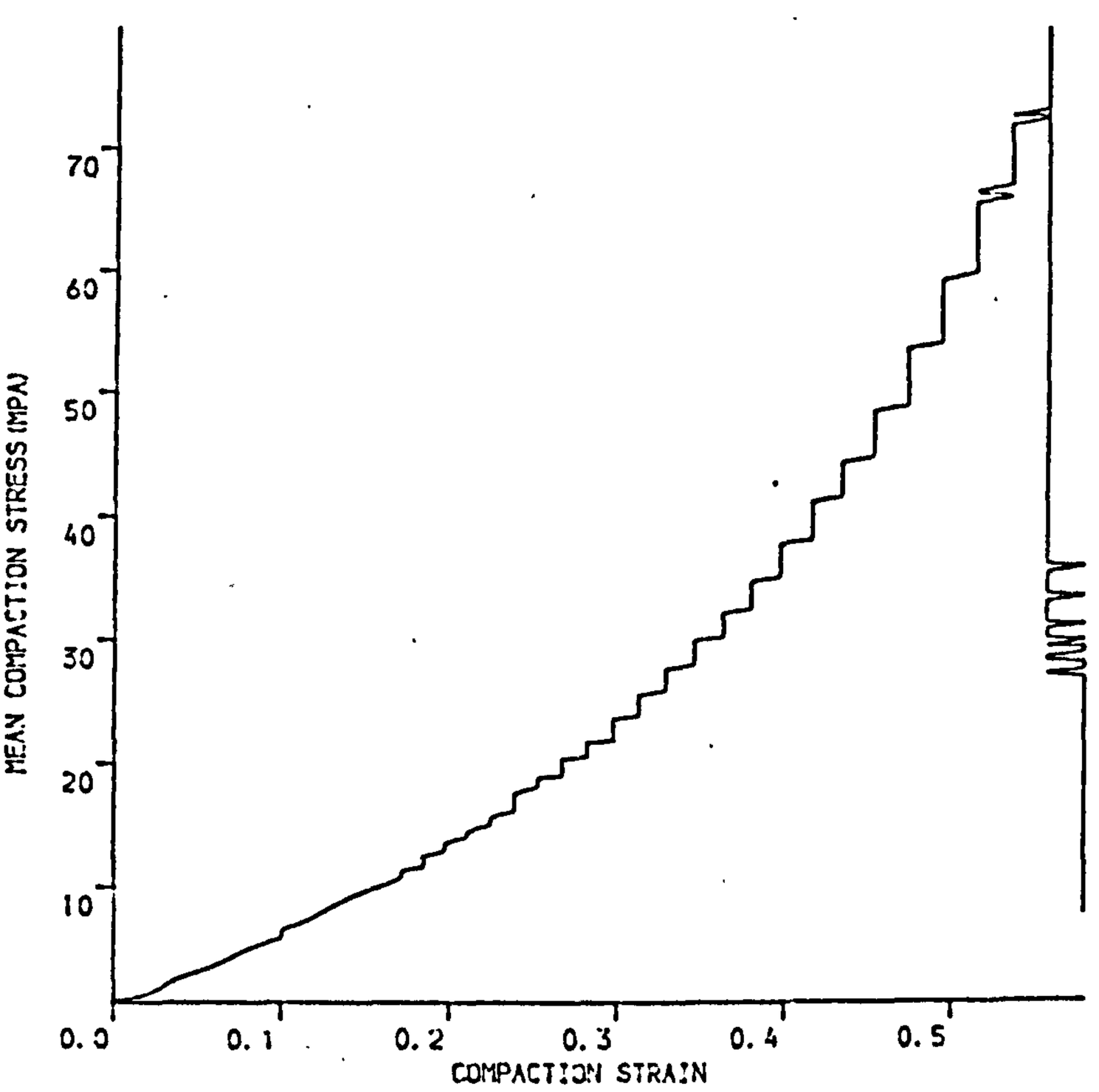

(B)

Figure 6.28 C-SODIUM CHLORIDE COMPACTED UNIAXIALLY AT 125MPA
(A) SHEAR STRESS VERSUS COMPACTION STRESS
(B) COMPACTION STRESS VERSUS NATURAL STRAIN

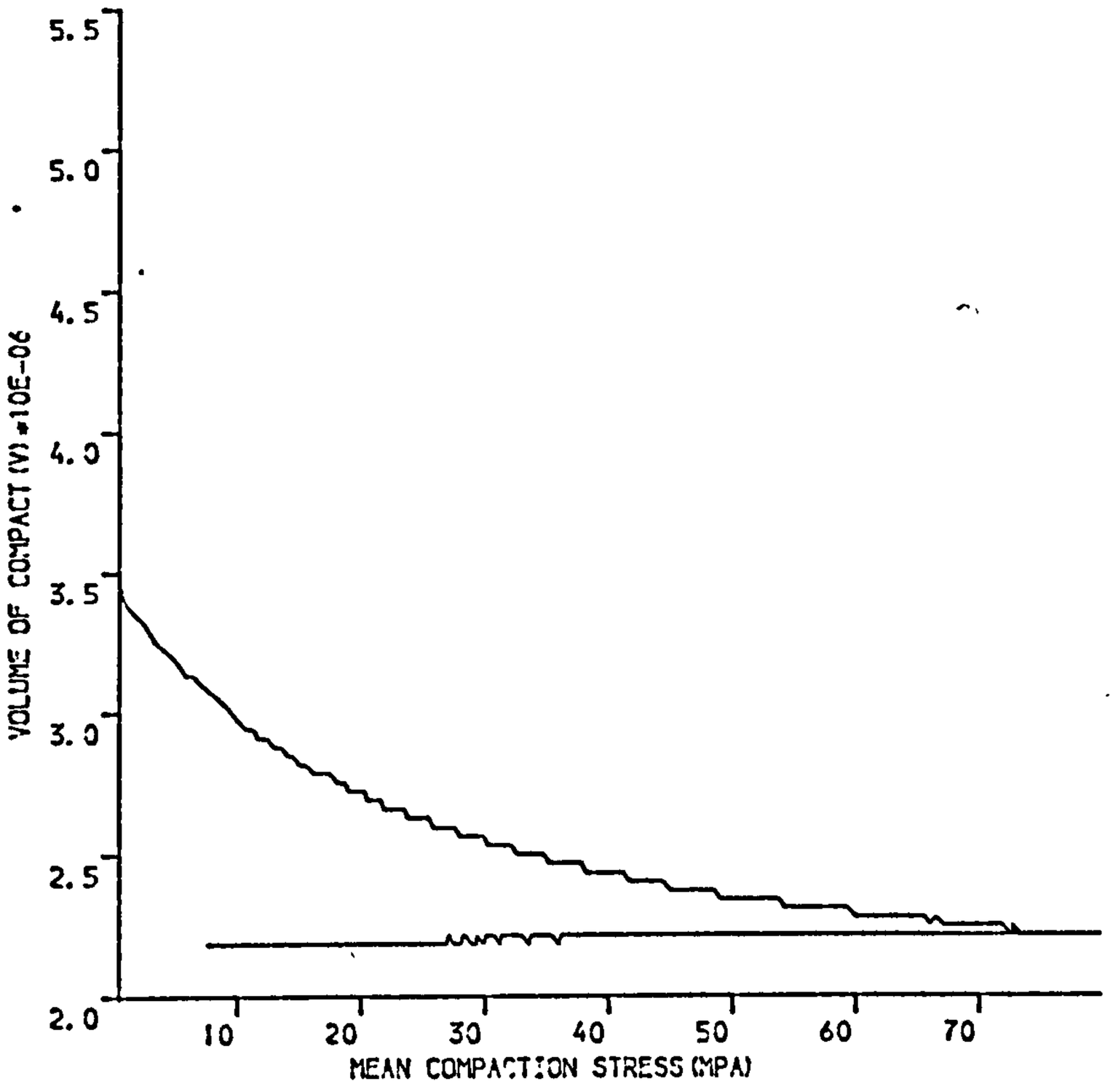

(A)

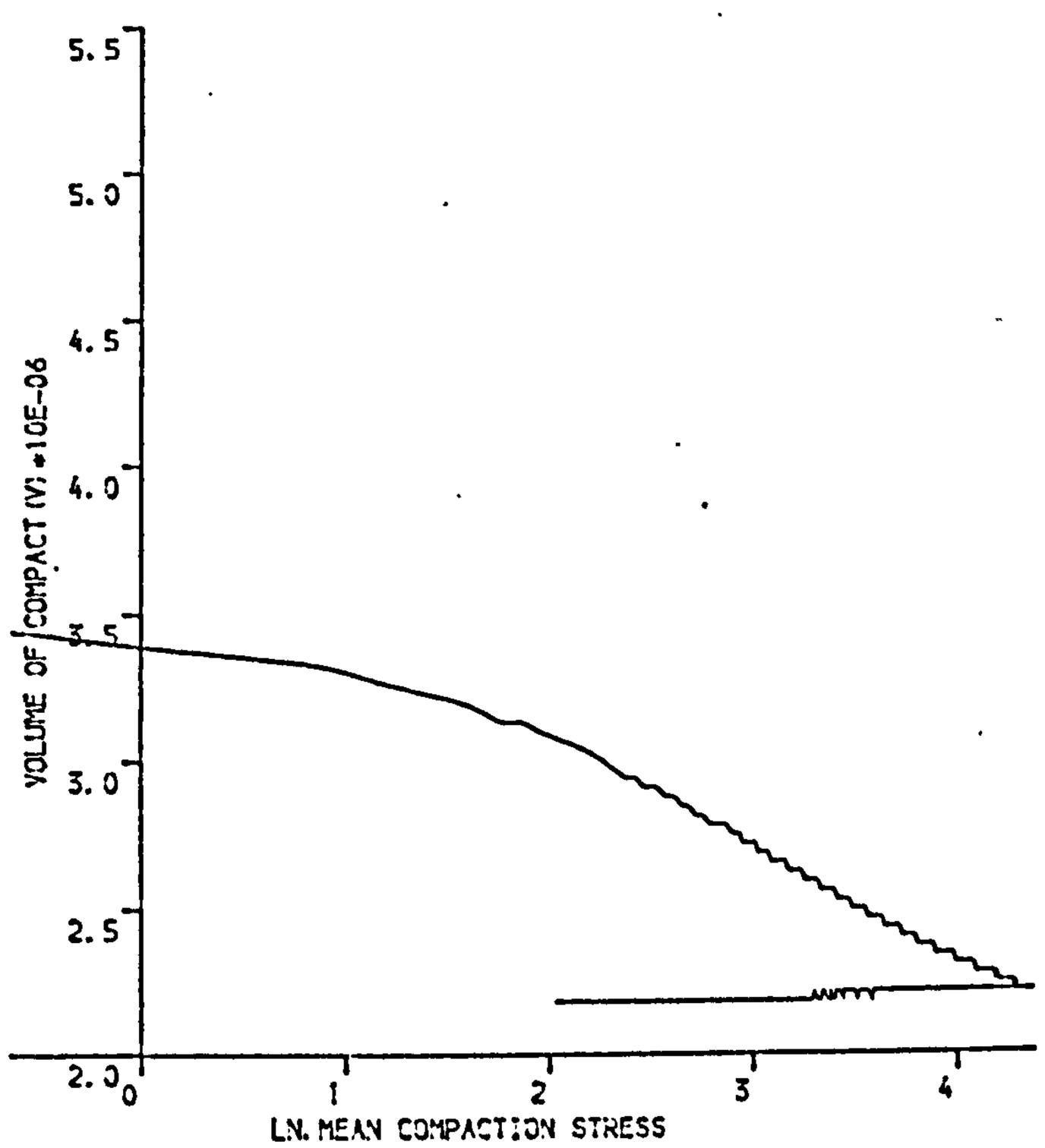

(B)

Figure 6.29 C-SODIUM CHLORIDE UNIAXIALLY COMPACTED AT 125MPA

(A) COMPACT VOLUME VERSUS MEAN COMPACTION STRESS

(B) COMPACT VOLUME VERSUS NATURAL LOGARITHMIC COMPACTION STRESS

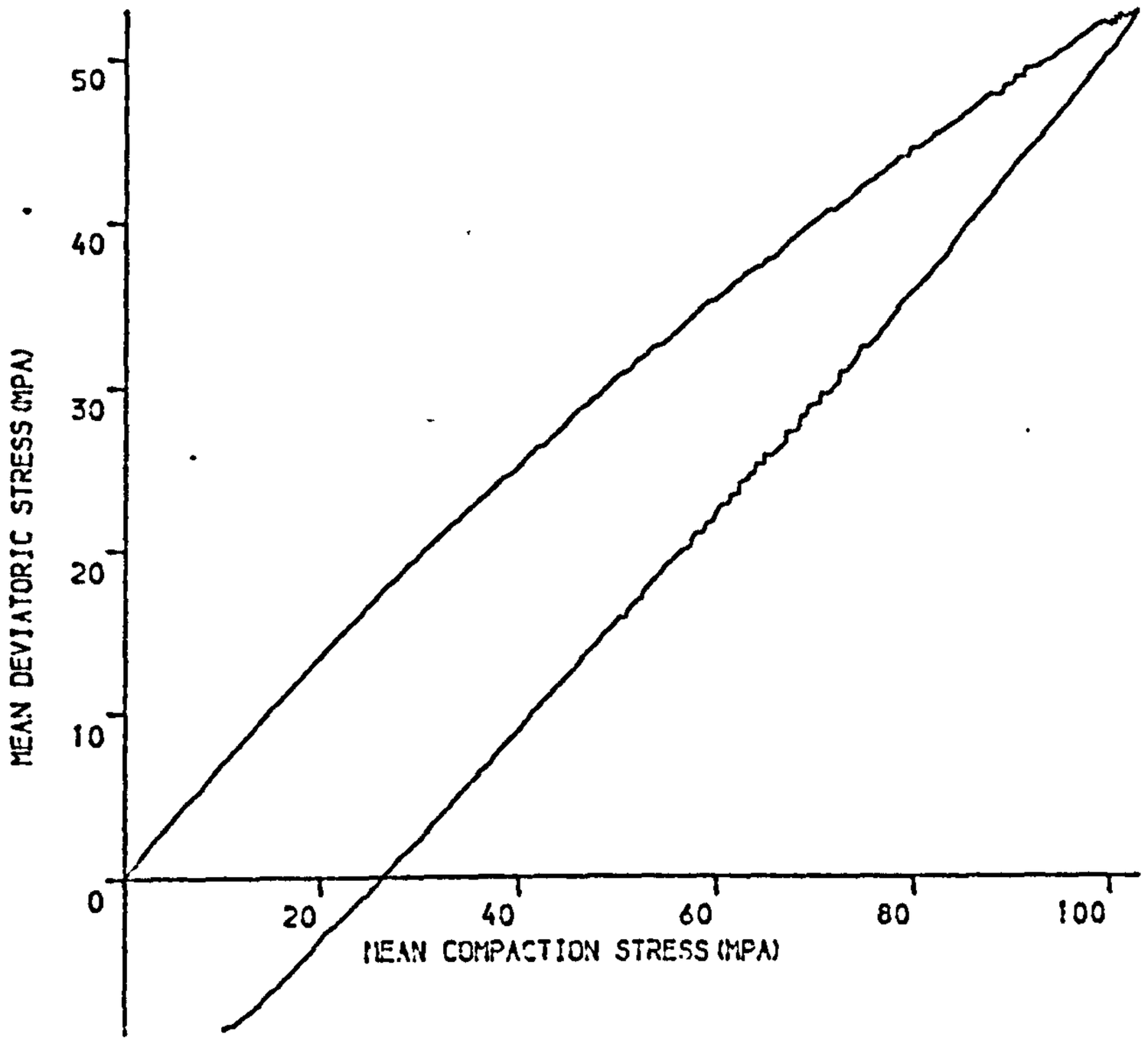

(A)

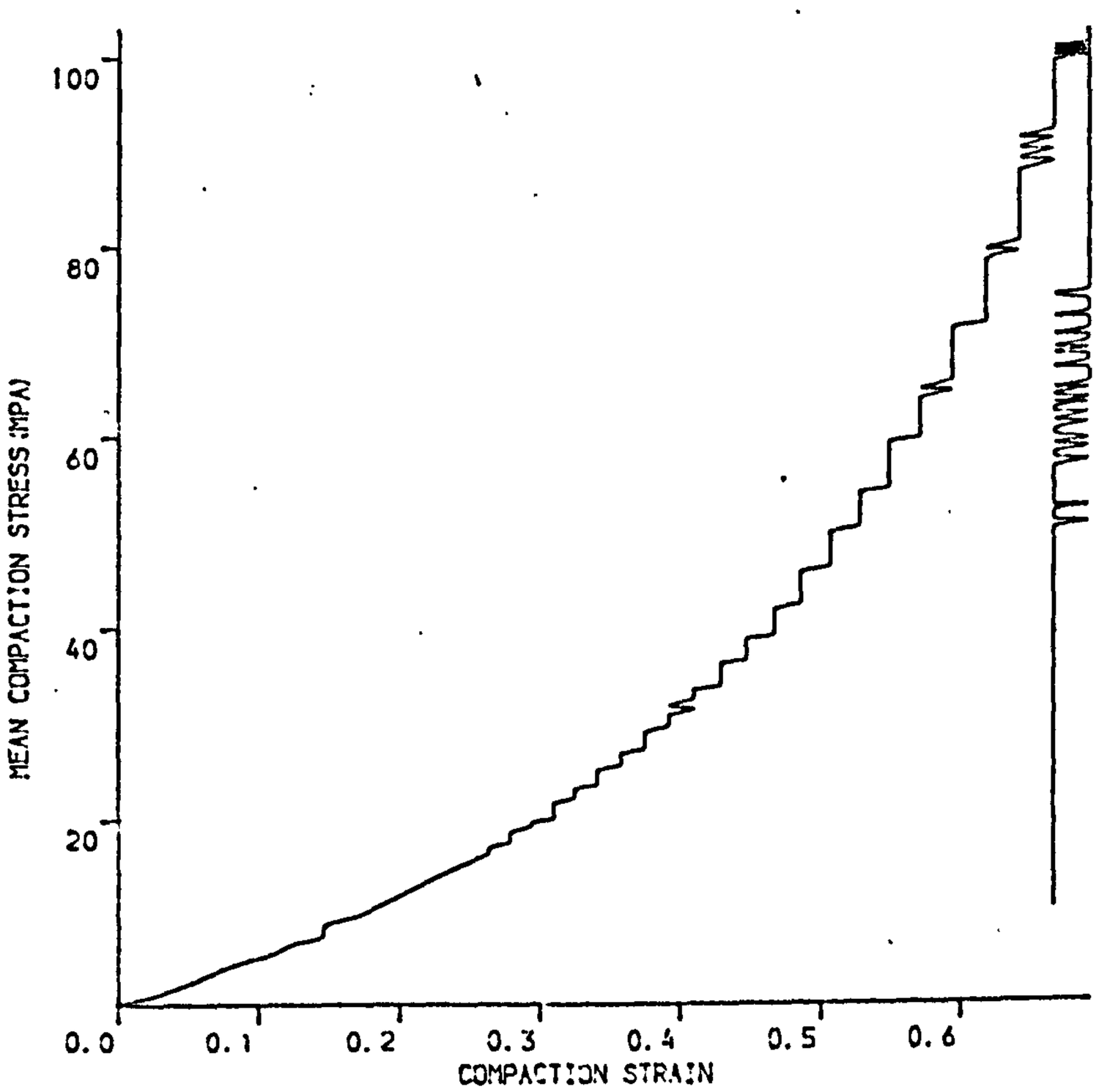

(B)

Figure 6.30 C-SODIUM CHLORIDE COMPACTED UNIAXIALLY AT 155MPA

(A) SHEAR STRESS VERSUS COMPACTION STRESS

(B) COMPACTION STRESS VERSUS NATURAL STRAIN

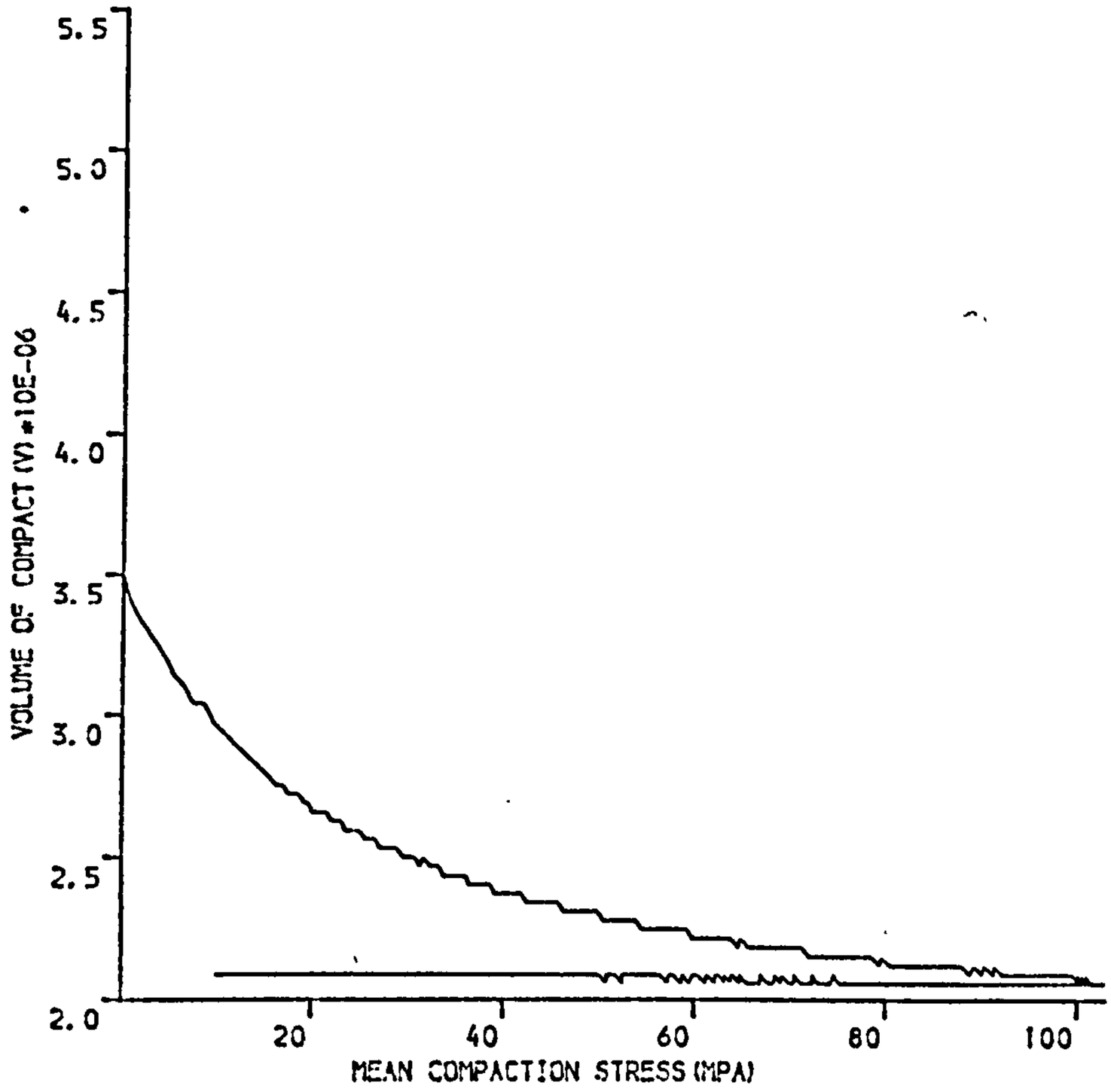

(A)

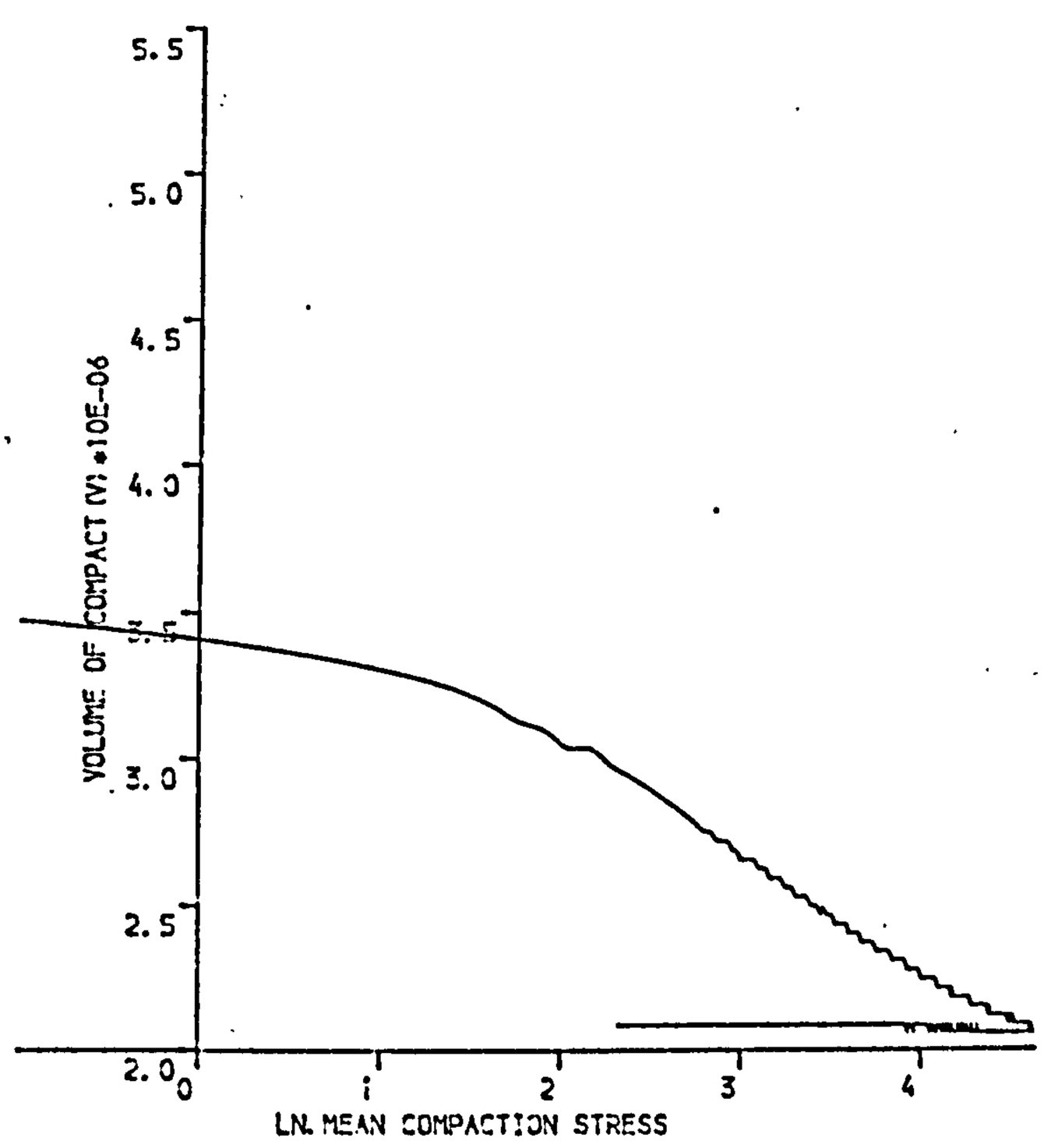

(B)

Figure 6.31 C-SODIUM CHLORIDE UNIAXIALLY COMPACTED AT 155MPA
(A) COMPACT VOLUME VERSUS MEAN COMPACTION STRESS
(B) COMPACT VOLUME VERSUS NATURAL LOGARITHMIC COMPACTION STRESS

Figure 6.32 3-D representation of compaction of C-sodium chloride compacted at 54 MPa

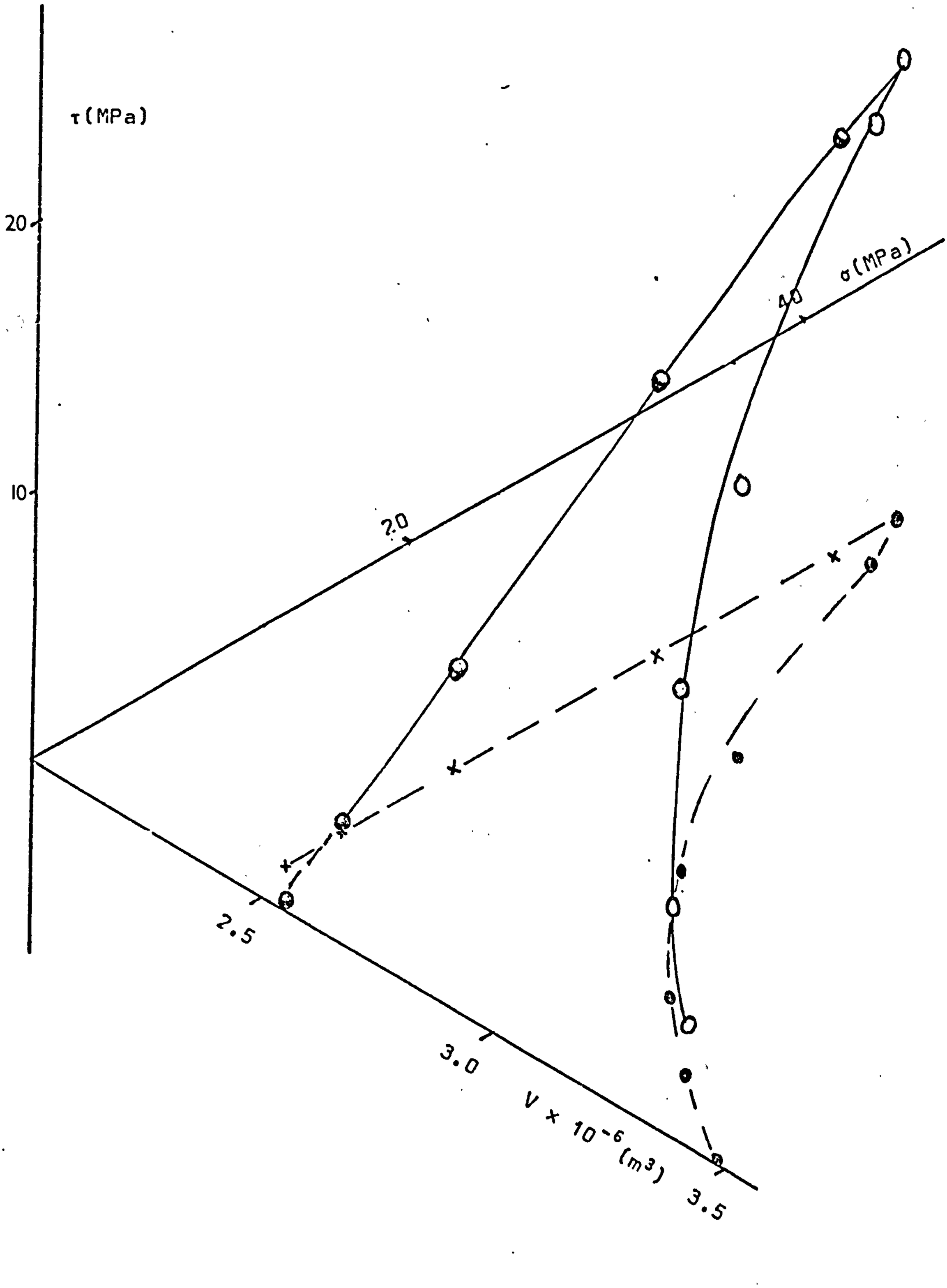

Figure 6.33 3-D representation of compaction of C-sodium chloride compacted at 77 MPa

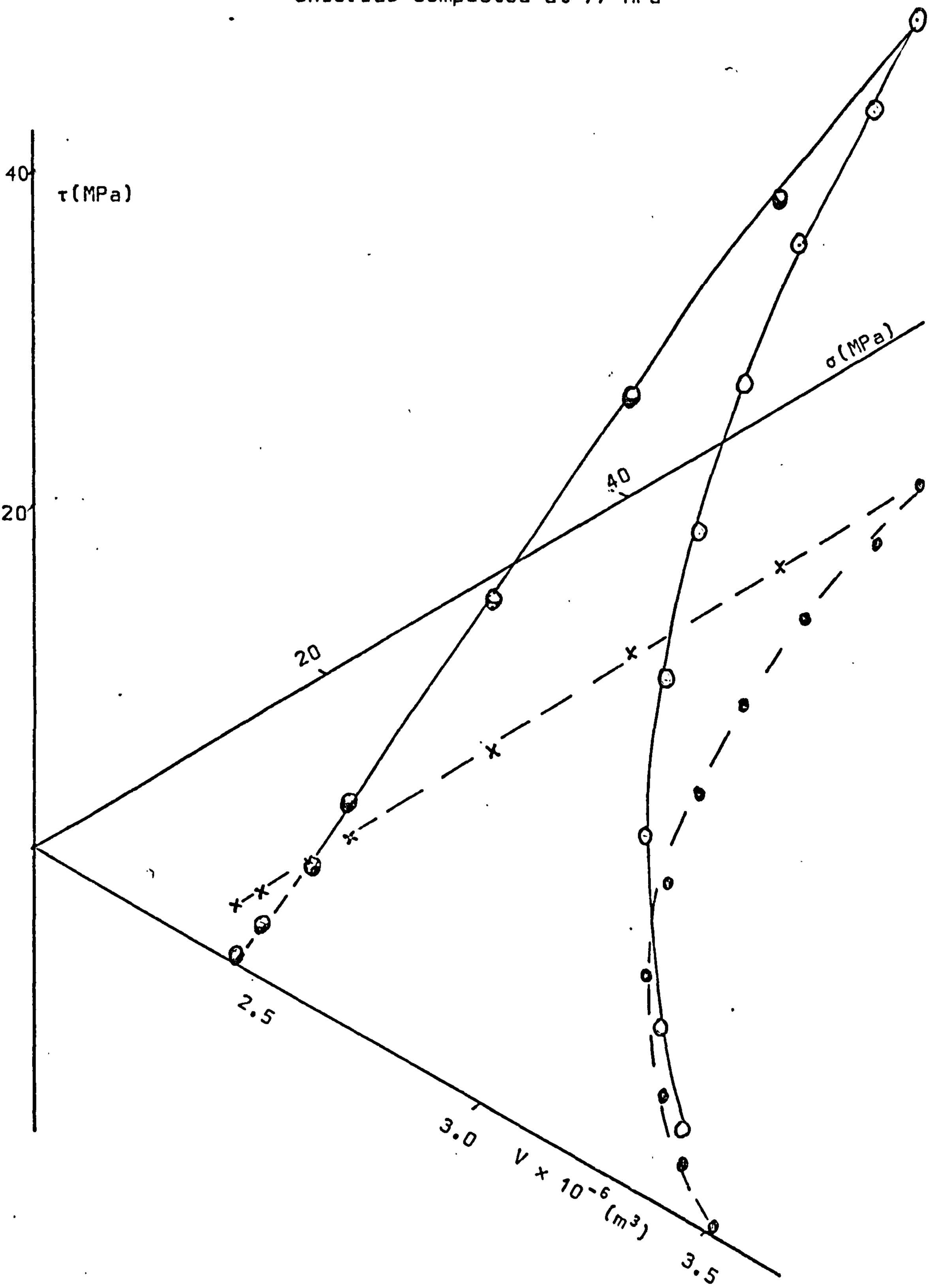

Figure 6.34 3-D representation of compaction of C-sodium chloride compacted at 125 MPa

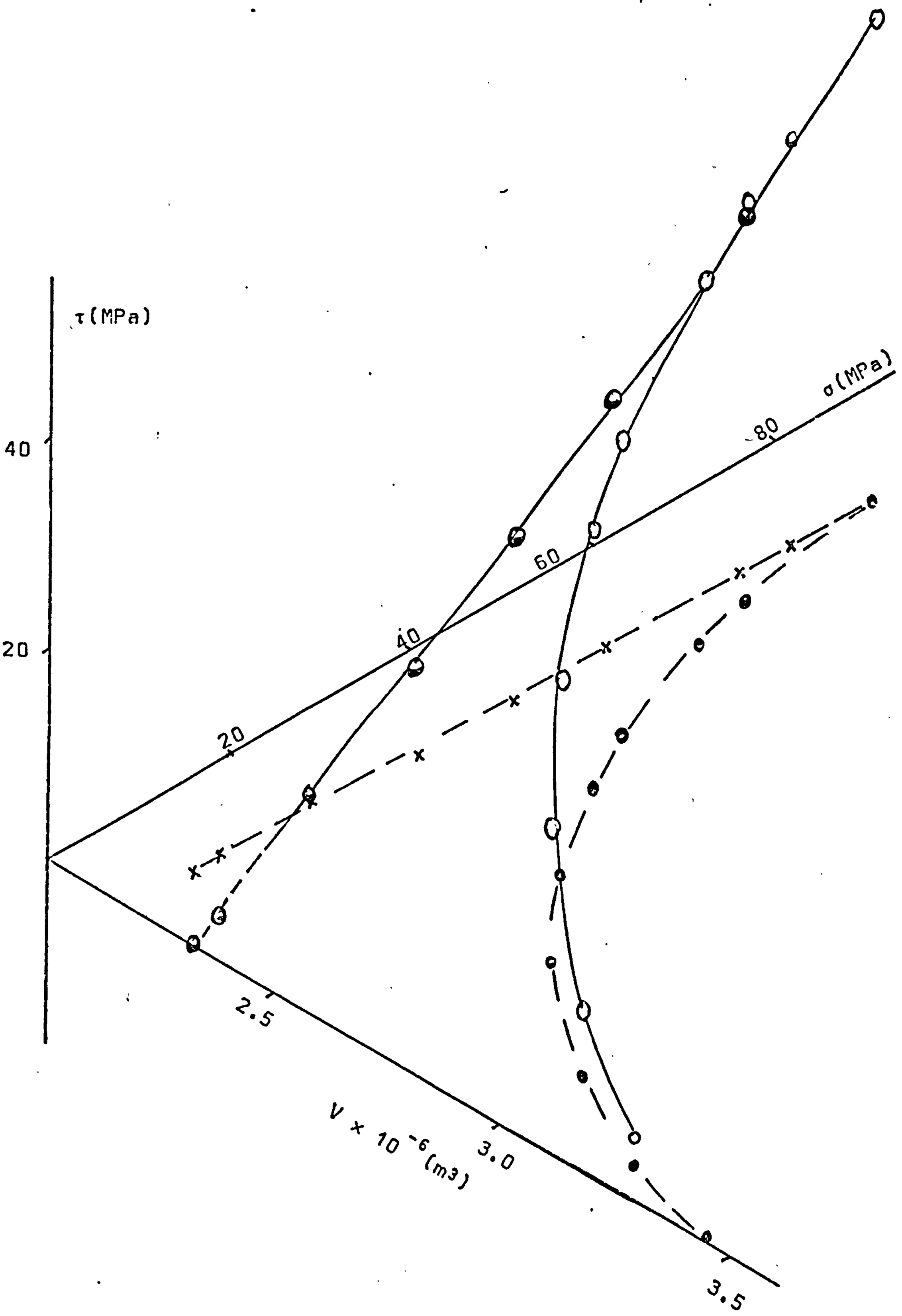

Figure 6.35 3-D representation of compaction of C-sodium chloride compacted at 155 MPa

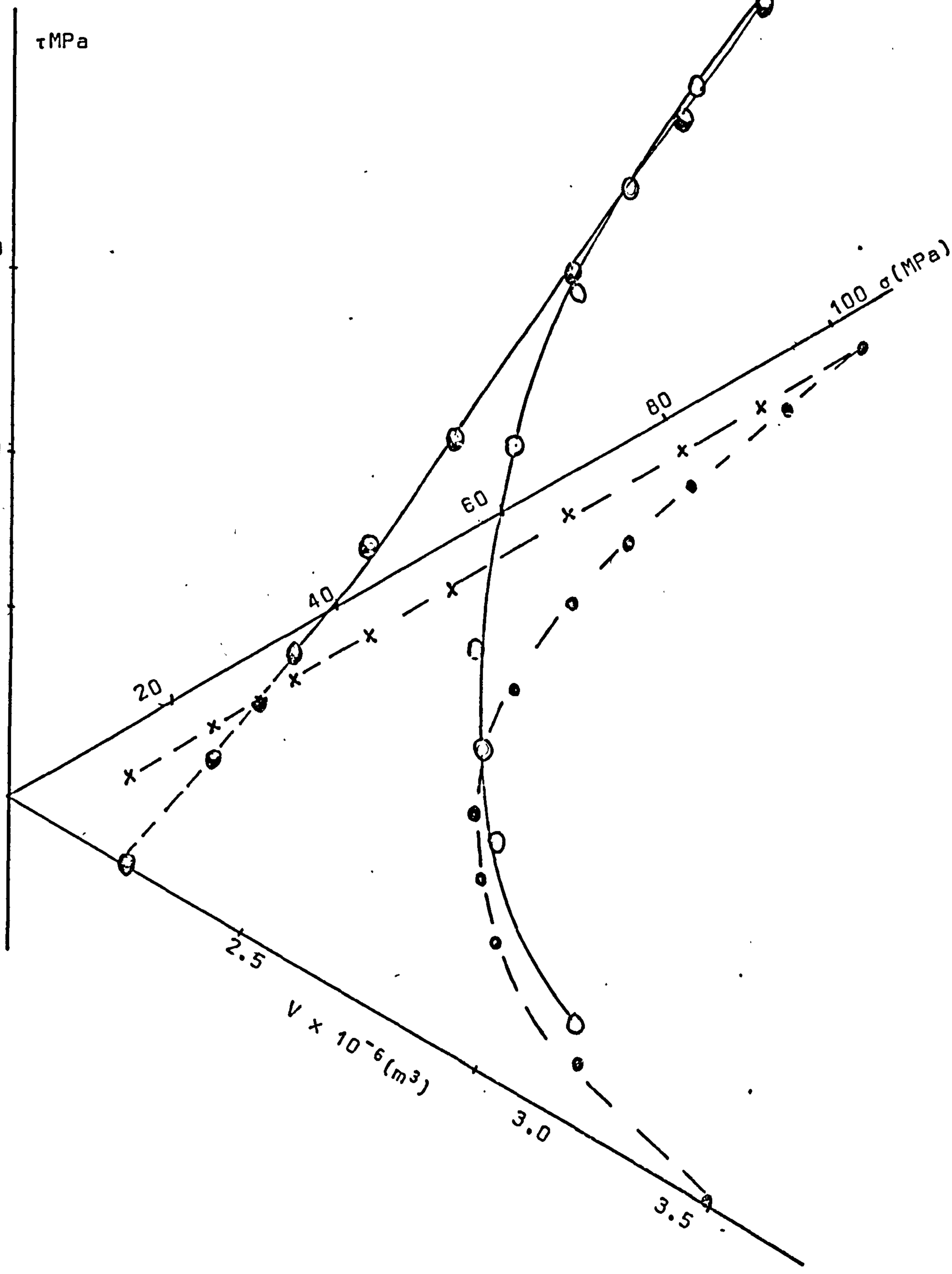

Figure 6.36 Mohr circles constructed for dicalcium phosphate compacted at 20 MPa

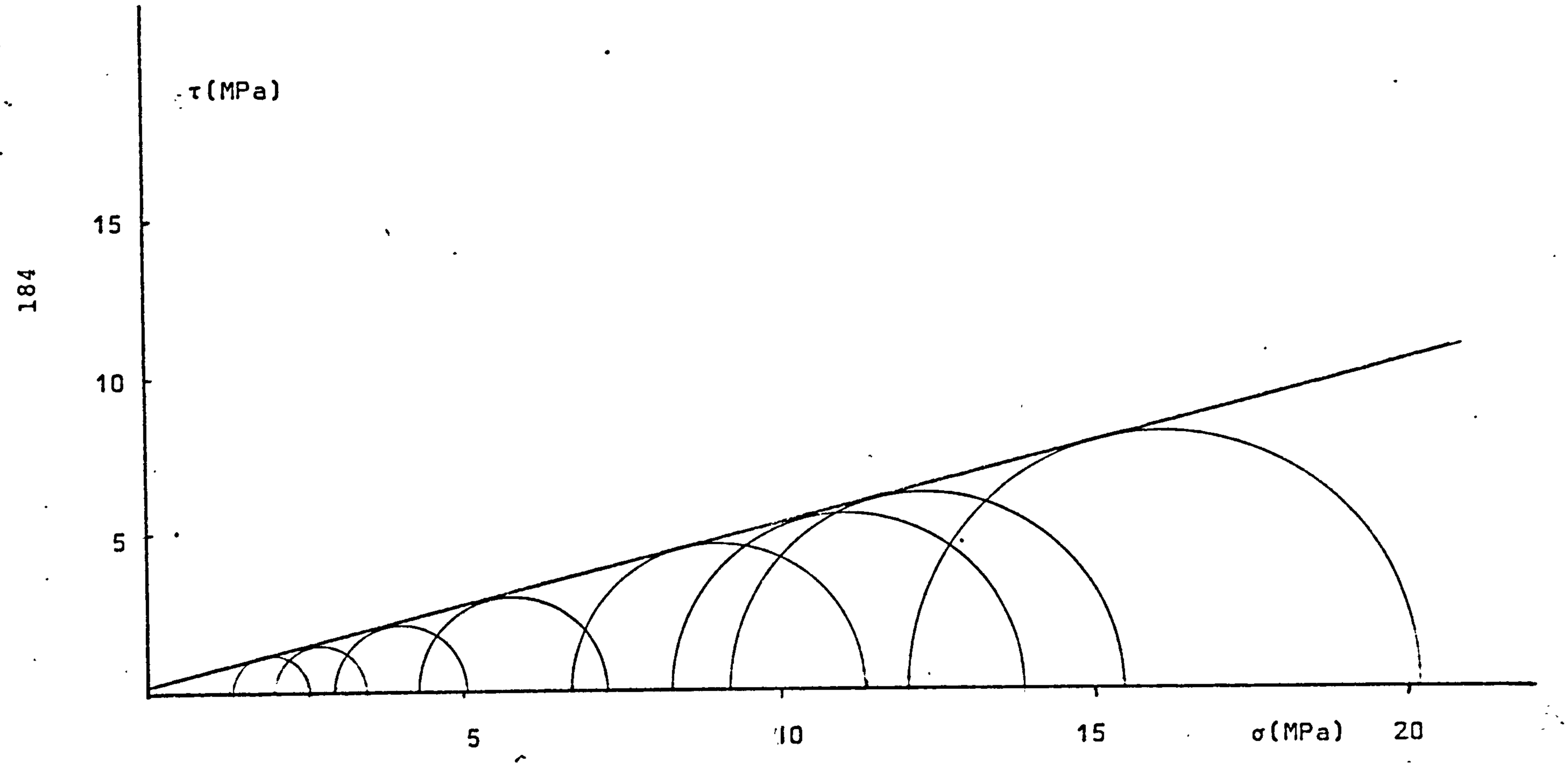

Figure 6.37 Mohr circles constructed for dicalcium phosphate compacted at 36 MPa

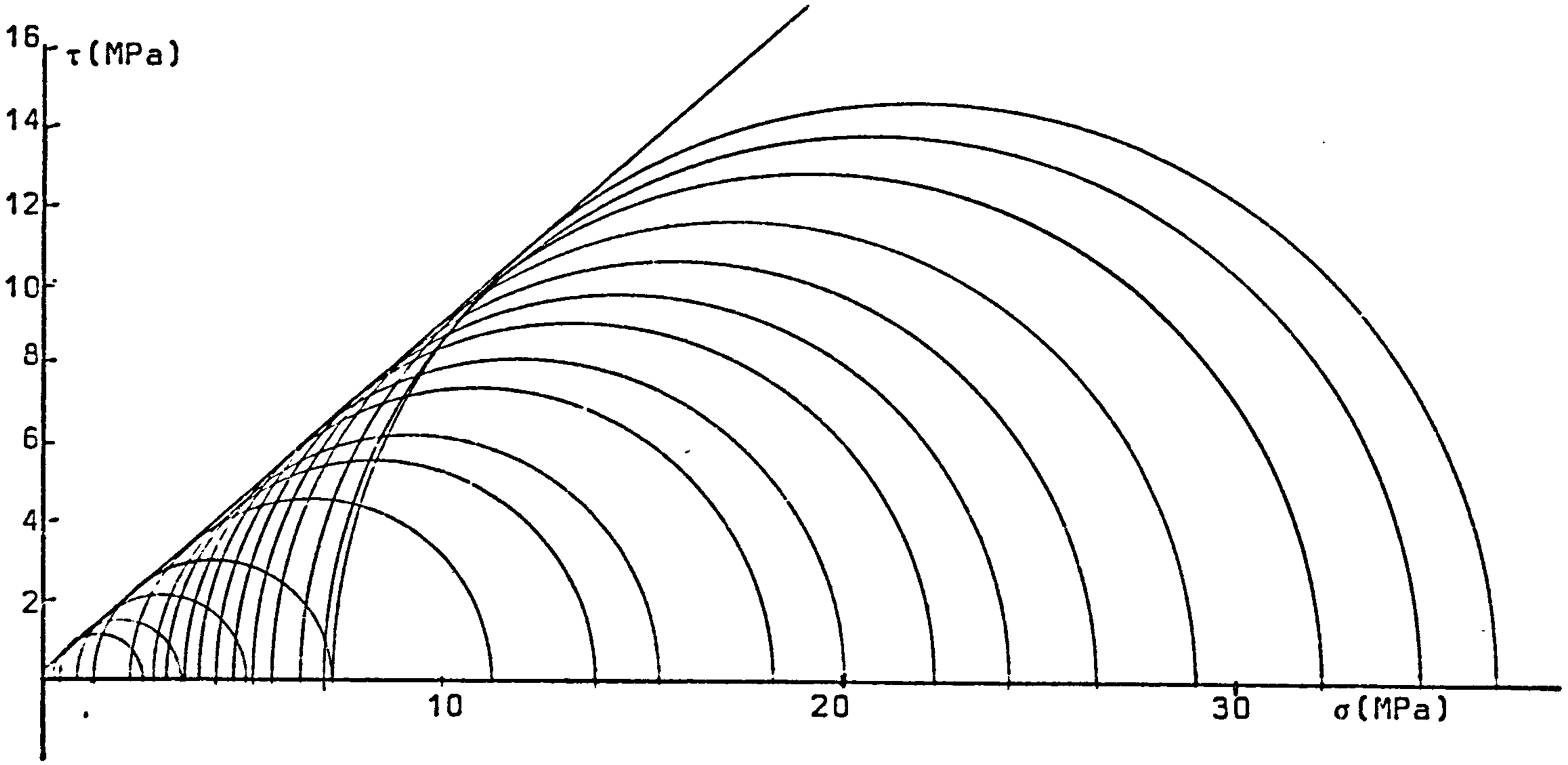

Figure 6.38 Mohr circles constructed for dicalcium phosphate compacted at 62 MPa

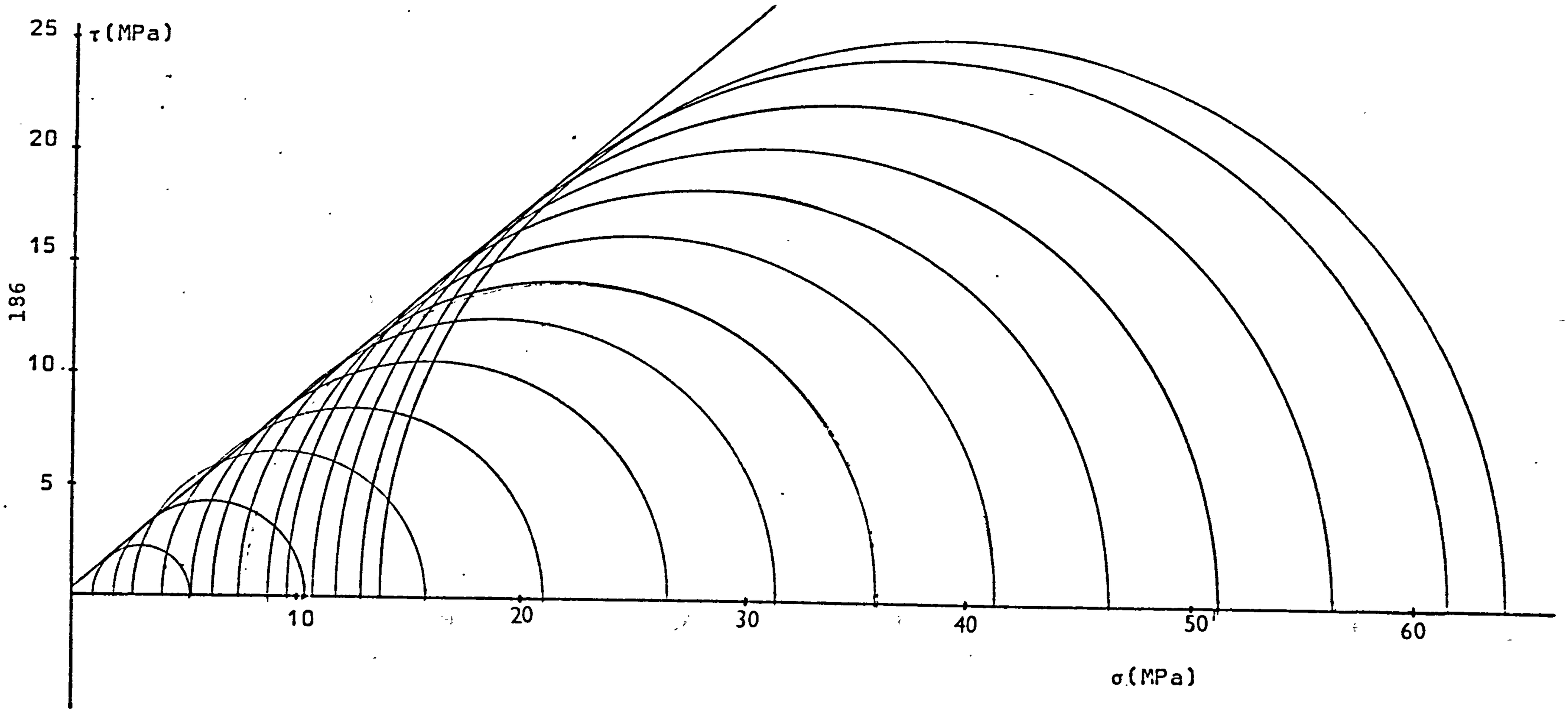

Figure 6.39 Mohr circles constructed for dicalcium phosphat ε compacted at 120 MPa

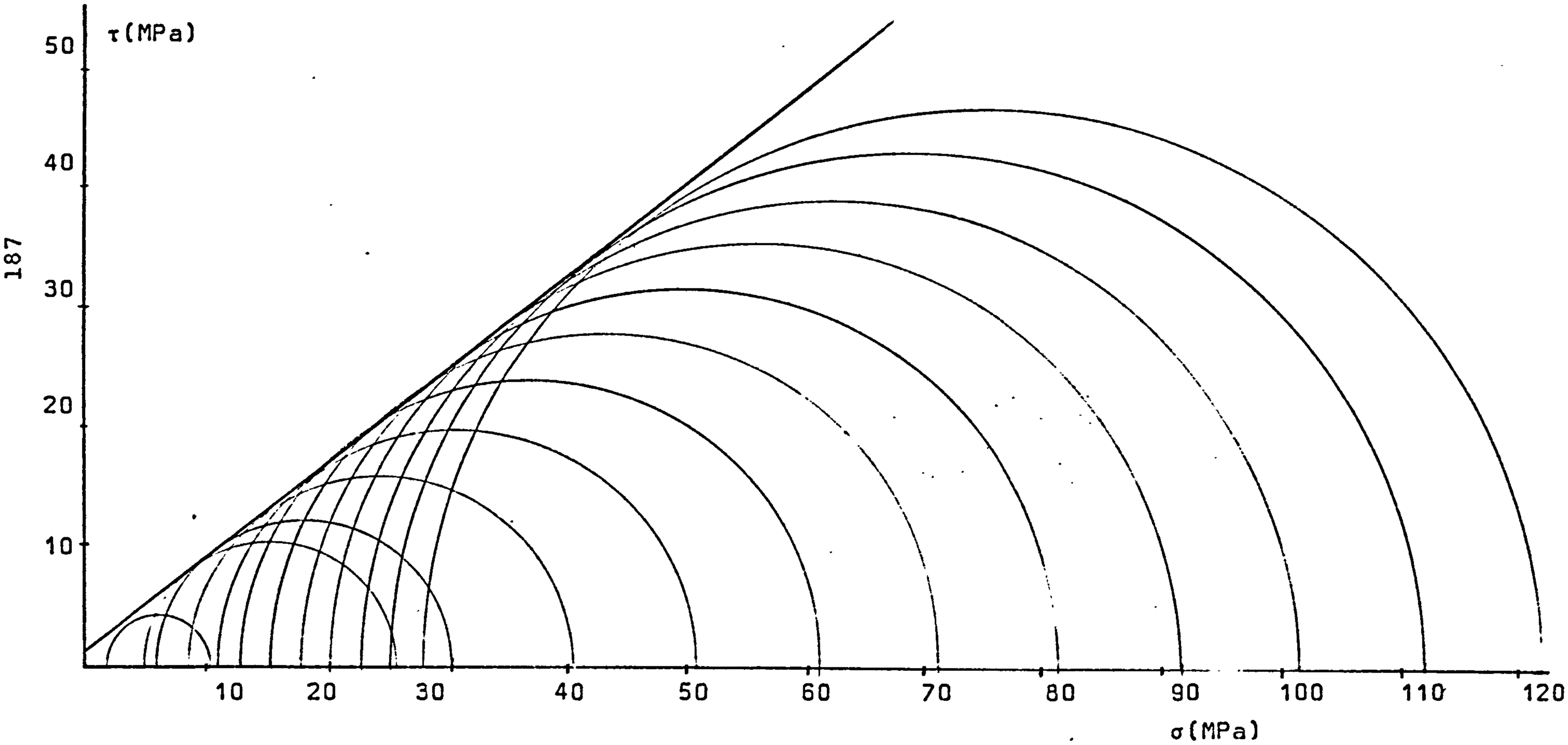

Figure 6.40 Mohr circles constructed for dicalcium phosphate compacted at 150 MPa

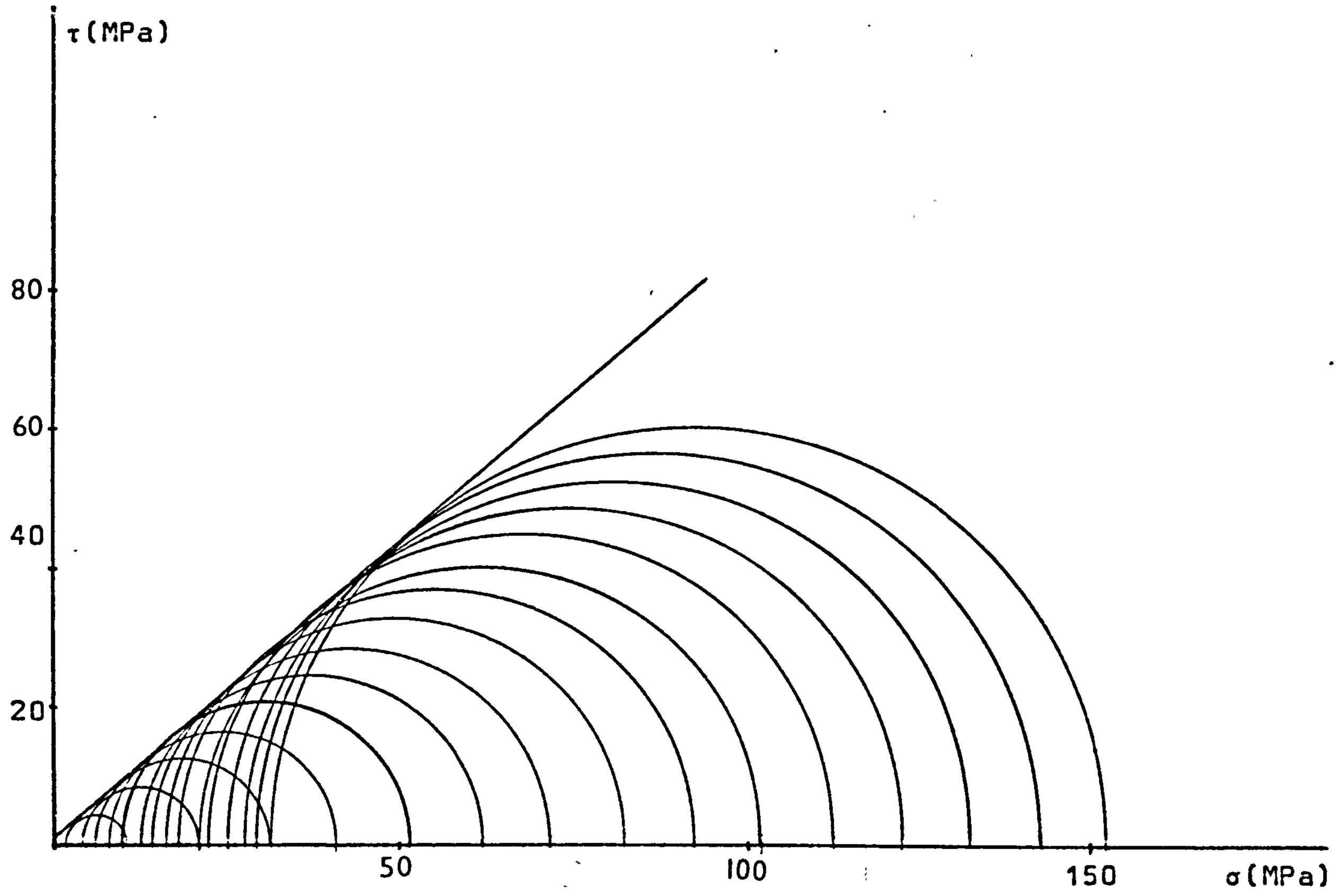

Figure 6.41 Mohr circles constructed for dicalcium phosphate compacted at 247 MPa

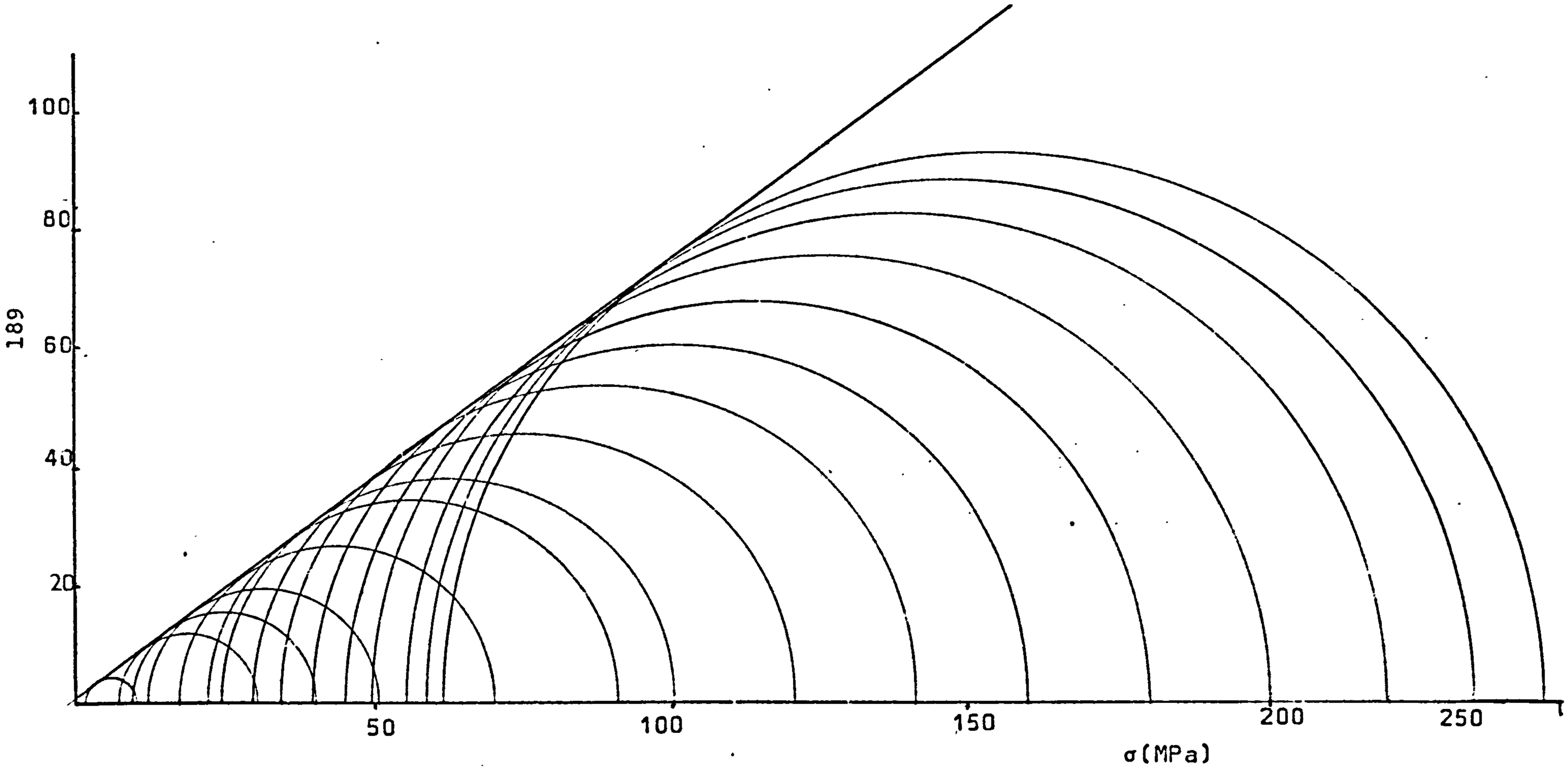

PAGE NUMBERS CUT OFF

IN

ORIGINAL

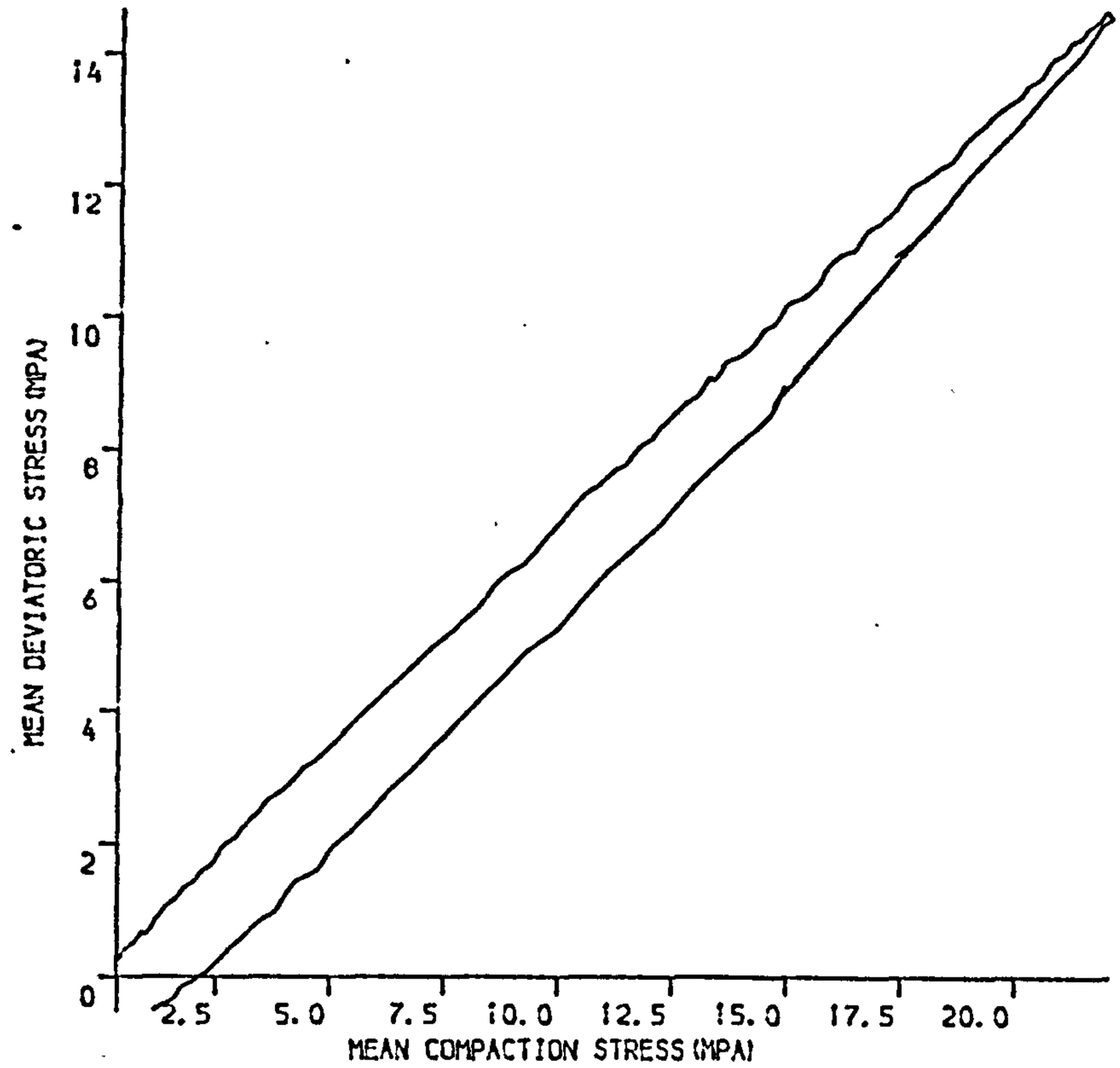

(A)

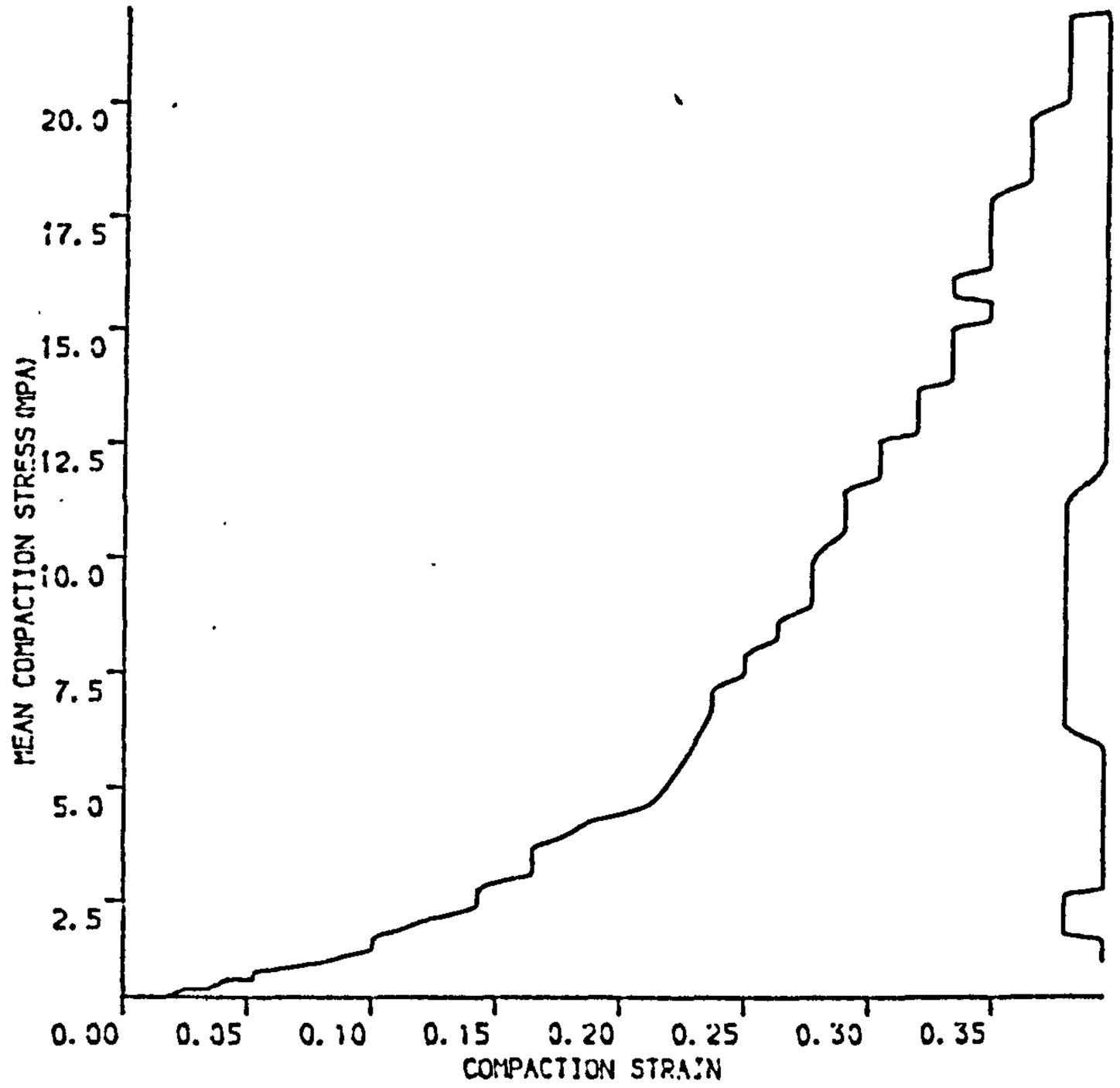

(B)

Figure 6.42 DICALCIUM PHOSPHATE COMPACTED UNIAXIALLY AT 36MPA
(A) SHEAR STRESS VERSUS COMPACTION STRESS
(B) COMPACTION STRESS VERSUS NATURAL STRAIN

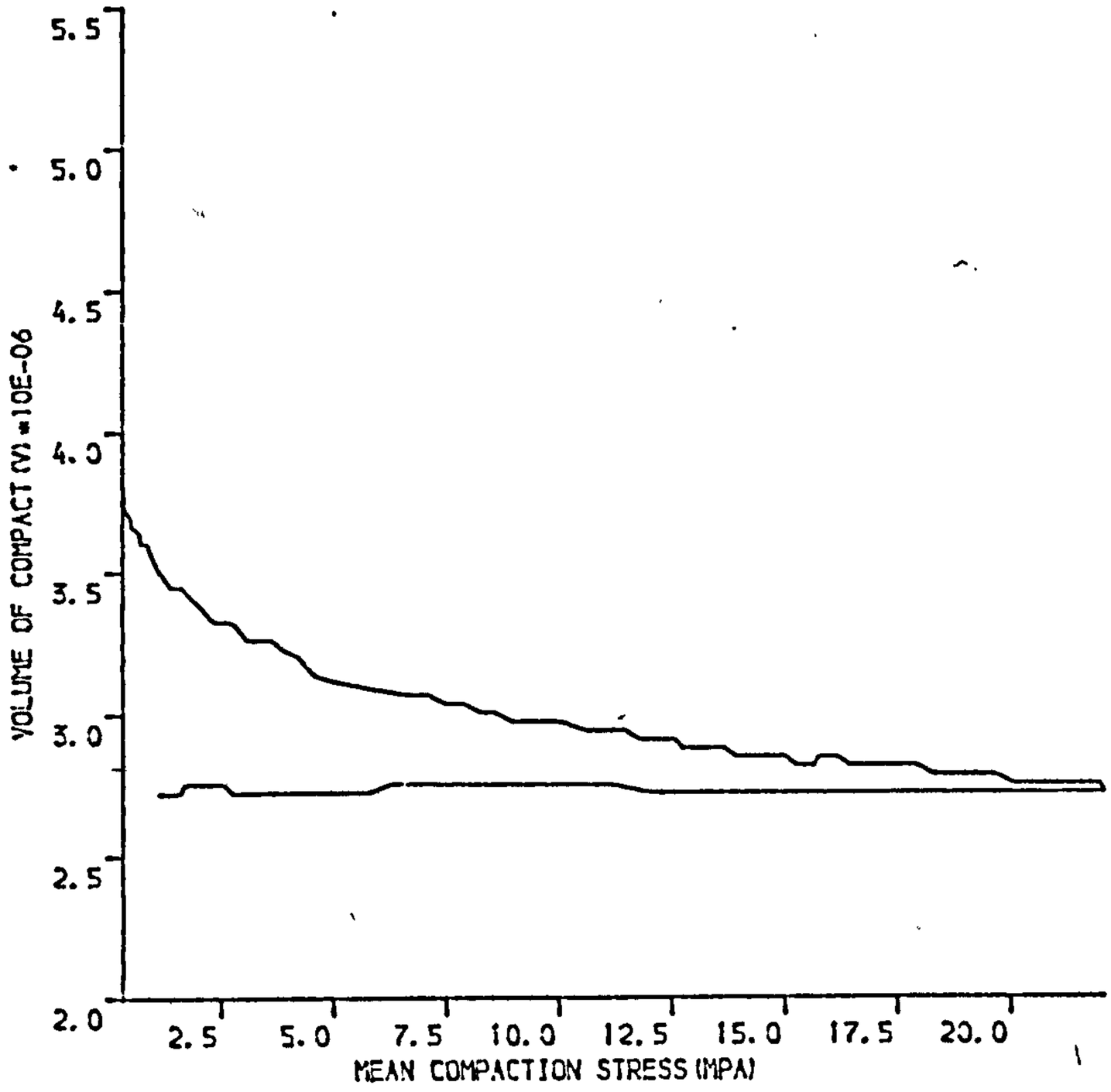

(A)

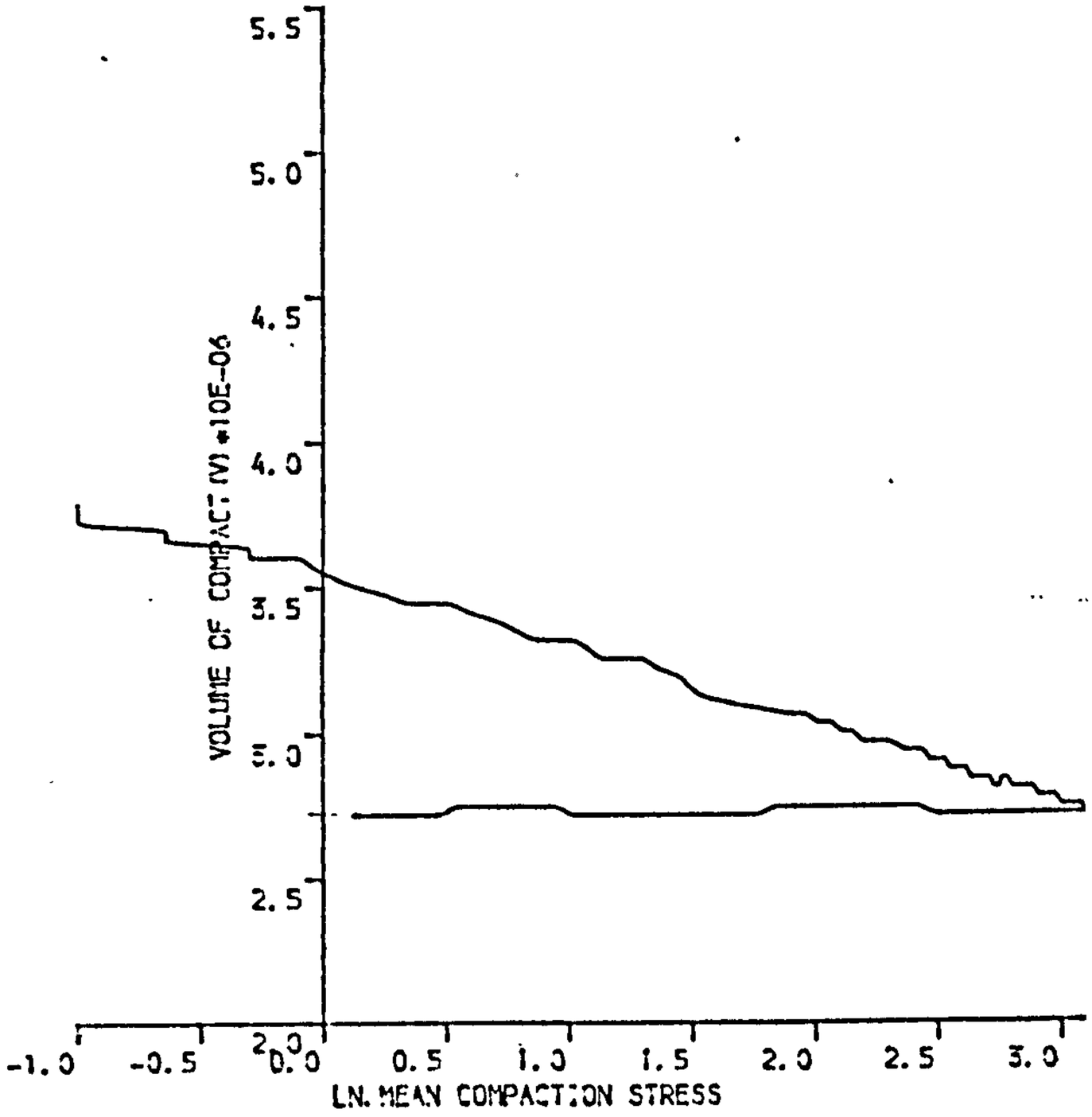

(B)

Figure 6.43 DICALCIUM PHOSPHATE UNIAXIALLY COMPACTED AT 36MPA

(A) COMPACT VOLUME VERSUS MEAN COMPACTION STRESS

(B) COMPACT VOLUME VERSUS NATURAL LOGARITHMIC COMPACTION STRESS

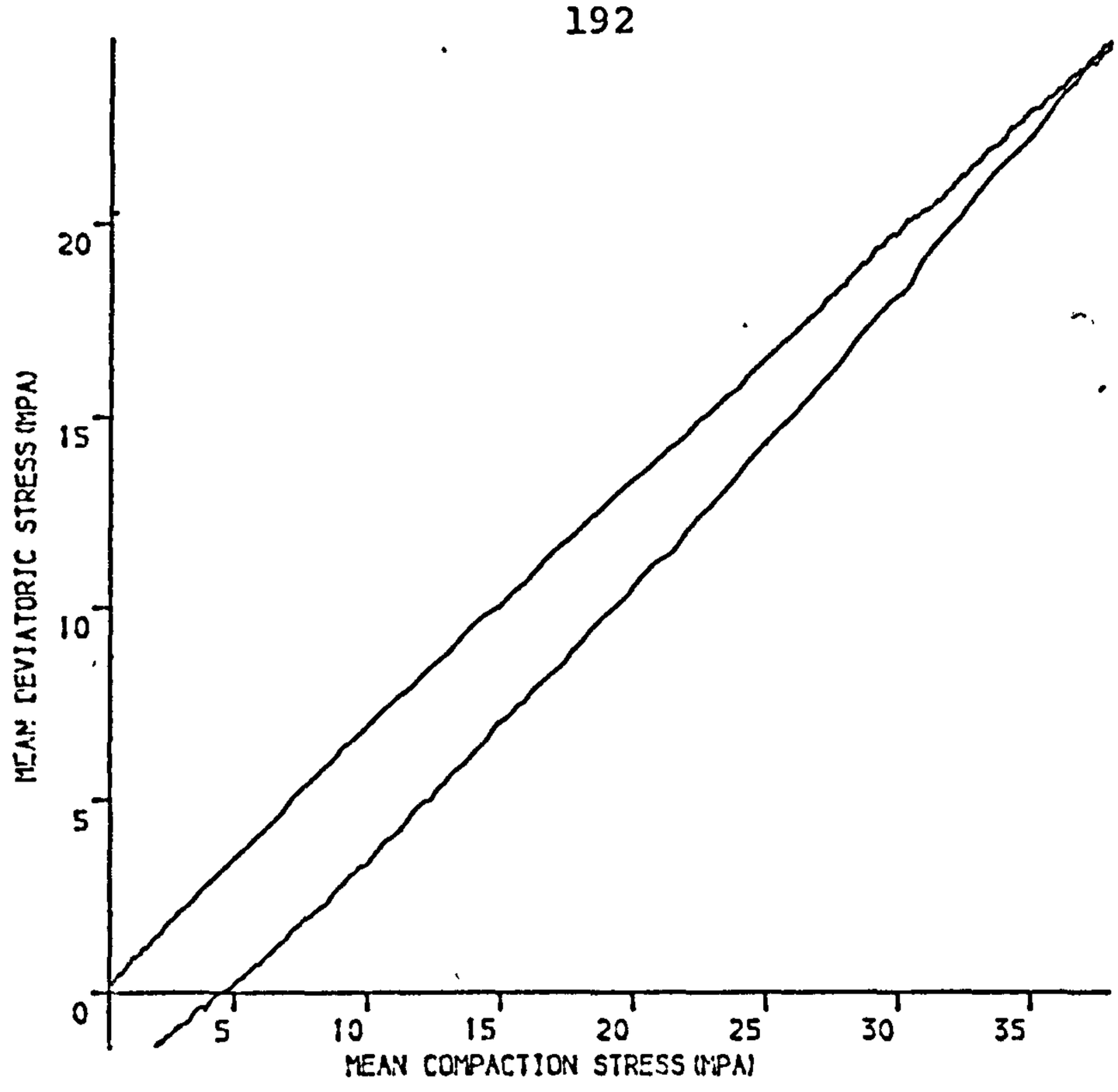

(A)

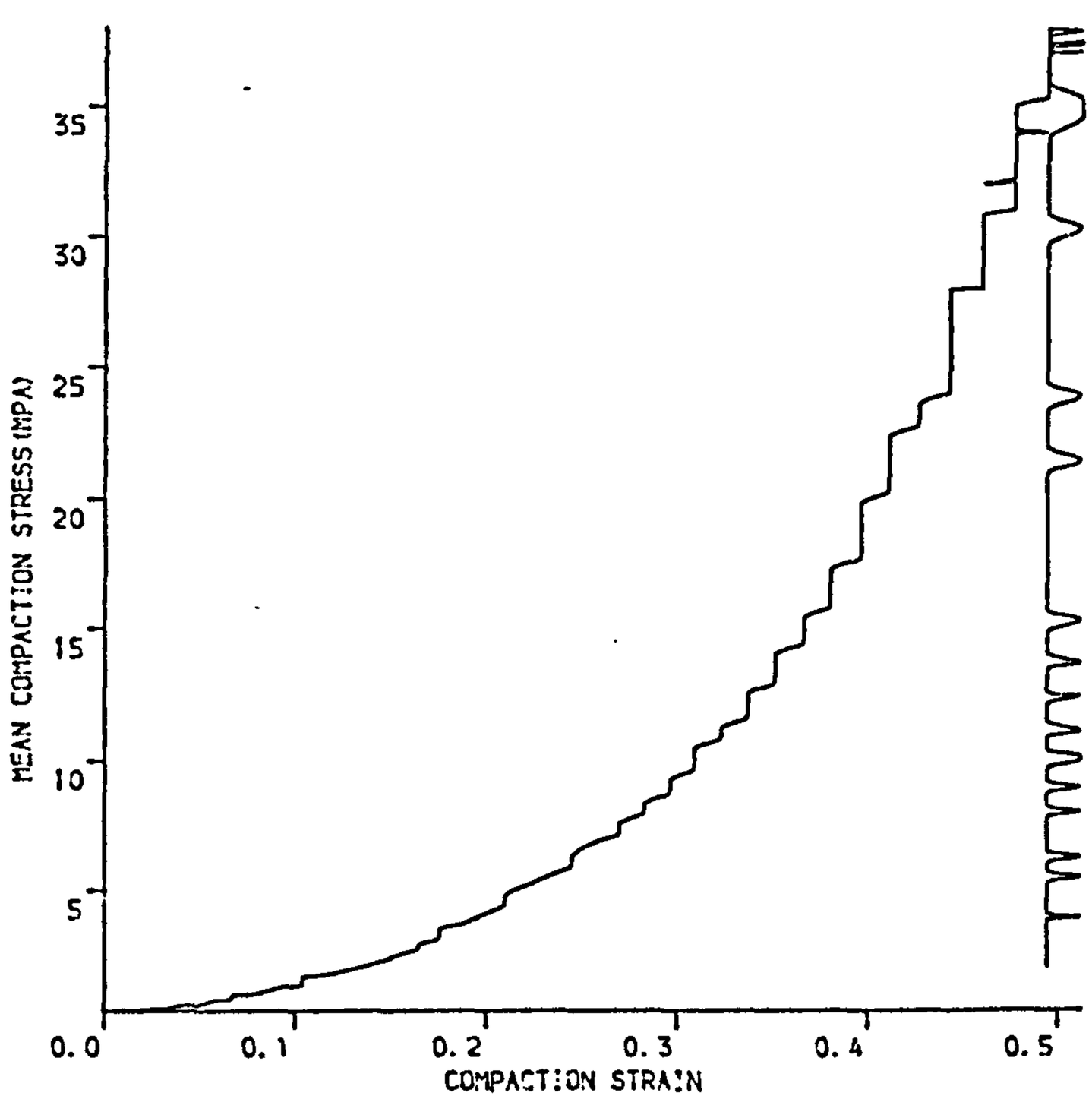

(B)

Figure 6.44 DICALCIUM PHOSPHATE COMPACTED UNIAXIALLY AT 62MPA
(A) SHEAR STRESS VERSUS COMPACTION STRESS
(B) COMPACTION STRESS VERSUS NATURAL STRAIN

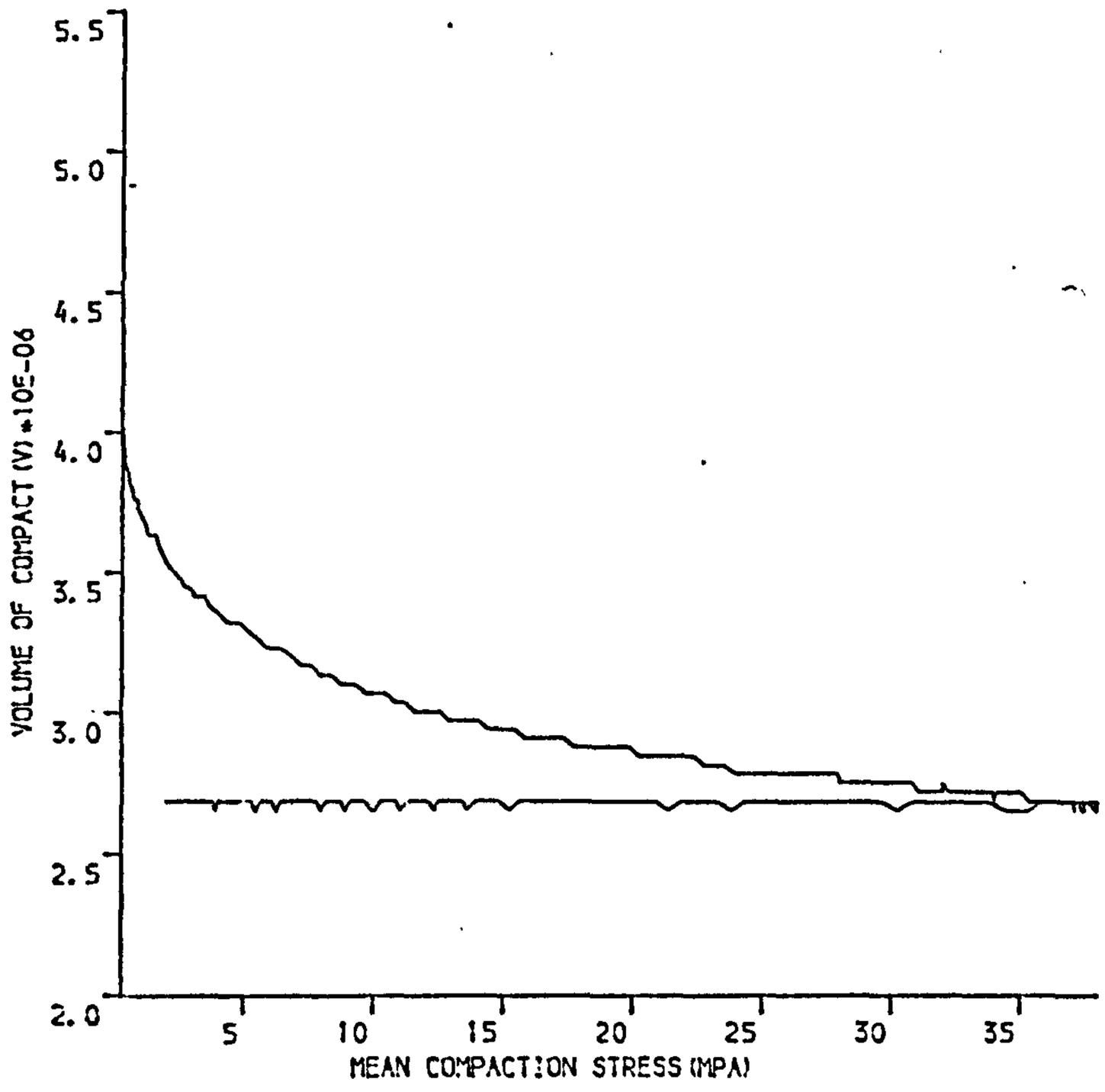

(A)

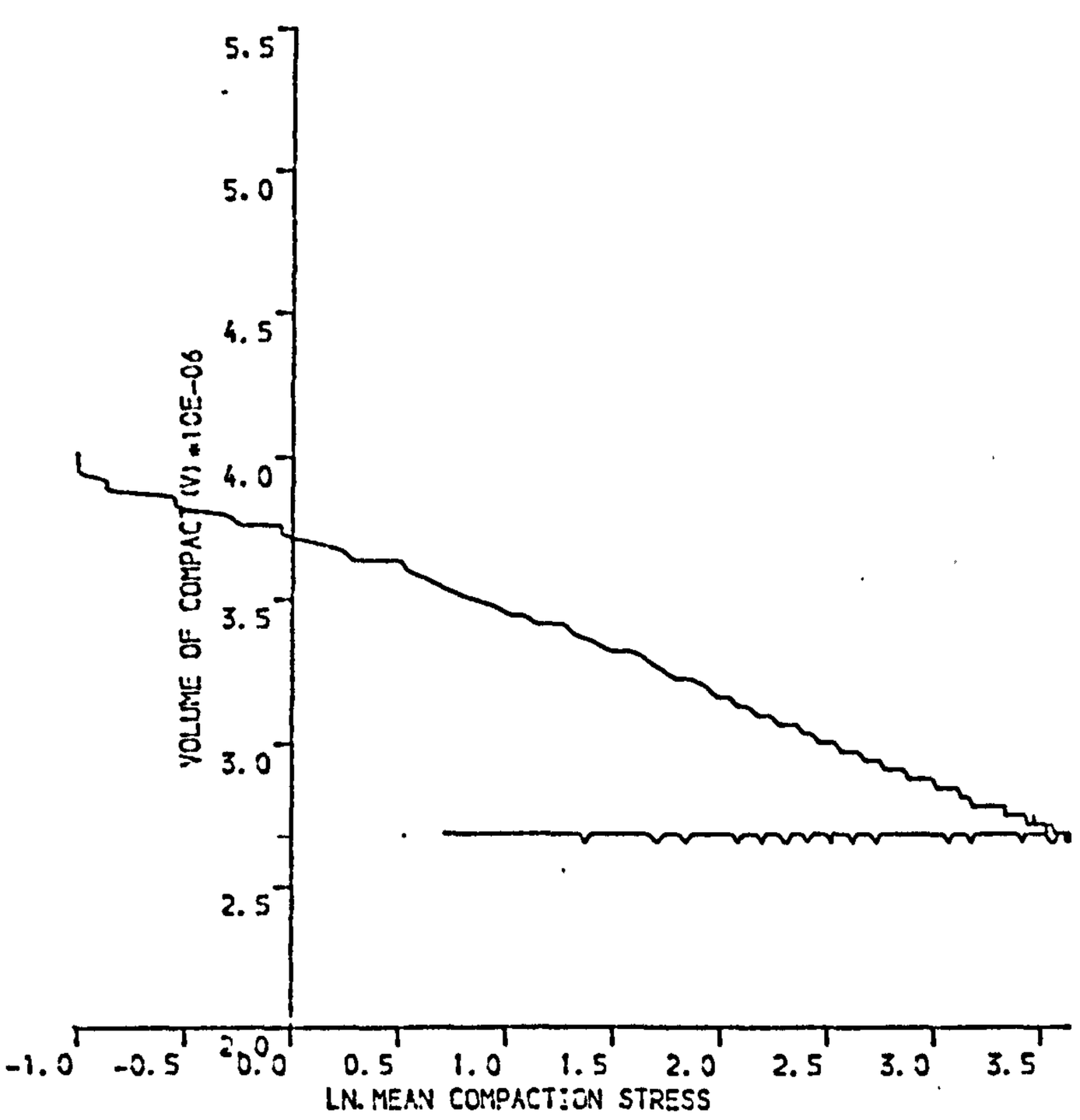

(B)

Figure 6.45 DICALCIUM PHOSPHATE UNIAXIALLY COMPACTED AT 62MPA
(A) COMPACT VOLUME VERSUS MEAN COMPACTION STRESS
(B) COMPACT VOLUME VERSUS NATURAL LOGARITHMIC COMPACTION STRESS

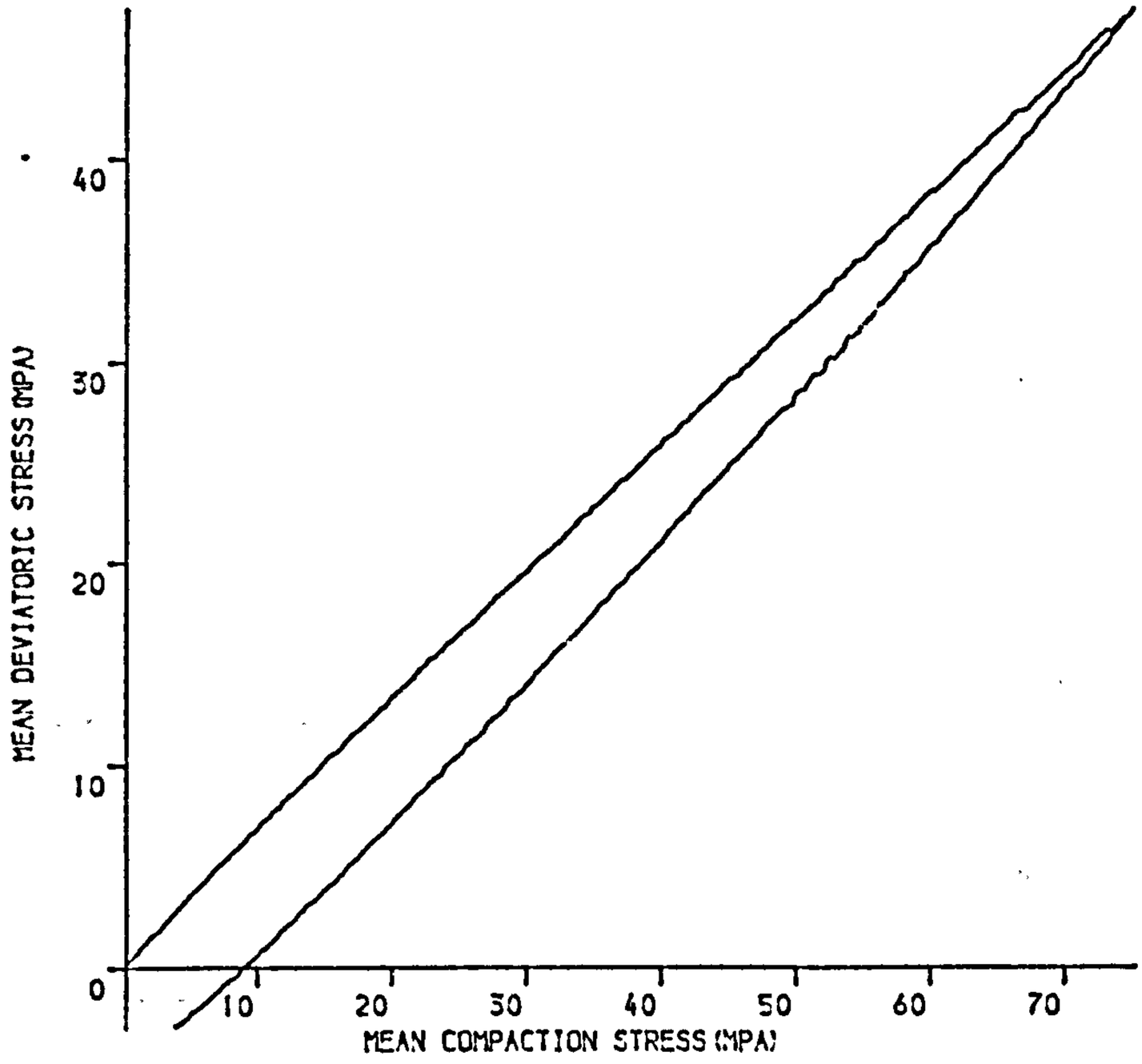

(A)

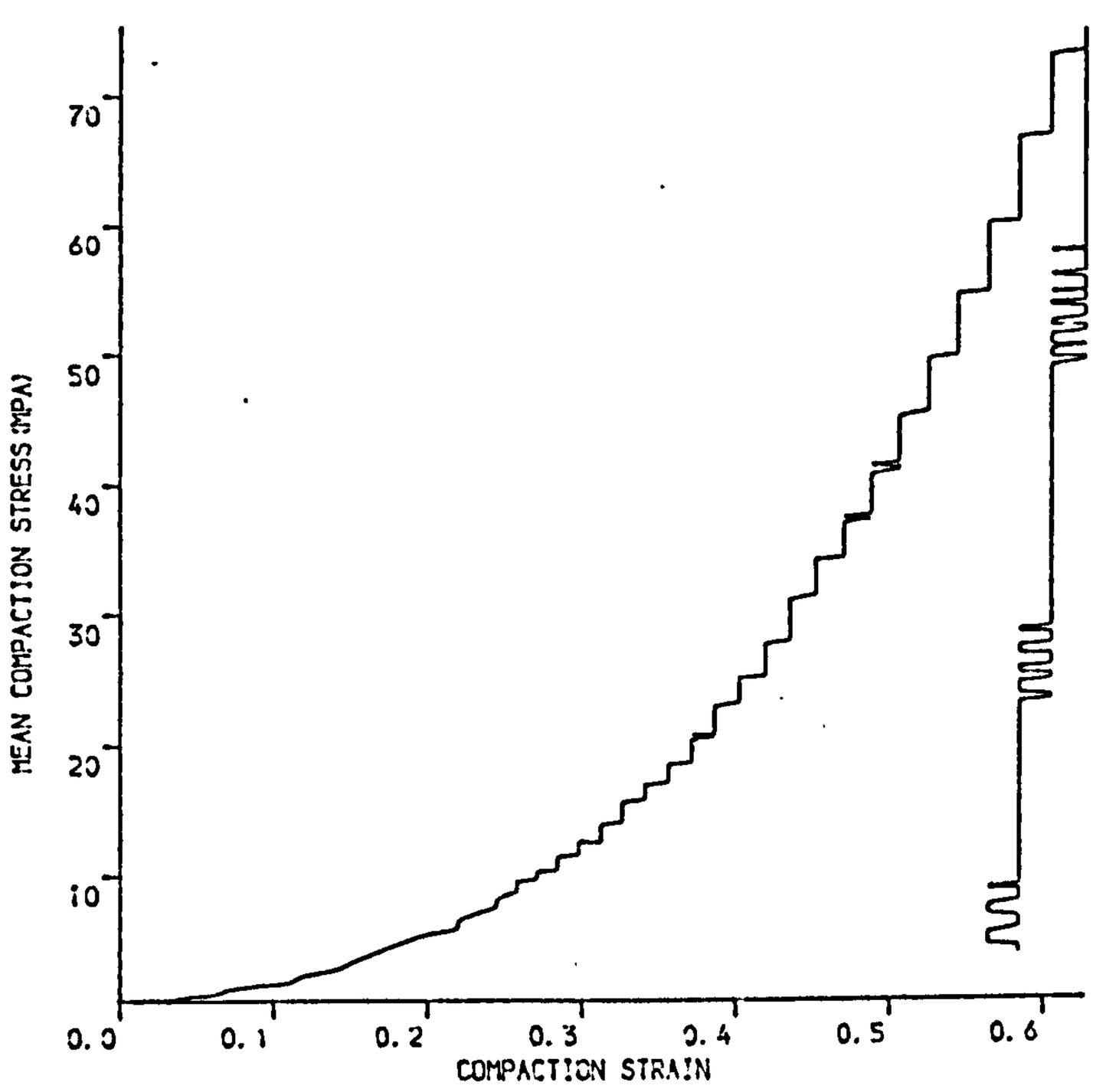

(B)

Figure 6.46 DICALCIUM PHOSPHATE COMPACTED UNIAXIALLY AT 122MPA

(A) SHEAR STRESS VERSUS COMPACTION STRESS

(B) COMPACTION STRESS VERSUS NATURAL STRAIN

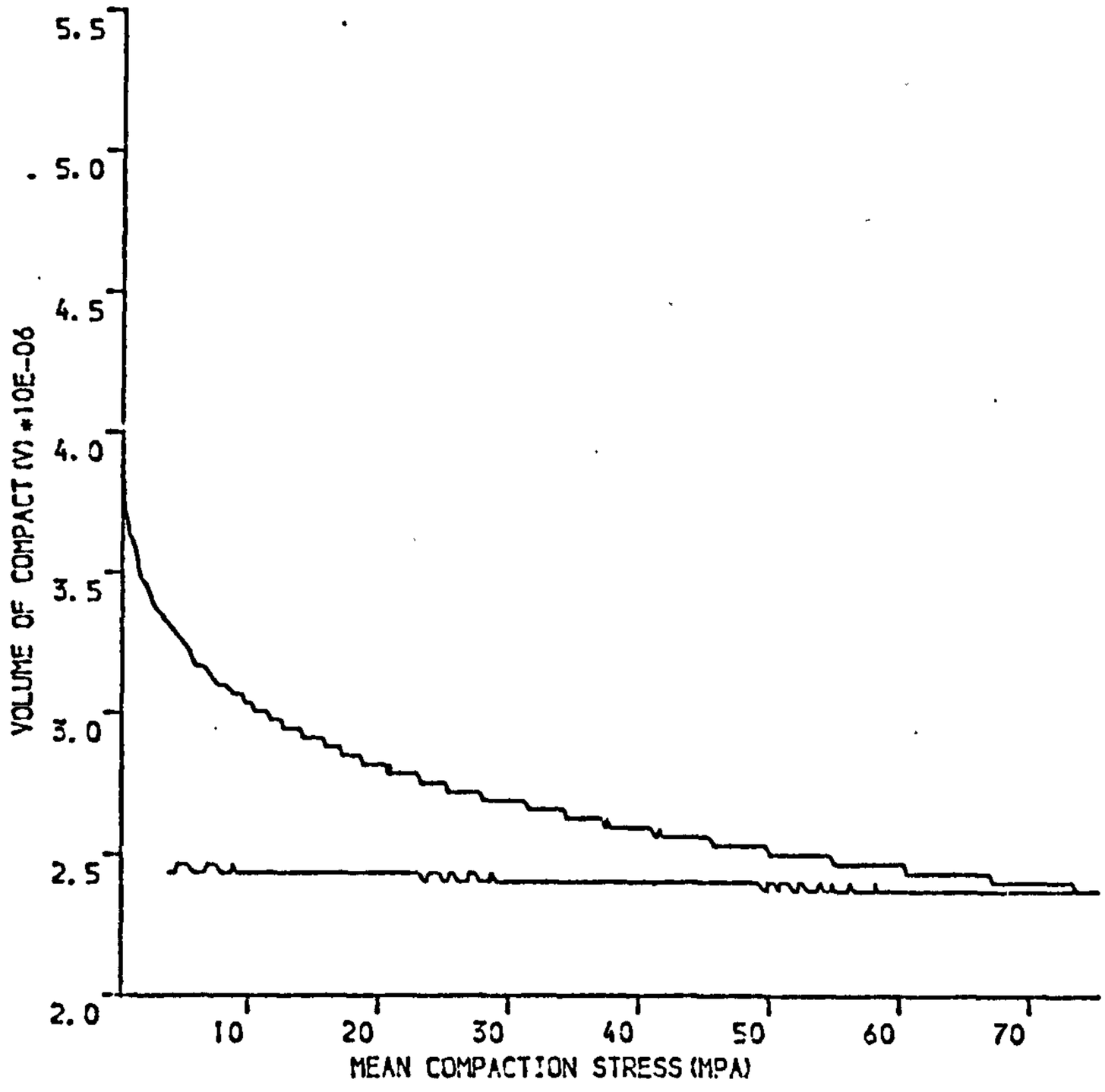

(A)

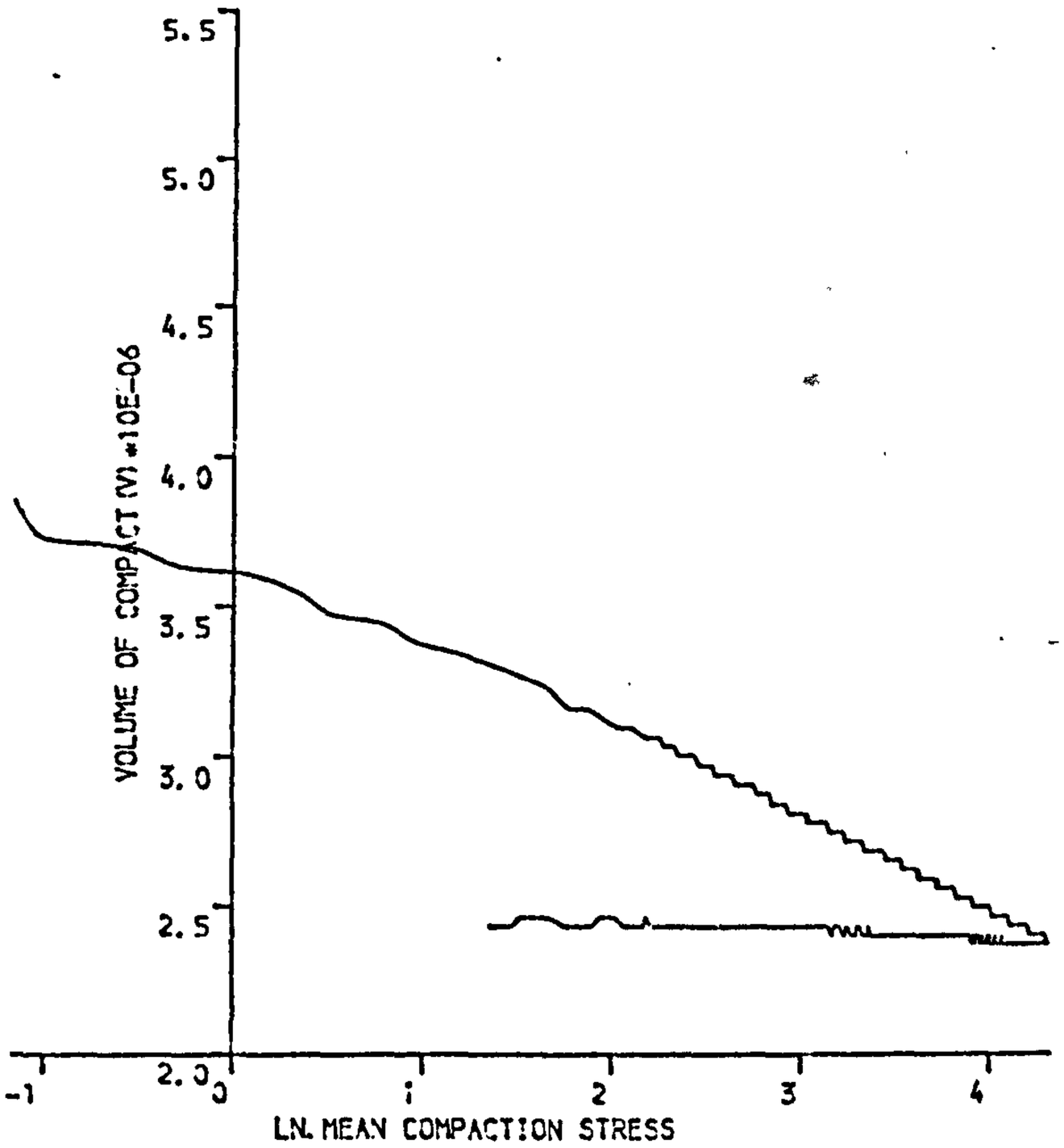

(B)

Figure 6.47 DICALCIUM PHOSPHATE UNIAXIALLY COMPACTED AT 122MPA
(A) COMPACT VOLUME VERSUS MEAN COMPACTION STRESS
(B) COMPACT VOLUME VERSUS NATURAL LOGARITHMIC COMPACTION STRESS

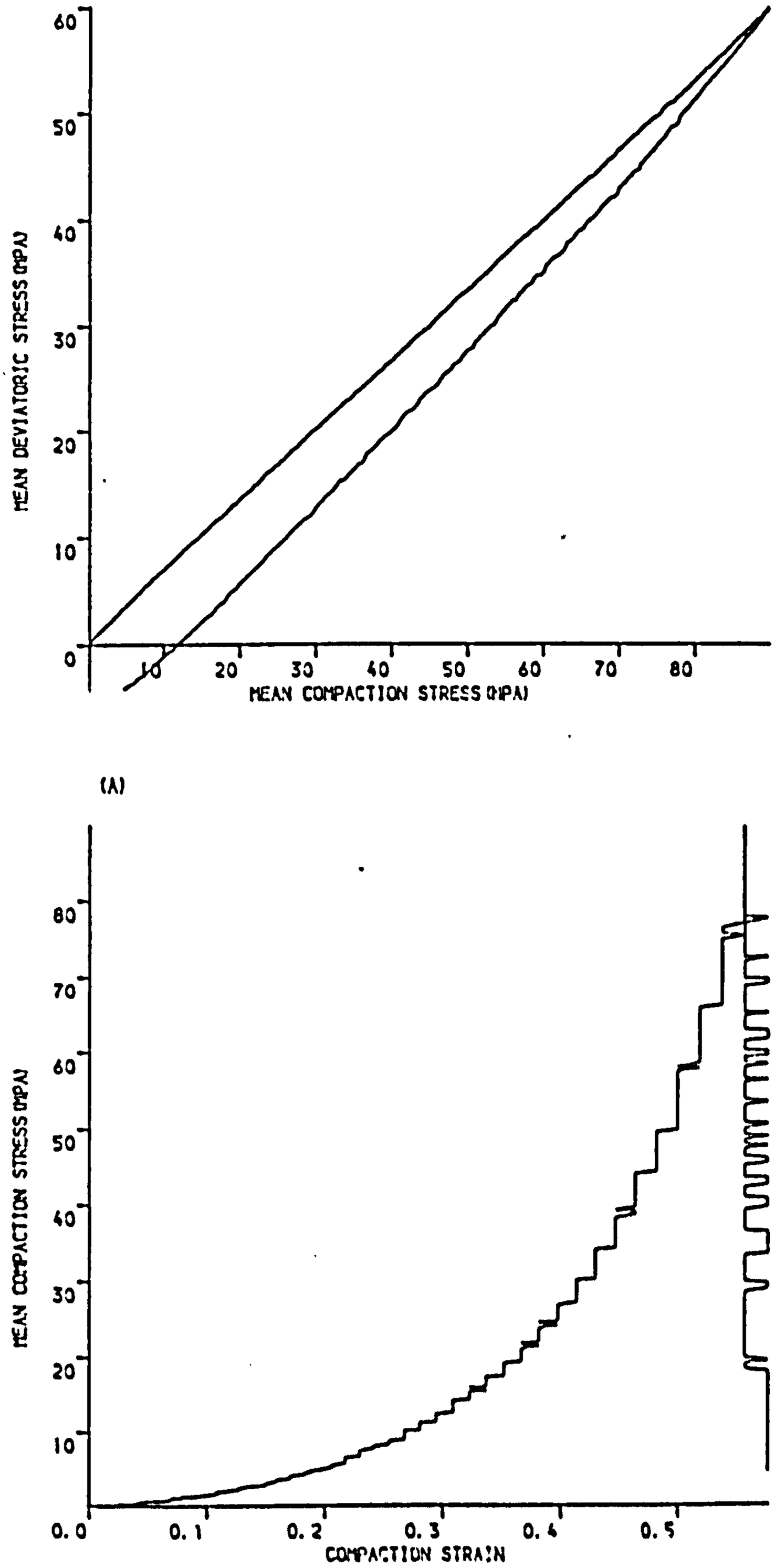

Figure 6.48 DICALCIUM PHOSPHATE COMPACTED UNIAXIALLY AT 150MPA
(A) SHEAR STRESS VERSUS COMPACTION STRESS
(B) COMPACTION STRESS VERSUS NATURAL STRAIN

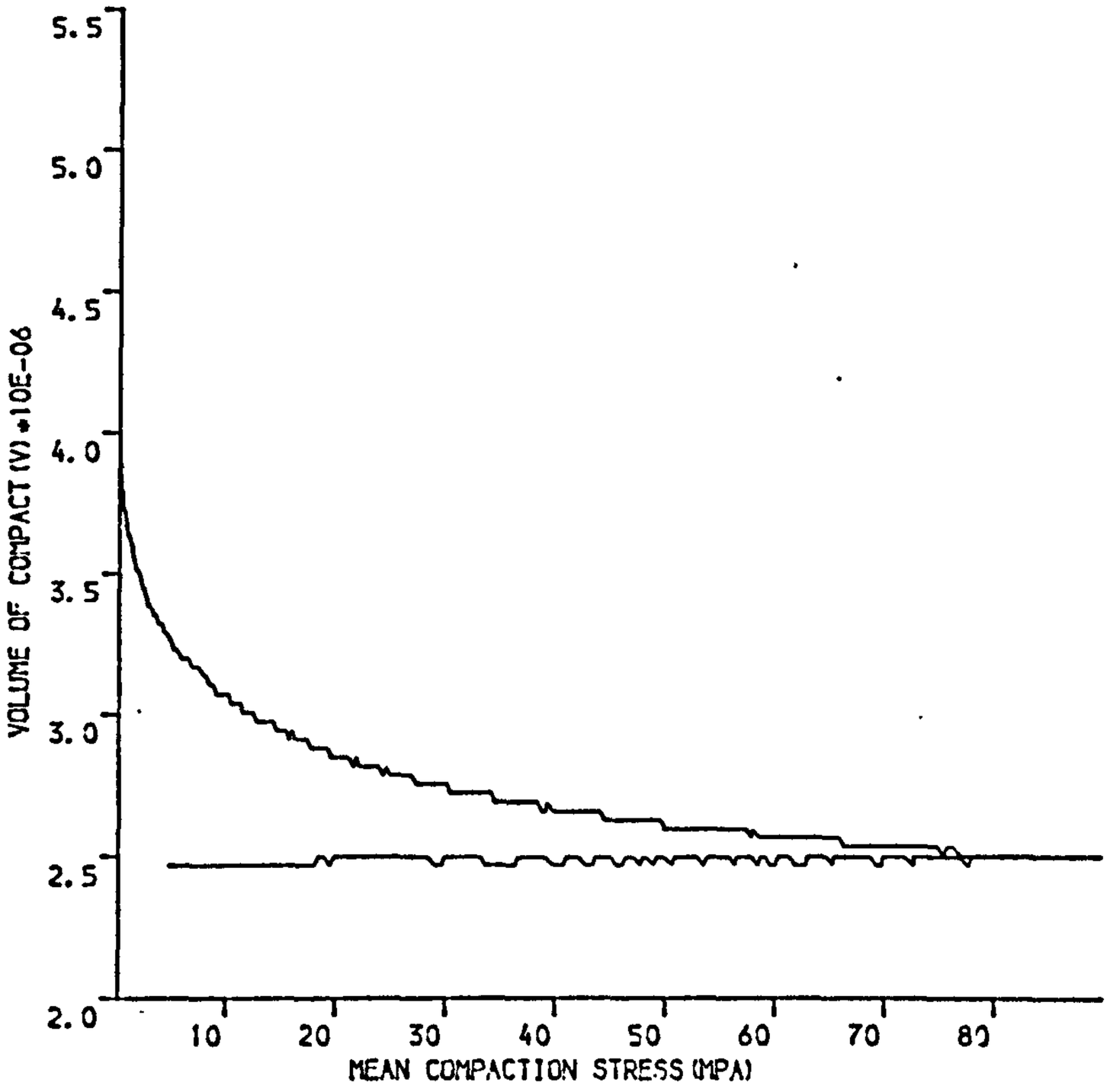

(A)

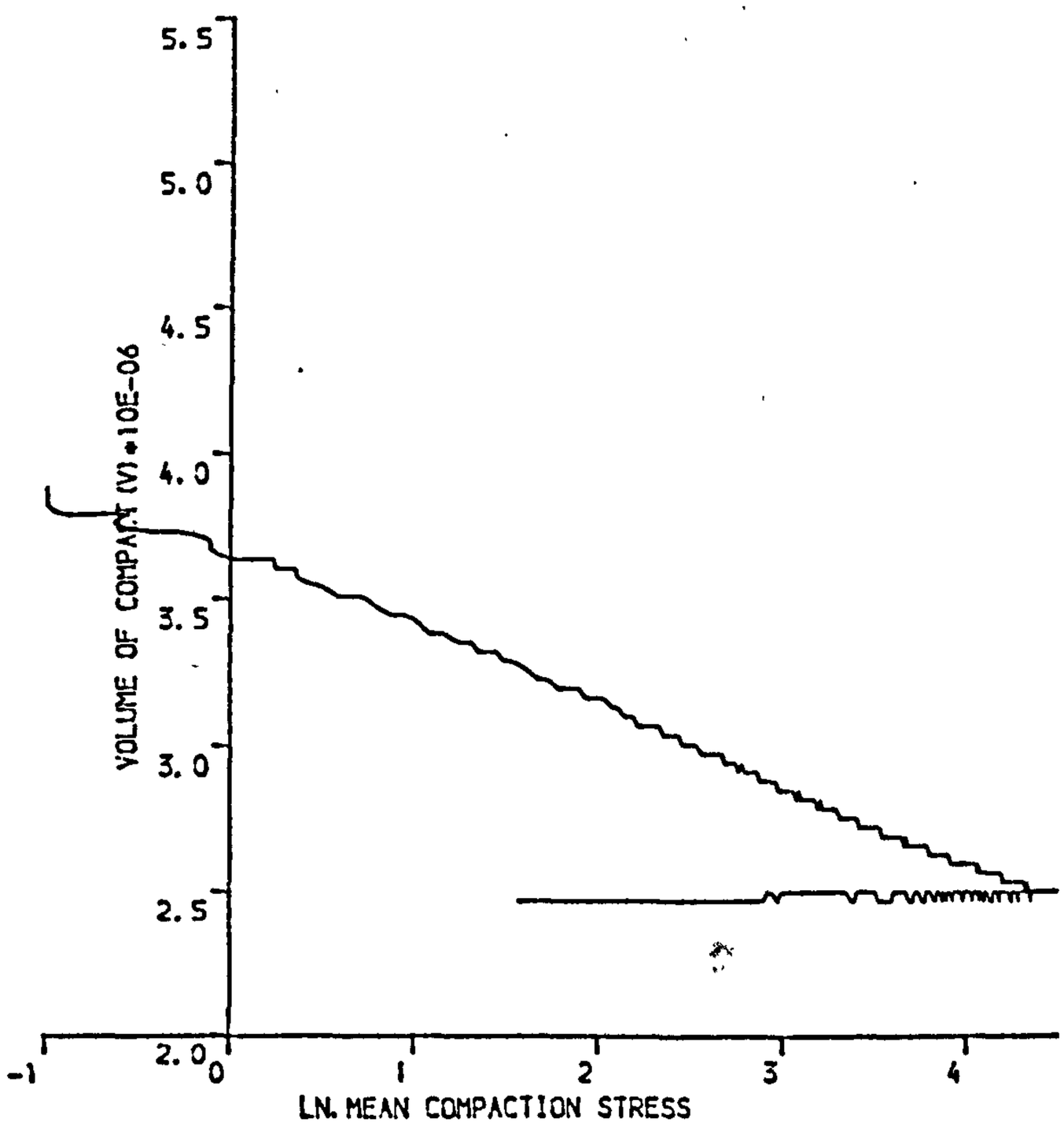

(B)

Figure 6.49 DICALCIUM PHOSPHATE UNIAXIALLY COMPACTED AT 150MPA
(A) COMPACT VOLUME VERSUS MEAN COMPACTION STRESS
(B) COMPACT VOLUME VERSUS NATURAL LOGARITHMIC COMPACTION STRESS

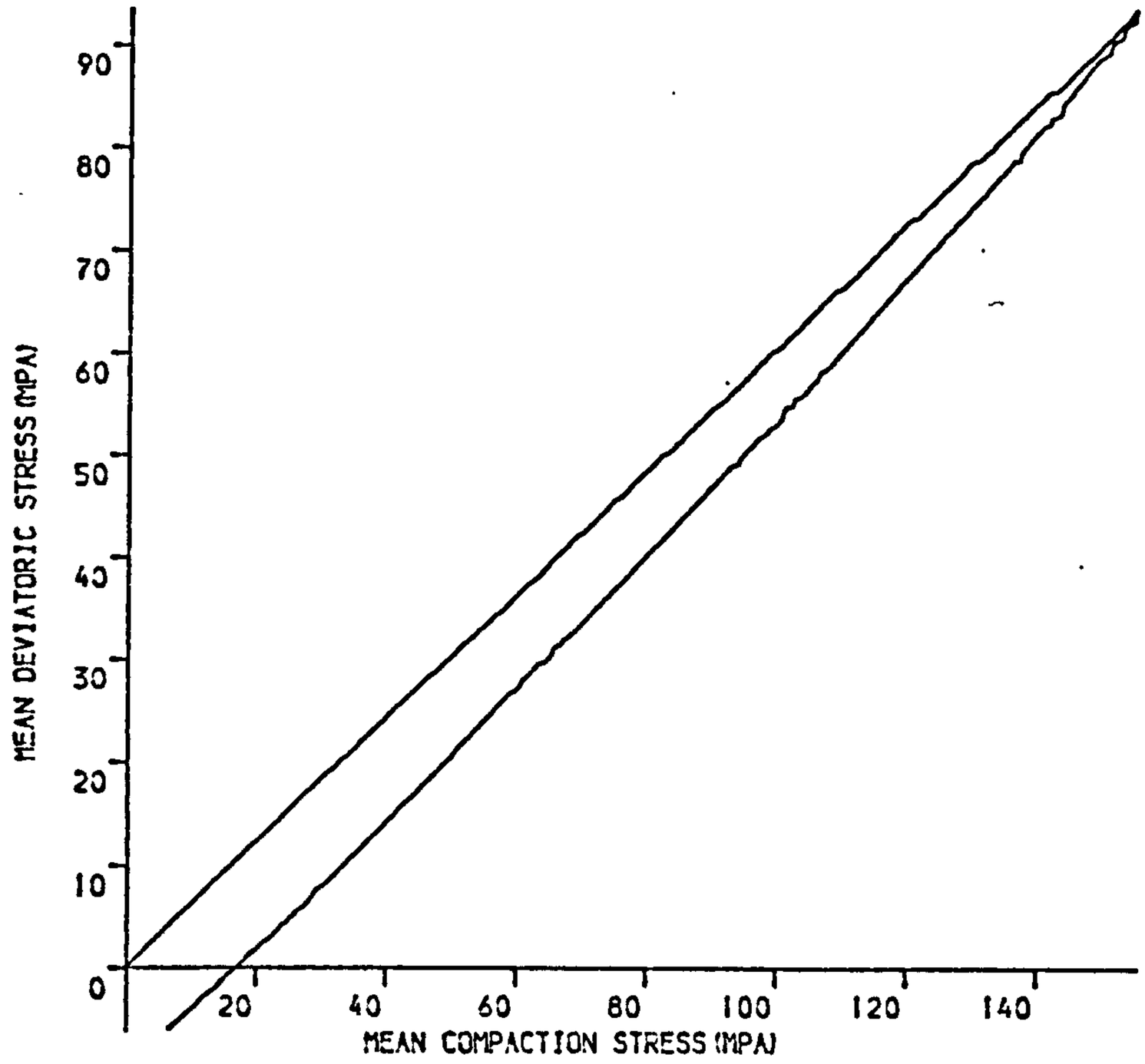

(A)

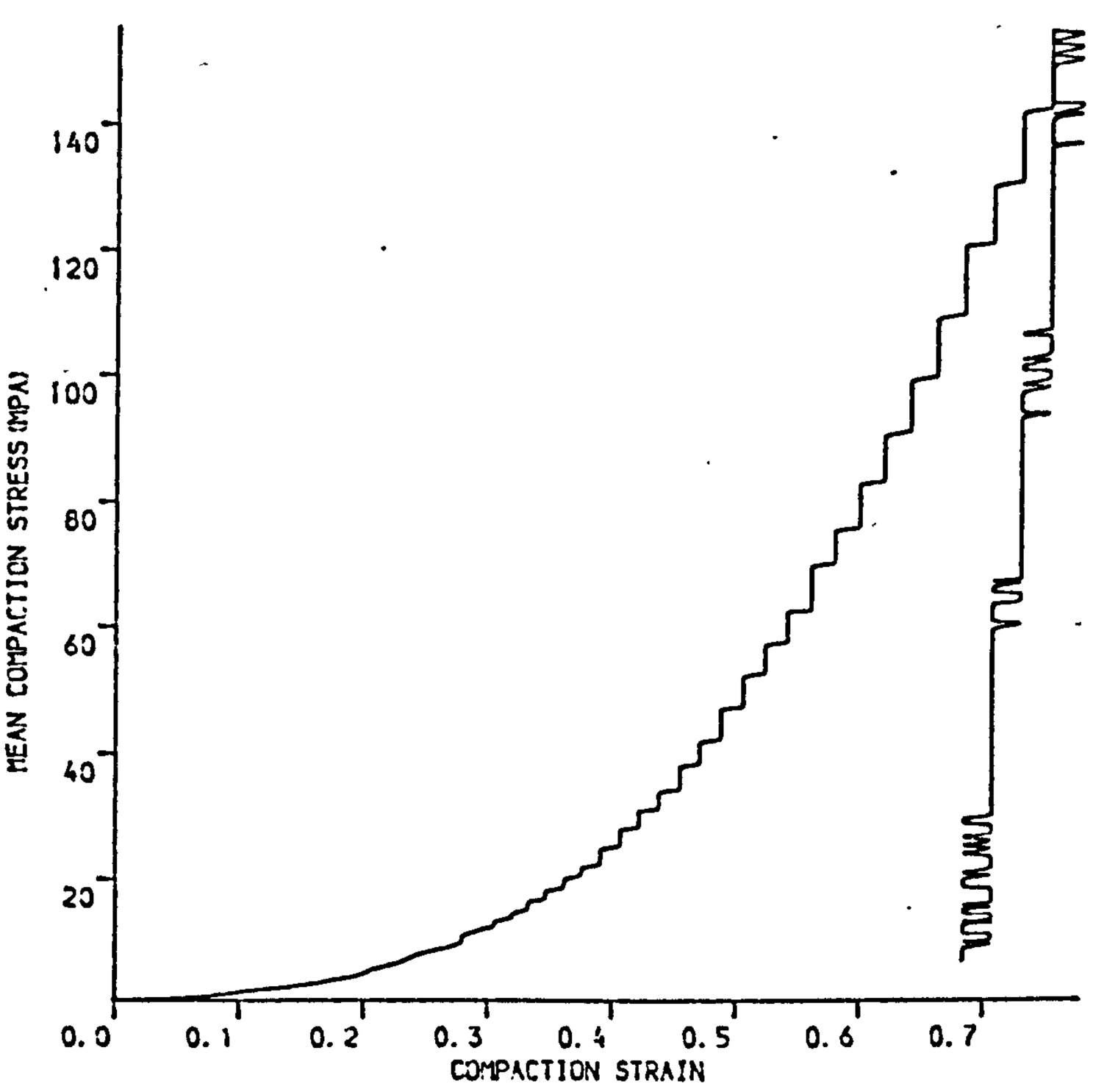

Figure 6.50 (B) DICALCIUM PHOSPHATE COMPACTED UNIAXIALLY AT 248MPA

(A) SHEAR STRESS VERSUS COMPACTION STRESS

(B) COMPACTION STRESS VERSUS NATURAL STRAIN

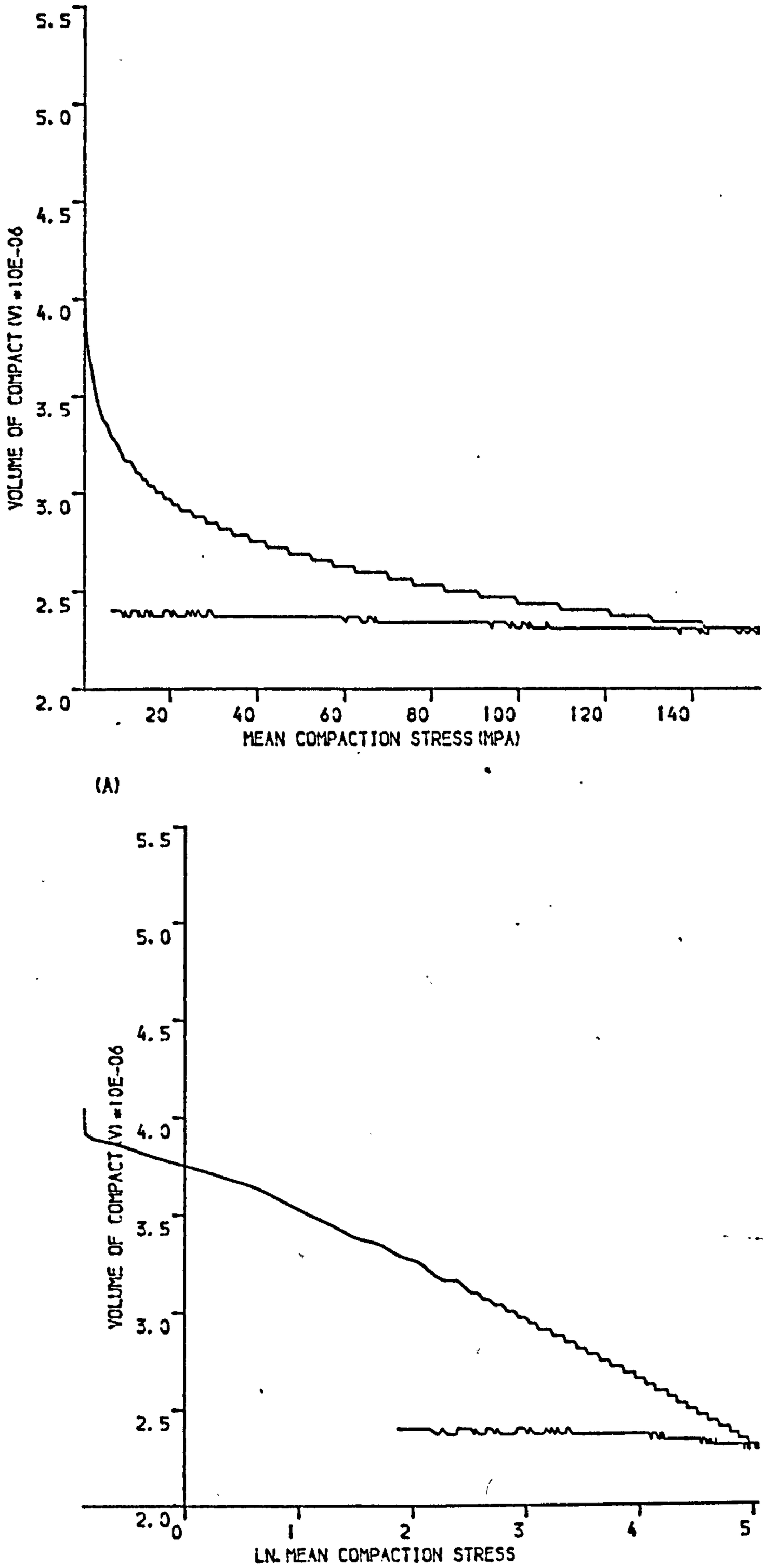

Figure 6.51 DICALCIUM PHOSPHATE UNIAXIALLY COMPACTED AT 248MPA
(A) COMPACT VOLUME VERSUS MEAN COMPACTION STRESS
(B) COMPACT VOLUME VERSUS NATURAL LOGARITHMIC COMPACTION STRESS

Figure 6.52 3-D representation of compaction of dicalcium phosphate compacted at 36 MPa

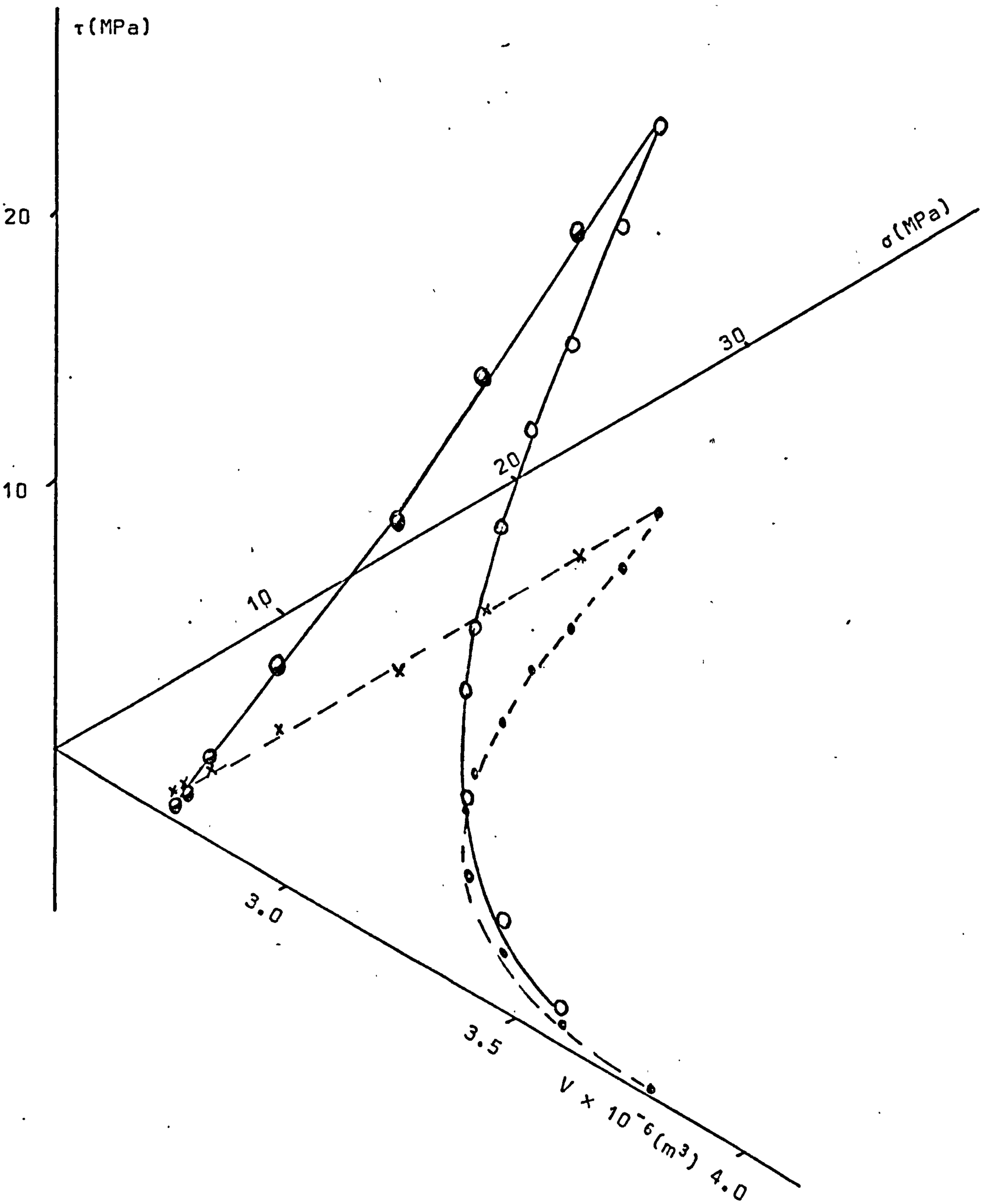

Figure 6.53 3-D representation of compaction of dicalcium phosphate compacted at 62 MPa

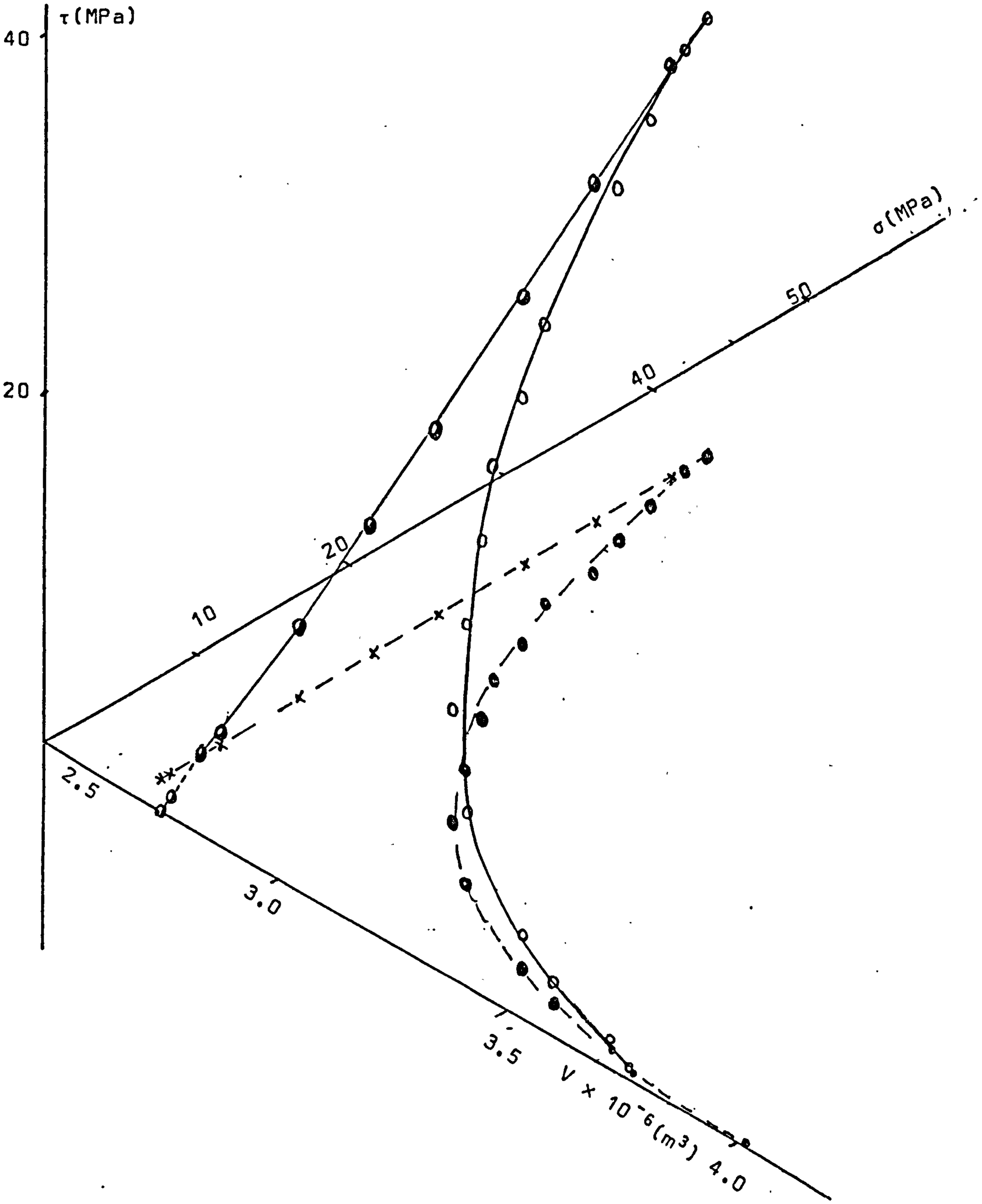

Figure 6.54 3-D representation of compaction of dicalcium phosphate compacted at 120 MPa

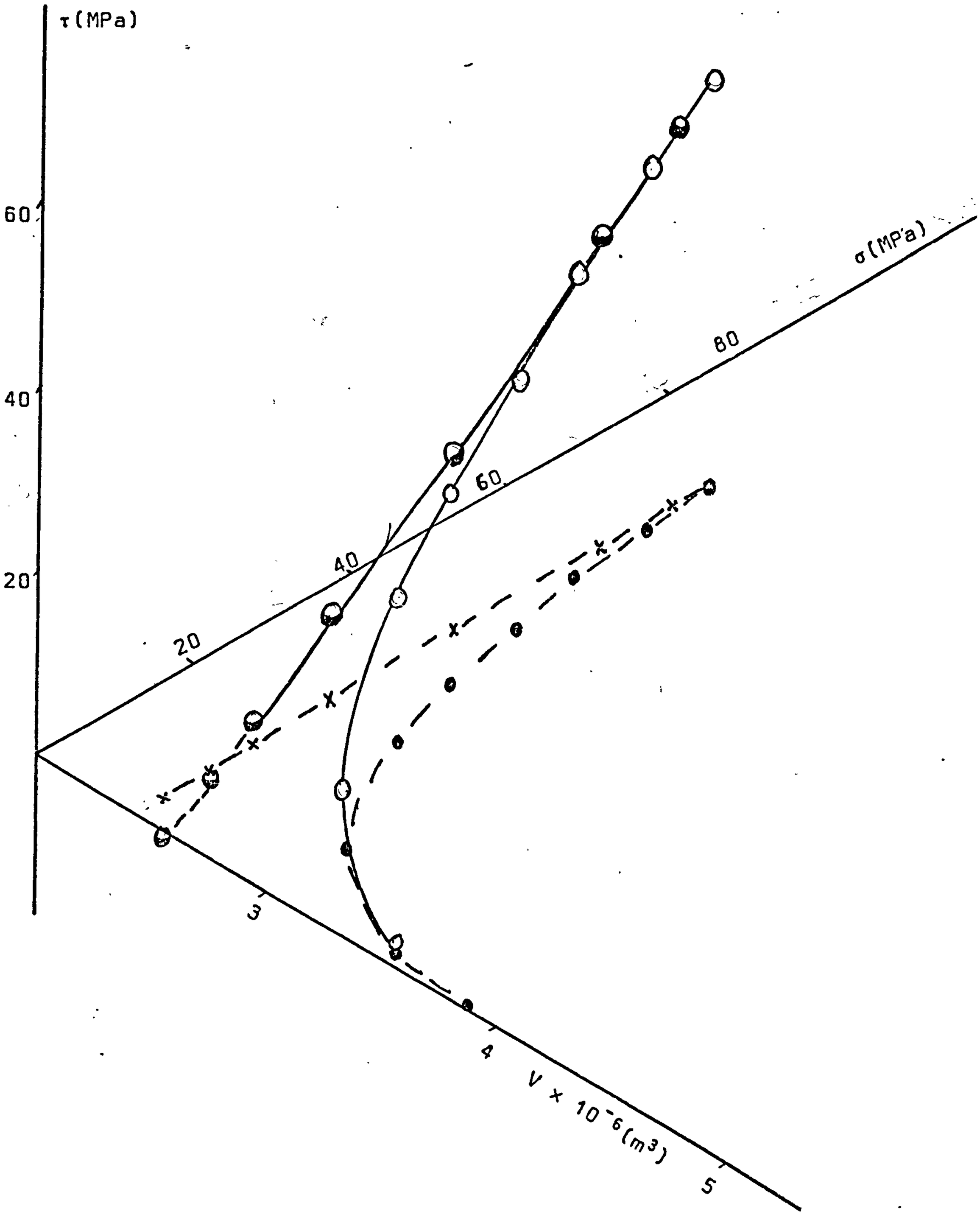

Figure 6.55 3-D representation of compaction of dicalcium phosphate compacted at 150 MPa

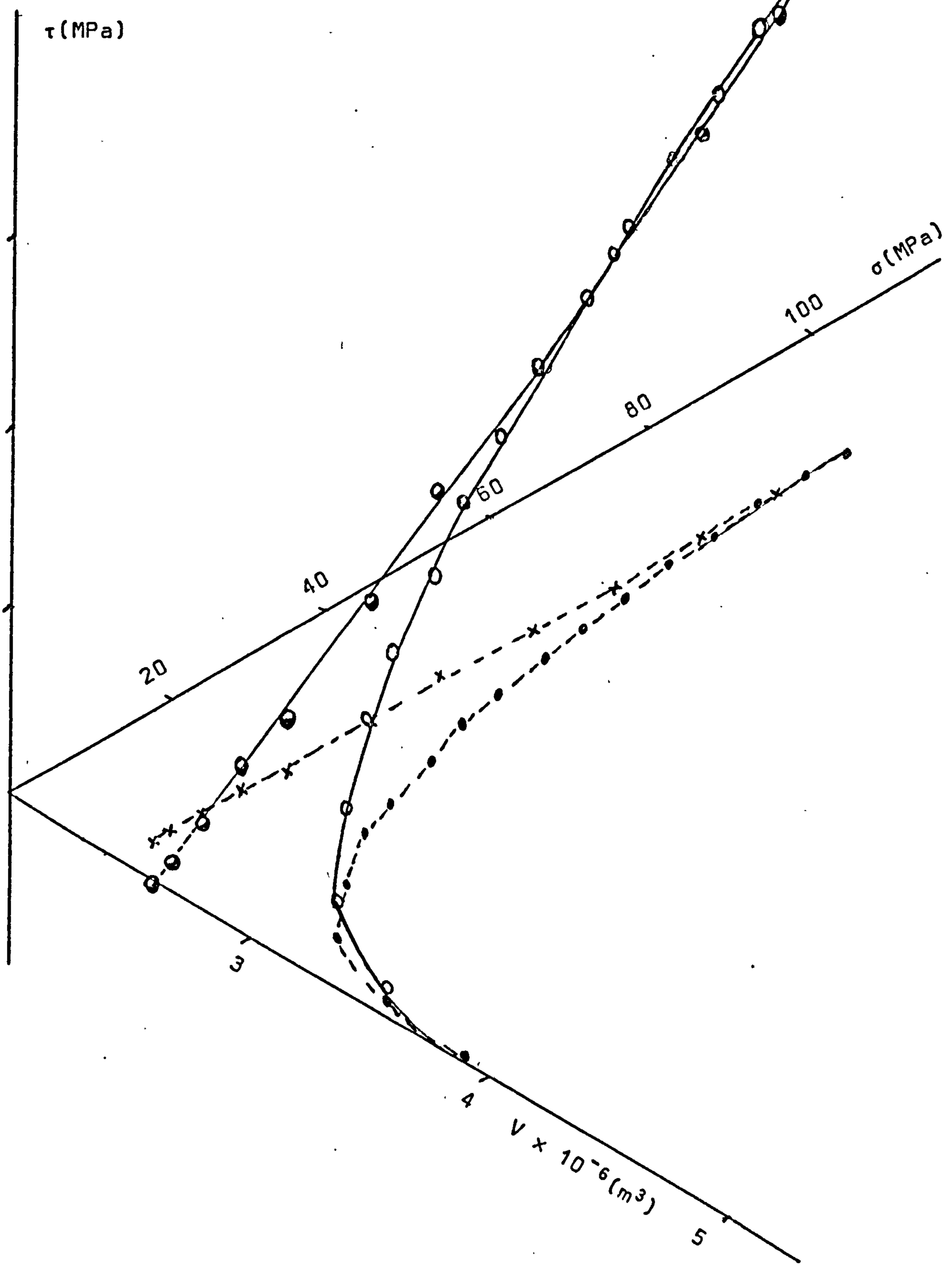

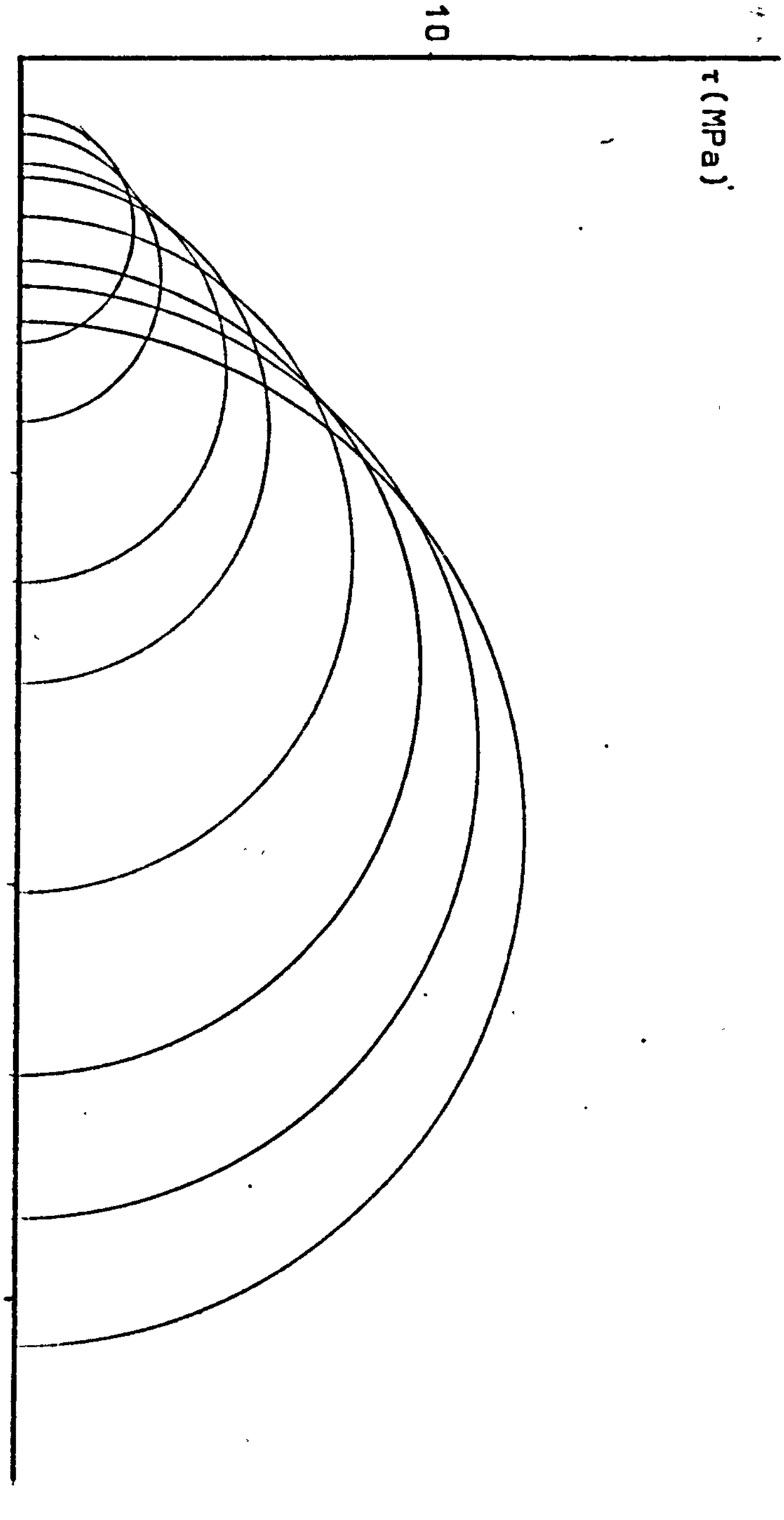

Figure 6.56 Mohr circles constructed for sugar compacted at 31 MPa

Figure 6.57 Mohr circles constructed for sugar compacted at 63 MPa

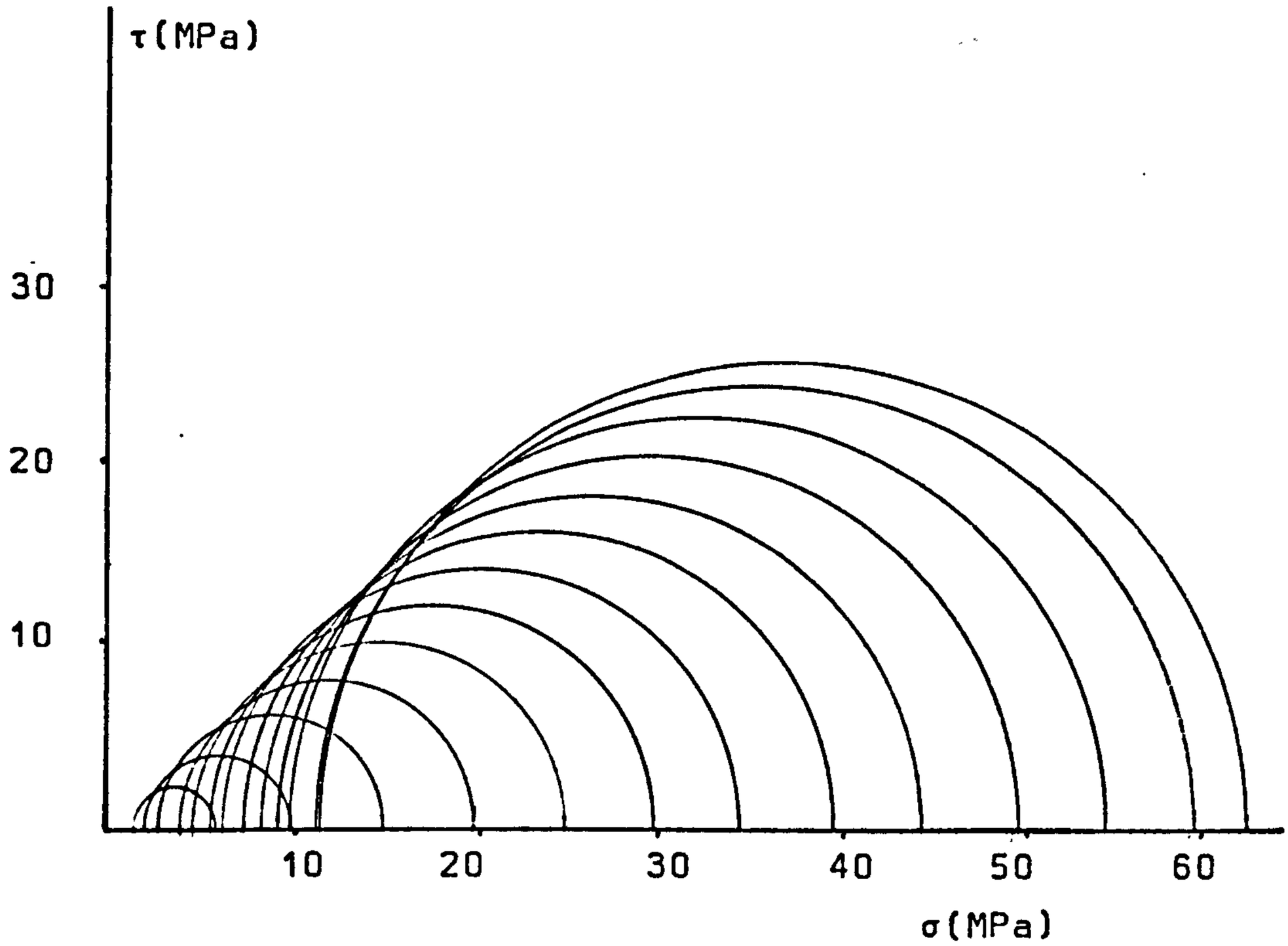

Figure 6.58 Mohr circles constructed for sugar compacted at 92 MPa

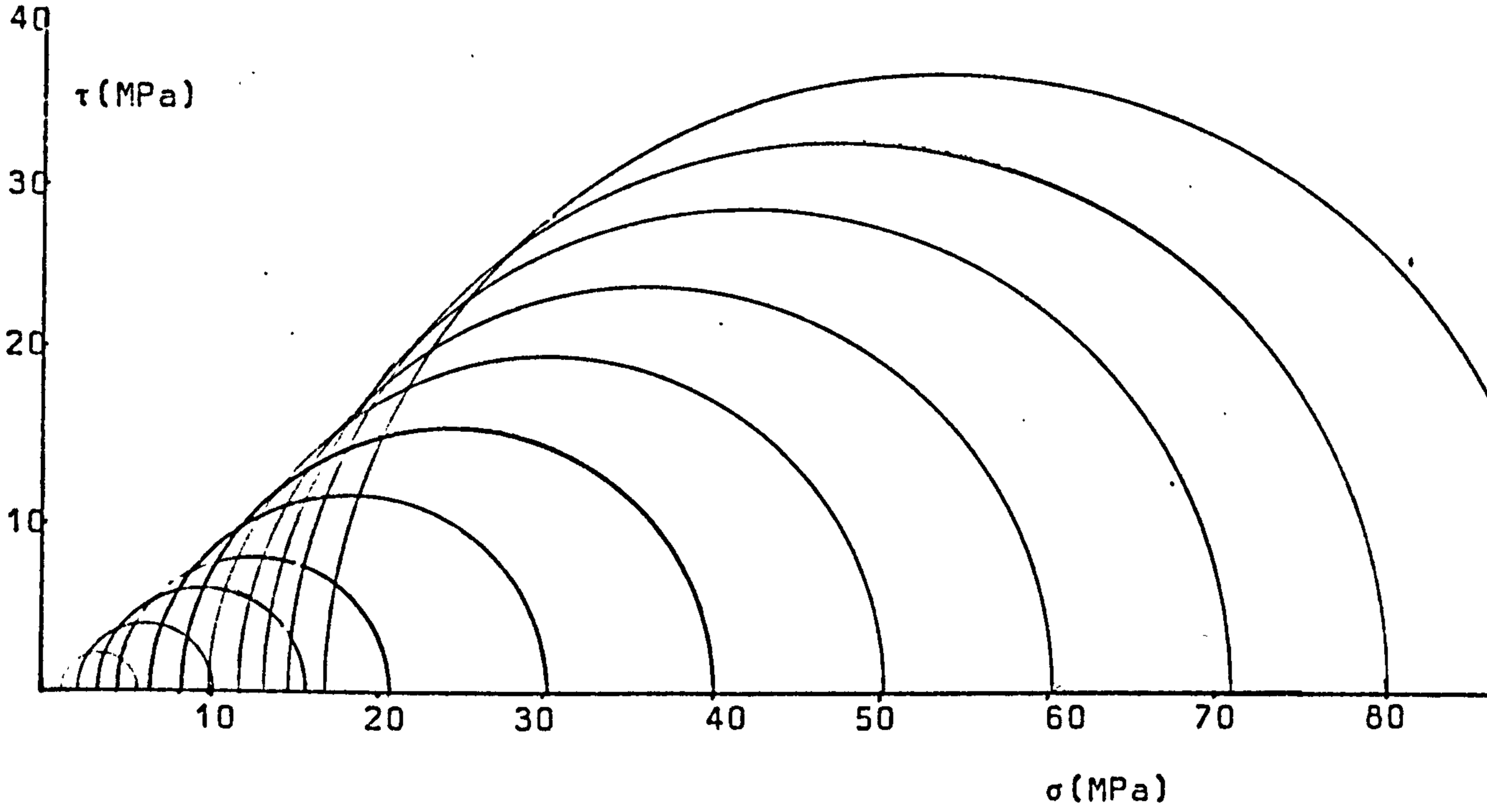

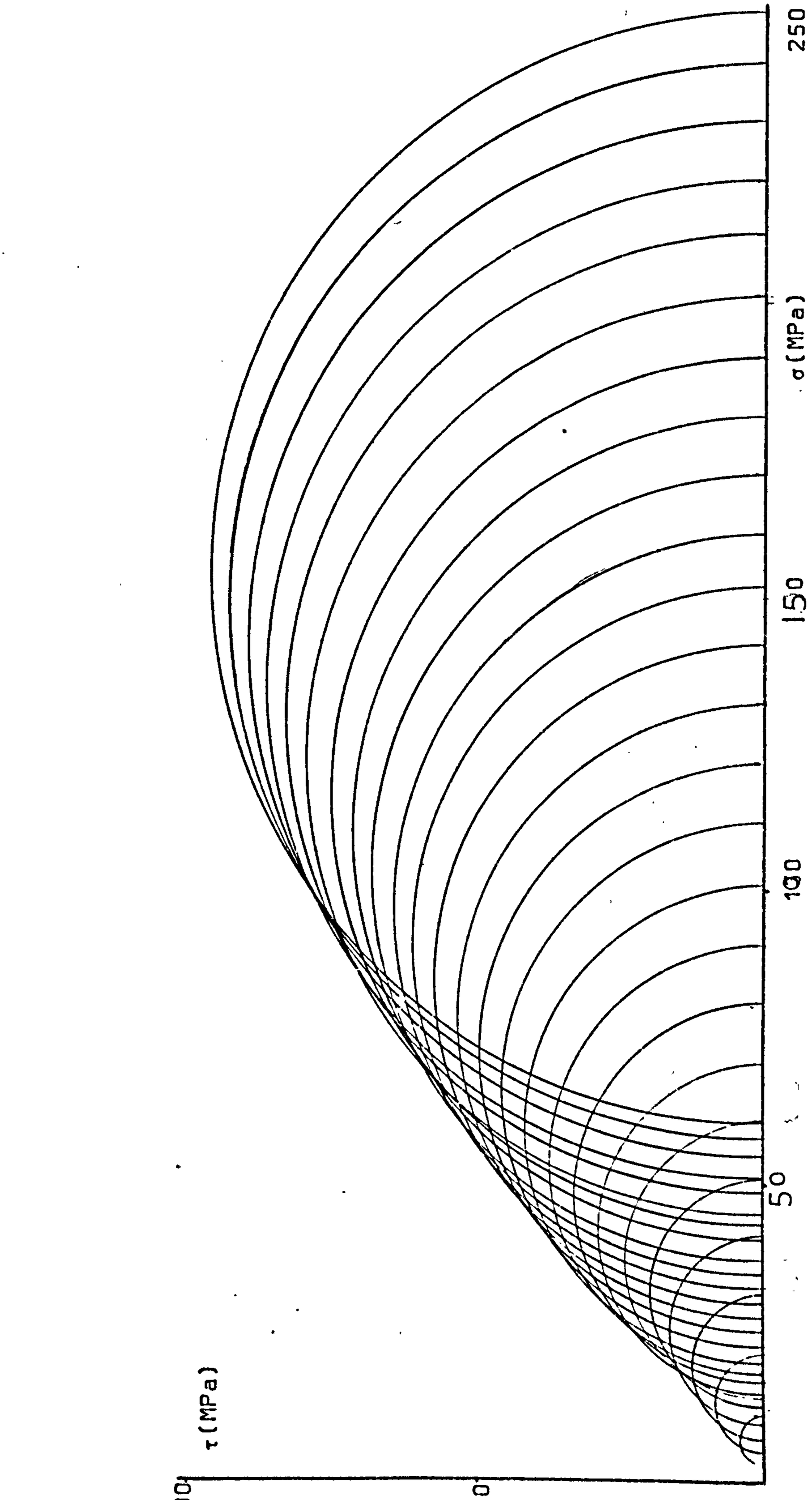
Mohr circles constructed for sugar compacted at 250 MPa
250
200
150
100
50
σ(MPa)
100
50
τ(MPa)

Figure 6.59

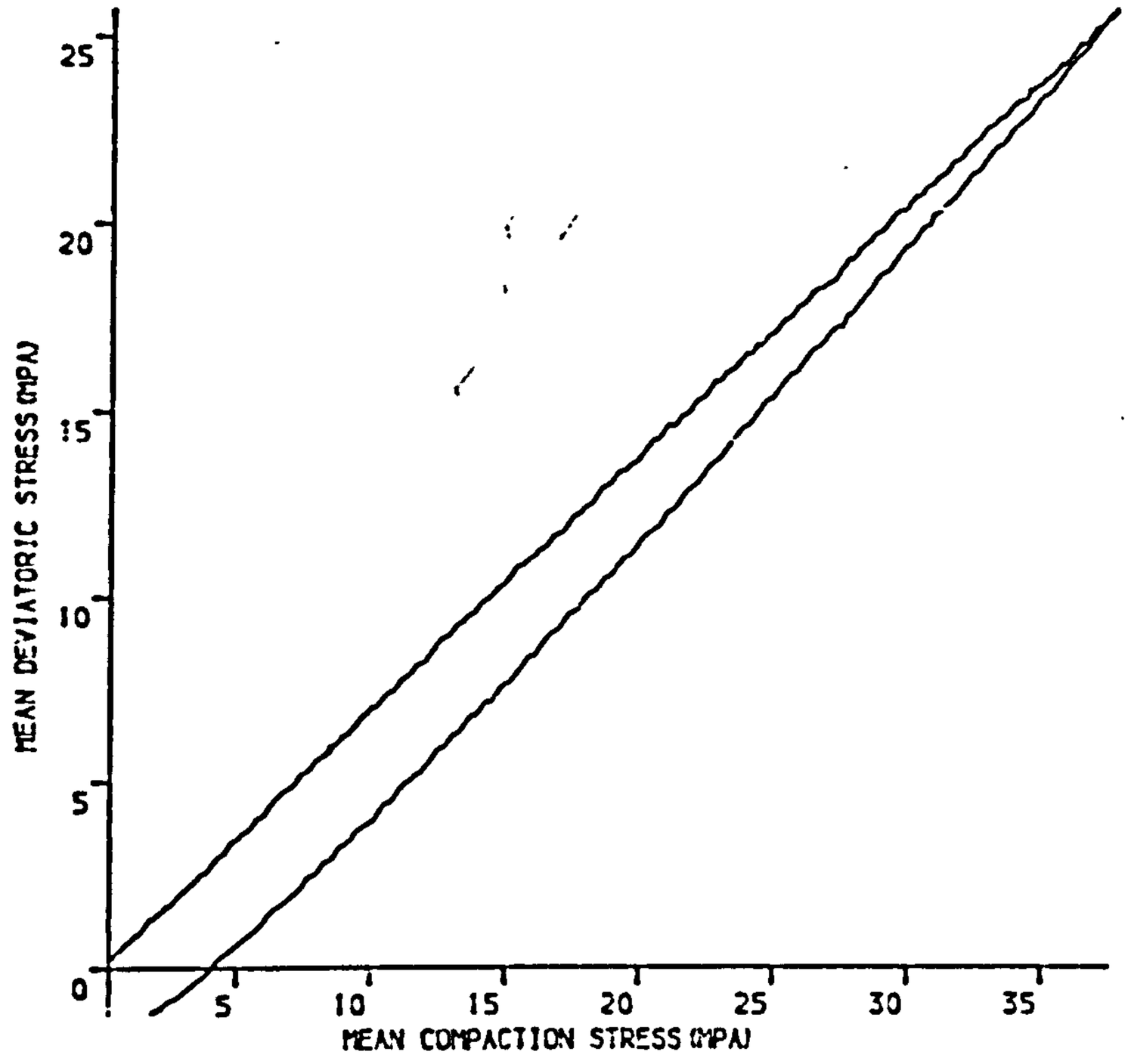

(A)

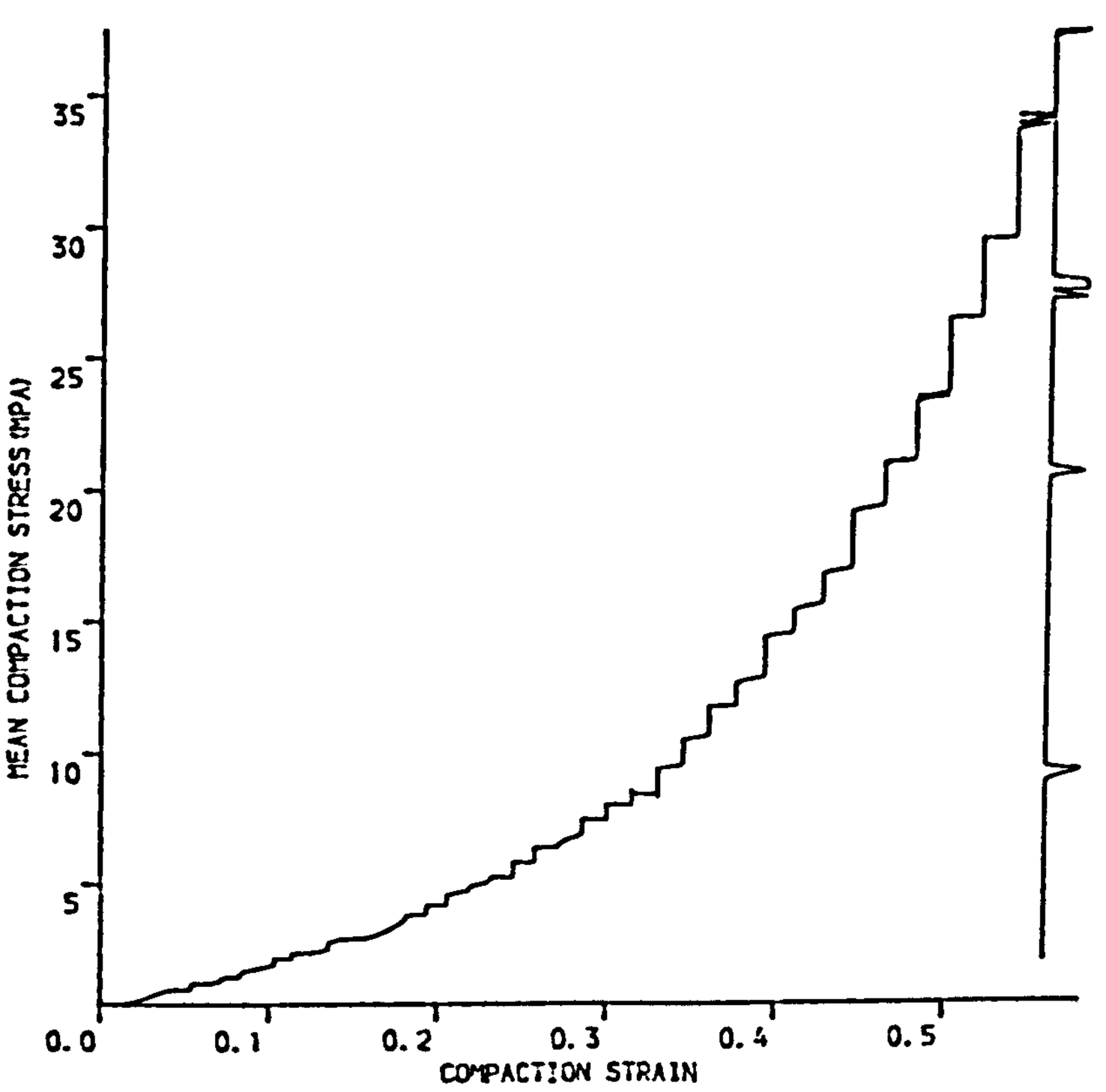

(B)

Figure 6.60 SUGAR COMPACTED UNIAXIALLY AT 63MPA
(A) SHEAR STRESS VERSUS COMPACTION STRESS
(B) COMPACTION STRESS VERSUS NATURAL STRAIN

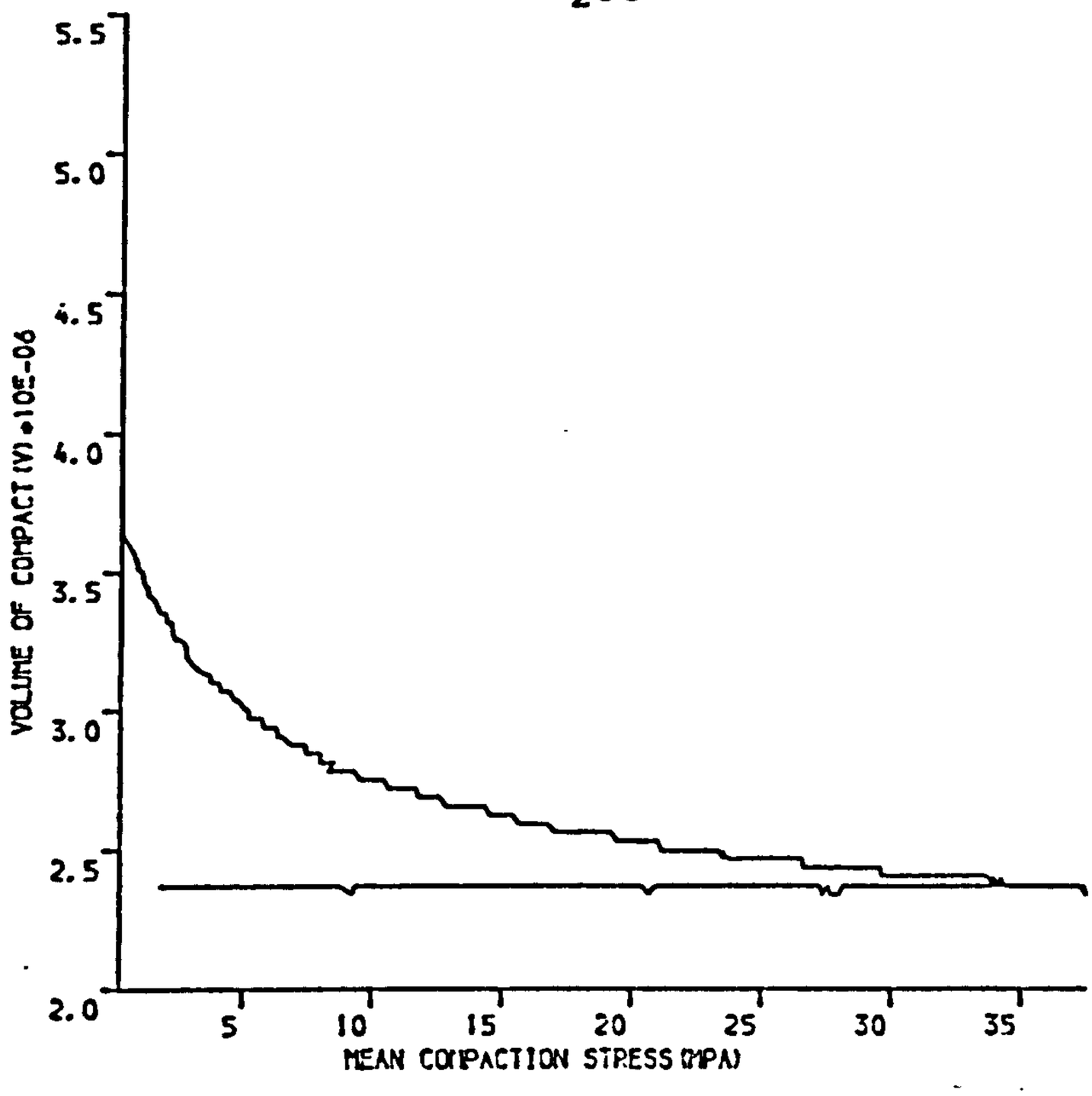

(A)

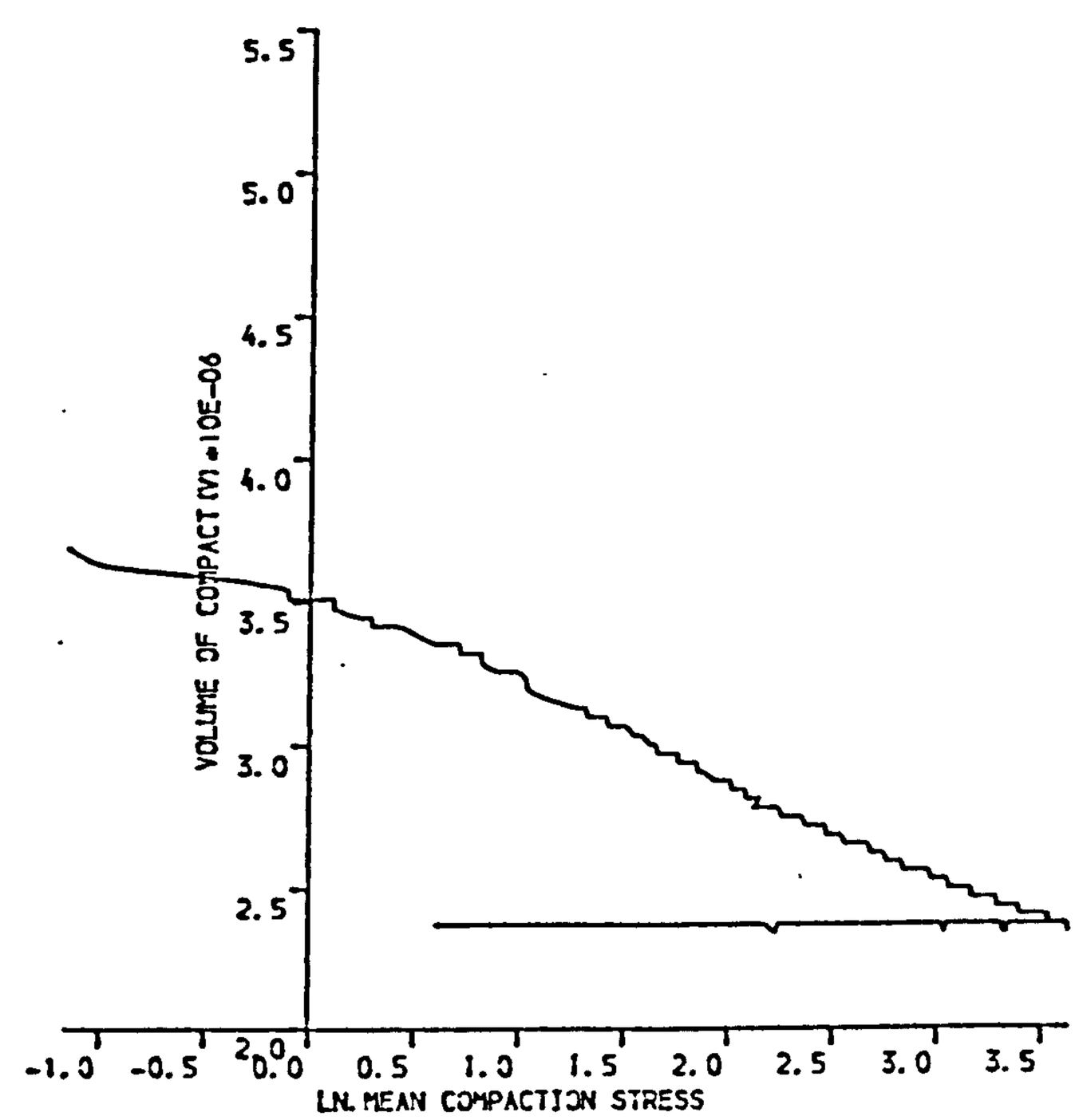

(B)

Figure 6.61 SUGAR UNIAXIALLY COMPACTED AT 63MPA
(A) COMPACT VOLUME VERSUS MEAN COMPACTION STRESS
(B) COMPACT VOLUME VERSUS NATURAL LOGARITHMIC COMPACTION STRESS

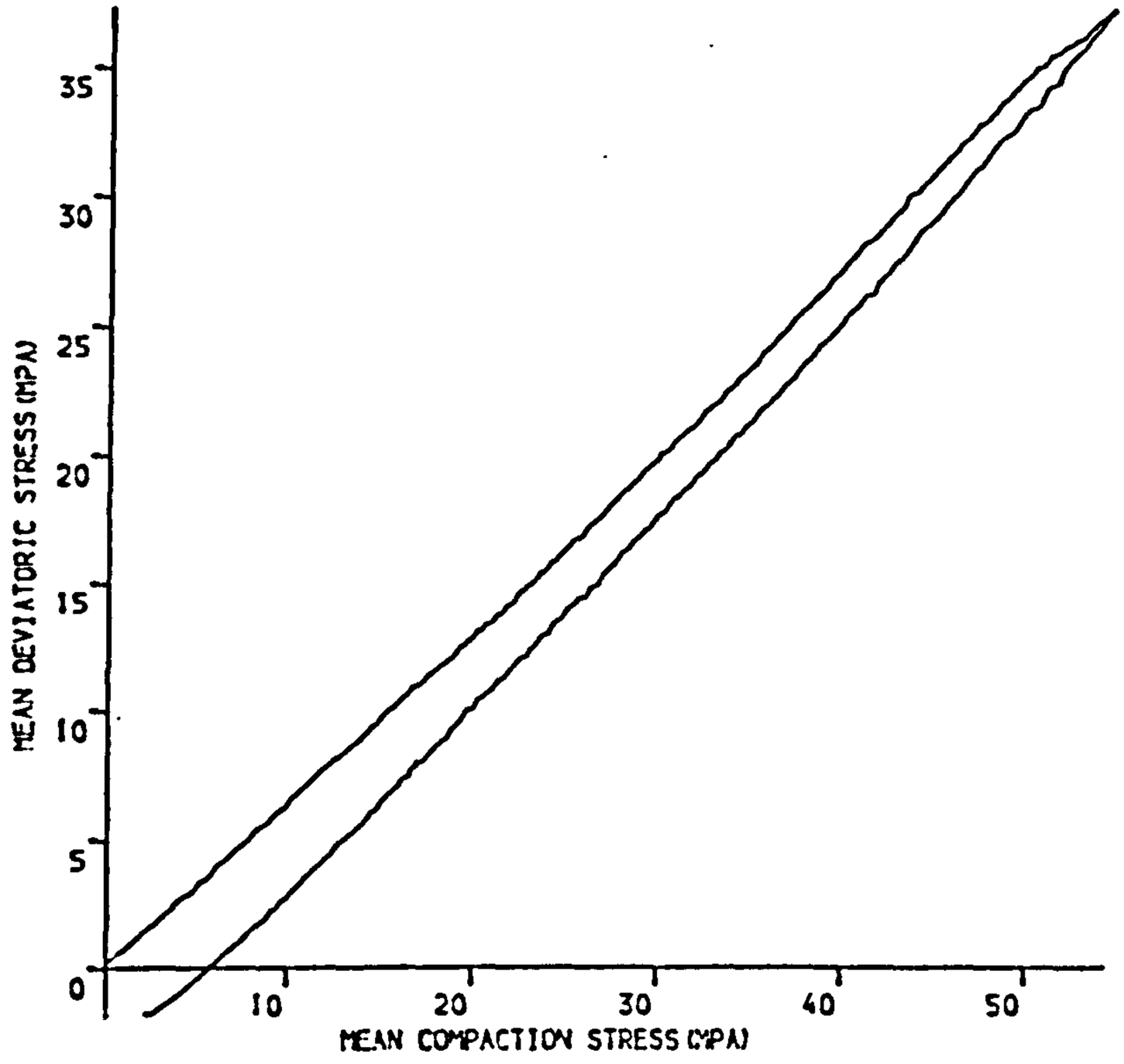

(A)

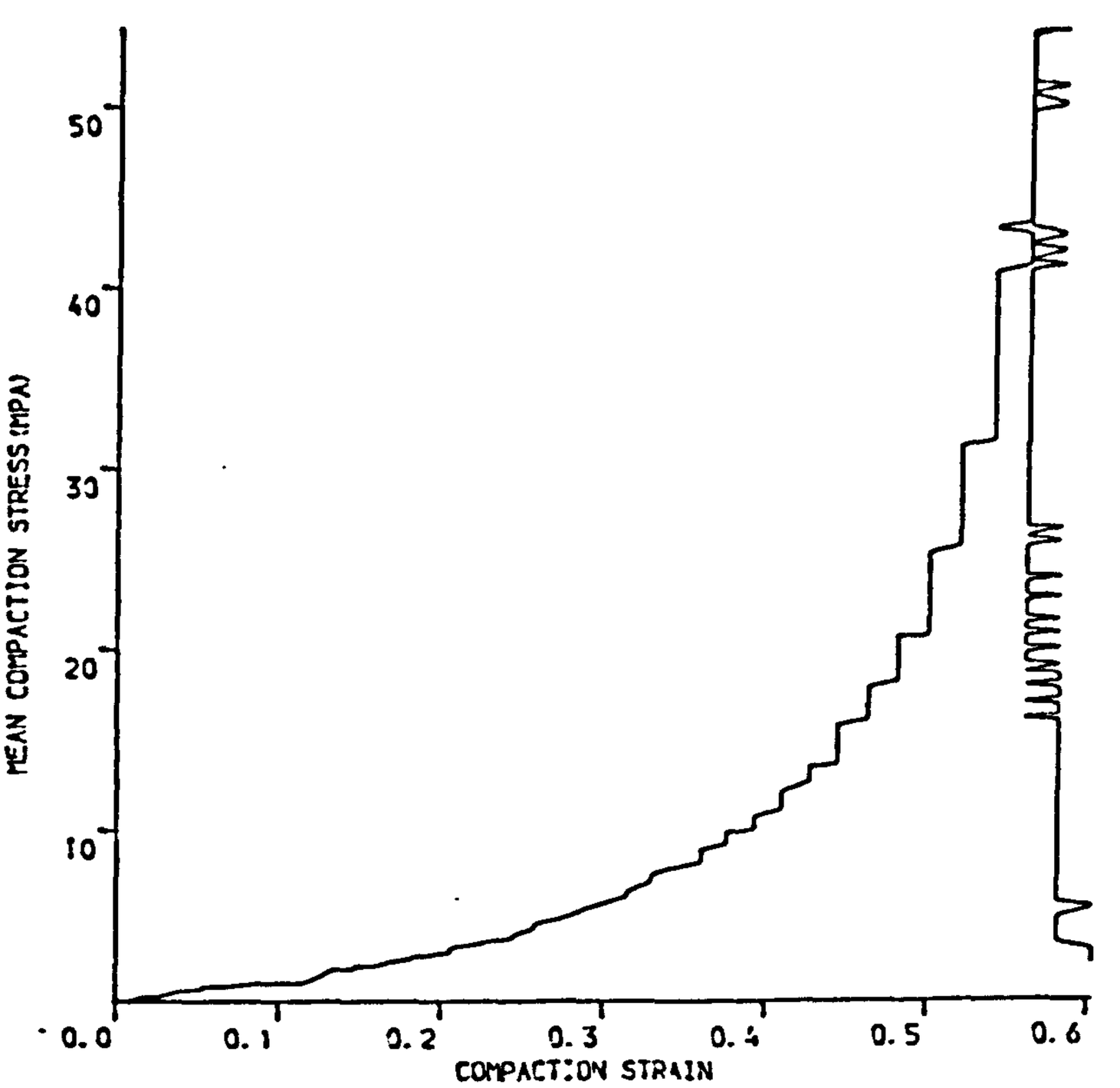

(B)

Figure6.62 SUGAR COMPACTED UNIAXIALLY AT 91MPA
(A) SHEAR STRESS VERSUS COMPACTION STRESS
(B) COMPACTION STRESS VERSUS NATURAL STRAIN

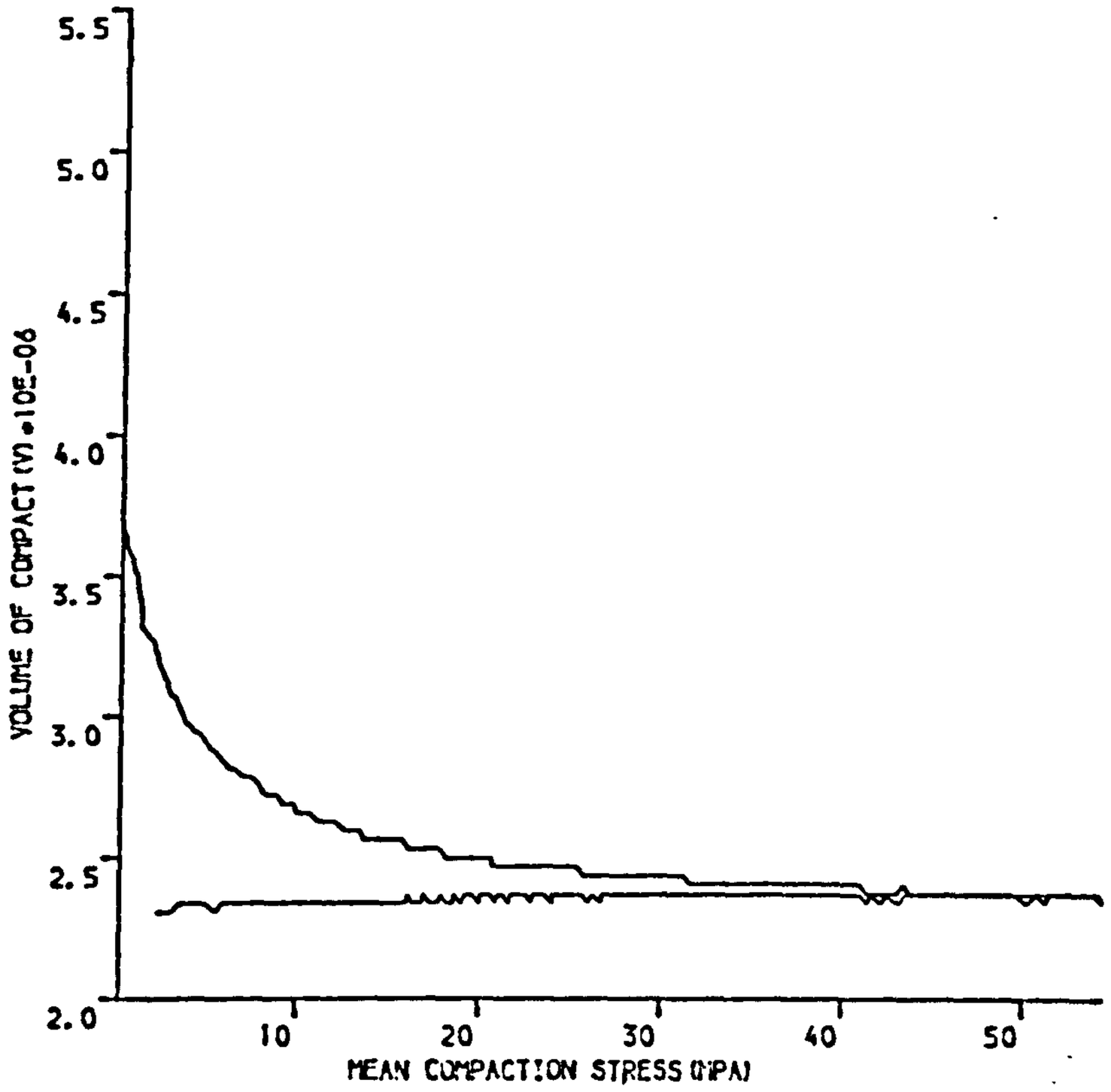

(A)

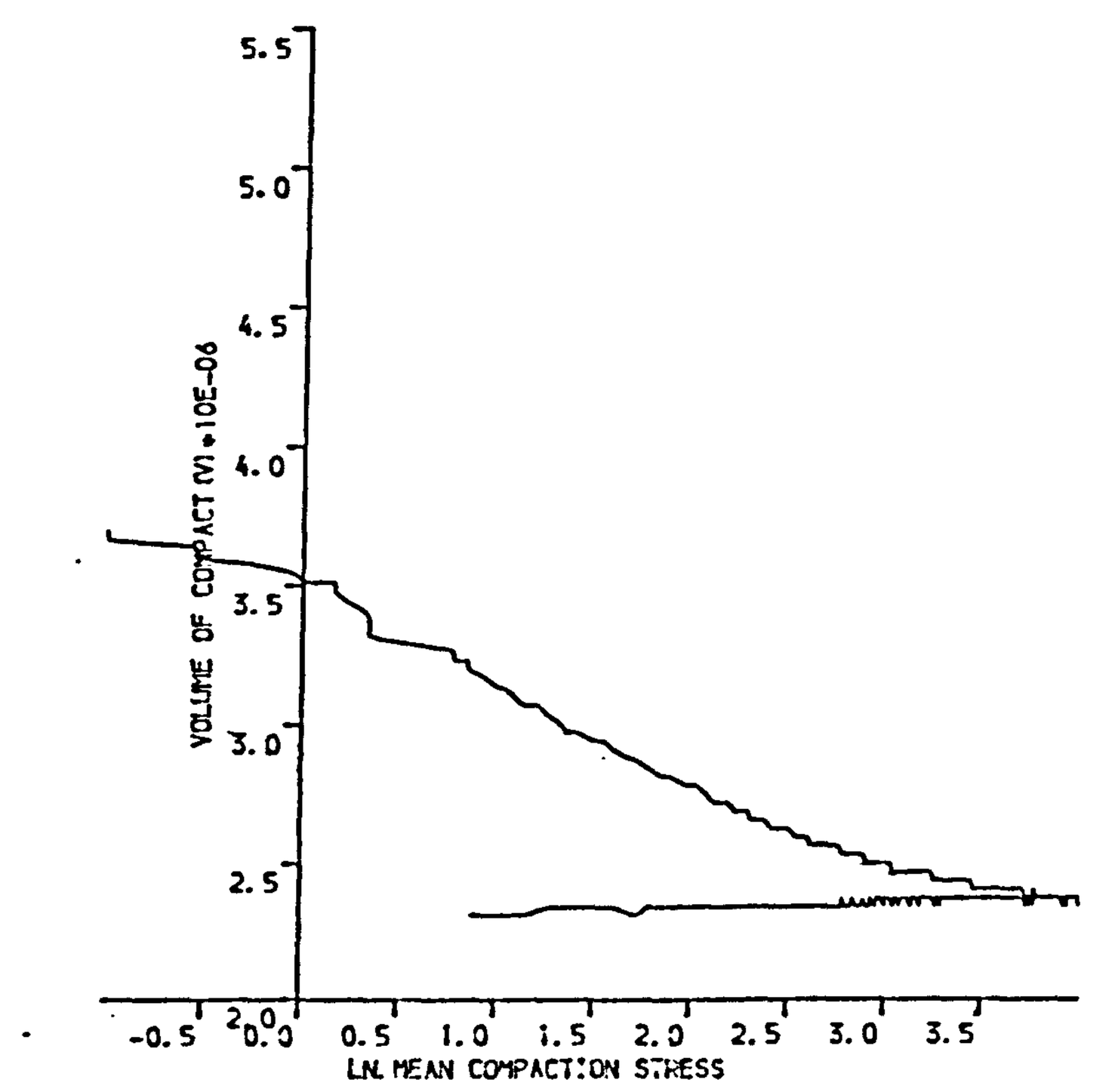

(B)

Figure 6.63 SUGAR UNIAXIALLY COMPACTED AT 91MPA
(A) COMPACT VOLUME VERSUS MEAN COMPACTION STRESS
(B) COMPACT VOLUME VERSUS NATURAL LOGARITHMIC COMPACTION STRESS

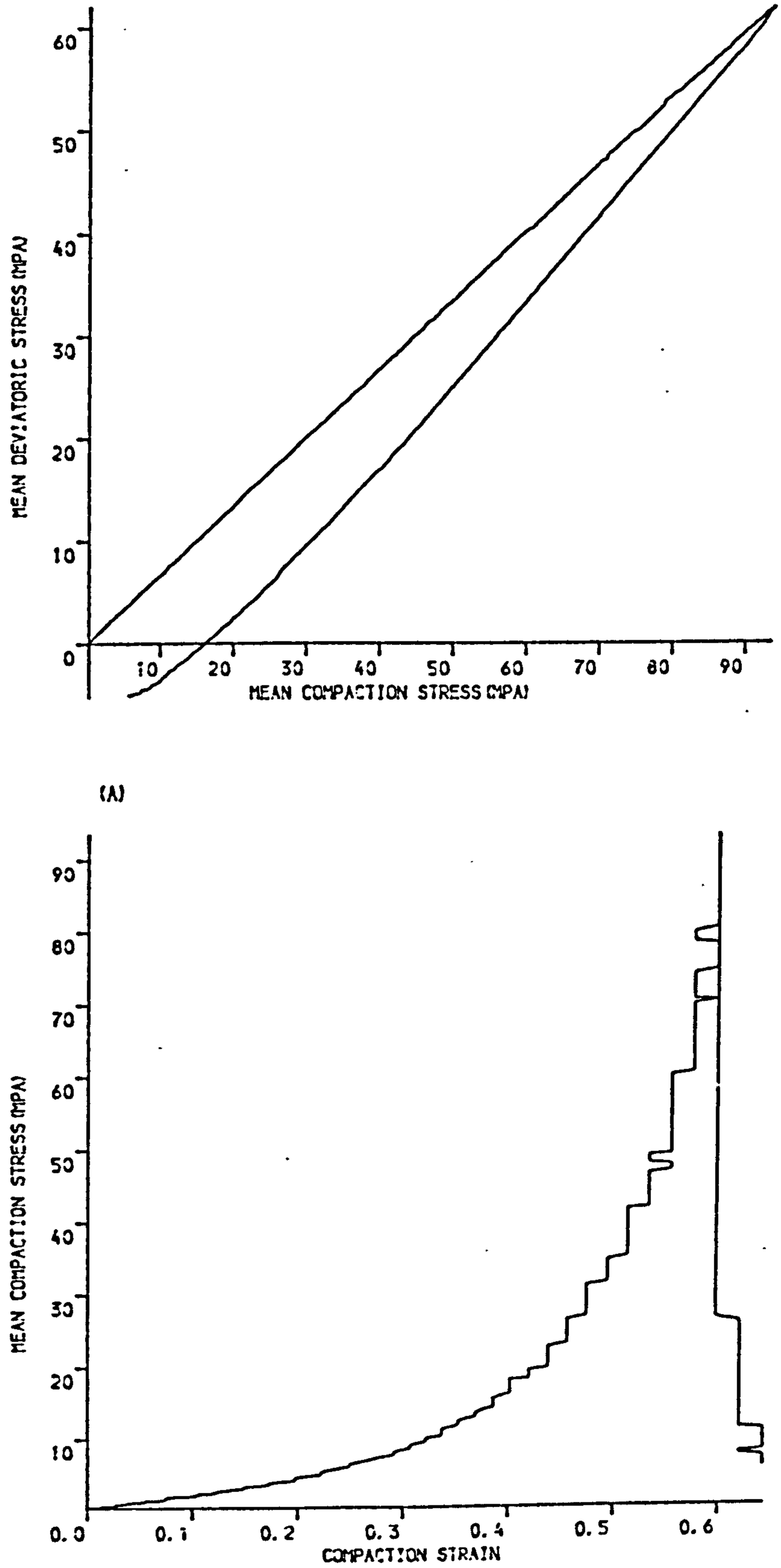

(A)

(B)

Figure 6.64 SUGAR COMPACTED UNIAXIALLY AT 155MPA
(A) SHEAR STRESS VERSUS COMPACTION STRESS
(B) COMPACTION STRESS VERSUS NATURAL STRAIN

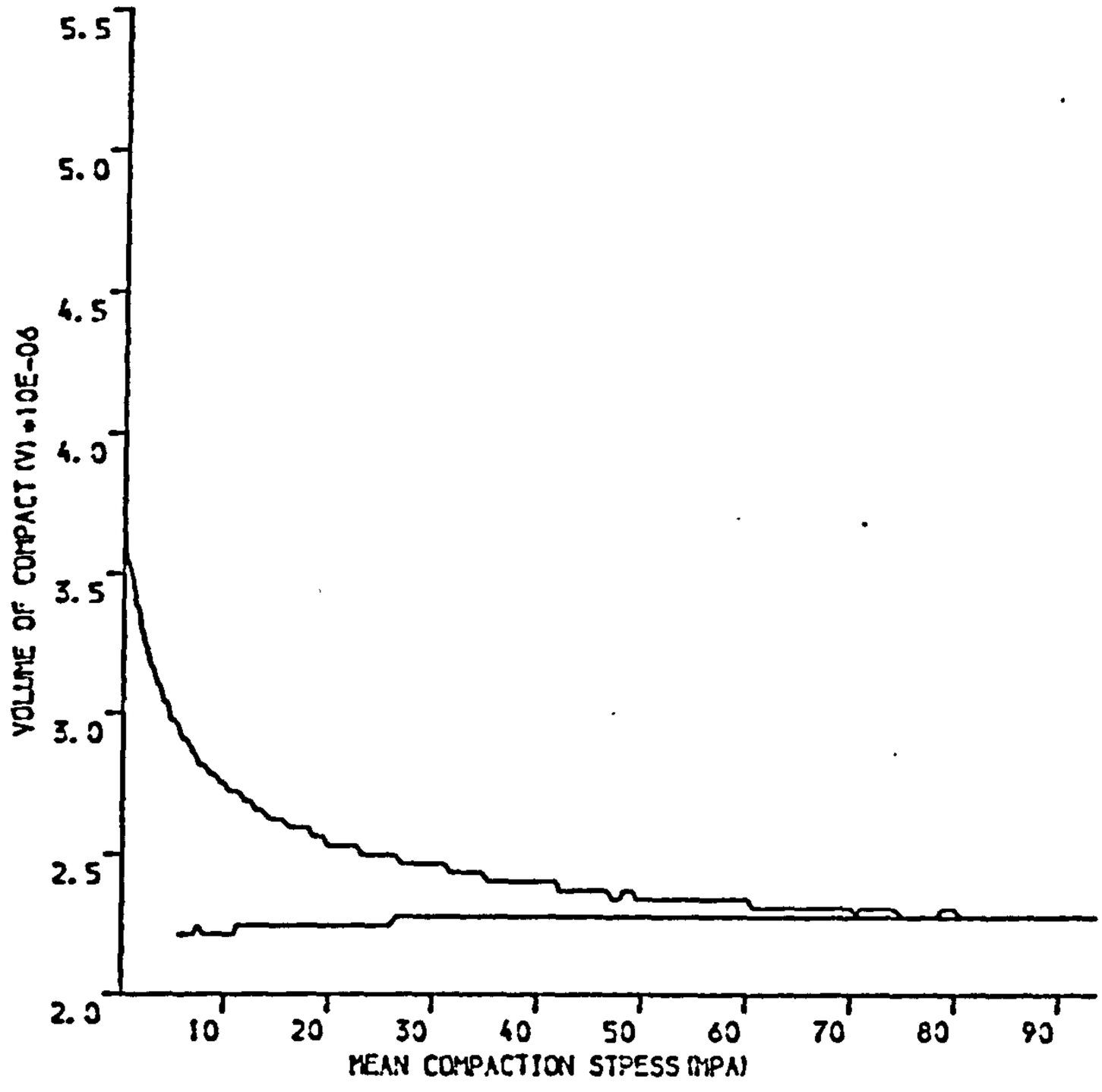

(A)

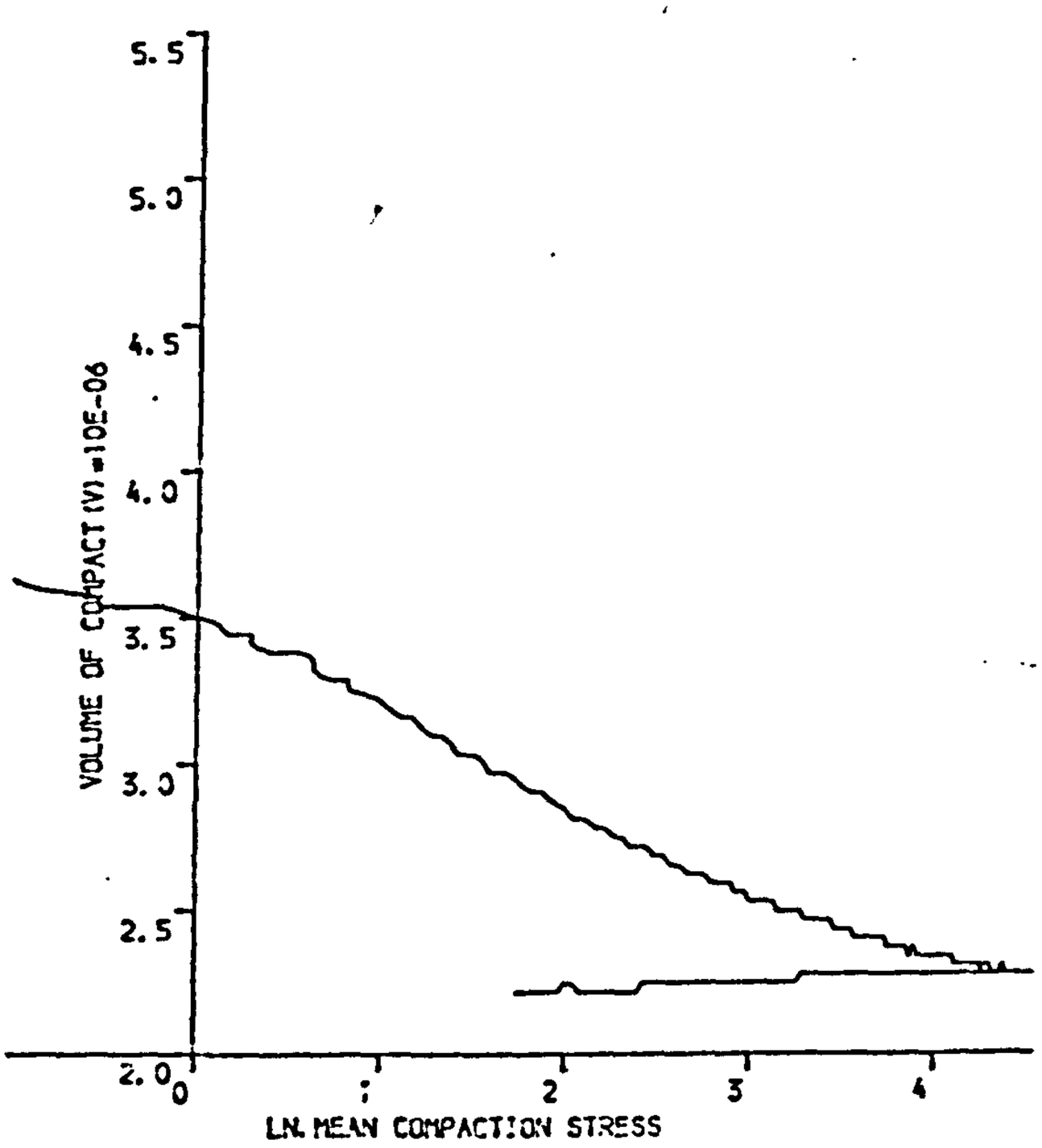

(B)

Figure 6.65 SUGAR UNIAXIALLY COMPACTED AT 155MPA
(A) COMPACT VOLUME VERSUS MEAN COMPACTION STRESS
(B) COMPACT VOLUME VERSUS NATURAL LOGARITHMIC COMPACTION STRESS

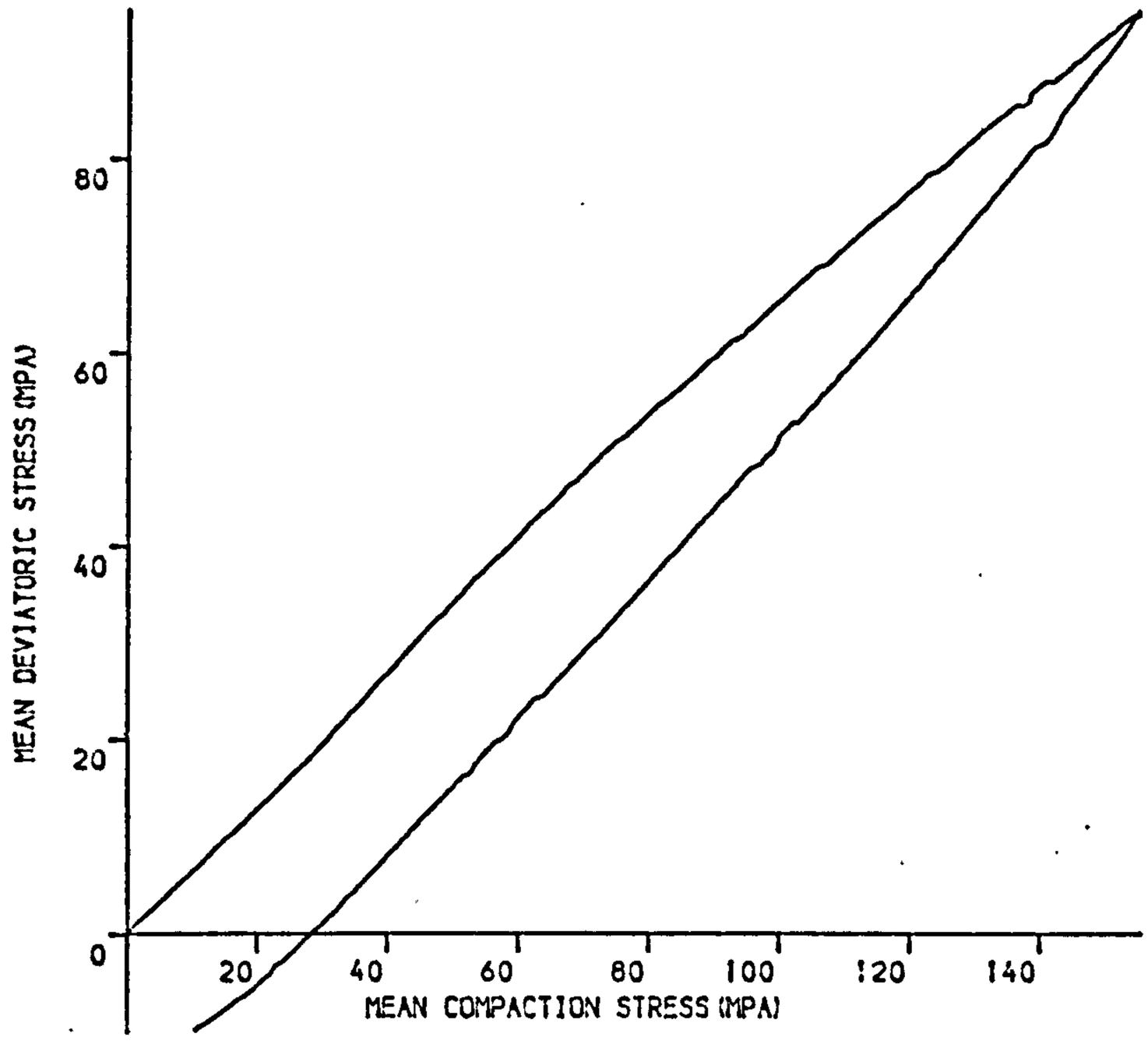

(A)

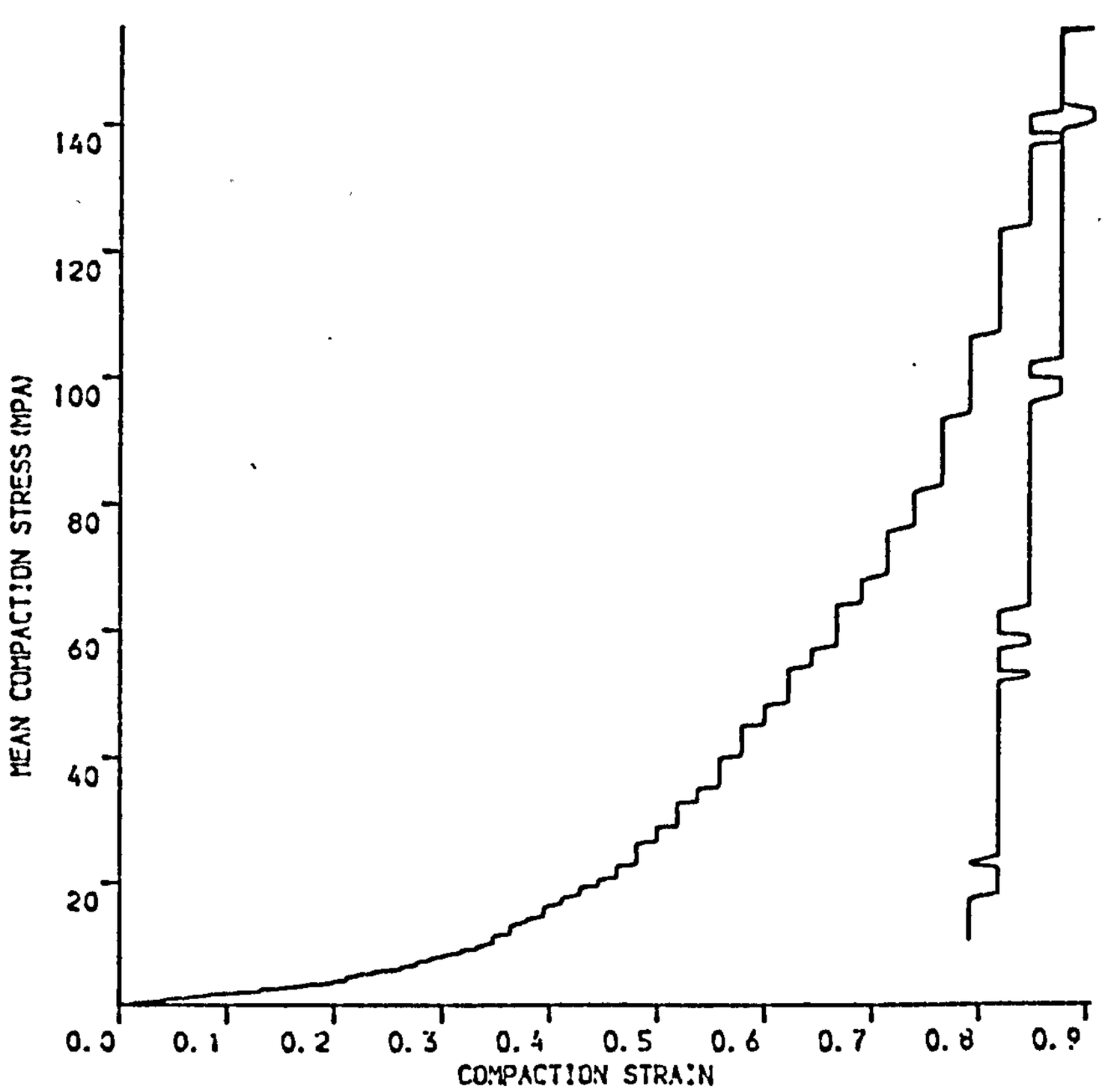

(B)

Figure 6.66 SUGAR COMPACTED UNIAXIALLY AT 250MPA
(A) SHEAR STRESS VERSUS COMPACTION STRESS
(B) COMPACTION STRESS VERSUS NATURAL STRAIN

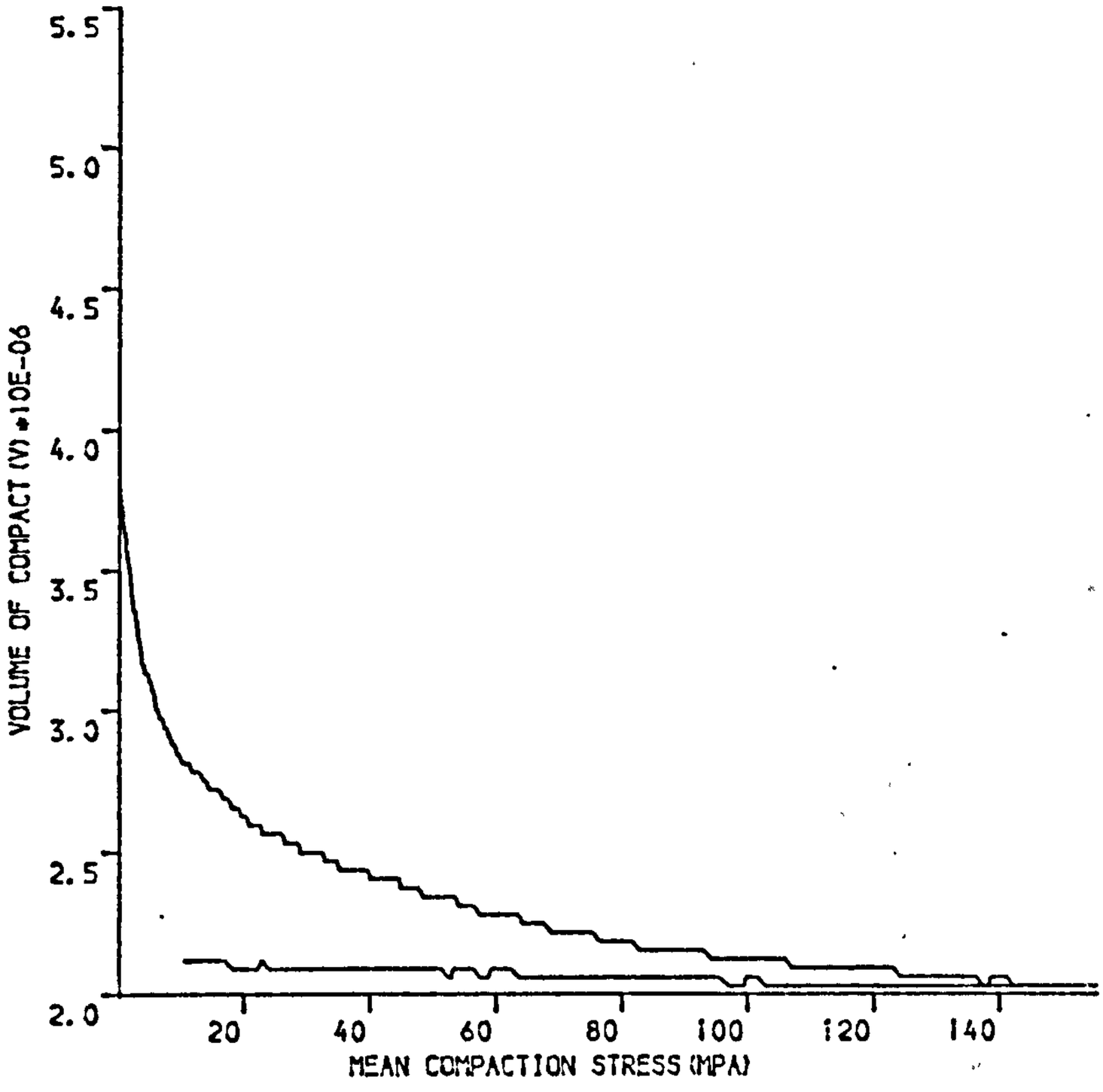

(A)

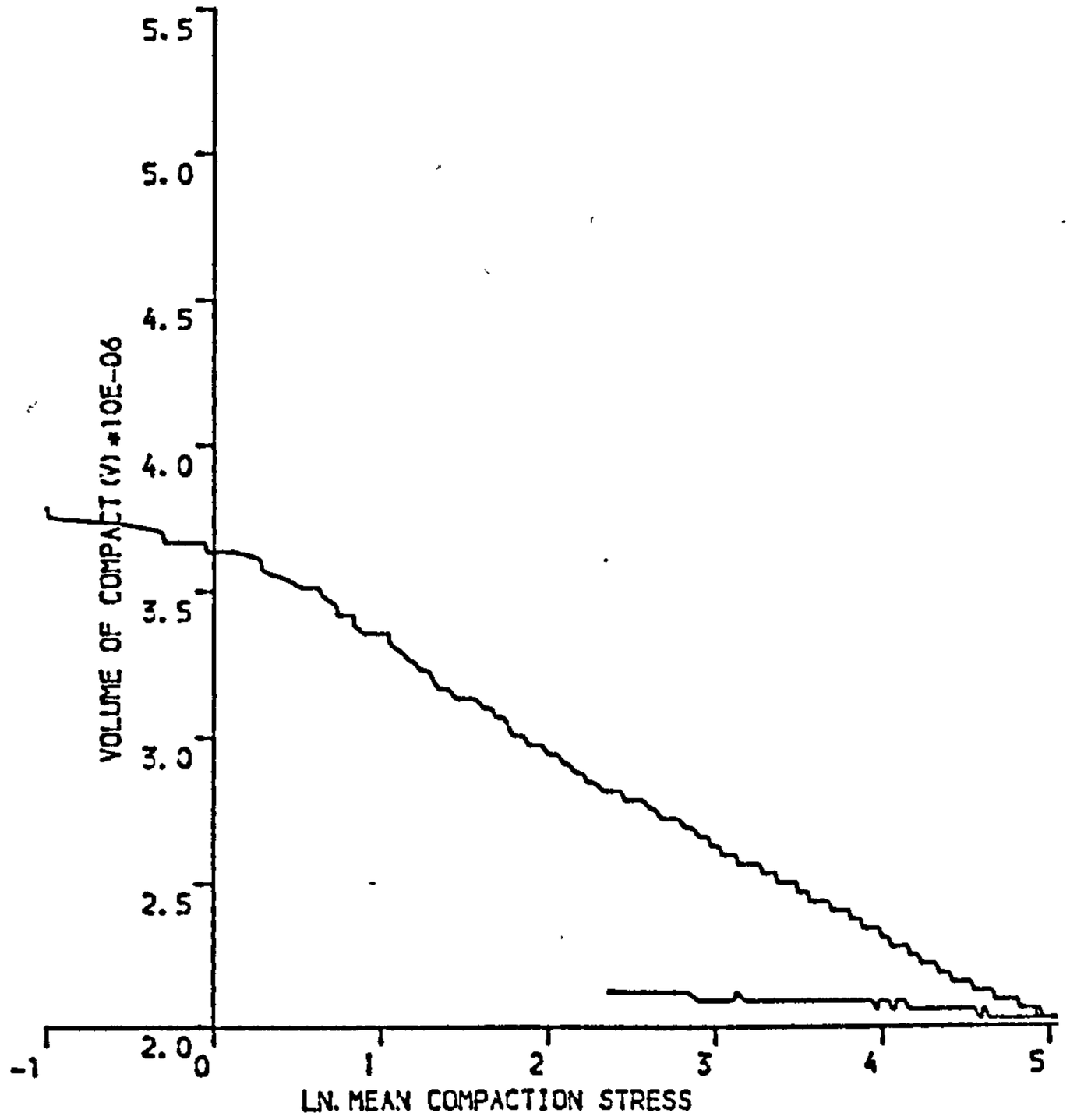

(B)

Figure 6.67 SUGAR UNIAXIALLY COMPACTED AT 250MPA
(A) COMPACT VOLUME VERSUS MEAN COMPACTION STRESS
(B) COMPACT VOLUME VERSUS NATURAL LOGARITHMIC COMPACTION STRESS

Figure 6.68 3-D representation of sugar compacted at 31 MPa

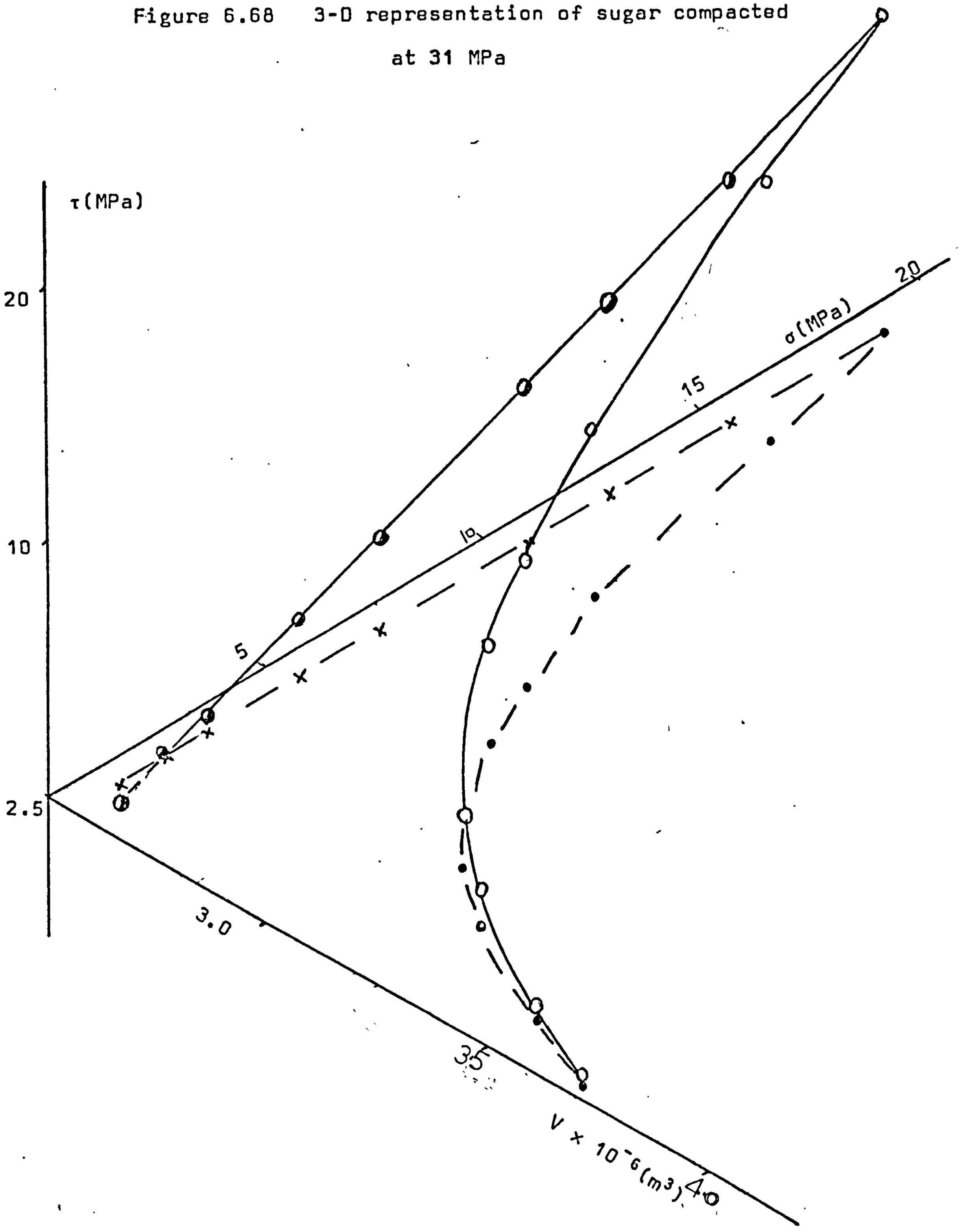

Figure 6.69 3-D representation of sugar compacted at 63 MPa

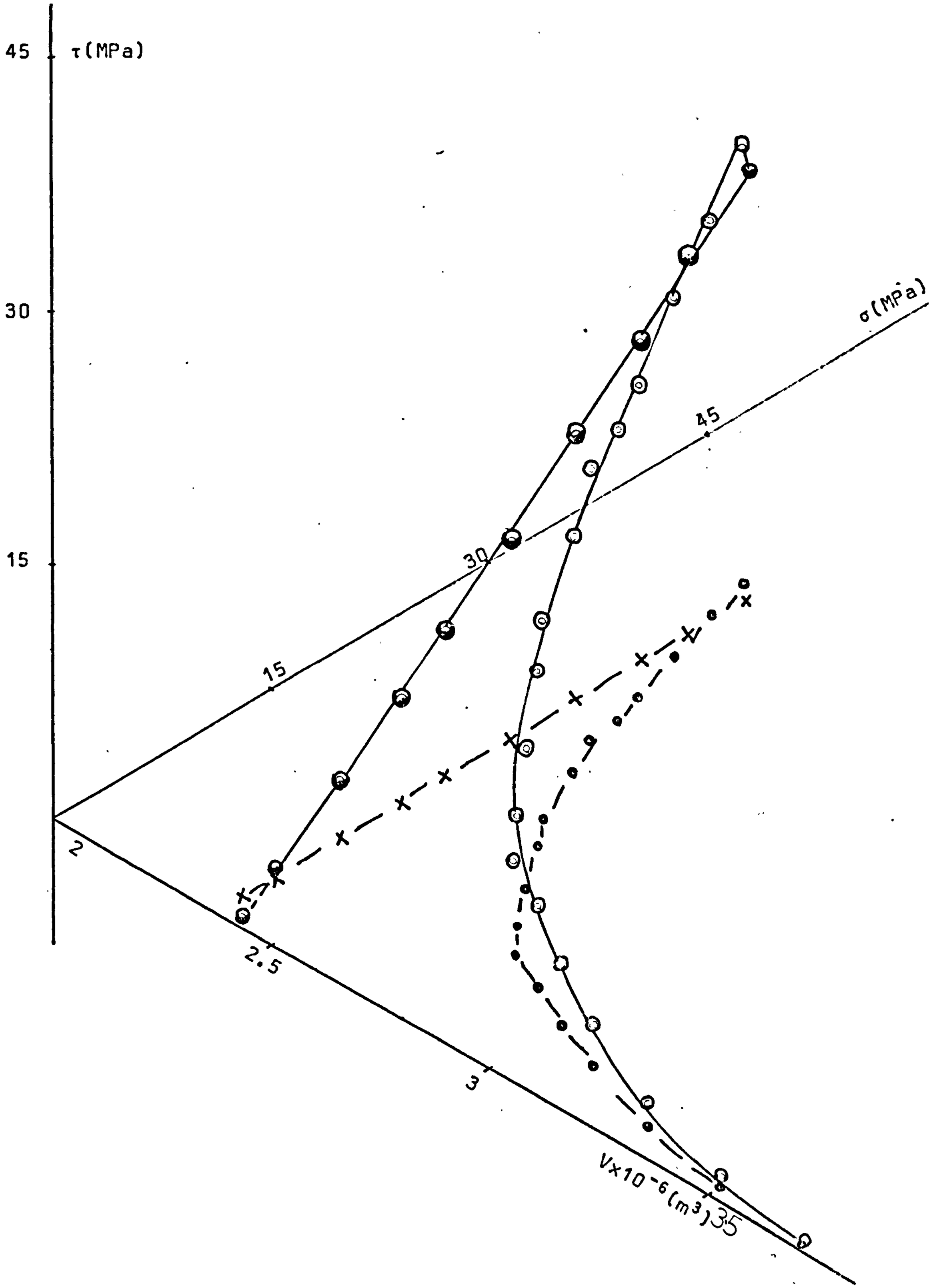

Figure 6.70 3-D representation of sugar compacted at 91 MPa

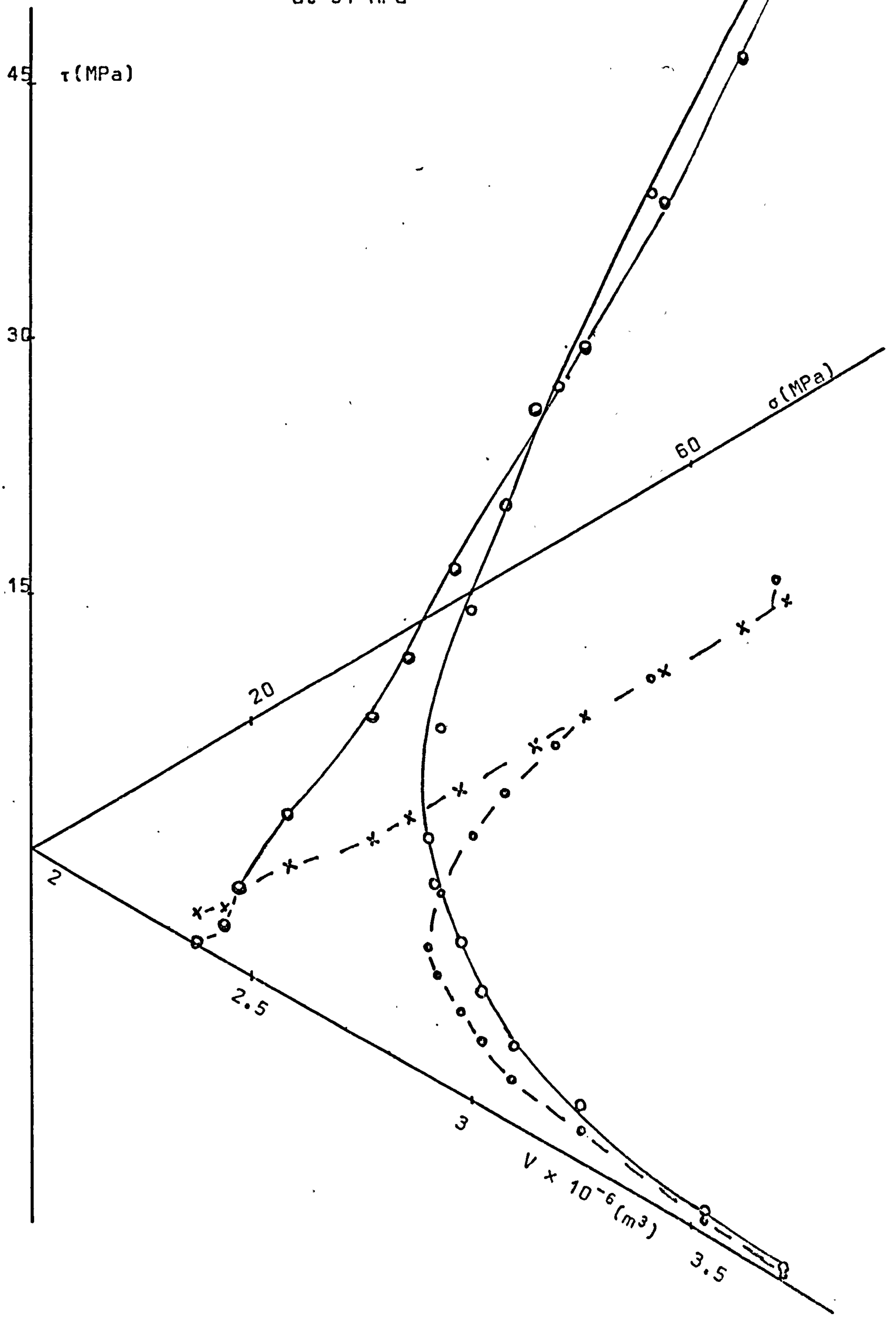

Figure 6.71 3-D representation of sugar compacted at 120 MPa

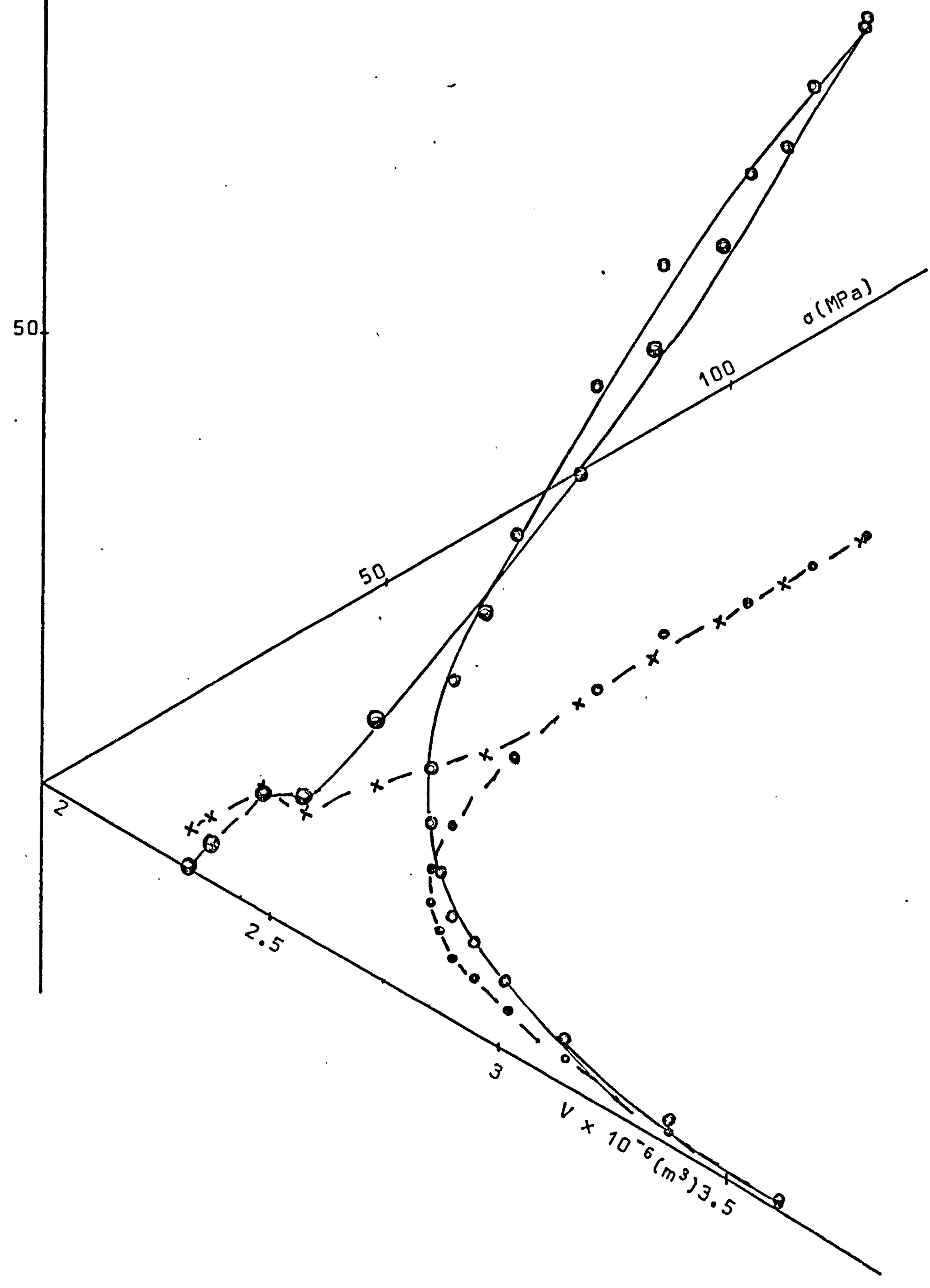

Figure 6.72 3-D representation of sugar compacted at 250 MPa

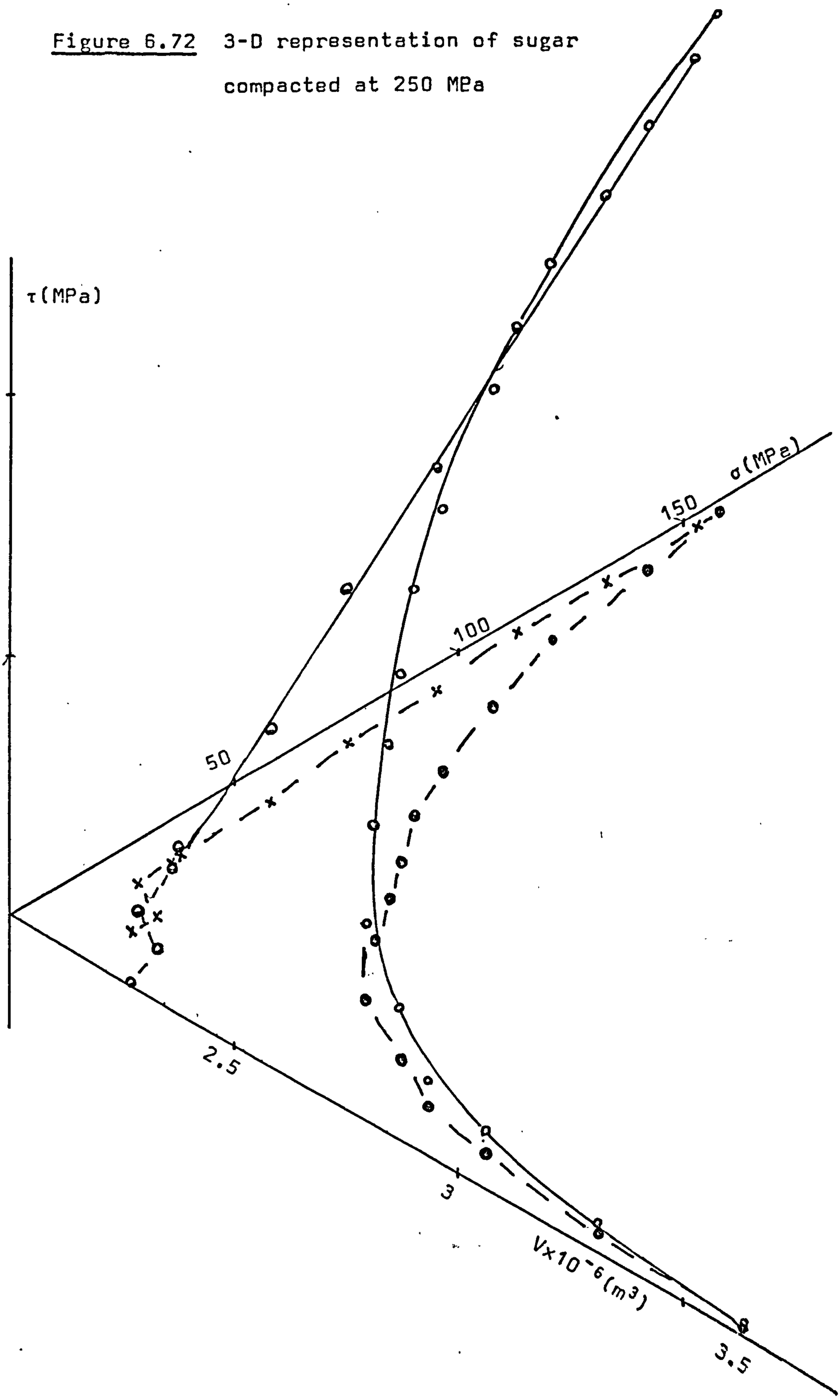

Figure 6.73 Mohr circles constructed for styrocell compacted at 56 MPa

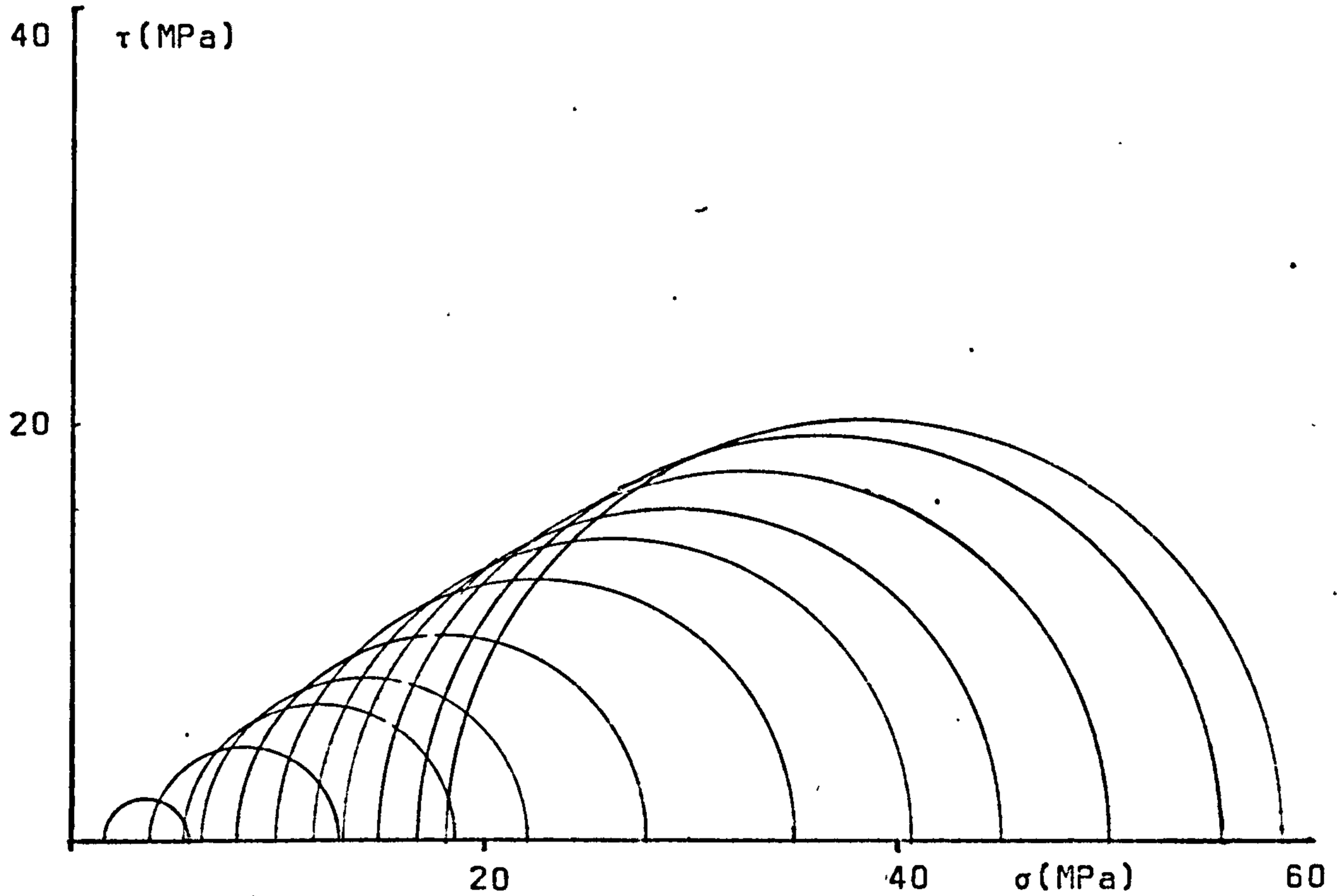

Figure 6.74 Mohr circles constructed for styrocell compacted at 153 MPa

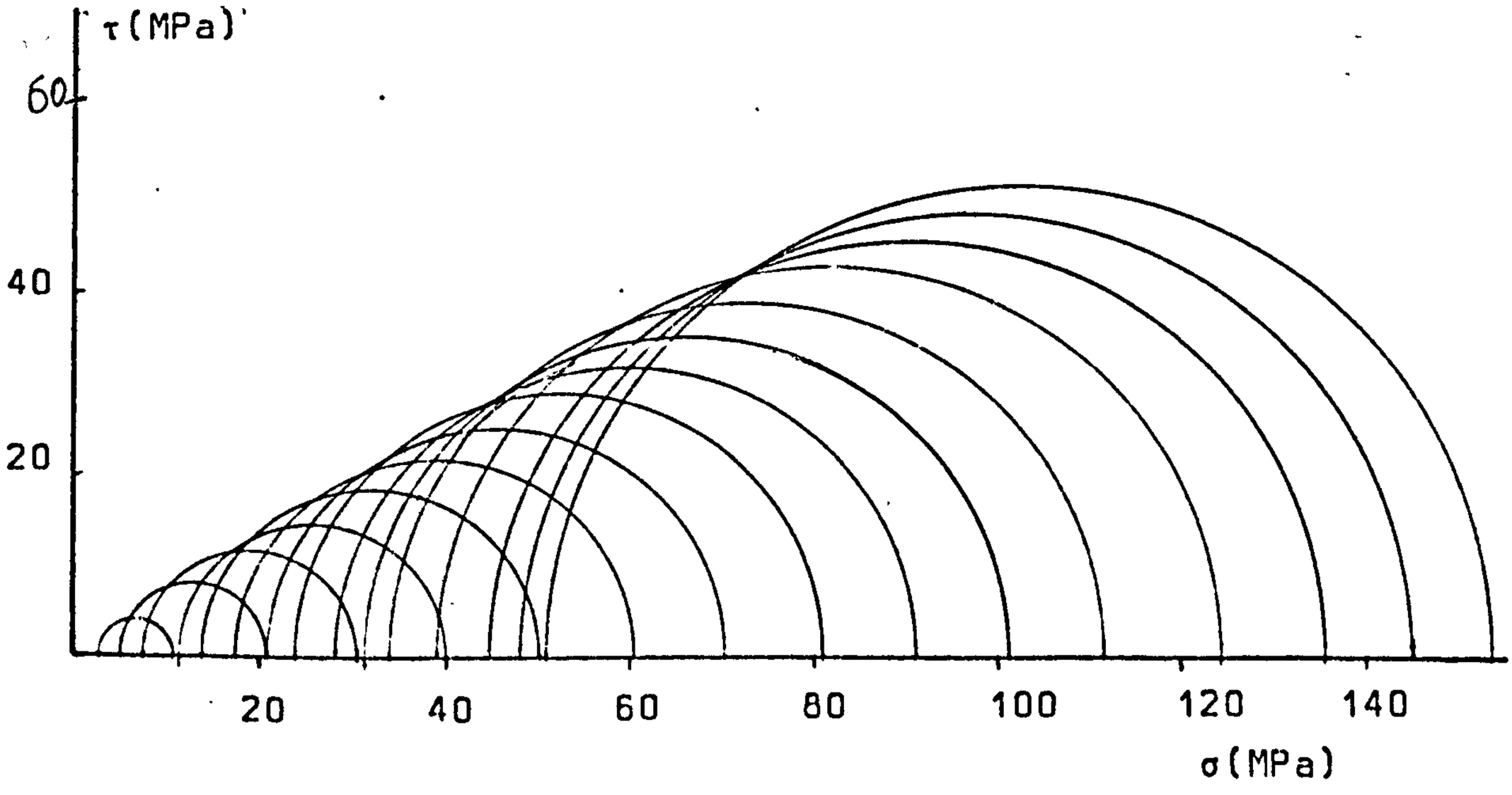

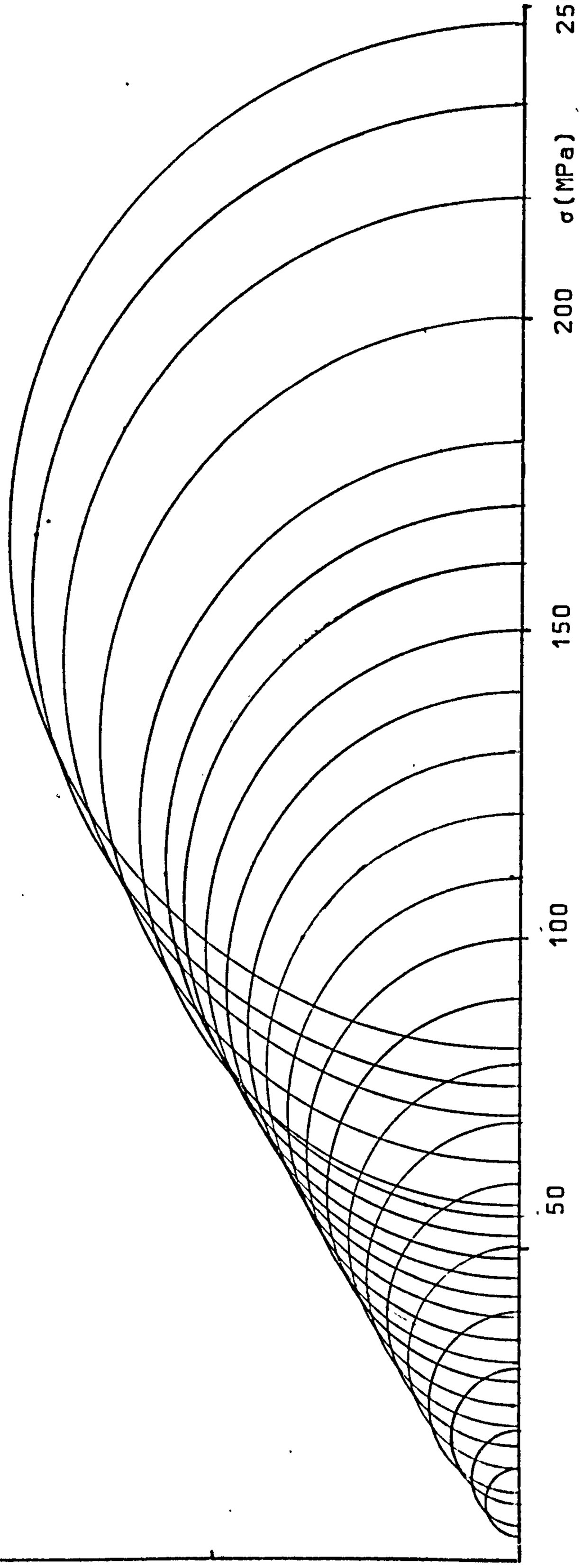

Figure 6.75 Mohr Circles constructed for Styrocell compacted at 247 MPa

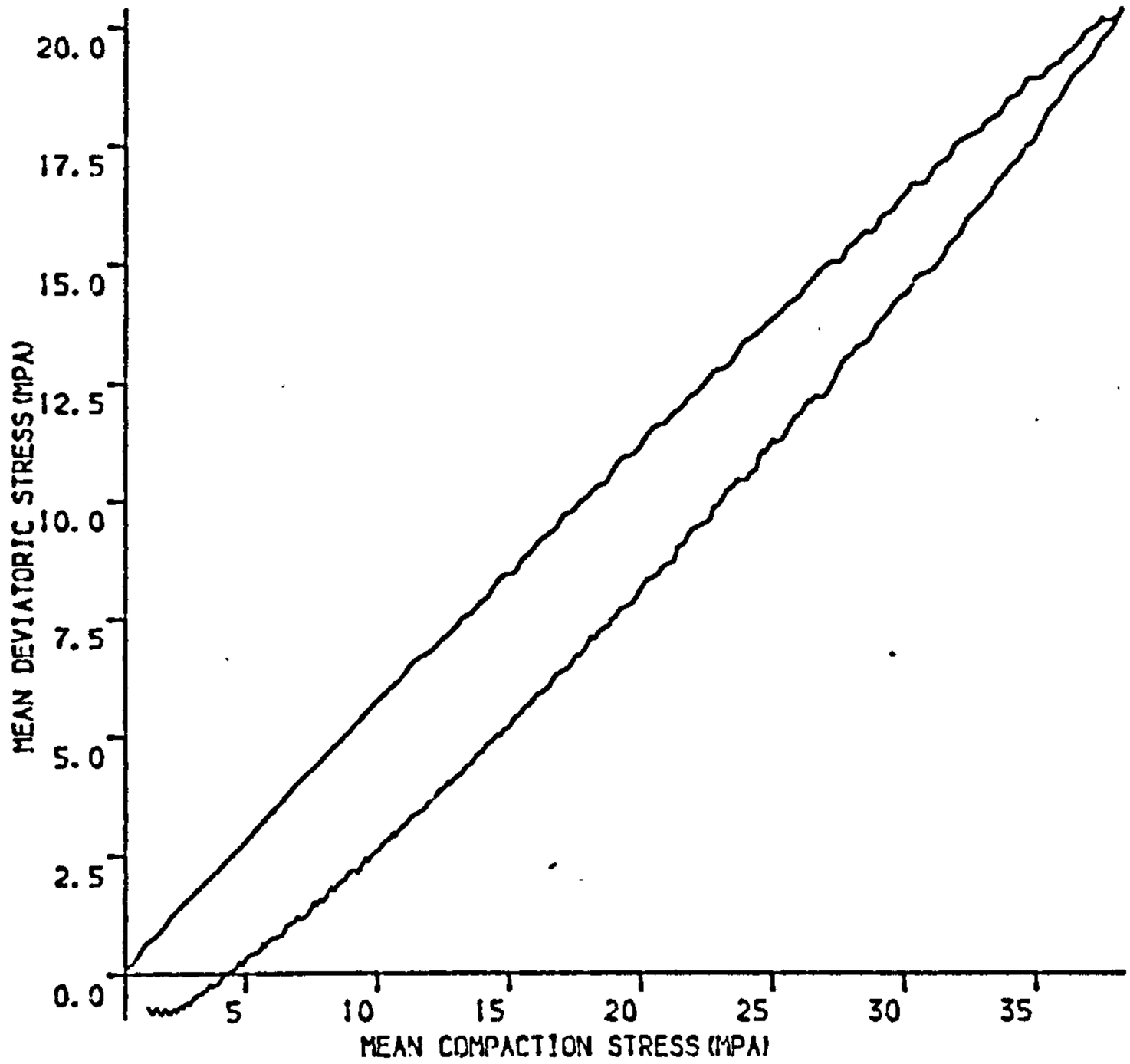

(A)

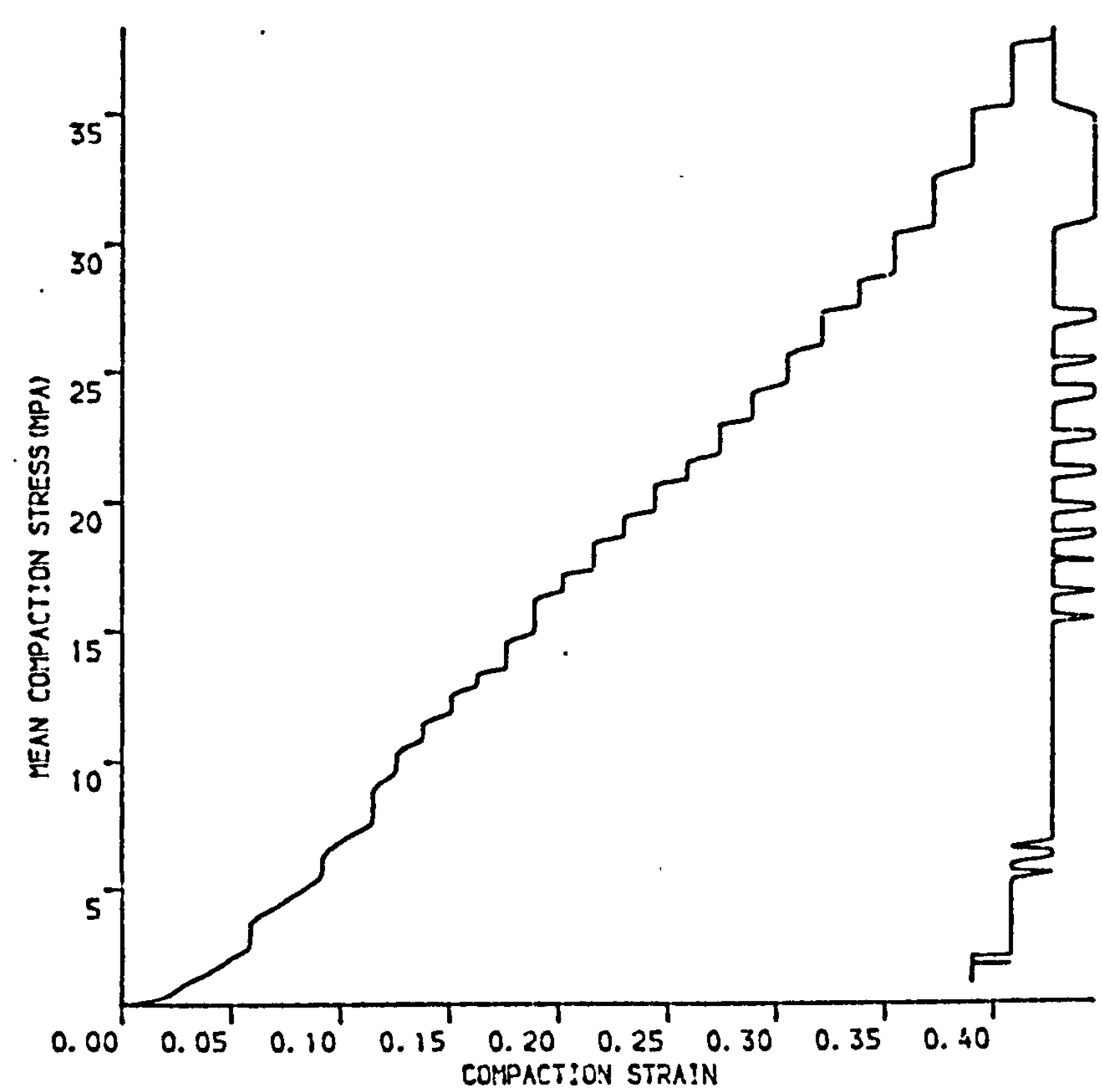

(B)

Figure 6.76 STYROCELL COMPACTED UNIAXIALLY AT 58MPA
(A) SHEAR STRESS VERSUS COMPACTION STRESS
(B) COMPACTION STRESS VERSUS NATURAL STRAIN

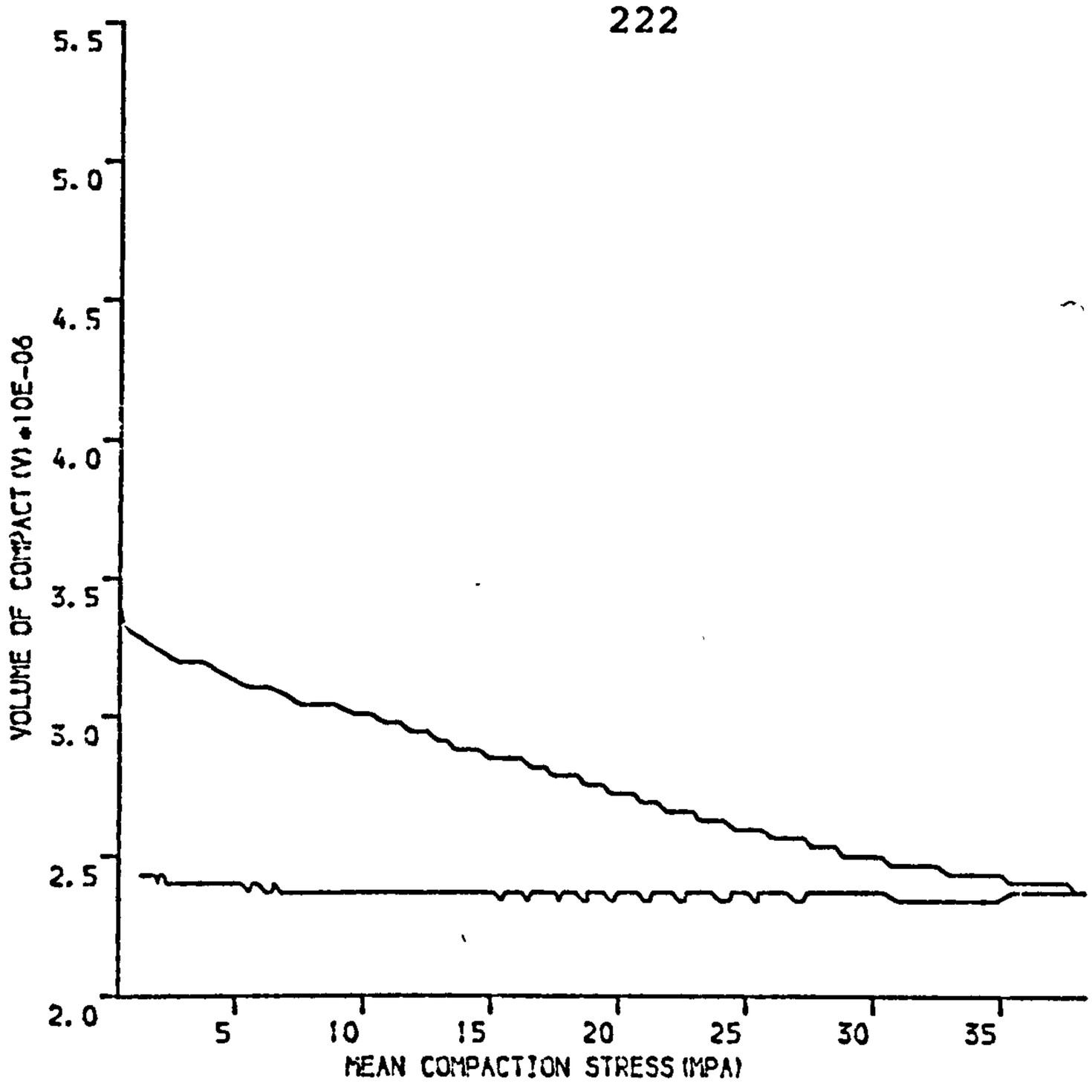

(A)

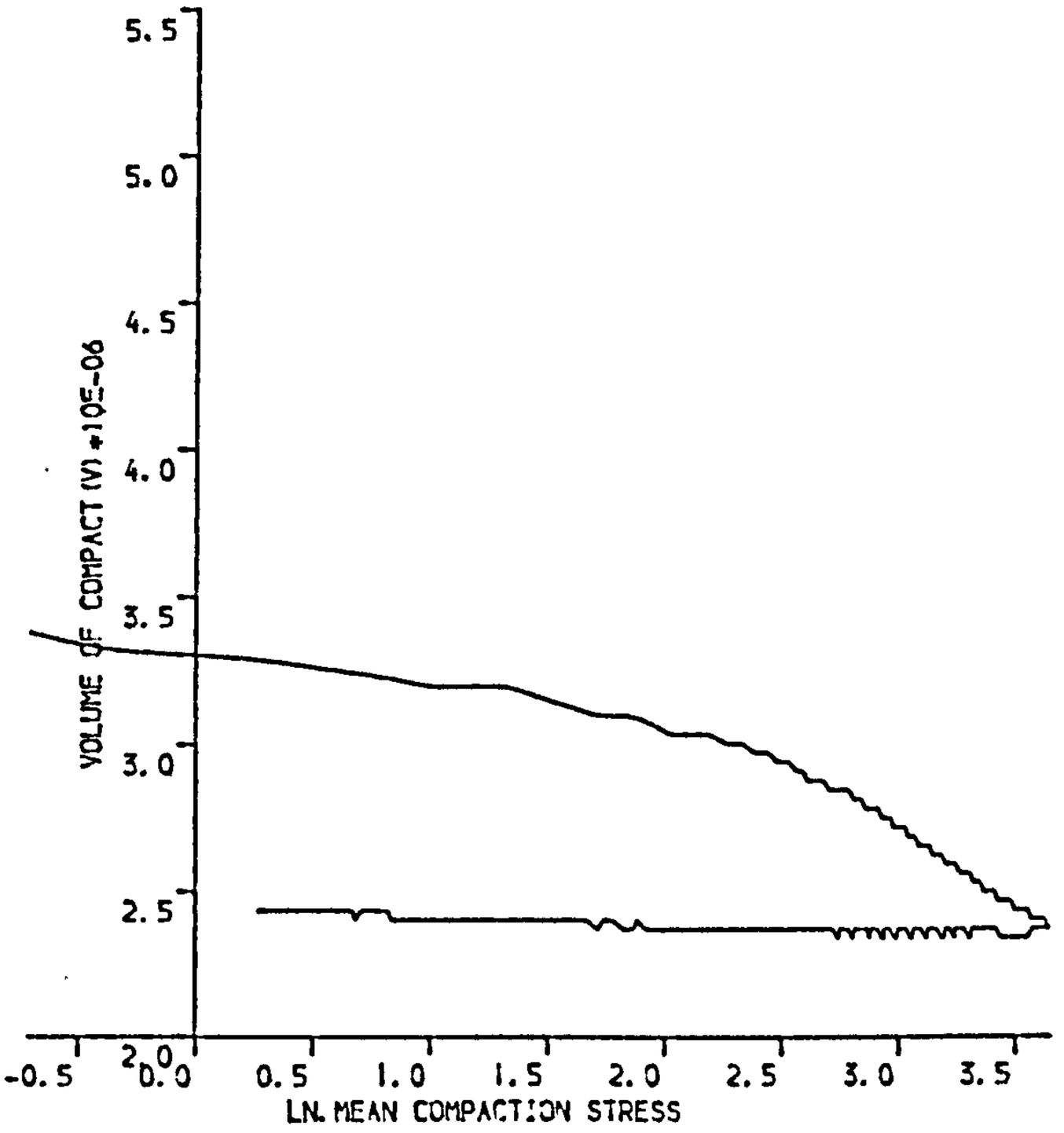

(B)

Figure 6.77 STYROCELL UNIAXIALLY COMPACTED AT 58MPA
(A) COMPACT VOLUME VERSUS MEAN COMPACTION STRESS
(B) COMPACT VOLUME VERSUS NATURAL LOGARITHMIC COMPACTION STRESS

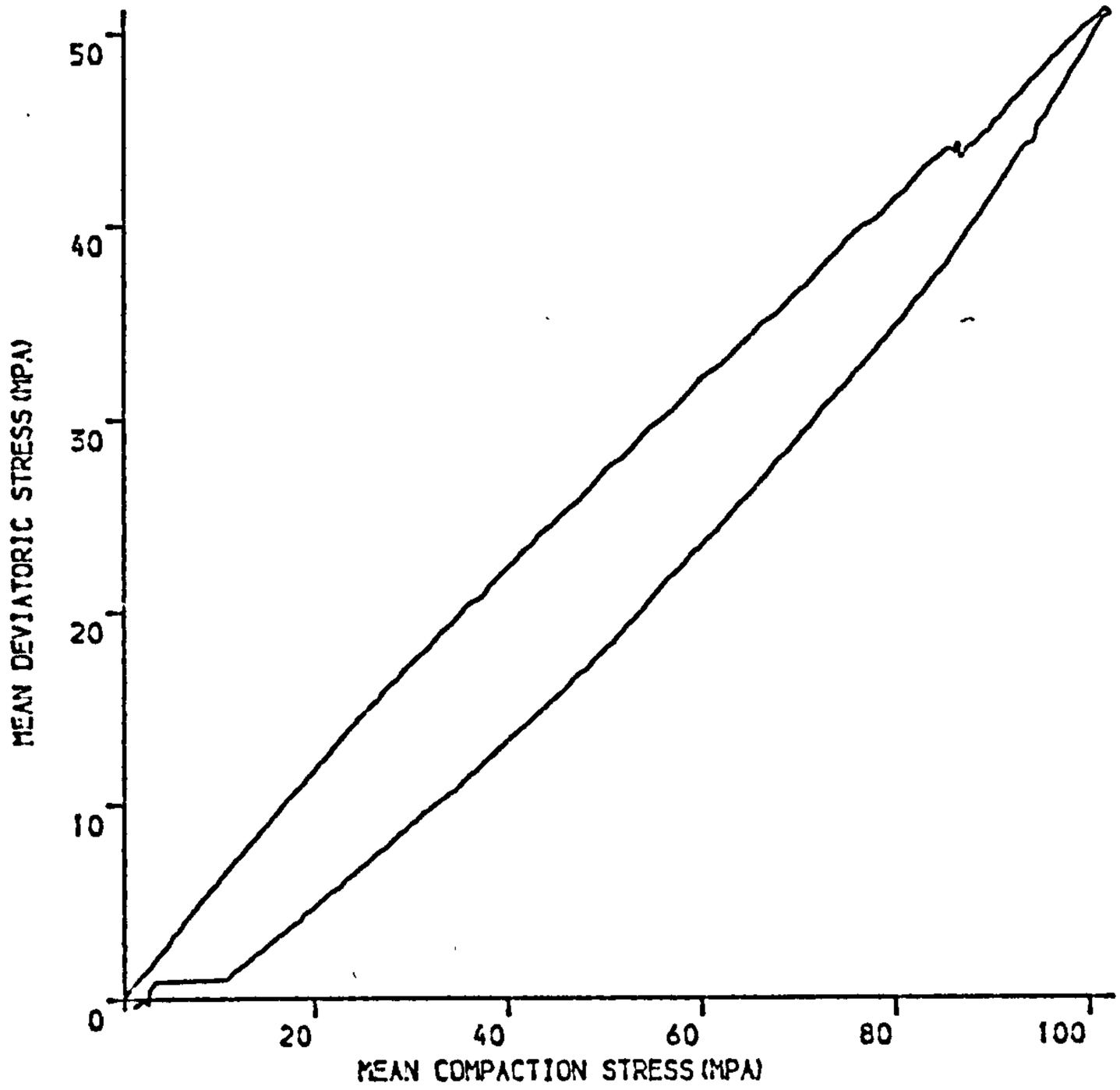

(A)

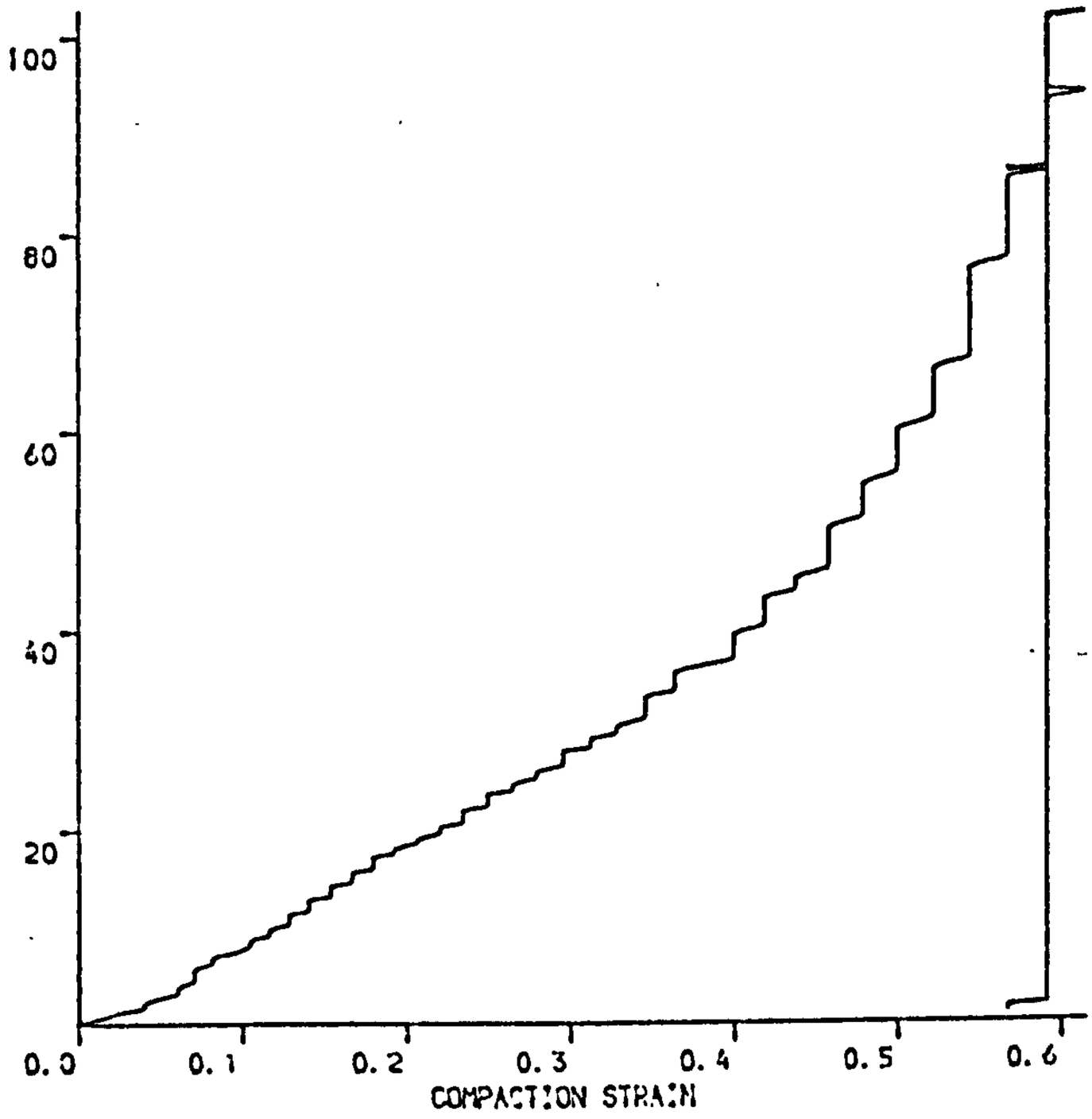

(B)

Figure 6.78 STYROCELL COMPACTED UNIAXIALLY AT 155MPA

(A) SHEAR STRESS VERSUS COMPACTION STRESS

(B) COMPACTION STRESS VERSUS NATURAL STRAIN

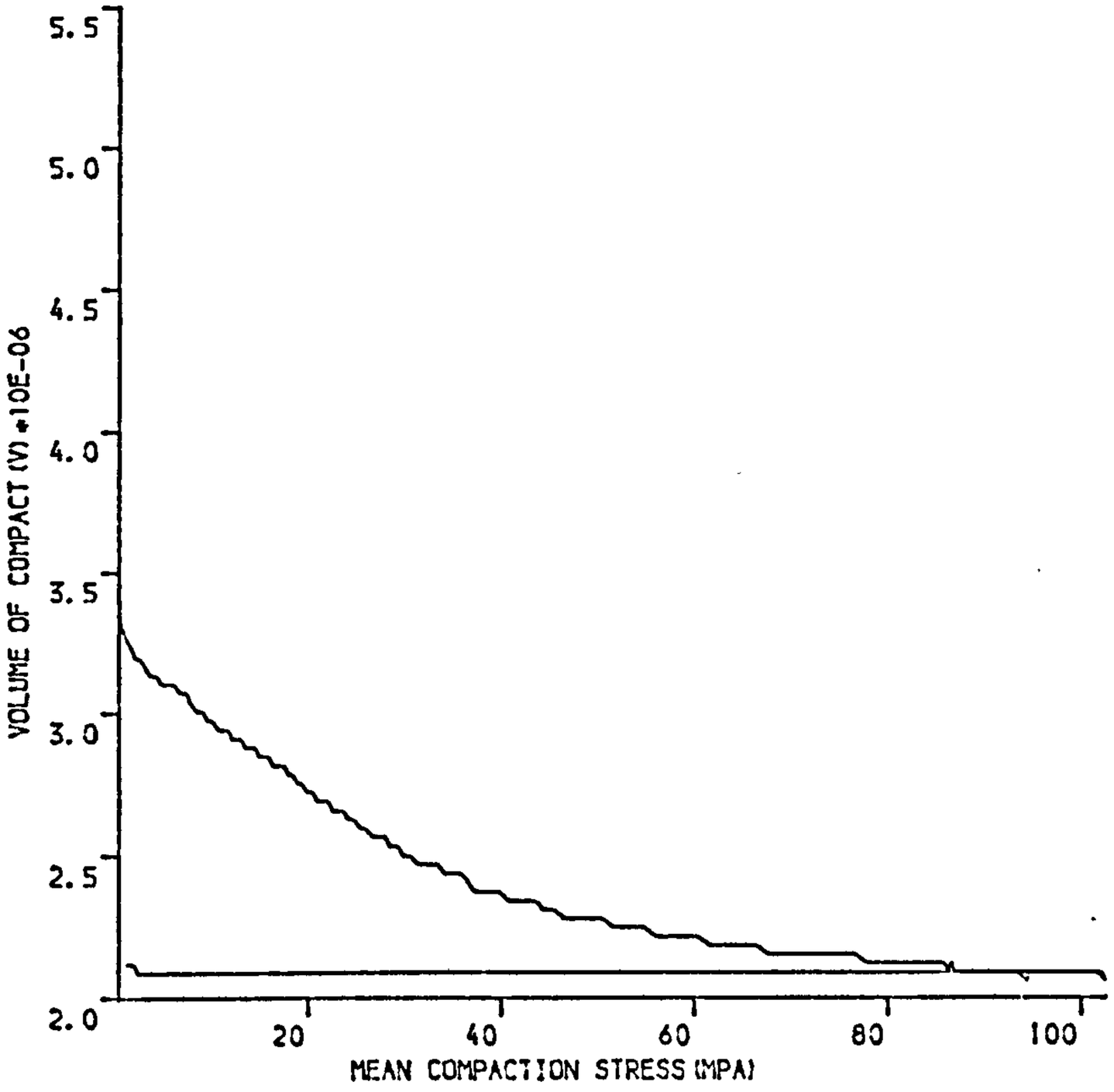

(A)

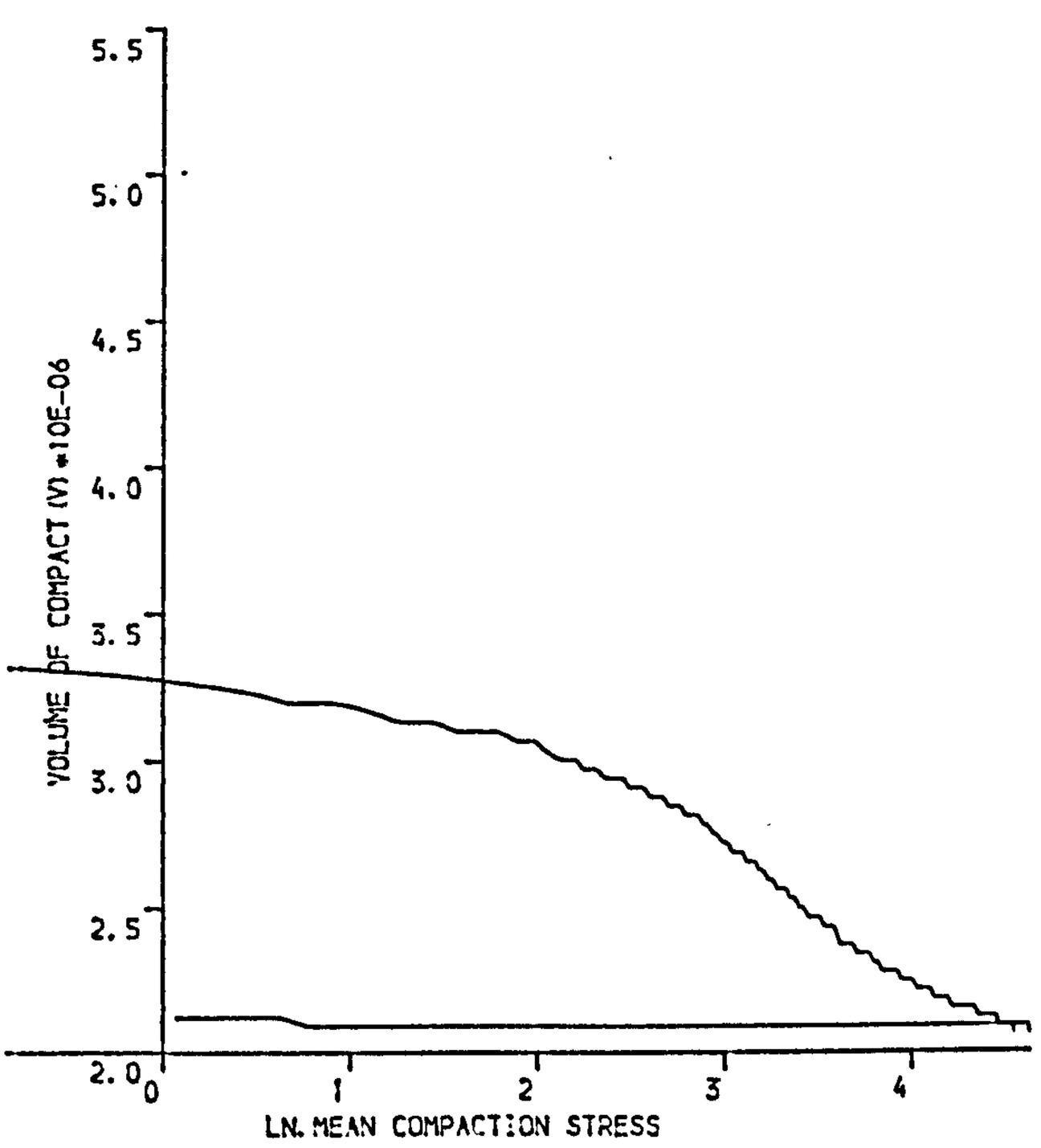

(B)

Figure 6.79 STYROCELL UNIAXIALLY COMPACTED AT 153MPA
(A) COMPACT VOLUME VERSUS MEAN COMPACTION STRESS
(B) COMPACT VOLUME VERSUS NATURAL LOGARITHMIC COMPACTION STRESS

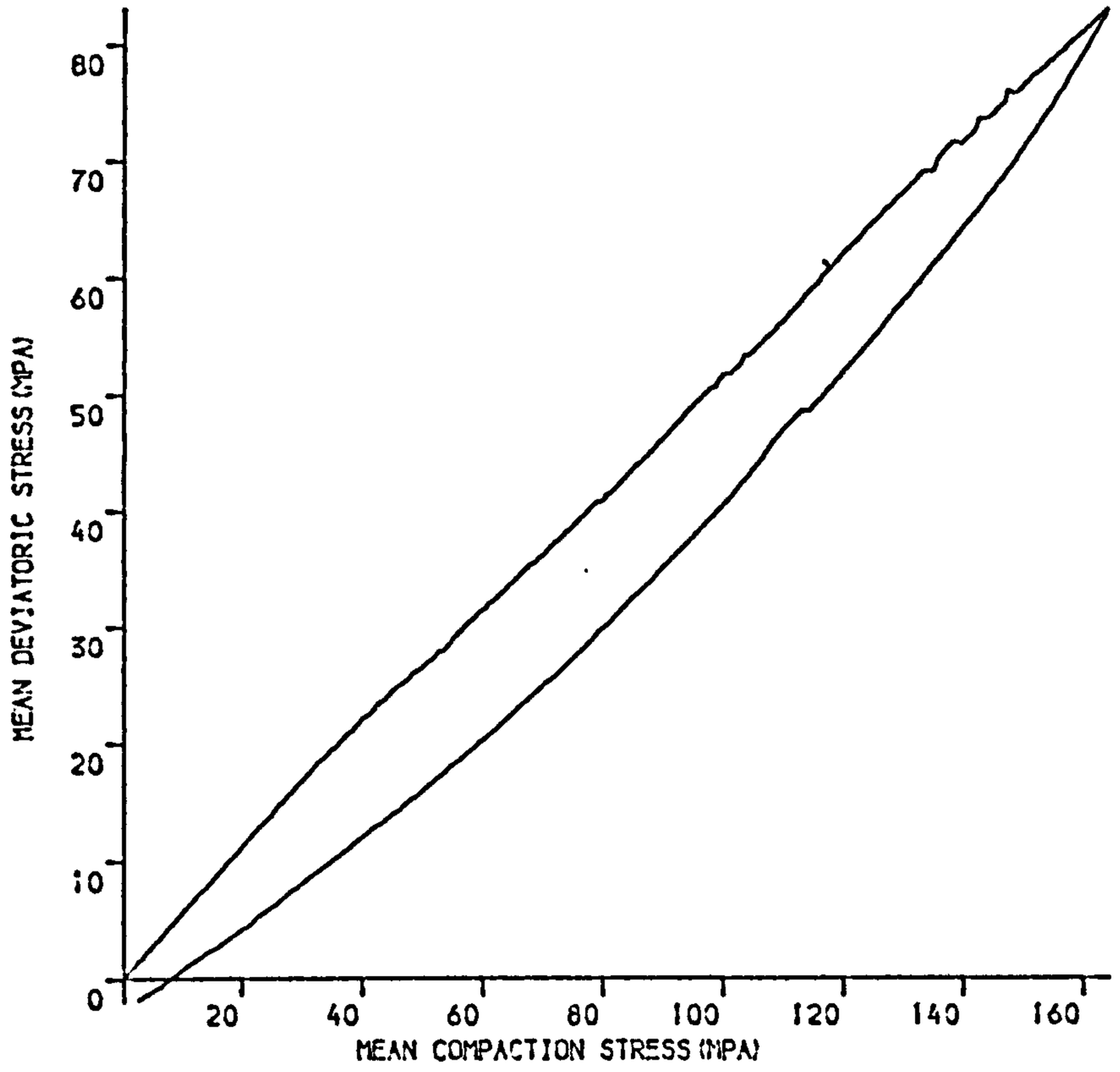

(A)

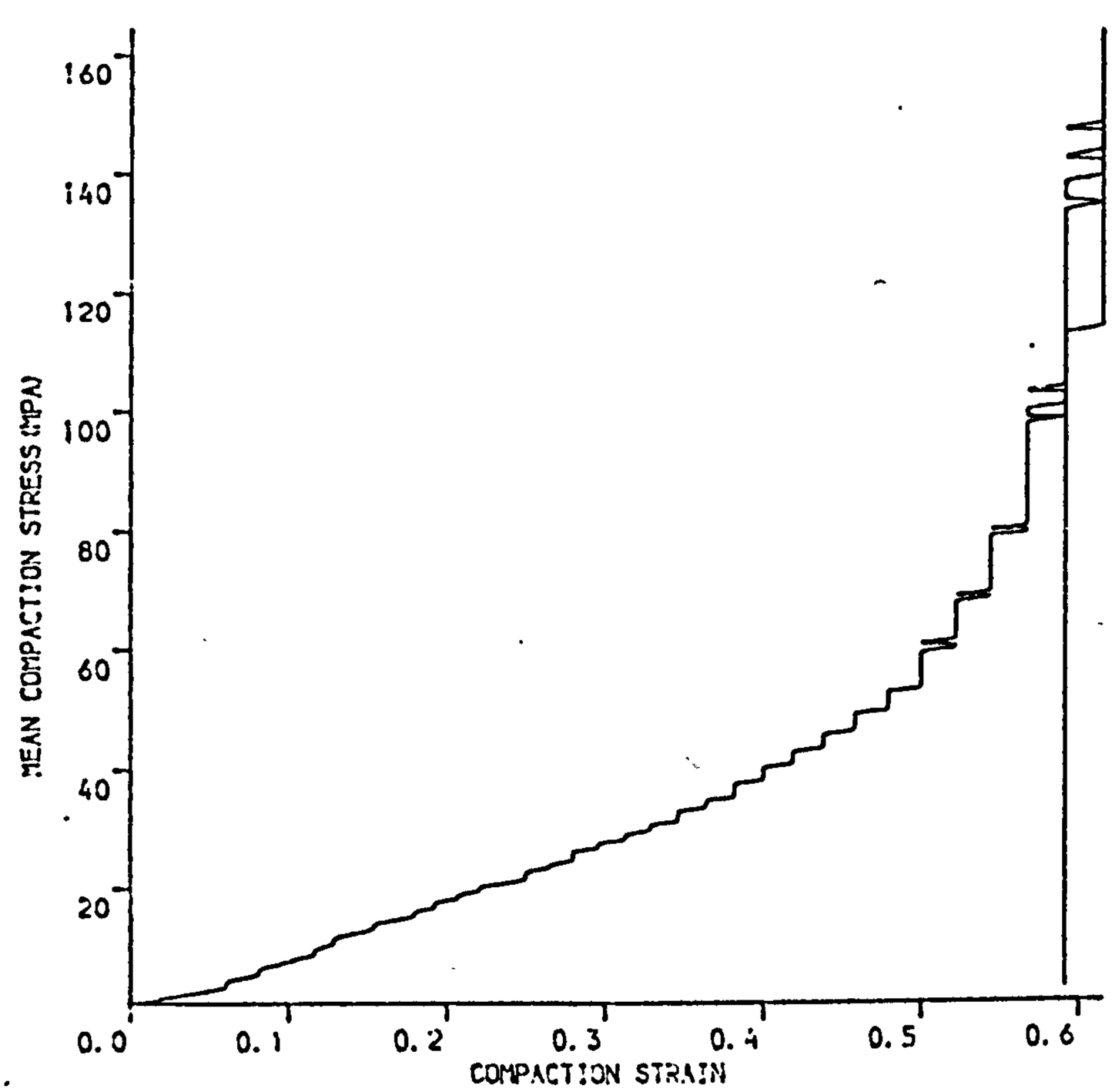

(B)

Figure 6.80 STYROCELL COMPACTED UNIAXIALLY AT 247MPA
(A) SHEAR STRESS VERSUS COMPACTION STRESS
(B) COMPACTION STRESS VERSUS NATURAL STRAIN

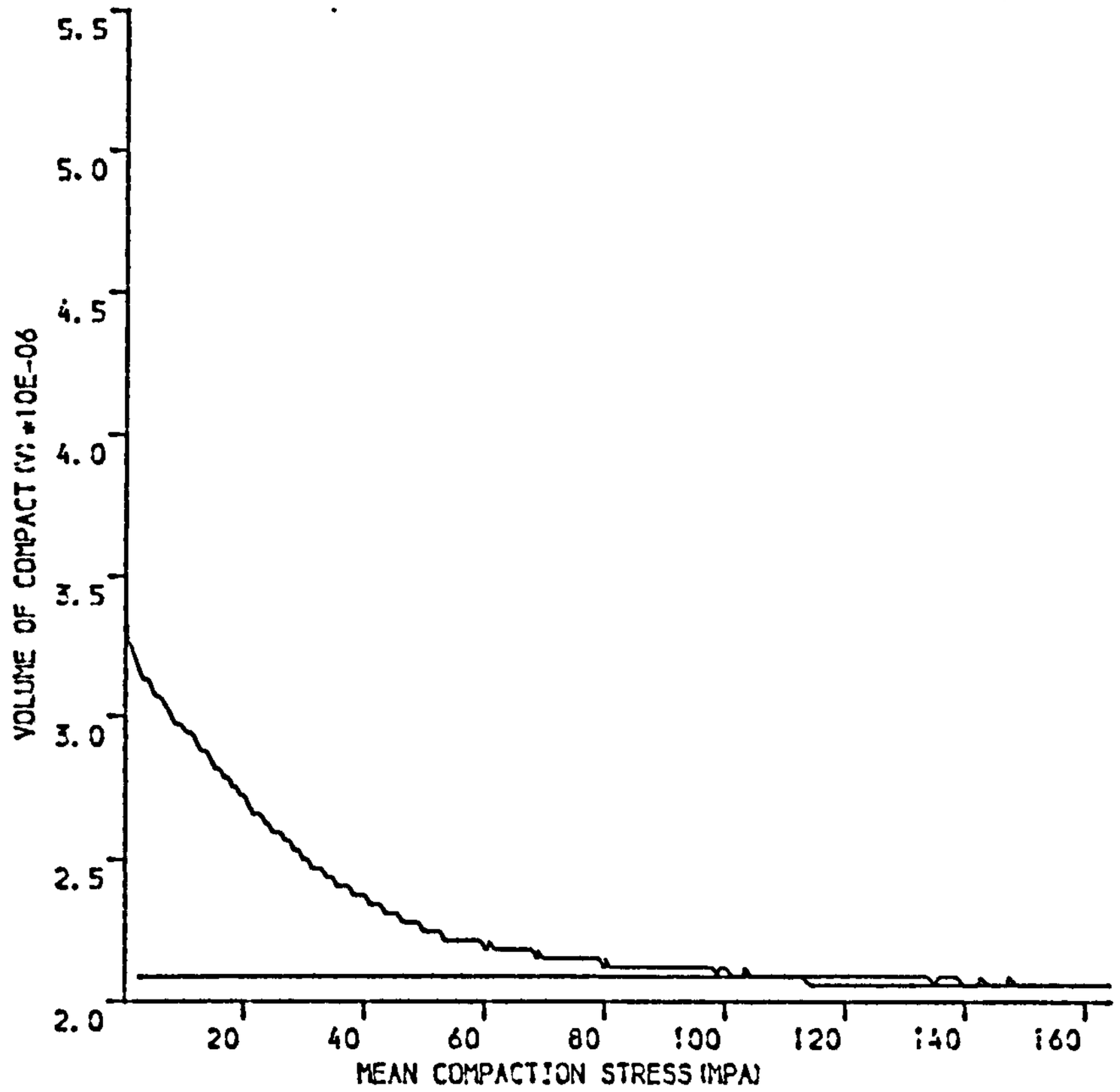

(A)

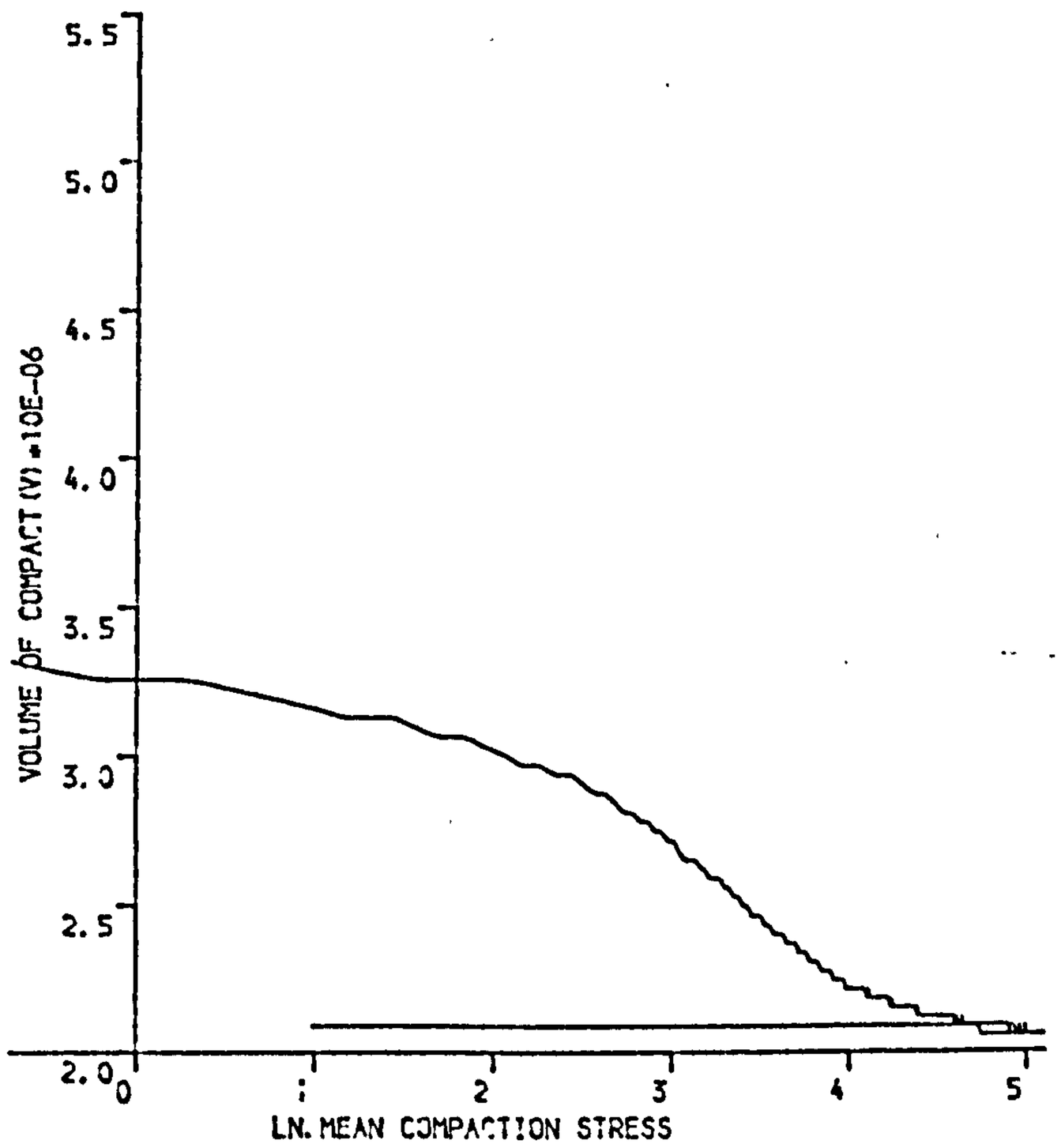

(B)

Figure. 6.81 STYROCELL UNIAXIALLY COMPACTED AT 247MPA
(A) COMPACT VOLUME VERSUS MEAN COMPACTION STRESS
(B) COMPACT VOLUME VERSUS NATURAL LOGARITHMIC COMPACTION STRESS

Figure 6.82 3-D Representation of Styrocell compacted at 155 MPa

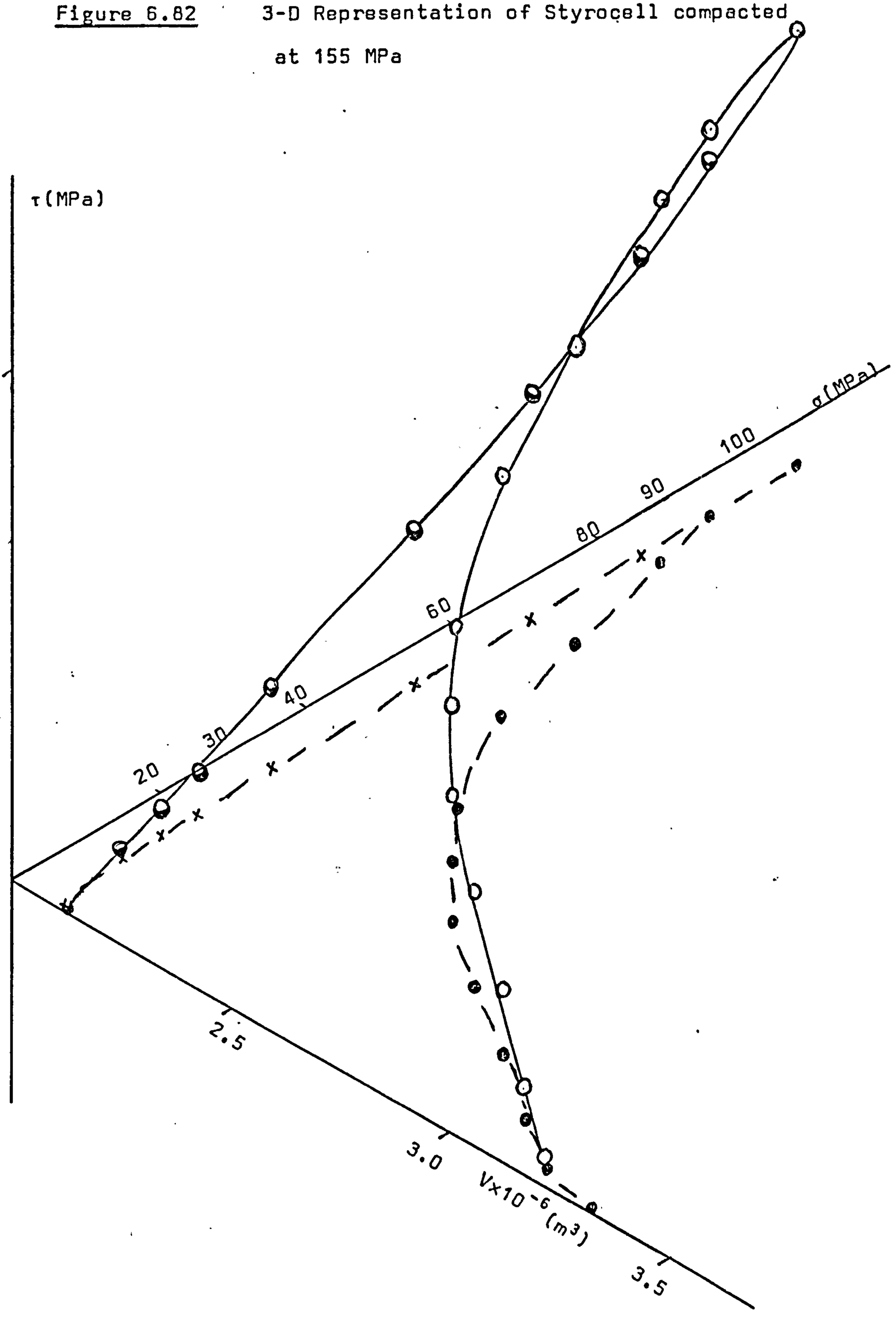

Figure 6.83 3-D representative of styrocell compacted at 247 MPa.

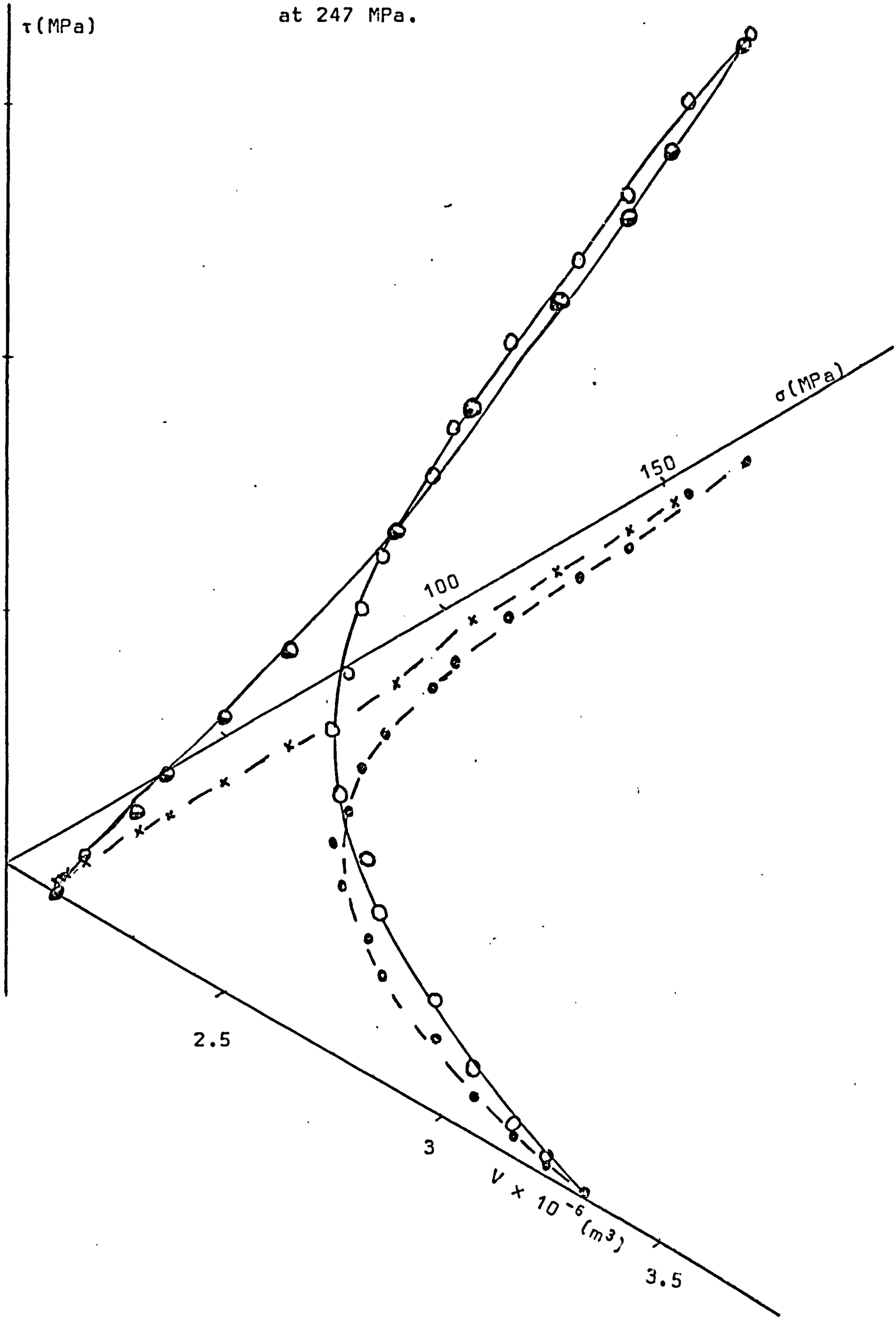

Figure 6.84 Mohr circles constructed for Homopolymer compacted at 250 MPa

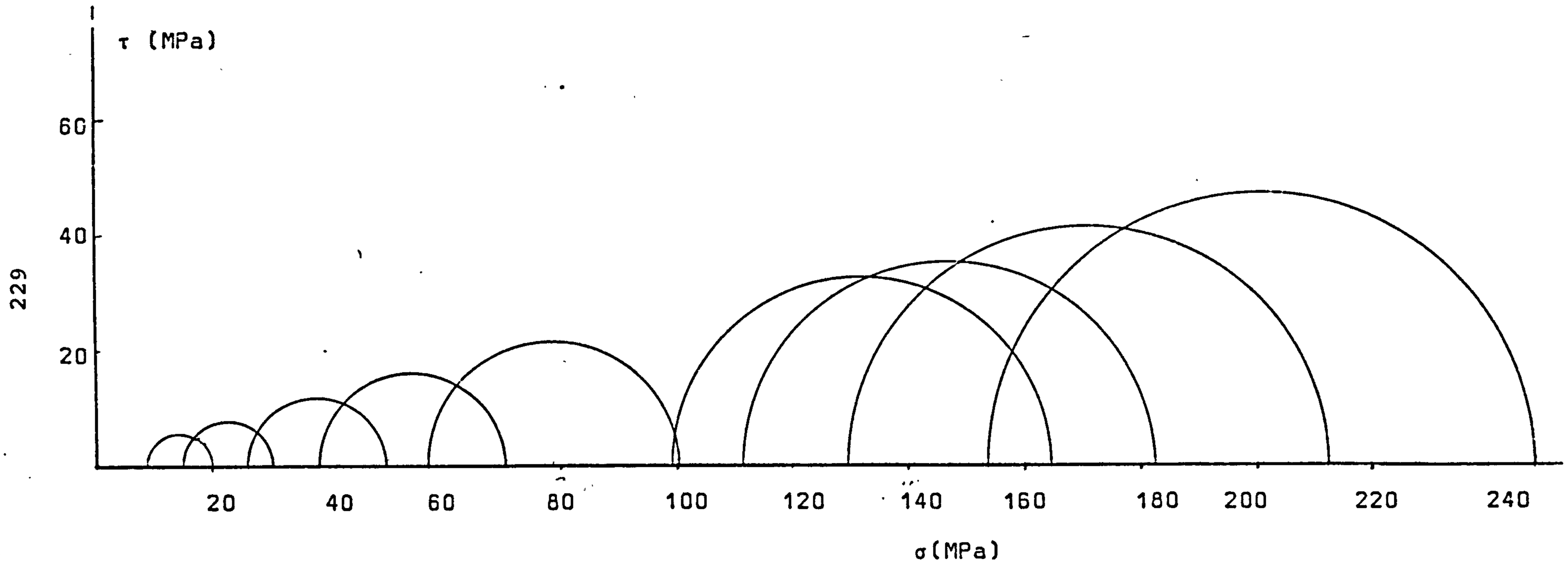

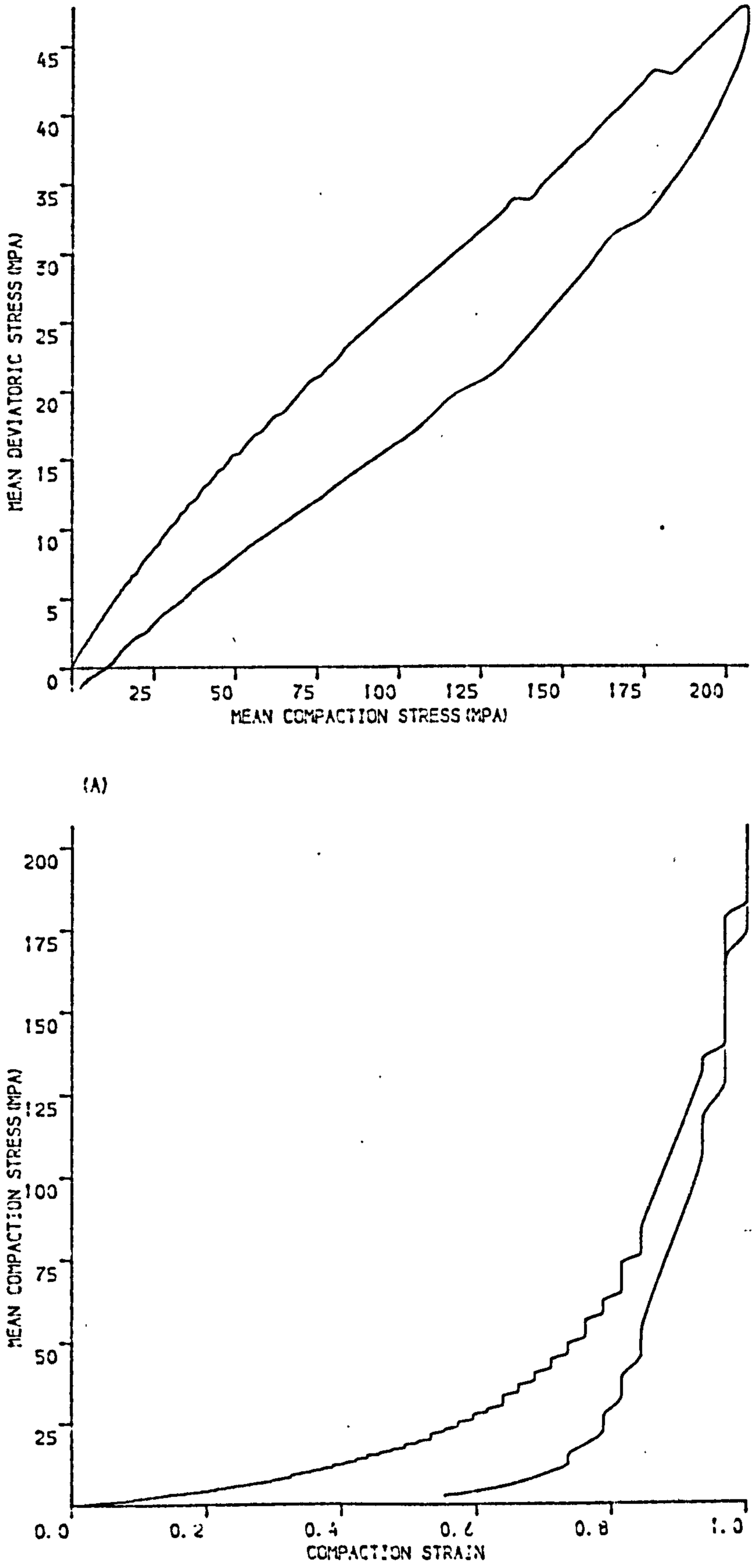

Figure 6.85 HOMOPOLYMER COMPACTED UNIAXIALLY AT 250MPA

(A) SHEAR STRESS VERSUS COMPACTION STRESS

(B) COMPACTION STRESS VERSUS NATURAL STRAIN

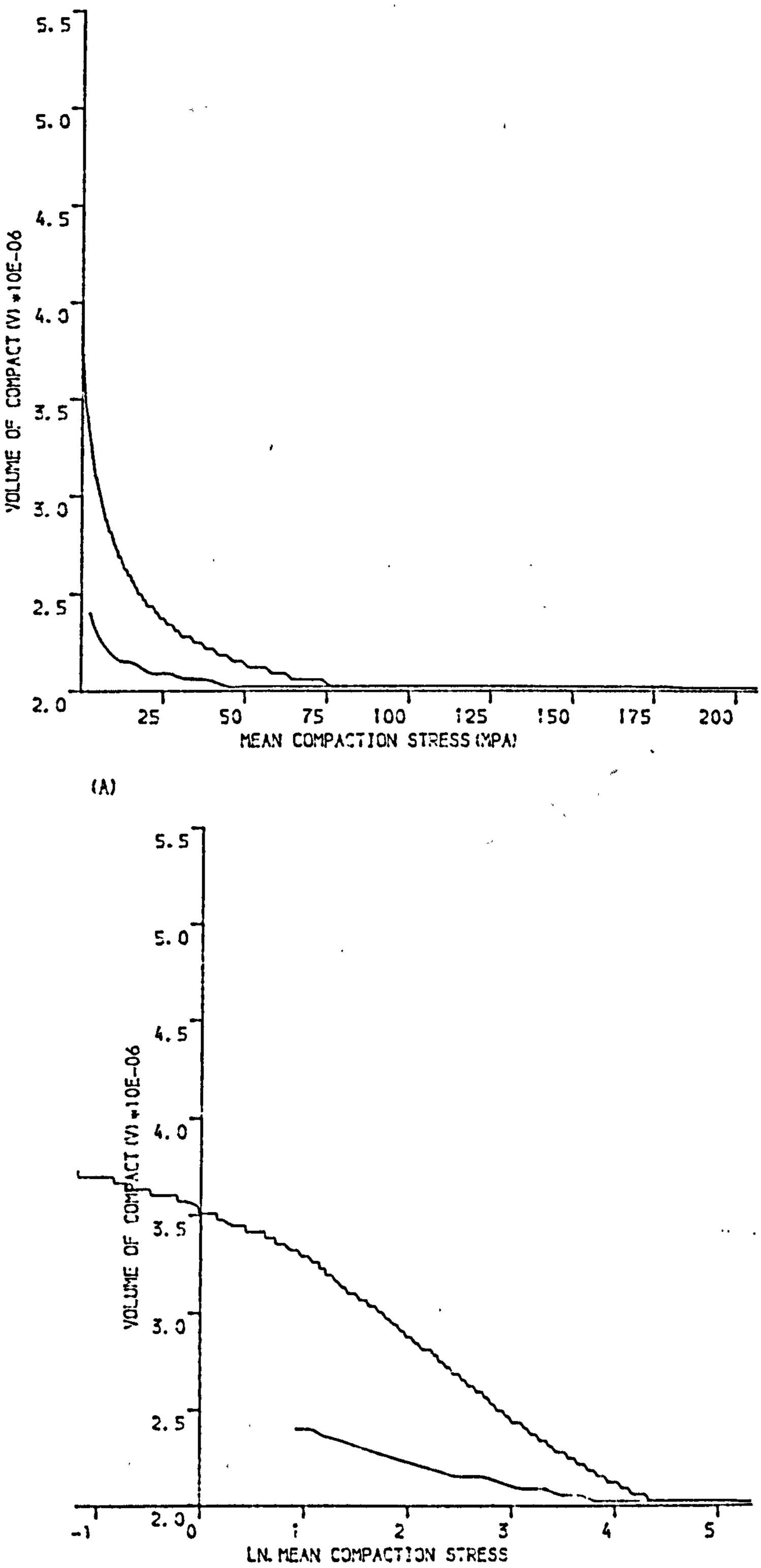

Figure . 6.86 HOMOPOLYMER UNIAXIALLY COMPACTED AT 250MPA

(A) COMPACT VOLUME VERSUS MEAN COMPACTION STRESS

(B) COMPACT VOLUME VERSUS NATURAL LOGARITHMIC COMPACTION STRESS

Figure 6.87 3-D representation of Homopolymer compacted at 250 MPa

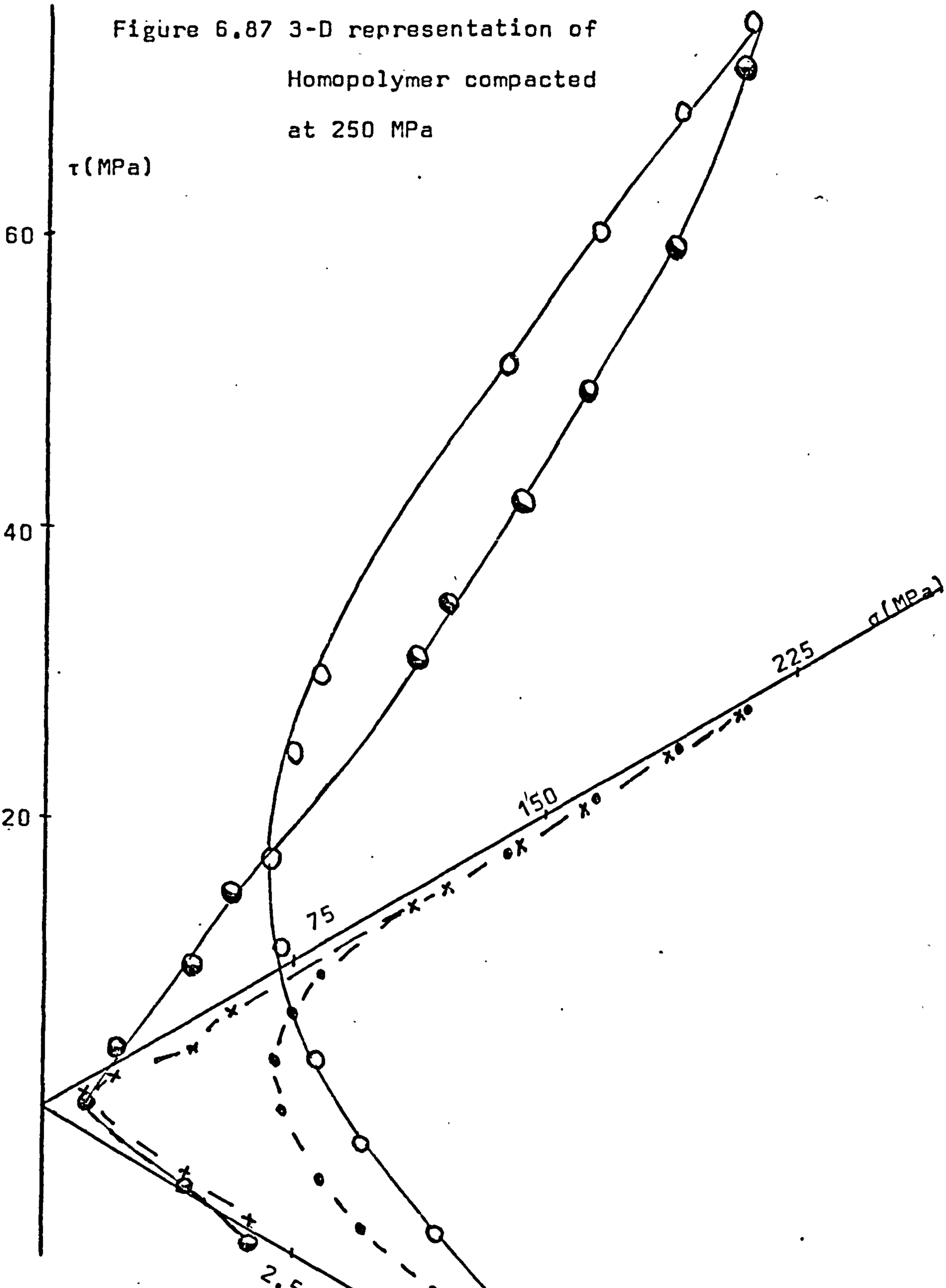

Figure. 6.88 Mohr Circles constructed for copolymer compacted at 250 MPa

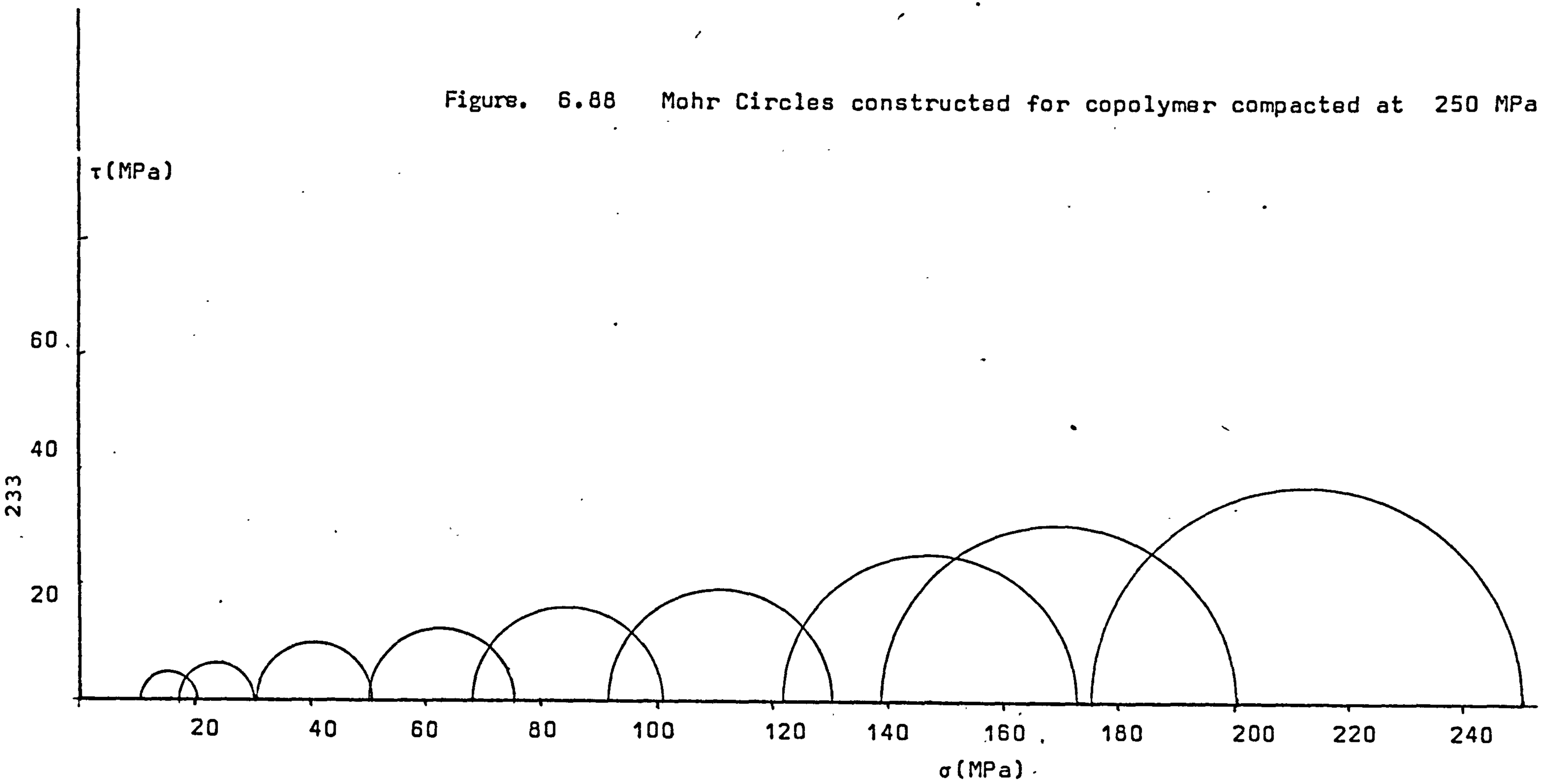

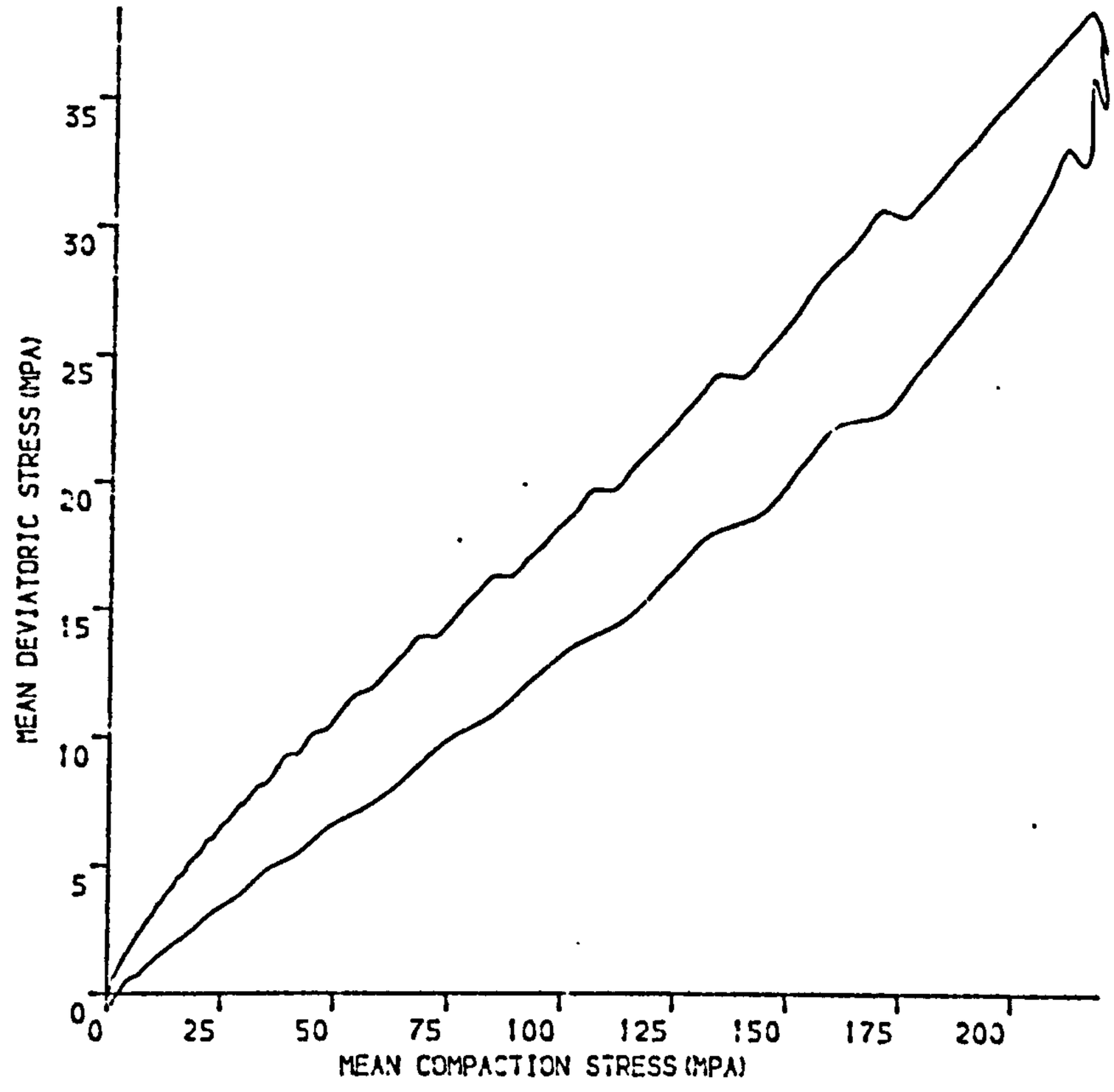

(A)

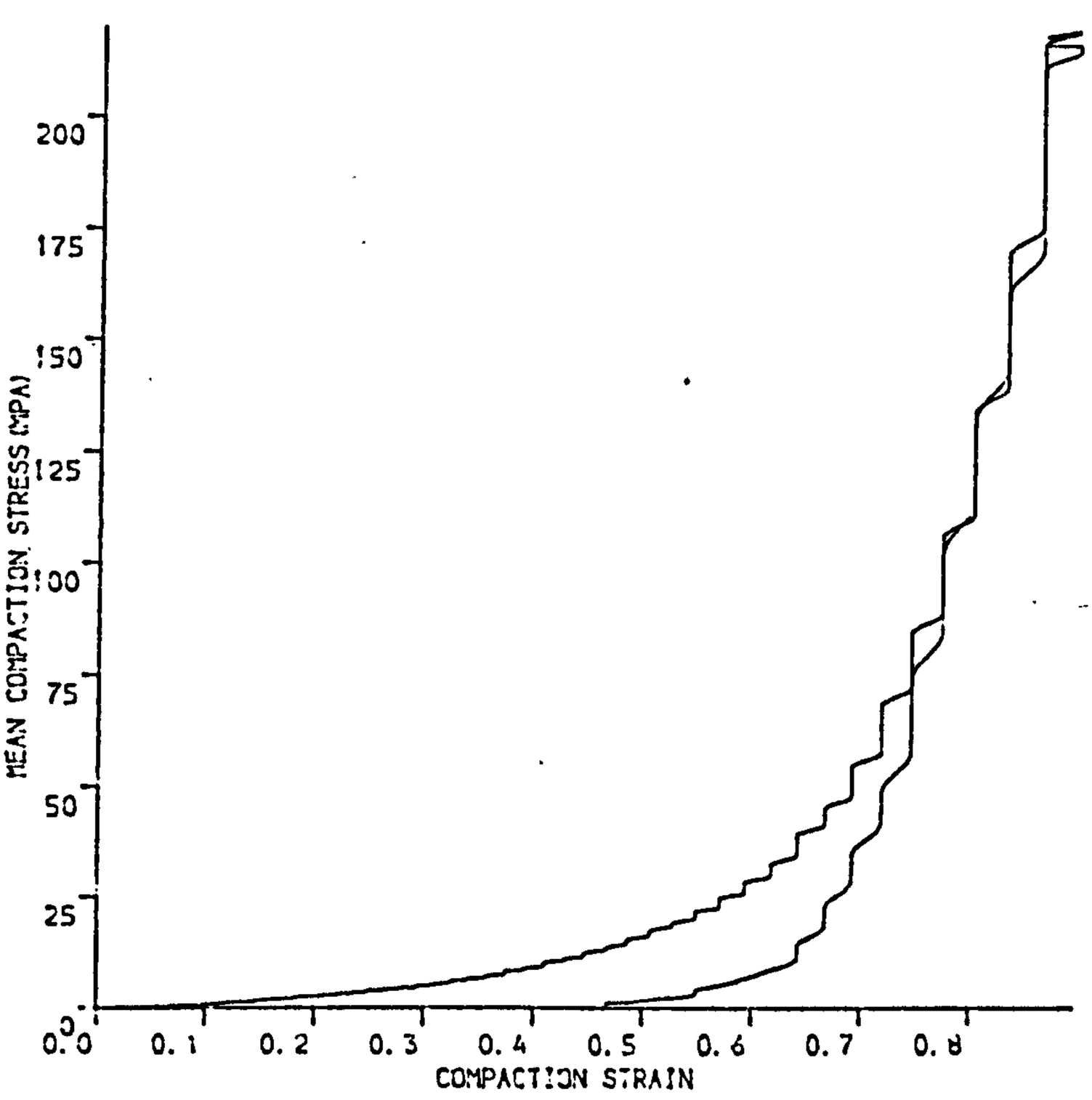

(B)

FIGURE. 6.89. COPOLYMER COMPACTED UNIAXIALLY AT 250MPA

(A) SHEAR STRESS VERSUS COMPACTION STRESS

(B) COMPACTION STRESS VERSUS NATURAL STRAIN

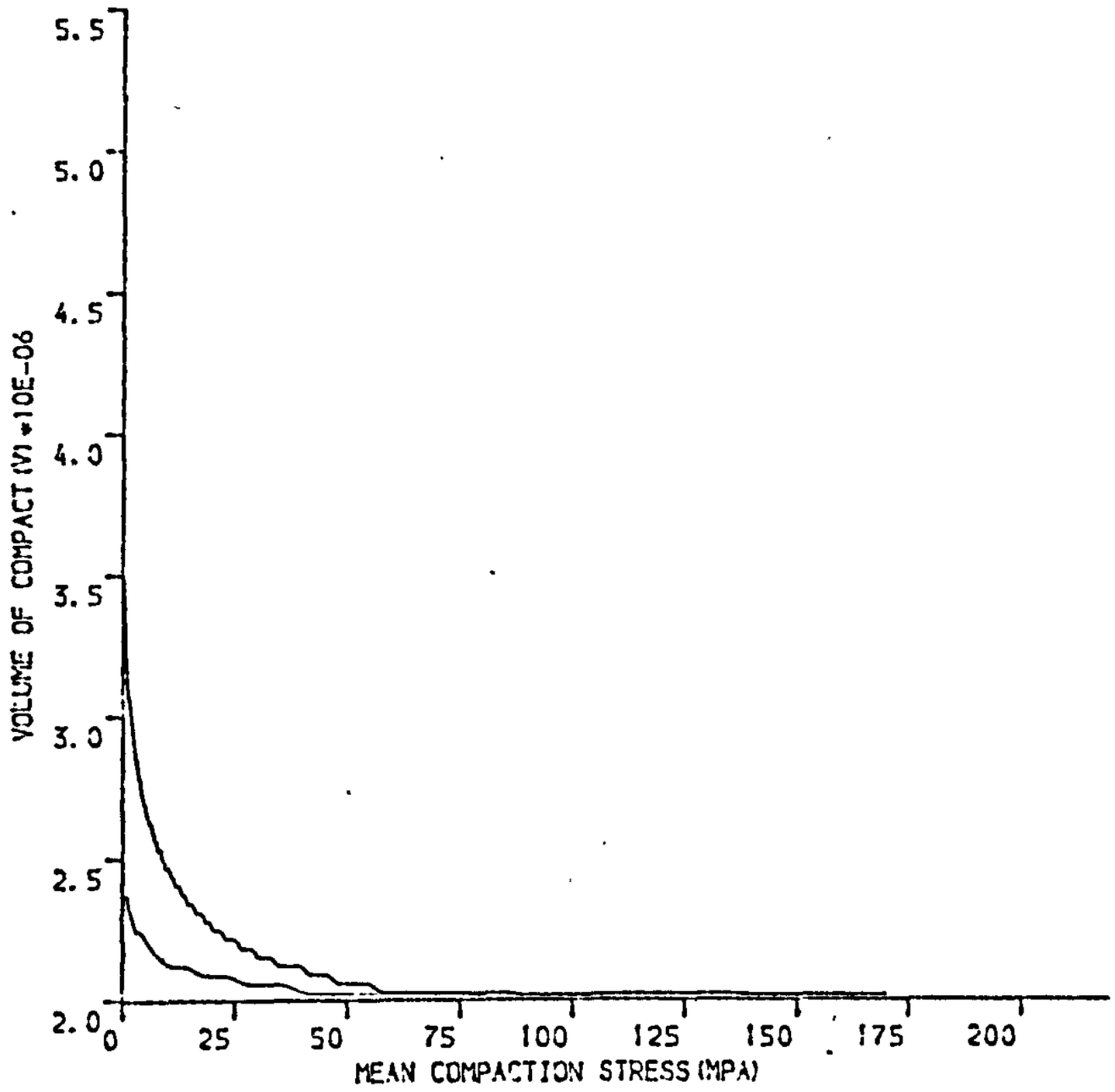

(A)

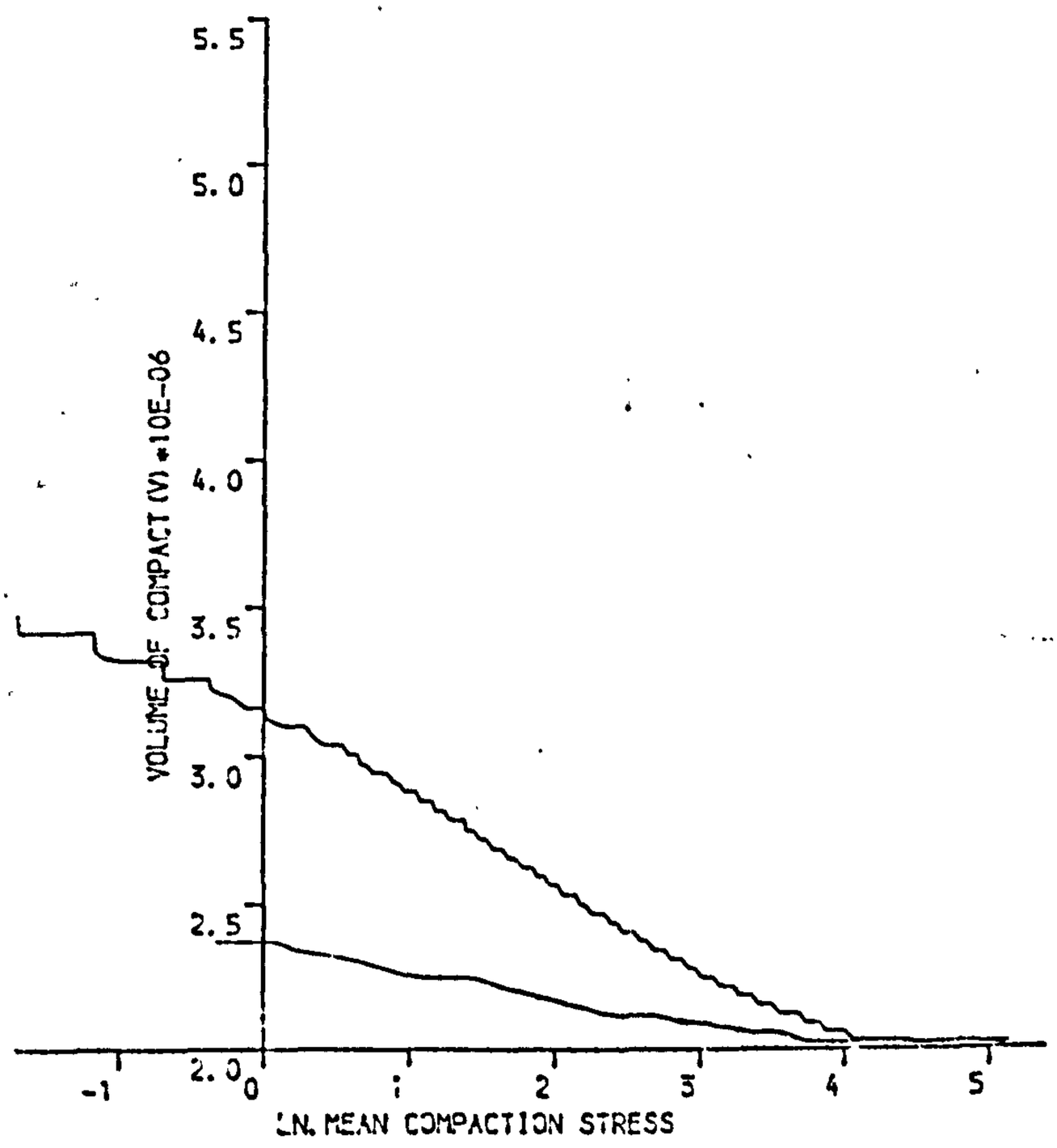

(B)

FIGURE. 6.90 COPOLYMER UNIAXIALLY COMPACTED AT 250MPA

(A) COMPACT VOLUME VERSUS MEAN COMPACTION STRESS

(B) COMPACT VOLUME VERSUS NATURAL LOGARITHMIC COMPACTION STRESS

Figure 6.91 3-D Representation of Co-polymer compacted at 250 MPa.

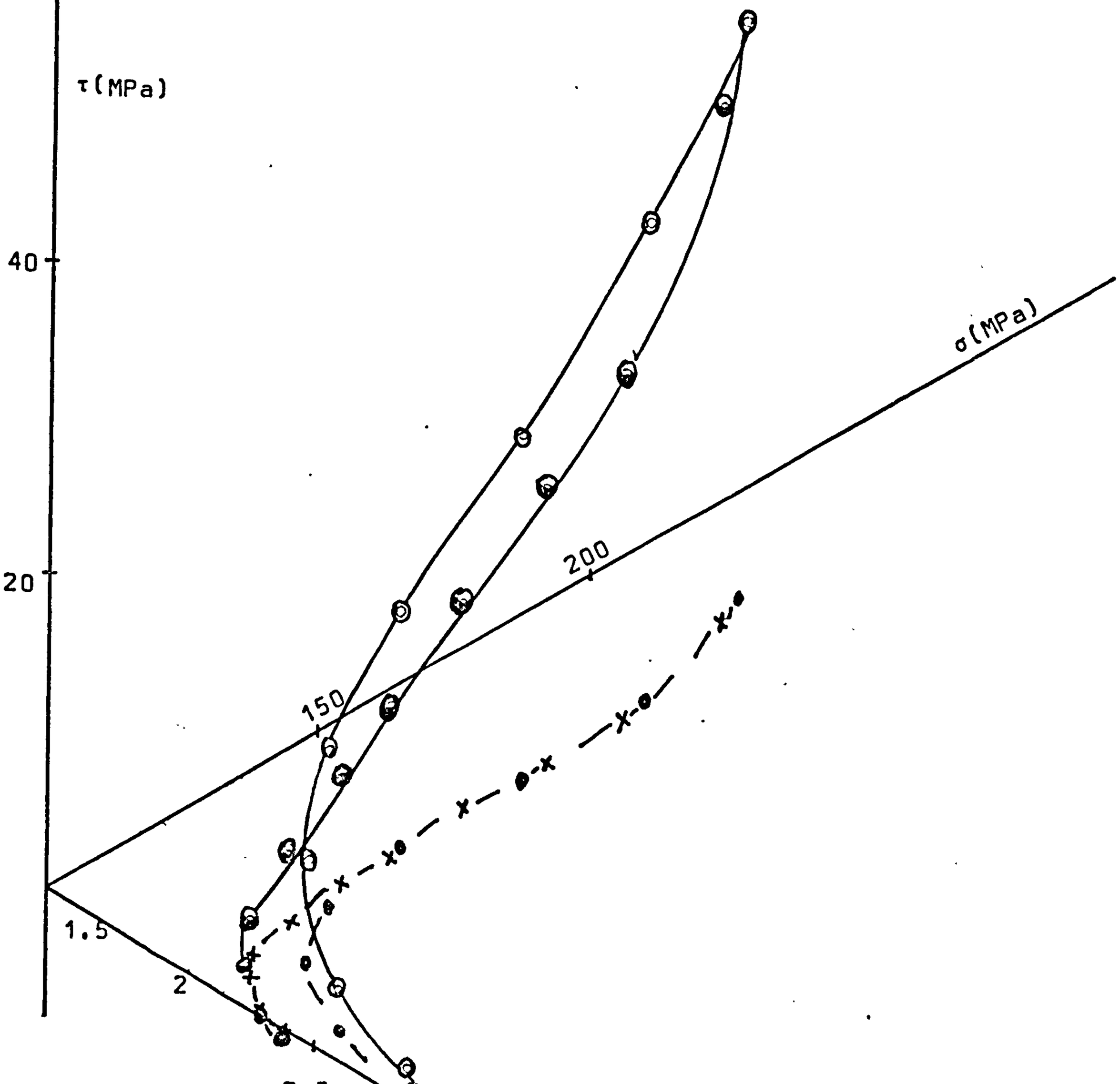

6.3 Surface area of compacts

The specific surface area of dicalcium phosphate compacts was determined from low temperature nitrogen adsorption isotherms using the B.E.T. and Huttig equations (section 2.2.4). The absorption data and the isotherms are presented in appendix 3.

The variation of B.E.T. surface area with maximum axial compaction pressure of dicalcium phosphate is presented in Figure 6.92 and Table 6.7.

The specific surface area of dentritic sodium chloride compacts were determined by Krypton adsorption isotherms (section 5.2). The adsorption data is presented in appendix 3.

The variation of specific surface areas with compaction pressure of dentritic sodium chloride is shown in Figure 6.93 and Table 6.7.

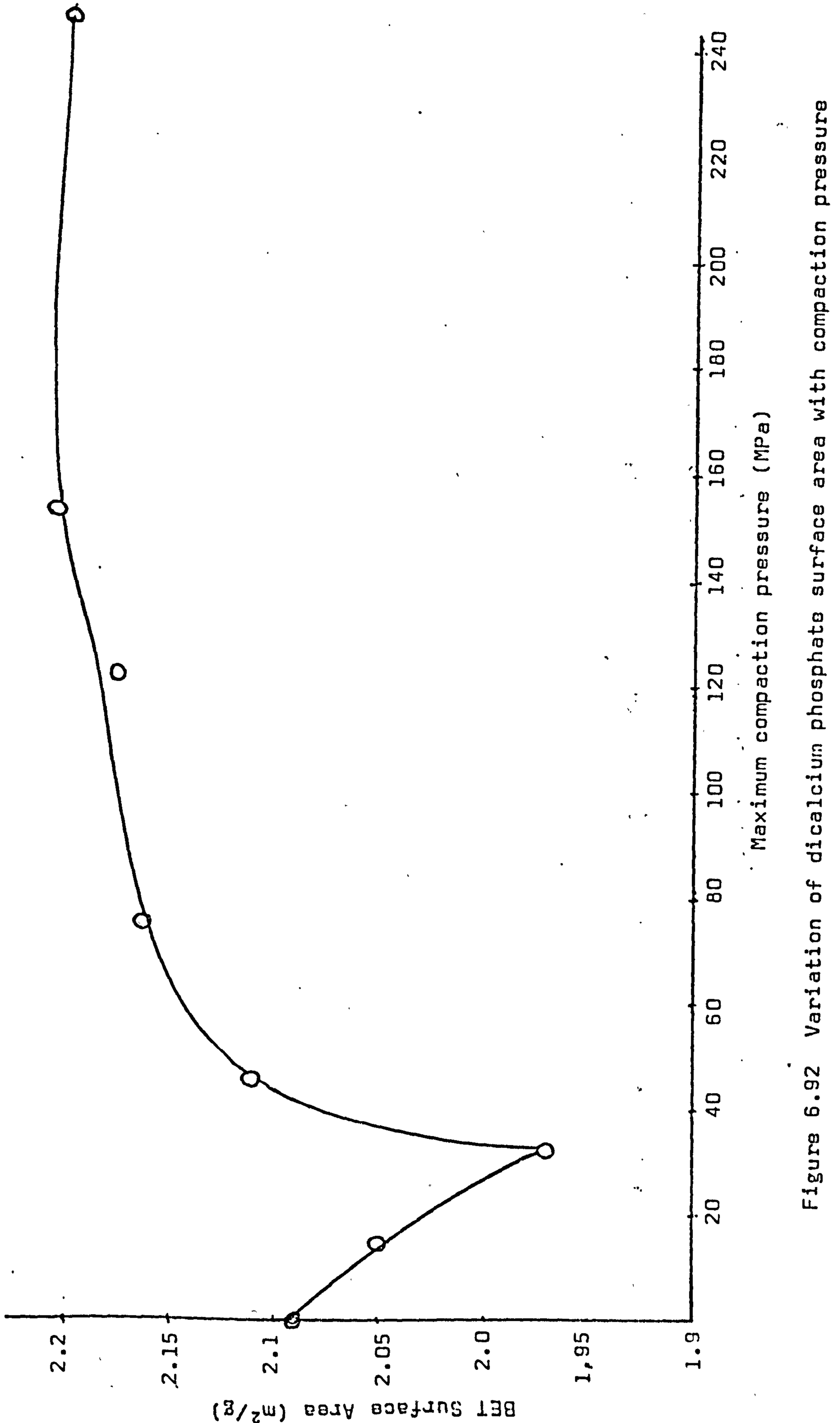

Figure 6.92 Variation of dicalcium phosphate surface area with compaction pressure

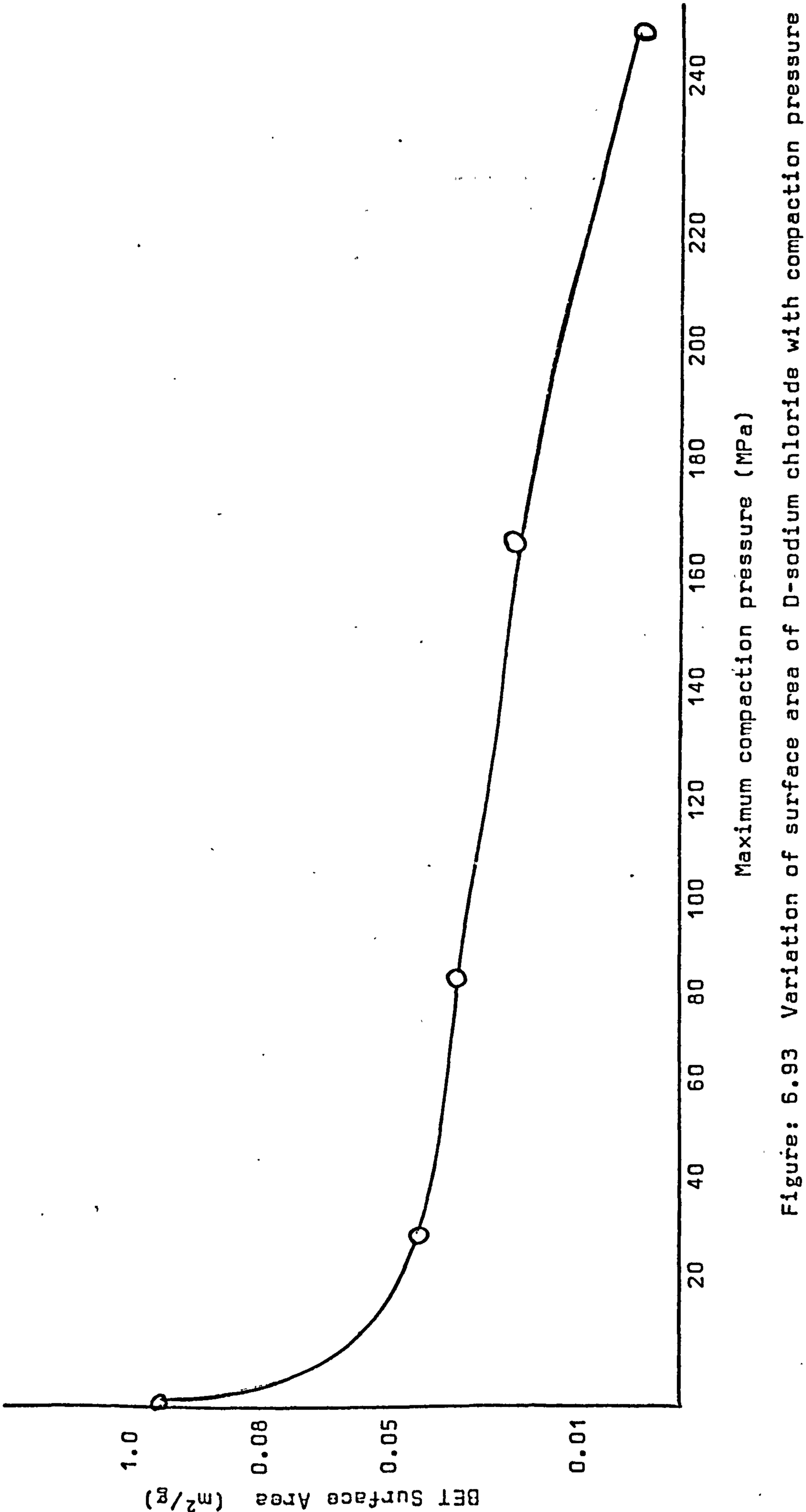

Figure: 6.93 Variation of surface area of D-sodium chloride with compaction pressure

Table 6.7 BET Surface area of compacts with degree of compaction.

Powder	Compaction stress units	BET * Surface area m^2g^{-1}	Degassing conditions
Dicalcium phosphate	0	2.09	2 0 hours at room temperature
	15	2.05	24 hours at 50°C
	32	1.97	"
	47	2.11	"
	77	2.16	"
	120	2.17	36 hours at 50°C
	155	2.20	"
	248	2.19	"
Dentritic sodium chloride	0	0.0945	36 hours at 50°C
	36	0.0471	
	77	0.0418	
	155	0.031	
	248	0.007	

* All surface area values are the mean of at least three experiments.

6.4 Porosity of Compacts

The porosities of the compacts were determined by a mercury penetration technique (Section 5.4) and direct measurements of the dimensions of the compacts. The experimental results from the porosimeter, were applied pressure and corresponding intrusion volume counter reading. By multiplication with a cell constant, the scale counter gave the penetration volume. The pore volume and surface area were also calculated from equations 1.39 and 1.40. The curve obtained from the volume-radius relationship was analysed to yield a relative frequency of pore sizes in compacts. The pore size distribution of dicalcium phosphate and dentritic sodium chloride compacts are shown in Figures 6.94 and 6.95 respectively, while the experimental and calculated data are presented in appendix 3.

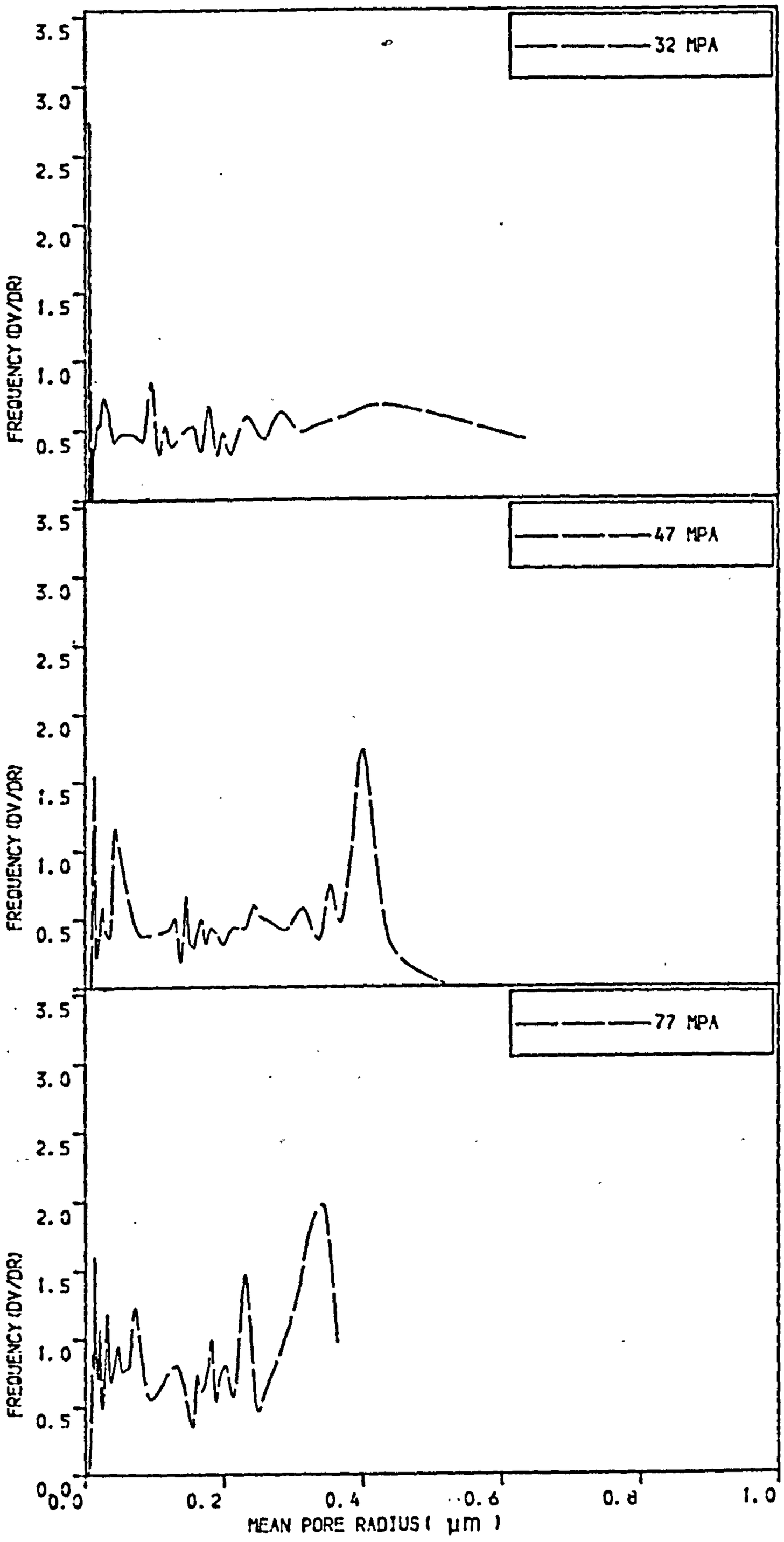

Figure 6.94 Interparticle pore size distribution of dicalcium phosphate compacts.

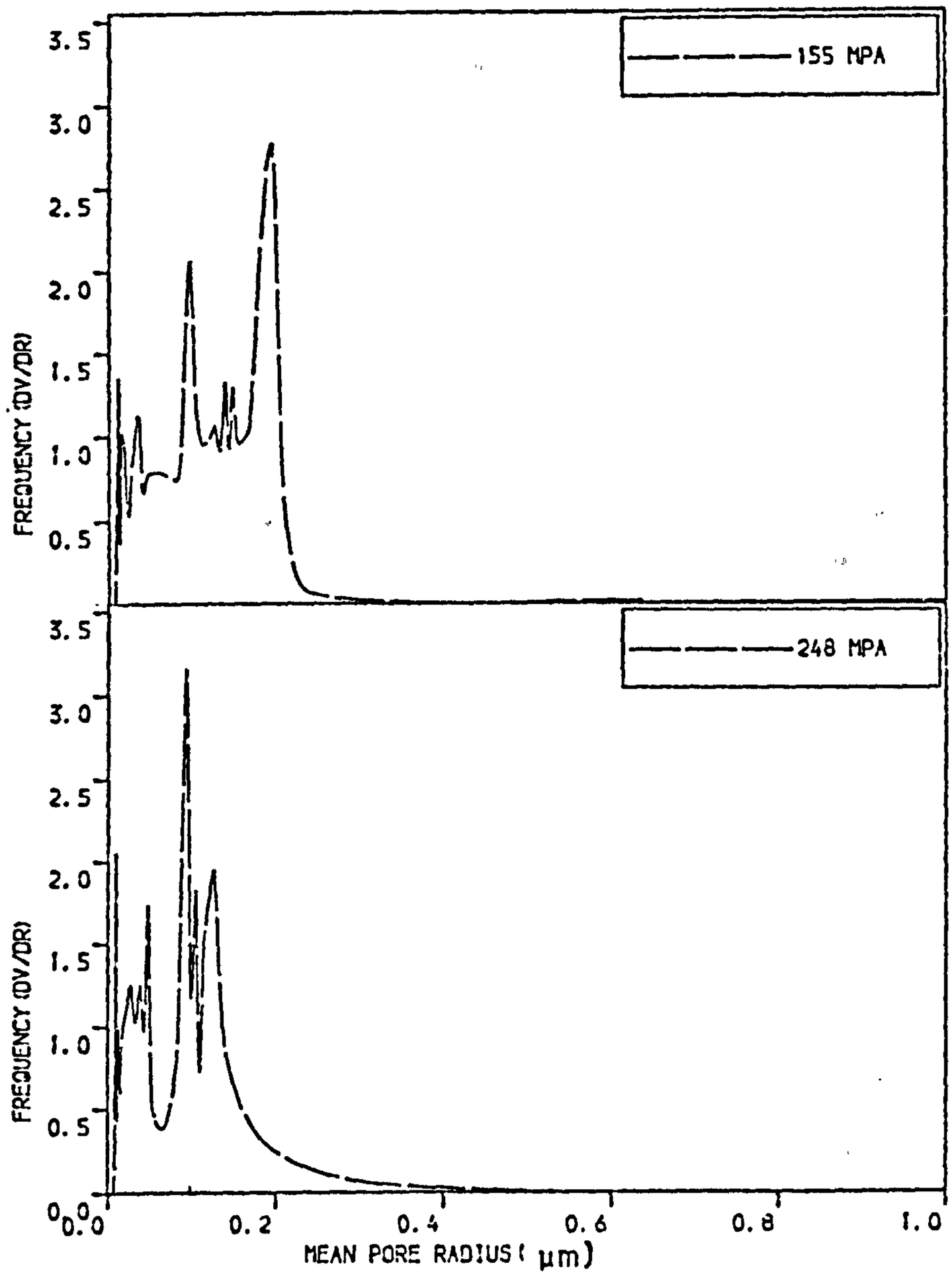

Figure 6.94 continued Interparticle pore size distribution of dicalcium phosphate compacts.

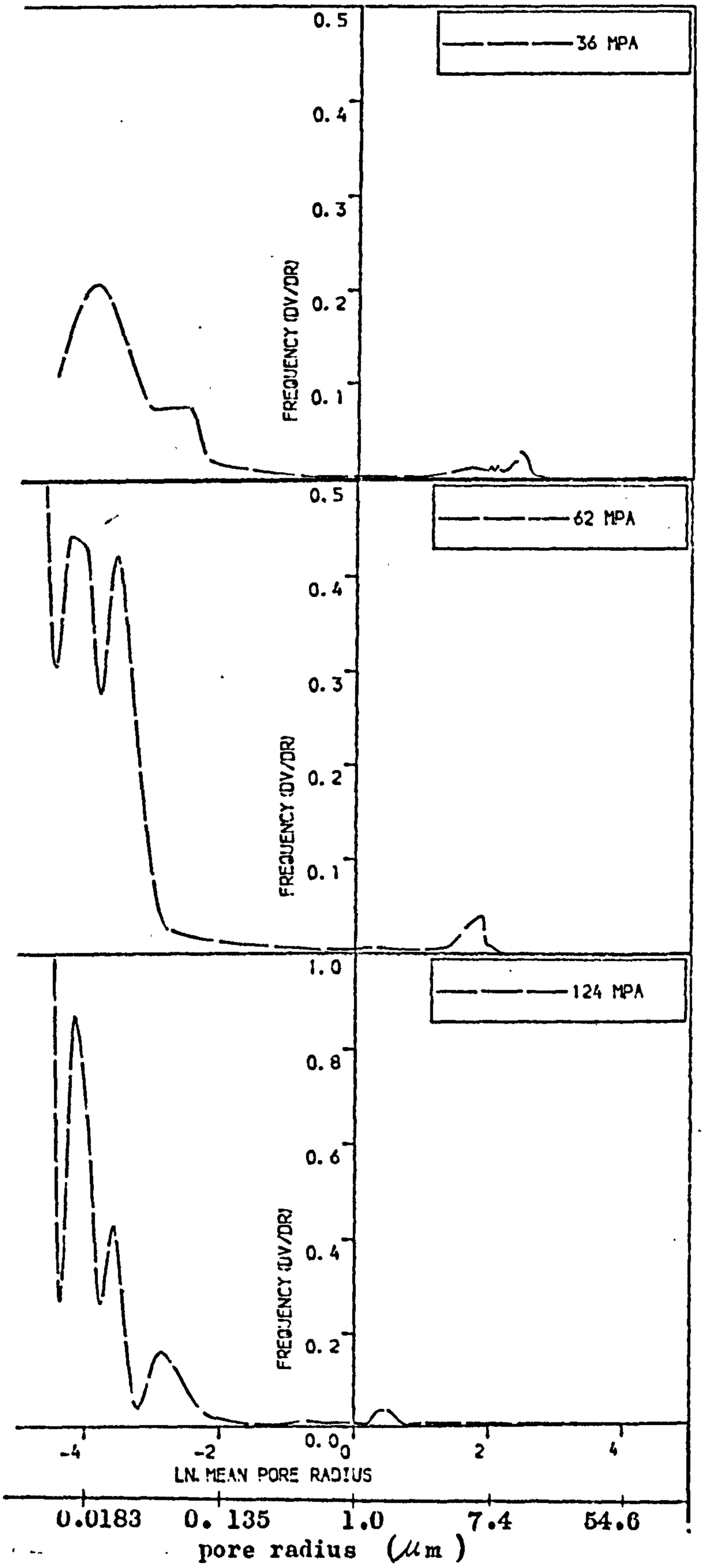

Figure 6.95 Interparticulate pore size distribution of dnetritic sodium chloride compacts.

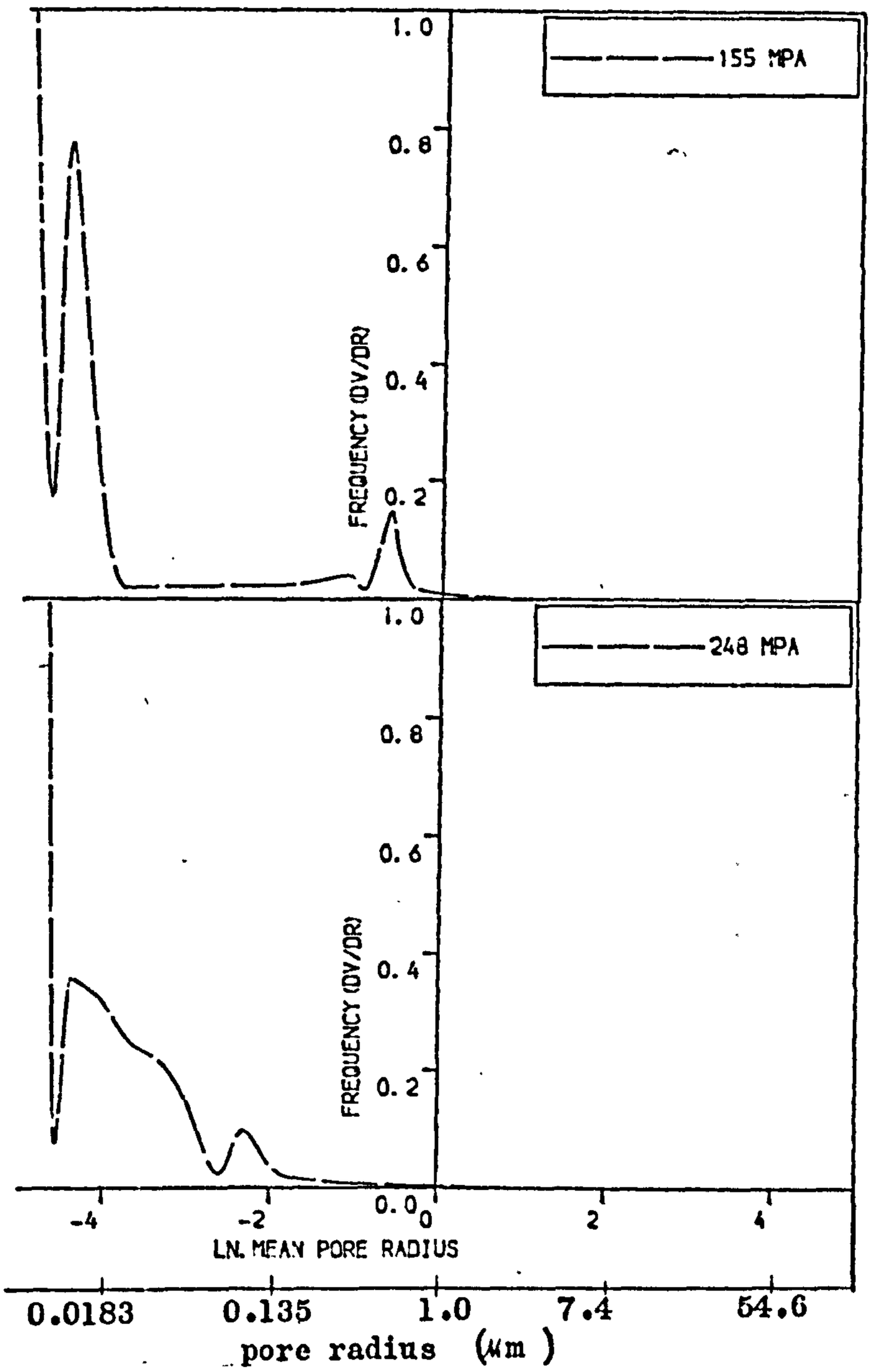

Figure 6.95 continued Interparticulate pore size distribution of dentritic sodium chloride compacts.

6.6 Mechanical Strength of Compacts

The mechanical strength of compacts was tested by a diametral crushing technique. (Section 5.5.1) The tensile strength was calculated in accord to the equation proposed by Frocht (1948) (equation 1.55). An alternative of measurement of mechanical strength of compacts, that of hardness, was also determined (section 1.6). Vickers hardness number, H_V, and Brinell hardness number, H_B, were evaluated for all compacts produced from compactable materials. Results from each materials group are presented in Figures 6.96-6.99 and 6.100 - 6.103 and table 6.8 and 6.9 for the plastically deforming and fragmenting materials respectively.

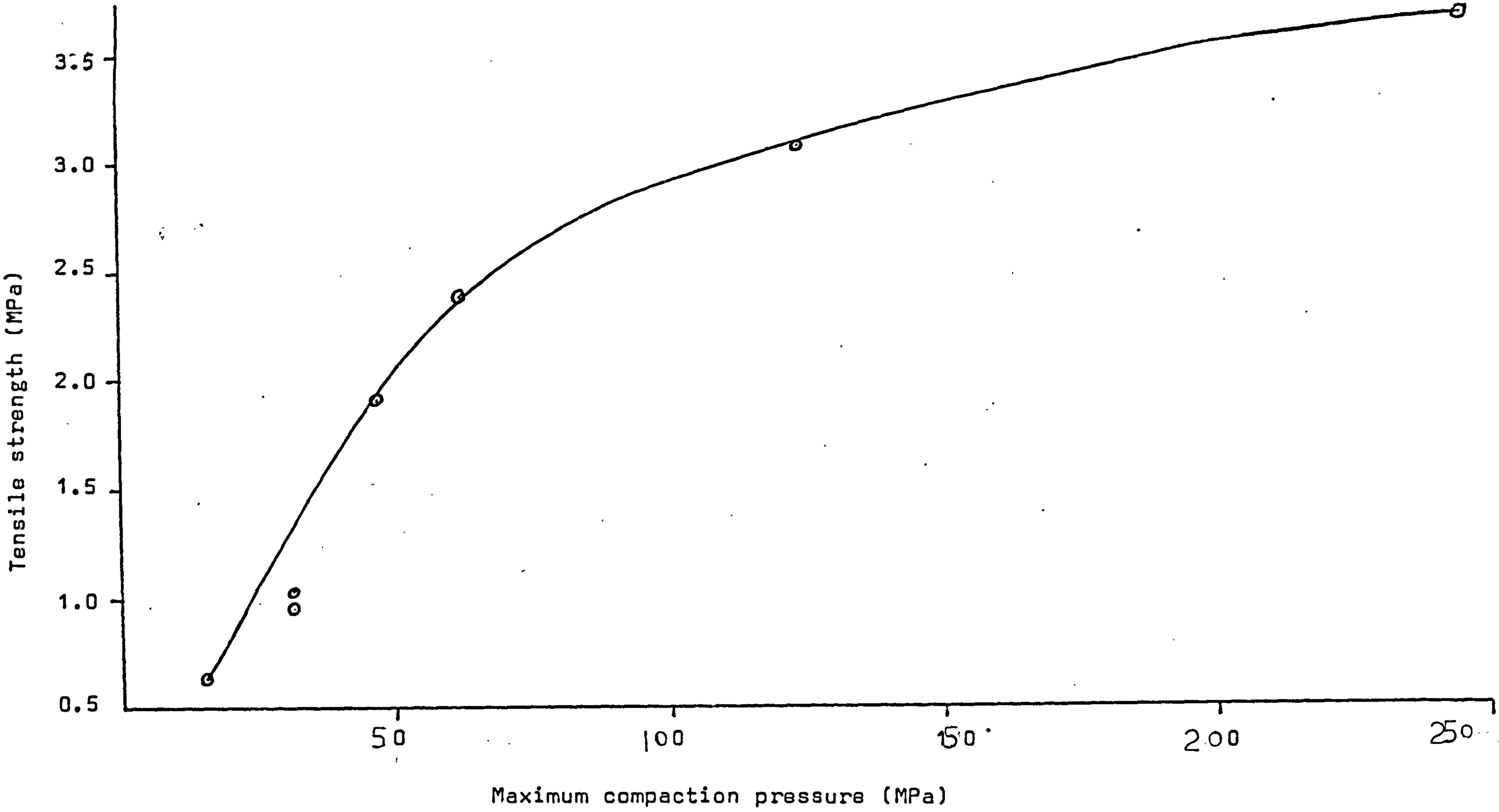

Figure 6.96 Variation of D-sodium chloride compact strength with compaction pressure

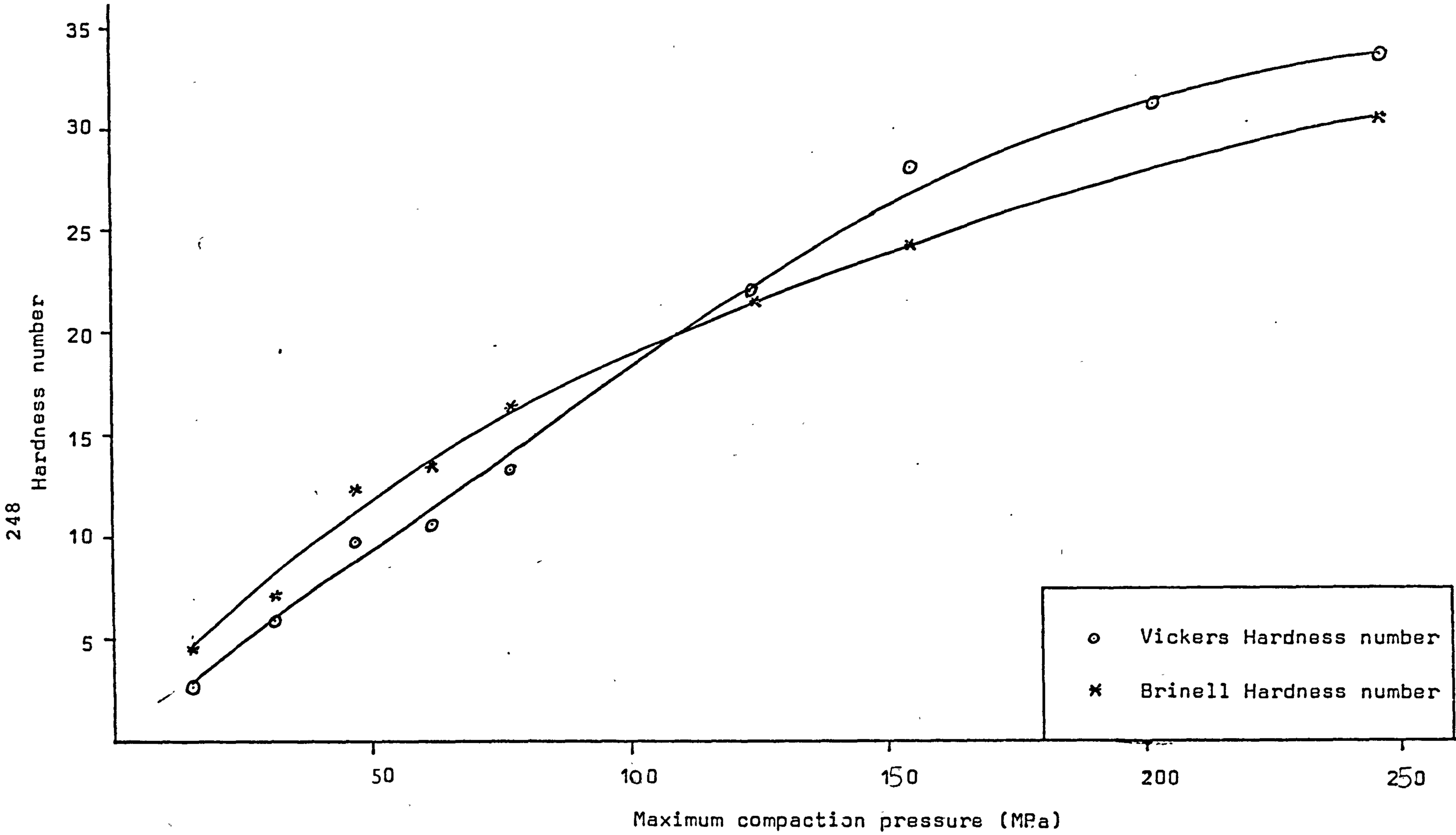

Figure 6.97 Variation of D-sodium chloride hardness with compaction pressure

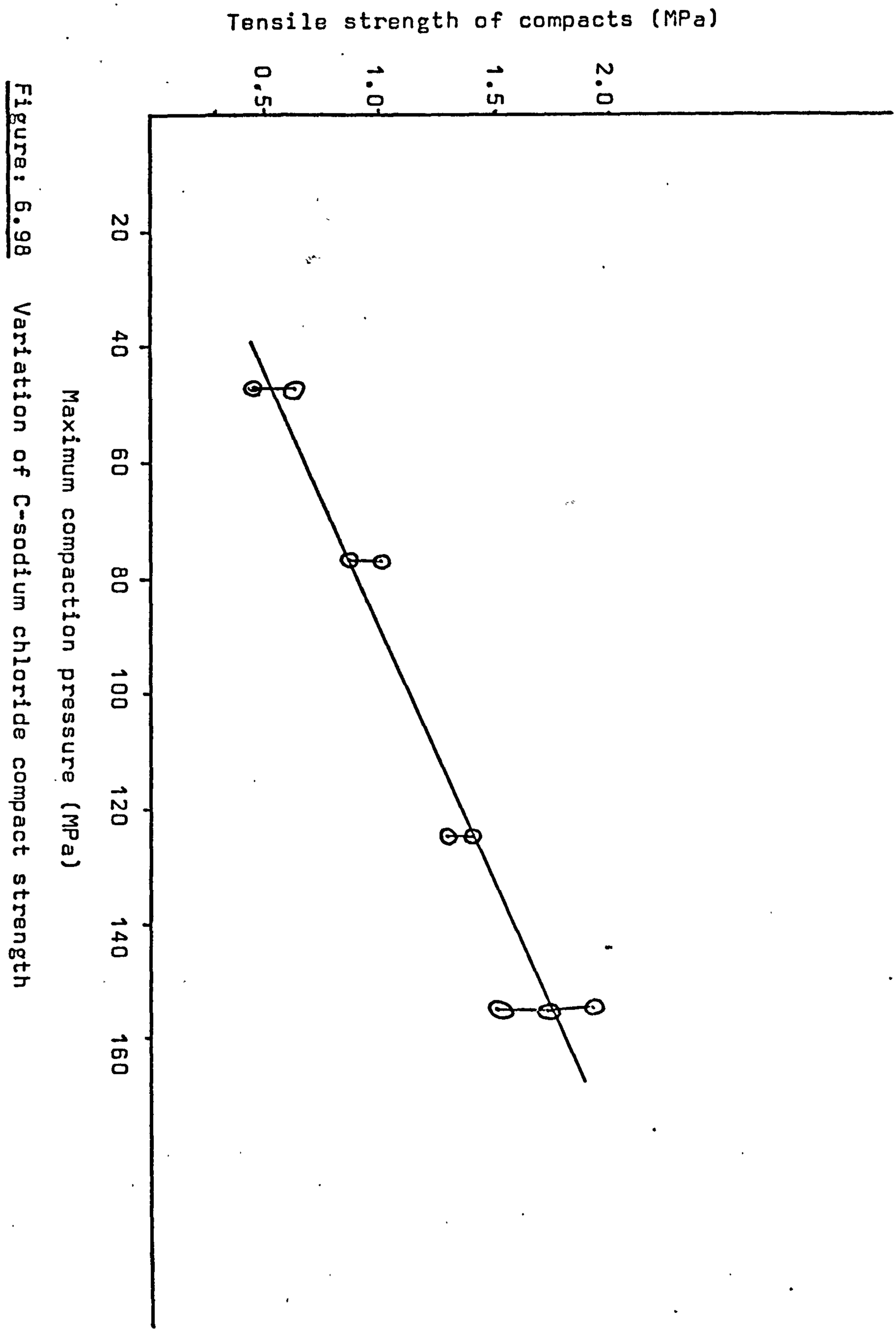

Figure: 6.98 Variation of C-sodium chloride compact strength with compaction pressure.

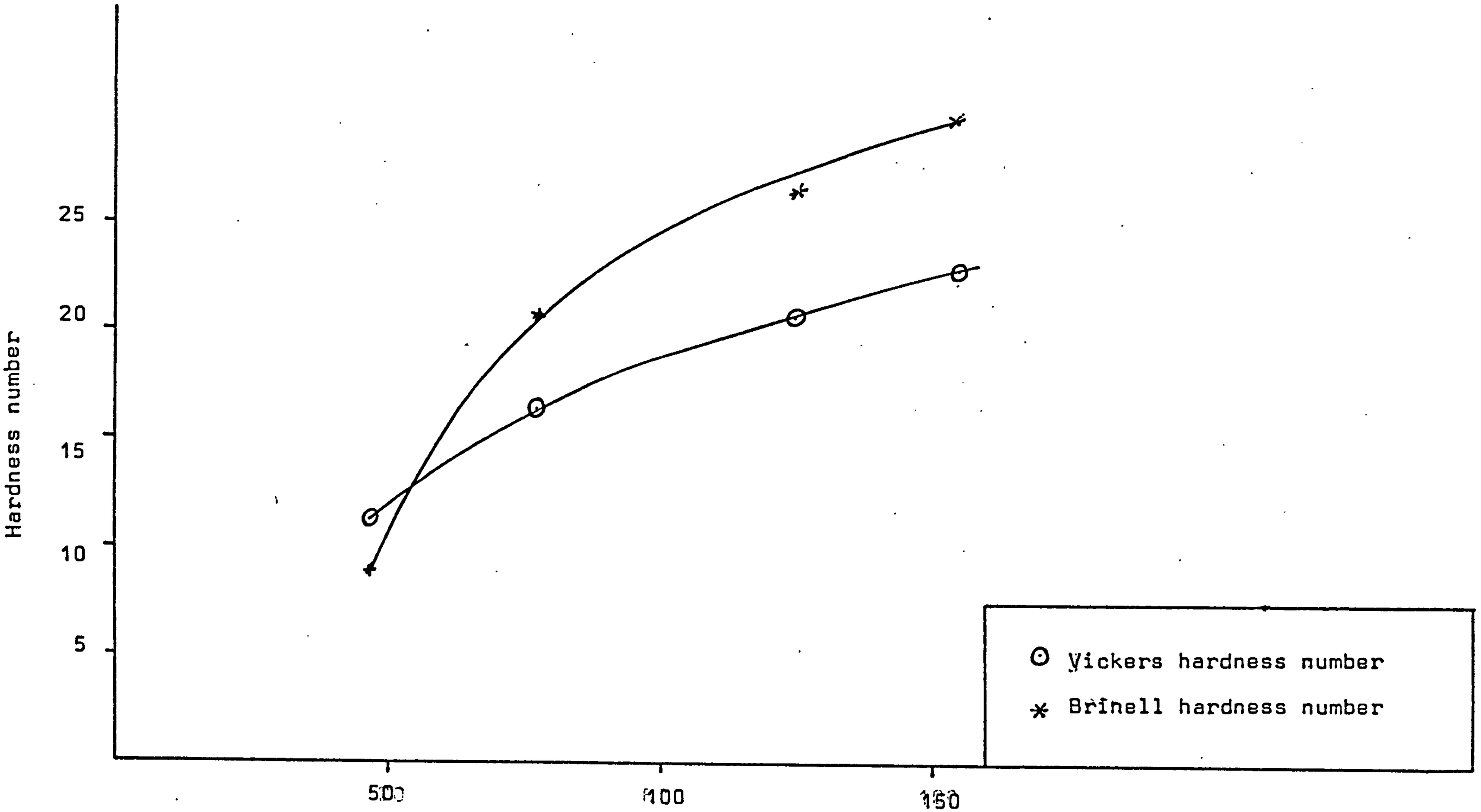

Figure 6.99 Variation of hardness of C-sodium chloride with compaction pressure

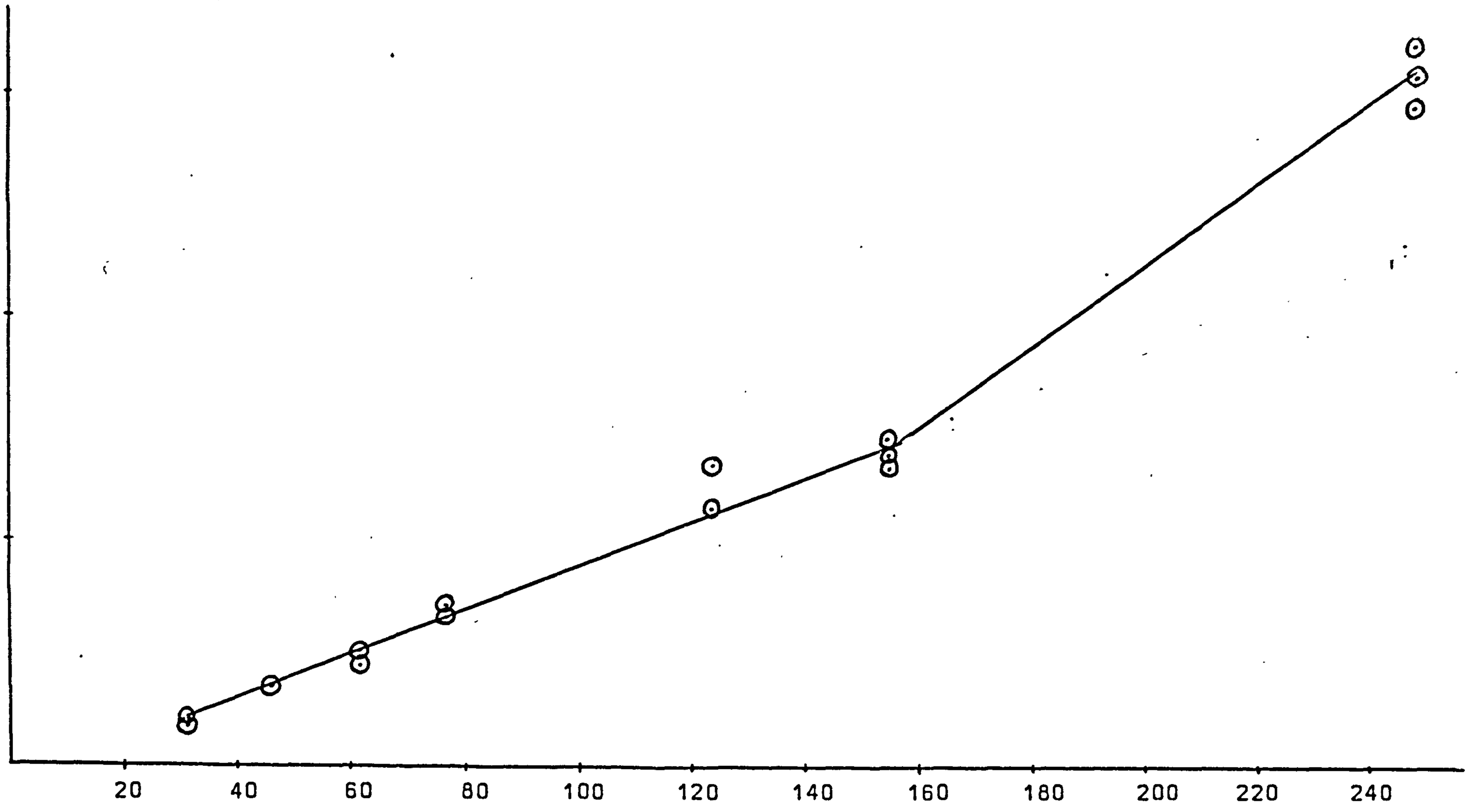

Figure: 6.100 Variation of dicalcium phosphate compact strength with compaction pressure.

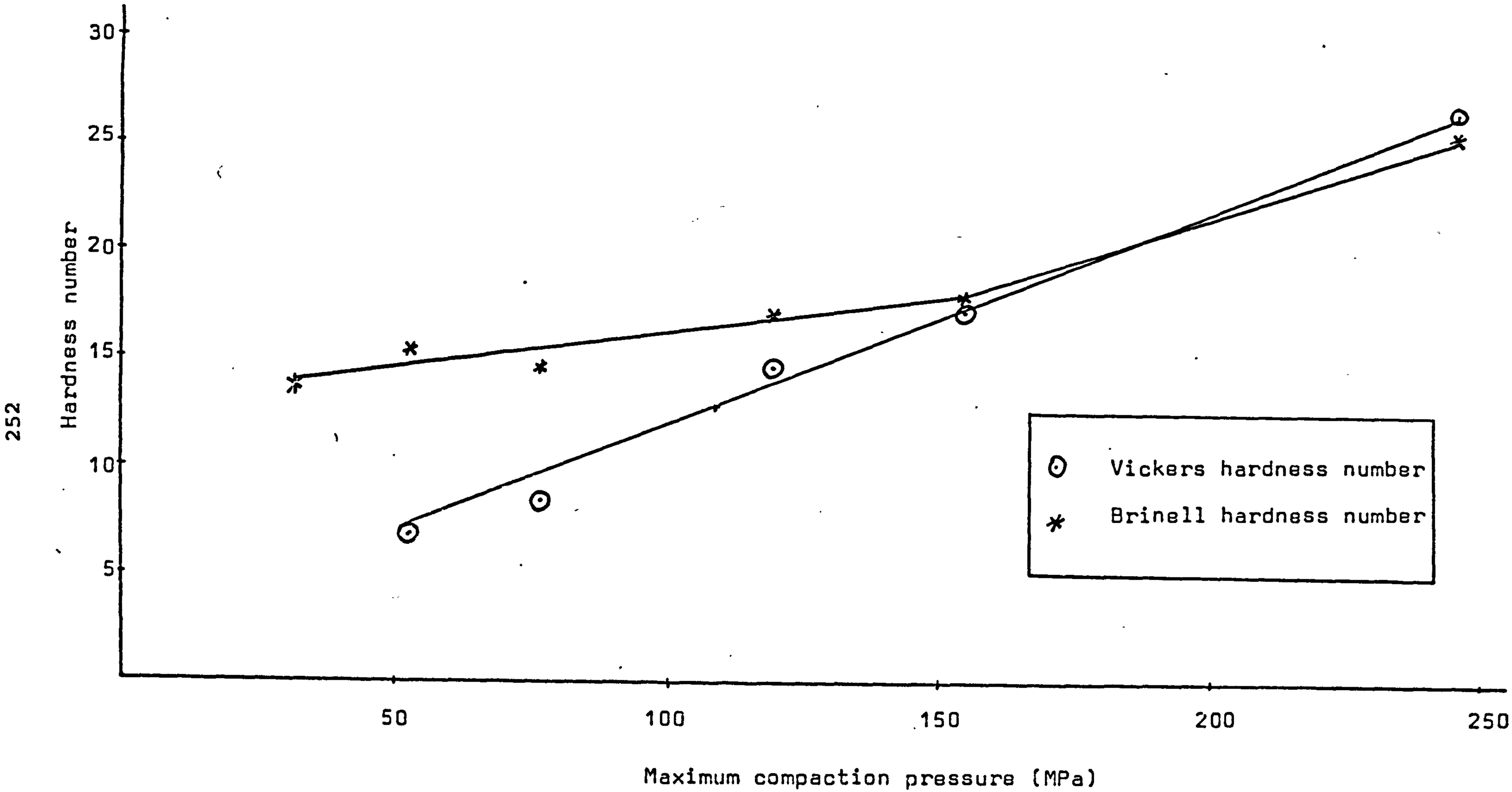

Figure:6.101 Variation of dicalcium phosphate compact hardness with compaction pressure

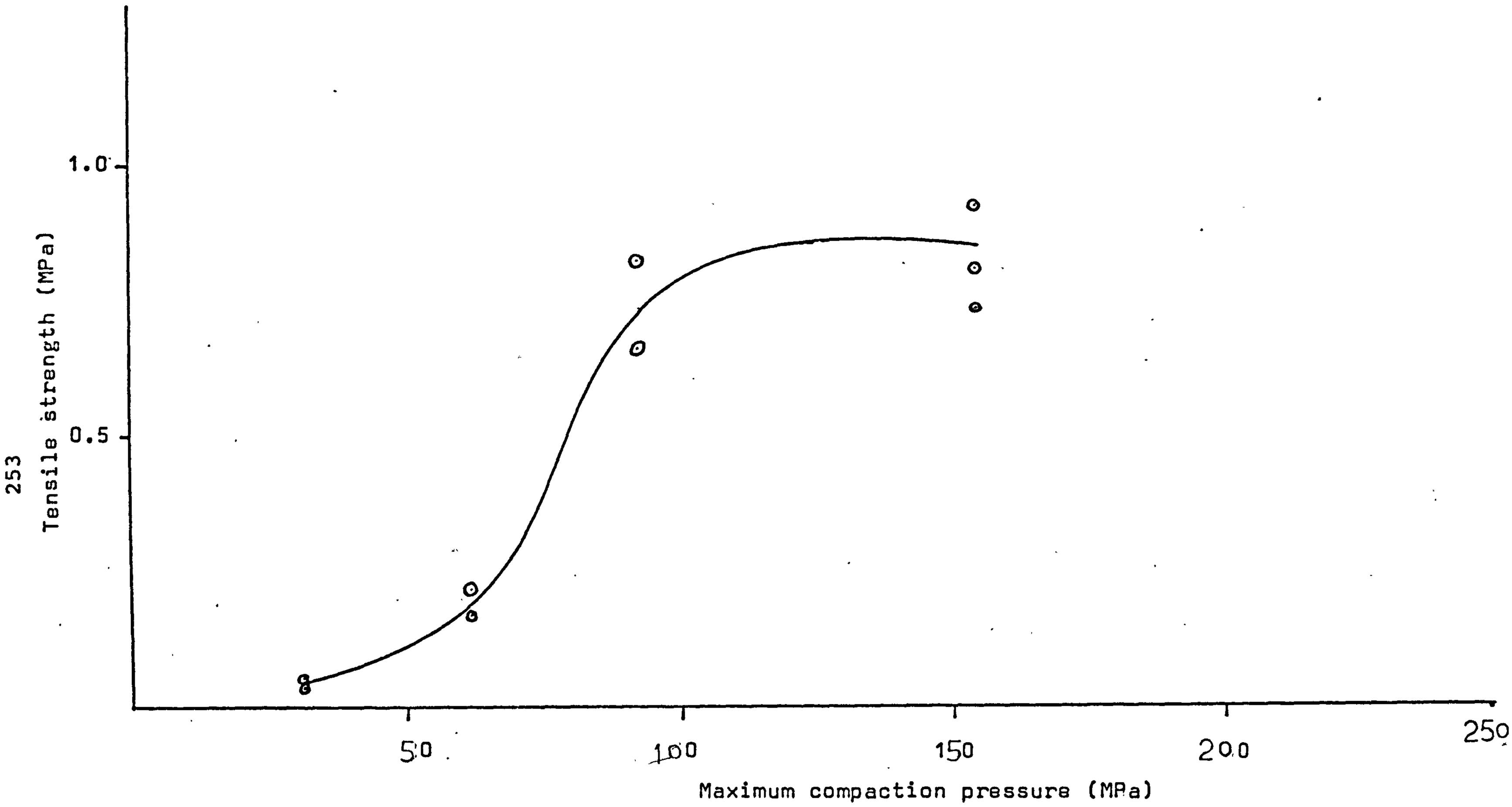

Figure: 6.102 Variation of sugar compact strength with compaction pressure

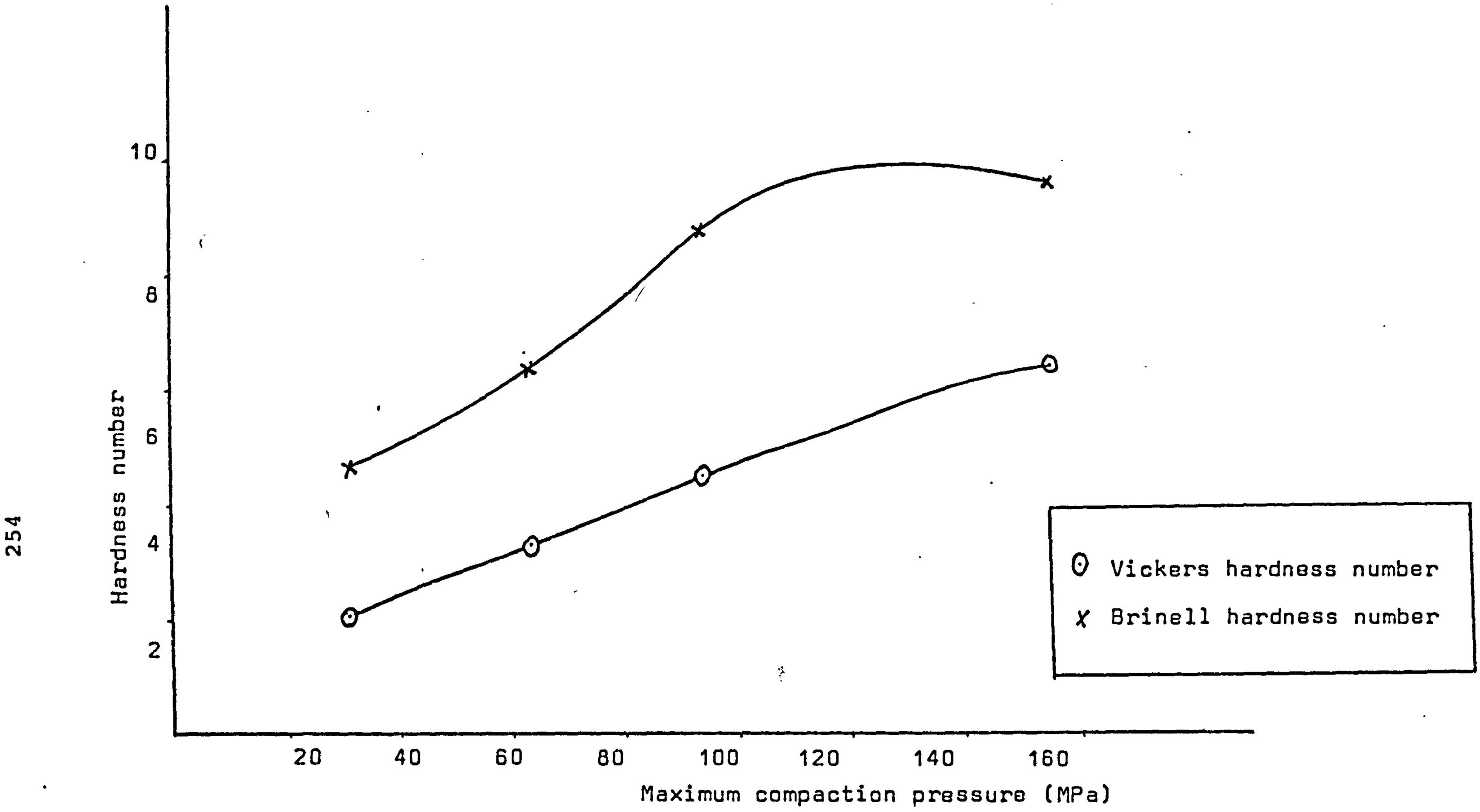

Figure 6.103 Variation of sugar compact hardness with compaction pressure.

Table 6.8 Variation of the Mechanical Strength of Sodium Chloride Compacts with Pressure

Powder	Maximum compaction stress	Mechanical Strength			Shear-Mean compaction stress parameters		
		Tensile strength	Hardness		Negative shear stress	Mean compaction stress	Area under unloading curve
	σ_{Amax}(MPa)	σt (MPa)	$H_{v(S)}$	$H_{B(S)}$	τmin (MPa)	σ^{o} (MPa)	a (cm^2)
Dentritic sodium chloride (250-300)μm	15	0.131	2.685	4.657	-	-	-
	32	0.532	5.943	7.1898	-0.940	3.5	0.03
	47	1.413	9.761	12.491	-2.708	8.5	0.186
	62	1.885	10.672	13.567	-	-	-
	77	2.071	13.325	16.488	-4.033	11.0	0.383
	124	2.58	22.0865	21.5335	-	-	-
	155	2.676	28.084	24.278	-9.557	27.0	2.583
	203	2.974	31.25	-	-13.713	40.5	5.459
	246	3.157	33.48	30.379	-16.741	53.0	8.756
Cubic sodium chloride (250-300)μm	47	0.572	11.258	8.794	-1,475	4.776	0.088
	77	0.853	16.374	20.62	-2.732	8.358	0.35
	125	1.295	20.578	26.522	-6.744	18.81	1.733
	155	1.616	22.814	30.101 29.975	-9.305	26.269	3.52

Table 6.9 Variation of Mechanical Strength of dicalcium phosphate and sugar compacts with pressure

Powder	Maximum compaction stress	Mechanical Strength			Shear - Mean compaction stress parameters		
		Tensile strength	Hardness		Negative shear stress	Compaction stress	Area under unloading curve
	σA_{max} (MPa)	σt (MPa)	H_V	H_B	τ_{min} (MPa)	σ^o (MPa)	a (cm^2)
Dicalcium phosphate	32	0.218 0.189	-	13.6196	-0.497	1.887	0.02
	47	0.35 0.311	6.905	15.4759	-0.969	3.75	0.08
	62	0.431 0.503	-	-	-	-	-
	77	0.661 0.705	8.3699	14.5099	-1.776	5.8125	0.26
	120	1.128 1.33	14.578	17.17 16.845	-3.725	11.25	1.26
	155	1.306 1.456 1.388	16.932	17.934 17.17	-4.162		
	246	3.205 3.073 2.415	26.6355	25.088 25.366	-5.867	-	-
Sugar (425-500) µm	31	0.039 0.0514	2.095	4.7	-.0468	1.739	0.014

cont.

Table 6.9 cont.

Sugar (425-500) µm	63	0.175 0.22	3.35	6.749	-1.208	3.913	0.04
	93	0.663 0.823	4.533	8.967	-1.772	6.087	0.154
	155	0.923 0.807 0.733	6.57	9.851	-5.036	14.78	1.02
	250	-	-	-	-9.919	27.83	4.0

Table 6.10 Variation of shear-mean compaction stress parameters of non-compactable materials with pressure.

Powder	Maximum compaction stress	Negative shear stress	Mean compaction stress	Area under unloading curve
	σ_{Amax} (MPa	τ_{min} (MPa)	σ^{o} (MPa)	a (cm^2)
Styrocell	62	-0.674		
	155	-0.443		
	248	-1.801		
Homopolymer	248	-1.589		
Copolymer	248	-0.468		

CHAPTER 7

DISCUSSION

7.1 Plastically Deforming Materials

7.1.1 Surface area

Sodium chloride is known as a plastically deforming powder (Hardman and Lilley 1973). The surface area of dentritic shaped sodium chloride used in this investigation was found to decrease continuously as the compaction pressure increased (fig 6.92). This kind of behaviour is expected from plastically deforming materials, since with plastic deformation the bonding of adjacent particles will increase the particle-particle contact area and decrease the accessible surface for adsorbates.

The results obtained in this thesis are in agreement with the work of Hardman and Lilley(1973), who found that the specific surface area of sodium chloride continuously decreased with increasing compaction pressures.

A similar pattern of change of surface area with compaction pressure was reported by Matsumaru (1957) when compacting aluminium silicate and by Avery and Ramsay (1973), who showed a marked decrease in surface area with increasing compaction pressure for both silica and zicronia powders. German (1985) compacted sub-micrometre palladium powders and found a decrease in surface area with increase in compaction pressure.

7.1.2 Porosity

Pore size distribution from mercury intrusion porosimetry analysis of dentritic sodium chloride compacts (appendix 3) showed consecutive elimination of the larger pore sizes or interparticle space as the compaction pressure increased (Fig.6.95). The mean pore radius decreased from an approximate value of 12 μm at the compaction pressure of 36 MPa to 0.13 μm at a compaction pressure of 248 MPa. Figure 7.1 shows the variation of the total pore volume of the compacts with compaction pressure. Below a pressure of approximately 80 MPa there is a very marked change in pore volume with compaction pressure, which can be attributed to particle deformation. The decrease in the rate of change in the pore volume above 80 MPa is intimately related to the decrease of pore sizes. Figure 7.1 indicates that the ultimate porosity of fragmentary dicalcium phosphate is much higher than that of plastic deforming dentritic sodium chloride. It is therefore concluded that only in the case of plastically deforming materials such as sodium chloride, can zero porosity or complete densification to the theoretical density be reached.

7.1.3 Mohr's Circles

The Mohr-Coulomb criterion is based on the idealization that particulate materials behave elastically up to a certain state of stress, after which yielding or failure of the material can occur.

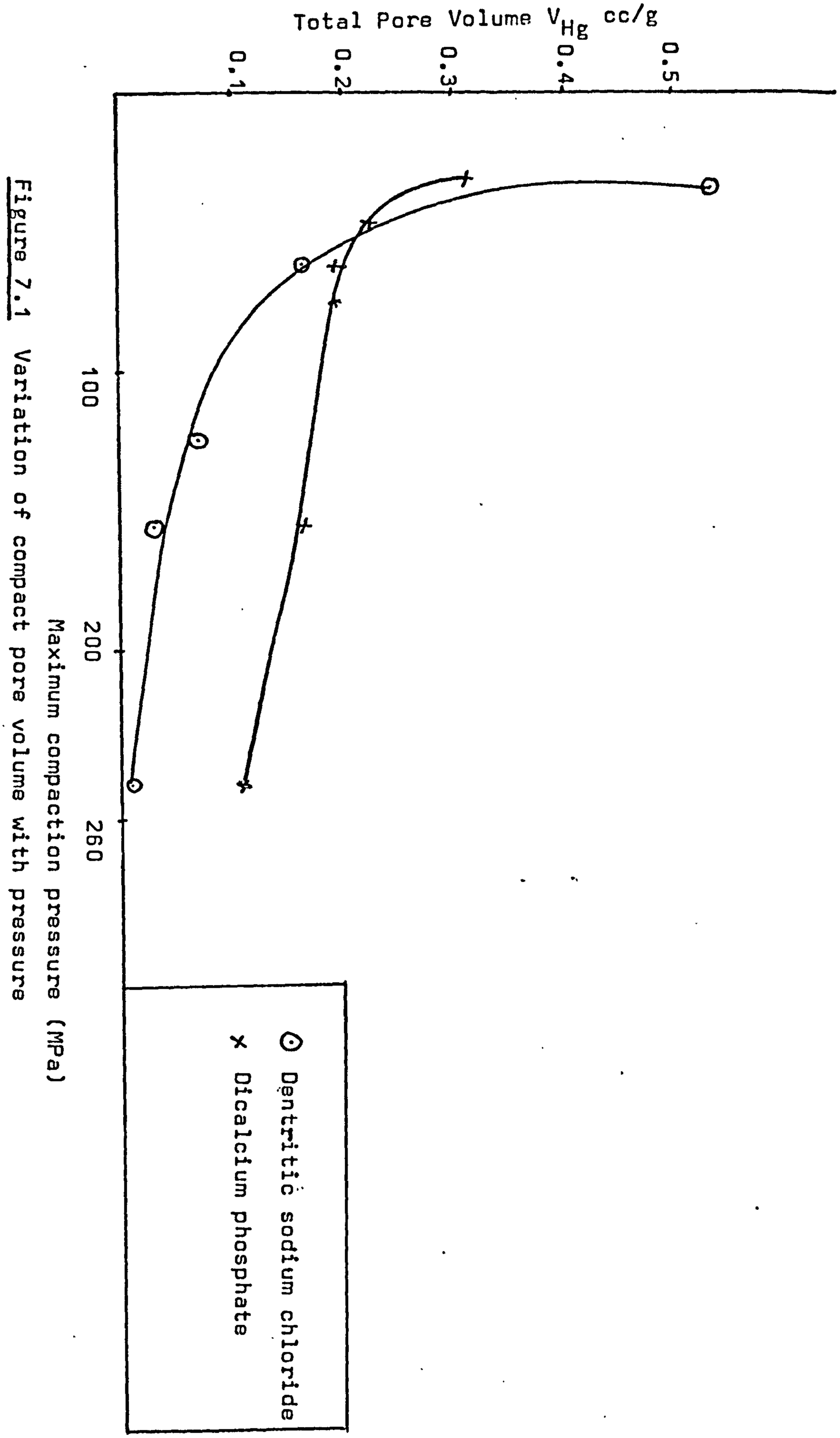

Figure 7.1 Variation of compact pore volume with pressure

The shear stress required for this yielding according to the Mohr-Coulomb relationship is considered to be a linear function of cohesion and the pressure normal to the slip surface. Schwartz and Weinstein (1969) compacted uranium dioxide powder over the range of 0 to 11.5 MPa and found that the relationship between shear stress and normal stress, was linear. The linearity of the powder yield locus, found in the compaction pressure range used, supported the assumption that Coulomb's equation, was tenable for the compaction of particulate solids and was satisfied for every point in the compact. Recent work by Strijbos et al (1977) and Fukumori and Okada (1977), who made use of the Mohr-Coulomb equation, however, showed that the yield locus of granular materials compacted at high pressures is not linear.

The Mohr's circles constructed for both dentritic and cubic sodium chloride compacts over the range of 0 to 250 MPa (Fig 6.2-6.5 and 6.20-6.23) indicate that the powder yield locus although initially linear at low compaction pressures, shows a power relationship between shear and compaction stress at higher compaction pressures.

The angle between the yield locus and the compaction stress axis of both dentritic and cubic sodium chloride, which is in effect the yield locus slope, tends to decrease continuously as the compaction pressure increases. This behaviour suggests that at high compaction pressures, or on extrapolation to complete densification-theoretical zero

porosity-the conditions for failure would depend on the material irrespective of the applied stress. The shear stress/strength will then be equal, at zero slope, to the cohesive strength of material and the state of failure could be defined by Tresca's yield criteria which was initially proposed for metals.

$$\tau = C \qquad (7.1)$$

where $\tau \equiv$ shear strength of the material

$C \equiv$ cohesive strength

At compaction pressures lower than those necessary to achieve complete densification the angle or slope of the yield locus varies in a similar manner to that seen by Suh(1969). This phenemenon expressed mathematically by Suh, who investigated the compaction of metal powders was attributed to the work hardening of the material. The similarity between the work of Suh and the data from both dentritic and cubic sodium chloride indicates that this material therefore undergo modification or work hardening. This change in the state of sodium chloride may be accomplished by the rearrangement of dislocations within the crystal habit.

7.1.4 Compaction stress pathways

The shear stress $(\sigma_A-\sigma_R)/2$ and the compaction stress $(\sigma_A+\sigma_R)/2$, relationships for the compressive curve - the powder yield locus - for each compaction pressure (Fig.7.2 and 7.3) were found to be of similar shape to the yield loci constructed from the Mohr's circles (Figs 6.2-6.5 and 6.20 - 6.23). The initial part of the

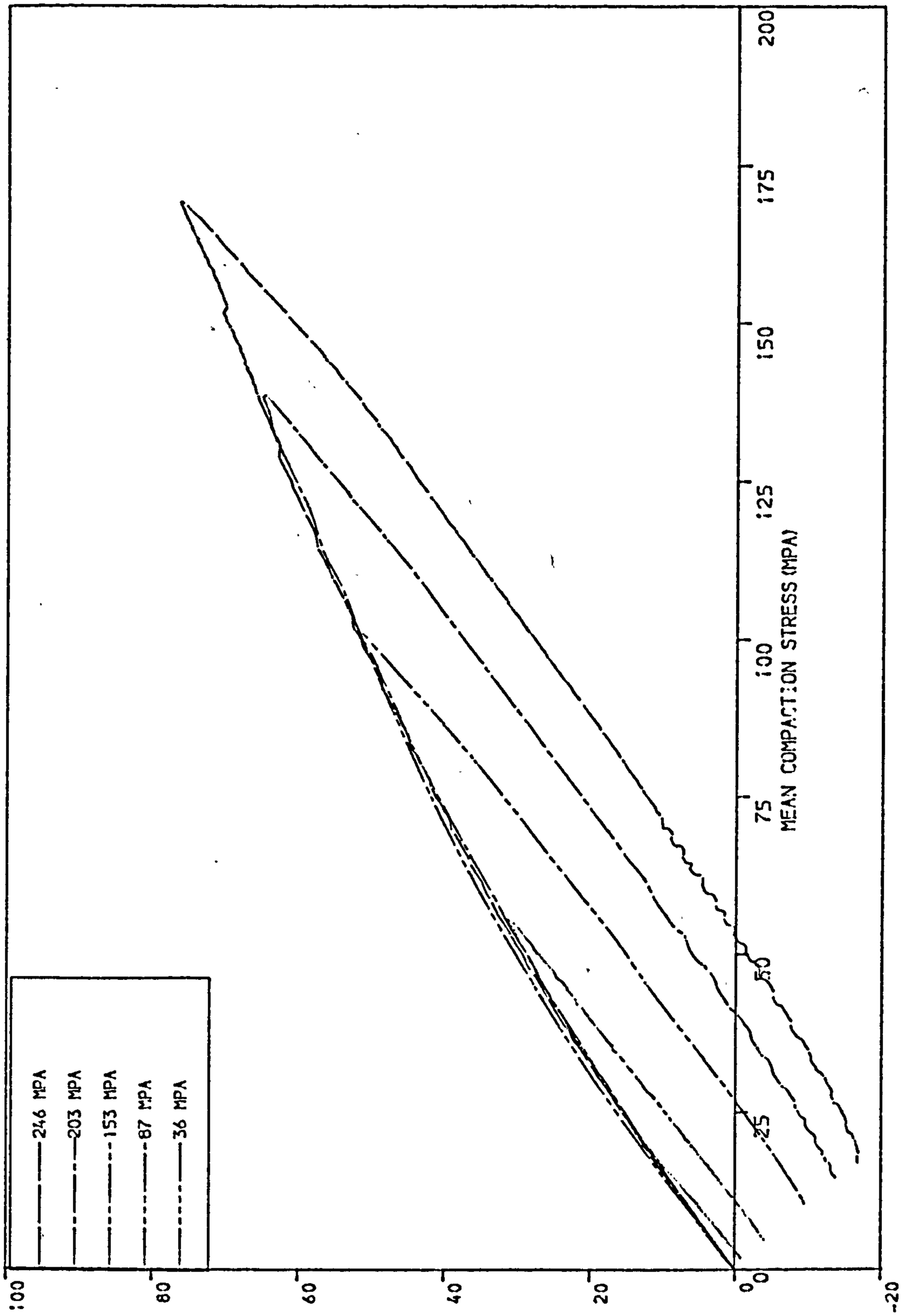

FIGURE 7.2 DENTRITIC SODIUM CHLORIDE
COMPACTED UNIAXIALLY AT DIFFERENT
COMPACTION PRESSURES

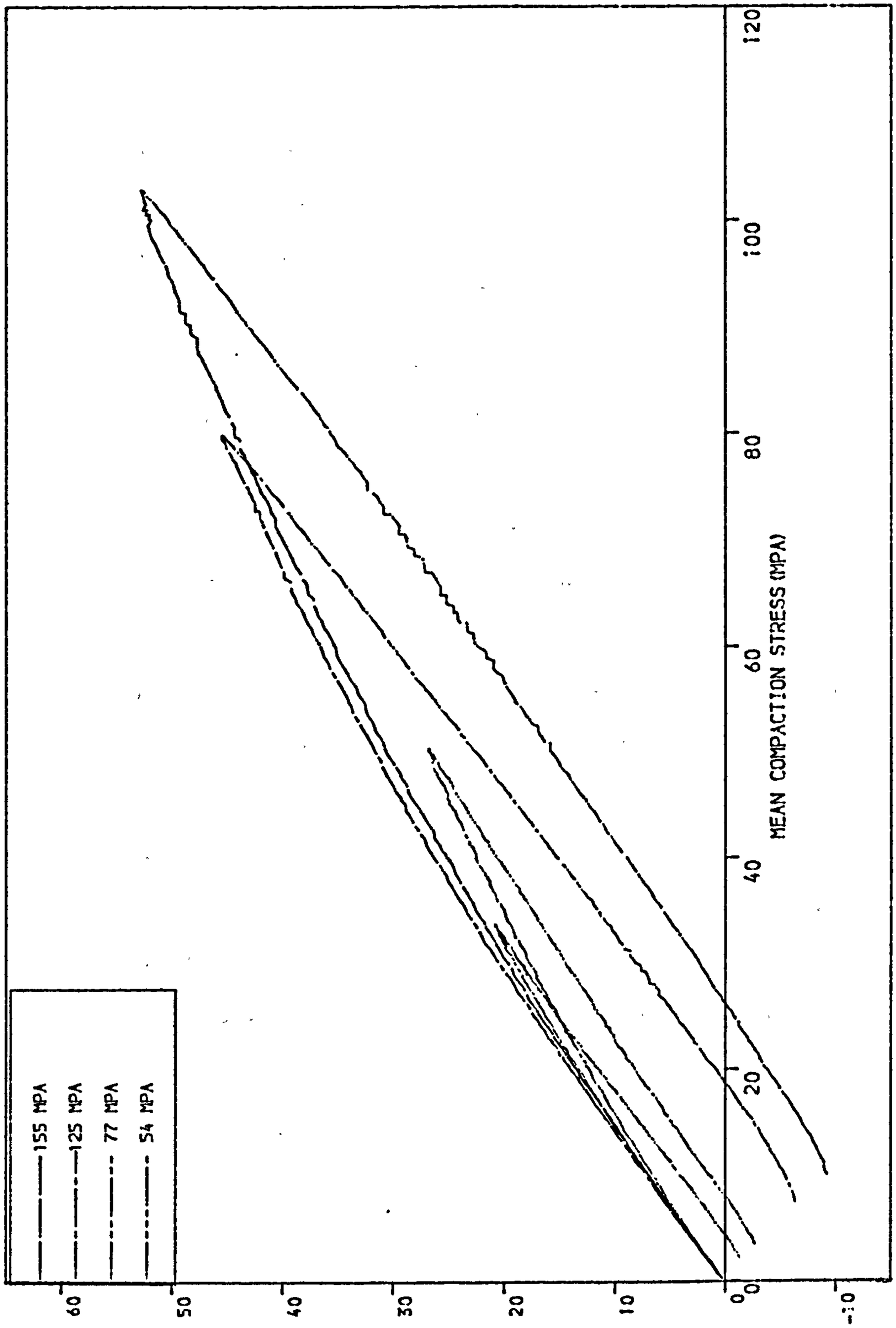

FIGURE 7.3 C-SODIUM CHLORIDE
COMPACTED UNIAXIALLY AT
DIFFERENT COMPACTION PRESSURES

yield loci from the Mohr circle figures and the stress pathway figures shows an approximate linear relationship between shear and compaction stress, which supports the assumption that the Coulomb yield equation is valid for the low pressure compaction of sodium chloride.

As the compaction pressure increases the slope of the powder yield locus decreases. Although an approximate linear relationship between shear and compaction pressures has been suggested for low compaction pressures, a power relationship therefore exists between these parameters. The conditions for failure of sodium chloride at high compaction pressures can not be defined by the linear Mohr-Coulomb equation (equation 1.11), because there is a continuous range of values of C and ϕ. The variation of C and ϕ seen with both dentritic and cubic sodium chloride is unlike the work of Fukumori and Okada (1977) who found for potassium chloride compacted to 100 MPa, that the yield locus for the compressive curve could be approximated by two linear relationships between shear and compaction stress.

$$\tau = 0.653\sigma_N \qquad (7.2)$$

$$\tau = 0.378\sigma_N + 33.8 \qquad (7.3)$$

where τ and σ_N are in MPa.

The relationships obtained for the yield loci for the compressive curves of both dentritic sodium chloride compacted at 248 MPa and cubic sodium chloride compacted at 155 MPa can be expressed by equations 7.4 and 7.5. respectively.

$$\tau = 0.6208\sigma - 0.0010501\sigma^2 + 0.3393 \qquad (7.4)$$

$$\tau = 0.6877\sigma - 0.0017038\sigma^2 + 0.2917 \qquad (7.5)$$

The experimental results show little scatter from the proposed equations (app:4)

7.1.5 Unloading:

All the unloading shear-compaction stress curves of sodium chloride compacts (fig.7.2 and 7.3) cross the compaction stress axis to give negative values of shear stress and reach a minimum value, τ_{min}. The magnitude of the point of crossing, σ_o and τ_{min} were always dependent on the maximum compaction pressure applied. The end points of the unloading stress paths for all the compaction pressures investigated were seen to terminate on a straight line in negative shear-compaction stress space. The unloading curves with the parameters of σ_o and τ_{min} thus may be more significant in ascertaining the stability of compacts than the yield compaction curves (Section 7.1.1 1).

7.1.6 Volumetric strain:

In a similar manner to the compaction and unloading stress path analysis, the history of the state of strain within the compacts investigated could be traced in terms of either the volumetric strain, ε (section 6.2) or simply the bulk volume of the compact during compaction.

The pressure-volume relationship of compacts has been studied by several authors (Train 1956), Shotton and Ganderton (1960), Marshall (1963) and Seelig and Wulff (1964)). It is now acknowledged that the mechanisms involved in the

compaction process are

a- Repacking or particle re-arrangement

b- Formation of bridges or supporting structures

c- Elastic-plastic deformation and/or brittle fracture

d- Bulk compression

Figure 7.4 shows the experimental results of dentritic sodium chloride stress paths replotted as compact volume change, V, against the natural logarithm of mean compaction pressure, $(\sigma_A+\sigma_R)/2$. This figure is similar in shape to the relationship between the compact stress and strain presented in Chapter 6, where strain is evaluated from expression

$$\varepsilon = \frac{V_o - V_i}{V_i}$$

where V_o and V_i are the initial and instantaneous states of volume respectively.

At the first sight, the volume change curves of dentritic sodium chloride with a particle size of 250-300μm (fig.7.4) compacted at different compaction pressures (36, 87, 153 and 246 MPa respectively), appear to depend on the initial die fill and the maximum compaction pressure. Each of the curves can easily be divided into two regions, with the possibility that a third region may also be identified at high compaction pressures.

The initial region occurring at compaction stresses of ln.mean values of -1 to 0 is regarded as a particle re-arrangement section. A second region exists between ln. stress values of 0 to 4.8 which is regarded as the

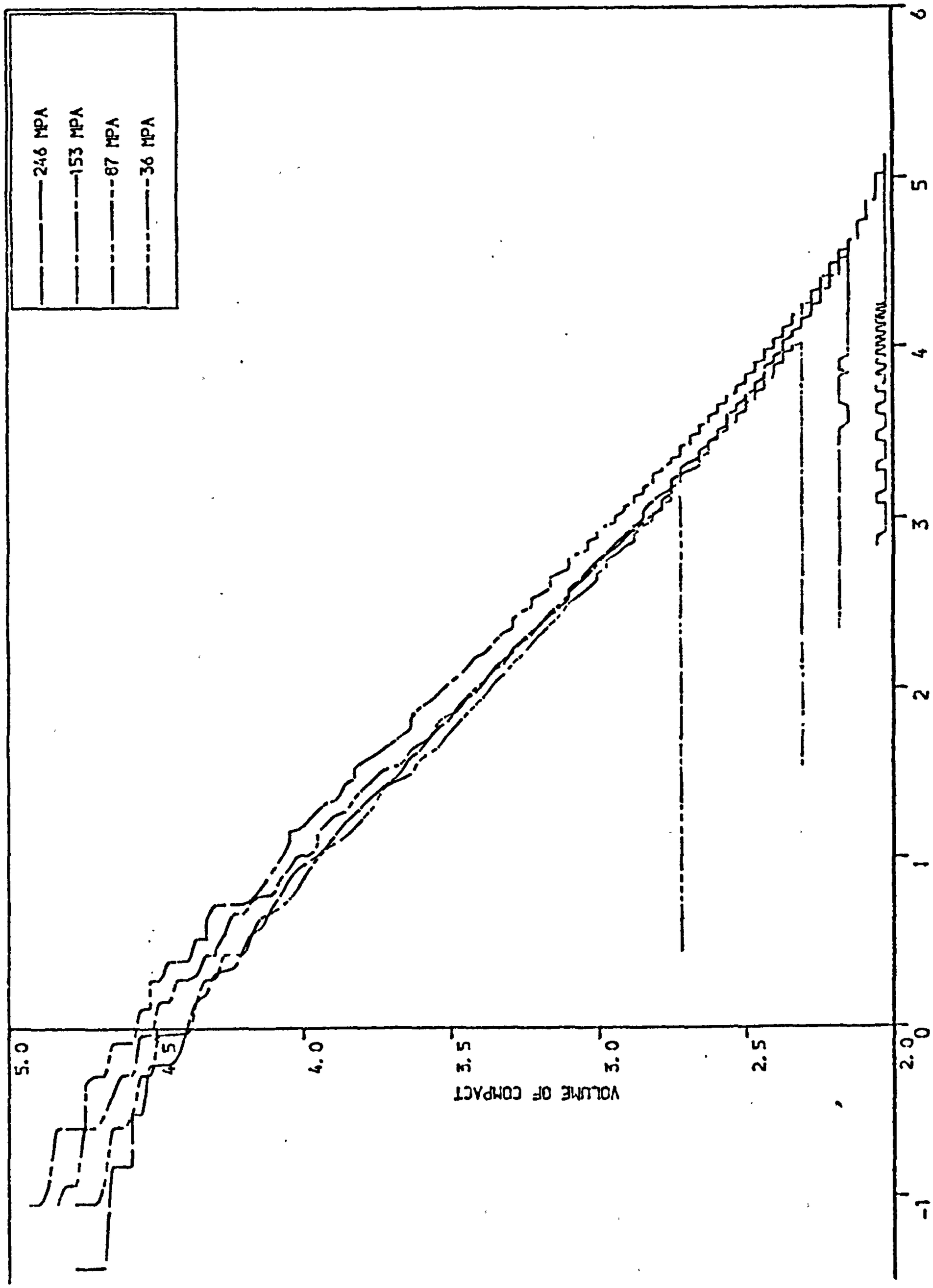

FIGURE 7.4 DENTRITIC SODIUM CHLORIDE COMPACTED UNIAXIALLY AT DIFFERENT COMPACTION PRESSURES

deformation and/or brittle fracture region, with a third possible region above ln. mean compaction stress value of 5. This third region may be designated as a bulk compaction region. In this third region densification of the particles became more and more difficult as the assembly behaves as a solid mass of material. Unlike the work of Hardman and Lilley(1973), who found no evidence of particle re-arrangement in the compaction of sodium chloride (63-90μm), the figures of dentritic sodium chloride in the size range of 250-300μm in this investigation show that there was a region which can be attributed to particle re-arrangement.

7.1.7 <u>The effect of particle size on the compaction of dentritic sodium chloride</u>

The effect of particle size on the stress paths is shown in figures 7.5 and 7.6 respectively, where particles of sodium chloride of different initial particle sizes were compacted at an applied pressure of 155 MPa. Although no significant difference was found in the shear compaction stress curves of the four different size ranges studies (Fig.7.5), the volume reduction curves (Fig.7.6) showed that the initial particle size is an important factor at the commencement of densification.

The effect of particle size was clearly observed in the initial stages of compaction. The size range of 355-425 μm showed no evidence of particle re-arrangement because there was no discontinuity in the shape of

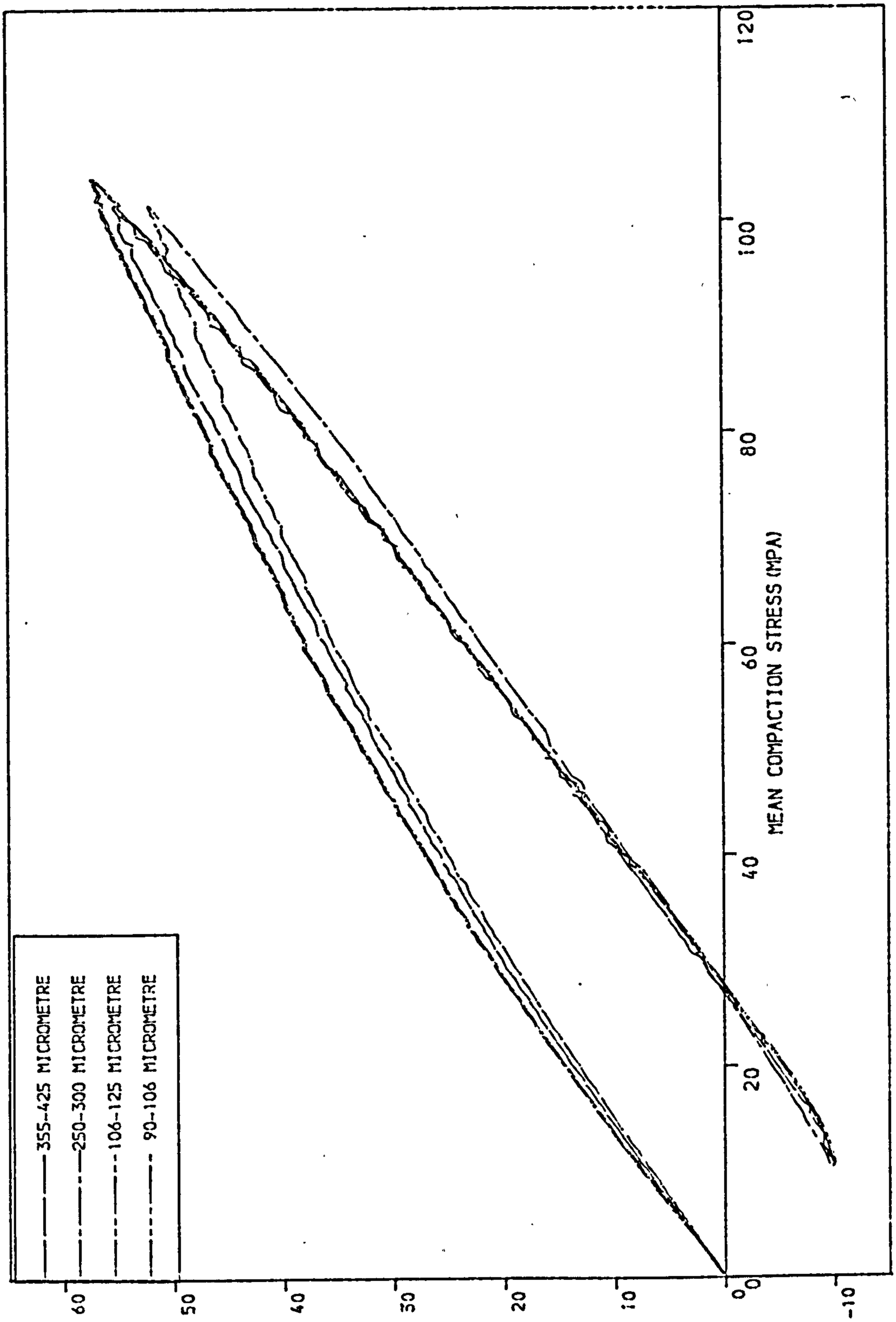

FIGURE 7.5 THE EFFECT OF PARTICLE SIZE ON THE COMPACTION OF DENTRITIC SODIUM CHLORIDE

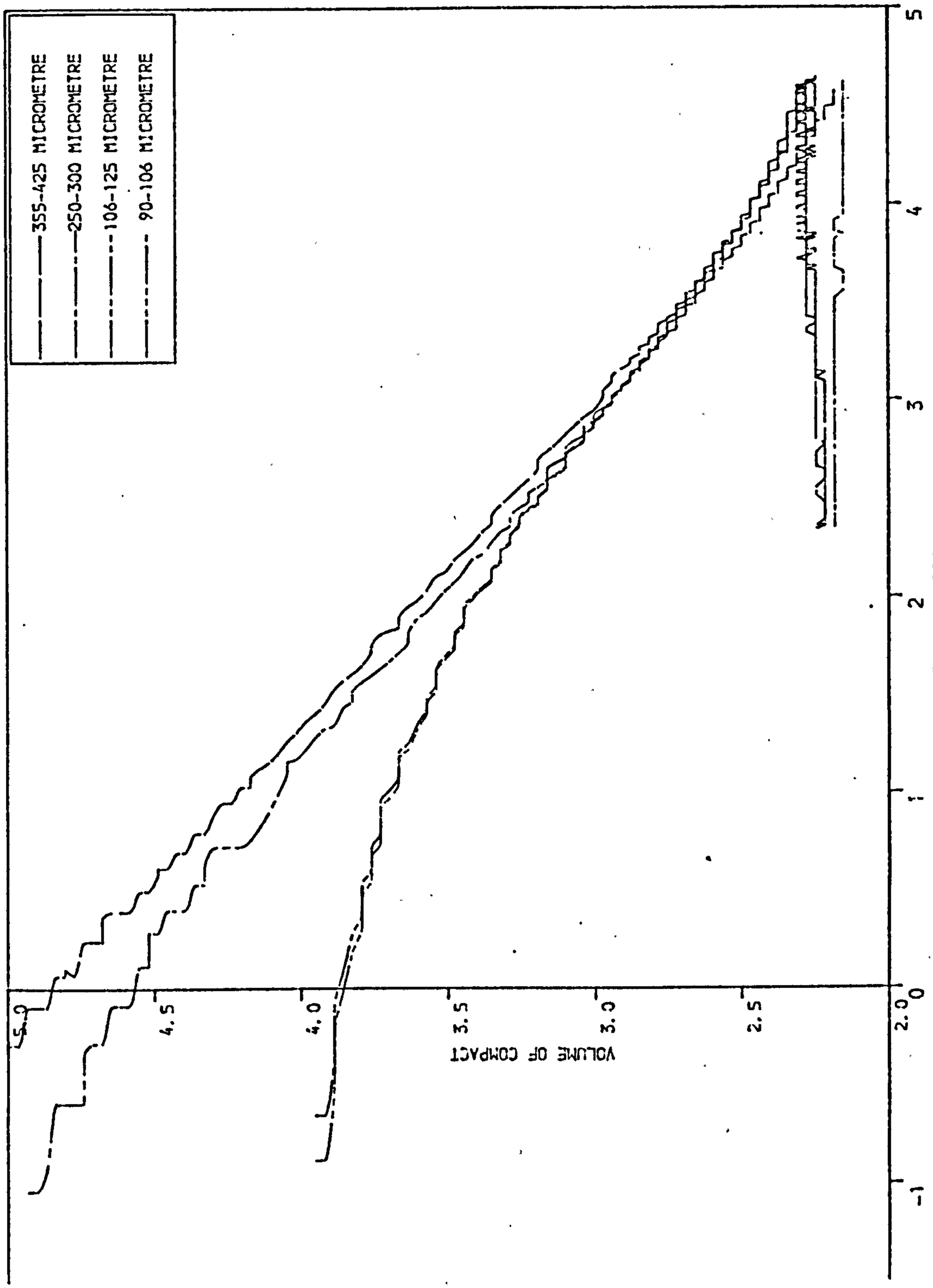

FIGURE 7.6 THE EFFECT OF PARTICLE SIZE ON THE COMPACTION OF DENTRITIC SODIUM CHLORIDE

the curve. The volume-pressure curve of the particle size range of 250-300μm however showed evidence of slippage or particle re-arrangement to an approximate value of compaction pressure of 1.5 MPa. The shape of curves plotted for the smaller sizes, namely 106-125 and 90-106μm of dentritic sodium chloride, indicate that the degree of particle re-arrangement and bridging increased as the particle size of the powder decreased. The pressure level at which particle slippage and bridging ceases as a compaction mechanism is higher for small particles than for large particles. This observation was in agreement with the findings of Huffine and Bonilla (1962) and York (1978) who studied the pressure-volume relationships of non-metallic powders in die compaction and found that the effect of size was similar to that found in this thesis.

7.1.8 Loading rate

The effect of the loading rate on the compaction of dentritic sodium chloride has also been studied. It was found that although there is some separation in the stress paths of different loading rates (Fig.7.7) the volume reduction curves (Fig.7.8) were identical. Caution must be used however in the pronouncement that the volume change of compacts is independent of loading rate because the loading rates used in this work varied from 4.25 to 13 MPa/sec., which is very much lower than the rates achieved with high speed commercial equipment . A general observation however indicates that at low rates of compaction, the final compacted volume seen from the mean compaction stress-volume figure is lower for the loading

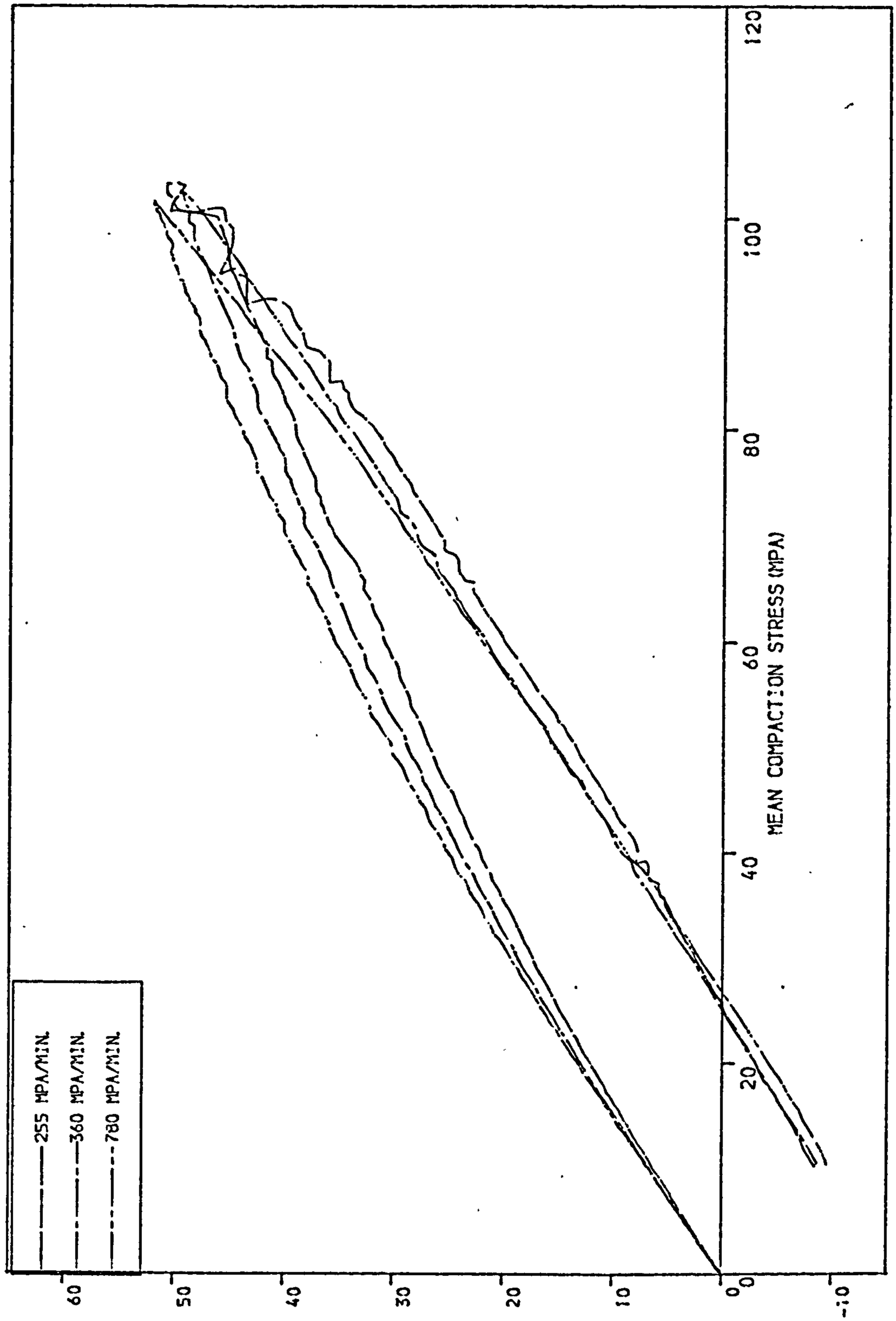

FIGURE 7.7 THE EFFECT OF LOADING RATE ON THE COMPACTION OF DENTRITIC SODIUM CHLORIDE

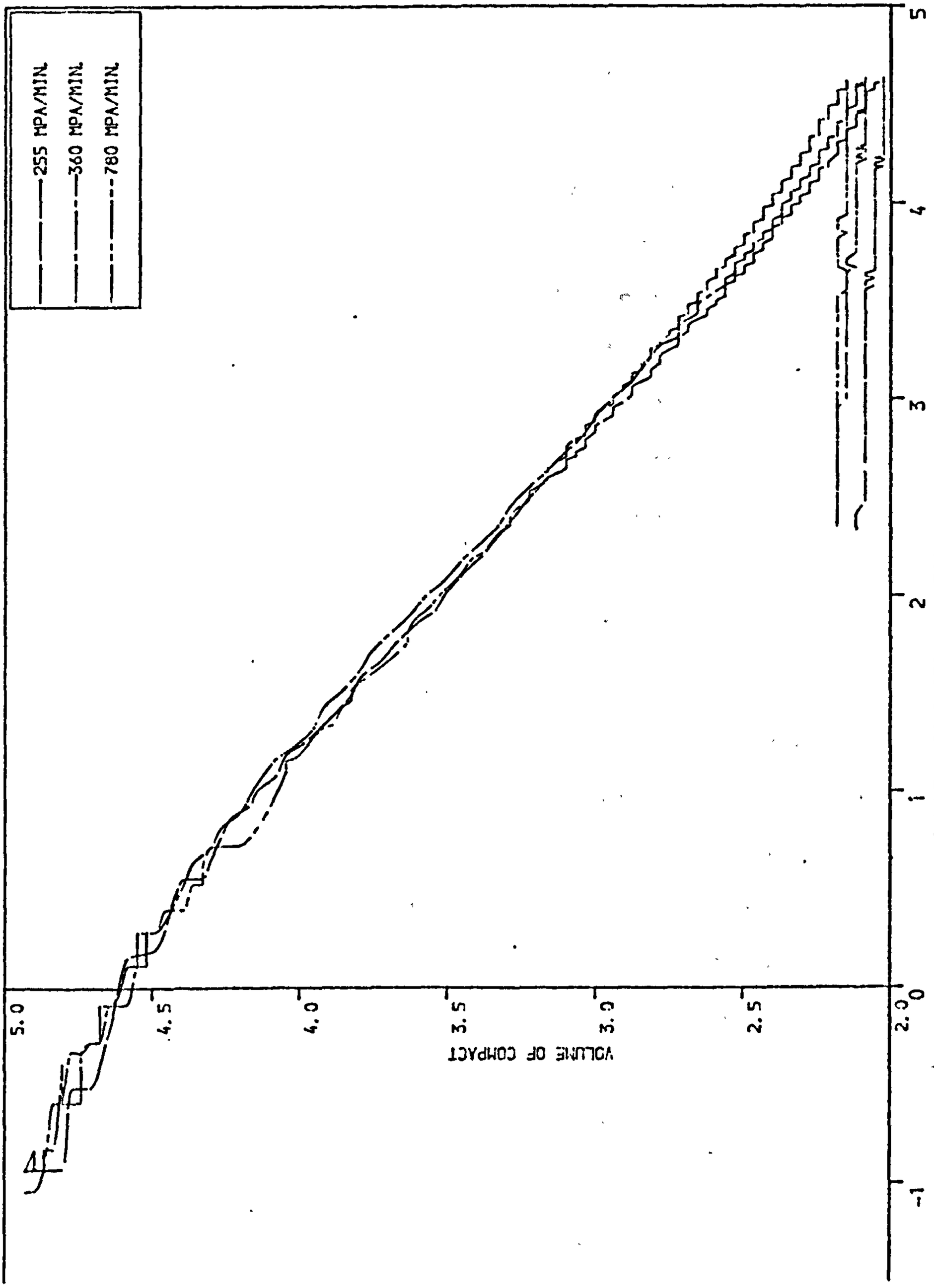

FIGURE 7.8 THE EFFECT OF LOADING RATE ON THE COMPACTION OF DENTRITIC SODIUM CHLORIDE

rate of 255 MPa/min than for 780 MPa/min.

7.1.9 Volume reduction curves of cubic sodium chloride

Figure 7.9 shows the experimental results obtained from cubic sodium chloride, of particle size range 250-300 μm, compacted at different compaction pressures (54, 77, 125 and 155 MPa. The shape of the initial volume reduction curves is different from that obtained with dentritic sodium chloride (Fig.7.4). The cubic sodium chloride curves could also be approximated to two regions. The two regions identified, represent different stages or mechanisms in the process of compaction.

Region (a) - Particle re-arrangement and bridge formation

The particle re-arrangement and bridge formation mechanisms in the compaction of cubic sodium chloride was found to occur at compaction stresses of ln-mean values of -1 to an approximate value of 1.5. This latter value was greater than that found for dentritic sodium chloride of the same particle size range. The above two mechanisms were seen to be followed by a third phenomenon in which the previously formed supporting structures begin to collapse leading to an increase in the rate of volume reduction.

Region (b) - Particle deformation.

The second region is the type of curve normally obtained by particle deformation and/or fragmentation mechanisms. There was no evidence of bulk compression of cubic sodium chloride in the range of compaction pressures investigated.

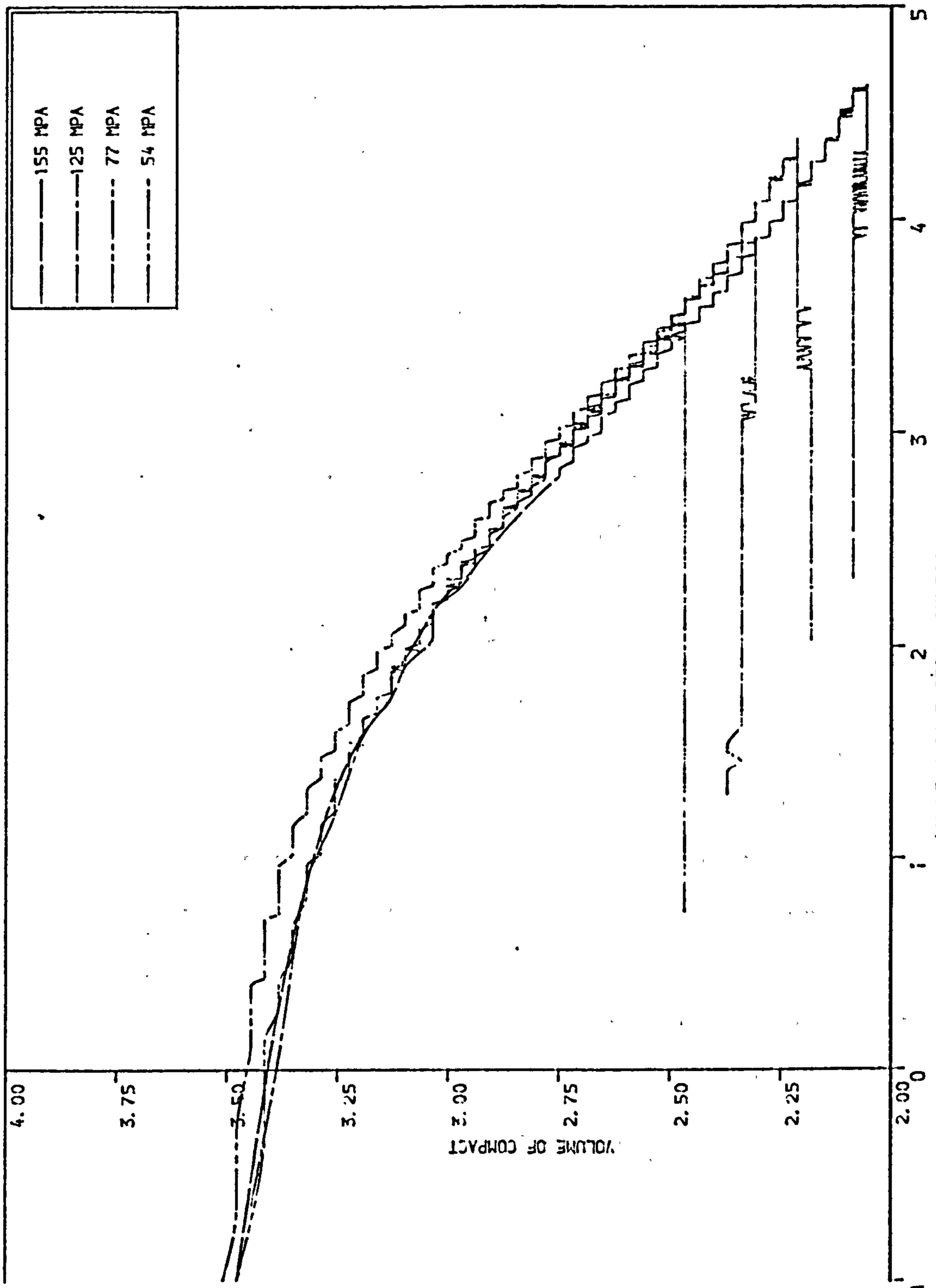

FIGURE 7.9 C-SODIUM CHLORIDE
COMPACTED UNIAXIALLY AT
DIFFERENT COMPACTION PRESSURES

7.1.10 The effect of particle size

The effect of the initial particle size on the densification process of cubic sodium ohloride is demonstrated in figures 7.10 and 7.11. The stress paths plotted in shear-compaction stress space of the three different size ranges, 425-500, 250-300 and 106-125 μm were identical. The volume reduction curves, however, showed a dependance on the initial particle size. As in the case of dentritic sodium chloride, the larger size range of cubic sodium chloride did not show any sign of particle slippage, while the domination by the mechanisms of particle rearrangement and bridging in the early stages of compaction increased with decreasing particle size.

From the comparison of the volume reduction curves obtained from dentritic and cubic sodium chloride, it can be concluded that the densification process of sodium chloride although dependent on the size of the particles is also dependent on the shape of the particles; The shape of the particles being more significant in the densification process.

7.1.11 Mechanical strength of compacts

7.1.11.1 Dentritic sodium chloride

(a) Tensile strength

The tensile strength of dentritic sodium chloride compacts, measured by diametral fracture showed an increase with increasing compaction pressure. Hardman and Lilley, found a linear relationship between compaction pressure and the tensile strength of sodium chloride. In this thesis compacts of dentritic sodium chloride

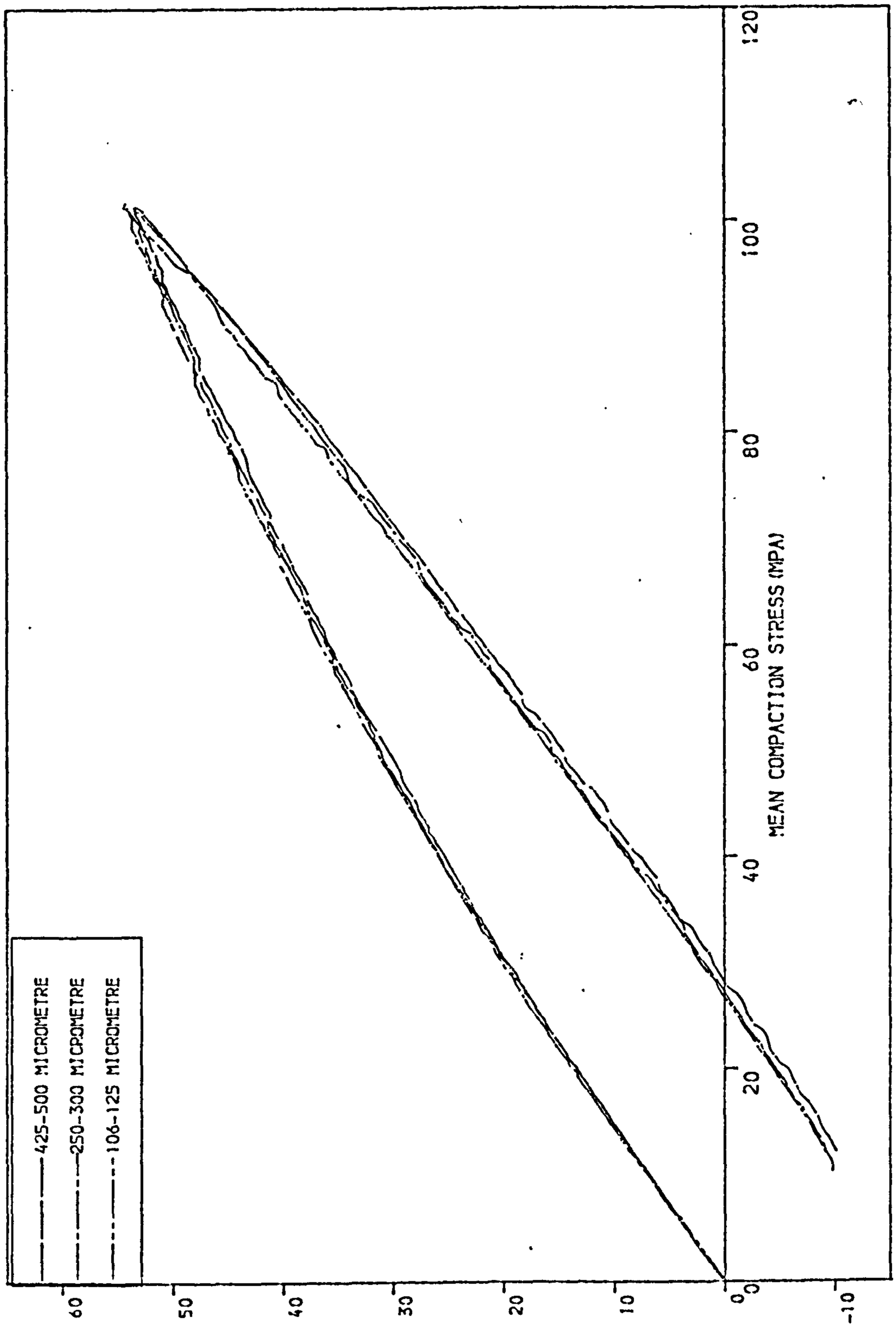

FIGURE 7.10 THE EFFECT OF PARTICLE SIZE ON THE COMPACTION OF C-SODIUM CHLORIDE

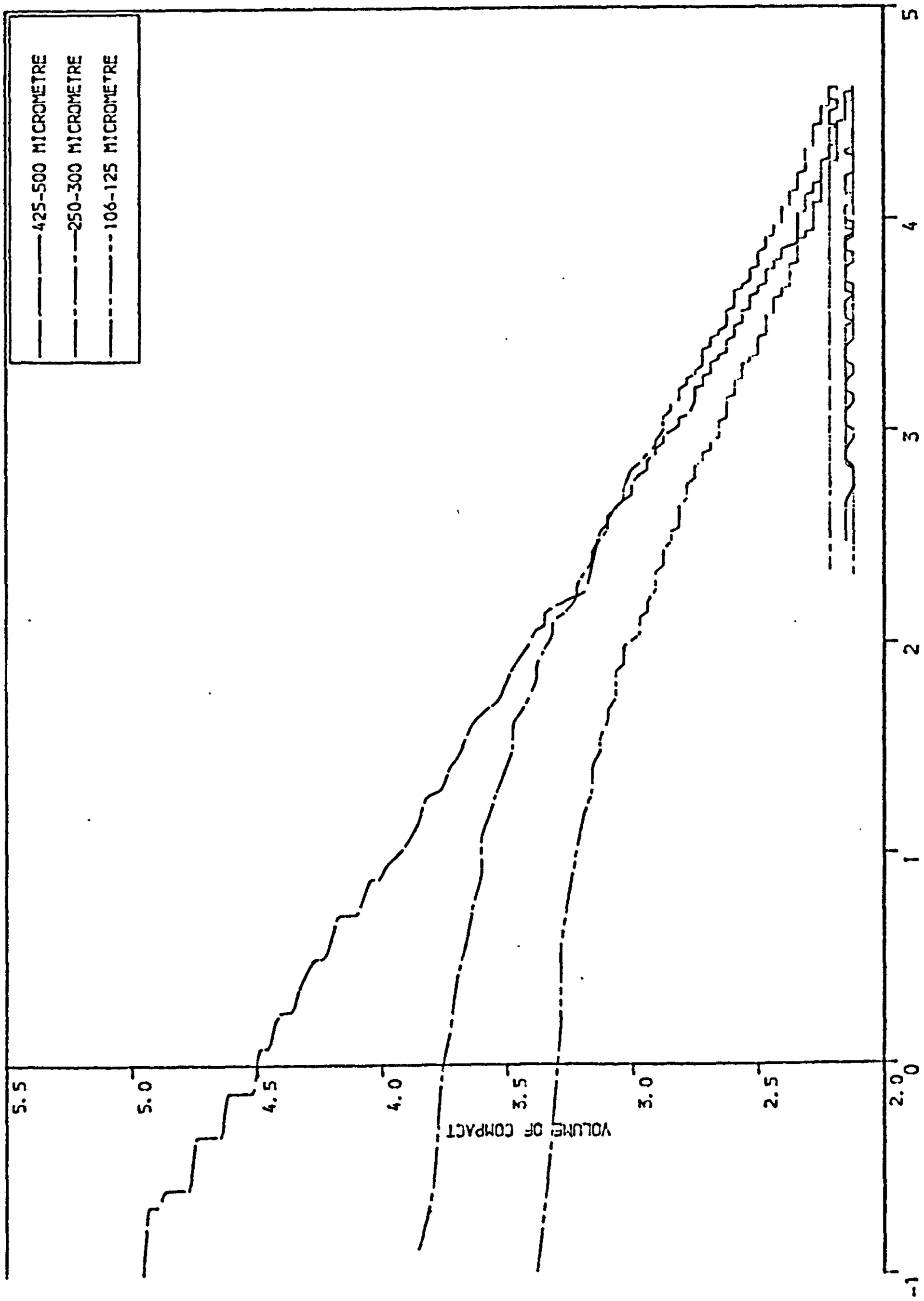

FIGURE 7.11 THE EFFECT OF PARTICLE SIZE ON THE COMPACTION OF C-SODIUM CHLORIDE

produced below a pressure of approximately 65 MPa showed an approximate linear relationship (Fig.7.12). With compacts produced at higher compaction pressures the slope of the curve, or the rate of increase in the compact strength decreases continuously.

A similar trend was observed in the relationship between the shear and mean compaction stress.

It is generally accepted that the strength of the bond between two surfaces depends on the area of contact between particle-particle surfaces.
In the case of dentritic sodium chloride the effect of increasing compaction pressure will cause particle deformation which increases the contact area and hence the production of a stronger compact. As the voids between the individual particles become smaller, more pressure will be needed for the material to be extruded plastically into these relatively small voids to occupy the void spaces.

(b) Hardness

The Vickers hardness number and the Brinell hardness number of dentritic sodium chloride were also found to increase with increasing compaction pressure (fig.6.97). A power relationship was also found between the compaction pressure and the hardness of compacts.

7.1.11.2 Cubic sodium chloride

(a) Tensile strength

The tensile strength of cubic sodium chloride compacts was found to increase linearly with increasing compaction pressure in the range of pressures, 47-155 MPa

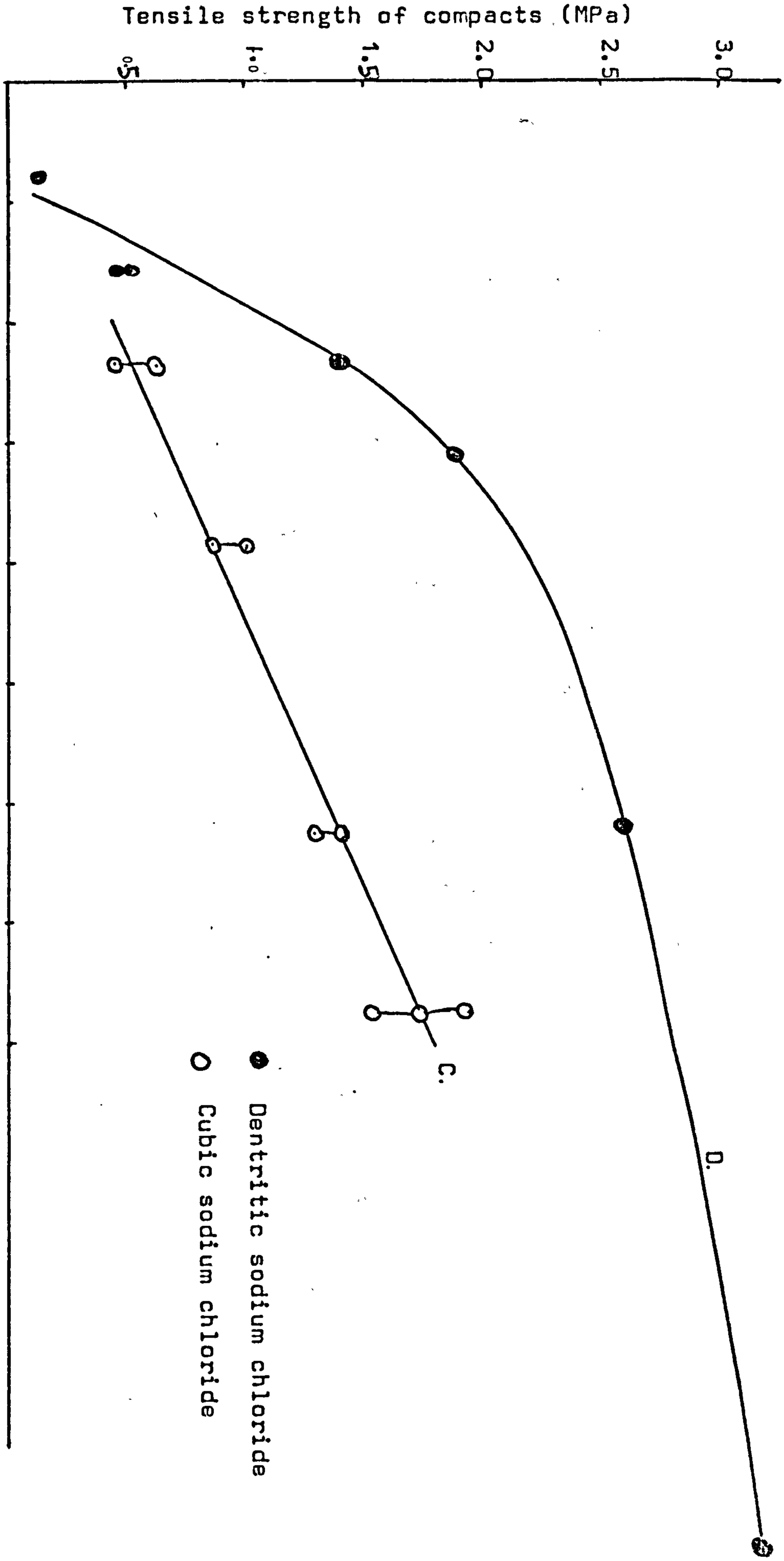

Figure 7.12 Effect of particle shape on the strength of sodium chloride compacts.

(fig. 6.98). It was also found that the strength of the cubic sodium chloride compacts is always lower than the strength of dentritic sodium chloride (fig.7.12).

(b) Hardness

Both Vickers and Brinell hardness numbers, were found to increase with increasing compaction pressure (fig 6.99).

From Figures 7.2 and 7.3 it was shown that all unloading shear-mean compaction stress curves of both dentritic and cubic sodium chloride compacts cross the mean compaction stress axis at σ_o to give negative values of shear stress and reach a minimum value of τmin. The area enclosed beneath the mean compaction stress axis and the unloading curve could also be evaluated. This area in terms of arbitrary units of square centimeters can be used for comparison between the compacts produced. These three values together with the dimetral fracture and hardness test values are shown in Table 6.9. Figures 7.13a, b and c and 7.14 a,b and c show the relationships of the parameters τ_{min}, $\sigma^o$and the area a, for both dentritic and cubic sodium chloride compacts with the tensile strength, σ_t, Vicker's hardness number V_N and Brinell hardness number H_N. A natural logarithmic relationship was found to exist between the evaluated parameters τ_{min}, σ^o and a and the tensile strength and hardness of the compacts, This observation suggests that the unloading stress paths are more informative than the compressive paths -yield loci- of sodium chloride.

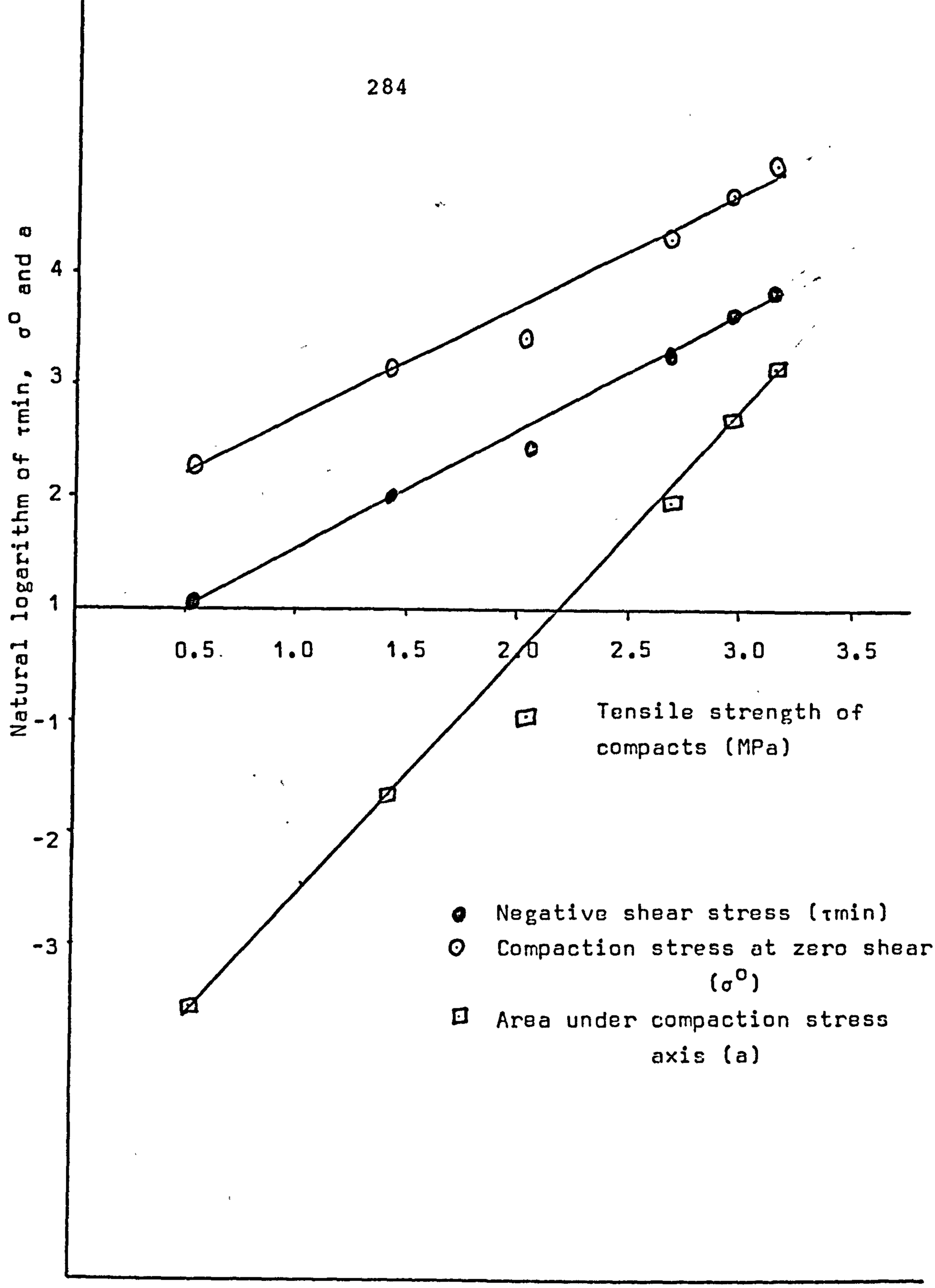

Figure : 7.13a Relationship between shear-compaction stress parameters and the tensile strength of D-sodium chloride compacts.

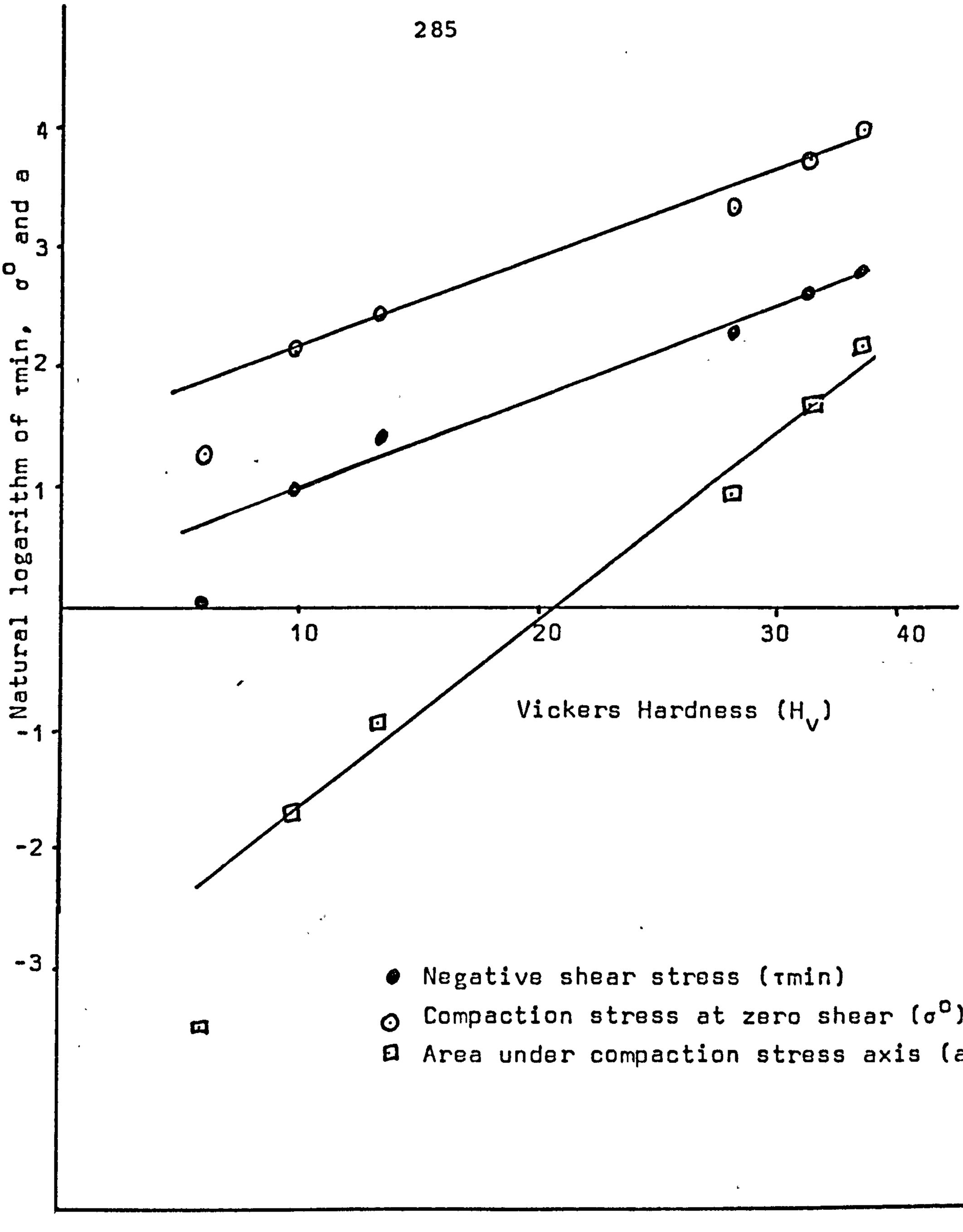

Figure: 7.13b Relationship between shear-compaction stress parameters and Vickers Hardness number of D-sodium chloride compacts.

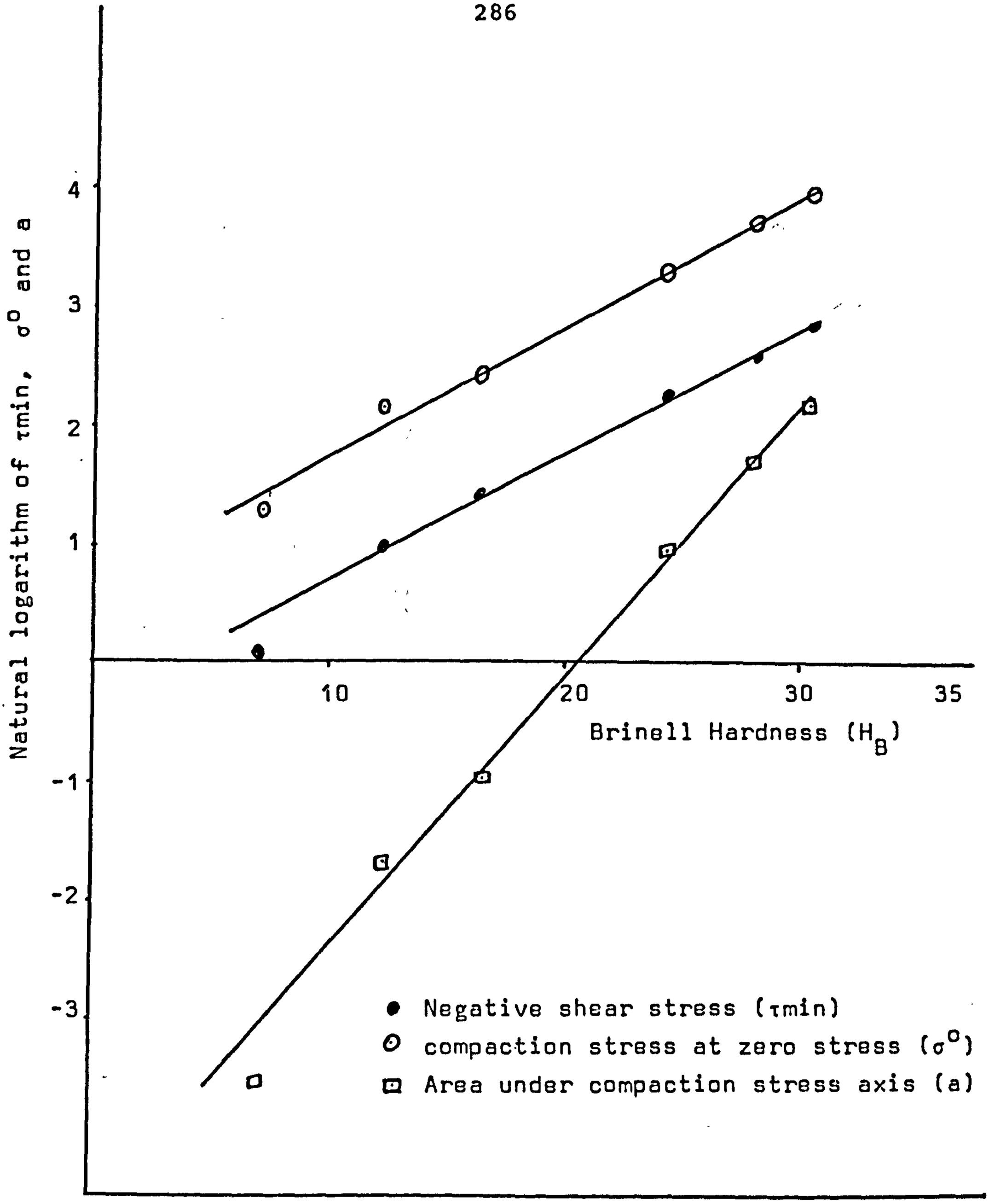

Figure : 7.13c Relationship between shear-compaction stress parameters and the Brinell Hardness number of D—sodium chloride compacts.

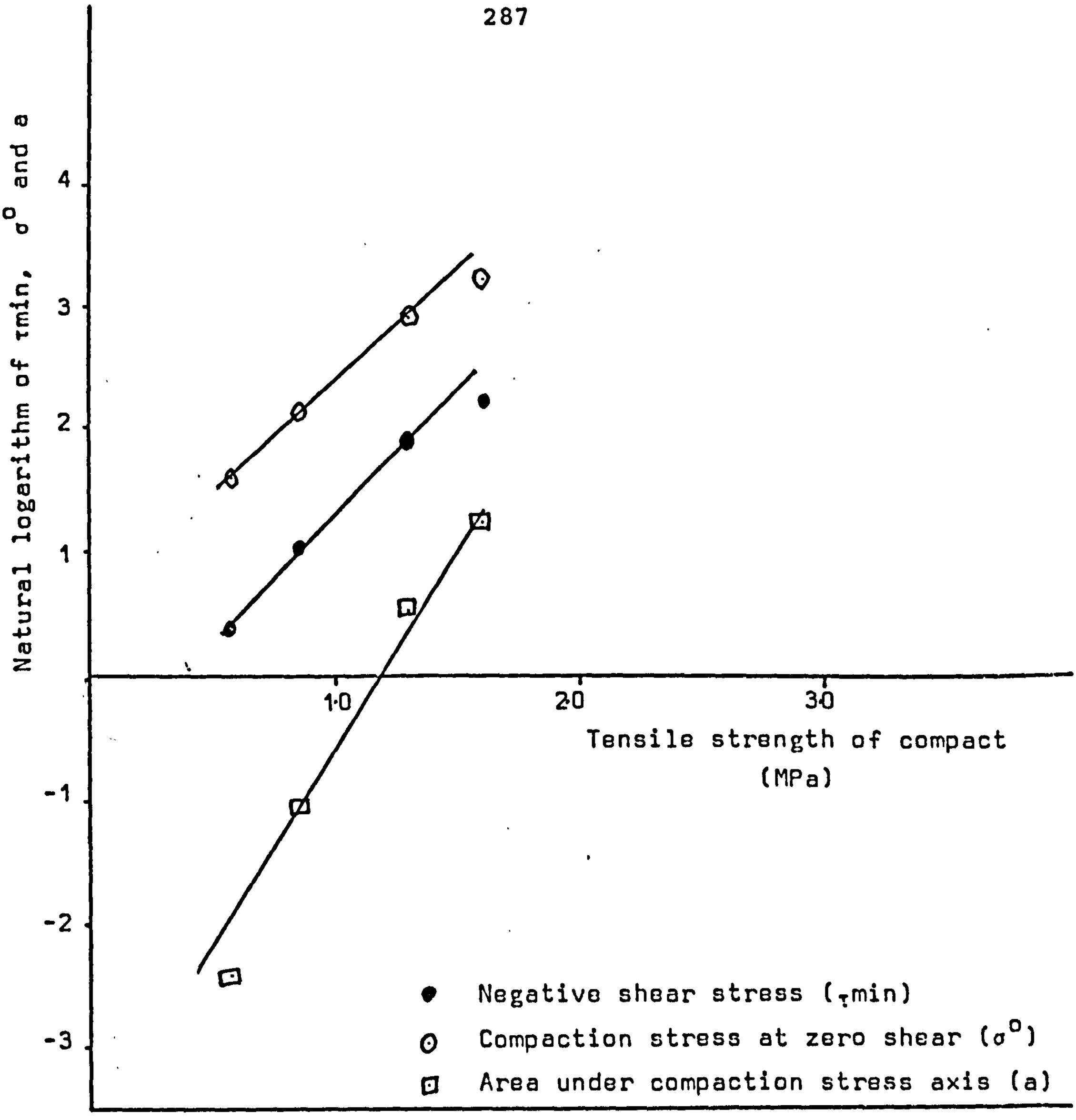

Figure : 7.14a Relationship between shear-compaction stress parameters and the tensile strength of C-sodium chloride compacts.

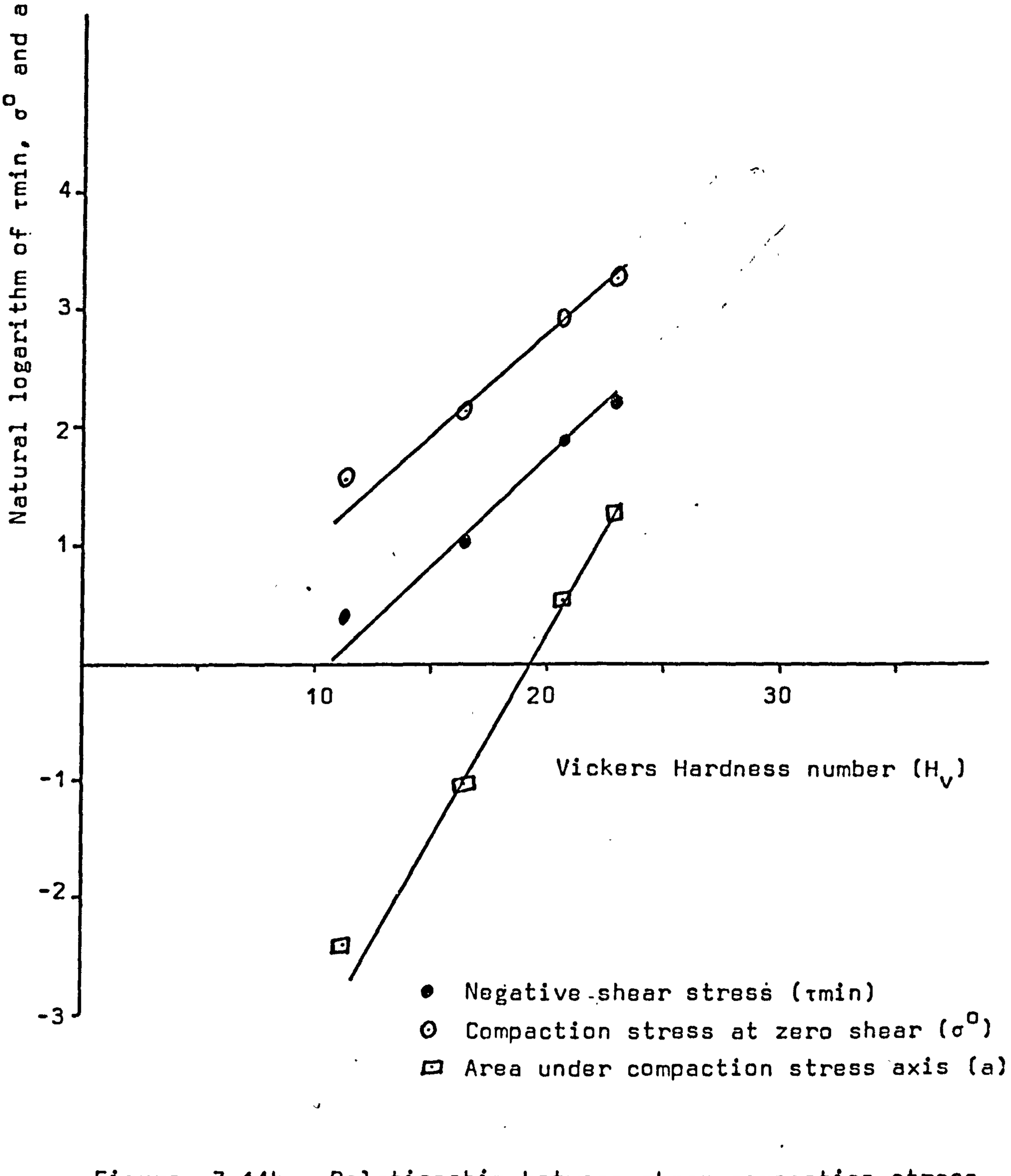

Figure: 7.14b Relationship between shear-compaction stress parameters and the Vickers hardness number of C-sodium chloride compacts.

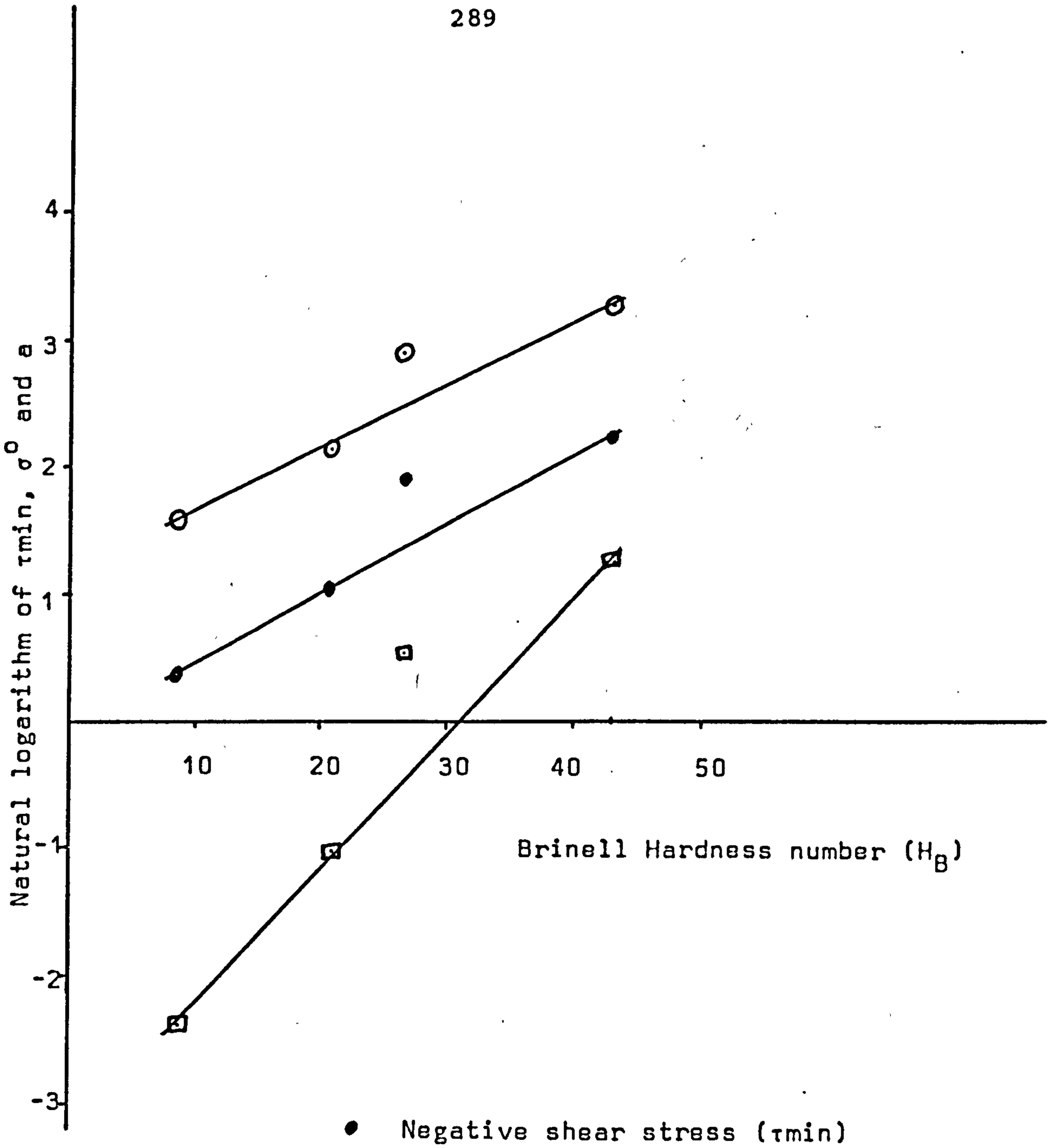

Figure: 7.14c Relationship between shear-compaction stress parameters and the Brinell hardness number of C-sodium chloride compacts.

7.2 Fragmenting Materials

7.2.1 Dicalcium phosphate

7.2.1.1 Surface area

Dicalcium phosphate is known to be a brittle powder, which fragments during compaction (de Boer et al 1978). The change in surface area with increasing compaction pressure may be affected by particle-particle bonding and the fracture of powder particles. As the two phenomena have contradicting effects on the surface area of the compacted material, the overall surface area will depend upon the predominance of one or other of these two phenomena.

The initial specific surface area of dicalcium phosphate (fig. 6.92) does not correspond to the curves of Hardman and Lilley (1973) which represent materials undergoing brittle fracture, such as coal and sucrose. It is apparent that both mechanisms of particle-particle bonding and fragmentation occur in the overall densification of dicalcium phosphate. The initial drop in surface area from the uncompacted powder to the compacts produced at 15 and 32 MPa is possibly due to bond formation between particles or simply because of closer packing, which decreases the accessible surface to the adsorbate molecules. At higher compaction pressures, above 32 MPa, the specific surface area increased with increase in compaction pressure. This increase in specific

surface area indicates that fragmentation of particles to produce new surfaces is predominant in this range of compaction pressures (32-155 MPa) and may also be responsible for the opening of previously blinded or closed intraparticle pores.

A slight decrease of specific surface area was found at a compaction pressure of 248 MPa. If particle fragmentation is the major mechanism of compaction, fracture can continue until a specific particle size is reached which will not undergo further fragmentation by compression. Increase in pressure on this specific limiting particle size will only cause particle deformation (Kedall 1978).

While the particles can undergo fragmentation, increase in compaction pressure will produce a wide range of particle size some of which could be small enough to pack between the interparticle spaces within the compact. The final surface area reduction can also be attributed to an increase of contact area between the particles caused by an increase in compaction pressure on particle size of a limiting value. The behaviour of dicalcium phosphate compacted above 32 MPa is similar to that reported by Hardman and Lilley (1973). They found that the surface area of sucrose increased with increase of compaction pressure and then decreased at a compaction pressure of approximately 170 MPa. The increase of the surface area was attributed to fragmentation of the powder particles, while the decrease of surface area above 170MPa was explained by the plastic flow.

Higuchi, Elowe and Busse (1954) also observed an initial increase in the surface area of sulphadiazine powder with increase in compaction pressure which reached a maximum at about 20 MPa, followed by a continuous decrease. Armstrong and Haines-Nutt (1970-1972) also observed- when compacting magnesium carbonate particles- that the surface area increased to a maximum then decreased with increase in compaction pressure. It was suggested that at low compaction pressures, a fracturing mechanism predominated and new surfaces were formed by fragmentation. A cold welding mechanism came into effect at higher compaction pressures resulting in decrease of surface area. Disintegration of compacts and particle size analysis of the resultant suspension showed an initial decrease of particle size followed by the increase in the number of larger particles at higher compaction pressures. This was consistent with the change of compact surface area but disintegration of the compact into the analysed particle size distribution is not necessarily the particle size distribution within the original compacted material. A further increase in surface area was also observed when magnesium carbonate and phenacetin were compacted above 250 MPa. This surface area increase was attributed to the elastic recovery which possibly caused microcracks within the compacts during ejection from the die.

7.2.1.2 Porosity

The analysis of the nitrogen adsorption isotherm and the Va-t curve of dicalcium phosphate powder

(appendix 3 TableA21 , Fig A 18) indicates that the powder is non-microporous. For non-micro and mesoporous solids, a graph of the amount of gas adsorbed (Va) against the film thickness (t) yields a straight line (Allen 1981).

Mercury intrusion porosimetry analysis of the dicalcium phosphate compacts gave pore space size distributions (Fig. 6.94) which showed consecutive elimination of larger pore space sizes as the compaction pressure increased. The mean pore space radius decreased from an approximate value of 0.45 μm at the compaction pressure of 32 MPa to 0.15 μm at a compaction pressure of 248 MPa. A similar decrease of total pore/void space volume, in the range of the compaction pressures investigated was also observed (Fig.7.1), which varied from 0.314 cm^3/g. to 0.11 cm^3/g. Since the decrease in the volume of compact with increase in compaction pressure is associated with an increase in specific surface area (section 7.2.1.1), it can be argued that the particle fracture of dicalcium phosphate discussed in the previous section may cause fragmented dicalcium phosphate to move into interparticle spaces within the particle assembly and thus reduce the total void volume. The surface area increase derived from the monolayer volume, indicated that dicalcium phosphate has fragmented to produce smaller particles of the original non-porous material, since production of smaller particles is the only way that surface area can increase with non-porous material. If the non-porous material had not undergone fragmentation, the surface area would be expected to decrease due to the increase in particle-particle contact. Generation of new surface in compaction with only

a limited decrease in compact pore/void volume, compared with the large decrease in compact pore/void volume seen with dentritic sodium chloride, suggest that the fragmented particles have moved into the interparticle space in the dicalcium phoshpate compacts. The filling of interparticle space by fragmented particles may produce microvoids.

The BET equation for surface area determination is valid up to a relative pressure, x, of 0.30-0.35. The size of a void or pore into which nitrogen can condense can be estimated from the Kelvin equation written by Gregg and Sing (1967) in the form:

$$r_K = - \frac{4.10 \times 10^{-10}}{\log x} \quad m \qquad (7.6)$$

At relative pressures of 0.30-0.35 the micro-void size would then be of the order of 0.8×10^{-3} μm which is smaller than the pore size (0.45-0.15 μm) determined by mercury porosimetry at compaction pressures between 32-248 MPa.

7.2.1.3 Mohr's circles

The Mohr circles constructed when dicalcium phosphate particles were compacted at 32,62,120, 150 and 248 MPa (Figs.6-36-6.41) indicated that the powder yield locus can be approximated by a straight line. The linearity of the powder yield locus suggest that the Mohr-Coulomb equation is applicable for this type of material. It is not possible to construct a straight line through the origin to approximate the yield locus at low compaction pressures as shown by Fukμmori and Okada (1977).

7.2.1.4 Compaction stress paths

The stress paths constructed in the shear compaction stress (Fig 6.42-6.51) at different compaction pressures were found to be of similar shape to the yield loci constructed from the Mohr's circles (Fig.6.35-6.41). The stress paths of dicalcium phosphate compacted at 36, 53,77, and 120 MPa(Fig.7.15) follow a common compaction curve as expected. The relationship between shear and mean compaction stresses can be expressed by equation 7.7 (appendix 4)

$$\tau = 0.614\sigma + 0.4738 \qquad (7.7)$$

Equation 7.7 obtained from fragmentary dicalcium phosphate is similar to the Mohr-Coulomb equation (eqn.1.11). The linear yield loci cannot however be correlated with the variation of surface area observed with increase in

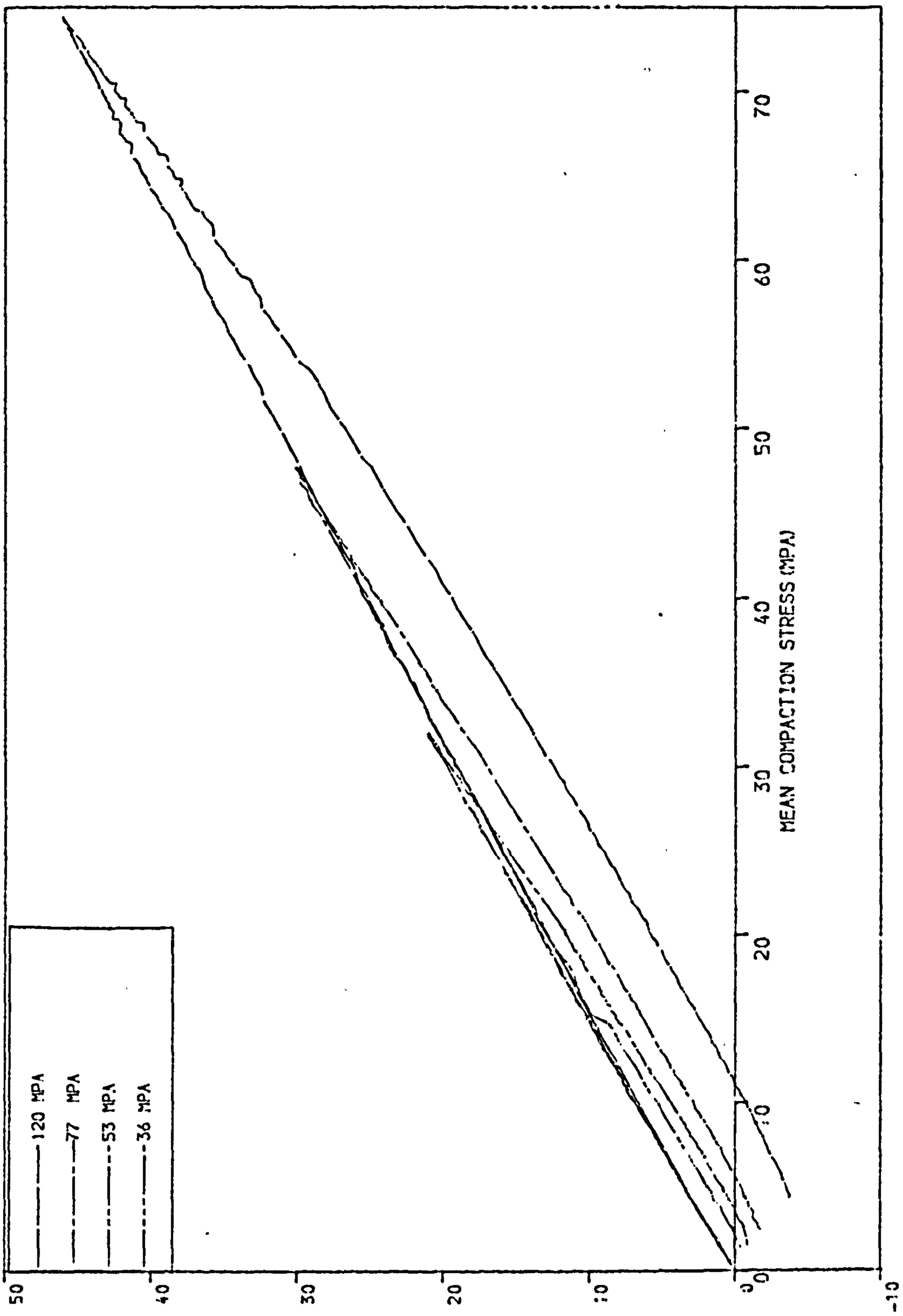

FIGURE 7.15 DICALCIUM PHOSPHATE
COMPACTED UNIAXIALLY AT DIFFERENT
COMPACTION PRESSURES

compaction pressure.

7.2.1.5 Unloading

The unloading curves of the stress pathways cross the mean compaction stress axis σ_o to give negative values of shear stress and reach a minimum value τ_{min}. The magnitude of τ_{min} and σ_o were dependent on the maximum applied pressure. The τ_{min} values of compacts at different compaction pressures were found to terminate on a straight line in the negative shear compaction stress space similar to that seen with sodium chloride.

7.2.1.6 Volumetric strain

The volume reduction curves of dicalcium phosphate plotted in V- ln. mean compaction stress space (Fig.7.16) do not show any sign of discontinuity. The curves are slightly convex to the ln. mean compaction stress axis. Birks and Muzaffar (1971) observed a similar behaviour, when compacting easily broken particles. The relationship between volume of compact and ln. mean compaction stress form a family of curves which is only dependent upon the initial volume of die fill. This is unlike the relationship found with sodium chloride which showed this type of dependancy only in the initial stages of compaction and followed a common compaction curve at higher compaction pressures.

7.2.1.7 Mechanical strength

(a) Tensile Strength

The tensile strength of dicalcium phosphate, measured by diametral fracture, showed a linear increase with increasing compaction pressure over the range, 32-155 MPa

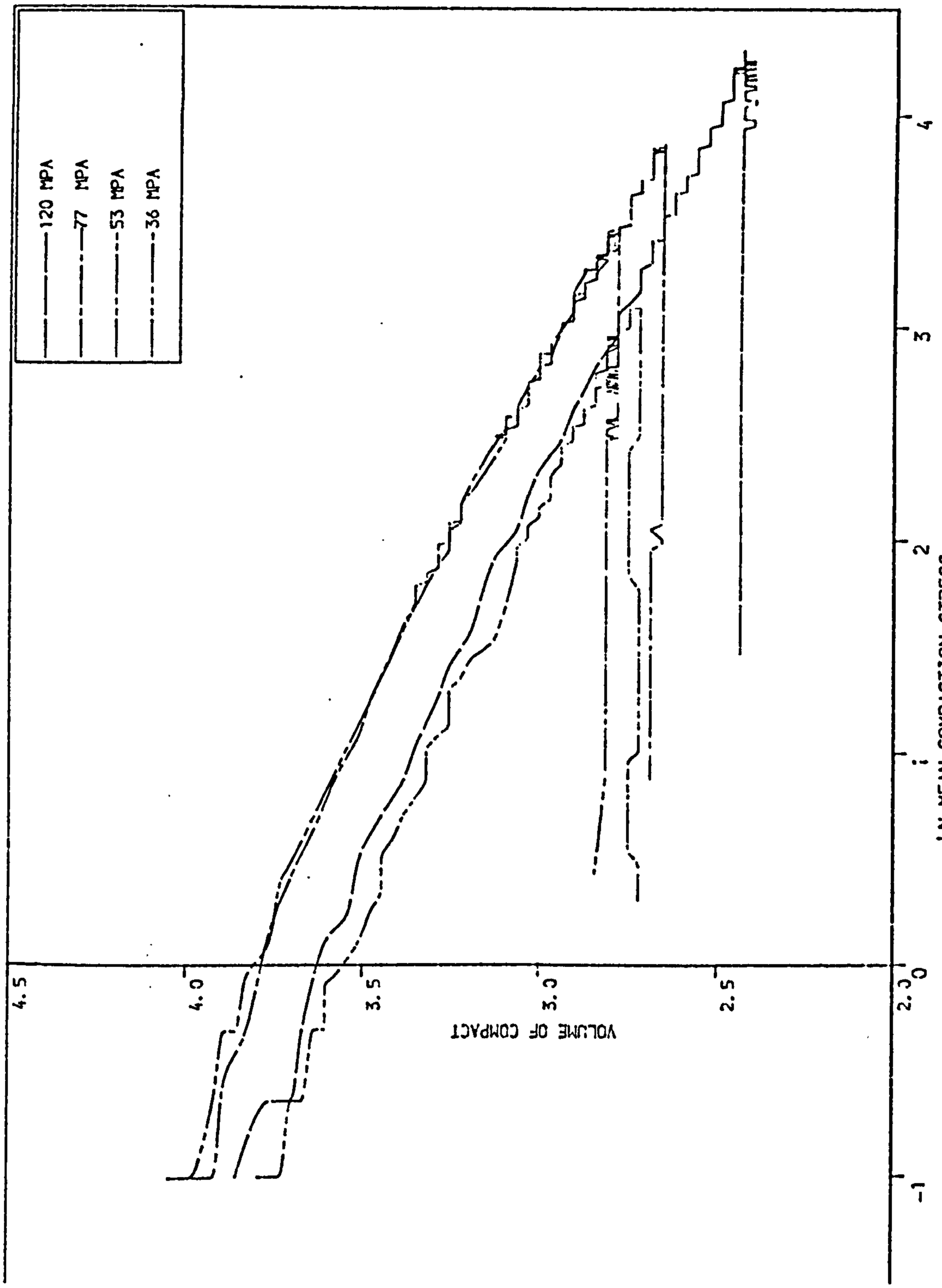

FIGURE 7.16 DICALCIUM PHOSPHATE
COMPACTED UNIAXIALLY AT DIFFERENT
COMPACTION PRESSURES

(fig.6.100).A significant increase in the strength of compacts, from an approximate value of 1.5 MPa for compacts produced at 155 MPa to a value of about 3 MPa for the compacts produced at a compaction pressure of 248 MPa was observed. This sharp increase was consistant with the decrease found in the surface area of compacts at the same compaction pressure. It is likely that this sharp increase in the tensile strength of the compacts is due to extensive increase in the particle-particle contact area by plastic flow of the material as already discussed.

(b) Hardness

Vickers hardness number and Brinell hardness number were found to increase with increasing compaction pressure (fig.6.101). Although some scatter in the data was observed, the shape of the Brinell hardness curve was similar to that of the tensile strength.

The relationships between the natural logarithm of the shear compaction stress parameters τ_{min} σ_o and a and the tensile strength and hardness of fragmentary dicalcium phosphate compacts were curved (Figs 7.17a, b and c), unlike the linear relationship found with plastic sodium chloride.

7.2.2 Sugar

7.2.2.1 Mohr's circles

The Mohr circles constructed for sugar, compacted at 31, 63 , 92 and 250 MPa, are presented in Figures 6.56-6.59. The yield locus of the material was found to be different from those obtained from the Mohr circles of

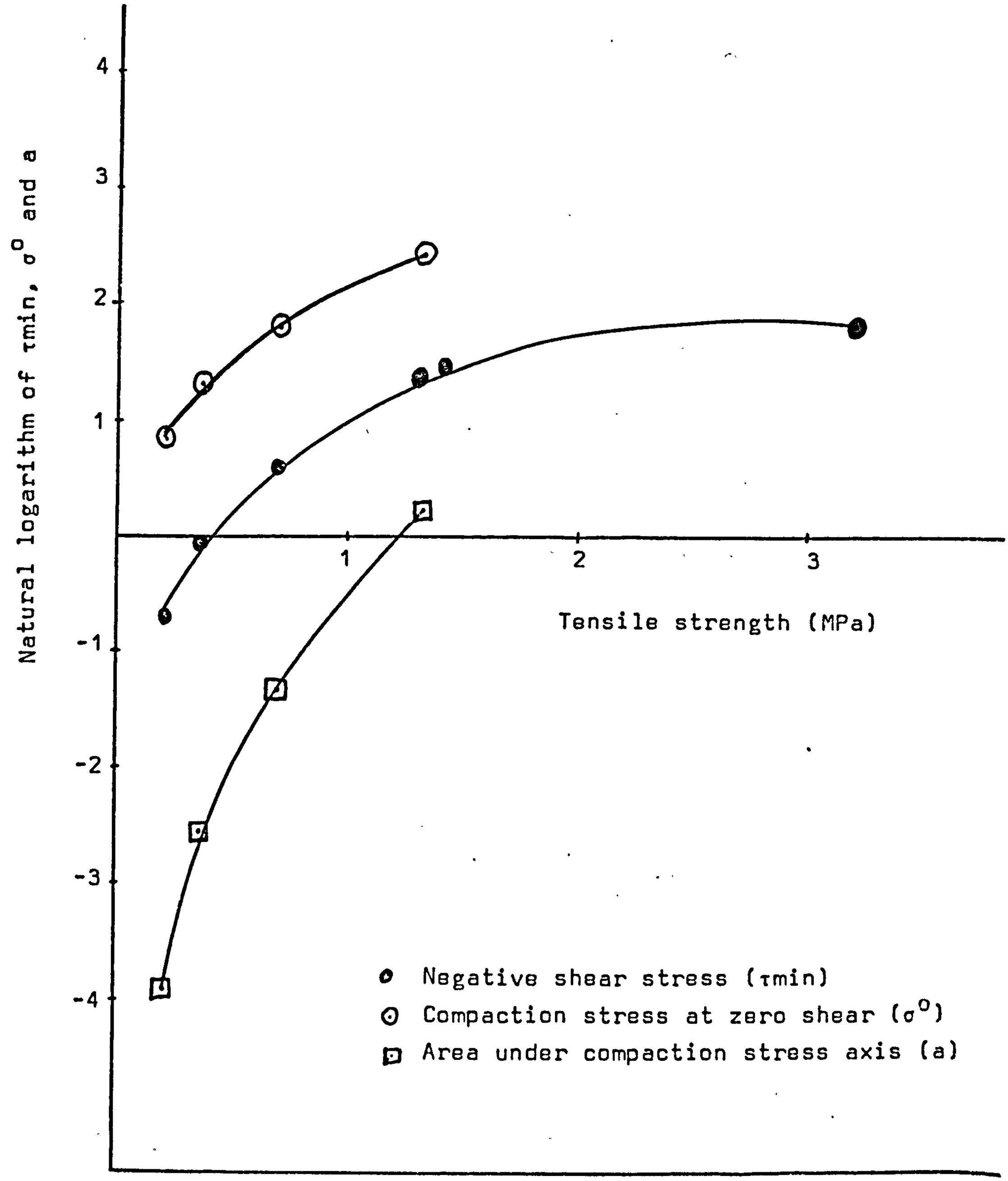

Figure: 7.17a Relationship between shear-compaction stress parameters and the tensile strength of dicalcium phosphate compacts.

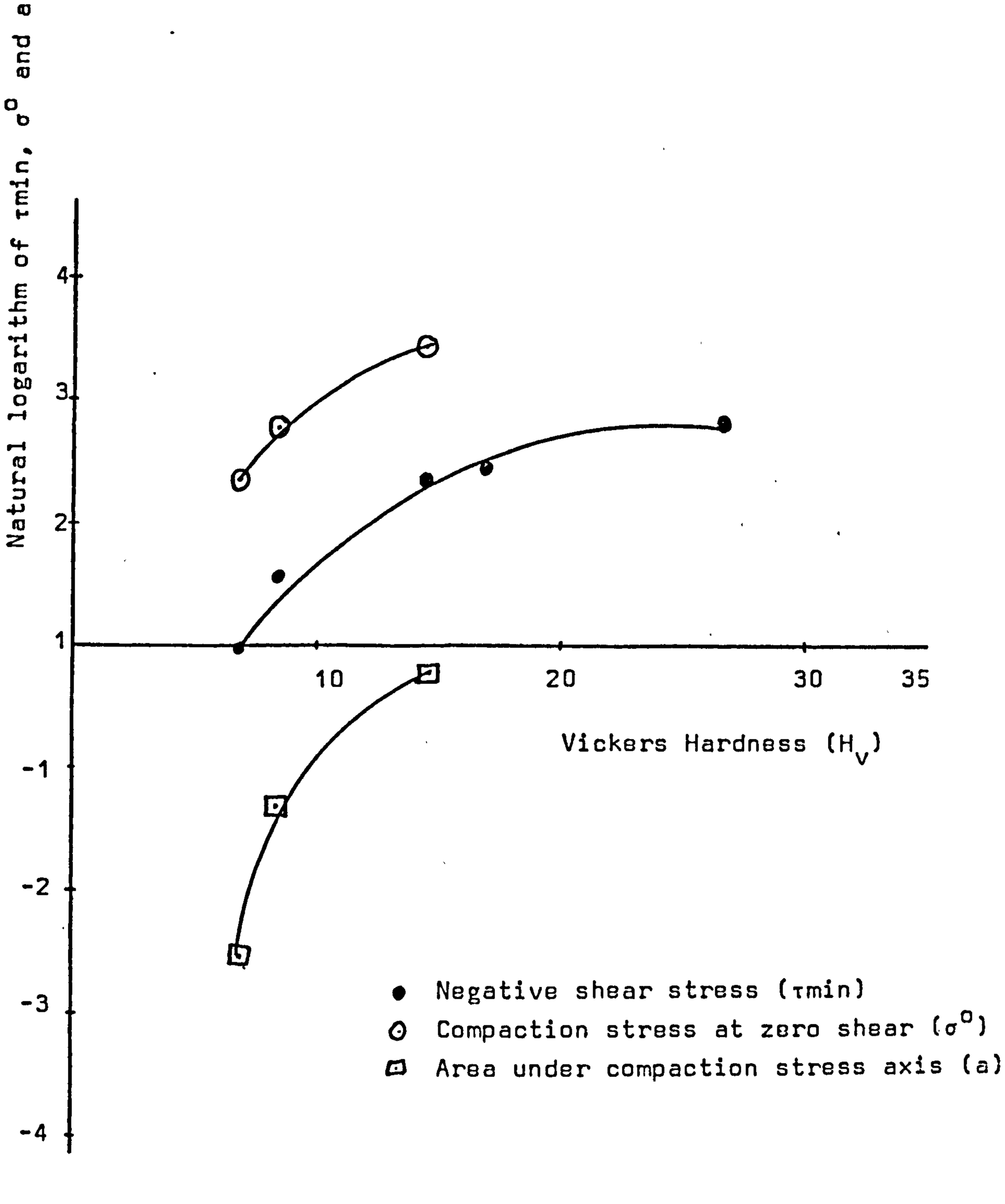

Figure : 7.17b Relationship between shear-compaction stress parameters and Vickers hardness of dicalcium phosphate compacts.

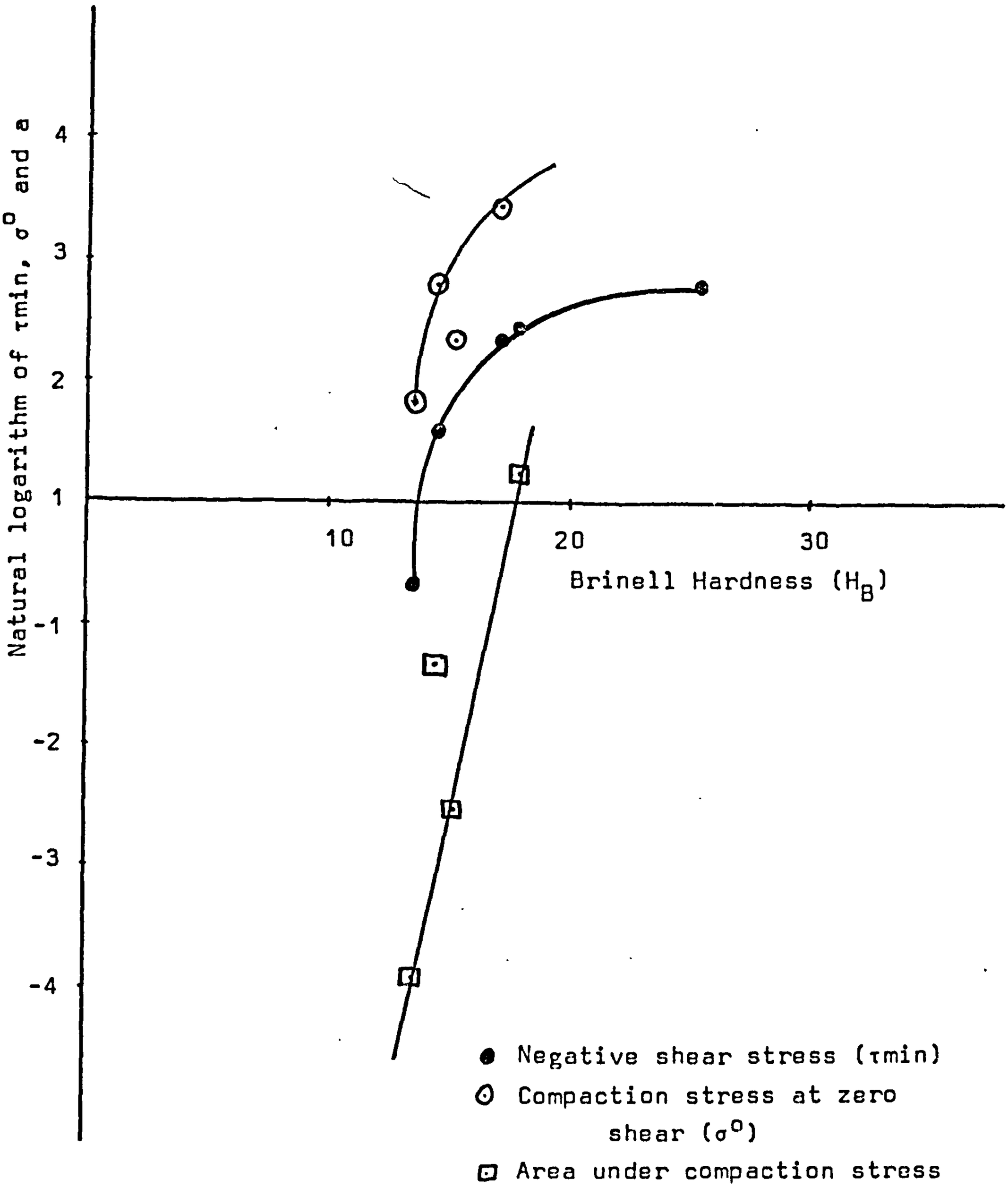

Figure: 7.17c Relationship between shear-compaction stress parameters and Brinell hardness of dicalcium phosphate compacts.

dicalcium phosphate. The yield locus of the material compacted at 250 MPa(fig 6.59) seems to have a sigmoidal shape. The slope of the line is nearly constant at low compaction pressures and begins to increase to a maximum before it decreases again. The yield locus can not be defined by straight lines as in the work of Fukumori, and the Coulomb yield equation is not applicable for the compaction of sugar.

7.2.2.2 Stress paths

The stress paths plotted in shear-mean compaction stress planes are shown in figures 6.60-6.67. The compressive curves of the different compacts are of similar pattern of the yield loci constructed from the Mohr circles of the compacts. The compressive curve of the compacts compacted uniaxially at 63 MPa(fig.6.60A) can be approximated to a straight line, while the curves of higher compaction pressures are convex to the mean compaction stress axis after an initial linear relationship.

Figure 7.18 represents the stress paths of sugar compacts, compacted at different compaction pressures - 31,63,91,155 and 250 MPa. The compressive curves follow the same path as expected. The relationship between shear and mean compaction stress of sugar compacts can be expressed by the following equation:

$$\tau = 0.7287\sigma - 0.00069591\sigma^2 - 0.9564 \qquad (7.8)$$

7.2.2.3 Unloading

The unloading curves of the stress paths cross the mean compaction stress axis to give negative values of shear. This behaviour was also observed with sodium

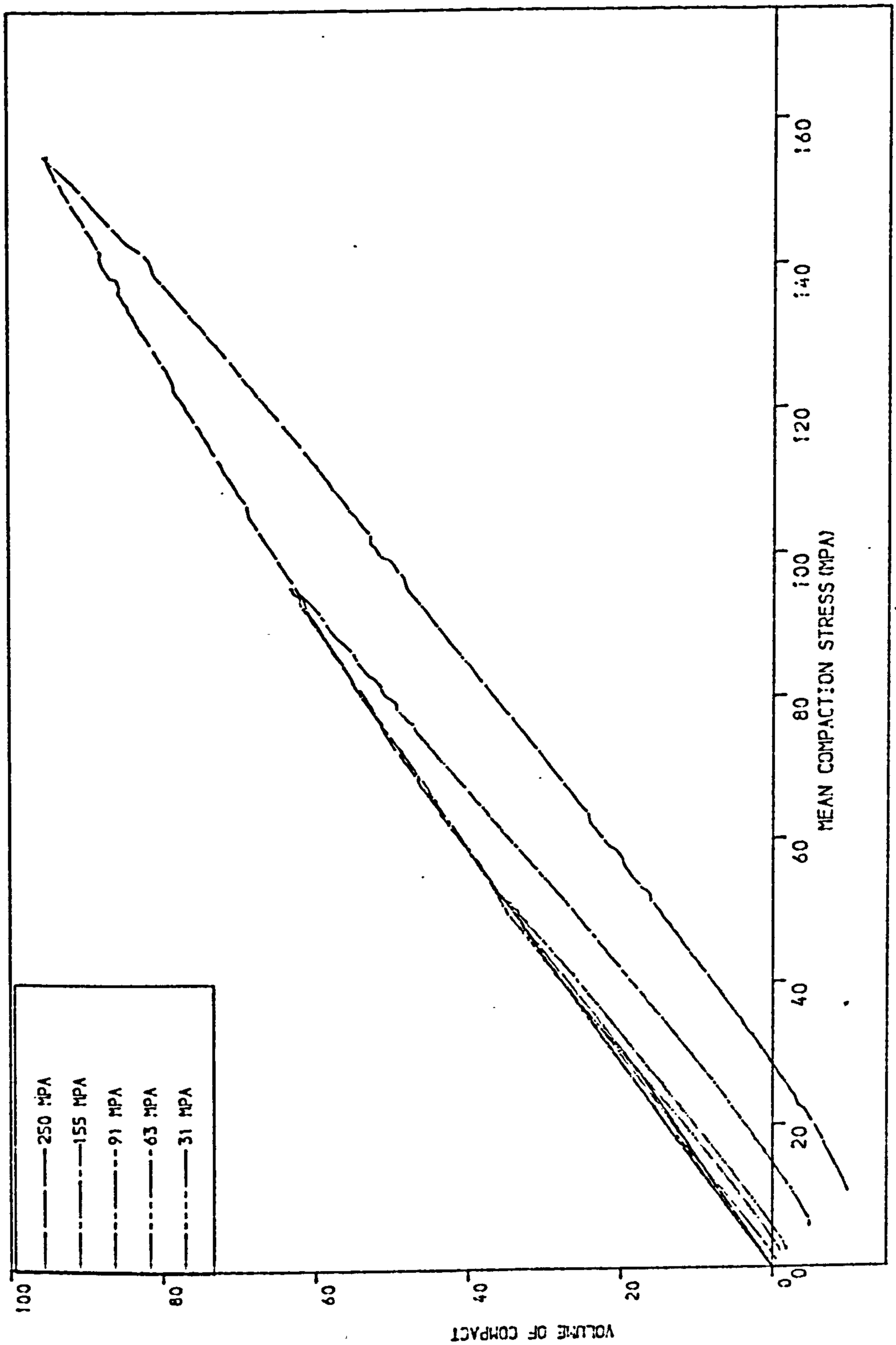

FIGURE 7.18 SUGAR GRANULES COMPACTED UNIAXIALLY AT DIFFERENT COMPACTION PRESSURES

chloride and dicalcium phosphate. The end points of the unloading curves terminate on a straight line.

7.2.2.4 Volume reduction curves

The volume reduction curves of sugar compacts plotted in the volume- mean compaction stress plane (fig.7.19) indicate that there is a progressive reduction of the volume with increase in pressure. The rate of volume decrease is very high at low pressures. Fig.7.20 is the volume reduction of sugar compacts replotted in the volume-ln. mean compaction stress plane. The discontinuity observed in these curves suggest the contribution of more than one mechanism in the densification process of this material. The existance of the straight line relationship at the very beginning of the compaction process to an approximate value of zero ln. mean compaction pressure can be explained by the re-arrangement of sugar particles. The existance of the bridging mechanism can not be ruled out because of the slight decrease observed in the rate of the volume reduction. It is obvious that as the pressure increases more and more point contacts between the particles will be achieved. This increase in number of contacts will lead to a decrease in the force acting per unit area leading to a decrease in the rate of the volume reduction. When the increase in pressure exceeds a critical value the above structure will collapse and plastic deformation and/or brittle fracture of the material will begin. As sugar is known to be a fragmenting material, the remaining behaviour of the curve can be attributed to fragmentation and densification by the filling of the voids by the finer particles. The steep decrease in the volume

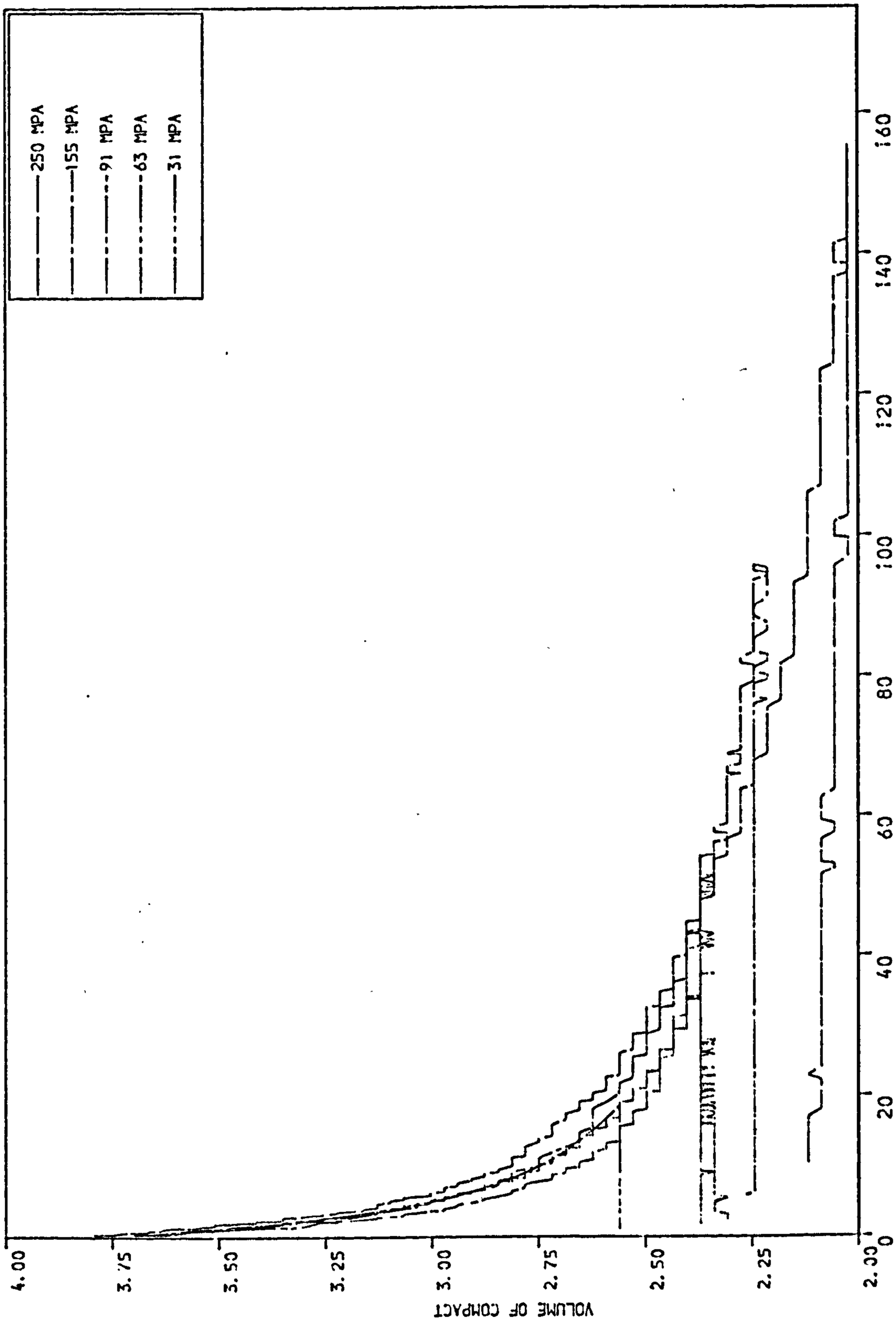

FIGURE 7.19 SUGAR GRANULES COMPACTED UNIAXIALLY AT DIFFERENT COMPACTION PRESSURES

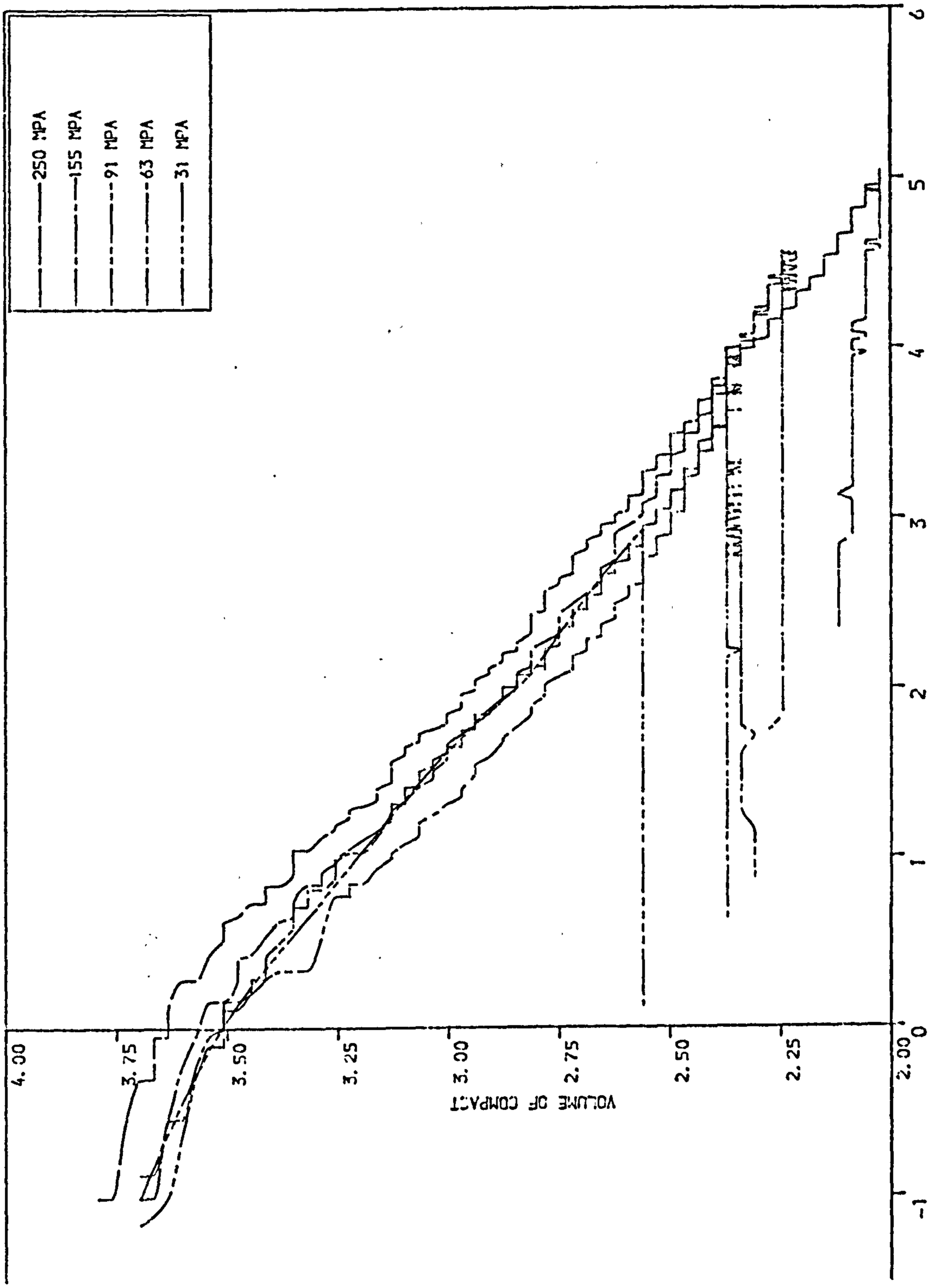

FIGURE 7.20SUGAR GRANULES
COMPACTED UNIAXIALLY AT DI
COMPACTION PRESSURES

reduction curve between ln. mean compaction values of 0.5 and 3 is most probably due to extensive fragmentation of large particles. It is also possible that plastic deformation or rebonding of the fragments contributes to the densification process at higher compaction pressures. As the particles become smaller and smaller the fragmentation process will become more difficult and thus this stage of compaction will be dominated by the bonding mechanism. The observed decrease in the rate of the volume reduction at high compaction pressure supports the above argument.

7.2.2.5 The effect of particle size on the compaction of sugar

Figure 7.21 and 7.22 represent the stress paths of three different particle sizes of sugar compacted to an axial pressure of 155 MPa. The stress paths plotted in shear - mean compaction stress space are similar. The volume reduction curves, however, show the difference in the densification process of the different sizes. The curves constructed from 300-355 μm and 425-500 μm show only a slight difference specially in the initial part of the compaction which is due to particle-particle re-arrangement. The volume reduction curve of 710-850 µm sieve fraction is obviously different, since the curve starts high-with higher initial die fill- and quickly drops below the curves of smaller sizes showing better densification. This behaviour can be explained by the fact that the fragmentation of the larger particles is greater than small particles, and that 710-850 µm particles fragmented even in the initial stages of compaction.

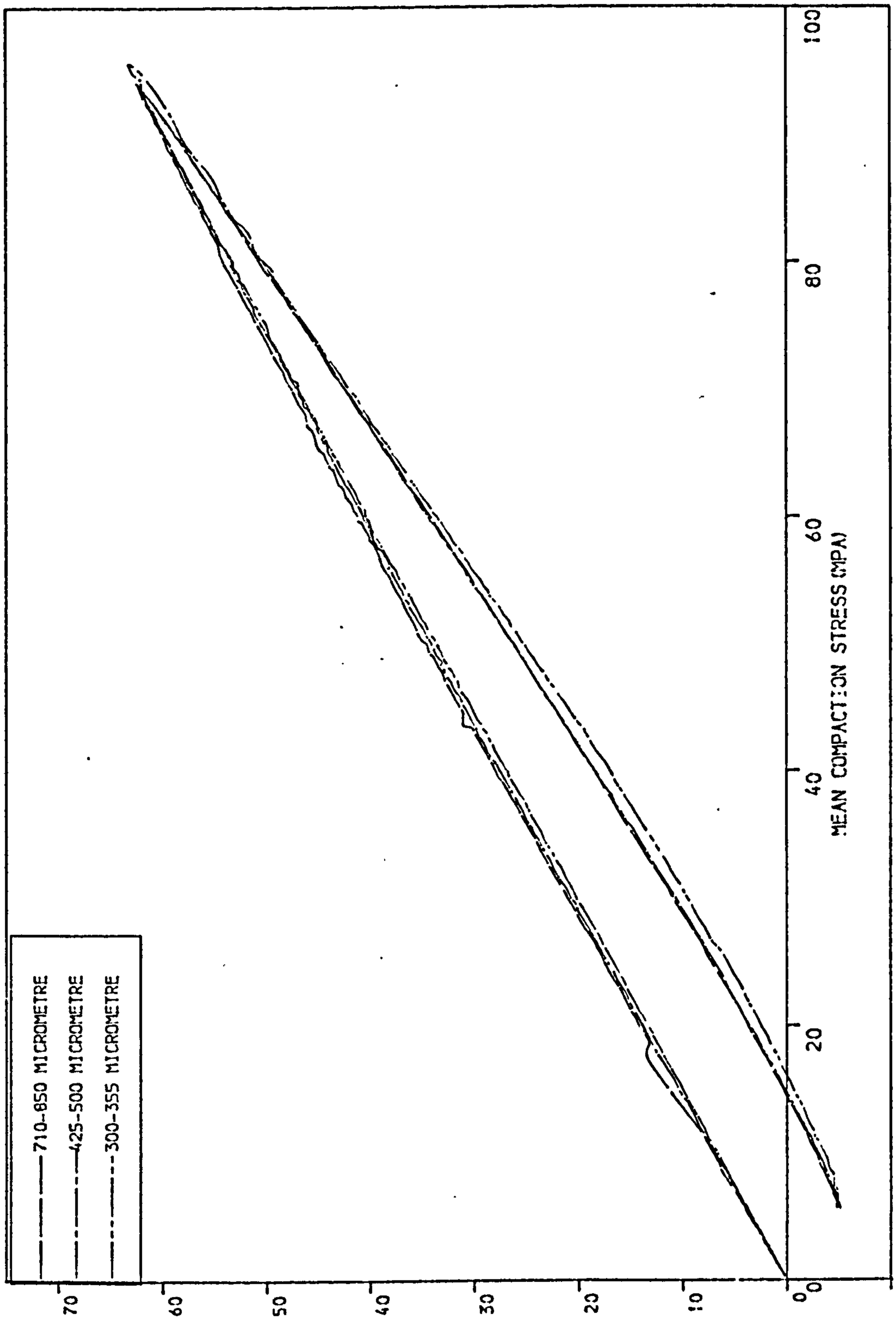

FIGURE 7.21:THE EFFECT OF PARTICLE SIZE ON THE COMPACTION OF SUGAR GRANULES

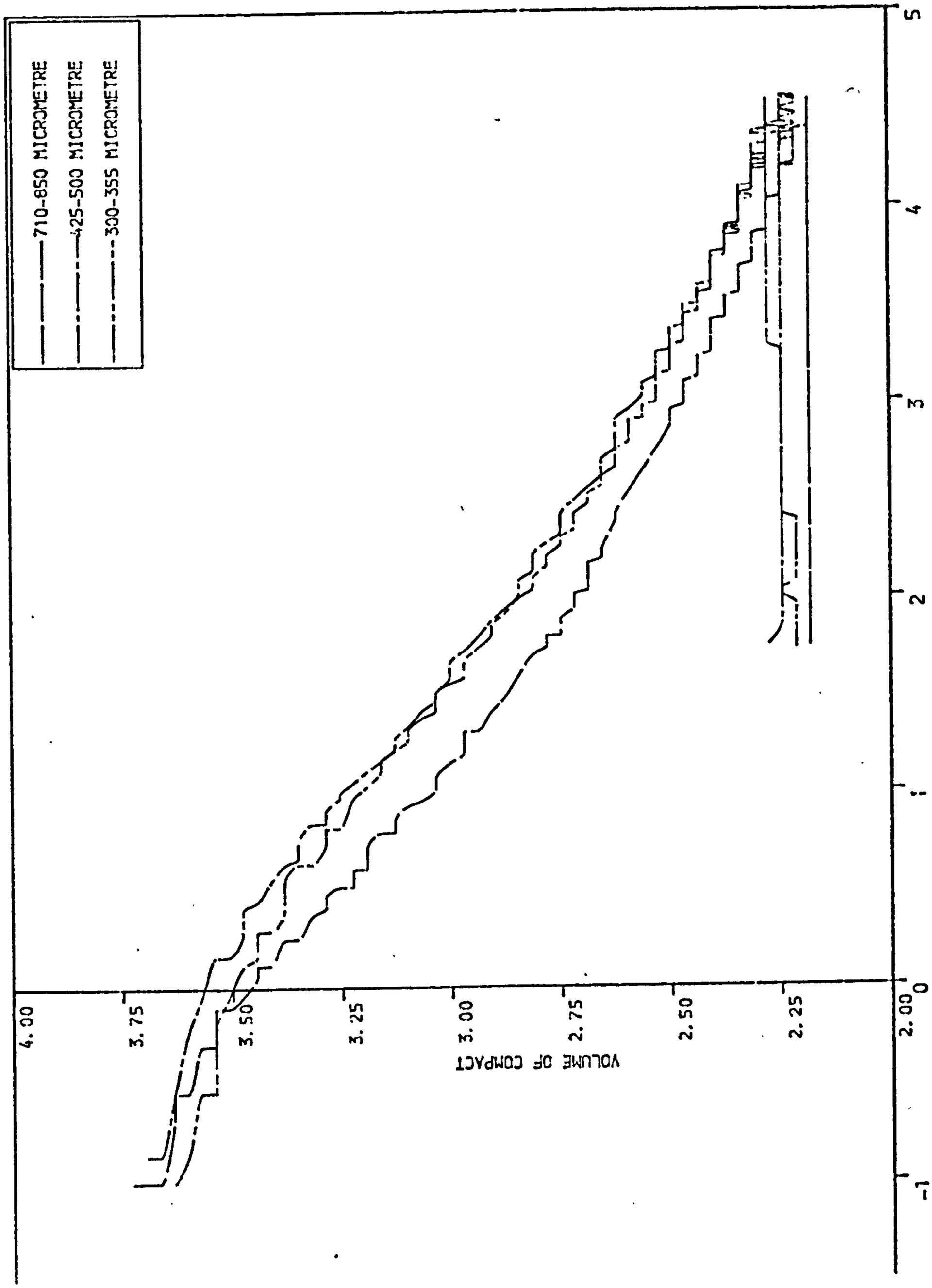

FIGURE 7.22 THE EFFECT OF PARTICLE SIZE ON THE COMPACTION OF SUGAR GRANULES

7.2.2.6 Mechanical strength of sugar compacts

The tensile strength of sugar compacts (fig.6.102) showed a continuous non-linear increase up to a maximum compaction pressure of 155 MPa. The sigmoidal shape of the curve suggest a change in the mechanism of the densification process. The tensile strength at low compaction pressure may be due to fragmentation followed at higher compaction pressures by the movement of particle fragments into the void spaces ultimately resulting in a more efficient packing of the particles. An increase in the compact strength was observed in the compaction range of 60-90 MPa. The only explanation for such behaviour is the corresponding increase in the contact area between the particles. These observations agree well with the explanations suggested for the volume reduction curve of fig.7.22.

The variation in the mechanism of densification of sugar compacts was shown in the relationship between the tensile strength and Brinell hardness number and the natural logarithm of the evaluated parameters τ_{min}, σ_o and a. Figures 7.23a and 7.23c show a similar pattern of curves between the three parameters and the tensile strength and Brinell number respectively. The first parts of the curves are similar in shape to the relationships found with the fragmenting material dicalcium phosphate. The second parts of the relationships suggest that the material is behaving like the plastically deforming materials- sodium chloride which shows a linear relationship (Stanley-Wood

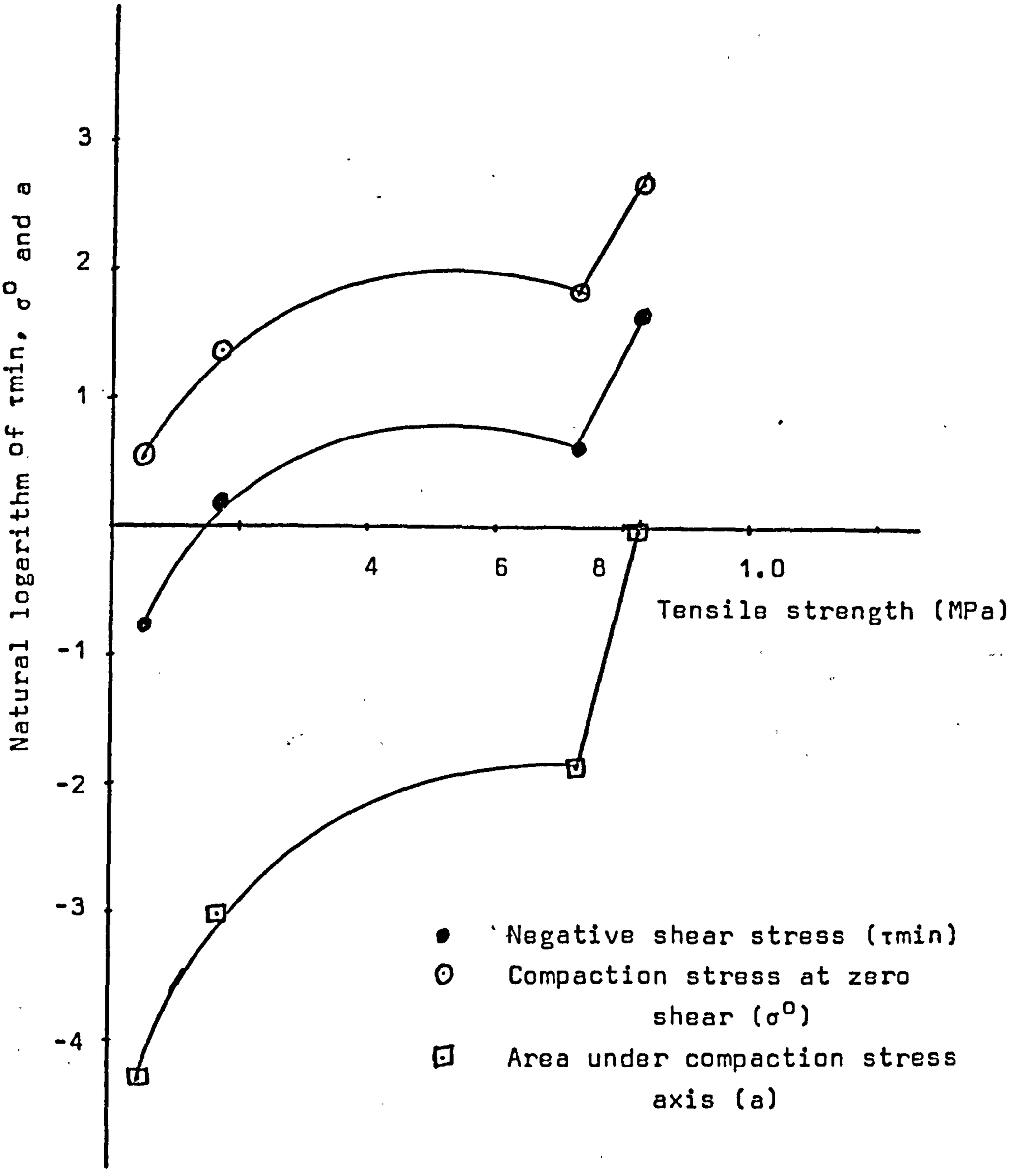

Figure:7.23a Relationship between shear-compaction stress parameters and the tensile strength of sugar compacts.

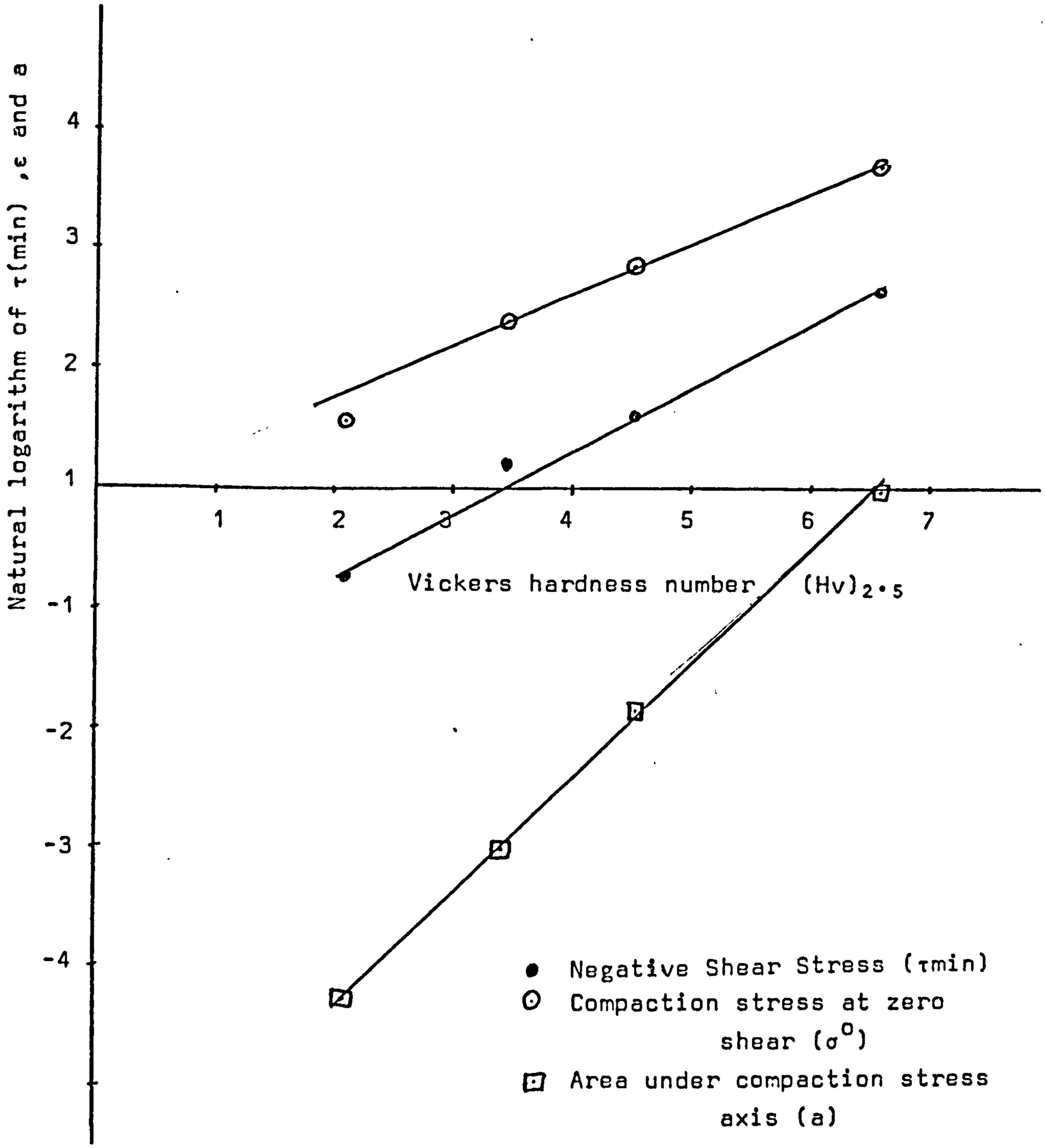

Figure : 7.23b Relationship between shear-compaction stress parameters and Vickers hardness of sugar compacts.

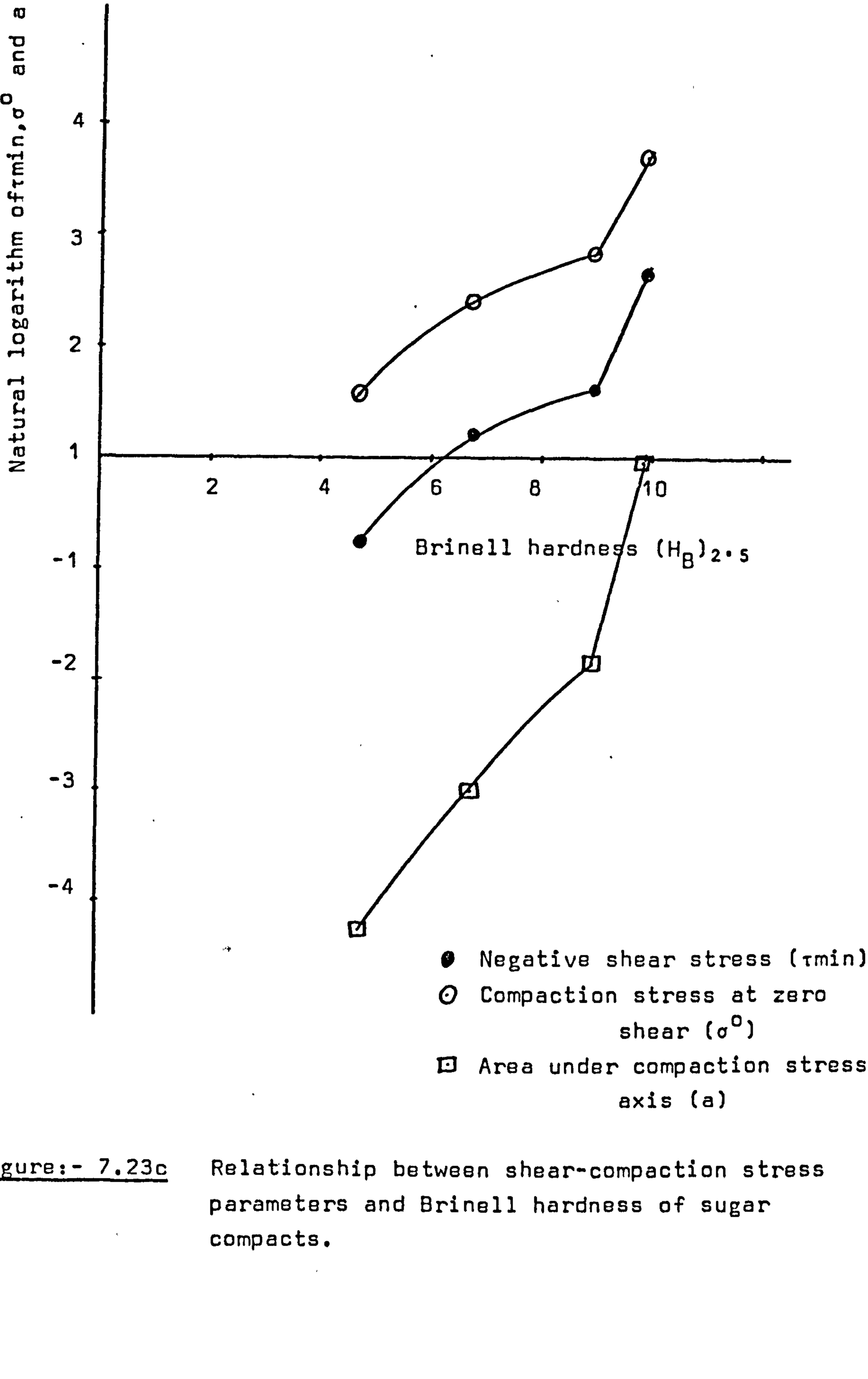

Figure:- 7.23c Relationship between shear-compaction stress parameters and Brinell hardness of sugar compacts.

and Abdelkarim 1982). This observation is again in agreement with the behaviour of the yield loci , volume reduction curves and the tensile strength of the compacts. Some doubts were, however, placed upon the relationship between the Vickers hardness and the three parameters (fig 7.23b) which show a linear relationship. This may be due to the shape of the indenter.

7.3 Non-compactable materials

7.3.1 Styrocell

7.3.1.1 Mohr circles

Mohr circles constructed for styrocell, compacted at different compaction pressure- (65,153,247, and 340 MPa), are shown in figures 6.73-6.75. The powder yield locus is similar in shape to that obtained from sodium chloride compacts which produce strong compacts when ejected from the die. Beddow (1968) studied pressure transfer characteristics of different shapes of copper powders and concluded that spherical powders transmit compaction pressures more effectively than non-spherical powders. Ridgway, Glasby and Rosser (1969) investigated the effect of crystal hardness on radial pressure at the wall of a tableting die and concluded that the pressure on the die wall increases as the hardness value of the compacted material decreases. It can be argued that, although the pressure transmission method can be useful in studying the stress history of a material during the compaction process, it can not predict the degree of bonding or the strength of the final product.

7.3.1.2 Compaction stress pathways

Typical cyclic relationships of the stress paths of styrocell compacts are presented in figures 6.76-6.81 The shear stress $(\sigma_A-\sigma_R)/2$ and the mean compaction stress $(\sigma_A+\sigma_R)/2$ relationship for the compressive curves- the yield locus- of different compaction pressures (fig.7.24) follow the same stress pathway as expected. The shape of yield locus of styrocell was similar in shape to that produced from plastically deforming materials. The yield locus of styrocell compacted at 247 MPa can be defined by:

$$\tau = 0.52\sigma - 0.00010397\sigma^2 + 0.6235$$

7.3.1.3 Unloading

The unloading curves or the decompression parts of the stress pathways fig (7.24) were however different from the unloading curves of sodium chloride. Parameters τ_{min}, σ_o and a are very small in the case of styrocell compacts (Table 6.10). The magnitude of the values of τ_{min}, σ_o and a also showed little dependancy on the maximum pressure of compaction.

7.3.1.4 Volume reduction

The volume reduction curves of styrocell are presented in fig.7.25. The shape of the curve was similar to that obtained from cubic sodium chloride. The existence of different mechanisms of compaction in the densification of this material is clearly shown by the shape of the volume reduction curve. There is no difference between the volume reduction

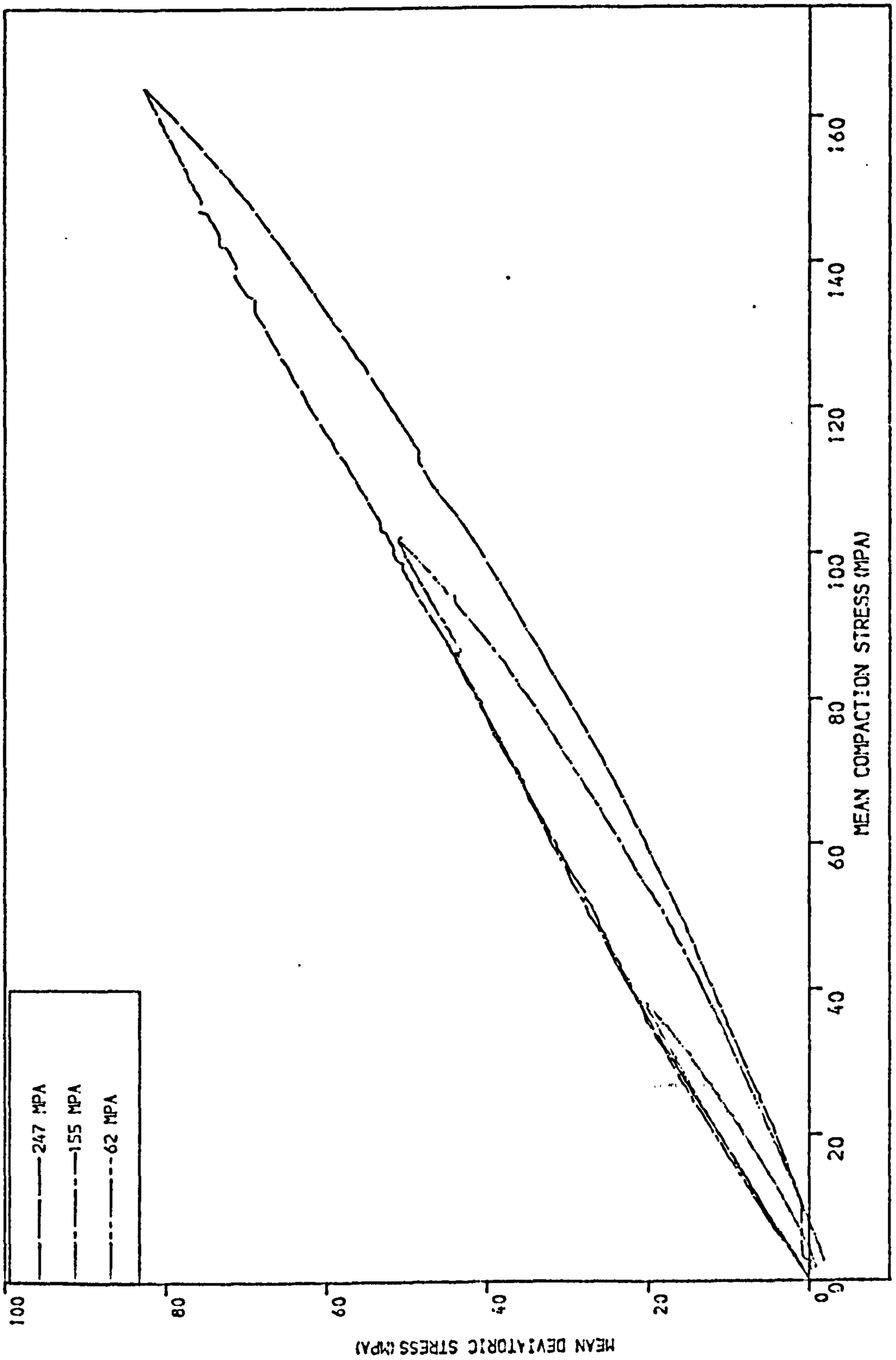

FIGURE 7.24:STYROCELL COMPACTED UNIAXIALLY AT DIFFERENT COMPACTION PRESSURES

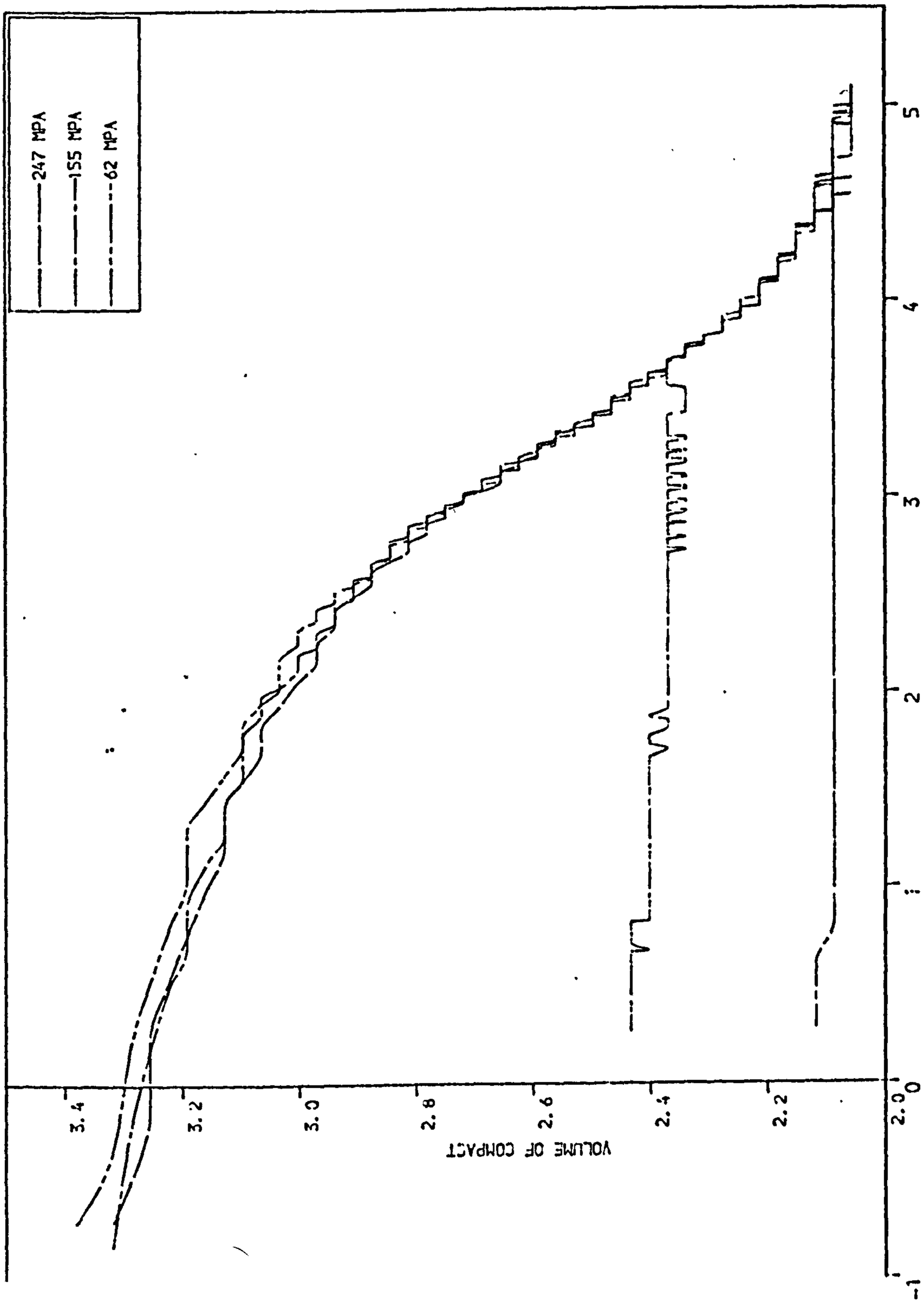

FIGURE 7.25 STYROCELL
COMPACTED UNIAXIALLY AT DIFFERENT
COMPACTION PRESSURES

curves of styrocell and other compactable solids. No reduction in the volume of the compact was achieved by increasing the compaction pressure from 155 to 247 MPa.

Figure 7.25 indicates that particle re-arrangement and deformation plays a major role in the densification of styrocell. The initial shape of styrocell is spherical but deformation of the particles and change in shape (Figure A.5) can be seen as the compaction pressure increases.

At low compaction pressures the mechanism suggested is that of particle re-arrangement and the formation of supporting structures. As compaction pressure increases generally the supporting structure will collapse and the material will undergo elastic and plastic deformation or fragmentation. Microscopic examination of styrocell (App.3. Fig.A.5) suggested that the volume reduction which occurred was due to individual particle-plastic deformation. It is also worth mentioning that a release of a yellow gas has always accompanied the compaction of this material. The densification and volume reduction is therefore possibly due to the deformation of the styrocell spheres which led to the release of gas entrapped inside the hollow spheres of the material.

7.3.2 Homopolymer and copolymer

7.3.2.1 Mohr's circles

The Mohr's circles of both homo and copolymers are presented in figures 6.84 and 6.88 respectively. The yield loci constructed from these Mohr's circles show that the relationship can be approximated by two straight lines. This type of behaviour was observed by Fukumori and Okada

(1977) who compacted potassium chloride and defined the failure properties by two different linear relationships.

7.3.2.2 Stress paths

The stress paths of homo and copolymers are shown in figures 6.85-6.86 and 6.89-6.90 respectively.

The yield loci evaluated from $(\sigma_A-\sigma_R)/2$ and $(\sigma_A+\sigma_R)/2$ (figs 6.85A and 6.89A) are similar in shape. The initial parts of the two curves are linear to an approximate mean compaction pressure of 15 MPa. As the pressure increases a decrease in the slope of the curve is observed.

7.3.2.3 Unloading

The unloading curves of the materials are different from the unloading curves of compactable materials. At zero mean compaction stress the corresponding shear values are almost zero (table 6.10). This behaviour is seen to be characteristic for non-compactable materials.

7.3.2.4 Volume reduction curves

The volume reduction curves are presented in the form of volume-mean compaction stress and volume-ln. mean compaction stress relationships. The compressive curves of homopolymer (fig 6.86 A and B) are similar in shape to the compressive curves of compactable material to an approximate mean compaction pressure of 77 MPa. Above this value the volume of the material is constant. The unloading curve, however, shows an increase in the volume of the compact. This increase in volume of the compacted material is due to the elastic recovery of the material.

A similar pattern of curves are observed in the

behaviour of copolymer (fig 6.90 A and B). A decrease in the volume of copolymer can be seen to an approximate mean compaction value of 60 MPa. Increasing the compaction pressure above 60 MPa does not effect the volume of the material. The unloading curves indicate the existance of elastic recovery of the material.

7.4 Three dimensional representation of stress pathways

Roscoe (1953) in his investigation of the failure or yielding of consolidated soils, measured the volume changes which occurred when soil samples were subjected to different shear and normal stress conditions. The experimental relationship, similar to that observed by Hvorslev (1937), related the shear stress τ at failure to the normal stress σ_N and the volume change V of the soil sample undergoing shear. This approach was used because the Mohr's-Coulomb criterion does not include the changes in volume of the sheared compact. Roscoe and co-workers (1953-1963) showed that for samples which could expand during shear(over-consolidated) the void ratio e which is a function of the compact volume, changed until it reached a critical value after which no volume change occurred. The locusof these critical values at which no change in volume occurred from different consolidated soil volumes formed a continuous line in τ, σ_N, V space. This line was termed the critical state line (C.S.L.) which is the limit of the Hvorslev surface. The space between this yield surface and the origin has been called the yield domain.

A second surface between the C.S.L. and the isotropic normal consolidation line named Roscoe or Rendulic surface has also been proposed by Roscoe et al (1957) and Ashton, Cheng, Farley and Valentin (1965).

The concept of the Hvorslev shear surface at low stresses has been used for the determination of the failure and flow properties of powders by Williams

and Birks (1965). In the compaction of powders, to produce a coherent body, the stresses used however are much higher than the stresses used in the field of soil mechanics and volume reduction occurs as opposed to volume expansion. The highest pressure reported in the field of soil mechanics was 10 MPa (Calladine (1971)) while the lowest pressure used in this investigation to produce a compact was of the order of 15 MPa, and the highest over 240 MPa. In the determination of the flow or failure properties of powders the state of the particle assembly usually undergoes a volume expansion and a Hvorslev shear surface can be recognised on one side of the critical state line in τ, σ_N and V space. In the compaction of a particle assembly there is a volume reduction which produces a Roscoe or Rendulic surface on the opposite side of the critical state line in τ, σ_N and V space.

The three dimensional representations of the stress paths of all materials used in this investigation are presented in chapter 6. The compressive stress paths of compactable and non-compactable materials, in τ,σ_N and V space, are similar in shape to the combination of the Rendulic and Hvorslev surfaces (Fig.1.20), which are separated by the critical state line. In soil mechanics nomenclature, isotropic compaction is defined as volume reduction without shear and the critical state line as the point of failure for isotropically compacted materials. Projection of the three dimensional isotropic compaction line onto τ:σ_N plane is coincidental with the normal stress axis because the shear stress in this type of compaction is zero.

From Figure 1.21 it was seen that the critical state line is below the isotropic compaction line in the volume-compaction stress plane. In uniaxial compaction the ratio of shear stress and mean compaction stress is different from the critical state and has a value less than the slope of the critical state but greater than zero. Since the critical state line lies on one edge of the Rendulic surface and the isotropic compaction line lies at the other edge at zero shear, it can be argued that the uniaxial compaction conditions lie between these two boundaries.

7.5 General Discussion and Conclusions

The compressive stress pathways constructed in shear-mean compaction stress and volume - ln mean compaction stress spaces of compactable (sodium chloride, sugar and dicalcium phosphate) and non-compactable (styrocell, homopolymer and copolymer) were found to be similar in shape. The production of coherent compacts is therefore not uniquely dependent upon the yield locus or the volume reduction curve. The unloading or decompression curves were however different. The unloading curves of non-compactable materials in the shear-mean compaction stress cycle reduced almost to zero. Unlike non-compactable materials, the unloading curves of all compactable materials cross the mean compaction stress axis to give negative values of shear stress and reach a minimum τ_{min}. The magnitudes of points of crossings σ_o and τ_{min} were found to be material and compaction pressure dependent. The end points of the unloading pathways determined at various material compaction stresses were seen to terminate on a straight line locus in the negative shear-mean compaction stress plane. The graphically evaluated parameters of τ_{min}, σ_o and the area measured between the mean compaction stress axis and the unloading curve a, were related to the mechanical strength of compacts. A linear relationship was found between the three parameters, τ_{min}, σ_o and a and tensile strength, Vickers hardness number and Brinell hardness number of plastically deforming sodium chloride.

For the fragmentary dicalcium phosphate compacts the relationships were curved. A combination of the

above two relationships was seen to exist for sugar compacts which was explained by fragmentation and a possible rebonding or plastic flow of the material during compaction. The following equations were found to define the relationship of shear-mean compaction stress of the materials investigated:

(a) Dentritic sodium chloride:-

$$\tau = 0.6208\sigma - 0.00105\sigma^2 + 0.3393$$

(b) Cubic sodium chloride:-

$$\tau = 0.6877\sigma - 0.0017038\sigma^2 + 0.2917$$

(c) Dicalcium phosphate:-

$$\tau = 0.614\sigma + 0.4738$$

(d) Sugar:-

$$\tau = 0.7287\sigma - 0.00069591\sigma^2 - 0.9564$$

(e) Styrocell:-

$$\tau = 0.52\sigma - 0.00010397\sigma^2 + 0.6235$$

(f) Homopolymer:

$$\tau = 0.306\sigma - 0.0004013\sigma^2 + 0.6394$$

(g) Copolymer:-

$$\tau = 0.1938\sigma - 0.00012165\sigma^2 + 0.8033$$

Comparison of the volume reduction curves of the compactable and non-compactable materials showed dependency on the initial size and shape of the particles. The volume change accompanying a given pressure increase was greater for small particles than for large particles. The unloading paths in the volume reduction curves of compactable materials were almost linear while the unloading curves of the uncompactable materials, homopolymer and copolymer, were curved due to the elastic recovery

of these materials. The linearity in the unloading curves of styrocell was explained by the individual particle deformation.

A continuous decrease in the surface area of dentritic sodium chloride with pressure was observed while the surface area of dicalcium phosphate compacts showed an initial decrease up to a compaction pressure of 32 MPa. This was then followed by an increase in the surface area on increase of compaction pressure. Comparison of mercury intrusion data for dentritic sodium chloride and dicalcium phosphate compacts showed a higher ultimate porosity for fragmentary dicalcium phosphate compacts than for the plastic deforming dentritic sodium chloride. The data suggested that to reach the theoretical density of sodium chloride is easier for sodium chloride than for dicalcium phosphate.

APENDIX 1

REFERENCES

APPENDIX 1

REFERENCES

1. ALLEN, T. (1981), Particle size measurement (3rd Ed.) Chapman and Hall, London.

2. AULTON, M.E., TEBBY, H.G.(1976), J.Pharm.Pharmac., 28, Suppl. 66p.

3. AULTON, M.E., TEBBY, H.G. WHITE, P.J.P. (1974), ibid, 26 Suppl. 69p.

4. ANDREASEN, A.H.M., LUNDBERG, J.J.V.(1930), Ber.Dt.Keram.Ges, 11,5, 312-23.

5. ANDERSON, R.B. (1946) J.Am.Chem.Soc., 68,686.

6. ARMSTRONG,N.A., GRIFFITH, R.V. (1970), Pharm Acta. Helv., 45, 583.

7. ARMSTRONG, N.A., HAINES-NUTT, R.F., (1972), J.Pharm.Pharmac., 24,Suppl. 135p.

8. ASHTON, M.D., CHENG, D.C.H., FARLEY, R., VALENTIN, F.H.H.(1965) Rheol. Acta., 4 206.

9. AVERY, R.G., RAMSAY, J.D.F.(1973), J.Colloid Interface Sci. 42,3.

10. AYER. J., SOPPETT, F. (1965), J.Am.Ceram. Soc., 48,180.

11. AYER, J., SOPPETT, F., (1966), ibid., 49, 207.

12. BARRETT, E.P., JOYNER, L.G., HALENDA, P.P. (1951) J.Am.Chem.Soc., 73,373.

13. BEEBE, R.A., BECKWITH, J.B., HONIG, J.M.(1945), J.Am.Chem.Soc., 67, 1554.

14. BEDDOW, J.K. (1968), Int.J.Powder Metall., 4 (1) 27.

15. BENETT, J.G., BROWN, R.L. (1940), J.Inst. Fuel 13,232-246.

16. BERNAL, J.D. (1964) Proc.Roy.Soc.280,299.

17. BERNAL, J.D. MASON, J. (1960), Nature, 188,910-11.

18. BOCKSTEIGEL, G. (1966), Int. J.Powder Metall, 2, 13.

19. BOCKSTEIGEL, G. (1967), ibid, 3,29.

20. BIRKS, A.H., MUZAFFAR, M. (1971), Symp.on Powder Flow and Storage, University of Bradford.

21. BROESE VAN GROENOU, A. (1978) Powder Metall.Int., 10,206.

22. BRUNAUER,S., EMMETT, P.H., TELLER, E. (1935) J. Am.Chem.Soc., 60, 309.

23. BRUNAUER,S., EMMETT,P.H.(1937), ibid, 59, 2682.

24. BRUNAUER,S. et al (1940), ibid, 62, 1723.

25. BRUNAUER,S. (1969), Chem. Eng.Progr. Sym. Ser. 65, 1.

26. BRINELL, J.A. (1900). Congr. Int. Method d'Essai, Paris, from Symposium of the Amircan Society of Metals, Oct. 1971.

27. BISHOP, A.W. (1971), Proc. Roscoe Memorial Symp., Cambridge University, March, 1971.

28. BRITISH STANDARD, 410 (1962) Parts 1-3.

29. BRITISH STANDARD, 3406(1936) Part 2.

30. BRITISH STANDARD, 4359 (1969) Part 1.

31. BRITISH STANDARD, 1902 (1952).

32. BRITISH STANDARD, 240 (1962) Part 1.

33. BRITISH STANDARD, 427(1961) Part 1.

34. BRITISH STANDARD, 891 (1940) Part 1.

35. BRITISH STANDARD, 1796(1976).

36. BRITISH STANDARD, 1881 (1970) Part 4.

37. CALLADINE,C.R. (1971), Geotechnique, 21, 391.

38. CAPPER,P.L., CASSIE, W.F.(1963), The Mechanics of Engineering Soils, E.and F.Spon, 22, Henrietta Street London, WC .

39. CHARLESS, J.E., LEIGH,S.(1974), J.Pharm. Pharmac. 26,289.

40. CARMAN,P.C., RAAL,E.A.(1951), Proc.Roy.Soc.A, 209, 59.

41. CARNEIRO,F., BARCILLOS,H. (1953), Rilem Report, 13,97-107, from Ridgeway ,K.(1970), Pharm J.,26, 709.

42. CHOWHAN,Z.T., AMARO, A.A.(1979), Drug. Devel. and Ind.Pharm, 5, 545.

43. CHOWHAN,Z.T. (1980), J.Pharm. Sci., 69, 1.

44. COLE,E.T., REES, J.E., HERSEY, J.A. (1975), Pharm.Acta. Helv, 50, 28.

45. COOPER, A.R., EATON, L.E. (1962), J.Amer.Ceram. Soc., 45,97.

46. COULOMB,C.H.(1776), Memoires Acadame Royal des Science, Paris, from WROTH,C.P., BASSETT, R.H.

47. CRANSTON,R.W., INKLEY,F.A.(1957), Advan.Catalysis,9,143.

PAGE NUMBERS CUT OFF

IN

ORIGINAL

48. DAESCHER,M.W., SEIBERT,E.E., PETERS,E.D. (1958), Symp. Particle Size Measurement, ASTM Sp. Publ. 234,26.

49. DE BLAEY,C.J., POLDERMAN,J. (1970). Pharm. Weekblad,105,241.

50. DE BLAEY, C.J., POLDERMAN,J.(1971). ibid, 106,57.

51. DE BOER,J.H., LINSEN,B.G., OSINGA,J. (1965), J.Catalysis, 4, 643.

52. DE BOER,A.H., BOLHUIS,G.K., LERK,C.F. (1978) Powder Technol. 20,75.

53. DE JOSSELIN DE JONG,G. (1959). Vitgiverij Walman Delft, from WROTH, C.P., BASSETT,R.H.

54. DUBININ, M.M.(1967), J. Colloid Interface Sci., 2, 217.

55. DUWEZ,P., ZWELL,L. (1949)., A.I.M.(Met.)E. Trans., 185;137.

56. DRUCKER,D.C. GIBSON,R.E., HENEKEL,D.J. (1957). Am. Soc. Civil. Eng. Trans., 122, 338.

57. DRAKE,L.C. (1948). Ind. Engng. Chem., 41, 780.

58. EASTWOOD, J., MATZEN, E.J.P., YOUNG,M.J., EPSTEIN, N. (1960), Brit. Chem. Engng. 14, 11, 1542.

59. FELL, J.T., NEWTON, J.M. (1970). J.Pharm.Sci., 59, 688.

60. FILLEBORN, V.M. (1948), Am.J.Pharm. 120, 233.

61. FROCHT, M.M. (1948). Photo-elasticity, Vol. 2, John Wiley and Sons Inc., New York.

62. FUKUMORI, Y., OKADA, J. (1977). Chem. Pharm. Bull, 25, 1610.

63. GERMAN, R.M. (1975). Int. J. Powder Metall. and Powder Tech. 11, 169.

64. GRATON, L.C., FRASER, J.H. (1935). J. Geol., 43, 785.

65. GREGG, S.J., LANGFORD, J.F. (1977), J.Chem.Sci., 73, 747.

66. GREGG, G.J., SING,K.S.W. (1967). Adsorption, Surface Area and Porosity, Academic Press, NY.

67. HARDMAN, J.S., LILLEY, B.A. (1973), Proc. Roy. Soc. A., 333, 183.

68. HARKIN, W.D., JURA,G. (1943), J.Chem.Phys., 11, 430.

69. HARKIN, W.D.,JURA,G. (1944), J.Am.Chem.Soc., 919, 1366.

70. HALSEY,G.D. (1948), J.Chem.Phys., 16, 931.

71. HAUSNER,H.H. (1981). Powder Technol., 30, 3.

72. HARRIS,N.S. (1981), M.Phil. Thesis, University of Bradford.

73. HEISTAND,E.N., BAINE,J.M., STREZELINSK, E.P.(1971), J.Pharm.Sci., 60, 758.

74. HEISTAND,E.N., WELLS,J.E., PEOT,C.B., OCHS,J.F. (1977), J.Pharm. Sci., 66, (4) 511.

75. HENDERSON,L.M., RIDGEWAY,C.M., ROSS,W.B.(1940), Refin.Natur.GasMfr., 19,(6) 69.

76. HERSEY,J.A., REES, J.E.(1971), Nature Phys. Sci., 230,(3)96.

77. HIGUCHI,T., ARNOLD, R.D., TUCKER,S.J., BUSSE,L.W.(1952), J.Am.Pharm.Ass.Sci.Ed., 41, 93.

78. HIGUCHI,T., MARISHMA,A, BUSSE,L.W., SWINTOVSKY, J.V.(1953), ibid, 42 194.

79. HIGUCHI,T., ELOWE,L.M., BUSSE,L.W.(1954), ibid,43,685.

80. HIGUCHI,T., SHIMAMOTO,T., ERIKSEN,S.P., YASHIKI,T.(1965), J.Pharm. Sci., 54(1).111.

81. HO, T., HERSEY,J.A.(1980), J.Pharm. Pharmac, 32,160.

82. HUFFINE,C.L., BONILLA,C.F.(1962), Am.Inst.Chem.Eng.J, 8, 490.

83. HUTTIG,C.F.(1948), Montash. Chem., 78, 177.

84. HVORSLEV, M.J.(1937), Ingeniorvidenskabelige Skrifter A, No.45, from WROTH, C.P., BASSETT,R.H.

85. IBRAHIM,K. (1979), Ph.D. Thesis, University of Bradford.

86. JAYCOCK,M.J.(1977), Private Communication, Chemistry Department, University of Technology, Loughborough, Leicestershire,LE11 3TU, England.

87. JENIKE,A.W., SHIELD,R.T.(1959), J.Appl. Mech., 81B, 599.

88. JENIKE,A.W.(1961), Gravity Flow of Bulk Solids, Utah,Engng. Exper. Station, University of Utah, Brit. 108.

89. KAMM,R., STEINBERG,M., WULFF,J.(1947), Am.Inst.Mining.Met. Eng., 171, 439.

90. KEDALL,K. (1978), Nature, 272, 710.

91. KHAN, K.A., RHODES, C.T. (1975), J.Pharm.Sci., 64, 445.

92. KOSTELNIK ,M.C., KLUDT,F.H., BEDDOW,J.K. (1968), Int.J. Powder Metall., 4, 19.

93. KUCZYNSKI, G.C., ZAPLATYNSKYJ,I. (1956), A.I.M.(Met)E.Trans., 206, 215.

94. LANGMUIR,I.(1917), J.Am.Chem.Soc., 39, 1848.

95. LAPLACE, (1806), from ALLEN (1981).

96. LIPPENS,B.C., LINSEN,B.G., DE BOER,J.H. (1964), J.Catalysis, 3,32.

97. LONG,W.M.(1960), Powder Metall., 6, 73.

98. LESSELLS,J.M. (1954), Strength and Resistance of Metals, Chapman and Hall, London.

99. MacLEOD, H.M., MARSHALL,K. (1977), Powder Technol., 16,107.

100. MARSHALL, K.(1977), The Physics of Tablet Compression, 12th Annual Arden House, Conf.

101. MATSUMARU,H. (1958), J.Pharm. Pharmac., 78, 1198.

102. MATSUMARU,H. (1958),ibid, 78, 1201.

103. MATSUMARU,H.(1958), ibid, 78 1205.

104. MATSUMARU,H.(1959), ibid, 79, 63.

105. McCLENNAN,A.L., HARNSBERGER,H.F. (1967), J.Colloid & Interface Sci.,23577.

106. McGEARY, R.K. (1961), J.Am. Ceram. Soc., 44, 513.

107. MEIHUIZEN,J.J., CROMMELIN,C.A. (1937), Physica, 4, 1, From JAYCOCK, M.J.

108. MEYER,E.(1908), "Untersuchungen über Hartepröfung und Härte", ZVer.Deut.Ing, 52, (17) 645,from LESSELLS,J.M.

109. MOHR,O. (1900), Z.Ver.Deut.Ing. 44 1524, from TIMOSHENKO,S.

110. NELSON,E., NAQVI,S.M., BUSSE,L.W., HIGUCHI,T.(1954), J.Am.Pharm. Assoc., Sci.Ed., 44, 494.

111. NUTTER-SMITH, A.(1949), Pharm. J., 163 227.

112. NUTTER-SMITH, A(1949), ibid, 163 477.

113. OBIORAH,B.A., SHOTTON,E.(1976),J.Pharm. Pharmac.,28 629.

114. PHILIPS,C.E.S.(1910), Proc. Roy. Inst., 19 742.

115. POLAKOWSKI,N.H.(1966), Strength and Structure of Engineering Materials, Prentice-Hall,Inc., Englewood Cliffs, New Jersey.

116. RAKOWSKI,V.S.(1935), Fundamental Considerations in the Production of Hard Alloys, Moscow, from COOPER, A.R., GOODNEW, W.H.

117. RANKINE,W.J.M.(1857), Proc.Roy.Soc., 147, 9.

118. REES,J.E., HERSEY,J.A., COLES, E.T.(1970), J.Pharm.Pharmac, 22,Suppl.645.

119. REES,J.E., SHOTTON,E.(1970), J.Pharm. Pharmac., 22 Suppl. 175.

120. REES,J.E., RUE,P.J., RICHARDSON,S.C.(1977), ibid, 29 Suppl. 38P.

121. REES,J.E., RUE,P.J. (1978), ibid, 30 601.

122. RENDULIC,L.(1937), Bauningeneur, 18, 459.

123. RIDGEWAY, K. (1966), J.Pharm.Pharmac., 18 Suppl. 176S.

124. RIDGEWAY,K. (1970), J.Pharm., 26 709.

125. RIDGEWAY, K., AULTON,M.E., ROSSER, P.H.(1970), J.Pharm.Pharmac., 22 Suppl. 70S.

126. RIDGEWAY,K., GLASBY, J., ROSSER, P.H.(1969), ibid, 21, Suppl. 24S.

127. RIDGEWAY, K. SHOTTON,E., GLASBY, J.(1969), ibid, 21 Suppl. 19S.

128. RITTER, H.L., DRAKE,L.C.(1945), Ind.Engng. Chem.Analyt.Edn., 17, 782.

129. ROOTARE,H.M.(1972), Powder Technol., 6,17.

130. ROSCOE,K.H.(1953), Proc.3rd Int. Conf., Soil Mech.,1, 186.

131. ROSCOE,K.H, SCHOFIELD,A.N., WROTH,C.P. (1957), Geotechnique,8,22.

132. RUDNICK,W.C., HUNTER,A.R., HOLDEN,F.C. (1963),Mater. Res. Stand.,1,283.

133. RUE,P.J. (1981), Symp.on Tablet Technology, Stockholm, Sweeden.

134. SCHOFIELD,A., WROTH,P.(1966), Critical State Soil Mechanics McGraw and HIll, London.

135. SCHWARTZ, E.G., WEINSTEIN,A.S.(1965), J.Am.Ceram.Soc., 48,346.

136. SCHWARTZ, E.G. HOLAND, A.R.(1969), J.Int. Powder Metall.,5,79.

137. SCHULL,C.G.(1948),J.Am.Chem.Soc.70,1405.

138. SEELIG,R.P., WULFF,J.(1947), A.I.M.(Met)E. Trans.171,506.

139. SETH,P.L., MUNZELL,K. (1960), Pharm.Ind., 22,7.

140. SHAXBY,T.H., EVANS, J.C.(1923), Trans. Farad. Soc., 19,60.

141. SHIELD, R.T.(1955), J.Mech.Phys. Solids, 4,10.

142. SHORE, A.F.(1910) Proc.A.S.T.M., 10,490, from LESSELLS.

143. SHOTTON, E., GANDERTON, D. (1960), J. Pharm. Pharmac., 12, 93T.

144. SHOTTON,E., GANDERTON,D.(1960), J.Pharm. Pharmac, 12, 87T,93T.

145. SHOTTON,E., GANDERTON,D.(1961), ibid, 13, 144T.

146. SHOTTON, E., OBIORAH,B.A.(1973), ibid, 25 Suppl. 37P.

147. SIXSMITH, D.G.(1975), Ph.D Thesis, University of Bradford.

148. SIXSMITH,D.G.(1977), Manuf. Chem., Aerozol News, 48,17.

149. SOKOLOVSKI,V.V.(1960), Statics of Soil Media, Butterworth, London.

150. SMAKULA,A., KALNAJS, J.(1955) Phys.Rev., 99, 1737.

151. SMITH,W.O., FOOTE, P.D., PUSANG,P.F. (1929), ibid, 34,1271.

152. SPENGLER,H., KAELIN,A. (1945), Pharm. Acta. Helv., 20219,239.

153. SPENCER, R.S., GILMORE,G.D., WILEY, R.M. (1950), J.Appl.Phs. 20,177 and 21,527.

154. STANLEY-WOOD, N.G.(1975), Powder Technol., 12, 225.

155. STANLEY-WOOD, N.G., JOHANSSON,M.E.(1977), 1st Int.Comf.of Pharm.Technol., Paris.

156. STANLEY-WOOD, N.G., SHUBAIR,M.S.(1979), Powder Technol., 25, 57.

157. STANLEY-WOOD, N.G. (1977), Powder Metall. Int., 9,27, 84, 138.

158. STANLEY-WOOD, N.G. (1982), Education Course, Sp. Inst.Chem.Eng.,Jan.1982, University of Bradford.

159. STANLEY-WOOD, N.G. ABDELKARIM, M.A.(1982), J.Powder Metall. Int., 14, 3.

160. SUH,N.P.(1969), Int.J.Powder Metall, 5,1.

161. TERZAGHI,K.(1943), Theoretical Soil Mechanics, Wiley, from SCHOFIELD,A., WROTH, P.

162. TIMOSHENKO,S.(1956), Strength of Materials, Part 2, 3rd Ed., D.VanNostrand. Comp. Inc., London.

163. TRAIN,D.(1956), J.Pharm. Pharmac., 8,745.

164. TRAIN,D.(1957), Trans.Inst.Chem.Eng., 35, 258.

165. TRAIN,D., HERSEY,J.A.(1960), Powder Metall, 6,20.

166. UNCKEL,H.(1945), Arch.Eisenhuttew, 18, 161, from MacLEOD.

167. VAN VLACK,L.H. (1961), Elements of Material Science, Second Ed., Addison Wesley Publishing Comp. Inc.,London.

168. WASHBURN,E.W.(1921), Proc.Natn.Acad. Sci., 7,115.

169. WHEELER,A.(1955), Catalysis, 2,118, Reinhold, N.Y. from ALLEN.

170. WILLIAMS, J.C., BIRKS, A.H.(1965), Rheol. Acta, 4,170.

171. WINDHEUSER,J.J., MISRA,J., ERIKSEN,S.P., HIGUCHI,T.(1963), J.Pharm. Sci., 52, 766.

172. WOLLASTON,W.H.(1828), Phil. Trans., 119, 1, from TRAIN,D. LEWIS, C.J.

173. WROTH,C.P., BASSETT,R.H.(1965), Geotechnique, 15, 32.

174. YORK,P., PILPEL,N. (1973), J.Pharm. Pharmac., 25, Suppl.1P.

175. YORK,P., BAILEY,E.D.(1977), ibid, 29, 70.

176. YORK,P.(1978), ibid, 30,6.

APENDIX 2

COMPACTION DATA

Symbols Used in Appendix 2

τ	Mean deviatoric stress
σ	Mean compaction stress
ε	Compaction strain
V	Compact volume
ln σ	Natural logarithm of mean compaction stress
σ_A	Axial stress
σ_R	Radial stress
σ_R/σ_A	Stress ratio

Table A1. Compaction data for Dentritic sodium chloride compacted uniaxially at 248 MPa

σ (MPa)	τ (MPa)	ε	V ($mx10^{-6}$)	ln σ	σ_A (MPa)	σ_R MPa	$\frac{\sigma_R}{\sigma_A}$
.242	.074	0.000	4.772	-1.419	.316	.168	.533
.243	.073	.013	4.708	-1.415	.316	.170	.540
.244	.072	.020	4.677	-1.412	.316	.172	.544
.445	.186	.027	4.645	-.809	.631	.259	.411
.447	.184	.041	4.582	-.805	.631	.263	.416
.605	.342	.041	4.582	-.503	.947	.263	.278
.606	.341	.049	4.550	-.502	.947	.265	.280
.809	.453	.056	4.519	-.212	1.262	.355	.281
.811	.451	.071	4.456	-.209	1.262	.360	.285
.858	.404	.079	4.424	-.153	1.262	.453	.359
1.017	.560	.086	4.392	.017	1.578	.457	.290
1.177	.716	.094	4.361	.163	1.893	.460	.243
1.225	.668	.102	4.329	.203	1.893	.556	.294
1.384	.824	.110	4.298	.325	2.209	.560	.254
1.436	.773	.127	4.234	.362	2.209	.663	.300
1.596	.928	.135	4.203	.468	2.524	.668	.265
1.756	1.083	.144	4.171	.563	2.840	.673	.237
1.808	1.032	.153	4.140	.592	2.840	.776	.273
2.017	1.138	.162	4.108	.702	3.155	.879	.279
2.178	1.292	.171	4.076	.779	3.471	.886	.255
2.389	1.397	.180	4.045	.871	3.786	.992	.262
2.551	1.551	.189	4.013	.936	4.102	1.000	.244
2.767	1.650	.208	3.950	1.018	4.417	1.117	.253
2.929	1.803	.218	3.918	1.075	4.732	1.126	.238
3.143	1.904	.228	3.887	1.145	5.048	1.239	.245
3.358	2.005	.238	3.855	1.211	5.363	1.353	.252
3.522	2.157	.248	3.824	1.259	5.679	1.364	.240
3.738	2.256	.258	3.792	1.319	5.994	1.482	.247

Table A1 cont.

4.120	2.506	.280	3.729	1.416	6.625	1.614	.244
4.284	2.656	.291	3.697	1.455	6.941	1.628	.235
4.504	2.752	.302	3.666	1.505	7.256	1.752	.241
4.882	3.005	.313	3.634	1.586	7.887	1.877	.238
5.104	3.099	.325	3.602	1.630	8.203	2.005	.244
5.484	3.349	.336	3.571	1.702	8.834	2.135	.242
5.866	3.599	.348	3.539	1.769	9.465	2.268	.240
6.091	3.689	.360	3.508	1.807	9.780	2.402	.246
6.633	4.094	.373	3.476	1.892	10.727	2.540	.237
7.019	4.339	.385	3.444	1.949	11.358	2.680	.236
7.248	4.426	.398	3.413	1.981	11.673	2.822	.242
7.793	4.827	.411	3.381	2.053	12.620	2.967	.235
8.340	5.226	.425	3.350	2.121	13.566	3.115	.230
8.573	5.308	.438	3.318	2.149	13.882	3.265	.235
9.342	5.801	.452	3.286	2.235	15.144	3.541	.234
9.737	6.038	.466	3.255	2.276	15.775	3.699	.234
10.133	6.273	.480	3.223	2.316	16.406	3.859	.235
10.845	6.822	.495	3.192	2.364	17.668	4.023	.228
11.308	6.991	.510	3.160	2.426	18.299	4.318	.236
11.867	7.378	.525	3.128	2.474	19.245	4.489	.233
12.651	7.856	.541	3.097	2.538	20.507	4.794	.234
13.189	8.265	.541	3.097	2.579	21.454	4.924	.230
13.818	8.582	.557	3.065	2.626	22.400	5.237	.234
14.767	9.211	.573	3.034	2.692	23.978	5.556	.232
15.561	9.679	.589	3.002	2.745	25.240	5.882	.233
16.358	10.144	.606	2.970	2.795	26.502	6.214	.234
17.317	10.762	.624	2.939	2.852	28.079	6.554	.233
18.121	11.220	.641	2.907	2.897	29.341	6.901	.235
19.087	11.831	.659	2.876	2.949	30.918	7.256	.235
20.058	12.438	.678	2.844	2.999	32.496	7.619	.234
20.830	12.928	.678	2.844	3.036	33.758	7.901	.234
22.035	13.616	.697	2.812	3.093	35.651	8.418	.236
23.015	14.213	.716	2.781	3.136	37.228	8.802	.236
23.843	14.647	.736	2.749	3.171	38.491	9.196	.239
24.935	15.448	.736	2.749	3.216	40.383	9.487	.235

Table A1 continued

25.927	16.034	.756	2.718	3.255	41.961	9.893	.236
26.706	16.517	.756	2.718	3.285	43.223	10.188	.236
27.778	17.022	.776	2.686	3.324	44.800	10.756	.240
28.549	17.513	.798	2.654	3.352	46.062	11.036	.240
29.489	18.151	.798	2.654	3.384	47.640	11.338	.238
30.657	18.876	.819	2.623	3.423	49.533	11.781	.238
31.283	19.196	.819	2.623	3.443	50.479	12.087	.239
32.300	19.756	.841	2.591	3.475	52.057	12.544	.241
33.479	20.471	.841	2.591	3.511	53.950	13.008	.241
34.347	20.865	.864	2.560	3.537	55.212	13.482	.244
35.529	21.576	.864	2.560	3.570	57.104	13.953	.244
36.632	22.366	.864	2.560	3.601	58.997	14.266	.242
37.590	22.669	.888	2.528	3.627	60.259	14.921	.248
38.695	23.457	.888	2.528	3.656	62.153	15.238	.245
40.137	24.224	.911	2.496	3.692	64.361	15.914	.247
41.167	24.771	.911	2.496	3.718	65.938	16.396	.249
42.621	25.526	.936	2.465	3.752	68.147	17.094	.251
44.050	26.305	.936	2.465	3.785	70.355	17.745	.252
45.360	26.889	.961	2.433	3.815	72.248	18.471	.256
46.794	27.663	.961	2.433	3.846	74.457	19.130	.257
48.303	28.678	.961	2.433	3.877	76.981	19.625	.255
49.713	29.161	.987	2.402	3.906	78.874	20.552	.261
51.309	30.089	.987	2.402	3.938	81.398	21.220	.261
53.209	31.028	1.013	2.370	3.974	84.237	22.180	.263
54.652	31.794	1.013	2.370	4.001	86.446	22.857	.264
56.252	32.717	1.013	2.370	4.030	88.970	23.535	.265
58.016	33.477	1.041	2.338	4.061	91.493	24.539	.268
59.464	34.238	1.041	2.338	4.085	93.702	25.226	.269
61.333	34.892	1.068	2.307	4.116	96.226	26.441	.275
62.699	35.736	1.068	2.307	4.138	98.434	26.963	.274
63.993	36.334	1.068	2.307	4.159	100.327	27.659	.276
65.642	36.894	1.097	2.275	4.184	102.536	28.748	.280
66.853	37.576	1.097	2.275	4.202	104.429	29.277	.280
67.906	38.100	1.097	2.275	4.218	106.006	29.806	.281
68.960	38.624	1.097	2.275	4.234	107.564	30.336	.282

Table A1 continued

106.133	53.823	1.254	2.117	4.665	159.956	52.311	.327
107.206	54.327	1.254	2.117	4.675	161.533	52.879	.327
108.532	54.894	1.254	2.117	4.687	163.426	53.638	.328
109.763	55.557	1.254	2.117	4.698	165.319	54.206	.328
110.931	55.966	1.254	2.117	4.709	166.897	54.964	.329
112.256	56.534	1.254	2.117	4.721	168.790	55.722	.330
113.329	57.038	1.254	2.117	4.730	170.367	56.291	.330
114.655	57.606	1.254	2.117	4.742	172.260	57.049	.331
116.322	57.831	1.288	2.086	4.756	174.153	58.491	.336
117.495	58.235	1.288	2.086	4.766	175.731	59.260	.337
118.827	58.797	1.288	2.086	4.778	177.623	60.030	.338
120.316	59.516	1.288	2.086	4.790	179.832	60.799	.338
121.489	59.920	1.288	2.086	4.800	181.409	61.569	.339
122.821	60.482	1.288	2.086	4.811	183.303	62.339	.340
123.898	60.982	1.288	2.086	4.819	184.880	62.916	.340
124.914	61.226	1.288	2.086	4.828	186.142	63.686	.342
128.908	62.913	1.288	2.086	4.859	191.821	65.994	.344
130.339	62.744	1.323	2.054	4.870	193.083	67.596	.350
131.263	63.082	1.323	2.054	4.877	194.345	68.182	.351
132.090	63.517	1.323	2.054	4.883	195.607	68.573	.351
133.014	63.855	1.323	2.054	4.890	196.869	69.159	.351
133.938	64.193	1.323	2.054	4.897	198.131	69.745	.352
134.862	64.531	1.323	2.054	4.904	199.393	70.331	.353
135.530	64.809	1.323	2.054	4.909	200.339	70.721	.353
136.454	65.147	1.323	2.054	4.916	201.601	71.308	.354
137.123	65.425	1.323	2.054	4.921	202.548	71.698	.354
137.792	65.702	1.323	2.054	4.926	203.494	72.089	.354
138.302	65.823	1.323	2.054	4.929	204.125	72.480	.355
138.971	66.101	1.323	2.054	4.934	205.072	72.870	.355
139.462	66.221	1.323	2.054	4.938	205.703	73.261	.356
139.835	66.183	1.323	2.054	4.940	206.018	73.652	.358
140.248	66.401	1.323	2.054	4.943	206.649	73.847	.357
140.661	66.619	1.323	2.054	4.946	207.280	74.043	.357
141.014	66.581	1.323	2.054	4.949	207.596	74.433	.359
141.428	66.799	1.323	2.054	4.952	208.227	74.629	.358

Table A1 continued

141.683	66.859	1.323	2.054	4.954	208.542	74.824	.359
142.096	67.077	1.323	2.054	4.957	209.173	75.020	.359
142.510	67.295	1.323	2.054	4.959	209.804	75.215	.359
143.020	67.415	1.323	2.054	4.963	210.435	75.605	.359
143.434	67.633	1.323	2.054	4.966	211.066	75.801	.359
143.787	67.595	1.323	2.054	4.968	211.382	76.192	.360
144.042	67.655	1.323	2.054	4.970	211.697	76.387	.361
144.455	67.873	1.323	2.054	4.973	212.328	76.582	.361
144.711	67.933	1.323	2.054	4.975	212.643	76.778	.361
145.124	68.151	1.323	2.054	4.978	213.274	76.973	.361
145.379	68.211	1.323	2.054	4.979	213.590	77.168	.361
145.890	68.331	1.323	2.054	4.983	214.221	77.559	.362
146.146	68.391	1.323	2.054	4.985	214.536	77.755	.362
146.559	68.609	1.323	2.054	4.987	215.167	77.950	.362
146.972	68.827	1.323	2.054	4.990	215.798	78.145	.362
147.227	68.887	1.323	2.054	4.992	216.114	78.341	.362
147.640	69.104	1.323	2.054	4.995	216.745	78.536	.362
147.896	69.165	1.323	2.054	4.997	217.060	78.731	.363
148.407	69.285	1.323	2.054	5.000	217.691	79.122	.363
148.820	69.502	1.323	2.054	5.003	218.322	79.318	.363
149.233	69.720	1.323	2.054	5.006	218.953	79.513	.363
149.489	69.780	1.323	2.054	5.007	219.269	79.708	.364
149.902	69.998	1.323	2.054	5.010	219.900	79.904	.363
150.315	70.216	1.323	2.054	5.013	220.531	80.099	.363
150.668	70.178	1.323	2.054	5.015	220.846	80.490	.364
151.081	70.396	1.323	2.054	5.018	221.477	80.685	.364
151.494	70.614	1.323	2.054	5.021	222.108	80.880	.364
152.383	70.041	1.359	2.022	5.026	222.424	82.342	.370
152.798	70.257	1.359	2.022	5.029	223.055	82.541	.370
153.055	70.315	1.359	2.022	5.031	223.370	82.739	.370
153.312	70.374	1.359	2.022	5.032	223.686	82.938	.371
153.727	70.590	1.359	2.022	5.035	224.317	83.136	.371
153.984	70.649	1.359	2.022	5.037	224.632	83.335	.371
154.240	70.707	1.359	2.022	5.039	224.948	83.533	.371
154.497	70.766	1.359	2.022	5.040	225.263	83.731	.372

Table A1 continued

154.912	70.982	1.359	2.022	5.043	225.894	83.930	.372
155.169	71.041	1.359	2.022	5.045	226.210	84.128	.372
155.426	71.099	1.359	2.022	5.046	226.525	84.327	.372
155.683	71.158	1.359	2.022	5.048	226.841	84.525	.373
155.841	71.316	1.359	2.022	5.049	227.156	84.525	.372
156.197	71.275	1.359	2.022	5.051	227.472	84.922	.373
156.355	71.433	1.359	2.022	5.052	227.787	84.922	.373
156.769	71.649	1.359	2.022	5.055	228.418	85.120	.373
157.026	71.708	1.359	2.022	5.056	228.734	85.319	.373
157.441	71.924	1.359	2.022	5.059	229.365	85.517	.373
157.698	71.982	1.359	2.022	5.061	229.680	85.716	.373
157.955	72.041	1.359	2.022	5.062	229.996	85.914	.374
158.212	72.099	1.359	2.022	5.064	230.311	86.113	.374
158.626	72.316	1.359	2.022	5.067	230.942	86.311	.374
159.041	72.532	1.359	2.022	5.069	231.573	86.509	.374
159.199	72.690	1.359	2.022	5.070	231.889	86.509	.373
159.456	72.748	1.359	2.022	5.072	232.204	86.708	.373
159.713	72.807	1.359	2.022	5.073	232.520	86.906	.374
160.227	72.924	1.359	2.022	5.077	233.151	87.303	.374
160.542	73.239	1.359	2.022	5.079	233.782	87.303	.373
160.799	73.298	1.359	2.022	5.080	234.097	87.501	.374
161.056	73.356	1.359	2.022	5.082	234.413	87.700	.374
161.471	73.573	1.359	2.022	5.084	235.044	87.898	.374
161.728	73.631	1.359	2.022	5.086	235.359	88.097	.374
161.985	73.690	1.359	2.022	5.088	235.675	88.295	.375
162.400	73.906	1.359	2.022	5.090	236.306	88.494	.374
162.814	74.122	1.359	2.022	5.093	236.937	88.692	.374
163.071	74.181	1.359	2.022	5.094	237.252	88.890	.375
163.328	74.240	1.359	2.022	5.096	237.568	89.089	.375
163.743	74.456	1.359	2.022	5.098	238.198	89.287	.375
164.000	74.514	1.359	2.022	5.100	238.514	89.486	.375
164.157	74.672	1.359	2.022	5.101	238.829	89.486	.375
164.671	74.789	1.359	2.022	5.104	239.460	89.882	.375
164.829	74.947	1.359	2.022	5.105	239.776	89.882	.375
165.185	74.906	1.359	2.022	5.107	240.091	90.279	.376

Table A1 continued

165.343	75.064	1.359	2.022	5.108	240.407	90.279	.376
165.758	75.280	1.359	2.022	5.111	241.038	90.478	.375
166.015	75.339	1.359	2.022	5.112	241.353	90.676	.376
166.272	75.397	1.359	2.022	5.114	241.669	90.874	.376
166.686	75.614	1.359	2.022	5.116	242.300	91.073	.376
166.943	75.672	1.359	2.022	5.118	242.616	91.271	.376
167.358	75.888	1.359	2.022	5.120	243.247	91.470	.376
167.615	75.947	1.359	2.022	5.122	243.562	91.668	.376
167.872	76.006	1.359	2.022	5.123	243.878	91.866	.377
168.030	76.163	1.359	2.022	5.124	244.193	91.866	.376
168.287	76.222	1.359	2.022	5.126	244.509	92.065	.377
168.701	76.438	1.359	2.022	5.128	245.140	92.263	.376
168.958	76.497	1.359	2.022	5.130	245.455	92.462	.377
169.058	76.397	1.359	2.022	5.130	245.455	92.660	.378
169.315	76.456	1.359	2.022	5.132	245.771	92.859	.378
169.157	76.298	1.359	2.022	5.131	245.455	92.859	.378
168.841	75.983	1.359	2.022	5.129	244.824	92.859	.379
168.368	75.509	1.359	2.022	5.126	243.878	92.859	.381
167.796	75.135	1.359	2.022	5.123	242.931	92.660	.381
167.165	74.504	1.359	2.022	5.119	241.669	92.660	.383
166.376	73.716	1.359	2.022	5.114	240.091	92.660	.386
165.488	73.026	1.359	2.022	5.109	238.514	92.462	.388
164.442	72.179	1.359	2.022	5.103	236.621	92.263	.390
163.397	71.332	1.359	2.022	5.096	234.728	92.065	.392
162.252	70.584	1.359	2.022	5.089	232.835	91.668	.394
161.048	69.578	1.359	2.022	5.082	230.627	91.470	.397
160.003	68.731	1.359	2.022	5.075	228.734	91.271	.399
158.957	67.884	1.359	2.022	5.069	226.841	91.073	.401
157.970	67.294	1.359	2.022	5.062	225.263	90.676	.403
156.766	66.289	1.359	2.022	5.055	223.055	90.478	.406
155.720	65.441	1.359	2.022	5.048	221.162	90.279	.408
154.675	64.594	1.359	2.022	5.041	219.269	90.081	.411
153.629	63.747	1.359	2.022	5.035	217.376	89.882	.413
152.583	62.899	1.359	2.022	5.028	215.483	89.664	.416
151.538	62.052	1.359	2.022	5.021	213.590	89.486	.419

Table A1 continued

150.393	61.304	1.359	2.022	5.013	211.697	89.089	.421
149.505	60.615	1.359	2.022	5.007	210.120	88.890	.423
148.459	59.767	1.359	2.022	5.000	208.227	88.692	.426
147.571	59.078	1.359	2.022	4.994	206.649	88.494	.428
146.683	58.388	1.359	2.022	4.988	205.072	88.295	.431
145.638	57.541	1.359	2.022	4.981	203.179	88.097	.434
144.907	57.009	1.359	2.022	4.976	201.917	87.898	.435
143.920	56.419	1.359	2.022	4.969	200.339	87.501	.437
143.131	55.630	1.359	2.022	4.964	198.762	87.501	.440
142.244	54.941	1.359	2.022	4.958	197.184	87.303	.443
141.256	54.350	1.359	2.022	4.951	195.607	86.906	.444
140.369	53.661	1.359	2.022	4.944	194.029	86.708	.447
139.638	53.129	1.359	2.022	4.939	192.767	86.509	.449
138.750	52.440	1.359	2.022	4.933	191.190	86.311	.451
138.020	51.908	1.359	2.022	4.927	189.928	86.113	.453
137.033	51.317	1.359	2.022	4.920	188.350	85.716	.455
136.204	50.885	1.359	2.022	4.914	187.088	85.319	.456
135.316	50.195	1.359	2.022	4.908	185.511	85.120	.459
134.585	49.664	1.359	2.022	4.902	184.249	84.922	.461
133.756	49.231	1.359	2.022	4.896	182.987	84.525	.462
133.026	48.699	1.359	2.022	4.891	181.725	84.327	.464
132.296	48.167	1.359	2.022	4.885	180.463	84.128	.466
131.565	47.636	1.359	2.022	4.880	179.201	83.930	.468
130.736	47.203	1.359	2.022	4.873	177.939	83.533	.469
130.006	46.671	1.359	2.022	4.868	176.677	83.335	.472
129.334	46.396	1.359	2.022	4.862	175.731	82.938	.472
128.604	45.865	1.359	2.022	4.857	174.469	82.739	.474
127.874	45.333	1.359	2.022	4.851	173.207	82.541	.477
127.301	44.959	1.359	2.022	4.847	172.260	82.342	.478
126.472	44.526	1.359	2.022	4.840	170.998	81.946	.479
125.899	44.152	1.359	2.022	4.835	170.052	81.747	.481
125.070	43.720	1.359	2.022	4.829	168.790	81.350	.482
124.498	43.346	1.359	2.022	4.824	167.843	81.152	.483
123.767	42.814	1.359	2.022	4.818	166.581	80.954	.486
123.195	42.440	1.359	2.022	4.814	165.635	80.755	.488

Table A1 continued

122.366	42.007	1.359	2.022	4.807	164.373	80.358	.489
121.635	41.475	1.359	2.022	4.801	163.111	80.160	.491
120.806	41.043	1.359	2.022	4.794	161.849	79.763	.493
120.076	40.511	1.359	2.022	4.788	160.587	79.565	.495
119.246	40.079	1.359	2.022	4.781	159.325	79.168	.497
118.259	39.488	1.359	2.022	4.773	157.747	78.771	.499
117.371	38.799	1.359	2.022	4.765	156.170	78.573	.503
116.384	38.208	1.359	2.022	4.757	154.592	78.176	.506
115.496	37.519	1.359	2.022	4.749	153.015	77.978	.510
114.509	36.929	1.359	2.022	4.741	151.438	77.581	.512
113.680	36.496	1.359	2.022	4.733	150.176	77.184	.514
112.792	35.806	1.359	2.022	4.726	148.598	76.985	.518
111.805	35.216	1.359	2.022	4.717	147.021	76.589	.521
110.817	34.626	1.359	2.022	4.708	145.443	76.192	.524
109.830	34.035	1.359	2.022	4.699	143.866	75.795	.527
108.942	33.346	1.359	2.022	4.691	142.288	75.596	.531
108.113	32.913	1.359	2.022	4.683	141.026	75.200	.533
107.225	32.224	1.359	2.022	4.675	139.449	75.001	.538
106.238	31.633	1.359	2.022	4.666	137.871	74.604	.541
105.408	31.201	1.359	2.022	4.658	136.609	74.207	.543
104.421	30.610	1.359	2.022	4.648	135.032	73.811	.547
103.533	29.921	1.359	2.022	4.640	133.454	73.612	.552
102.546	29.331	1.359	2.022	4.630	131.877	73.215	.555
101.559	28.740	1.359	2.022	4.621	130.299	72.819	.559
100.671	28.051	1.359	2.022	4.612	128.722	72.620	.564
99.684	27.460	1.359	2.022	4.602	127.144	72.223	.568
98.539	26.713	1.359	2.022	4.590	125.252	71.827	.573
97.552	26.122	1.359	2.022	4.580	123.674	71.430	.578
96.565	25.532	1.359	2.022	4.570	122.097	71.033	.582
95.578	24.941	1.359	2.022	4.560	120.519	70.636	.586
94.847	24.410	1.359	2.022	4.552	119.257	70.438	.591
93.860	23.819	1.359	2.022	4.542	117.679	70.041	.595
92.972	23.130	1.359	2.022	4.532	116.102	69.842	.602
91.985	22.540	1.359	2.022	4.522	114.525	69.446	.606
91.156	22.107	1.359	2.022	4.513	113.263	69.049	.610

Table A1 continued

90.425	21.575	1.359	2.022	4.505	112.001	68.850	.615
89.438	20.985	1.359	2.022	4.494	110.423	68.454	.620
88.609	20.552	1.359	2.022	4.484	109.161	68.057	.623
87.879	20.021	1.359	2.022	4.476	107.899	67.858	.629
86.892	19.430	1.359	2.022	4.465	106.322	67.461	.635
86.161	18.898	1.359	2.022	4.456	105.060	67.263	.640
85.490	18.624	1.359	2.022	4.448	104.113	66.866	.642
84.760	18.092	1.359	2.022	4.440	102.851	66.668	.648
84.029	17.560	1.359	2.022	4.431	101.589	66.469	.654
83.200	17.127	1.359	2.022	4.421	100.327	66.072	.659
82.627	16.754	1.359	2.022	4.414	99.381	65.874	.663
82.055	16.379	1.359	2.022	4.407	98.434	65.676	.667
81.226	15.947	1.359	2.022	4.397	97.172	65.279	.672
80.653	15.573	1.359	2.022	4.390	96.226	65.080	.676
80.081	15.199	1.359	2.022	4.383	95.279	64.882	.681
79.409	14.924	1.359	2.022	4.375	94.333	64.485	.684
78.679	14.392	1.359	2.022	4.365	93.071	64.287	.691
78.264	14.176	1.359	2.022	4.360	92.440	64.088	.693
77.534	13.644	1.359	2.022	4.351	91.178	63.890	.701
76.862	13.369	1.359	2.022	4.342	90.232	63.493	.704
76.290	12.995	1.359	2.022	4.335	89.285	63.295	.709
75.875	12.779	1.359	2.022	4.329	88.654	63.096	.712
75.303	12.405	1.359	2.022	4.322	87.708	62.898	.717
74.730	12.031	1.359	2.022	4.314	86.761	62.699	.723
74.158	11.657	1.359	2.022	4.306	85.815	62.501	.728
73.585	11.283	1.359	2.022	4.298	84.868	62.303	.734
73.171	11.066	1.359	2.022	4.293	84.237	62.104	.737
72.657	10.949	1.359	2.022	4.286	83.606	61.707	.738
72.183	10.476	1.359	2.022	4.279	82.659	61.707	.747
71.512	10.201	1.359	2.022	4.270	81.713	61.311	.750
71.097	9.985	1.359	2.022	4.264	81.082	61.112	.754
70.056	10.080	1.323	2.054	4.249	80.136	59.976	.748
70.110	9.395	1.359	2.022	4.250	79.505	60.715	.764
69.537	9.021	1.359	2.022	4.242	78.558	60.517	.770
69.123	8.804	1.359	2.022	4.236	77.927	60.319	.774

Table A1 continued

68.246	9.051	1.323	2.054	4.223	77.296	59.195	.766
67.675	8.675	1.323	2.054	4.215	76.350	59.000	.773
67.262	8.457	1.323	2.054	4.209	75.719	58.804	.777
67.306	7.781	1.359	2.022	4.209	75.068	59.525	.793
66.833	7.308	1.359	2.022	4.202	74.141	59.525	.803
66.319	7.191	1.359	2.022	4.194	73.510	59.128	.804
65.451	7.428	1.323	2.054	4.181	72.879	58.023	.796
65.136	7.113	1.323	2.054	4.176	72.248	58.023	.803
64.625	6.993	1.323	2.054	4.169	71.617	57.632	.805
64.503	6.168	1.359	2.022	4.167	70.671	58.334	.825
63.641	6.399	1.323	2.054	4.153	70.040	57.241	.817
63.070	6.024	1.323	2.054	4.144	69.093	57.046	.826
62.656	5.806	1.323	2.054	4.138	68.462	56.851	.830
62.528	4.988	1.359	2.022	4.136	67.516	57.541	.852
61.956	4.614	1.359	2.022	4.126	66.569	57.342	.861
60.944	4.679	1.323	2.054	4.110	65.623	56.265	.857
60.275	4.401	1.323	2.054	4.099	64.677	55.874	.864
59.704	4.026	1.323	2.054	4.089	63.730	55.678	.874
59.567	3.217	1.359	2.022	4.087	62.784	56.350	.898
59.152	3.000	1.359	2.022	4.080	62.153	56.152	.903
58.480	2.726	1.359	2.022	4.069	61.206	55.755	.911
57.481	2.779	1.323	2.054	4.051	60.259	54.702	.908
57.067	2.561	1.323	2.054	4.044	59.628	54.506	.914
56.921	1.761	1.359	2.022	4.042	58.682	55.160	.940
56.506	1.545	1.359	2.022	4.034	58.051	54.961	.947
55.512	1.592	1.323	2.054	4.017	57.104	53.920	.944
55.099	1.374	1.323	2.054	4.009	56.473	53.725	.951
54.686	1.157	1.323	2.054	4.002	55.843	53.530	.959
54.532	.364	1.359	2.022	3.999	54.896	54.167	.987
53.860	.090	1.359	2.022	3.986	53.950	53.771	.997
53.033	.285	1.323	2.054	3.971	53.319	52.748	.989
52.462	-.090	1.323	2.054	3.960	52.372	52.553	1.003
51.892	-.466	1.323	2.054	3.949	51.426	52.357	1.018
51.629	-1.150	1.359	2.022	3.944	50.479	52.779	1.046
51.214	-1.366	1.359	2.022	3.936	49.848	52.560	1.055

Table A1 continued

50.239	-1.337	1.323	2.054	3.917	48.902	51.576	1.055
49.668	-1.713	1.323	2.054	3.905	47.955	51.381	1.071
48.999	-1.990	1.323	2.054	3.892	47.009	50.990	1.085
48.825	-2.763	1.359	2.022	3.888	46.062	51.588	1.120
48.410	-2.979	1.359	2.022	3.880	45.431	51.390	1.131
47.739	-3.254	1.359	2.022	3.866	44.485	50.993	1.146
46.776	-3.237	1.323	2.054	3.845	43.538	50.013	1.149
46.205	-3.613	1.323	2.054	3.833	42.592	49.818	1.170
46.080	-4.119	1.359	2.022	3.830	41.961	50.199	1.196
45.350	-4.651	1.359	2.022	3.814	40.699	50.001	1.229
44.935	-4.867	1.359	2.022	3.805	40.068	49.802	1.243
44.263	-5.142	1.359	2.022	3.790	39.121	49.406	1.263
43.313	-5.138	1.323	2.054	3.768	38.175	48.450	1.269
42.644	-5.415	1.323	2.054	3.753	37.228	48.059	1.291
42.073	-5.791	1.323	2.054	3.739	36.282	47.864	1.319
42.032	-6.381	1.359	2.022	3.738	35.651	48.413	1.358
41.361	-6.656	1.359	2.022	3.722	34.704	48.017	1.384
40.788	-7.030	1.359	2.022	3.708	33.758	47.818	1.417
40.116	-7.305	1.359	2.022	3.692	32.811	47.421	1.445
39.544	-7.679	1.359	2.022	3.677	31.865	47.223	1.482
38.767	-7.534	1.323	2.054	3.658	31.234	46.301	1.482
38.099	-7.811	1.323	2.054	3.640	30.288	45.910	1.516
37.528	-8.187	1.323	2.054	3.625	29.341	45.715	1.558
36.957	-8.563	1.323	2.054	3.610	28.395	45.520	1.603
36.641	-9.193	1.359	2.022	3.601	27.448	45.834	1.670
35.969	-9.468	1.359	2.022	3.583	26.502	45.437	1.715
35.555	-9.684	1.359	2.022	3.571	25.871	45.239	1.749
34.982	-10.058	1.359	2.022	3.555	24.924	45.040	1.807
34.468	-10.175	1.359	2.022	3.540	24.293	44.644	1.838
34.054	-10.392	1.359	2.022	3.528	23.662	44.445	1.878
33.141	-10.425	1.323	2.054	3.501	22.716	43.566	1.918
32.728	-10.643	1.323	2.054	3.486	22.084	43.371	1.964
32.157	-11.019	1.323	2.054	3.471	21.138	43.175	2.043
31.646	-11.139	1.323	2.054	3.455	20.507	42.785	2.086
31.308	-11.748	1.359	2.022	3.444	19.561	43.056	2.201

Table A1 continued

30.736	-12.122	1.359	2.022	3.425	18.614	42.858	2.302
30.321	-12.338	1.359	2.022	3.412	17.983	42.660	2.372
29.650	-12.613	1.359	2.022	3.389	17.037	42.263	2.481
29.235	-12.829	1.359	2.022	3.375	16.406	42.064	2.564
28.820	-13.046	1.359	2.022	3.361	15.775	41.866	2.654
28.405	-13.262	1.359	2.022	3.347	15.144	41.667	2.751
27.672	-13.159	1.323	2.054	3.320	14.513	40.831	2.813
27.416	-13.219	1.323	2.054	3.311	14.197	40.636	2.862
27.003	-13.437	1.323	2.054	3.296	13.566	40.440	2.981
26.492	-13.557	1.323	2.054	3.277	12.935	40.049	3.096
26.391	-14.086	1.359	2.022	3.273	12.304	40.477	3.290
26.134	-14.145	1.359	2.022	3.263	11.989	40.278	3.360
25.719	-14.361	1.359	2.022	3.247	11.358	40.080	3.529
25.304	-14.577	1.359	2.022	3.231	10.727	39.882	3.718
25.047	-14.636	1.359	2.022	3.221	10.411	39.683	3.812
24.633	-14.852	1.359	2.022	3.204	9.780	39.485	4.037
24.218	-15.068	1.359	2.022	3.187	9.149	39.286	4.294
23.961	-15.127	1.359	2.022	3.176	8.834	39.088	4.425
23.546	-15.343	1.359	2.022	3.159	8.203	38.889	4.741
22.992	-15.104	1.323	2.054	3.135	7.887	38.096	4.830
22.578	-15.322	1.323	2.054	3.117	7.256	37.901	5.223
22.323	-15.382	1.323	2.054	3.106	6.941	37.705	5.432
21.812	-15.502	1.323	2.054	3.082	6.310	37.314	5.914
21.847	-15.852	1.359	2.022	3.084	5.994	37.699	6.289
21.432	-16.069	1.359	2.022	3.065	5.363	37.500	6.992
21.175	-16.127	1.359	2.022	3.053	5.048	37.302	7.390
20.760	-16.344	1.359	2.022	3.033	4.417	37.104	8.401
20.346	-16.560	1.359	2.022	3.013	3.786	36.905	9.748
19.990	-16.519	1.359	2.022	2.995	3.471	36.508	10.519
19.575	-16.735	1.359	2.022	2.974	2.840	36.310	12.787
19.318	-16.794	1.359	2.022	2.961	2.524	36.112	14.307
18.804	-16.911	1.359	2.022	2.934	1.893	35.715	18.866
18.547	-16.969	1.359	2.022	2.920	1.578	35.516	22.514
18.018	-16.756	1.323	2.054	2.891	1.262	34.775	27.555
17.665	-16.719	1.323	2.054	2.872	.947	34.384	36.327

Table A1 continued

17.410	-16.779	1.323	2.054	2.857	.631	34.188	54.180
17.057	-16.741	1.323	2.054	2.837	.316	33.798	107.123

Table A2. Compaction data for cubic sodium chloride compacted uniaxially at 155 MPa

σ (MPa)	τ (MPa)	ε	V ($m \times 10^{-6}$)	$\ln \sigma$	σ_A (MPa)	σ_R MPa	$\frac{\sigma_R}{\sigma_A}$
.3730	.2580	0.0000	3.4760	-.9860	.6310	.1150	.1830
1.3420	.8670	.0280	3.3810	.2940	2.2090	.4750	.2150
2.4140	1.6880	.0480	3.3180	.8810	4.1020	.7260	.1770
3.7100	2.6000	.0680	3.2550	1.3110	6.3100	1.1100	.1760
4.8560	3.3470	.0890	3.1920	1.5800	8.2030	1.5090	.1840
5.7880	3.9920	.1110	3.1280	1.7560	9.7800	1.7960	.1840
6.7160	4.6420	.1220	3.0970	1.9040	11.3580	2.0730	.1830
7.7240	5.2110	.1460	3.0340	2.0440	12.9350	2.5130	.1940
8.6450	5.8670	.1460	3.0340	2.1570	14.5130	2.7780	.1910
9.7560	6.6490	.1700	2.9700	2.2780	16.4060	3.1070	.1890
10.6980	7.2850	.1830	2.9390	2.3700	17.9830	3.4140	.1900
11.6440	7.9170	.1960	2.9070	2.4550	19.5610	3.7270	.1910
12.5930	8.5460	.2090	2.8760	2.5330	21.1380	4.0470	.1910
13.5450	9.1710	.2220	2.8440	2.6060	22.7160	4.3740	.1930
14.5010	9.7920	.2360	2.8120	2.6740	24.2930	4.7080	.1940
15.4610	10.4100	.2500	2.7810	2.7380	25.8710	5.0510	.1950
16.4240	11.0240	.2640	2.7490	2.7990	27.4480	5.4010	.1970
16.9710	11.4240	.2640	2.7490	2.8310	28.3950	5.5460	.1950
17.5500	11.7910	.2790	2.7180	2.8650	29.3410	5.7590	.1960
17.9390	12.0330	.2790	2.7180	2.8870	29.9720	5.9060	.1970
18.3280	12.2740	.2790	2.7180	2.9080	30.6030	6.0540	.1980
18.6440	12.5900	.2790	2.7180	2.9260	31.2340	6.0540	.1940
19.2280	12.9530	.2940	2.6860	2.9560	32.1800	6.2750	.1950
19.6180	13.1940	.2940	2.6860	2.9760	32.8110	6.4240	.1960
20.0470	13.3950	.3100	2.6540	2.9980	33.4420	6.6520	.1990
20.5960	13.7930	.3100	2.6540	3.0250	34.3690	6.8030	.1980
20.9870	14.0330	.3100	2.6540	3.0440	35.0200	6.9540	.1990
21.5360	14.4310	.3100	2.6540	3.0700	35.9660	7.1050	.1980

Table A2 continued

22.1280	14.7850	.3250	2.6230	3.0970	36.9130	7.3440	.1990
22.5200	15.0240	.3250	2.6230	3.1140	37.5440	7.4970	.2000
23.0700	15.4200	.3250	2.6230	3.1390	38.4910	7.6500	.1990
23.5100	15.6120	.3410	2.5910	3.1570	39.1210	7.8980	.2020
24.0600	16.0080	.3410	2.5910	3.1810	40.0680	8.0530	.2010
24.6110	16.4030	.3410	2.5910	3.2030	41.0140	8.2080	.2000
25.0040	16.6410	.3410	2.5910	3.2190	41.6450	8.3620	.2010
25.6070	16.9850	.3580	2.5600	3.2430	42.5920	8.6230	.2020
26.1590	17.3790	.3580	2.5600	3.2640	43.5380	8.7790	.2020
26.7100	17.7740	.3580	2.5600	3.2850	44.4850	8.9360	.2010
27.1610	17.9550	.3750	2.5280	3.3020	45.1160	9.2070	.2040
27.7930	18.2690	.3750	2.5280	3.3250	46.0620	9.5240	.2070
28.3460	18.6630	.3750	2.5280	3.3440	47.0090	9.6830	.2060
28.8980	19.0570	.3750	2.5280	3.3640	47.9550	9.8410	.2050
29.5950	19.3070	.3920	2.4960	3.3860	48.9020	10.2860	.2100
30.1480	19.7000	.3920	2.4960	3.4060	49.8480	10.4480	.2100
30.7020	20.0930	.3920	2.4960	3.4240	50.7950	10.6090	.2090
31.3240	20.4170	.4100	2.4650	3.4440	51.7410	10.9060	.2110
31.7320	20.6400	.3920	2.4960	3.4570	52.3720	11.0910	.2120
32.3570	20.9610	.4100	2.4650	3.4770	53.3190	11.3960	.2140
32.7540	21.1950	.4100	2.4650	3.4890	53.9500	11.5590	.2140
33.3090	21.5870	.4100	2.4650	3.5060	54.8960	11.7220	.2140
33.7830	21.7440	.4290	2.4330	3.5200	55.5270	12.0390	.2170
34.3390	22.1350	.4290	2.4330	3.5360	56.4730	12.2040	.2160
34.7370	22.3680	.4290	2.4330	3.5480	57.1040	12.3690	.2170
35.1350	22.6010	.4290	2.4330	3.5590	57.7350	12.5340	.2170
35.6150	22.7510	.4290	2.4330	3.5730	58.3660	12.8640	.2200
36.1710	23.1420	.4290	2.4330	3.5880	59.3130	13.0280	.2200
36.4140	23.2140	.4470	2.4020	3.5950	59.6280	13.2000	.2210
36.8130	23.4460	.4470	2.4020	3.6060	60.2590	13.3670	.2220
37.2120	23.6780	.4470	2.4020	3.6170	60.8910	13.5340	.2220
37.6110	23.9100	.4470	2.4020	3.6270	61.5220	13.7010	.2230
38.0100	24.1420	.4470	2.4020	3.6360	62.1530	13.8680	.2230
38.4090	24.3740	.4470	2.4020	3.6480	62.7840	14.0350	.2240
38.6510	24.4480	.4470	2.4020	3.6550	63.0990	14.2020	.2250

Table A2 continued

39.1460	24.5850	.4670	2.3700	3.6670	63.7300	14.5610	.2280
39.5460	24.8150	.4670	2.3700	3.6770	64.3610	14.7300	.2290
39.7880	24.8880	.4670	2.3700	3.6840	64.6770	14.9000	.2300
40.1030	25.2040	.4670	2.3700	3.6910	65.3070	14.9000	.2280
40.3460	25.2770	.4670	2.3700	3.6970	65.6230	15.0690	.2300
40.6610	25.5920	.4670	2.3700	3.7050	66.2540	15.0690	.2270
40.9040	25.6650	.4670	2.3700	3.7110	66.5690	15.2380	.2290
41.3040	25.8960	.4670	2.3700	3.7210	67.2000	15.4080	.2290
41.8620	26.2850	.4670	2.3700	3.7340	68.1470	15.5770	.2290
42.4540	26.3240	.4860	2.3380	3.7480	68.7780	16.1310	.2350
43.0130	26.7110	.4860	2.3380	3.7620	69.7240	16.3020	.2340
43.4150	26.9410	.4860	2.3380	3.7710	70.3550	16.4740	.2340
43.8160	27.1700	.4860	2.3380	3.7800	70.9860	16.6460	.2340
44.2170	27.4000	.4860	2.3380	3.7890	71.6170	16.8170	.2350
44.6190	27.6300	.4860	2.3380	3.7980	72.2480	16.9890	.2350
45.1760	28.0170	.4860	2.3380	3.8110	73.1950	17.1600	.2340
45.7360	28.4050	.4860	2.3380	3.8230	74.1410	17.3320	.2340
46.4150	28.6720	.5070	2.3070	3.8380	75.0880	17.7430	.2360
46.9050	28.8140	.5070	2.3070	3.8480	75.7190	18.0910	.2390
47.4650	29.2000	.5070	2.3070	3.8600	76.6650	18.2650	.2380
47.9550	29.3420	.5070	2.3070	3.8700	77.2960	18.6130	.2410
48.5150	29.7280	.5070	2.3070	3.8820	78.2430	18.7870	.2400
48.9170	29.9560	.5070	2.3070	3.8900	78.8740	18.9610	.2400
49.4780	30.3430	.5070	2.3070	3.9020	79.8200	19.1350	.2400
49.8800	30.5710	.5070	2.3070	3.9100	80.4510	19.3090	.2400
50.5760	30.8220	.5280	2.2750	3.9230	81.3980	19.7530	.2430
51.0670	30.9610	.5280	2.2750	3.9330	82.0290	20.1060	.2450
51.6290	31.3460	.5280	2.2750	3.9440	82.9750	20.2820	.2440
52.0320	31.5740	.5280	2.2750	3.9520	83.6060	20.4590	.2450
52.5240	31.7130	.5280	2.2750	3.9610	84.2370	20.8120	.2470
52.9280	31.9400	.5280	2.2750	3.9690	84.8680	20.9880	.2470
53.4890	32.3250	.5280	2.2750	3.9790	85.8150	21.1640	.2470
53.9810	32.4640	.5280	2.2750	3.9890	86.4460	21.5170	.2490
54.5380	32.5390	.5490	2.2440	3.9990	87.0770	21.9990	.2530
54.9430	32.7650	.5490	2.2440	4.0060	87.7080	22.1780	.2530

Table A2 continued

55.5050	33.1490	.5490	2.2440	4.0160	88.6540	22.3570	.2520
56.0000	33.2850	.5490	2.2440	4.0250	89.2650	22.7140	.2540
56.5620	33.6690	.5490	2.2440	4.0350	90.2320	22.8930	.2540
56.9670	33.8950	.5490	2.2440	4.0420	90.8630	23.0720	.2540
57.6190	34.1890	.5490	2.2440	4.0540	91.8090	23.4300	.2550
58.1820	34.5730	.5490	2.2440	4.0640	92.7550	23.6090	.2550
58.5870	34.7990	.5490	2.2440	4.0710	93.3860	23.7880	.2550
59.2390	35.0940	.5490	2.2440	4.0820	94.3330	24.1450	.2560
59.8180	35.1460	.5710	2.2120	4.0910	94.9640	24.6720	.2600
60.2240	35.3710	.5710	2.2120	4.0980	95.5950	24.8530	.2600
60.8790	35.6630	.5710	2.2120	4.1090	96.5410	25.2160	.2610
61.2850	35.8880	.5710	2.2120	4.1160	97.1720	25.3970	.2610
61.8490	36.2700	.5710	2.2120	4.1250	98.1190	25.5790	.2610
62.3460	36.4040	.5710	2.2120	4.1330	98.7500	25.9410	.2630
62.9100	36.7870	.5710	2.2120	4.1420	99.6960	26.1230	.2620
63.4060	36.9210	.5710	2.2120	4.1500	100.3270	26.4860	.2640
63.8130	37.1460	.5710	2.2120	4.1560	100.9580	26.6670	.2640
64.6630	37.2420	.5940	2.1800	4.1690	101.9050	27.4220	.2690
64.8740	37.6620	.5710	2.2120	4.1720	102.5360	27.2110	.2650
65.7280	37.7540	.5940	2.1800	4.1860	103.4820	27.9740	.2700
66.2930	38.1350	.5940	2.1800	4.1940	104.4290	28.1580	.2700
66.9510	38.4250	.5940	2.1800	4.2040	105.3750	28.5260	.2710
67.5160	38.8060	.5940	2.1800	4.2120	106.3220	28.7100	.2700
68.1730	39.0950	.5940	2.1800	4.2220	107.2680	29.0780	.2710
68.5810	39.3190	.5940	2.1800	4.2280	107.8990	29.2620	.2710
69.2380	39.6080	.5940	2.1800	4.2380	108.8460	29.6300	.2720
69.6450	39.8310	.5940	2.1800	4.2430	109.4770	29.8140	.2720
70.3030	40.1200	.5940	2.1800	4.2530	110.4230	30.1820	.2730
70.7100	40.3440	.5940	2.1800	4.2590	111.0540	30.3660	.2730
71.3680	40.6330	.5940	2.1800	4.2680	112.0010	30.7340	.2740
72.0020	40.6290	.6180	2.1490	4.2770	112.6320	31.3730	.2790
72.5690	41.0090	.6180	2.1490	4.2850	113.5780	31.5600	.2780
73.0710	41.1380	.6180	2.1490	4.2910	114.2090	31.9330	.2800
73.7310	41.4240	.6180	2.1490	4.3000	115.1560	32.3070	.2810
74.2980	41.8040	.6180	2.1490	4.3080	116.1020	32.4940	.2800

Table A2 continued

74.7070	42.0270	.6180	2.1490	4.3140	116.7330	32.6800	.2800
75.3670	42.3130	.6180	2.1490	4.3220	117.6790	33.0540	.2810
75.8690	42.4420	.6180	2.1490	4.3290	118.3100	33.4270	.2830
76.4360	42.8210	.6180	2.1490	4.3360	119.2570	33.6140	.2820
76.9380	42.9500	.6180	2.1490	4.3430	119.8880	33.9870	.2830
77.5040	43.3300	.6180	2.1490	4.3500	120.8340	34.1740	.2830
78.0070	43.4590	.6180	2.1490	4.3570	121.4660	34.5480	.2840
78.5730	43.8390	.6180	2.1490	4.3640	122.4120	34.7340	.2840
79.4950	43.8630	.6420	2.1170	4.3760	123.3590	35.6320	.2890
79.6420	44.3470	.6180	2.1490	4.3780	123.9900	35.2950	.2850
80.5680	44.3680	.6420	2.1170	4.3890	124.9360	36.2010	.2900
80.9780	44.5880	.6420	2.1170	4.3940	125.5670	36.3900	.2900
81.6410	44.8720	.6420	2.1170	4.4020	126.5130	36.7690	.2910
82.2090	45.2510	.6420	2.1170	4.4090	127.4600	36.9590	.2900
82.7140	45.3770	.6420	2.1170	4.4150	128.0910	37.3380	.2910
82.9670	45.4400	.6420	2.1170	4.4180	128.4060	37.5270	.2920
83.3770	45.6600	.6420	2.1170	4.4230	129.0370	37.7170	.2920
84.0400	45.9440	.6420	2.1170	4.4310	129.9840	38.0960	.2930
84.5450	46.0700	.6420	2.1170	4.4370	130.6150	38.4750	.2950
85.1130	46.4490	.6420	2.1170	4.4440	131.5610	38.6640	.2940
85.7760	46.7320	.6420	2.1170	4.4520	132.5080	39.0440	.2950
86.1860	46.9530	.6420	2.1170	4.4570	133.1390	39.2330	.2950
86.8490	47.2370	.6420	2.1170	4.4640	134.0850	39.6120	.2950
87.4170	47.6150	.6420	2.1170	4.4710	135.0320	39.8020	.2950
87.9220	47.7410	.6420	2.1170	4.4760	135.6630	40.1810	.2960
88.8920	47.7170	.6670	2.0860	4.4870	136.6090	41.1740	.3010
89.2470	48.3080	.6420	2.1170	4.4910	137.5560	40.9390	.2980
90.1270	48.3750	.6670	2.0860	4.5010	138.5020	41.7510	.3010
90.3200	48.8130	.6420	2.1170	4.5030	139.1330	41.5070	.2980
91.3000	48.7790	.6670	2.0860	4.5140	140.0800	42.5210	.3040
91.3930	49.3170	.6420	2.1170	4.5150	140.7110	42.0760	.2990
92.2820	49.3760	.6670	2.0860	4.5250	141.6570	42.9060	.3030
92.7890	49.4990	.6670	2.0860	4.5300	142.2880	43.2910	.3040
93.2010	49.7180	.6670	2.0860	4.5350	142.9190	43.4830	.3040
93.7090	49.8410	.6670	2.0860	4.5400	143.5500	43.8680	.3060

Table A2 continued

94.2170	49.9640	.6670	2.0860	4.5460	144.1810	44.2530	.3070
94.7860	50.3410	.6670	2.0860	4.5520	145.1280	44.4450	.3060
95.2940	50.4640	.6670	2.0860	4.5570	145.7590	44.8300	.3080
95.8020	50.5870	.6670	2.0860	4.5620	146.3900	45.2150	.3090
96.3720	50.9650	.6670	2.0860	4.5680	147.3360	45.4070	.3080
97.0370	51.2450	.6670	2.0860	4.5750	148.2830	45.7920	.3090
97.7030	51.5260	.6670	2.0860	4.5820	149.2290	46.1770	.3090
98.1150	51.7450	.6670	2.0860	4.5860	149.8600	46.3690	.3090
98.5260	51.9650	.6670	2.0860	4.5900	150.4910	46.5620	.3090
99.0340	52.0880	.6670	2.0860	4.5950	151.1220	46.9460	.3110
99.2880	52.1490	.6670	2.0860	4.5980	151.4380	47.1390	.3110
99.5420	52.2110	.6670	2.0860	4.6010	151.7530	47.3310	.3120
99.6380	52.1150	.6670	2.0860	4.6020	151.7530	47.5240	.3130
100.1620	51.9070	.6920	2.0540	4.6070	152.0680	48.2550	.3170
100.1460	52.2380	.6670	2.0860	4.6070	152.3840	47.9080	.3140
100.6720	52.0270	.6920	2.0540	4.6120	152.6990	48.6460	.3190
100.5580	52.4570	.6670	2.0860	4.6110	153.0150	48.1010	.3140
101.0860	52.2450	.6920	2.0540	4.6160	153.3300	48.8410	.3190
100.9700	52.6760	.6670	2.0860	4.6150	153.6460	48.2930	.3140
101.5960	52.3650	.6920	2.0540	4.6210	153.9610	49.2320	.3200
101.7540	52.5230	.6920	2.0540	4.6230	154.2770	49.2320	.3190
102.0100	52.5830	.6920	2.0540	4.6250	154.5920	49.4270	.3200
102.2650	52.6430	.6920	2.0540	4.6280	154.9080	49.6220	.3200
102.5210	52.7030	.6920	2.0540	4.6300	155.2230	49.8180	.3210
102.7760	52.7630	.6920	2.0540	4.6330	155.5390	50.0130	.3220
102.9340	52.9210	.6920	2.0540	4.6340	155.8540	50.0130	.3210
102.8740	52.6650	.6920	2.0540	4.6340	155.5390	50.2080	.3230
102.3030	52.2900	.6920	2.0540	4.6280	154.5920	50.0130	.3240
101.6720	51.6590	.6920	2.0540	4.6220	153.3300	50.0130	.3260
100.9430	51.1250	.6920	2.0540	4.6150	152.0680	49.8180	.3280
100.4700	50.6520	.6920	2.0540	4.6100	151.1220	49.8180	.3300
99.8990	50.2770	.6920	2.0540	4.6040	150.1760	49.6220	.3300
99.4860	50.0590	.6920	2.0540	4.6000	149.5450	49.4270	.3310
99.0130	49.5860	.6920	2.0540	4.5950	148.5980	49.4270	.3330
98.5990	49.3680	.6920	2.0540	4.5910	147.9670	49.2320	.3330

Table A2 continued

98.2840	49.0520	.6920	2.0540	4.5880	147.3360	49.2320	.3340
97.8710	48.8340	.6920	2.0540	4.5840	146.7050	49.0360	.3340
97.5550	48.5190	.6920	2.0540	4.5800	146.0740	49.0360	.3360
97.3970	48.3610	.6920	2.0540	4.5790	145.7590	49.0360	.3360
96.9840	48.1430	.6920	2.0540	4.5750	145.1280	48.8410	.3370
96.6690	47.8280	.6920	2.0540	4.5710	144.4970	48.8410	.3380
96.0980	47.4520	.6920	2.0540	4.5650	143.5500	48.6460	.3390
95.7820	47.1370	.6920	2.0540	4.5620	142.9190	48.6460	.3400
95.3690	46.9190	.6920	2.0540	4.5580	142.2880	48.4500	.3410
94.7980	46.5440	.6920	2.0540	4.5520	141.3420	48.2550	.3410
94.4830	46.2280	.6920	2.0540	4.5480	140.7110	48.2550	.3430
93.9120	45.8520	.6920	2.0540	4.5420	139.7640	48.0590	.3440
93.1830	45.3190	.6920	2.0540	4.5350	138.5020	47.8640	.3460
92.8680	45.0040	.6920	2.0540	4.5310	137.8710	47.8640	.3470
91.3130	44.0350	.6920	2.0540	4.5140	135.3470	47.2780	.3490
91.1550	43.8770	.6920	2.0540	4.5130	135.0320	47.2780	.3500
90.7420	43.6590	.6920	2.0540	4.5080	134.4010	47.0830	.3500
90.4260	43.3440	.6920	2.0540	4.5050	133.7700	47.0830	.3520
90.1710	43.2840	.6920	2.0540	4.5020	133.4540	46.8870	.3510
89.8550	42.9680	.6920	2.0540	4.4980	132.8230	46.8870	.3530
89.6980	42.8100	.6920	2.0540	4.4960	132.5080	46.8870	.3540
89.2840	42.5930	.6920	2.0540	4.4920	131.8770	46.6920	.3540
88.2400	41.7440	.6920	2.0540	4.4800	129.9840	46.4960	.3580
86.7830	40.6770	.6920	2.0540	4.4630	127.4600	46.1060	.3620
85.3260	39.6110	.6920	2.0540	4.4460	124.9360	45.7150	.3660
84.1240	38.6040	.6920	2.0540	4.4320	122.7280	45.5200	.3710
82.9220	37.5970	.6920	2.0540	4.4180	120.5190	45.3240	.3760
81.9370	37.0040	.6920	2.0540	4.4060	118.9410	44.9330	.3780
81.7800	36.8460	.6920	2.0540	4.4040	118.6260	44.9330	.3790
81.6220	36.6880	.6920	2.0540	4.4020	118.3100	44.9330	.3800
81.2090	36.4710	.6920	2.0540	4.3970	117.6790	44.7380	.3800
81.0510	36.3130	.6920	2.0540	4.3950	117.3640	44.7380	.3810
80.7960	36.2530	.6920	2.0540	4.3920	117.0480	44.5430	.3810
80.6380	36.0950	.6920	2.0540	4.3900	116.7330	44.5430	.3820
80.4800	35.9370	.6920	2.0540	4.3880	116.4180	44.5430	.3830

Table A2 continued

80.0670	35.7200	.6920	2.0540	4.3830	115.7870	44.3480	.3830
80.0670	35.7200	.6920	2.0540	4.3830	115.7870	44.3480	.3830
79.6540	35.5020	.6920	2.0540	4.3760	115.1560	44.1520	.3830
79.4960	35.3440	.6920	2.0540	4.3760	114.8400	44.1520	.3840
79.0830	35.1260	.6920	2.0540	4.3700	114.2090	43.9570	.3850
78.8270	35.0660	.6920	2.0540	4.3670	113.8940	43.7610	.3840
78.3540	34.5930	.6920	2.0540	4.3610	112.9470	43.7610	.3870
78.0390	34.2770	.6920	2.0540	4.3570	112.3160	43.7610	.3900
77.4680	33.9020	.6920	2.0540	4.3500	111.3700	43.5660	.3910
77.1520	33.5860	.6920	2.0540	4.3460	110.7390	43.5660	.3930
76.7390	33.3680	.6920	2.0540	4.3400	110.1080	43.3710	.3940
76.2660	32.8950	.6920	2.0540	4.3340	109.1610	43.3710	.3970
75.8530	32.6770	.6920	2.0540	4.3290	108.5300	43.1750	.3980
75.2820	32.3020	.6920	2.0540	4.3210	107.5840	42.9800	.4000
74.6410	32.3120	.6670	2.0860	4.3130	106.9530	42.3290	.3960
74.2980	31.7090	.6920	2.0540	4.3080	106.0060	42.5890	.4020
73.9820	31.3930	.6920	2.0540	4.3040	105.3750	42.5890	.4040
73.5690	31.1750	.6920	2.0540	4.2980	104.7440	42.3940	.4050
72.9980	30.8000	.6920	2.0540	4.2900	103.7980	42.1980	.4070
72.3630	30.8040	.6670	2.0860	4.2820	103.1670	41.5590	.4030
72.3670	30.1690	.6920	2.0540	4.2820	102.5360	42.1980	.4120
71.9540	29.9510	.6920	2.0540	4.2760	101.9050	42.0030	.4120
71.6380	29.6350	.6920	2.0540	4.2720	101.2740	42.0030	.4150
71.2250	29.4170	.6920	2.0540	4.2660	100.6430	41.8080	.4150
70.4970	29.5150	.6670	2.0860	4.2560	100.0120	40.9820	.4100
70.4970	28.8840	.6920	2.0540	4.2560	99.3810	41.6120	.4190
69.9860	28.7640	.6920	2.0540	4.2480	98.7500	41.2220	.4170
69.2000	28.6030	.6670	2.0860	4.2370	97.8030	40.5970	.4150
69.0990	28.0730	.6920	2.0540	4.2360	97.1720	41.0260	.4220
68.4730	28.0680	.6670	2.0860	4.2260	96.5410	40.4050	.4190
68.3710	27.5400	.6920	2.0540	4.2250	95.9100	40.8310	.4260
67.8000	27.1640	.6920	2.0540	4.2170	94.9640	40.6360	.4280
66.9220	27.0950	.6670	2.0860	4.2040	94.0170	39.8280	.4240
66.9130	26.4730	.6920	2.0540	4.2030	93.3860	40.4400	.4330
66.5000	26.2550	.6920	2.0540	4.1970	92.7550	40.2450	.4340

Table A2 continued

65.9290	25.8800	.6920	2.0540	4.1890	91.8090	40.0490	.4360
65.5160	25.6620	.6920	2.0540	4.1820	91.1780	39.8540	.4370
64.8020	25.7450	.6670	2.0860	4.1710	90.5470	39.0580	.4310
64.7870	25.1290	.6920	2.0540	4.1710	89.9160	39.6590	.4410
64.0750	25.2100	.6670	2.0860	4.1600	89.2850	38.8650	.4350
63.9170	25.0520	.6670	2.0860	4.1580	88.9700	38.8650	.4370
63.8030	24.5350	.6920	2.0540	4.1560	88.3390	39.2680	.4450
63.1900	24.5170	.6670	2.0860	4.1460	87.7080	38.6730	.4410
63.2320	24.1600	.6920	2.0540	4.1470	87.3920	39.0730	.4470
62.6210	24.1400	.6670	2.0860	4.1370	86.7610	38.4810	.4440
62.2090	23.9210	.6670	2.0860	4.1310	86.1300	38.2880	.4450
62.1880	23.3110	.6920	2.0540	4.1300	85.4990	38.8770	.4550
61.3240	23.2280	.6670	2.0860	4.1160	84.5530	38.0960	.4510
61.2040	22.7180	.6920	2.0540	4.1140	83.9220	38.4870	.4590
60.3430	22.6320	.6670	2.0860	4.1000	82.9750	37.7110	.4540
59.8700	22.1590	.6670	2.0860	4.0920	82.0290	37.7110	.4600
59.4910	21.5910	.6920	2.0540	4.0860	81.0820	37.9010	.4670
58.8890	21.5620	.6670	2.0860	4.0760	80.4510	37.3260	.4640
58.6050	20.9000	.6920	2.0540	4.0710	79.5050	37.7050	.4740
57.9080	20.9660	.6670	2.0860	4.0590	78.8740	36.9410	.4680
57.4340	20.4930	.6670	2.0860	4.0510	77.9270	36.9410	.4740
57.2080	20.0890	.6920	2.0540	4.0470	77.2960	37.1190	.4800
56.4530	19.8970	.6670	2.0860	4.0330	76.3500	36.5570	.4790
56.0410	19.6770	.6670	2.0860	4.0260	75.7190	36.3640	.4800
55.4720	19.3000	.6670	2.0860	4.0160	74.7720	36.1720	.4840
55.0600	19.0810	.6670	2.0860	4.0080	74.1410	35.9790	.4850
54.6490	18.8620	.6670	2.0860	4.0010	73.5100	35.7870	.4870
54.1750	18.3880	.6670	2.0860	3.9920	72.5640	35.7870	.4930
53.7640	18.1690	.6670	2.0860	3.9850	71.9330	35.5950	.4950
53.3520	17.9500	.6670	2.0860	3.9770	71.3020	35.4020	.4970
53.0370	17.6340	.6670	2.0860	3.9710	70.6710	35.4020	.5010
52.7830	17.5730	.6670	2.0860	3.9660	70.3550	35.2100	.5000
52.4670	17.2570	.6670	2.0860	3.9600	69.7240	35.2100	.5050
52.4820	16.9260	.6920	2.0540	3.9600	69.4090	35.5560	.5120
51.8980	16.8800	.6670	2.0860	3.9490	68.7780	35.0170	.5090

Table A2 continued

51.4860	16.6610	.6670	2.0860	3.9410	68.1470	34.8250	.5110
51.3280	16.5030	.6670	2.0860	3.9380	67.8310	34.8250	.5130
50.9160	16.2840	.6670	2.0860	3.9300	67.2000	34.6330	.5150
50.7700	15.8000	.6920	2.0540	3.9270	66.5690	34.9700	.5250
50.0930	15.8450	.6670	2.0860	3.9140	65.9380	34.2480	.5190
49.7780	15.5300	.6670	2.0860	3.9080	65.3070	34.2480	.5240
49.2080	15.1530	.6670	2.0860	3.8960	64.3610	34.0550	.5290
48.7960	14.9340	.6670	2.0860	3.8880	63.7300	33.8630	.5310
48.3850	14.7140	.6670	2.0860	3.8790	63.0990	33.6700	.5340
47.9110	14.2410	.6670	2.0860	3.8690	62.1530	33.6700	.5420
47.5000	14.0220	.6670	2.0860	3.8610	61.5220	33.4780	.5440
46.9300	13.6450	.6670	2.0860	3.8490	60.5750	33.2860	.5490
46.5190	13.4250	.6670	2.0860	3.8400	59.9440	33.0930	.5520
45.9490	13.0480	.6670	2.0860	3.8260	58.9970	32.9010	.5580
45.4760	12.5750	.6670	2.0860	3.8170	58.0510	32.9010	.5670
45.0640	12.3560	.6670	2.0860	3.8080	57.4200	32.7090	.5700
44.6520	12.1360	.6670	2.0860	3.7990	56.7890	32.5160	.5730
44.3370	11.8210	.6670	2.0860	3.7920	56.1580	32.5160	.5790
43.9250	11.6020	.6670	2.0860	3.7820	55.5270	32.3240	.5820
43.5140	11.3820	.6670	2.0860	3.7730	54.8960	32.1310	.5850
43.1980	11.0670	.6670	2.0860	3.7660	54.2650	32.1310	.5920
42.7870	10.8480	.6670	2.0860	3.7560	53.6340	31.9390	.5950
42.3750	10.6280	.6670	2.0860	3.7470	53.0030	31.7470	.5990
42.0590	10.3130	.6670	2.0860	3.7390	52.3720	31.7470	.6060
41.6480	10.0940	.6670	2.0860	3.7290	51.7410	31.5540	.6100
41.2360	9.8740	.6670	2.0860	3.7190	51.1100	31.3620	.6140
40.9200	9.5590	.6670	2.0860	3.7120	50.4790	31.3620	.6210
40.5090	9.3390	.6670	2.0860	3.7020	49.8480	31.1690	.6250
40.0350	8.8660	.6670	2.0860	3.6900	48.9020	31.1690	.6370
39.6240	8.6470	.6670	2.0860	3.6790	48.2710	30.9770	.6420
39.0540	8.2700	.6670	2.0860	3.6650	47.3240	30.7850	.6510
38.6430	8.0510	.6670	2.0860	3.6540	46.6930	30.5920	.6550
38.0730	7.6740	.6670	2.0860	3.6400	45.7470	30.4000	.6650
37.5040	7.2970	.6670	2.0860	3.6240	44.8000	30.2070	.6740
37.1880	6.9810	.6670	2.0860	3.6160	44.1690	30.2070	.6840

Table A2 continued

36.6190	6.6040	.6670	2.0860	3.6010	43.2230	30.0150	.6940
36.3650	6.5420	.6670	2.0860	3.5940	42.9070	29.8220	.6950
35.9530	6.3230	.6670	2.0860	3.5820	42.2760	29.6300	.7010
35.6380	6.0080	.6670	2.0860	3.5730	41.6450	29.6300	.7110
35.2260	5.7880	.6670	2.0860	3.5620	41.0140	29.4380	.7180
34.6570	5.4110	.6670	2.0860	3.5450	40.0680	29.2450	.7300
34.0870	5.0340	.6670	2.0860	3.5290	39.1210	29.0530	.7430
33.5180	4.6570	.6670	2.0860	3.5120	38.1750	28.8600	.7560
32.7910	4.1220	.6670	2.0860	3.4900	36.9130	28.6680	.7770
32.2210	3.7450	.6670	2.0860	3.4730	35.9660	28.4760	.7920
31.6520	3.3680	.6670	2.0860	3.4550	35.0200	28.2830	.8080
30.9240	2.8330	.6670	2.0860	3.4320	33.7580	28.0910	.8320
30.3550	2.4560	.6670	2.0860	3.4130	32.8110	27.8990	.8500
29.9430	2.2370	.6670	2.0860	3.3990	32.1800	27.7060	.8610
29.5320	2.0180	.6670	2.0860	3.3850	31.5490	27.5140	.8720
28.9620	1.6410	.6670	2.0860	3.3660	30.6030	27.3210	.8930
28.5500	1.4220	.6670	2.0860	3.3520	29.9720	27.1290	.9050
28.1390	1.2020	.6670	2.0860	3.3370	29.3410	26.9370	.9180
27.7270	.9830	.6670	2.0860	3.3220	28.7100	26.7440	.9320
27.4120	.6670	.6670	2.0860	3.3110	28.0790	26.7440	.9520
26.8420	.2900	.6670	2.0860	3.2900	27.1330	26.5520	.9790
26.5880	.2290	.6670	2.0860	3.2800	26.8170	26.3590	.9830
26.2730	-.0870	.6670	2.0860	3.2690	26.1860	26.3590	1.0070
25.8610	-.3060	.6670	2.0860	3.2530	25.5550	26.1670	1.0240
25.5450	-.6210	.6670	2.0860	3.2400	24.9240	26.1670	1.0500
25.2910	-.6830	.6670	2.0860	3.2300	24.6090	25.9740	1.0560
24.8800	-.9020	.6670	2.0860	3.2140	23.9780	25.7820	1.0750
24.5540	-1.2180	.6670	2.0860	3.2010	23.3470	25.7820	1.1040
24.2140	-1.1830	.6670	2.0860	3.1870	23.0310	25.3970	1.1030
23.8990	-1.4990	.6670	2.0860	3.1740	22.4000	25.3970	1.1340
23.6450	-1.5600	.6670	2.0860	3.1630	22.0840	25.2050	1.1410
23.3290	-1.8760	.6670	2.0860	3.1500	21.4540	25.2050	1.1750
22.9180	-2.0950	.6670	2.0860	3.1320	20.8230	25.0120	1.2010
22.3480	-2.4720	.6670	2.0860	3.1070	19.8760	24.8200	1.2490
21.9360	-2.6910	.6670	2.0860	3.0880	19.2450	24.6280	1.2800

Table A2 continued

21.3670	-3.0680	.6670	2.0860	3.0620	18.2990	24.4350	1.3350
21.1130	-3.1300	.6670	2.0860	3.0500	17.9830	24.2430	1.3480
20.7010	-3.3490	.6670	2.0860	3.0300	17.3520	24.0500	1.3860
20.2900	-3.5680	.6670	2.0860	3.0100	16.7210	23.8580	1.4270
19.9740	-3.8840	.6670	2.0860	2.9940	16.0900	23.8580	1.4830
19.5620	-4.1030	.6670	2.0860	2.9740	15.4590	23.6660	1.5310
18.8350	-4.6380	.6670	2.0860	2.9360	14.1970	23.4730	1.6530
17.8540	-5.2340	.6670	2.0860	2.8820	12.6200	23.0880	1.8300
17.1270	-5.7690	.6670	2.0860	2.8410	11.3580	22.8960	2.0160
16.3040	-6.2080	.6670	2.0860	2.7910	10.0960	22.5110	2.2300
15.5760	-6.7420	.6670	2.0860	2.7460	8.8340	22.3190	2.5270
14.9110	-7.0230	.6670	2.0860	2.7020	7.8870	21.9340	2.7810
14.3410	-7.4000	.6670	2.0860	2.6630	6.9410	21.7410	3.1320
13.7720	-7.7770	.6670	2.0860	2.6230	5.9940	21.5490	3.5950
13.1060	-8.0580	.6670	2.0860	2.5730	5.0480	21.1640	4.1930
12.6940	-8.2780	.6670	2.0860	2.5410	4.4170	20.9720	4.7480
12.0290	-8.5580	.6670	2.0860	2.4870	3.4710	20.5870	5.9320
11.6170	-8.7780	.6670	2.0860	2.4520	2.8400	20.3950	7.1820
11.2050	-8.9970	.6670	2.0860	2.4160	2.2090	20.2020	9.1470
10.8550	-8.9620	.6670	2.0860	2.3850	1.8930	19.8180	10.4690
10.6010	-9.0240	.6670	2.0860	2.3610	1.5780	19.6250	12.4400
10.1900	-9.2430	.6670	2.0860	2.3210	.9470	19.4330	20.5310
9.9360	-9.3050	.6670	2.0860	2.2960	.6310	19.2400	30.4910

Table A3 Compaction data for dicalcium phosphate compacted uniaxially at 122 Mpa

σ (MPa)	τ (MPa)	ε	$V_{mx10^{-6}}$	$\ln\sigma$	σ_A (MPa)	σ_R (MPa)	σ_R/σ_A
.3160	.3160	0.0000	3.8550	-1.1540	.6310	0.0000	0.0000
.7410	.5210	.0610	3.8340	-.2990	1.2620	.2210	.1750
1.6510	1.1890	.1090	3.4760	.5010	2.8400	.4620	.1630
3.1610	2.2020	.1510	3.3500	1.1510	5.3630	.9580	.1790
4.7790	3.4230	.1840	3.2550	1.5640	8.2030	1.3560	.1650
6.4740	4.5690	.2200	3.1600	1.8680	11.0420	1.9050	.1730
8.1720	5.7100	.2450	3.0970	2.1010	13.8820	2.4620	.1770
9.4850	6.6050	.2580	3.0650	2.2500	16.0900	2.8800	.1790
10.2630	7.0890	.2710	3.0340	2.3290	17.3520	3.1750	.1830
10.8870	7.4120	.2840	3.0020	2.3860	18.2990	3.4750	.1900
11.4270	7.8180	.2840	3.0020	2.4360	19.2450	3.6090	.1880
12.0550	8.1370	.2980	2.9700	2.4890	20.1920	3.9180	.1940
12.6170	8.5210	.3120	2.9390	2.5350	21.1380	4.0960	.1940
13.3850	9.0150	.3120	2.9390	2.5940	22.4000	4.3690	.1950
14.1770	9.4850	.3260	2.9070	2.6520	23.6620	4.6930	.1980
14.8780	10.0470	.3260	2.9070	2.7000	24.9240	4.8310	.1940
15.6470	10.5390	.3260	2.9070	2.7500	26.1860	5.1070	.1950
16.4450	11.0030	.3410	2.8760	2.8000	27.4480	5.4420	.1980
17.1770	11.5330	.3560	2.8440	2.8440	28.7100	5.6440	.1970
17.7910	11.8650	.3560	2.8440	2.8790	29.6570	5.9260	.2000
18.5630	12.3550	.3560	2.8440	2.9210	30.9180	6.2060	.2010
19.3000	12.8800	.3710	2.8120	2.9600	32.1600	6.4210	.2000
20.0740	13.3680	.3710	2.8120	2.9990	33.4420	6.7060	.2010
20.7300	13.6590	.3860	2.7810	3.0320	34.3690	7.0710	.2060
21.1180	13.9020	.3860	2.7810	3.0500	35.0200	7.2150	.2060
21.6630	14.3030	.3860	2.7810	3.0760	35.9660	7.3600	.2050
22.2080	14.7050	.3860	2.7810	3.1000	36.9130	7.5040	.2030
22.7540	15.1060	.3860	2.7810	3.1250	37.8590	7.6460	.2020

Table A3 continued

23.4170	15.3890	.4020	2.7490	3.1530	38.8060	8.0280	.2070
24.1210	15.9470	.4020	2.7490	3.1830	40.0680	8.1740	.2040
25.1280	16.5170	.4020	2.7490	3.2240	41.6450	8.6120	.2070
25.9570	16.9500	.4190	2.7180	3.2560	42.9070	9.0070	.2100
26.6620	17.5070	.4190	2.7180	3.2830	44.1690	9.1550	.2070
27.4410	17.9910	.4190	2.7180	3.3120	45.4310	9.4500	.2080
27.7560	18.3060	.4190	2.7180	3.3230	46.0620	9.4500	.2050
28.5920	18.7320	.4350	2.6860	3.3530	47.3240	9.8600	.2080
28.9820	18.9730	.4350	2.6860	3.3670	47.9550	10.0090	.2090
29.5300	19.3710	.4350	2.6860	3.3850	48.9020	10.1590	.2080
29.9950	19.5370	.4350	2.6860	3.4010	49.5330	10.4580	.2110
30.5430	19.9360	.4350	2.6860	3.4190	50.4790	10.6070	.2100
31.0910	20.3350	.4350	2.6860	3.4370	51.4260	10.7560	.2090
31.7790	20.5930	.4520	2.6540	3.4590	52.3720	11.1870	.2140
32.7190	21.2300	.4520	2.6540	3.4880	53.9500	11.4890	.2130
33.6590	21.8680	.4520	2.6540	3.5160	55.5270	11.7920	.2120
34.4380	22.3510	.4700	2.6230	3.5390	56.7890	12.0870	.2130
35.2220	22.8290	.4700	2.6230	3.5620	58.0510	12.3930	.2130
36.3980	23.5460	.4700	2.6230	3.5950	59.9440	12.8520	.2140
37.1050	24.1010	.4700	2.6230	3.6140	61.2060	13.0050	.2120
37.8130	24.3400	.4880	2.5910	3.6330	62.1530	13.4730	.2170
38.5210	24.8930	.4880	2.5910	3.6510	63.4150	13.6280	.2150
39.0720	25.2890	.4880	2.5910	3.6650	64.3610	13.7830	.2140
39.7000	25.6070	.4880	2.5910	3.6810	65.3070	14.0920	.2160
40.2510	26.0030	.4880	2.5910	3.6950	66.2540	14.2470	.2150
40.6430	26.2410	.4880	2.5910	3.7050	66.8850	14.4020	.2150
41.4420	26.7050	.5060	2.5600	3.7240	68.1470	14.7370	.2160
42.0720	27.0220	.5060	2.5600	3.7390	69.0930	15.0500	.2180
42.7810	27.5740	.5060	2.5600	3.7560	70.3550	15.2070	.2160
43.4110	27.8910	.5060	2.5600	3.7710	71.3020	15.5210	.2180
43.9630	28.2860	.5060	2.5600	3.7830	72.2480	15.6770	.2170
44.6720	28.8380	.5060	2.5600	3.7990	73.5100	15.8340	.2150
45.3020	29.1550	.5060	2.5600	3.8130	74.4570	16.1480	.2170
45.9560	29.4470	.5250	2.5280	3.8280	75.4030	16.5080	.2190
46.5080	29.8410	.5250	2.5280	3.8400	76.3500	16.6670	.2180

Table A3 continued

46.9830	29.9980	.5250	2.5280	3.8500	76.9810	16.9840	.2210
47.6930	30.5500	.5250	2.5280	3.8650	78.2430	17.1430	.2190
48.4030	31.1010	.5250	2.5280	3.8800	79.5050	17.3020	.2180
49.0350	31.4160	.5250	2.5280	3.8930	80.4510	17.6190	.2190
49.6670	31.7310	.5250	2.5280	3.9050	81.3980	17.9370	.2200
50.2540	32.0900	.5440	2.4960	3.9170	82.3440	18.1640	.2210
51.0460	32.5600	.5440	2.4960	3.9330	83.6060	18.4850	.2210
52.1530	33.3460	.5440	2.4960	3.9540	85.4990	18.8070	.2200
52.7870	33.6590	.5440	2.4960	3.9660	86.4460	19.1280	.2210
53.3410	34.0520	.5440	2.4960	3.9770	87.3920	19.2890	.2210
53.8940	34.4440	.5440	2.4960	3.9870	88.3390	19.4500	.2200
54.4480	34.8370	.5440	2.4960	3.9970	89.2850	19.6100	.2200
54.9700	34.9460	.5640	2.4650	4.0070	89.9160	20.0250	.2230
55.5250	35.3380	.5640	2.4650	4.0170	90.8630	20.1880	.2220
56.3190	35.8060	.5640	2.4650	4.0310	92.1240	20.5130	.2230
57.0310	36.3550	.5640	2.4650	4.0440	93.3860	20.6760	.2210
57.6670	36.6660	.5640	2.4650	4.0550	94.3330	21.0020	.2230
58.3630	36.9760	.5640	2.4650	4.0660	95.2790	21.3270	.2240
59.0160	37.5260	.5640	2.4650	4.0780	96.5410	21.4900	.2230
59.5700	37.9180	.5640	2.4650	4.0870	97.4880	21.6530	.2220
59.9670	38.1520	.5640	2.4650	4.0940	98.1190	21.8150	.2220
60.5070	38.2430	.5840	2.4330	4.1030	98.7500	22.2640	.2250
61.0620	38.6340	.5840	2.4330	4.1120	99.6960	22.4290	.2250
61.6180	39.0250	.5840	2.4330	4.1210	100.6430	22.5940	.2240
62.1740	39.4150	.5840	2.4330	4.1300	101.5890	22.7590	.2240
62.7300	39.8060	.5840	2.4330	4.1390	102.5360	22.9240	.2240
63.1280	40.0390	.5840	2.4330	4.1450	103.1670	23.0880	.2240
63.9230	40.5050	.5840	2.4330	4.1580	104.4290	23.4180	.2240
64.8770	41.1290	.5840	2.4330	4.1720	106.0060	23.7480	.2240
66.0710	41.8280	.5840	2.4330	4.1910	107.8990	24.2430	.2250
66.8670	42.2940	.5840	2.4330	4.2030	109.1610	24.5730	.2250
67.5850	42.5220	.6050	2.4020	4.2130	110.1080	25.0630	.2280
68.3830	42.9860	.6050	2.4020	4.2250	111.3700	25.3970	.2280
68.9400	43.3760	.6050	2.4020	4.2330	112.3160	25.5640	.2280
69.4970	43.7660	.6050	2.4020	4.2410	113.2630	25.7310	.2270

Table A3 continued

69.8960	43.9980	.6050	2.4020	4.2470	113.8940	25.8980	.2270
70.4530	44.3870	.6050	2.4020	4.2550	114.8400	26.0660	.2270
70.8520	44.6190	.6050	2.4020	4.2610	115.4710	26.2330	.2270
71.4090	45.0090	.6050	2.4020	4.2660	116.4180	26.4000	.2270
71.9650	45.3990	.6050	2.4020	4.2760	117.3640	26.5670	.2260
72.2810	45.7140	.6050	2.4020	4.2810	117.9950	26.5670	.2250
72.8380	46.1040	.6050	2.4020	4.2880	118.9410	26.7340	.2250
73.6580	46.2300	.6270	2.3700	4.2990	119.8880	27.4290	.2290
74.2160	46.6180	.6270	2.3700	4.3070	120.8340	27.5980	.2280
74.5320	46.9340	.6270	2.3700	4.3110	121.4660	27.5980	.2270
74.7740	47.0070	.6270	2.3700	4.3140	121.7810	27.7680	.2280
75.0170	47.0800	.6270	2.3700	4.3180	122.0970	27.9370	.2290
75.0170	47.0800	.6270	2.3700	4.3180	122.0970	27.9370	.2290
75.3320	47.3950	.6270	2.3700	4.3220	122.7280	27.9370	.2280
75.3320	47.3950	.6270	2.3700	4.3220	122.7280	27.9370	.2280
74.4590	46.6910	.6270	2.3700	4.3100	121.1500	27.7680	.2290
73.7430	46.1450	.6270	2.3700	4.3010	119.8880	27.5980	.2300
73.2700	45.6720	.6270	2.3700	4.2940	118.9410	27.5980	.2320
72.7120	45.2830	.6270	2.3700	4.2870	117.9950	27.4290	.2320
72.5540	45.1250	.6270	2.3700	4.2840	117.6790	27.4290	.2330
71.8390	44.5790	.6270	2.3700	4.2740	116.4180	27.2600	.2340
70.7230	43.8020	.6270	2.3700	4.2590	114.5250	26.9210	.2350
70.2500	43.3290	.6270	2.3700	4.2520	113.5780	26.9210	.2370
69.6920	42.9400	.6270	2.3700	4.2440	112.6320	26.7520	.2380
69.3760	42.6240	.6270	2.3700	4.2400	112.0010	26.7520	.2390
68.8180	42.2360	.6270	2.3700	4.2310	111.0540	26.5820	.2390
68.4180	42.0050	.6270	2.3700	4.2260	110.4230	26.4130	.2390
67.7870	41.3740	.6270	2.3700	4.2160	109.1610	26.4130	.2420
66.9870	40.9120	.6270	2.3700	4.2040	107.8990	26.0740	.2420
66.3560	40.2810	.6270	2.3700	4.1950	106.6370	26.0740	.2450
65.9560	40.0510	.6270	2.3700	4.1890	106.0060	25.9050	.2440
65.4830	39.5770	.6270	2.3700	4.1820	105.0600	25.9050	.2470
64.6820	39.1160	.6270	2.3700	4.1690	103.7980	25.5670	.2460
64.2090	38.6420	.6270	2.3700	4.1620	102.8510	25.5670	.2490
63.4930	38.0960	.6270	2.3700	4.1510	101.5890	25.3970	.2500

Table A3 continued

62.6200	37.3920	.6270	2.3700	4.1370	100.0120	25.2280	.2520
61.9770	37.0880	.6270	2.3700	4.1270	99.0660	24.8690	.2510
61.5040	36.6150	.6270	2.3700	4.1190	98.1190	24.8890	.2540
60.9460	36.2260	.6270	2.3700	4.1100	97.1720	24.7200	.2540
60.2310	35.6800	.6270	2.3700	4.0980	95.9100	24.5510	.2560
59.3570	34.9760	.6270	2.3700	4.0840	94.3330	24.3810	.2580
58.6410	34.4290	.6270	2.3700	4.0710	93.0710	24.2120	.2600
58.0630	34.3570	.6050	2.4020	4.0620	92.4400	23.7260	.2570
57.8410	33.9680	.6270	2.3700	4.0580	91.8090	23.8730	.2600
57.3680	33.4950	.6270	2.3700	4.0490	90.8630	23.8730	.2630
56.8100	33.1060	.6270	2.3700	4.0400	89.9160	23.7040	.2640
55.9370	32.4020	.6270	2.3700	4.0240	88.3390	23.5350	.2660
55.0630	31.6980	.6270	2.3700	4.0080	86.7610	23.3650	.2690
54.7480	31.3820	.6270	2.3700	4.0030	86.1300	23.3650	.2710
54.1050	31.0780	.6270	2.3700	3.9910	85.1840	23.0270	.2700
53.6320	30.6050	.6270	2.3700	3.9820	84.2370	23.0270	.2730
52.9160	30.0590	.6270	2.3700	3.9690	82.9750	22.8570	.2750
52.2010	29.5130	.6270	2.3700	3.9550	81.7130	22.6880	.2780
51.2530	29.1980	.6050	2.4020	3.9370	80.4510	22.0560	.2740
50.6650	28.5040	.6270	2.3700	3.9260	79.1890	22.1800	.2800
49.9820	28.2610	.6050	2.4020	3.9120	78.2430	21.7210	.2780
49.5690	27.7270	.6270	2.3700	3.9030	77.2960	21.8420	.2830
48.7110	27.3240	.6050	2.4020	3.8860	76.0340	21.3870	.2810
47.9130	26.8600	.6050	2.4020	3.8690	74.7720	21.0530	.2820
47.1240	26.0710	.6050	2.4020	3.8530	73.1950	21.0530	.2880
46.3260	25.6070	.6050	2.4020	3.8360	71.9330	20.7190	.2880
45.7690	25.2170	.6050	2.4020	3.8240	70.9860	20.5520	.2900
45.3700	24.9850	.6050	2.4020	3.8150	70.3550	20.3850	.2900
44.8130	24.5960	.6050	2.4020	3.8030	69.4090	20.2170	.2910
44.0990	24.0480	.6050	2.4020	3.7860	68.1470	20.0500	.2940
43.5420	23.6580	.6050	2.4020	3.7740	67.2000	19.8830	.2960
42.8270	23.1110	.6050	2.4020	3.7570	65.9380	19.7160	.2990
42.2700	22.7210	.6050	2.4020	3.7440	64.9920	19.5490	.3010
41.5560	22.1740	.6050	2.4020	3.7270	63.7300	19.3820	.3040
41.1570	21.9420	.6050	2.4020	3.7170	63.0990	19.2150	.3050

Table A3 continued

40.6000	21.5520	.6050	2.4020	3.7040	62.1530	19.0480	.3060
39.7280	20.8470	.6050	2.4020	3.6820	60.5750	18.8810	.3120
38.8560	20.1420	.6050	2.4020	3.6600	58.9970	18.7140	.3170
38.2990	19.7520	.6050	2.4020	3.6450	58.0510	18.5470	.3190
37.9000	19.5200	.6050	2.4020	3.6350	57.4200	18.3800	.3200
37.1850	18.9730	.6050	2.4020	3.6160	56.1580	18.2120	.3240
36.5450	18.6670	.6050	2.4020	3.5990	55.2120	17.8780	.3240
36.0720	18.1930	.6050	2.4020	3.5860	54.2650	17.8780	.3290
35.6730	17.9620	.6050	2.4020	3.5740	53.6340	17.7110	.3300
35.2740	17.7290	.6050	2.4020	3.5630	53.0030	17.5440	.3310
34.5590	17.1820	.6050	2.4020	3.5430	51.7410	17.3770	.3360
33.8450	16.6350	.6050	2.4020	3.5220	50.4790	17.2100	.3410
33.1300	16.0870	.6050	2.4020	3.5000	49.2170	17.0430	.3460
32.4900	15.7810	.6050	2.4020	3.4810	48.2710	16.7090	.3460
32.1740	15.4650	.6050	2.4020	3.4710	47.6400	16.7090	.3510
31.7750	15.2340	.6050	2.4020	3.4590	47.0090	16.5420	.3520
31.2180	14.8440	.6050	2.4020	3.4410	46.0620	16.3750	.3550
30.6620	14.4540	.6050	2.4020	3.4230	45.1160	16.2070	.3590
29.9470	13.9070	.6050	2.4020	3.3990	43.8540	16.0400	.3660
29.3900	13.5170	.6050	2.4020	3.3810	42.9070	15.8730	.3700
28.7310	13.2290	.5840	2.4330	3.3580	41.9610	15.5020	.3690
28.2770	12.7380	.6050	2.4020	3.3420	41.0140	15.5390	.3790
27.4620	12.2900	.5840	2.4330	3.3130	39.7520	15.1720	.3820
26.8480	11.6430	.6050	2.4020	3.2900	38.4910	15.2050	.3950
26.0500	11.1790	.6050	2.4020	3.2600	37.2280	14.8710	.3990
25.6380	10.9600	.5840	2.4330	3.2440	36.5970	14.6780	.4010
25.0940	10.5570	.6050	2.4020	3.2230	35.6510	14.5370	.4080
24.5260	10.1780	.5840	2.4330	3.2000	34.7040	14.3480	.4130
23.8880	9.8700	.5840	2.4330	3.1730	33.7580	14.0180	.4150
23.1740	9.3210	.5840	2.4330	3.1430	32.4960	13.8530	.4260
22.6190	8.9310	.5840	2.4330	3.1190	31.5490	13.6880	.4340
22.0630	8.5400	.5840	2.4330	3.0940	30.6030	13.5230	.4420
21.6650	8.3070	.5840	2.4330	3.0760	29.9720	13.3580	.4460
20.5540	7.5250	.5840	2.4330	3.0230	28.0790	13.0280	.4640
19.6000	6.9010	.5840	2.4330	2.9760	26.5020	12.6990	.4790

Table A3 continued

18.8870	6.3530	.5840	2.4330	2.9380	25.2400	12.5340	.4970
18.2480	6.0450	.5840	2.4330	2.9040	24.2930	12.2040	.5020
17.6930	5.6540	.5840	2.4330	2.8730	23.3470	12.0390	.5160
17.1370	5.2630	.5840	2.4330	2.8410	22.4000	11.8740	.5300
16.4240	4.7150	.5840	2.4330	2.7990	21.1380	11.7090	.5540
15.7100	4.1660	.5840	2.4330	2.7540	19.8760	11.5440	.5810
14.8320	3.7820	.5840	2.4330	2.6970	18.6140	11.0490	.5940
14.1180	3.2340	.5840	2.4330	2.6470	17.3520	10.8840	.6270
13.6380	3.0830	.5840	2.4330	2.6130	16.7210	10.5550	.6310
12.6090	2.2190	.5840	2.4330	2.5340	14.8280	10.3900	.7010
11.5730	1.6780	.5840	2.4330	2.4490	13.2510	9.8950	.7470
10.4620	.8960	.5840	2.4330	2.3480	11.3580	9.5650	.8420
9.9060	.5060	.5840	2.4330	2.2930	10.4110	9.4000	.9030
9.2680	.1970	.5840	2.4330	2.2270	9.4650	9.0700	.9580
8.8130	.0210	.5640	2.4650	2.1760	8.8340	8.7910	.9950
8.5540	-.3510	.5840	2.4330	2.1460	8.2030	8.9050	1.0860
7.9160	-.6600	.5840	2.4330	2.0690	7.2560	8.5760	1.1820
6.9090	-1.2310	.5640	2.4650	1.9330	5.6790	8.1400	1.4330
5.9260	-1.8250	.5840	2.4330	1.7790	4.1020	7.7510	1.8900
5.2410	-2.0850	.5640	2.4650	1.6560	3.1550	7.3260	2.3220
4.5280	-2.6350	.5640	2.4650	1.5100	1.8930	7.1630	3.7840
3.8540	-2.9080	.5840	2.4330	1.3490	.9470	6.7620	7.1440

Table A4 Compaction data for dicalcium phosphate compcated uniaxially at 248 MPa

σ (MPa)	τ (MPa)	ε	V ($mx10^{-6}$)	ln σ	σ_A (MPa)	σ_R MPa	$\frac{\sigma_R}{\sigma_A}$
.414	.216	0.000	4.045	-.882	.630	.198	.315
.417	.212	.032	3.918	-.874	.630	.205	.325
.577	.369	.049	3.855	-.550	.946	.208	.220
.790	.473	.067	3.792	-.236	1.263	.318	.251
1.161	.731	.085	3.729	.150	1.892	.430	.227
1.376	.833	.094	3.697	.319	2.209	.543	.246
1.909	1.246	.113	3.634	.646	3.155	.663	.210
2.342	1.443	.133	3.571	.851	3.785	.899	.238
2.880	1.851	.153	3.508	1.058	4.731	1.030	.218
3.638	2.356	.174	3.444	1.291	5.994	1.281	.214
4.459	2.797	.196	3.381	1.495	7.256	1.662	.229
5.434	3.396	.208	3.350	1.693	8.832	2.037	.231
6.585	4.143	.231	3.286	1.885	10.728	2.442	.228
7.728	4.892	.243	3.255	2.045	12.620	2.836	.225
8.891	5.622	.267	3.192	2.185	14.513	3.269	.225
9.887	6.205	.280	3.160	2.291	16.092	3.683	.229
10.866	6.802	.280	3.160	2.386	17.668	4.064	.230
11.646	7.285	.293	3.128	2.455	18.930	4.361	.230
12.429	7.764	.306	3.097	2.520	20.193	4.665	.231
13.032	8.108	.306	3.097	2.567	21.139	4.924	.233
13.752	8.647	.320	3.065	2.621	22.399	5.106	.228
14.423	8.925	.320	3.065	2.669	23.348	5.498	.235
15.148	9.460	.333	3.034	2.718	24.608	5.688	.231
15.753	9.801	.333	3.034	2.757	25.554	5.952	.233
16.359	10.141	.333	3.034	2.795	26.500	6.217	.235
16.933	10.517	.347	3.002	2.829	27.449	6.416	.234
17.540	10.856	.347	3.002	2.864	28.396	6.684	.235
18.146	11.196	.347	3.002	2.898	29.342	6.951	.237

Table A4 continued

18.724	11.564	.362	2.970	2.930	30.288	7.160	.236
19.332	11.902	.362	2.970	2.962	31.234	7.430	.238
19.940	12.240	.362	2.970	2.993	32.180	7.700	.239
20.750	12.693	.376	2.939	3.033	33.443	8.056	.241
21.359	13.030	.376	2.939	3.061	34.389	8.329	.242
21.901	13.435	.376	2.939	3.087	35.335	8.466	.240
22.489	13.793	.391	2.907	3.113	36.282	8.696	.240
23.258	14.286	.391	2.907	3.147	37.544	8.972	.239
23.711	14.463	.391	2.907	3.166	38.174	9.248	.242
24.253	14.867	.391	2.907	3.189	39.120	9.386	.240
24.864	15.202	.391	2.907	3.213	40.066	9.662	.241
25.462	15.554	.407	2.876	3.237	41.016	9.908	.242
25.846	15.799	.407	2.876	3.252	41.646	10.047	.241
26.231	16.044	.407	2.876	3.267	42.275	10.187	.241
26.774	16.448	.407	2.876	3.267	43.222	10.326	.239
27.160	16.694	.407	2.876	3.302	43.854	10.466	.239
27.545	16.939	.407	2.876	3.316	44.484	10.605	.238
27.931	17.186	.407	2.876	3.330	45.117	10.745	.238
28.376	17.371	.422	2.844	3.346	45.747	11.006	.241
28.990	17.703	.422	2.844	3.367	46.693	11.288	.242
29.149	17.861	.422	2.844	3.372	47.009	11.288	.240
29.763	18.193	.422	2.844	3.393	47.956	11.570	.241
30.148	18.437	.422	2.844	3.406	48.585	11.711	.241
30.535	18.683	.422	2.844	3.419	49.218	11.852	.241
30.921	18.927	.422	2.844	3.431	49.848	11.993	.241
31.374	19.104	.438	2.812	3.446	50.478	12.270	.243
31.992	19.436	.438	2.812	3.465	51.427	12.556	.244
32.378	19.679	.438	2.812	3.477	52.057	12.699	.244
32.922	20.081	.438	2.812	3.494	53.003	12.841	.242
33.467	20.483	.438	2.812	3.511	53.949	12.984	.241
33.924	20.655	.438	2.812	3.524	54.579	13.269	.243
34.546	20.982	.455	2.781	3.542	55.528	13.564	.244
35.164	21.311	.455	2.781	3.560	56.475	13.853	.245
35.551	21.554	.455	2.781	3.571	57.104	13.997	.245
36.254	22.113	.455	2.781	3.591	58.367	14.142	.242

Table A4 continued

36.714	22.283	.455	2.781	3.603	58.997	14.430	.245
37.259	22.684	.455	2.781	3.618	59.943	14.575	.243
37.876	23.013	.455	2.781	3.634	60.889	14.863	.244
38.508	23.328	.471	2.749	3.651	61.835	15.180	.245
39.055	23.729	.471	2.749	3.665	62.785	15.326	.244
39.516	23.898	.471	2.749	3.677	63.415	15.618	.246
40.062	24.299	.471	2.749	3.690	64.361	15.764	.245
40.608	24.699	.471	2.749	3.704	65.307	15.910	.244
41.227	25.026	.471	2.749	3.719	66.253	16.202	.245
41.774	25.426	.471	2.749	3.732	67.199	16.348	.243
42.259	25.573	.488	2.718	3.744	67.832	16.685	.246
42.880	25.899	.488	2.718	3.758	68.778	16.981	.247
43.427	26.298	.488	2.718	3.771	69.725	17.128	.246
43.815	26.539	.488	2.718	3.780	70.354	17.276	.246
44.362	26.938	.488	2.718	3.792	71.301	17.424	.244
44.983	27.264	.488	2.718	3.806	72.247	17.719	.245
45.373	27.507	.488	2.718	3.815	72.880	17.867	.245
45.920	27.906	.488	2.718	3.827	73.826	18.014	.244
46.541	28.231	.488	2.718	3.840	74.772	18.310	.245
46.930	28.472	.488	2.718	3.849	75.402	18.457	.245
47.429	28.605	.506	2.686	3.859	76.035	18.824	.248
47.977	29.004	.506	2.686	3.871	76.981	18.973	.246
48.367	29.244	.506	2.686	3.879	77.611	19.123	.246
48.914	29.642	.506	2.686	3.890	78.557	19.272	.245
49.306	29.884	.506	2.686	3.898	79.190	19.421	.245
49.928	30.208	.506	2.686	3.911	80.136	19.720	.246
50.243	30.523	.506	2.686	3.917	80.766	19.720	.244
50.709	30.690	.506	2.686	3.926	81.399	20.019	.246
51.257	31.088	.506	2.686	3.937	82.345	20.168	.245
51.646	31.328	.506	2.686	3.944	82.975	20.318	.245
52.037	31.570	.506	2.686	3.952	83.608	20.467	.245
52.708	31.846	.524	2.654	3.965	84.554	20.862	.247
53.098	32.085	.524	2.654	3.972	85.184	21.013	.247
53.489	32.324	.524	2.654	3.979	85.813	21.164	.247
53.881	32.565	.524	2.654	3.987	86.446	21.315	.247

Table A4 continued

54.430	32.963	.524	2.654	3.997	87.392	21.467	.246
54.739	32.970	.524	2.654	4.003	87.709	21.769	.248
55.288	33.367	.524	2.654	4.013	88.655	21.920	.247
55.678	33.607	.524	2.654	4.020	89.285	22.071	.247
56.069	33.846	.524	2.654	4.027	89.915	22.222	.247
56.619	34.245	.524	2.654	4.036	90.864	22.374	.246
57.009	34.484	.524	2.654	4.043	91.494	22.525	.246
57.536	34.587	.542	2.623	4.052	92.123	22.949	.249
57.929	34.827	.542	2.623	4.059	92.756	23.102	.249
58.321	35.065	.542	2.623	4.066	93.366	23.255	.249
58.870	35.462	.542	2.623	4.075	94.332	23.408	.248
59.263	35.702	.542	2.623	4.082	94.965	23.561	.248
59.655	35.940	.542	2.623	4.089	95.595	23.714	.248
60.046	36.179	.542	2.623	4.095	96.225	23.867	.248
60.362	36.495	.542	2.623	4.100	96.858	23.867	.246
60.754	36.734	.542	2.623	4.107	97.487	24.020	.246
61.147	36.973	.542	2.623	4.113	98.120	24.173	.246
61.538	37.212	.542	2.623	4.120	98.750	24.326	.246
61.930	37.450	.542	2.623	4.126	99.380	24.479	.246
62.322	37.690	.542	2.623	4.132	100.013	24.632	.246
62.629	37.697	.561	2.591	4.137	100.326	24.933	.249
63.023	37.936	.561	2.591	4.144	100.959	25.087	.248
63.415	38.173	.561	2.591	4.150	101.589	25.242	.248
63.809	38.412	.561	2.591	4.156	102.222	25.397	.248
64.202	38.650	.561	2.591	4.162	102.851	25.552	.248
64.360	38.808	.561	2.591	4.164	103.166	25.552	.248
64.752	39.045	.561	2.591	4.171	103.797	25.707	.248
65.145	39.283	.561	2.591	4.177	104.427	25.862	.248
65.461	39.599	.561	2.591	4.181	105.060	25.862	.246
65.853	39.837	.561	2.591	4.187	105.690	26.017	.246
66.247	40.076	.561	2.591	4.193	106.323	26.171	.246
66.639	40.313	.561	2.591	4.199	106.953	26.326	.246
67.032	40.551	.561	2.591	4.205	107.582	26.481	.246
67.267	40.631	.561	2.591	4.209	107.899	26.636	.247
67.426	40.790	.561	2.591	4.211	108.215	26.636	.246

Table A4 continued

67.818	41.027	.561	2.591	4.217	108.845	26.791	.246
68.212	41.266	.561	2.591	4.223	109.478	26.946	.246
68.527	41.581	.561	2.591	4.227	110.108	26.946	.245
68.919	41.818	.561	2.591	4.233	110.737	27.101	.245
69.155	41.899	.561	2.591	4.236	111.054	27.256	.245
69.313	42.057	.561	2.591	4.239	111.370	27.256	.245
69.705	42.295	.561	2.591	4.244	112.000	27.410	.245
70.269	42.364	.580	2.560	4.252	112.633	27.906	.248
70.426	42.520	.580	2.560	4.255	112.946	27.906	.247
70.821	42.758	.580	2.560	4.260	113.579	28.062	.247
71.214	42.995	.580	2.560	4.266	114.209	28.219	.247
71.372	43.153	.580	2.560	4.268	114.525	28.219	.246
71.607	43.231	.580	2.560	4.271	114.839	28.376	.247
72.002	43.469	.580	2.560	4.277	115.472	28.533	.247
72.395	43.706	.580	2.560	4.282	116.101	28.689	.247
72.554	43.864	.580	2.560	4.284	116.418	28.689	.246
72.947	44.101	.580	2.560	4.290	117.047	28.846	.246
73.342	44.339	.580	2.560	4.295	117.680	29.003	.246
73.735	44.575	.580	2.560	4.300	118.310	29.160	.246
74.130	44.813	.580	2.560	4.306	118.943	29.317	.246
74.445	45.128	.580	2.560	4.310	119.573	29.317	.245
74.838	45.365	.580	2.560	4.315	120.203	29.473	.245
75.389	45.759	.580	2.560	4.323	121.149	29.630	.245
75.970	45.811	.600	2.528	4.330	121.782	30.159	.248
76.365	46.047	.600	2.528	4.336	122.411	30.318	.248
76.760	46.284	.600	2.528	4.341	123.044	30.477	.248
77.155	46.519	.600	2.528	4.346	123.674	30.635	.248
77.707	46.913	.600	2.528	4.353	124.620	30.794	.247
78.260	47.307	.600	2.528	4.360	125.566	30.953	.247
79.050	47.779	.600	2.528	4.370	126.829	31.270	.247
79.602	48.173	.600	2.528	4.377	127.775	31.429	.246
79.996	48.409	.600	2.528	4.382	128.405	31.588	.246
80.630	48.725	.600	2.528	4.390	129.354	31.905	.247
81.182	49.118	.600	2.528	4.397	130.301	32.064	.246
81.577	49.354	.600	2.528	4.402	130.930	32.223	.246

Table A4 continued

82.129	49.748	.600	2.528	4.408	131.877	32.381	.246
82.681	50.141	.600	2.528	4.415	132.823	32.540	.245
83.284	50.171	.620	2.496	4.422	133.456	33.113	.248
83.838	50.564	.620	2.496	4.429	134.402	33.274	.248
84.313	50.718	.620	2.496	4.435	135.032	33.595	.249
84.786	51.191	.620	2.496	4.440	135.978	33.595	.247
85.264	51.347	.620	2.496	4.446	136.611	33.917	.248
85.974	51.896	.620	2.496	4.454	137.870	34.077	.247
86.527	52.289	.620	2.496	4.460	138.816	34.238	.247
87.161	52.602	.620	2.496	4.468	139.763	34.560	.247
87.873	53.153	.620	2.496	4.476	141.025	34.720	.246
88.507	53.465	.620	2.496	4.483	141.972	35.042	.247
89.060	53.858	.620	2.496	4.489	142.918	35.202	.246
89.615	54.252	.620	2.496	4.496	143.867	35.363	.246
90.010	54.486	.620	2.496	4.500	144.497	35.524	.246
90.406	54.721	.620	2.496	4.504	145.127	35.685	.246
91.347	55.042	.641	2.465	4.515	146.389	36.305	.248
91.745	55.277	.641	2.465	4.519	147.022	36.468	.248
92.381	55.587	.641	2.465	4.526	147.968	36.793	.249
92.935	55.979	.641	2.465	4.532	148.915	36.956	.248
93.490	56.371	.641	2.465	4.538	149.861	37.119	.248
94.126	56.681	.641	2.465	4.545	150.807	37.445	.248
94.680	57.073	.641	2.465	4.551	151.753	37.607	.248
95.235	57.465	.641	2.465	4.556	152.699	37.770	.247
95.631	57.698	.641	2.465	4.560	153.329	37.933	.247
96.187	58.091	.641	2.465	4.566	154.278	38.096	.247
96.583	58.325	.641	2.465	4.570	154.908	38.259	.247
96.898	58.640	.641	2.465	4.574	155.538	38.259	.246
97.296	58.875	.641	2.465	4.578	156.171	38.421	.246
97.692	59.108	.641	2.465	4.582	156.801	38.584	.246
98.089	59.342	.641	2.465	4.586	157.430	38.747	.246
98.563	59.816	.641	2.465	4.591	158.380	38.747	.245
98.883	59.810	.641	2.465	4.594	158.693	39.073	.246
99.199	60.127	.641	2.465	4.597	159.326	39.073	.245
100.009	60.264	.662	2.433	4.605	160.272	39.745	.248

Table A4 continued

100.406	60.496	.662	2.433	4.609	160.902	39.910	.248
100.805	60.730	.662	2.433	4.613	161.535	40.075	.248
101.202	60.962	.662	2.433	4.617	162.165	40.240	.248
101.517	61.277	.662	2.433	4.620	162.794	40.240	.247
101.758	61.353	.662	2.433	4.623	163.111	40.405	.248
102.313	61.744	.662	2.433	4.628	164.057	40.570	.247
102.711	61.976	.662	2.433	4.632	164.687	40.735	.247
103.110	62.210	.662	2.433	4.636	165.320	40.899	.247
103.747	62.518	.662	2.433	4.642	166.266	41.229	.248
104.221	62.991	.662	2.433	4.647	167.212	41.229	.247
104.461	63.067	.662	2.433	4.649	167.528	41.394	.247
105.017	63.458	.662	2.433	4.654	166.475	41.559	.247
105.414	63.690	.662	2.433	4.658	169.104	41.724	.247
105.813	63.924	.662	2.433	4.662	169.737	41.889	.247
106.210	64.157	.662	2.433	4.665	170.367	42.054	.247
106.606	64.389	.662	2.433	4.669	170.997	42.219	.247
107.083	64.864	.662	2.433	4.674	171.946	42.219	.246
107.562	65.014	.662	2.433	4.678	172.576	42.549	.247
108.673	65.795	.662	2.433	4.688	174.468	42.878	.246
109.071	66.027	.662	2.433	4.692	175.098	43.043	.246
109.912	66.135	.684	2.402	4.700	176.047	43.777	.249
110.311	66.367	.684	2.402	4.703	176.677	43.944	.249
110.867	66.756	.684	2.402	4.708	177.623	44.111	.248
111.266	66.988	.684	2.402	4.712	178.253	44.278	.248
111.907	67.295	.684	2.402	4.718	179.203	44.612	.249
112.306	67.526	.684	2.402	4.721	179.832	44.779	.249
112.621	67.841	.684	2.402	4.724	180.462	44.779	.248
113.021	68.074	.684	2.402	4.728	181.095	44.946	.248
113.419	68.306	.684	2.402	4.731	181.725	45.114	.248
113.817	68.537	.684	2.402	4.735	182.354	45.280	.248
114.376	68.928	.684	2.402	4.739	183.304	45.448	.248
114.932	69.318	.684	2.402	4.744	184.250	45.615	.248
115.573	69.624	.684	2.402	4.750	185.196	45.949	.248
116.287	70.171	.684	2.402	4.756	186.459	46.116	.247
117.084	70.634	.684	2.402	4.763	187.718	46.450	.247

Table A4 continued

117.641	71.024	.684	2.402	4.768	188.665	46.617	.247
118.356	71.571	.684	2.402	4.774	189.927	46.784	.246
118.839	71.721	.684	2.402	4.778	190.560	47.119	.247
119.396	72.110	.684	2.402	4.782	191.506	47.286	.247
119.711	72.425	.684	2.402	4.785	192.136	47.286	.246
120.351	72.731	.684	2.402	4.790	193.082	47.620	.247
120.751	72.964	.684	2.402	4.794	193.715	47.787	.247
121.384	72.960	.707	2.370	4.799	194.345	48.424	.249
121.869	73.106	.707	2.370	4.803	194.975	48.763	.250
122.185	73.422	.707	2.370	4.806	195.608	48.763	.249
122.743	73.811	.707	2.370	4.810	196.554	48.932	.249
123.142	74.041	.707	2.370	4.813	197.184	49.101	.249
123.543	74.273	.707	2.370	4.817	197.816	49.271	.249
124.343	74.733	.707	2.370	4.823	199.076	49.609	.249
125.059	75.280	.707	2.370	4.829	200.339	49.779	.248
125.616	75.668	.707	2.370	4.833	201.285	49.948	.248
126.259	75.972	.707	2.370	4.838	202.231	50.267	.249
126.660	76.204	.707	2.370	4.842	202.864	50.456	.249
127.218	76.593	.707	2.370	4.846	203.810	50.625	.248
127.617	76.823	.707	2.370	4.849	204.440	50.794	.248
128.175	77.211	.707	2.370	4.853	205.386	50.964	.248
128.576	77.443	.707	2.370	4.857	206.019	51.133	.248
129.134	77.831	.707	2.370	4.861	206.965	51.302	.248
129.449	78.146	.707	2.370	4.863	207.595	51.302	.247
129.850	78.378	.707	2.370	4.866	208.226	51.472	.247
130.249	78.608	.707	2.370	4.869	208.858	51.641	.247
131.157	78.647	.730	2.338	4.876	209.804	52.510	.250
131.558	78.876	.730	2.338	4.879	210.434	52.682	.250
131.960	79.106	.730	2.338	4.882	211.066	52.854	.250
132.275	79.421	.730	2.338	4.885	211.696	52.854	.250
132.763	79.566	.730	2.338	4.889	212.329	53.197	.251
133.164	79.795	.730	2.338	4.892	212.959	53.369	.251
133.637	80.268	.730	2.338	4.895	213.905	53.369	.249
134.039	80.499	.730	2.338	4.898	214.538	53.540	.250
134.440	80.728	.730	2.338	4.901	215.168	53.712	.250

Table A4 continued

134.840	80.957	.730	2.338	4.904	215.797	53.883	.250
135.399	81.344	.730	2.338	4.908	216.744	54.055	.249
135.802	81.575	.730	2.338	4.911	217.377	54.227	.249
136.202	81.804	.730	2.338	4.914	218.006	54.398	.250
136.761	82.191	.730	2.338	4.918	218.953	54.570	.249
137.163	82.422	.730	2.338	4.921	219.585	54.741	.249
137.722	82.809	.730	2.338	4.925	220.532	54.913	.249
138.123	83.038	.730	2.338	4.928	221.161	55.085	.249
138.367	83.111	.730	2.338	4.930	221.478	55.256	.249
138.682	83.426	.730	2.338	4.932	222.108	55.256	.249
139.084	83.656	.730	2.338	4.935	222.741	55.428	.249
139.485	83.885	.730	2.338	4.938	223.370	55.599	.249
139.800	84.200	.730	2.338	4.940	224.000	55.599	.248
140.129	84.187	.730	2.338	4.943	224.316	55.942	.249
140.446	84.503	.730	2.338	4.945	224.949	55.942	.249
140.847	84.733	.730	2.338	4.948	225.579	56.114	.249
141.091	84.805	.730	2.338	4.949	225.896	56.286	.249
141.564	85.278	.730	2.338	4.953	226.842	56.286	.248
142.050	85.421	.730	2.338	4.956	227.472	56.629	.249
142.998	85.419	.753	2.307	4.963	228.418	57.579	.252
143.315	85.736	.753	2.307	4.965	229.051	57.579	.251
143.962	86.035	.753	2.307	4.970	229.997	57.926	.252
144.522	86.421	.753	2.307	4.973	230.943	58.100	.252
144.924	86.649	.753	2.307	4.976	231.573	58.274	.252
145.327	86.879	.753	2.307	4.979	232.206	58.448	.252
145.642	87.194	.753	2.307	4.981	232.835	58.448	.251
146.044	87.421	.753	2.307	4.984	233.465	58.622	.251
146.289	87.493	.753	2.307	4.986	233.782	58.796	.252
146.604	87.807	.753	2.307	4.988	234.411	58.796	.251
147.007	88.037	.753	2.307	4.990	235.044	58.970	.251
147.251	88.107	.753	2.307	4.992	235.358	59.144	.251
147.654	88.336	.753	2.307	4.995	235.991	59.318	.251
147.969	88.651	.753	2.307	4.997	236.620	59.318	.251
148.056	88.564	.753	2.307	4.998	236.620	59.492	.251
148.460	88.794	.753	2.307	5.000	237.253	59.666	.251

Table A4 continued

148.862	89.021	.753	2.307	5.003	237.883	59.840	.252
149.176	89.336	.753	2.307	5.005	238.513	59.840	.251
149.422	89.408	.753	2.307	5.007	236.829	60.014	.251
149.825	89.637	.753	2.307	5.009	239.462	60.188	.251
149.982	89.794	.753	2.307	5.011	239.775	60.188	.251
150.298	90.110	.753	2.307	5.013	240.408	60.188	.250
150.542	90.180	.753	2.307	5.014	240.722	60.362	.251
150.787	90.251	.753	2.307	5.016	241.038	60.536	.251
151.102	90.566	.753	2.307	5.018	241.668	60.536	.250
151.347	90.637	.753	2.307	5.020	241.984	60.710	.251
151.592	90.708	.753	2.307	5.021	242.301	60.884	.251
151.749	90.865	.753	2.307	5.022	242.614	60.884	.251
152.065	91.182	.753	2.307	5.024	243.247	60.884	.250
152.224	91.340	.753	2.307	5.025	243.563	60.884	.250
152.467	91.409	.753	2.307	5.027	243.877	61.058	.250
152.871	91.639	.753	2.307	5.030	244.509	61.232	.250
153.027	91.796	.753	2.307	5.031	244.823	61.232	.250
153.186	91.954	.753	2.307	5.032	245.139	61.232	.250
153.431	92.025	.753	2.307	5.033	245.456	61.406	.250
153.674	92.095	.753	2.307	5.035	245.769	61.580	.251
153.832	92.253	.753	2.307	5.036	246.085	61.580	.250
154.236	92.482	.753	2.307	5.038	246.718	61.754	.250
154.393	92.639	.753	2.307	5.039	247.032	61.754	.250
154.393	92.639	.753	2.307	5.039	247.032	61.754	.250
154.551	92.797	.753	2.307	5.041	247.348	61.754	.250
154.796	92.869	.753	2.307	5.042	247.665	61.927	.250
154.953	93.025	.753	2.307	5.043	247.978	61.927	.250
155.111	93.183	.753	2.307	5.044	248.294	61.927	.249
155.356	93.255	.753	2.307	5.046	248.611	62.101	.250
155.513	93.411	.753	2.307	5.047	248.924	62.101	.249
155.513	93.411	.753	2.307	5.047	248.924	62.101	.249
155.356	93.255	.753	2.307	5.046	248.611	62.101	.250
154.910	92.122	.778	2.275	5.043	247.032	62.788	.254
153.446	91.693	.753	2.307	5.033	245.139	61.754	.252
152.753	90.494	.778	2.275	5.029	243.247	62.258	.256

Table A4 continued

151.450	90.218	.753	2.307	5.020	241.668	61.232	.253
150.841	88.935	.778	2.275	5.016	239.775	61.906	.258
149.542	88.658	.753	2.307	5.008	238.199	60.884	.256
148.665	87.955	.753	2.307	5.002	236.620	60.710	.257
147.703	87.341	.753	2.307	4.995	235.044	60.362	.257
147.072	86.710	.753	2.307	4.991	233.782	60.362	.258
146.353	86.166	.753	2.307	4.986	232.519	60.188	.259
145.635	85.621	.753	2.307	4.981	231.256	60.014	.260
145.005	84.991	.753	2.307	4.977	229.997	60.014	.261
144.445	84.605	.753	2.307	4.973	229.051	59.840	.261
143.640	84.148	.753	2.307	4.967	227.788	59.492	.261
143.580	83.262	.778	2.275	4.967	226.842	60.318	.266
143.019	82.877	.778	2.275	4.963	225.896	60.142	.266
141.889	82.744	.753	2.307	4.955	224.633	59.144	.263
141.895	82.105	.778	2.275	4.955	224.000	59.789	.267
141.012	82.042	.753	2.307	4.949	223.054	58.970	.264
140.452	81.656	.753	2.307	4.945	222.108	58.796	.265
140.050	81.428	.753	2.307	4.942	221.478	58.622	.265
139.490	81.042	.753	2.307	4.938	220.532	58.448	.265
139.174	80.725	.753	2.307	4.936	219.899	58.448	.266
138.613	80.339	.753	2.307	4.932	218.953	58.274	.266
138.299	80.024	.753	2.307	4.929	218.323	58.274	.267
137.895	79.795	.753	2.307	4.926	217.690	58.100	.267
137.493	79.567	.753	2.307	4.924	217.060	57.926	.267
137.178	79.252	.753	2.307	4.921	216.430	57.926	.268
137.176	78.621	.778	2.275	4.921	215.797	58.555	.271
136.460	78.708	.753	2.307	4.916	215.168	57.752	.268
136.215	78.636	.753	2.307	4.914	214.851	57.579	.268
136.058	78.480	.753	2.307	4.913	214.538	57.579	.268
135.584	78.005	.753	2.307	4.910	213.589	57.579	.270
135.340	77.935	.753	2.307	4.908	213.275	57.405	.269
135.024	77.619	.753	2.307	4.905	212.642	57.405	.270
134.622	77.391	.753	2.307	4.902	212.013	57.231	.270
134.463	77.233	.753	2.307	4.901	211.696	57.231	.270
134.062	77.005	.753	2.307	4.898	211.066	57.057	.270
133.658	76.775	.753	2.307	4.895	210.434	56.883	.270

Table A4 continued

133.343	76.461	.753	2.307	4.893	209.804	56.883	.271
132.783	76.074	.753	2.307	4.889	208.858	56.709	.272
132.223	75.688	.753	2.307	4.884	207.911	56.535	.272
131.908	75.373	.753	2.307	4.882	207.282	56.535	.273
131.505	75.144	.753	2.307	4.879	206.649	56.361	.273
130.945	74.758	.753	2.307	4.875	205.703	56.187	.273
130.385	74.372	.753	2.307	4.870	204.756	56.013	.274
129.983	74.144	.753	2.307	4.867	204.127	55.839	.274
129.579	73.914	.753	2.307	4.864	203.494	55.665	.274
129.106	73.441	.753	2.307	4.861	202.547	55.665	.275
128.704	73.213	.753	2.307	4.858	201.918	55.491	.275
128.144	72.827	.753	2.307	4.853	200.972	55.317	.275
127.741	72.598	.753	2.307	4.850	200.339	55.143	.275
127.339	72.370	.753	2.307	4.847	199.709	54.969	.275
126.866	71.897	.753	2.307	4.843	198.763	54.969	.277
126.621	71.825	.753	2.307	4.841	198.446	54.795	.276
126.463	71.667	.753	2.307	4.840	198.130	54.795	.277
126.061	71.439	.753	2.307	4.837	197.500	54.621	.277
125.659	71.211	.753	2.307	4.834	196.870	54.447	.277
125.501	71.053	.753	2.307	4.832	196.554	54.447	.277
124.941	70.667	.753	2.307	4.828	195.608	54.273	.277
124.222	70.123	.753	2.307	4.822	194.345	54.100	.278
123.575	69.824	.753	2.307	4.817	193.399	53.752	.278
122.857	69.279	.753	2.307	4.811	192.136	53.578	.279
122.139	68.735	.753	2.307	4.805	190.873	53.404	.280
121.578	68.349	.753	2.307	4.801	189.927	53.230	.280
121.018	67.963	.753	2.307	4.796	188.981	53.056	.281
120.300	67.418	.753	2.307	4.790	187.718	52.882	.282
119.898	67.190	.753	2.307	4.787	187.089	52.708	.282
119.336	66.804	.753	2.307	4.782	186.142	52.534	.282
118.935	66.575	.753	2.307	4.779	185.509	52.360	.282
118.462	66.102	.753	2.307	4.775	184.563	52.360	.284
118.060	65.874	.753	2.307	4.771	183.934	52.186	.284
117.500	65.488	.753	2.307	4.766	182.987	52.012	.284
117.341	65.329	.753	2.307	4.765	182.671	52.012	.285

Table A4 continued

116.781	64.943	.753	2.307	4.760	181.725	51.838	.285
116.467	64.628	.753	2.307	4.758	181.095	51.838	.286
116.063	64.399	.753	2.307	4.754	180.462	51.664	.286
115.503	64.013	.753	2.307	4.749	179.516	51.490	.287
115.101	63.785	.753	2.307	4.746	178.886	51.316	.287
114.698	63.555	.753	2.307	4.742	178.253	51.142	.287
114.225	63.082	.753	2.307	4.738	177.307	51.142	.288
113.823	62.854	.753	2.307	4.735	176.677	50.968	.288
113.104	62.310	.753	2.307	4.728	175.415	50.794	.290
112.544	61.924	.753	2.307	4.723	174.468	50.620	.290
111.826	61.380	.753	2.307	4.717	173.206	50.447	.291
111.266	60.993	.753	2.307	4.712	172.259	50.273	.292
110.706	60.607	.753	2.307	4.707	171.313	50.099	.292
110.146	60.221	.753	2.307	4.702	170.367	49.925	.293
109.586	59.835	.753	2.307	4.697	169.421	49.751	.294
108.867	59.291	.753	2.307	4.690	168.158	49.577	.295
108.307	58.905	.753	2.307	4.685	167.212	49.403	.295
107.747	58.518	.753	2.307	4.680	166.266	49.229	.296
107.346	58.291	.753	2.307	4.676	165.636	49.055	.296
106.539	58.147	.730	2.338	4.669	164.687	48.392	.294
106.382	57.675	.753	2.307	4.667	164.057	48.707	.297
105.909	57.202	.753	2.307	4.663	163.111	48.707	.299
105.507	56.974	.753	2.307	4.659	162.481	48.533	.299
105.104	56.745	.753	2.307	4.655	161.848	48.359	.299
104.543	56.358	.753	2.307	4.650	160.902	48.185	.299
104.229	56.044	.753	2.307	4.647	160.272	48.185	.301
103.825	55.814	.753	2.307	4.643	159.639	48.011	.301
103.423	55.586	.753	2.307	4.639	159.009	47.837	.301
102.541	55.522	.730	2.338	4.630	158.063	47.019	.297
102.390	54.727	.753	2.307	4.629	157.117	47.663	.303
101.423	54.747	.730	2.338	4.619	156.171	46.676	.299
100.950	54.274	.730	2.338	4.615	155.225	46.676	.301
100.710	53.569	.753	2.307	4.612	154.278	47.141	.306
100.148	53.181	.753	2.307	4.607	153.329	46.968	.306
99.588	52.795	.753	2.307	4.601	152.383	46.794	.307

Table A4 continued

98.557	52.567	.730	2.338	4.591	151.123	45.990	.304
98.223	51.951	.753	2.307	4.587	150.174	46.272	.308
97.195	51.720	.730	2.338	4.577	148.915	45.475	.305
96.477	51.174	.730	2.338	4.569	147.652	45.303	.307
95.919	50.787	.730	2.338	4.564	146.706	45.132	.308
95.360	50.400	.730	2.338	4.558	145.759	44.960	.308
94.801	50.012	.730	2.338	4.552	144.813	44.788	.309
94.242	49.625	.730	2.338	4.546	143.867	44.617	.310
93.899	49.019	.753	2.307	4.542	142.918	44.880	.314
93.281	49.007	.730	2.338	4.536	142.288	44.273	.311
92.636	48.706	.730	2.338	4.529	141.342	43.930	.311
92.321	48.391	.730	2.338	4.525	140.712	43.930	.312
91.919	48.160	.730	2.338	4.521	140.079	43.759	.312
91.518	47.931	.730	2.338	4.517	139.449	43.587	.313
91.202	47.615	.730	2.338	4.513	138.816	43.587	.314
90.801	47.386	.730	2.338	4.509	138.187	43.416	.314
90.242	46.998	.730	2.338	4.502	137.241	43.244	.315
89.597	46.697	.730	2.338	4.495	136.294	42.901	.315
89.281	46.380	.730	2.338	4.492	135.661	42.901	.316
88.566	45.836	.730	2.338	4.484	134.402	42.729	.318
88.163	45.606	.730	2.338	4.479	133.769	42.558	.318
87.604	45.218	.730	2.338	4.473	132.823	42.386	.319
87.045	44.831	.730	2.338	4.466	131.877	42.214	.320
86.645	44.602	.730	2.338	4.462	131.247	42.043	.320
86.086	44.215	.730	2.338	4.455	130.301	41.871	.321
85.527	43.828	.730	2.336	4.449	129.354	41.699	.322
84.967	43.439	.730	2.338	4.442	128.405	41.528	.323
84.408	43.051	.730	2.338	4.436	127.459	41.356	.324
83.849	42.664	.730	2.338	4.429	126.513	41.185	.326
83.290	42.277	.730	2.338	4.422	125.566	41.013	.327
82.889	42.048	.730	2.338	4.418	124.937	40.841	.327
82.330	41.660	.730	2.338	4.411	123.991	40.670	.328
81.613	41.115	.730	2.338	4.402	122.728	40.498	.330
81.125	40.970	.730	2.338	4.396	122.095	40.155	.329
80.652	40.497	.730	2.338	4.390	121.149	40.155	.331

Table A4 continued

80.007	40.195	.730	2.338	4.382	120.203	39.812	.331
79.692	39.880	.730	2.338	4.378	119.573	39.812	.333
79.133	39.493	.730	2.338	4.371	118.627	39.640	.334
78.574	39.106	.730	2.338	4.364	117.680	39.469	.335
78.172	38.875	.730	2.338	4.359	117.047	39.297	.336
77.613	38.488	.730	2.338	4.352	116.101	39.126	.337
77.054	38.101	.730	2.338	4.345	115.155	38.954	.338
76.654	37.872	.730	2.338	4.339	114.525	38.782	.339
76.095	37.484	.730	2.338	4.332	113.579	38.611	.340
75.693	37.254	.730	2.338	4.327	112.946	38.439	.340
75.292	37.025	.730	2.338	4.321	112.316	38.267	.341
74.733	36.637	.730	2.338	4.314	111.370	38.096	.342
74.331	36.407	.730	2.338	4.309	110.737	37.924	.342
74.016	36.092	.730	2.338	4.304	110.108	37.924	.344
73.529	35.948	.730	2.338	4.298	109.478	37.581	.343
73.056	35.475	.730	2.338	4.291	108.532	37.581	.346
72.654	35.245	.730	2.338	4.286	107.899	37.409	.347
72.253	35.016	.730	2.338	4.280	107.269	37.238	.347
71.851	34.785	.730	2.338	4.275	106.636	37.066	.348
71.536	34.470	.730	2.338	4.270	106.006	37.066	.350
71.136	34.241	.730	2.338	4.265	105.377	36.895	.350
70.733	34.010	.730	2.338	4.259	104.744	36.723	.351
70.418	33.695	.730	2.338	4.254	104.114	36.723	.353
70.016	33.465	.730	2.338	4.249	103.481	36.551	.353
69.860	33.308	.730	2.338	4.246	103.168	36.551	.354
69.457	33.078	.730	2.338	4.241	102.535	36.380	.355
69.142	32.763	.730	2.338	4.236	101.905	36.380	.357
68.898	32.690	.730	2.338	4.233	101.589	36.208	.356
68.498	32.461	.730	2.338	4.227	100.959	36.037	.357
68.254	32.389	.730	2.338	4.223	100.642	35.865	.356
67.695	32.001	.730	2.338	4.215	99.696	35.693	.358
67.142	31.924	.707	2.370	4.207	99.066	35.218	.355
66.978	31.456	.730	2.338	4.204	98.434	35.522	.361
66.183	31.304	.707	2.370	4.192	97.487	34.879	.358
65.541	31.000	.707	2.370	4.183	96.541	34.540	.358

Table A4 continued

65.301	30.294	.730	2.338	4.179	95.595	35.007	.366
64.656	29.993	.730	2.338	4.169	94.649	34.664	.366
64.097	29.605	.730	2.338	4.160	93.703	34.492	.368
63.466	29.603	.707	2.370	4.151	93.070	33.863	.364
63.067	29.373	.707	2.370	4.144	92.440	33.694	.364
62.752	29.058	.707	2.370	4.139	91.810	33.694	.367
62.194	28.670	.707	2.370	4.130	90.864	33.524	.369
61.635	28.280	.707	2.370	4.121	89.915	33.355	.371
60.836	27.819	.707	2.370	4.108	88.655	33.016	.372
60.342	27.051	.730	2.338	4.100	87.392	33.291	.381
59.404	26.726	.707	2.370	4.084	86.130	32.678	.379
58.518	26.349	.707	2.370	4.069	84.867	32.170	.379
58.045	25.876	.707	2.370	4.061	83.921	32.170	.383
57.245	25.414	.707	2.370	4.047	82.658	31.831	.385
56.687	25.025	.707	2.370	4.038	81.712	31.662	.387
56.129	24.637	.707	2.370	4.028	80.766	31.493	.390
55.571	24.248	.707	2.370	4.018	79.820	31.323	.392
55.014	23.860	.707	2.370	4.008	78.873	31.154	.395
54.614	23.630	.707	2.370	4.000	78.244	30.985	.396
54.056	23.241	.707	2.370	3.990	77.297	30.815	.399
53.571	23.094	.707	2.370	3.981	76.665	30.477	.398
53.256	22.779	.707	2.370	3.975	76.035	30.477	.401
52.698	22.391	.707	2.370	3.965	75.089	30.307	.404
52.297	22.159	.707	2.370	3.957	74.456	30.138	.405
51.897	21.929	.707	2.370	3.949	73.826	29.969	.406
51.498	21.698	.707	2.370	3.942	73.196	29.799	.407
50.938	21.308	.707	2.370	3.931	72.247	29.630	.410
50.539	21.078	.707	2.370	3.923	71.617	29.461	.411
50.066	20.605	.707	2.370	3.913	70.671	29.461	.417
49.508	20.217	.707	2.370	3.902	69.725	29.292	.420
49.109	19.986	.707	2.370	3.894	69.095	29.122	.421
48.549	19.596	.707	2.370	3.883	68.146	28.953	.425
47.991	19.208	.707	2.370	3.871	67.199	28.783	.428
47.434	18.820	.707	2.370	3.859	66.253	28.614	.432
47.034	18.589	.707	2.370	3.851	65.623	28.445	.433

Table A4 continued

45.676	17.739	.707	2.370	3.822	63.415	27.937	.441
45.118	17.350	.707	2.370	3.809	62.468	27.768	.445
44.560	16.962	.707	2.370	3.797	61.522	27.598	.449
44.159	16.730	.707	2.370	3.788	60.889	27.429	.450
43.760	16.500	.707	2.370	3.779	60.259	27.260	.452
43.360	16.270	.707	2.370	3.770	59.630	27.090	.454
42.959	16.038	.707	2.370	3.760	58.997	26.921	.456
42.559	15.808	.707	2.370	3.751	58.367	26.752	.458
42.002	15.419	.707	2.370	3.738	57.421	26.582	.463
41.444	15.031	.707	2.370	3.724	56.475	26.413	.468
40.886	14.642	.707	2.370	3.711	55.528	26.244	.473
40.485	14.411	.707	2.370	3.701	54.896	26.074	.475
40.086	14.180	.707	2.370	3.691	54.266	25.905	.477
39.528	13.792	.707	2.370	3.677	53.320	25.736	.483
39.127	13.560	.707	2.370	3.667	52.687	25.567	.485
38.569	13.172	.707	2.370	3.652	51.741	25.397	.491
38.169	12.941	.707	2.370	3.642	51.111	25.228	.494
37.768	12.710	.707	2.370	3.631	50.478	25.059	.496
37.210	12.321	.707	2.370	3.617	49.532	24.889	.502
36.653	11.933	.707	2.370	3.601	48.585	24.720	.509
36.095	11.544	.707	2.370	3.586	47.639	24.551	.515
35.695	11.314	.707	2.370	3.575	47.009	24.381	.519
35.294	11.082	.707	2.370	3.564	46.377	24.212	.522
34.895	10.852	.707	2.370	3.552	45.747	24.043	.526
34.495	10.622	.707	2.370	3.541	45.117	23.873	.529
34.094	10.390	.707	2.370	3.529	44.484	23.704	.533
33.536	10.002	.707	2.370	3.513	43.538	23.535	.541
33.137	9.771	.707	2.370	3.501	42.908	23.365	.545
32.579	9.383	.707	2.370	3.484	41.962	23.196	.553
32.021	8.995	.707	2.370	3.466	41.016	23.027	.561
31.620	8.763	.707	2.370	3.454	40.383	22.857	.566
31.062	8.374	.707	2.370	3.436	39.437	22.688	.575
30.505	7.986	.707	2.370	3.418	38.491	22.519	.585
30.021	7.840	.707	2.370	3.402	37.861	22.180	.586
29.316	7.595	.684	2.402	3.378	36.911	21.721	.588

Table A4 continued

28.760	7.205	.684	2.402	3.359	35.965	21.554	.599
28.346	6.673	.707	2.370	3.344	35.019	21.672	.619
27.788	6.285	.707	2.370	3.325	34.073	21.503	.631
26.987	5.823	.707	2.370	3.295	32.810	21.164	.645
26.450	5.731	.684	2.402	3.275	32.180	20.719	.644
25.787	5.131	.707	2.370	3.250	30.918	20.656	.668
25.094	4.877	.684	2.402	3.223	29.972	20.217	.675
24.671	4.354	.707	2.370	3.206	29.025	20.318	.700
23.898	4.181	.684	2.402	3.174	28.079	19.716	.702
23.471	3.662	.707	2.370	3.156	27.133	19.810	.730
22.829	3.358	.707	2.370	3.128	26.187	19.471	.744
22.271	2.969	.707	2.370	3.103	25.241	19.302	.765
21.629	2.665	.707	2.370	3.074	24.294	18.963	.781
20.706	2.326	.684	2.402	3.030	23.032	18.380	.798
20.270	1.815	.707	2.370	3.009	22.085	18.455	.836
19.749	1.704	.684	2.402	2.983	21.453	18.045	.841
19.109	1.398	.684	2.402	2.950	20.506	17.711	.864
18.552	1.008	.684	2.402	2.921	19.560	17.544	.897
18.270	.661	.707	2.370	2.905	18.930	17.609	.930
17.784	.514	.707	2.370	2.878	18.297	17.270	.944
17.226	.125	.707	2.370	2.846	17.351	17.101	.986
16.826	-.105	.707	2.370	2.823	16.722	16.931	1.013
16.427	-.335	.707	2.370	2.799	16.092	16.762	1.042
16.026	-.567	.707	2.370	2.774	15.459	16.593	1.073
15.518	-.689	.684	2.402	2.742	14.829	16.207	1.093
15.225	-1.029	.707	2.370	2.723	14.196	16.254	1.145
14.803	-1.237	.684	2.402	2.695	13.566	16.040	1.182
14.562	-1.312	.684	2.402	2.678	13.250	15.873	1.198
14.163	-1.543	.684	2.402	2.651	12.620	15.706	1.245
14.025	-1.721	.707	2.370	2.641	12.304	15.746	1.280
13.710	-2.036	.707	2.370	2.618	11.674	15.746	1.349
13.467	-2.110	.707	2.370	2.600	11.358	15.577	1.372
13.224	-2.183	.707	2.370	2.582	11.041	15.408	1.395
12.808	-2.397	.684	2.402	2.550	10.411	15.205	1.460
12.667	-2.572	.707	2.370	2.539	10.095	15.238	1.510

Table A4 continued

12.326	-2.545	.684	2.402	2.512	9.782	14.871	1.520
12.064	-2.619	.684	2.402	2.492	9.465	14.704	1.553
11.768	-2.936	.684	2.402	2.465	8.832	14.704	1.665
11.528	-3.009	.684	2.402	2.445	8.519	14.537	1.706
11.286	-3.083	.684	2.402	2.424	8.203	14.369	1.752
10.971	-3.398	.684	2.402	2.395	7.573	14.369	1.898
10.824	-3.568	.707	2.370	2.382	7.256	14.392	1.983
10.425	-3.798	.707	2.370	2.344	6.627	14.223	2.146
10.023	-4.030	.707	2.370	2.305	5.994	14.053	2.345
9.616	-4.252	.684	2.402	2.263	5.364	13.868	2.585
9.223	-4.492	.707	2.370	2.222	4.731	13.714	2.899
8.576	-4.791	.684	2.402	2.149	3.785	13.367	3.532
8.177	-5.022	.684	2.402	2.101	3.155	13.200	4.184
7.779	-5.254	.684	2.402	2.051	2.525	13.033	5.161
7.379	-5.487	.684	2.402	1.999	1.892	12.866	6.799
6.981	-5.718	.684	2.402	1.943	1.263	12.699	10.057
6.581	-5.951	.684	2.402	1.884	.630	12.532	19.899
6.497	-5.867	.684	2.402	1.871	.630	12.364	19.634

Table A5 Compaction data for sugar compacted uniaxially at 250 MPa

σ (MPa)	τ (MPa)	ε	V ($mx10^{-6}$)	ln σ	σ_A (MPa)	σ_R MPa	$\frac{\sigma_R}{\sigma_A}$
.368	.263	0.000	3.792	-.999	.631	.106	.168
.369	.262	.008	3.760	-.997	.631	.107	.169
.581	.366	.017	3.729	-.543	.947	.215	.227
.740	.522	.026	3.697	-.302	1.262	.217	.172
.741	.522	.034	3.666	-.300	1.262	.219	.174
.953	.625	.034	3.666	-.048	1.578	.328	.208
.954	.623	.043	3.634	-.047	1.578	.331	.210
1.112	.781	.043	3.634	.106	1.893	.331	.175
1.327	.882	.053	3.602	.283	2.209	.446	.202
1.329	.880	.062	3.571	.284	2.209	.449	.204
1.329	.880	.062	3.571	.284	2.209	.449	.204
1.545	.979	.071	3.539	.435	2.524	.567	.225
1.706	1.134	.081	3.508	.534	2.840	.572	.201
1.706	1.134	.081	3.508	.534	2.840	.572	.201
1.706	1.134	.081	3.508	.534	2.840	.572	.201
1.864	1.292	.081	3.508	.622	3.155	.572	.181
1.924	1.231	.091	3.476	.654	3.155	.693	.220
2.085	1.386	.101	3.444	.735	3.471	.699	.201
2.085	1.386	.101	3.444	.735	3.471	.699	.201
2.088	1.383	.111	3.413	.736	3.471	.705	.203
2.305	1.482	.111	3.413	.835	3.786	.823	.217
2.308	1.478	.121	3.381	.837	3.786	.831	.219
2.470	1.631	.132	3.350	.904	4.102	.839	.204
2.530	1.572	.132	3.350	.928	4.102	.958	.234
2.628	1.789	.132	3.350	.966	4.417	.839	.190
2.845	1.887	.132	3.350	1.046	4.732	.958	.203
2.850	1.882	.143	3.318	1.047	4.732	.968	.204
2.850	1.882	.143	3.318	1.047	4.732	.968	.204

Table A5 continued

3.073	1.974	.154	3.286	1.123	5.048	1.099	.218
3.236	2.127	.165	3.255	1.174	5.363	1.110	.207
3.298	2.065	.165	3.255	1.193	5.363	1.233	.230
3.462	2.217	.176	3.223	1.242	5.679	1.245	.219
3.620	2.375	.176	3.223	1.286	5.994	1.245	.208
3.689	2.306	.188	3.192	1.305	5.994	1.383	.231
3.853	2.457	.200	3.160	1.349	6.310	1.397	.221
4.075	2.551	.200	3.160	1.405	6.625	1.524	.230
4.240	2.701	.212	3.128	1.445	6.941	1.539	.222
4.462	2.794	.212	3.128	1.496	7.256	1.667	.230
4.620	2.952	.212	3.128	1.530	7.572	1.667	.220
4.777	3.110	.212	3.128	1.564	7.887	1.667	.211
5.008	3.194	.224	3.097	1.611	8.203	1.814	.221
5.231	3.287	.224	3.097	1.655	8.518	1.944	.228
5.399	3.435	.237	3.065	1.686	8.834	1.964	.222
5.622	3.527	.237	3.065	1.727	9.149	2.095	.229
5.791	3.674	.250	3.034	1.756	9.465	2.116	.224
6.026	3.754	.263	3.002	1.796	9.780	2.272	.232
6.342	4.069	.263	3.002	1.847	10.411	2.272	.218
6.579	4.148	.277	2.970	1.864	10.727	2.432	.227
6.805	4.238	.277	2.970	1.918	11.042	2.567	.232
7.120	4.553	.277	2.970	1.963	11.673	2.567	.220
7.360	4.629	.290	2.939	1.996	11.989	2.731	.228
7.744	4.876	.290	2.939	2.047	12.620	2.867	.227
8.075	5.176	.304	2.907	2.089	13.251	2.899	.219
8.301	5.265	.304	2.907	2.116	13.566	3.037	.224
8.703	5.494	.319	2.876	2.164	14.197	3.210	.226
9.089	5.740	.319	2.876	2.207	14.828	3.349	.226
9.265	5.879	.333	2.844	2.226	15.144	3.386	.224
9.651	6.124	.333	2.844	2.267	15.775	3.527	.224
10.215	6.506	.348	2.812	2.324	16.721	3.710	.222
10.445	6.592	.348	2.812	2.346	17.037	3.852	.226
10.831	6.836	.348	2.812	2.362	17.668	3.995	.226
11.376	7.238	.348	2.812	2.432	18.614	4.138	.222
11.629	7.300	.364	2.781	2.454	18.930	4.329	.229

Table A5 continued

12.175	7.701	.364	2.781	2.499	19.876	4.473	.225
12.720	8.103	.364	2.781	2.543	20.823	4.618	.222
12.950	8.188	.364	2.781	2.561	21.138	4.762	.225
13.681	8.719	.379	2.749	2.616	22.400	4.963	.222
14.070	8.961	.379	2.749	2.644	23.031	5.109	.222
14.489	9.173	.395	2.718	2.673	23.662	5.316	.225
15.036	9.573	.395	2.718	2.710	24.609	5.463	.222
15.583	9.972	.395	2.718	2.746	25.555	5.611	.220
16.046	10.140	.395	2.718	2.775	26.186	5.906	.226
16.787	10.661	.412	2.686	2.821	27.448	6.125	.223
17.177	10.902	.412	2.686	2.844	28.079	6.275	.223
17.567	11.143	.412	2.686	2.866	28.710	6.424	.224
18.154	11.502	.429	2.654	2.899	29.657	6.652	.224
18.545	11.742	.429	2.654	2.920	30.288	6.803	.225
18.936	11.982	.429	2.654	2.941	30.918	6.954	.225
19.252	12.298	.429	2.654	2.958	31.549	6.954	.220
19.528	12.337	.446	2.623	2.972	31.865	7.191	.226
19.762	12.418	.446	2.623	2.984	32.180	7.344	.228
19.920	12.576	.446	2.623	2.992	32.496	7.344	.226
20.078	12.734	.446	2.623	3.000	32.811	7.344	.224
20.235	12.892	.446	2.623	3.007	33.127	7.344	.222
20.470	12.973	.446	2.623	3.019	33.442	7.497	.224
20.470	12.973	.446	2.623	3.019	33.442	7.497	.224
20.908	13.165	.463	2.591	3.040	34.073	7.743	.227
21.066	13.323	.463	2.591	3.048	34.389	7.743	.225
21.066	13.323	.463	2.591	3.048	34.389	7.743	.225
21.617	13.719	.463	2.591	3.073	35.335	7.898	.224
21.852	13.799	.463	2.591	3.084	35.651	8.053	.226
22.010	13.957	.463	2.591	3.091	35.966	8.053	.224
22.403	14.195	.463	2.591	3.109	36.597	8.208	.224
22.718	14.510	.463	2.591	3.123	37.228	8.208	.220
23.005	14.539	.481	2.560	3.136	37.544	8.466	.225
23.320	14.855	.481	2.560	3.149	38.175	8.466	.222
23.557	14.934	.481	2.560	3.159	38.491	8.623	.224
23.714	15.092	.481	2.560	3.166	38.806	8.623	.222

Table A5 continued

24.108	15.329	.481	2.560	3.183	39.437	8.779	.223
24.266	15.486	.481	2.560	3.189	39.752	8.779	.221
24.344	15.408	.481	2.560	3.192	39.752	8.936	.225
24.817	15.881	.481	2.560	3.212	40.699	8.936	.220
24.896	15.803	.481	2.560	3.215	40.699	9.093	.223
25.211	16.118	.481	2.560	3.227	41.330	9.093	.220
25.605	16.356	.481	2.560	3.243	41.961	9.250	.220
25.605	16.356	.481	2.560	3.243	41.961	9.250	.220
25.841	16.435	.481	2.560	3.252	42.276	9.406	.222
26.157	16.750	.481	2.560	3.264	42.907	9.406	.219
26.157	16.750	.481	2.560	3.264	42.907	9.406	.219
26.610	16.928	.500	2.528	3.281	43.538	9.683	.222
26.768	17.086	.500	2.528	3.287	43.854	9.683	.221
26.926	17.243	.500	2.528	3.293	44.169	9.683	.219
27.163	17.322	.500	2.526	3.302	44.485	9.841	.221
27.558	17.558	.500	2.528	3.316	45.116	10.000	.222
27.716	17.716	.500	2.528	3.322	45.431	10.000	.220
27.874	17.873	.500	2.528	3.328	45.747	10.000	.219
28.268	18.109	.500	2.528	3.342	46.378	10.159	.219
28.426	18.267	.500	2.528	3.347	46.693	10.159	.218
28.821	18.503	.500	2.528	3.361	47.324	10.318	.218
29.044	18.596	.519	2.496	3.369	47.640	10.448	.219
29.202	18.753	.519	2.496	3.374	47.955	10.448	.218
29.597	18.989	.519	2.496	3.388	48.586	10.609	.218
29.755	19.146	.519	2.496	3.393	48.902	10.609	.217
29.913	19.304	.519	2.496	3.398	49.217	10.609	.216
30.151	19.381	.519	2.496	3.406	49.533	10.770	.217
30.309	19.539	.519	2.496	3.411	49.846	10.770	.216
30.547	19.617	.519	2.496	3.419	50.164	10.930	.218
30.863	19.932	.519	2.496	3.430	50.795	10.930	.215
30.863	19.932	.519	2.496	3.430	50.795	10.930	.215
31.258	20.167	.519	2.496	3.442	51.426	11.091	.216
31.416	20.325	.519	2.496	3.447	51.741	11.091	.214
31.574	20.483	.519	2.496	3.452	52.057	11.091	.213
31.732	20.640	.519	2.496	3.457	52.372	11.091	.212

Table A5 continued

31.970	20.718	.519	2.496	3.465	52.688	11.252	.214
32.285	21.033	.519	2.496	3.475	53.319	11.252	.211
32.523	21.111	.519	2.496	3.482	53.634	11.413	.213
32.681	21.268	.519	2.496	3.487	53.950	11.413	.212
32.912	21.353	.538	2.465	3.494	54.265	11.559	.213
33.228	21.669	.538	2.465	3.503	54.896	11.559	.211
33.309	21.587	.538	2.465	3.506	54.896	11.722	.214
33.624	21.903	.538	2.465	3.515	55.527	11.722	.211
33.940	22.218	.538	2.465	3.525	56.158	11.722	.209
34.179	22.294	.538	2.465	3.532	56.473	11.885	.210
34.337	22.452	.538	2.465	3.536	56.789	11.885	.209
34.652	22.768	.538	2.465	3.545	57.420	11.885	.207
34.734	22.686	.536	2.465	3.548	57.420	12.047	.210
34.891	22.844	.538	2.465	3.552	57.735	12.047	.209
35.285	23.081	.558	2.433	3.563	58.366	12.204	.209
35.285	23.081	.558	2.433	3.563	58.366	12.204	.209
35.443	23.239	.558	2.433	3.568	58.682	12.204	.208
35.841	23.472	.558	2.433	3.579	59.313	12.369	.209
35.999	23.630	.558	2.433	3.583	59.628	12.369	.207
35.999	23.630	.558	2.433	3.583	59.628	12.369	.207
36.314	23.945	.558	2.433	3.592	60.259	12.369	.205
36.554	24.021	.558	2.433	3.599	60.575	12.534	.207
36.870	24.336	.558	2.433	3.607	61.206	12.534	.205
37.028	24.494	.558	2.433	3.612	61.522	12.534	.204
37.426	24.727	.558	2.433	3.622	62.153	12.699	.204
37.741	25.042	.558	2.433	3.631	62.784	12.699	.202
38.297	25.433	.558	2.433	3.645	63.730	12.864	.202
38.612	25.749	.558	2.433	3.654	64.361	12.864	.200
39.010	25.982	.558	2.433	3.664	64.992	13.028	.200
39.566	26.372	.558	2.433	3.678	65.938	13.193	.200
39.724	26.530	.558	2.433	3.682	66.254	13.193	.199
40.126	26.759	.579	2.402	3.692	66.885	13.367	.200
40.683	27.149	.579	2.402	3.706	67.831	13.534	.200
40.840	27.306	.579	2.402	3.710	68.147	13.534	.199
41.397	27.696	.579	2.402	3.723	69.093	13.701	.198

Table A5 continued

41.871	28.169	.579	2.402	3.735	70.040	13.701	.196
42.427	28.559	.579	2.402	3.748	70.986	13.868	.195
42.984	28.949	.579	2.402	3.761	71.933	14.035	.195
43.457	29.422	.579	2.402	3.772	72.879	14.035	.193
43.699	29.496	.579	2.402	3.777	73.195	14.202	.194
44.255	29.886	.579	2.402	3.790	74.141	14.369	.194
44.729	30.359	.579	2.402	3.801	75.088	14.369	.191
44.982	30.421	.600	2.370	3.806	75.403	14.561	.193
45.540	30.810	.600	2.370	3.819	76.350	14.730	.193
46.013	31.283	.600	2.370	3.829	77.296	14.730	.191
46.729	31.829	.600	2.370	3.844	78.556	14.900	.190
47.287	32.218	.600	2.370	3.856	79.505	15.069	.190
47.845	32.606	.600	2.370	3.868	80.451	15.238	.189
48.507	32.891	.622	2.338	3.882	81.398	15.616	.192
49.066	33.278	.622	2.338	3.893	82.344	15.788	.192
49.381	33.594	.622	2.338	3.900	82.975	15.788	.190
49.940	33.981	.622	2.338	3.911	83.922	15.959	.190
50.342	34.211	.622	2.338	3.919	84.553	16.131	.191
50.815	34.684	.622	2.338	3.928	85.499	16.131	.189
51.460	34.986	.622	2.338	3.941	86.446	16.474	.191
52.248	35.775	.622	2.338	3.956	88.023	16.474	.187
52.808	36.162	.622	2.338	3.967	88.970	16.646	.187
53.524	36.707	.622	2.338	3.980	90.232	16.817	.186
54.200	36.978	.644	2.307	3.993	91.178	17.222	.189
54.760	37.365	.644	2.307	4.003	92.124	17.395	.189
55.478	37.909	.644	2.307	4.016	93.386	17.569	.188
56.038	38.295	.644	2.307	4.026	94.333	17.743	.188
56.598	38.681	.644	2.307	4.036	95.279	17.917	.188
57.442	39.099	.667	2.275	4.051	96.541	18.342	.190
58.161	39.642	.667	2.275	4.063	97.803	18.519	.189
58.968	40.097	.667	2.275	4.077	99.066	18.871	.190
59.845	40.797	.667	2.275	4.092	100.643	19.048	.189
60.407	41.182	.667	2.275	4.101	101.589	19.224	.189
60.968	41.568	.667	2.275	4.110	102.536	19.401	.189
61.845	42.268	.667	2.275	4.125	104.113	19.577	.188

Table A5 continued

62.407	42.653	.667	2.275	4.134	105.060	19.753	.188
62.968	43.038	.667	2.275	4.143	106.006	19.930	.188
63.687	43.581	.667	2.275	4.154	107.268	20.106	.187
64.234	43.666	.690	2.244	4.163	107.899	20.568	.191
64.954	44.207	.690	2.244	4.174	109.161	20.747	.190
66.079	44.975	.690	2.244	4.191	111.054	21.105	.190
66.800	45.516	.690	2.244	4.202	112.316	21.284	.189
67.678	46.216	.690	2.244	4.215	113.894	21.462	.188
68.802	46.670	.714	2.212	4.231	115.471	22.132	.192
69.523	47.210	.714	2.212	4.242	116.733	22.313	.191
70.493	47.817	.714	2.212	4.256	118.310	22.676	.192
71.373	48.515	.714	2.212	4.268	119.888	22.858	.191
72.185	48.965	.714	2.212	4.279	121.150	23.220	.192
73.065	49.663	.714	2.212	4.291	122.728	23.402	.191
74.283	50.337	.714	2.212	4.308	124.621	23.946	.192
75.253	50.945	.714	2.212	4.321	126.198	24.309	.193
76.560	51.531	.739	2.180	4.338	128.091	25.029	.195
77.533	52.136	.739	2.180	4.351	129.668	25.397	.196
78.506	52.740	.739	2.180	4.363	131.246	25.765	.196
79.636	53.503	.739	2.180	4.377	133.139	26.133	.196
80.609	54.107	.739	2.180	4.390	134.716	26.501	.197
81.582	54.712	.739	2.180	4.402	136.294	26.870	.197
82.912	55.274	.765	2.149	4.418	138.187	27.638	.200
83.888	55.876	.765	2.149	4.429	139.764	28.012	.200
85.115	56.543	.765	2.149	4.444	141.657	28.572	.202
86.090	57.145	.765	2.149	4.455	143.234	28.945	.202
87.065	57.747	.765	2.149	4.467	144.812	29.319	.202
88.199	58.506	.765	2.149	4.480	146.705	29.692	.202
89.174	59.108	.765	2.149	4.491	148.283	30.066	.203
90.243	59.617	.765	2.149	4.503	149.860	30.626	.204
91.219	60.219	.765	2.149	4.513	151.438	31.000	.205
92.101	60.914	.765	2.149	4.523	153.015	31.186	.204
93.012	61.265	.765	2.149	4.533	154.277	31.746	.206
94.227	61.627	.791	2.117	4.546	155.854	32.599	.209
95.110	62.321	.791	2.117	4.555	157.432	32.789	.208

Table A5 continued

95.773	62.605	.791	2.117	4.562	158.378	33.168	.209
96.909	63.362	.791	2.117	4.574	160.271	33.547	.209
97.477	63.741	.791	2.117	4.580	161.218	33.737	.209
98.298	64.182	.791	2.117	4.588	162.480	34.116	.210
99.434	64.939	.791	2.117	4.599	164.373	34.495	.210
100.254	65.381	.791	2.117	4.608	165.635	34.874	.211
101.233	65.980	.791	2.117	4.617	167.212	35.253	.211
102.368	66.737	.791	2.117	4.629	169.105	35.632	.211
103.347	67.336	.791	2.117	4.638	170.683	36.011	.211
104.167	67.777	.791	2.117	4.646	171.945	36.390	.212
105.303	68.534	.791	2.117	4.657	173.838	36.769	.212
105.966	68.818	.791	2.117	4.663	174.784	37.148	.213
107.071	68.975	.818	2.086	4.673	176.046	38.096	.216
108.052	69.571	.818	2.086	4.683	177.623	38.481	.217
108.779	70.106	.818	2.086	4.689	178.885	38.673	.216
109.603	70.545	.818	2.086	4.697	180.147	39.058	.217
110.584	71.141	.818	2.086	4.706	181.725	39.443	.217
111.153	71.518	.818	2.086	4.711	182.672	39.635	.217
112.135	72.115	.818	2.086	4.720	184.249	40.020	.217
112.800	72.395	.818	2.086	4.726	185.196	40.405	.218
113.369	72.772	.818	2.086	4.731	186.142	40.597	.218
114.193	73.211	.818	2.086	4.738	187.404	40.982	.219
114.762	73.588	.818	2.086	4.743	188.350	41.174	.219
115.428	73.869	.818	2.086	4.749	189.297	41.559	.220
115.997	74.246	.818	2.086	4.754	190.243	41.751	.219
116.409	74.465	.818	2.086	4.757	190.874	41.944	.220
116.979	74.842	.818	2.086	4.762	191.821	42.136	.220
117.644	75.123	.818	2.086	4.768	192.767	42.521	.221
118.214	75.500	.818	2.086	4.772	193.714	42.714	.220
118.783	75.877	.818	2.086	4.777	194.660	42.906	.220
119.195	76.096	.818	2.086	4.781	195.291	43.098	.221
119.764	76.473	.818	2.086	4.786	196.238	43.291	.221
120.334	76.851	.818	2.086	4.790	197.184	43.483	.221
120.999	77.131	.818	2.086	4.796	198.131	43.868	.221
121.569	77.509	.818	2.086	4.800	199.077	44.060	.221

Table A5 continued

122.454	78.201	.818	2.086	4.808	200.655	44.253	.221
123.119	78.482	.818	2.086	4.813	201.601	44.638	.221
124.191	78.672	.846	2.054	4.822	202.863	45.520	.224
125.018	79.107	.846	2.054	4.828	204.125	45.910	.225
125.686	79.385	.846	2.054	4.834	205.072	46.301	.226
126.415	79.919	.846	2.054	4.840	206.334	46.496	.225
126.986	80.294	.846	2.054	4.844	207.280	46.692	.225
127.557	80.670	.846	2.054	4.849	208.227	46.887	.225
128.383	81.105	.846	2.054	4.855	209.489	47.278	.226
129.367	81.699	.846	2.054	4.863	211.066	47.669	.226
130.194	82.134	.846	2.054	4.869	212.328	48.059	.226
130.922	82.668	.846	2.054	4.875	213.590	48.255	.226
131.749	83.103	.846	2.054	4.881	214.852	48.646	.226
132.575	83.539	.846	2.054	4.887	216.114	49.036	.227
133.244	83.817	.846	2.054	4.892	217.060	49.427	.228
133.972	84.350	.846	2.054	4.898	218.322	49.622	.227
134.483	84.470	.846	2.054	4.901	218.953	50.013	.228
135.212	85.004	.846	2.054	4.907	220.216	50.208	.228
135.880	85.281	.846	2.054	4.912	221.162	50.599	.229
136.451	85.657	.846	2.054	4.916	222.108	50.794	.229
137.263	85.476	.875	2.022	4.922	222.739	51.787	.232
137.935	85.751	.875	2.022	4.927	223.686	52.183	.233
138.507	86.125	.875	2.022	4.931	224.632	52.382	.233
138.517	86.746	.846	2.054	4.931	225.263	51.771	.230
138.930	86.964	.846	2.054	4.934	225.894	51.967	.230
139.344	87.182	.846	2.054	4.937	226.525	52.162	.230
139.915	87.557	.846	2.054	4.941	227.472	52.357	.230
140.328	87.775	.846	2.054	4.944	228.103	52.553	.230
140.996	88.053	.846	2.054	4.949	229.049	52.943	.231
141.252	88.113	.846	2.054	4.951	229.365	53.139	.232
142.082	87.914	.875	2.022	4.956	229.996	54.167	.236
142.397	88.230	.875	2.022	4.959	230.627	54.167	.235
142.812	88.446	.875	2.022	4.962	231.258	54.366	.235
143.069	88.504	.875	2.022	4.963	231.573	54.564	.236
143.641	88.878	.875	2.022	4.967	232.520	54.763	.236

Table A5 continued

143.898	88.937	.875	2.022	4.969	232.835	54.961	.236
144.313	89.153	.875	2.022	4.972	233.466	55.160	.236
144.628	89.469	.875	2.022	4.974	234.097	55.160	.236
144.885	89.527	.875	2.022	4.976	234.413	55.358	.236
145.201	89.843	.875	2.022	4.978	235.044	55.358	.236
145.873	90.118	.875	2.022	4.983	235.990	55.755	.236
146.130	90.176	.875	2.022	4.984	236.306	55.953	.237
146.702	90.550	.875	2.022	4.988	237.252	56.152	.237
147.117	90.767	.875	2.022	4.991	237.883	56.350	.237
147.432	91.082	.875	2.022	4.993	238.514	56.350	.236
147.847	91.298	.875	2.022	4.996	239.145	56.548	.236
148.419	91.672	.875	2.022	5.000	240.091	56.747	.236
148.676	91.731	.875	2.022	5.002	240.407	56.945	.237
149.249	92.105	.875	2.022	5.006	241.353	57.144	.237
149.663	92.321	.875	2.022	5.008	241.984	57.342	.237
149.920	92.380	.875	2.022	5.010	242.300	57.541	.237
150.236	92.695	.875	2.022	5.012	242.931	57.541	.237
150.650	92.912	.875	2.022	5.015	243.562	57.739	.237
150.907	92.970	.875	2.022	5.017	243.878	57.937	.238
151.322	93.186	.875	2.022	5.019	244.509	58.136	.238
151.579	93.245	.875	2.022	5.021	244.824	58.334	.238
152.052	93.718	.875	2.022	5.024	245.771	58.334	.237
152.467	93.934	.875	2.022	5.027	246.402	58.533	.238
152.724	93.993	.875	2.022	5.029	246.717	58.731	.238
152.981	94.051	.875	2.022	5.030	247.032	58.930	.239
153.139	94.209	.875	2.022	5.031	247.348	58.930	.238
153.553	94.425	.875	2.022	5.034	247.979	59.128	.238
153.810	94.484	.875	2.022	5.036	248.294	59.326	.239
153.968	94.642	.875	2.022	5.037	248.610	59.326	.239
154.225	94.700	.875	2.022	5.038	248.925	59.525	.239
154.383	94.858	.875	2.022	5.039	249.241	59.525	.239
154.640	94.917	.875	2.022	5.041	249.556	59.723	.239
155.429	94.758	.905	2.022	5.046	250.187	60.671	.243
155.212	95.291	.875	2.022	5.045	250.503	59.922	.239
155.370	95.448	.875	2.022	5.046	250.818	59.922	.239

Table A5 continued

155.212	95.291	.875	2.022	5.045	250.503	59.922	.239
154.897	94.975	.875	2.022	5.043	249.872	59.922	.240
153.950	94.029	.875	2.022	5.037	247.979	59.922	.242
153.004	93.082	.875	2.022	5.030	246.086	59.922	.243
151.584	91.662	.875	2.022	5.021	243.247	59.922	.246
149.907	90.184	.875	2.022	5.010	240.091	59.723	.249
148.131	88.805	.875	2.022	4.998	236.937	59.326	.250
146.455	87.327	.875	2.022	4.987	233.782	59.128	.253
144.778	85.848	.875	2.022	4.975	230.627	58.930	.256
143.259	84.528	.875	2.022	4.965	227.787	58.731	.258
142.104	82.844	.905	2.022	4.957	224.948	59.260	.263
140.583	81.525	.905	2.022	4.946	222.108	59.059	.266
138.919	80.981	.875	2.022	4.934	219.900	57.937	.263
137.557	79.819	.875	2.022	4.924	217.376	57.739	.266
136.512	78.971	.875	2.022	4.916	215.483	57.541	.267
135.466	78.124	.875	2.022	4.909	213.590	57.342	.268
134.420	77.277	.875	2.022	4.901	211.697	57.144	.270
133.375	76.429	.875	2.022	4.893	209.804	56.945	.271
132.644	75.898	.875	2.022	4.888	208.542	56.747	.272
131.698	74.951	.875	2.022	4.881	206.649	56.747	.275
131.125	74.577	.875	2.022	4.876	205.703	56.548	.275
130.395	74.045	.875	2.022	4.871	204.441	56.350	.276
129.508	73.356	.875	2.022	4.864	202.863	56.152	.277
129.034	72.883	.875	2.022	4.860	201.917	56.152	.278
128.462	72.508	.875	2.022	4.856	200.970	55.953	.278
127.989	72.035	.875	2.022	4.852	200.024	55.953	.280
127.416	71.661	.875	2.022	4.847	199.077	55.755	.280
126.785	71.030	.875	2.022	4.842	197.815	55.755	.282
126.055	70.498	.875	2.022	4.837	196.553	55.556	.283
125.482	70.124	.875	2.022	4.832	195.607	55.358	.283
124.594	69.435	.875	2.022	4.825	194.029	55.160	.284
123.864	68.903	.875	2.022	4.819	192.767	54.961	.285
123.233	68.272	.875	2.022	4.814	191.505	54.961	.287
122.246	67.682	.875	2.022	4.806	189.928	54.564	.287
121.457	66.893	.875	2.022	4.800	188.350	54.564	.290

Table A5 continued

120.727	66.361	.875	2.022	4.794	187.088	54.366	.291
119.682	65.514	.875	2.022	4.785	185.196	54.167	.292
118.794	64.824	.875	2.022	4.777	183.618	53.969	.294
117.748	63.977	.875	2.022	4.769	181.725	53.771	.296
116.860	63.288	.875	2.022	4.761	180.147	53.572	.297
115.972	62.598	.875	2.022	4.753	178.570	53.374	.299
115.084	61.909	.875	2.022	4.746	176.993	53.175	.300
114.196	61.219	.875	2.022	4.738	175.415	52.977	.302
113.466	60.687	.875	2.022	4.732	174.153	52.779	.303
112.578	59.998	.875	2.022	4.724	172.576	52.580	.305
111.848	59.466	.875	2.022	4.717	171.314	52.382	.306
111.118	58.934	.875	2.022	4.711	170.052	52.183	.307
110.230	58.245	.875	2.022	4.703	168.474	51.985	.309
109.400	57.812	.875	2.022	4.695	167.212	51.588	.309
108.927	57.339	.875	2.022	4.691	166.266	51.588	.310
108.039	56.649	.875	2.022	4.682	164.688	51.390	.312
107.151	55.960	.875	2.022	4.674	163.111	51.191	.314
106.322	55.527	.875	2.022	4.666	161.849	50.795	.314
105.533	54.738	.875	2.022	4.659	160.271	50.795	.317
104.546	54.148	.875	2.022	4.650	158.694	50.398	.318
103.658	53.459	.875	2.022	4.641	157.116	50.199	.320
102.770	52.769	.875	2.022	4.632	155.539	50.001	.321
101.814	52.778	.846	2.054	4.623	154.592	49.036	.317
101.183	52.147	.846	2.054	4.617	153.330	49.036	.320
100.357	51.711	.846	2.054	4.609	152.068	48.646	.320
99.726	51.081	.846	2.054	4.602	150.807	48.646	.323
99.534	50.326	.875	2.022	4.600	149.860	49.207	.328
98.646	49.637	.875	2.022	4.592	148.283	49.009	.331
97.816	49.204	.875	2.022	4.583	147.021	48.612	.331
97.027	48.416	.875	2.022	4.575	145.443	48.612	.334
95.512	48.038	.846	2.054	4.559	143.550	47.473	.331
94.783	47.505	.846	2.054	4.552	142.288	47.278	.332
93.739	46.656	.846	2.054	4.541	140.395	47.083	.335
92.695	45.808	.846	2.054	4.529	138.502	46.887	.339
91.966	45.274	.846	2.054	4.521	137.240	46.692	.340

Table A5 continued

90.824	44.523	.846	2.054	4.509	135.347	46.301	.342
89.938	43.832	.846	2.054	4.499	133.770	46.106	.345
89.051	43.141	.846	2.054	4.489	132.192	45.910	.347
87.910	42.390	.846	2.054	4.476	130.299	45.520	.349
86.865	41.541	.846	2.054	4.464	128.406	45.324	.353
85.979	40.850	.846	2.054	4.454	126.829	45.129	.356
84.935	40.001	.846	2.054	4.442	124.936	44.933	.360
84.048	39.310	.846	2.054	4.431	123.359	44.738	.363
83.064	38.717	.846	2.054	4.420	121.781	44.348	.364
81.862	37.710	.846	2.054	4.405	119.572	44.152	.369
80.720	36.959	.846	2.054	4.391	117.679	43.761	.372
79.676	36.110	.846	2.054	4.378	115.787	43.566	.376
78.377	35.201	.846	2.054	4.362	113.578	43.175	.380
77.175	34.195	.846	2.054	4.346	111.370	42.980	.386
76.033	33.444	.846	2.054	4.331	109.477	42.589	.389
74.831	32.437	.846	2.054	4.315	107.268	42.394	.395
73.689	31.686	.846	2.054	4.300	105.375	42.003	.399
72.487	30.679	.846	2.054	4.283	103.167	41.808	.405
71.345	29.928	.846	2.054	4.268	101.274	41.417	.409
70.204	29.177	.846	2.054	4.251	99.381	41.026	.413
69.159	28.329	.846	2.054	4.236	97.488	40.831	.419
67.860	27.420	.846	2.054	4.217	95.279	40.440	.424
66.816	26.571	.846	2.054	4.202	93.386	40.245	.431
65.674	25.820	.846	2.054	4.185	91.493	39.854	.436
64.630	24.971	.846	2.054	4.169	89.601	39.659	.443
63.743	24.280	.846	2.054	4.155	88.023	39.463	.448
62.463	23.982	.818	2.086	4.135	86.446	38.481	.445
61.578	23.290	.818	2.086	4.120	84.868	38.288	.451
60.851	22.755	.818	2.086	4.108	83.606	38.096	.456
59.966	22.063	.818	2.086	4.094	82.029	37.903	.462
59.239	21.528	.818	2.086	4.082	80.767	37.711	.467
58.800	20.705	.846	2.054	4.074	79.505	38.096	.479
58.072	20.171	.846	2.054	4.062	78.243	37.901	.484
57.501	19.796	.846	2.054	4.052	77.296	37.705	.488
56.488	19.546	.818	2.086	4.034	76.034	36.941	.486

Table A5 continued

55.761	19.012	.818	2.086	4.021	74.772	36.749	.491
55.349	18.792	.818	2.086	4.014	74.141	36.557	.493
54.780	18.415	.818	2.086	4.003	73.195	36.364	.497
54.052	17.881	.818	2.086	3.990	71.933	36.172	.503
53.737	17.565	.818	2.086	3.984	71.302	36.172	.507
53.167	17.188	.818	2.086	3.973	70.355	35.979	.511
52.873	16.536	.846	2.054	3.968	69.409	36.338	.524
52.302	16.160	.846	2.054	3.957	68.462	36.142	.528
51.459	16.057	.818	2.086	3.941	67.516	35.402	.524
50.986	15.584	.818	2.086	3.932	66.569	35.402	.532
50.574	15.364	.818	2.086	3.923	65.938	35.210	.534
50.101	14.891	.818	2.086	3.914	64.992	35.210	.542
49.689	14.672	.818	2.086	3.906	64.361	35.017	.544
49.278	14.452	.818	2.086	3.897	63.730	34.825	.546
48.550	13.918	.818	2.086	3.883	62.468	34.633	.554
48.235	13.602	.818	2.086	3.876	61.837	34.633	.560
47.823	13.383	.818	2.086	3.868	61.206	34.440	.563
47.254	13.006	.818	2.086	3.856	60.259	34.248	.568
46.938	12.690	.818	2.086	3.849	59.628	34.248	.574
46.684	12.629	.818	2.086	3.843	59.313	34.055	.574
46.211	12.156	.818	2.086	3.833	58.366	34.055	.583
45.957	12.094	.818	2.086	3.828	58.051	33.863	.583
45.545	11.875	.818	2.086	3.819	57.420	33.670	.586
45.387	11.717	.818	2.086	3.815	57.104	33.670	.590
44.818	11.340	.818	2.086	3.803	56.158	33.478	.596
44.503	11.024	.818	2.086	3.796	55.527	33.478	.603
44.091	10.805	.818	2.086	3.786	54.896	33.286	.606
43.679	10.586	.818	2.086	3.777	54.265	33.093	.610
43.206	10.113	.818	2.086	3.766	53.319	33.093	.621
42.637	9.736	.818	2.086	3.753	52.372	32.901	.628
42.067	9.359	.818	2.086	3.739	51.426	32.709	.636
41.594	8.885	.818	2.086	3.728	50.479	32.709	.648
41.024	8.508	.818	2.086	3.714	49.533	32.516	.656
40.455	8.131	.818	2.086	3.700	48.586	32.324	.665
39.885	7.754	.818	2.086	3.686	47.640	32.131	.674

Table A5 continued

39.158	7.219	.818	2.086	3.668	46.376	31.939	.689
38.589	6.842	.818	2.086	3.653	45.431	31.747	.699
38.019	6.465	.818	2.086	3.638	44.485	31.554	.709
37.292	5.931	.818	2.086	3.619	43.223	31.362	.726
36.723	5.554	.818	2.086	3.603	42.276	31.169	.737
35.996	5.019	.818	2.086	3.583	41.014	30.977	.755
35.426	4.642	.818	2.086	3.567	40.068	30.785	.768
34.953	4.168	.818	2.086	3.554	39.121	30.785	.787
34.287	3.886	.818	2.086	3.535	38.175	30.400	.796
33.718	3.511	.818	2.086	3.518	37.228	30.207	.811
33.148	3.134	.818	2.086	3.501	36.282	30.015	.827
32.675	2.660	.818	2.086	3.487	35.335	30.015	.849
32.106	2.283	.818	2.086	3.469	34.389	29.822	.867
31.536	1.906	.818	2.086	3.451	33.442	29.630	.886
30.713	1.468	.818	2.086	3.425	32.180	29.245	.909
30.397	1.152	.818	2.086	3.414	31.549	29.245	.927
29.828	.775	.818	2.086	3.395	30.603	29.053	.949
29.005	.337	.818	2.086	3.367	29.341	28.668	.977
28.435	-.040	.818	2.086	3.348	28.395	28.476	1.003
27.866	-.418	.818	2.086	3.327	27.448	28.283	1.030
27.042	-.856	.818	2.086	3.297	26.186	27.899	1.065
26.315	-1.391	.818	2.086	3.270	24.924	27.706	1.112
25.588	-1.926	.818	2.086	3.242	23.662	27.514	1.163
24.764	-2.364	.818	2.086	3.209	22.400	27.129	1.211
24.037	-2.899	.818	2.086	3.180	21.138	26.937	1.274
22.858	-3.297	.791	2.117	3.129	19.561	26.155	1.337
22.171	-4.188	.818	2.086	3.099	17.983	26.359	1.466
21.348	-4.627	.818	2.086	3.061	16.721	25.974	1.553
20.524	-5.065	.818	2.086	3.022	15.459	25.590	1.655
19.797	-5.600	.818	2.086	2.966	14.197	25.397	1.789
18.974	-6.038	.818	2.086	2.943	12.935	25.012	1.934
18.150	-6.477	.818	2.086	2.899	11.673	24.628	2.110
16.988	-6.893	.791	2.117	2.833	10.096	23.861	2.365
16.168	-7.334	.791	2.117	2.763	8.834	23.502	2.660
15.347	-7.775	.791	2.117	2.731	7.572	23.123	3.054

Table A5 continued

14.274	-8.280	.791	2.117	2.658	5.994	22.554	3.763
13.454	-8.721	.791	2.117	2.599	4.732	22.175	4.686
12.381	-9.226	.791	2.117	2.516	3.155	21.607	6.848
11.466	-9.573	.791	2.117	2.439	1.893	21.038	11.113
10.550	-9.919	.791	2.117	2.356	.631	20.469	32.439

Table A6 Compaction data for Styrocell compacted uniaxially at 247 MPa

σ (MPa)	τ (MPa)	ε	$V_{mx10^{-6}}$	$\ln\sigma$	σ_A (MPa)	σ_R (MPa)	σ_R/σ_A
.497	.134	0.000	3.318	-.699	.631	.363	.575
.497	.134	0.000	3.318	-.699	.631	.363	.575
.878	.384	.019	3.255	-.131	1.262	.493	.391
1.255	.638	.019	3.255	.227	1.893	.616	.326
1.698	.826	.029	3.223	.529	2.524	.871	.345
2.143	1.012	.040	3.192	.762	3.155	1.132	.359
2.686	1.416	.050	3.160	.988	4.102	1.270	.310
3.358	1.690	.061	3.128	1.211	5.048	1.667	.330
4.117	2.193	.061	3.128	1.415	6.310	1.924	.305
4.730	2.527	.071	3.097	1.554	7.256	2.203	.304
5.503	3.016	.082	3.065	1.705	8.518	2.487	.292
6.173	3.292	.082	3.065	1.820	9.465	2.880	.304
6.951	3.776	.094	3.034	1.939	10.727	3.175	.296
7.890	4.415	.105	3.002	2.066	12.304	3.475	.282
8.742	4.824	.117	2.970	2.168	13.566	3.918	.289
9.508	5.320	.117	2.970	2.252	14.828	4.168	.282
10.524	5.882	.129	2.939	2.354	16.406	4.642	.283
11.360	6.308	.129	2.939	2.430	17.668	5.052	.286
12.156	6.773	.141	2.907	2.498	18.930	5.383	.284
13.114	7.393	.154	2.876	2.574	20.507	5.721	.279
13.797	7.657	.154	2.876	2.624	21.454	6.140	.286
14.603	8.113	.167	2.844	2.681	22.716	6.490	.286
15.413	8.564	.180	2.812	2.735	23.978	6.849	.286
16.029	8.895	.180	2.812	2.774	24.924	7.134	.286
16.845	9.341	.193	2.781	2.824	26.186	7.504	.287
17.620	9.828	.193	2.781	2.869	27.448	7.792	.284
18.211	10.183	.207	2.749	2.902	28.395	8.028	.283
18.830	10.511	.207	2.749	2.935	29.341	8.320	.284

Table A6 continued

19.657	10.946	.221	2.718	2.978	30.603	8.712	.285
20.204	11.345	.221	2.718	3.006	31.549	8.859	.281
20.804	11.691	.235	2.686	3.035	32.496	9.113	.280
21.641	12.117	.250	2.654	3.075	33.758	9.524	.282
22.032	12.357	.250	2.654	3.092	34.389	9.675	.281
22.814	12.837	.250	2.654	3.127	35.651	9.977	.280
23.658	13.255	.265	2.623	3.164	36.913	10.404	.282
24.050	13.494	.265	2.623	3.180	37.544	10.557	.281
24.901	13.905	.280	2.591	3.215	38.806	10.995	.283
25.609	14.459	.280	2.591	3.243	40.068	11.150	.278
26.237	14.777	.280	2.591	3.267	41.014	11.460	.279
26.938	15.023	.296	2.560	3.294	41.961	11.915	.284
27.647	15.576	.296	2.560	3.320	43.223	12.072	.279
28.355	15.815	.313	2.528	3.345	44.169	12.540	.284
29.065	16.366	.313	2.528	3.370	45.431	12.699	.280
29.937	16.756	.329	2.496	3.399	46.693	13.181	.282
30.729	17.226	.329	2.496	3.425	47.955	13.502	.282
31.370	17.532	.346	2.465	3.446	48.902	13.838	.283
32.321	18.158	.346	2.465	3.476	50.479	14.164	.281
32.958	18.468	.346	2.465	3.495	51.426	14.489	.282
33.848	18.840	.364	2.433	3.522	52.688	15.008	.285
34.801	19.464	.364	2.433	3.550	54.265	15.337	.283
35.542	19.669	.382	2.402	3.571	55.212	15.873	.287
36.498	20.291	.382	2.402	3.597	56.789	16.207	.285
37.536	20.829	.382	2.402	3.625	58.366	16.709	.286
38.292	21.021	.400	2.370	3.645	59.313	17.270	.291
39.250	21.641	.400	2.370	3.670	60.891	17.609	.289
40.208	22.260	.400	2.370	3.694	62.468	17.947	.287
41.060	22.355	.419	2.338	3.715	63.415	18.705	.295
42.020	22.972	.419	2.338	3.738	64.992	19.048	.293
42.822	23.431	.419	2.338	3.757	66.254	19.391	.293
43.602	23.598	.438	2.307	3.775	67.200	20.005	.298
44.407	24.055	.438	2.307	3.793	68.462	20.353	.297
45.212	24.512	.438	2.307	3.811	69.724	20.701	.297
45.615	24.741	.438	2.307	3.820	70.355	20.874	.297

Table A6 continued

46.567	25.050	.458	2.275	3.841	71.617	21.517	.300
47.217	25.347	.458	2.275	3.855	72.564	21.870	.301
47.709	25.486	.458	2.275	3.865	73.195	22.223	.304
48.270	25.871	.458	2.275	3.877	74.141	22.399	.302
48.674	26.098	.458	2.275	3.885	74.772	22.575	.302
49.166	26.238	.458	2.275	3.895	75.403	22.928	.304
49.890	26.460	.479	2.244	3.910	76.350	23.430	.307
50.295	26.686	.479	2.244	3.918	76.981	23.609	.307
50.542	26.754	.479	2.244	3.923	77.296	23.788	.308
50.947	26.980	.479	2.244	3.931	77.927	23.966	.306
51.194	27.049	.479	2.244	3.936	78.243	24.145	.309
51.194	27.049	.479	2.244	3.936	78.243	24.145	.309
51.441	27.117	.479	2.244	3.940	78.558	24.324	.310
51.441	27.117	.479	2.244	3.940	78.558	24.324	.310
51.688	27.185	.479	2.244	3.945	78.874	24.503	.311
51.846	27.343	.479	2.244	3.948	79.189	24.503	.309
52.093	27.411	.479	2.244	3.953	79.505	24.682	.310
52.409	27.727	.479	2.244	3.959	80.136	24.682	.308
52.814	27.953	.479	2.244	3.967	80.767	24.861	.308
53.488	27.910	.500	2.212	3.979	81.398	25.579	.314
54.210	28.450	.500	2.212	3.993	82.659	25.760	.312
55.022	28.899	.500	2.212	4.008	83.922	26.123	.311
55.586	29.282	.500	2.212	4.018	84.868	26.304	.310
56.241	29.574	.500	2.212	4.030	85.815	26.667	.311
56.805	29.956	.500	2.212	4.040	86.761	26.848	.309
57.459	30.248	.500	2.212	4.051	87.708	27.211	.310
57.866	30.473	.500	2.212	4.058	88.339	27.393	.310
58.520	30.765	.500	2.212	4.069	89.285	27.756	.311
58.926	30.990	.500	2.212	4.076	89.916	27.937	.311
59.490	31.372	.500	2.212	4.086	90.863	28.118	.309
60.259	31.549	.522	2.180	4.099	91.809	28.710	.313
60.667	31.773	.522	2.180	4.105	92.440	28.894	.313
60.957	32.113	.500	2.212	4.110	93.071	28.844	.310
61.732	32.286	.522	2.180	4.123	94.017	29.446	.313
61.981	32.351	.522	2.180	4.127	94.333	29.630	.314

Table A6 continued

62.547	32.733	.522	2.180	4.136	95.279	29.814	.313
63.204	33.022	.522	2.180	4.146	96.226	30.182	.314
63.454	33.088	.522	2.180	4.150	96.541	30.366	.315
64.019	33.469	.522	2.180	4.159	97.488	30.550	.313
64.427	33.692	.522	2.180	4.166	98.119	30.734	.313
64.676	33.758	.522	2.180	4.169	98.434	30.918	.314
65.084	33.982	.522	2.180	4.176	99.066	31.102	.314
65.491	34.205	.522	2.180	4.182	99.696	31.286	.314
65.899	34.428	.522	2.180	4.188	100.327	31.470	.314
66.306	34.652	.522	2.180	4.194	100.958	31.655	.314
66.714	34.875	.522	2.180	4.200	101.589	31.839	.313
66.964	34.941	.522	2.180	4.204	101.905	32.023	.314
67.371	35.165	.522	2.180	4.210	102.536	32.207	.314
67.779	35.388	.522	2.180	4.216	103.167	32.391	.314
68.028	35.454	.522	2.180	4.220	103.482	32.575	.315
68.835	35.594	.544	2.149	4.232	104.429	33.240	.318
69.086	35.659	.544	2.149	4.235	104.744	33.427	.319
69.093	35.966	.522	2.180	4.235	105.060	33.127	.315
69.904	36.103	.544	2.149	4.247	106.006	33.801	.319
70.312	36.325	.544	2.149	4.253	106.637	33.987	.319
70.721	36.547	.544	2.149	4.259	107.268	34.174	.319
71.288	36.927	.544	2.149	4.267	108.215	34.361	.318
71.697	37.149	.544	2.149	4.272	108.846	34.548	.317
72.106	37.371	.544	2.149	4.278	109.477	34.734	.317
72.608	37.500	.544	2.149	4.285	110.108	35.108	.319
73.017	37.722	.544	2.149	4.291	110.739	35.295	.319
73.425	37.944	.544	2.149	4.296	111.370	35.481	.319
73.992	38.324	.544	2.149	4.304	112.316	35.668	.318
74.337	38.295	.544	2.149	4.309	112.632	36.042	.320
74.746	38.517	.544	2.149	4.314	113.263	36.228	.320
75.312	38.897	.544	2.149	4.322	114.209	36.415	.319
75.563	38.961	.544	2.149	4.325	114.525	36.602	.320
76.130	39.341	.544	2.149	4.332	115.471	36.789	.319
76.381	39.406	.544	2.149	4.336	115.787	36.975	.319
76.790	39.628	.544	2.149	4.341	116.418	37.162	.319

Table A6 continued

77.199	39.850	.544	2.149	4.346	117.048	37.349	.319
77.608	40.072	.544	2.149	4.352	117.679	37.536	.319
78.016	40.294	.544	2.149	4.357	118.310	37.722	.319
78.425	40.516	.544	2.149	4.362	118.941	37.909	.319
78.834	40.738	.544	2.149	4.367	119.572	38.096	.319
79.243	40.960	.544	2.149	4.373	120.203	38.283	.318
79.781	40.738	.567	2.117	4.379	120.519	39.044	.324
80.349	41.116	.567	2.117	4.386	121.466	39.233	.323
80.312	41.469	.544	2.149	4.386	121.781	38.643	.319
81.012	41.400	.567	2.117	4.395	122.412	39.612	.324
81.580	41.778	.567	2.117	4.402	123.359	39.802	.323
81.833	41.841	.567	2.117	4.405	123.674	39.991	.323
82.243	42.062	.567	2.117	4.410	124.305	40.181	.323
82.811	42.441	.567	2.117	4.417	125.252	40.370	.322
83.063	42.503	.567	2.117	4.420	125.567	40.560	.323
83.474	42.724	.567	2.117	4.425	126.198	40.749	.323
84.042	43.103	.567	2.117	4.431	127.144	40.939	.322
84.452	43.324	.567	2.117	4.436	127.775	41.128	.322
84.862	43.544	.567	2.117	4.441	128.406	41.318	.322
85.430	43.923	.567	2.117	4.448	129.353	41.507	.321
85.683	43.986	.567	2.117	4.451	129.668	41.697	.322
86.188	44.112	.567	2.117	4.457	130.299	42.076	.323
86.756	44.490	.567	2.117	4.463	131.246	42.265	.322
86.913	44.648	.567	2.117	4.465	131.561	42.265	.321
87.418	44.774	.567	2.117	4.471	132.192	42.645	.323
87.987	45.152	.567	2.117	4.477	133.139	42.834	.322
88.239	45.215	.567	2.117	4.480	133.454	43.024	.322
88.807	45.594	.567	2.117	4.486	134.401	43.213	.322
89.217	45.815	.567	2.117	4.491	135.032	43.403	.321
89.627	46.035	.567	2.117	4.496	135.663	43.592	.321
90.038	46.256	.567	2.117	4.500	136.294	43.782	.321
90.701	46.540	.567	2.117	4.508	137.240	44.161	.322
91.016	46.855	.567	2.117	4.511	137.871	44.161	.320
91.837	47.297	.567	2.117	4.520	139.133	44.540	.320
92.405	47.675	.567	2.117	4.526	140.080	44.729	.319

Table A6 continued

92.910	47.801	.567	2.117	4.532	140.711	45.108	.321
93.635	48.337	.567	2.117	4.539	141.973	45.298	.319
94.456	48.779	.567	2.117	4.548	143.234	45.677	.319
94.866	48.999	.567	2.117	4.552	143.866	45.867	.319
95.687	49.441	.567	2.117	4.561	145.128	46.246	.319
96.192	49.567	.567	2.117	4.566	145.759	46.625	.320
96.917	50.103	.567	2.117	4.574	147.021	46.814	.318
97.423	50.229	.567	2.117	4.579	147.652	47.193	.320
97.990	50.608	.567	2.117	4.585	148.598	47.383	.319
98.919	50.626	.591	2.086	4.594	149.545	48.293	.323
99.064	51.112	.567	2.117	4.596	150.176	47.951	.319
99.632	51.491	.567	2.117	4.601	151.122	48.141	.319
100.294	51.774	.567	2.117	4.608	152.068	48.520	.319
101.231	51.784	.591	2.086	4.617	153.015	49.448	.323
101.801	52.161	.591	2.086	4.623	153.961	49.640	.322
102.466	52.442	.591	2.086	4.630	154.908	50.025	.323
103.132	52.722	.591	2.086	4.636	155.854	50.410	.323
103.419	53.382	.567	2.117	4.639	156.801	50.036	.319
104.367	53.380	.591	2.086	4.648	157.747	50.987	.323
105.033	53.661	.591	2.086	4.654	158.694	51.372	.324
105.602	54.038	.591	2.086	4.660	159.641	51.564	.323
106.426	54.477	.591	2.086	4.667	160.902	51.949	.323
107.249	54.915	.591	2.086	4.675	162.164	52.334	.323
107.915	55.196	.591	2.086	4.681	163.111	52.718	.323
108.738	55.635	.591	2.086	4.689	164.373	53.103	.323
109.307	56.012	.591	2.086	4.694	165.319	53.296	.322
109.973	56.293	.591	2.086	4.700	166.266	53.680	.323
110.797	56.731	.591	2.086	4.708	167.528	54.065	.323
111.366	57.108	.591	2.086	4.713	168.474	54.258	.322
112.443	57.608	.591	2.086	4.722	170.052	54.835	.322
113.582	58.362	.591	2.086	4.733	171.945	55.220	.321
114.563	58.959	.591	2.086	4.741	173.522	55.605	.320
115.641	59.459	.591	2.086	4.750	175.100	56.182	.321
116.937	60.371	.591	2.086	4.762	177.308	56.567	.319
118.015	60.871	.591	2.086	4.771	178.885	57.144	.319

Table A6 continued

118.996	61.467	.591	2.086	4.779	180.463	57.528	.319
120.389	62.283	.591	2.086	4.791	182.672	58.106	.318
121.466	62.783	.591	2.086	4.800	184.249	58.683	.318
122.543	63.283	.591	2.086	4.808	185.827	59.260	.319
123.682	64.037	.591	2.086	4.818	187.719	59.645	.318
124.759	64.537	.591	2.086	4.826	189.297	60.222	.318
125.837	65.037	.591	2.086	4.835	190.874	60.799	.319
126.976	65.792	.591	2.086	4.844	192.767	61.184	.317
127.895	66.134	.591	2.086	4.851	194.029	61.761	.318
128.876	66.730	.591	2.086	4.859	195.607	62.146	.318
129.954	67.230	.591	2.086	4.867	197.184	62.723	.318
130.777	67.669	.591	2.086	4.873	198.446	63.108	.318
131.855	68.169	.591	2.086	4.882	200.024	63.686	.318
132.836	68.766	.591	2.086	4.889	201.601	64.070	.318
133.755	69.108	.591	2.086	4.896	202.863	64.648	.319
135.079	69.046	.615	2.054	4.906	204.125	66.033	.323
135.656	70.047	.591	2.086	4.910	205.703	65.609	.319
136.479	70.485	.591	2.086	4.916	206.965	65.994	.319
137.461	71.081	.591	2.086	4.923	208.542	66.379	.318
138.538	71.582	.591	2.086	4.931	210.120	66.956	.319
139.722	71.344	.615	2.054	4.940	211.066	68.377	.324
140.548	71.780	.615	2.054	4.946	212.328	68.768	.324
141.630	72.276	.615	2.054	4.953	213.905	69.354	.324
142.201	72.651	.615	2.054	4.957	214.852	69.549	.324
142.593	73.521	.591	2.086	4.960	216.114	69.073	.320
144.109	73.583	.615	2.054	4.971	217.691	70.526	.324
144.777	73.861	.615	2.054	4.975	218.638	70.917	.324
145.604	74.296	.615	2.054	4.981	219.900	71.308	.324
146.430	74.732	.615	2.054	4.987	221.162	71.698	.324
147.099	75.010	.615	2.054	4.991	222.108	72.089	.325
147.376	75.994	.591	2.086	4.993	223.370	71.382	.320
148.594	75.723	.615	2.054	5.001	224.317	72.870	.325
149.104	75.843	.615	2.054	5.005	224.948	73.261	.326
149.931	76.279	.615	2.054	5.010	226.210	73.652	.326
150.502	76.654	.615	2.054	5.014	227.156	73.847	.325

Table A6 continued

151.013	76.775	.615	2.054	5.017	227.787	74.238	.326
151.741	77.308	.615	2.054	5.022	229.049	74.433	.325
152.252	77.428	.615	2.054	5.026	229.680	74.824	.326
152.763	77.548	.615	2.054	5.029	230.311	75.215	.327
153.334	77.924	.615	2.054	5.033	231.258	75.410	.326
153.845	78.044	.615	2.054	5.036	231.889	75.801	.327
154.416	78.419	.615	2.054	5.040	232.835	75.996	.326
154.927	78.540	.615	2.054	5.043	233.466	76.387	.327
155.340	78.757	.615	2.054	5.046	234.097	76.582	.327
155.753	78.975	.615	2.054	5.048	234.728	76.778	.327
156.166	79.193	.615	2.054	5.051	235.359	76.973	.327
156.677	79.313	.615	2.054	5.054	235.990	77.364	.328
157.248	79.689	.615	2.054	5.058	236.937	77.559	.327
157.661	79.907	.615	2.054	5.060	237.568	77.755	.327
158.074	80.124	.615	2.054	5.063	238.198	77.950	.327
158.487	80.342	.615	2.054	5.066	238.829	78.145	.327
158.743	80.402	.615	2.054	5.067	239.145	78.341	.328
159.254	80.522	.615	2.054	5.070	239.776	78.731	.328
159.569	80.838	.615	2.054	5.072	240.407	78.731	.327
159.825	80.898	.615	2.054	5.074	240.722	78.927	.328
160.336	81.018	.615	2.054	5.077	241.353	79.318	.329
160.906	81.394	.615	2.054	5.081	242.300	79.513	.328
161.162	81.454	.615	2.054	5.082	242.616	79.708	.329
161.260	81.356	.615	2.054	5.083	242.616	79.904	.329
161.733	81.829	.615	2.054	5.086	243.562	79.904	.328
161.988	81.889	.615	2.054	5.088	243.878	80.099	.328
162.244	81.949	.615	2.054	5.089	244.193	80.294	.329
162.657	82.167	.615	2.054	5.092	244.824	80.490	.329
162.815	82.325	.615	2.054	5.093	245.140	80.490	.328
163.070	82.385	.615	2.054	5.094	245.455	80.685	.329
163.483	82.603	.615	2.054	5.097	246.086	80.880	.329
163.739	82.663	.615	2.054	5.098	246.402	81.076	.329
164.152	82.881	.615	2.054	5.101	247.032	81.271	.329
164.309	83.038	.615	2.054	5.102	247.348	81.271	.329
163.934	82.468	.615	2.054	5.099	246.402	81.466	.331

Table A6 continued

163.205	81.934	.615	2.054	5.095	245.140	81.271	.332
162.417	81.145	.615	2.054	5.090	243.562	81.271	.334
161.372	80.297	.615	2.054	5.084	241.669	81.076	.335
160.584	79.508	.615	2.054	5.079	240.091	81.076	.338
159.539	78.659	.615	2.054	5.072	238.198	80.880	.340
158.495	77.810	.615	2.054	5.066	236.306	80.685	.341
157.609	77.119	.615	2.054	5.060	234.728	80.490	.343
156.620	76.330	.615	2.054	5.055	233.151	80.490	.345
155.934	75.639	.615	2.054	5.049	231.573	80.294	.347
155.205	75.106	.615	2.054	5.045	230.311	80.099	.348
154.574	74.475	.615	2.054	5.041	229.049	80.099	.350
153.845	73.942	.615	2.054	5.036	227.787	79.904	.351
153.117	73.409	.615	2.054	5.031	226.525	79.708	.352
152.388	72.875	.615	2.054	5.026	225.263	79.513	.353
151.915	72.402	.615	2.054	5.023	224.317	79.513	.354
151.344	72.026	.615	2.054	5.020	223.370	79.318	.355
150.773	71.651	.615	2.054	5.016	222.424	79.122	.356
150.044	71.117	.615	2.054	5.011	221.162	78.927	.357
149.729	70.802	.615	2.054	5.009	220.531	78.927	.358
149.158	70.427	.615	2.054	5.005	219.584	78.731	.359
148.527	69.796	.615	2.054	5.001	218.322	78.731	.361
148.114	69.578	.615	2.054	4.998	217.691	78.536	.361
147.543	69.202	.615	2.054	4.994	216.745	78.341	.361
146.972	68.827	.615	2.054	4.990	215.798	78.145	.362
146.656	68.511	.615	2.054	4.988	215.167	78.145	.363
146.243	68.293	.615	2.054	4.985	214.536	77.950	.363
145.830	68.075	.615	2.054	4.982	213.905	77.755	.364
145.672	67.918	.615	2.054	4.981	213.590	77.755	.364
145.259	67.700	.615	2.054	4.979	212.959	77.559	.364
144.944	67.384	.615	2.054	4.976	212.328	77.559	.365
144.530	67.167	.615	2.054	4.973	211.697	77.364	.365
144.117	66.949	.615	2.054	4.971	211.066	77.168	.366
143.704	66.731	.615	2.054	4.968	210.435	76.973	.366
143.389	66.416	.615	2.054	4.966	209.804	76.973	.367
142.818	66.040	.615	2.054	4.962	208.856	76.778	.368

Table A6 continued

142.247	65.664	.615	2.054	4.958	207.911	76.582	.368
141.834	65.446	.615	2.054	4.955	207.280	76.387	.369
141.263	65.071	.615	2.054	4.951	206.334	76.192	.369
140.692	64.695	.615	2.054	4.947	205.387	75.996	.370
140.278	64.478	.615	2.054	4.944	204.756	75.801	.370
139.707	64.102	.615	2.054	4.940	203.809	75.605	.371
139.137	63.726	.615	2.054	4.935	202.863	75.410	.372
138.566	63.351	.615	2.054	4.931	201.917	75.215	.373
137.995	62.975	.615	2.054	4.927	200.970	75.020	.373
137.424	62.600	.615	2.054	4.923	200.024	74.824	.374
136.853	62.224	.615	2.054	4.919	199.077	74.629	.375
136.184	61.946	.615	2.054	4.914	198.131	74.238	.375
135.869	61.631	.615	2.054	4.912	197.500	74.238	.376
135.200	61.353	.615	2.054	4.907	196.553	73.847	.376
134.629	60.977	.615	2.054	4.903	195.607	73.652	.377
134.059	60.602	.615	2.054	4.898	194.660	73.457	.377
133.330	60.069	.615	2.054	4.893	193.398	73.261	.379
132.917	59.851	.615	2.054	4.890	192.767	73.066	.379
132.188	59.317	.615	2.054	4.884	191.505	72.870	.381
131.677	59.197	.615	2.054	4.880	190.874	72.480	.380
131.204	58.724	.615	2.054	4.877	189.928	72.480	.382
130.633	58.348	.615	2.054	4.872	188.981	72.284	.382
129.964	58.071	.615	2.054	4.867	188.035	71.894	.382
129.236	57.537	.615	2.054	4.862	186.773	71.698	.384
128.567	57.259	.615	2.054	4.856	185.827	71.308	.384
127.838	56.726	.615	2.054	4.851	184.565	71.112	.385
127.012	56.291	.615	2.054	4.844	183.303	70.721	.386
126.283	55.757	.615	2.054	4.839	182.041	70.526	.387
125.555	55.224	.615	2.054	4.833	180.778	70.331	.389
124.886	54.946	.615	2.054	4.827	179.832	69.940	.389
124.157	54.413	.615	2.054	4.822	178.570	69.745	.391
123.331	53.977	.615	2.054	4.815	177.308	69.354	.391
122.760	53.602	.615	2.054	4.810	176.362	69.159	.392
122.189	53.226	.615	2.054	4.806	175.415	68.963	.393
121.363	52.790	.615	2.054	4.799	174.153	68.573	.394

Table A6 continued

120.792	52.415	.615	2.054	4.794	173.207	68.377	.395
119.966	51.979	.615	2.054	4.787	171.945	67.986	.395
119.237	51.446	.615	2.054	4.781	170.683	67.791	.397
118.568	51.168	.615	2.054	4.775	169.736	67.400	.397
117.840	50.635	.615	2.054	4.769	168.474	67.205	.399
117.171	50.357	.615	2.054	4.764	167.528	66.814	.399
116.442	49.823	.615	2.054	4.757	166.266	66.619	.401
115.774	49.546	.615	2.054	4.752	165.319	66.228	.401
114.947	49.110	.615	2.054	4.744	164.057	65.837	.401
114.219	48.577	.615	2.054	4.738	162.795	65.642	.403
112.898	48.635	.591	2.086	4.726	161.533	64.263	.399
112.074	48.197	.591	2.086	4.719	160.271	63.878	.399
111.251	47.758	.591	2.086	4.712	159.009	63.493	.399
110.428	47.320	.591	2.086	4.704	157.747	63.108	.400
109.604	46.881	.591	2.086	4.697	156.485	62.723	.401
108.877	46.346	.591	2.086	4.690	155.223	62.531	.403
108.054	45.908	.591	2.086	4.683	153.961	62.146	.404
107.011	45.057	.591	2.086	4.673	152.068	61.954	.407
106.264	44.523	.591	2.086	4.666	150.807	61.761	.410
105.557	43.988	.591	2.086	4.659	149.545	61.569	.412
104.576	43.391	.591	2.086	4.650	147.967	61.184	.413
103.848	42.857	.591	2.086	4.643	146.705	60.992	.416
103.025	42.418	.591	2.086	4.635	145.443	60.607	.417
102.044	41.822	.591	2.086	4.625	143.866	60.222	.419
101.317	41.287	.591	2.086	4.618	142.604	60.030	.421
100.493	40.848	.591	2.086	4.610	141.342	59.645	.422
99.670	40.410	.591	2.086	4.602	140.080	59.260	.423
98.847	39.971	.591	2.086	4.594	138.818	58.875	.424
97.865	39.375	.591	2.086	4.584	137.240	58.491	.426
97.042	38.936	.591	2.086	4.575	135.978	58.106	.427
96.219	38.498	.591	2.086	4.567	134.716	57.721	.428
95.395	38.059	.591	2.086	4.558	133.454	57.336	.430
94.572	37.620	.591	2.086	4.549	132.192	56.951	.431
93.748	37.182	.591	2.086	4.541	130.930	56.567	.432
92.925	36.743	.591	2.086	4.532	129.668	56.182	.433

Table A6 continued

92.102	36.305	.591	2.086	4.523	128.406	55.797	.435
91.278	35.866	.591	2.086	4.514	127.144	55.412	.436
90.455	35.428	.591	2.086	4.505	125.882	55.027	.437
89.789	35.147	.591	2.086	4.497	124.936	54.642	.437
88.966	34.708	.591	2.086	4.488	123.674	54.258	.439
87.985	34.112	.591	2.086	4.477	122.097	53.873	.441
87.161	33.673	.591	2.086	4.468	120.834	53.488	.443
86.338	33.235	.591	2.086	4.458	119.572	53.103	.444
85.260	32.734	.591	2.086	4.446	117.995	52.526	.445
84.183	32.234	.591	2.086	4.433	116.418	51.949	.446
83.202	31.638	.591	2.086	4.421	114.840	51.564	.449
81.967	30.980	.591	2.086	4.406	112.947	50.987	.451
80.986	30.384	.591	2.086	4.394	111.370	50.602	.454
79.908	29.884	.591	2.086	4.381	109.792	50.025	.456
78.831	29.384	.591	2.086	4.367	108.215	49.448	.457
77.850	28.787	.591	2.086	4.355	106.637	49.063	.460
76.773	28.287	.591	2.086	4.341	105.060	48.486	.462
75.949	27.849	.591	2.086	4.330	103.798	48.101	.463
74.872	27.348	.591	2.086	4.316	102.220	47.524	.465
72.814	26.252	.591	2.086	4.288	99.066	46.562	.470
71.578	25.594	.591	2.086	4.271	97.172	45.984	.473
70.405	25.190	.591	2.086	4.254	95.595	45.215	.473
69.170	24.532	.591	2.086	4.237	93.702	44.638	.476
68.092	24.032	.591	2.086	4.221	92.124	44.060	.478
67.015	23.532	.591	2.086	4.205	90.547	43.483	.480
65.938	23.032	.591	2.086	4.189	88.970	42.906	.482
64.860	22.532	.591	2.086	4.172	87.392	42.329	.484
63.783	22.032	.591	2.086	4.155	85.815	41.751	.487
62.863	21.689	.591	2.086	4.141	84.553	41.174	.487
61.882	21.093	.591	2.086	4.125	82.975	40.789	.492
60.963	20.751	.591	2.086	4.110	81.713	40.212	.492
60.139	20.312	.591	2.086	4.097	80.451	39.828	.495
59.377	20.127	.591	2.086	4.084	79.505	39.250	.494
58.554	19.689	.591	2.086	4.070	78.243	38.865	.497
57.634	19.346	.591	2.086	4.054	76.981	38.288	.497

Table A6 continued

56.969	19.065	.591	2.086	4.043	76.034	37.903	.499
56.145	18.627	.591	2.086	4.028	74.772	37.519	.502
55.226	18.285	.591	2.086	4.011	73.510	36.941	.503
54.560	18.004	.591	2.086	3.999	72.564	36.557	.504
53.737	17.565	.591	2.086	3.984	71.302	36.172	.507
53.071	17.284	.591	2.086	3.972	70.355	35.787	.509
52.406	17.003	.591	2.086	3.959	69.409	35.402	.510
51.486	16.661	.591	2.086	3.941	68.147	34.825	.511
50.820	16.380	.591	2.086	3.928	67.200	34.440	.513
50.155	16.099	.591	2.086	3.915	66.254	34.055	.514
49.331	15.661	.591	2.086	3.899	64.992	33.670	.518
48.666	15.380	.591	2.086	3.885	64.046	33.286	.520
48.158	15.257	.591	2.086	3.874	63.415	32.901	.519
47.492	14.976	.591	2.086	3.861	62.468	32.516	.521
46.826	14.695	.591	2.086	3.846	61.522	32.131	.522
46.415	14.476	.591	2.086	3.838	60.891	31.939	.525
45.749	14.195	.591	2.086	3.823	59.944	31.554	.526
45.241	14.072	.591	2.086	3.812	59.313	31.169	.526
44.733	13.949	.591	2.086	3.801	58.682	30.785	.525
44.068	13.668	.591	2.086	3.786	57.735	30.400	.527
43.656	13.449	.591	2.086	3.776	57.104	30.207	.529
42.990	13.168	.591	2.086	3.761	56.158	29.822	.531
42.482	13.045	.591	2.086	3.749	55.527	29.438	.530
41.975	12.922	.591	2.086	3.737	54.896	29.053	.529
41.563	12.702	.591	2.086	3.727	54.265	28.860	.532
40.897	12.422	.591	2.086	3.711	53.319	28.476	.534
40.485	12.202	.591	2.086	3.701	52.688	28.283	.537
39.820	11.921	.591	2.086	3.684	51.741	27.899	.539
39.312	11.798	.591	2.086	3.672	51.110	27.514	.538
38.646	11.517	.591	2.086	3.654	50.164	27.129	.541
38.138	11.394	.591	2.086	3.641	49.533	26.744	.540
37.569	11.017	.591	2.086	3.626	48.586	26.552	.546
37.061	10.894	.591	2.086	3.613	47.955	26.167	.546
36.395	10.613	.591	2.086	3.594	47.009	25.782	.548
35.984	10.394	.591	2.086	3.583	46.378	25.590	.552

Table A6 continued

35.476	10.271	.591	2.086	3.569	45.747	25.205	.551
34.968	10.148	.591	2.086	3.554	45.116	24.820	.550
34.398	9.771	.591	2.086	3.538	44.169	24.628	.558
33.891	9.648	.591	2.086	3.523	43.538	24.243	.557
33.479	9.428	.591	2.086	3.511	42.907	24.050	.561
32.971	9.305	.591	2.086	3.496	42.276	23.666	.560
32.559	9.086	.591	2.086	3.483	41.645	23.473	.564
32.051	8.963	.591	2.086	3.467	41.014	23.088	.563
31.640	8.744	.591	2.086	3.454	40.383	22.896	.567
31.132	8.621	.591	2.086	3.438	39.752	22.511	.566
30.466	8.340	.591	2.086	3.417	38.806	22.126	.570
29.800	8.059	.591	2.086	3.395	37.859	21.741	.574
29.135	7.778	.591	2.086	3.372	36.913	21.357	.579
28.627	7.655	.591	2.086	3.354	36.282	20.972	.578
27.961	7.374	.591	2.086	3.331	35.335	20.587	.583
27.296	7.093	.591	2.086	3.307	34.389	20.202	.587
26.630	6.812	.591	2.086	3.282	33.442	19.818	.593
25.964	6.532	.591	2.086	3.257	32.496	19.433	.598
25.395	6.155	.591	2.086	3.235	31.549	19.240	.610
24.791	6.128	.591	2.086	3.210	30.918	18.663	.604
24.379	5.908	.591	2.086	3.194	30.288	18.471	.610
23.713	5.628	.591	2.086	3.166	29.341	18.086	.616
23.206	5.504	.591	2.086	3.144	28.710	17.701	.617
22.794	5.285	.591	2.086	3.126	28.079	17.509	.624
22.286	5.162	.591	2.086	3.104	27.448	17.124	.624
21.717	4.785	.591	2.086	3.078	26.502	16.931	.639
21.051	4.504	.591	2.086	3.047	25.555	16.547	.647
20.543	4.381	.591	2.086	3.023	24.924	16.162	.648
20.035	4.258	.591	2.086	2.997	24.293	15.777	.649
19.623	4.039	.591	2.086	2.977	23.662	15.585	.659
19.115	3.916	.591	2.086	2.950	23.031	15.200	.660
18.704	3.696	.591	2.086	2.929	22.400	15.008	.670
18.196	3.573	.591	2.086	2.901	21.769	14.623	.672
17.784	3.354	.591	2.086	2.878	21.138	14.430	.683
17.276	3.231	.591	2.086	2.849	20.507	14.045	.685

Table A6 continued

16.865	3.012	.591	2.086	2.825	19.876	13.853	.697
16.357	2.888	.591	2.086	2.795	19.245	13.468	.700
15.945	2.669	.591	2.086	2.769	18.614	13.276	.713
15.437	2.546	.591	2.086	2.737	17.983	12.891	.717
14.929	2.423	.591	2.086	2.703	17.352	12.506	.721
14.675	2.361	.591	2.086	2.686	17.037	12.314	.723
14.167	2.238	.591	2.086	2.651	16.406	11.929	.727
13.756	2.019	.591	2.086	2.621	15.775	11.737	.744
13.248	1.896	.591	2.086	2.584	15.144	11.352	.750
12.994	1.834	.591	2.086	2.564	14.828	11.160	.753
12.582	1.615	.591	2.086	2.532	14.197	10.967	.772
12.074	1.492	.591	2.086	2.491	13.566	10.582	.780
11.820	1.430	.591	2.086	2.470	13.251	10.390	.784
11.409	1.211	.591	2.086	2.434	12.620	10.197	.808
11.155	1.150	.591	2.086	2.412	12.304	10.005	.813
10.647	1.027	.591	2.086	2.365	11.673	9.620	.824
10.235	.807	.591	2.086	2.326	11.042	9.428	.854
9.981	.746	.591	2.086	2.301	10.727	9.235	.861
9.727	.684	.591	2.086	2.275	10.411	9.043	.869
9.315	.465	.591	2.086	2.232	9.780	8.850	.905
8.904	.246	.591	2.086	2.186	9.149	8.658	.946
8.396	.122	.591	2.086	2.128	8.518	8.273	.971
8.142	.061	.591	2.086	2.097	8.203	8.081	.985
7.730	-.158	.591	2.086	2.045	7.572	7.889	1.042
7.222	-.281	.591	2.086	1.977	6.941	7.504	1.081
6.811	-.501	.591	2.086	1.918	6.310	7.311	1.159
6.399	-.720	.591	2.086	1.856	5.679	7.119	1.254
6.145	-.782	.591	2.086	1.816	5.363	6.927	1.291
5.637	-.905	.591	2.086	1.729	4.732	6.542	1.382
5.383	-.966	.591	2.086	1.683	4.417	6.349	1.438
4.971	-1.185	.591	2.086	1.604	3.786	6.157	1.626
4.717	-1.247	.591	2.086	1.551	3.471	5.964	1.719
4.464	-1.309	.591	2.086	1.496	3.155	5.772	1.830
4.210	-1.370	.591	2.086	1.437	2.840	5.580	1.965
3.956	-1.432	.591	2.086	1.375	2.524	5.387	2.134

Table A6 continued

3.702	-1.493	.591	2.086	1.309	2.209	5.195	2.352
3.290	-1.712	.591	2.086	1.191	1.578	5.002	3.171
3.036	-1.774	.591	2.086	1.111	1.262	4.810	3.811
2.782	-1.836	.591	2.086	1.023	.947	4.618	4.878
2.666	-1.739	.591	2.086	.988	.947	4.425	4.675
2.432	-1.801	.591	2.086	.889	.631	4.233	6.708

Table A7 Compaction data for homopolymer compacted uniaxially at 250 MPa

σ (MPa)	$\dot{\varepsilon}$ (MPa)	ε	V ($mx10^{-6}$)	ln σ	σ_A (MPa)	σ_R MPa	$\frac{\sigma_R}{\sigma_A}$
.305	.197	0.000	3.729	-1.187	.502	.108	.215
.305	.197	.009	3.697	-1.186	.502	.109	.216
.305	.197	.009	3.697	-1.186	.502	.109	.216
.431	.322	.009	3.697	-.842	.753	.109	.144
.431	.322	.017	3.666	-.841	.753	.110	.146
.486	.267	.017	3.666	-.721	.753	.219	.291
.467	.266	.026	3.634	-.719	.753	.221	.293
.613	.392	.026	3.634	-.490	1.004	.221	.220
.614	.391	.035	3.602	-.488	1.004	.223	.222
.614	.391	.035	3.602	-.488	1.004	.223	.222
.795	.460	.035	3.602	-.229	1.255	.335	.266
.796	.459	.044	3.571	-.228	1.255	.337	.269
.796	.459	.044	3.571	-.228	1.255	.337	.269
.853	.403	.044	3.571	-.159	1.255	.450	.358
.980	.526	.054	3.539	-.020	1.507	.454	.301
.982	.524	.063	3.508	-.018	1.507	.458	.304
1.165	.593	.063	3.508	.153	1.758	.573	.326
1.168	.590	.073	3.476	.155	1.758	.578	.329
1.225	.532	.073	3.476	.203	1.756	.693	.394
1.354	.655	.083	3.444	.303	2.009	.700	.348
1.354	.655	.083	3.444	.303	2.009	.700	.348
1.538	.722	.083	3.444	.430	2.260	.816	.361
1.542	.718	.093	3.413	.433	2.260	.824	.365
1.667	.844	.093	3.413	.511	2.511	.824	.328
1.667	.844	.093	3.413	.511	2.511	.824	.328
1.852	.910	.093	3.413	.616	2.762	.942	.341
1.856	.906	.103	3.381	.619	2.762	.950	.344

Table A7 continued

2.041	.972	.103	3.381	.714	3.013	1.069	.355
2.046	.967	.113	3.350	.716	3.013	1.079	.358
2.232	1.033	.113	3.350	.803	3.264	1.199	.367
2.363	1.152	.124	3.318	.860	3.516	1.211	.344
2.424	1.092	.124	3.318	.885	3.516	1.332	.379
2.549	1.217	.124	3.318	.936	3.766	1.332	.354
2.617	1.150	.135	3.286	.962	3.766	1.467	.389
2.742	1.275	.135	3.286	1.009	4.017	1.467	.365
2.803	1.214	.135	3.286	1.031	4.017	1.589	.395
2.936	1.352	.146	3.255	1.077	4.269	1.604	.375
3.124	1.396	.146	3.255	1.139	4.520	1.728	.382
3.132	1.387	.157	3.223	1.142	4.520	1.745	.386
3.320	1.451	.157	3.223	1.200	4.771	1.869	.392
3.329	1.442	.168	3.192	1.203	4.771	1.888	.396
3.518	1.504	.168	3.192	1.258	5.022	2.014	.401
3.653	1.620	.180	3.160	1.296	5.273	2.034	.386
3.717	1.556	.180	3.160	1.313	5.273	2.161	.410
3.918	1.607	.192	3.128	1.365	5.524	2.311	.418
4.043	1.732	.192	3.128	1.397	5.775	2.311	.400
4.120	1.655	.204	3.097	1.416	5.775	2.464	.427
4.245	1.781	.204	3.097	1.446	6.026	2.464	.409
4.436	1.842	.204	3.097	1.490	6.278	2.594	.413
4.640	1.888	.216	3.065	1.535	6.528	2.752	.422
4.766	2.014	.216	3.065	1.561	6.780	2.752	.406
4.957	2.074	.216	3.065	1.601	7.031	2.883	.410
5.038	1.993	.229	3.034	1.617	7.031	3.045	.433
5.230	2.052	.229	3.034	1.654	7.282	3.178	.436
5.355	2.178	.229	3.034	1.678	7.533	3.178	.422
5.565	2.220	.242	3.002	1.716	7.784	3.345	.430
5.757	2.278	.242	3.002	1.750	8.035	3.479	.433
5.969	2.318	.255	2.970	1.787	8.286	3.651	.441
6.094	2.443	.255	2.970	1.807	8.537	3.651	.428
6.433	2.606	.269	2.939	1.861	9.040	3.827	.423
6.627	2.663	.269	2.939	1.891	9.291	3.964	.427
6.843	2.699	.283	2.907	1.923	9.542	4.145	.434

Table A7 continued

7.038	2.755	.283	2.907	1.951	9.793	4.283	.437
7.257	2.787	.297	2.876	1.982	10.044	4.470	.445
7.382	2.913	.297	2.876	1.999	10.295	4.470	.434
7.578	2.968	.297	2.876	2.025	10.546	4.609	.437
7.925	3.123	.311	2.844	2.070	11.046	4.802	.435
8.121	3.178	.311	2.844	2.094	11.299	4.943	.437
8.471	3.330	.326	2.812	2.137	11.802	5.141	.436
8.668	3.384	.326	2.812	2.160	12.053	5.284	.438
8.865	3.438	.326	2.812	2.182	12.304	5.427	.441
9.188	3.618	.326	2.812	2.218	12.806	5.570	.435
9.489	3.567	.341	2.781	2.250	13.057	5.922	.454
9.741	3.819	.341	2.781	2.276	13.559	5.922	.437
9.973	3.837	.356	2.749	2.300	13.810	6.136	.444
10.297	4.015	.356	2.749	2.332	14.313	6.282	.439
10.733	4.082	.372	2.718	2.373	14.815	6.651	.449
11.058	4.259	.372	2.718	2.403	15.317	6.799	.444
11.298	4.270	.388	2.686	2.425	15.568	7.028	.451
11.624	4.446	.388	2.686	2.453	16.070	7.178	.447
12.025	4.548	.388	2.686	2.487	16.572	7.477	.451
12.396	4.679	.405	2.654	2.517	17.075	7.717	.452
12.723	4.854	.405	2.654	2.543	17.577	7.869	.448
13.174	4.905	.422	2.623	2.578	18.079	8.270	.457
13.502	5.079	.422	2.623	2.603	18.581	8.423	.453
13.906	5.177	.422	2.623	2.632	19.084	8.729	.457
14.288	5.298	.439	2.591	2.659	19.586	8.991	.459
14.694	5.394	.439	2.591	2.687	20.088	9.301	.463
15.148	5.693	.439	2.591	2.718	20.841	9.455	.454
15.489	5.603	.457	2.560	2.740	21.092	9.886	.469
15.944	5.901	.457	2.560	2.769	21.846	10.043	.460
16.543	6.056	.475	2.528	2.806	22.599	10.486	.464
16.953	6.148	.475	2.528	2.830	23.101	10.804	.468
17.433	6.170	.494	2.496	2.858	23.603	11.263	.477
17.970	6.386	.494	2.496	2.889	24.356	11.564	.476
18.428	6.682	.494	2.496	2.914	25.110	11.745	.468
18.998	6.614	.513	2.465	2.944	25.612	12.385	.484

Table A7 continued

19.538	6.827	.513	2.465	2.972	26.365	12.711	.482
20.162	6.956	.532	2.433	3.004	27.119	13.206	.487
20.829	7.293	.532	2.433	3.036	28.123	13.536	.481
21.371	7.505	.532	2.433	3.062	28.876	13.866	.480
21.913	7.717	.532	2.433	3.087	29.629	14.196	.479
22.759	7.874	.553	2.402	3.125	30.634	14.885	.486
23.303	8.084	.553	2.402	3.149	31.387	15.219	.485
24.161	8.230	.573	2.370	3.185	32.391	15.931	.492
24.707	8.438	.573	2.370	3.207	33.145	16.270	.491
25.464	8.686	.573	2.370	3.237	34.149	16.778	.491
26.337	8.817	.595	2.338	3.271	35.154	17.520	.498
27.222	9.187	.595	2.338	3.304	36.409	18.035	.495
27.896	9.517	.595	2.338	3.328	37.414	18.379	.491
28.786	9.632	.616	2.307	3.360	38.418	19.153	.499
29.674	9.999	.616	2.307	3.390	39.673	19.675	.496
30.704	10.225	.639	2.275	3.424	40.929	20.478	.500
31.559	10.374	.639	2.275	3.452	41.933	21.185	.505
32.452	10.737	.639	2.275	3.480	43.189	21.714	.503
33.558	11.137	.639	2.275	3.513	44.695	22.420	.502
34.702	11.249	.662	2.244	3.547	45.951	23.452	.510
35.723	11.734	.662	2.244	3.576	47.458	23.989	.505
36.799	11.914	.662	2.244	3.605	48.713	24.884	.511
38.093	12.127	.686	2.212	3.640	50.220	25.966	.517
39.335	12.642	.686	2.212	3.672	51.977	26.692	.514
40.451	13.032	.686	2.212	3.700	53.484	27.419	.513
41.989	13.252	.710	2.180	3.737	55.241	28.737	.520
43.329	13.670	.710	2.180	3.769	56.999	29.658	.520
44.668	14.089	.710	2.180	3.799	58.757	30.579	.520
46.239	14.275	.735	2.149	3.834	60.515	31.964	.528
47.804	14.719	.735	2.149	3.867	62.523	33.085	.529
49.276	15.256	.735	2.149	3.897	64.532	34.020	.527
51.198	15.343	.761	2.117	3.936	66.541	35.856	.539
52.897	15.903	.761	2.117	3.968	68.801	36.994	.538
54.471	16.339	.761	2.117	3.998	70.809	38.132	.539
56.265	16.805	.761	2.117	4.030	73.069	39.460	.540

Table A7 continued

58.271	17.058	.788	2.086	4.065	75.329	41.213	.547
60.201	17.639	.788	2.086	4.098	77.840	42.562	.547
62.227	18.124	.788	2.086	4.131	80.351	44.102	.549
64.506	18.356	.815	2.054	4.167	82.862	46.150	.557
66.669	18.955	.815	2.054	4.200	85.624	47.714	.557
68.832	19.554	.815	2.054	4.232	88.386	49.279	.558
70.996	20.153	.815	2.054	4.263	91.148	50.843	.558
73.362	20.779	.815	2.054	4.296	94.162	52.603	.559
76.094	21.081	.844	2.022	4.332	97.175	55.014	.566
78.495	21.693	.844	2.022	4.363	100.188	56.801	.567
80.994	22.207	.844	2.022	4.394	103.201	58.787	.570
83.645	23.071	.844	2.022	4.427	106.716	60.574	.568
131.744	32.976	.934	2.022	4.881	164.720	98.768	.600
135.359	33.881	.934	2.022	4.908	169.240	101.477	.600
139.716	33.793	.967	2.020	4.940	173.509	105.923	.610
143.247	34.782	.967	2.020	4.965	178.028	108.465	.609
146.883	35.665	.967	2.020	4.990	182.548	111.219	.609
150.395	36.422	.967	2.020	5.013	186.617	113.973	.610
153.800	37.285	.967	2.020	5.036	191.085	116.515	.610
157.186	37.917	.967	2.020	5.057	195.103	119.269	.611
160.717	38.906	.967	2.020	5.080	199.623	121.811	.610
164.122	39.769	.967	2.020	5.101	203.891	124.353	.610
167.634	40.526	.967	2.020	5.122	208.160	127.107	.611
171.271	41.409	.967	2.020	5.143	212.680	129.861	.611
174.676	42.273	.967	2.020	5.163	216.948	132.403	.610
178.313	43.155	.967	2.020	5.184	221.468	135.157	.610
183.118	42.870	1.000	2.015	5.210	225.988	140.249	.621
186.653	43.604	1.000	2.015	5.229	230.257	143.049	.621
190.313	44.463	1.000	2.015	5.249	234.776	145.850	.621
193.973	45.323	1.000	2.015	5.268	239.296	148.651	.621
197.634	46.182	1.000	2.015	5.286	243.816	151.451	.621
201.294	47.042	1.000	2.015	5.305	248.336	154.252	.621
204.829	47.776	1.000	2.015	5.322	252.604	157.053	.622
206.569	47.793	1.000	2.015	5.331	254.362	158.776	.624
206.641	47.219	1.000	2.015	5.331	253.860	159.423	.628

Table A7 continued

206.606	46.752	1.000	2.015	5.331	253.358	159.853	.631
206.444	46.160	1.000	2.015	5.330	252.604	160.284	.635
206.068	45.783	1.000	2.015	5.328	251.851	160.284	.636
205.565	45.281	1.000	2.015	5.326	250.847	160.284	.639
204.938	44.653	1.000	2.015	5.323	249.591	160.284	.642
203.467	43.613	1.000	2.015	5.316	247.080	159.853	.647
201.655	42.663	1.000	2.015	5.307	244.318	158.992	.651
199.358	41.444	1.000	2.015	5.295	240.803	157.914	.656
194.425	39.096	1.000	2.015	5.270	233.521	155.329	.665
189.043	36.945	1.000	2.015	5.242	225.988	152.098	.673
182.979	34.974	1.000	2.015	5.209	217.953	148.004	.679
174.672	32.484	1.000	2.015	5.163	207.156	142.188	.686
165.585	31.275	.967	2.020	5.109	196.860	134.310	.682
157.452	28.862	.967	2.020	5.059	186.315	128.590	.690
147.805	26.206	.967	2.020	4.996	174.011	121.599	.699
138.158	23.549	.967	2.020	4.928	161.707	114.608	.709
128.298	21.105	.967	2.020	4.854	149.403	107.194	.717
116.724	19.622	.934	2.022	4.760	136.346	97.101	.712
106.843	17.451	.934	2.022	4.671	124.293	89.392	.719
52.653	8.364	.844	2.022	3.964	61.017	44.289	.726
45.280	6.949	.844	2.022	3.813	52.228	38.331	.734
38.551	5.894	.815	2.054	3.652	44.444	32.657	.735
32.563	4.599	.815	2.054	3.483	37.162	27.964	.752
26.968	3.665	.788	2.086	3.295	30.634	23.303	.761
22.347	2.511	.788	2.086	3.107	24.859	19.836	.798
18.201	1.886	.761	2.117	2.902	20.088	16.315	.812
14.732	1.087	.735	2.149	2.690	15.819	13.645	.863
12.165	.389	.735	2.149	2.499	12.555	11.776	.938
9.870	-.077	.710	2.180	2.290	9.793	9.947	1.016
8.068	-.284	.686	2.212	2.088	7.784	8.353	1.073
6.594	-.567	.662	2.244	1.866	6.026	7.161	1.188
5.475	-.704	.639	2.275	1.700	4.771	6.179	1.295
4.562	-.816	.616	2.307	1.522	3.766	5.398	1.433
3.872	-1.110	.595	2.338	1.354	2.762	4.981	1.803
3.208	-1.199	.573	2.370	1.166	2.009	4.406	2.193

Table A7 continued

2.844	-1.337	.553	2.402	1.045	1.507	4.181	2.775
2.509	-1.505	.553	2.402	.920	1.004	4.014	3.996
2.091	-1.589	.553	2.402	.738	.502	3.680	7.327

Table A8 Compaction data for copolymer compacted uniaxially at 256 MPa

σ (MPa)	τ (MPa)	ε	V ($mx10^{-6}$)	ln σ	σ_A (MPa)	σ_R (MPa)	σ_R/σ_A
.183	.068	0.000	3.476	-1.697	.251	.116	.461
.184	.067	.009	3.444	-1.694	.251	.117	.465
.184	.067	.009	3.444	-1.694	.251	.117	.465
.184	.067	.019	3.413	-1.691	.251	.118	.469
.184	.067	.019	3.413	-1.691	.251	.118	.469
.310	.192	.019	3.413	-1.171	.502	.118	.234
.311	.192	.028	3.381	-1.169	.502	.119	.237
.311	.192	.028	3.381	-1.169	.502	.119	.237
.311	.191	.038	3.350	-1.168	.502	.120	.239
.311	.191	.038	3.350	-1.168	.502	.120	.239
.372	.130	.048	3.318	-.988	.502	.242	.482
.372	.130	.048	3.318	-.988	.502	.242	.482
.498	.256	.048	3.318	-.698	.753	.242	.321
.499	.254	.058	3.286	-.696	.753	.244	.324
.499	.254	.058	3.286	-.696	.753	.244	.324
.499	.254	.058	3.286	-.696	.753	.244	.324
.500	.253	.068	3.255	-.693	.753	.247	.328
.687	.317	.068	3.255	-.375	1.004	.370	.369
.689	.315	.078	3.223	-.372	1.004	.374	.372
.689	.315	.078	3.223	-.372	1.004	.374	.372
.816	.439	.089	3.192	-.203	1.255	.378	.301
.816	.439	.089	3.192	-.203	1.255	.378	.301
.882	.374	.100	3.160	-.126	1.255	.508	.405
1.008	.499	.100	3.160	.007	1.507	.508	.337
1.008	.499	.100	3.160	.007	1.507	.508	.337
1.010	.497	.111	3.128	.010	1.507	.513	.341
1.010	.497	.111	3.128	.010	1.507	.513	.341
1.203	.555	.122	3.097	.185	1.758	.648	.369

Table A8 continued

1.203	.555	.122	3.097	.185	1.758	.648	.369
1.329	.680	.122	3.097	.284	2.009	.648	.323
1.398	.611	.134	3.065	.335	2.009	.786	.391
1.398	.611	.134	3.065	.335	2.009	.786	.391
1.527	.733	.146	3.034	.423	2.260	.794	.352
1.593	.667	.146	3.034	.466	2.260	.927	.410
1.719	.792	.146	3.034	.542	2.511	.927	.369
1.791	.720	.158	3.002	.583	2.511	1.070	.426
1.916	.846	.158	3.002	.650	2.762	1.070	.388
1.922	.840	.170	2.970	.653	2.762	1.082	.392
1.990	.772	.170	2.970	.688	2.762	1.217	.441
2.122	.892	.183	2.939	.752	3.013	1.230	.408
2.315	.949	.183	2.939	.840	3.264	1.367	.419
2.315	.949	.183	2.939	.840	3.264	1.367	.419
2.449	1.067	.196	2.907	.895	3.516	1.382	.393
2.518	.998	.196	2.907	.923	3.516	1.520	.432
2.651	1.115	.209	2.876	.975	3.766	1.537	.408
2.847	1.171	.209	2.876	1.046	4.017	1.676	.417
2.927	1.091	.222	2.844	1.074	4.017	1.836	.457
3.052	1.216	.222	2.844	1.116	4.269	1.836	.430
3.178	1.342	.222	2.844	1.156	4.520	1.836	.406
3.260	1.260	.236	2.812	1.182	4.520	2.000	.442
3.457	1.314	.236	2.812	1.240	4.771	2.142	.449
3.594	1.428	.250	2.781	1.279	5.022	2.167	.431
3.792	1.481	.250	2.781	1.333	5.273	2.311	.438
3.990	1.534	.250	2.781	1.384	5.524	2.455	.444
4.004	1.520	.264	2.749	1.387	5.524	2.484	.450
4.203	1.573	.264	2.749	1.436	5.775	2.630	.455
4.417	1.609	.279	2.718	1.486	6.026	2.808	.466
4.617	1.661	.279	2.718	1.530	6.278	2.956	.471
4.834	1.694	.294	2.686	1.576	6.528	3.140	.481
4.960	1.820	.294	2.686	1.601	6.780	3.140	.463
5.160	1.870	.294	2.686	1.641	7.031	3.290	.468
5.381	1.901	.310	2.654	1.663	7.282	3.460	.478
5.582	1.951	.310	2.654	1.720	7.533	3.632	.482

Table A8 continued

5.932	2.103	.325	2.623	1.780	8.035	3.828	.476
6.134	2.152	.325	2.623	1.814	8.286	3.982	.481
6.336	2.201	.325	2.623	1.846	8.537	4.135	.484
6.564	2.224	.341	2.591	1.882	8.788	4.340	.494
6.893	2.398	.341	2.591	1.930	9.291	4.495	.484
7.125	2.417	.358	2.560	1.964	9.542	4.708	.493
7.533	2.511	.358	2.560	2.019	10.044	5.022	.500
7.769	2.526	.375	2.528	2.050	10.295	5.243	.509
8.100	2.698	.375	2.528	2.092	10.797	5.402	.500
8.510	2.790	.375	2.528	2.141	11.299	5.720	.506
8.752	2.799	.392	2.496	2.169	11.551	5.953	.515
9.083	2.969	.392	2.496	2.206	12.053	6.114	.507
9.537	3.018	.410	2.465	2.255	12.555	6.518	.519
9.951	3.106	.410	2.465	2.298	13.057	6.844	.524
10.365	3.195	.410	2.465	2.338	13.559	7.170	.529
10.871	3.442	.429	2.433	2.386	14.313	7.428	.519
11.287	3.528	.429	2.433	2.424	14.815	7.759	.524
11.756	3.561	.447	2.402	2.464	15.317	8.195	.535
12.300	3.770	.447	2.402	2.510	16.070	8.529	.531
12.718	3.854	.447	2.402	2.543	16.572	8.864	.535
13.323	4.002	.467	2.370	2.590	17.326	9.321	.538
13.954	4.125	.467	2.370	2.636	18.079	9.830	.544
14.569	4.263	.486	2.338	2.679	18.832	10.306	.547
15.118	4.468	.486	2.338	2.716	19.586	10.650	.544
15.752	4.587	.486	2.338	2.757	20.339	11.165	.549
16.466	4.626	.507	2.307	2.801	21.092	11.840	.561
17.230	4.867	.507	2.307	2.847	22.097	12.363	.559
17.780	5.070	.507	2.307	2.878	22.850	12.711	.556
18.636	5.219	.528	2.275	2.925	23.854	13.417	.562
19.491	5.368	.528	2.275	2.970	24.859	14.123	.568
20.361	5.502	.549	2.244	3.014	25.863	14.859	.575
21.132	5.736	.549	2.244	3.051	26.867	15.396	.573
22.117	6.005	.549	2.244	3.096	28.123	16.112	.573
23.098	6.029	.571	2.212	3.140	29.127	17.069	.586
24.089	6.294	.571	2.212	3.182	30.383	17.795	.586

Table A8 continued

25.296	6.593	.571	2.212	3.231	31.890	18.703	.586
26.428	6.717	.594	2.180	3.274	33.145	19.711	.595
27.642	7.010	.594	2.180	3.319	34.652	20.632	.595
28.855	7.302	.594	2.180	3.362	36.158	21.553	.596
30.235	7.430	.618	2.149	3.409	37.665	22.805	.605
31.674	7.748	.618	2.149	3.456	39.422	23.926	.607
33.114	8.066	.618	2.149	3.500	41.180	25.048	.608
34.749	8.189	.642	2.117	3.548	42.938	26.560	.619
36.197	8.499	.642	2.117	3.589	44.695	27.698	.620
37.991	8.965	.642	2.117	3.637	46.955	29.026	.618
39.659	9.305	.642	2.117	3.680	48.964	30.354	.620
41.664	9.309	.667	2.086	3.730	50.973	32.355	.635
43.690	9.794	.667	2.086	3.777	53.484	33.895	.634
45.590	10.154	.667	2.086	3.820	55.744	35.436	.636
47.998	10.257	.692	2.054	3.871	58.255	37.741	.648
50.259	10.758	.692	2.054	3.917	61.017	39.501	.647
52.520	11.259	.692	2.054	3.961	63.779	41.261	.647
54.879	11.662	.692	2.054	4.005	66.541	43.216	.649
57.716	11.838	.719	2.022	4.056	69.554	45.878	.660
60.315	12.252	.719	2.022	4.100	72.567	48.062	.662
63.039	12.792	.719	2.022	4.144	75.832	50.247	.663
65.764	13.332	.719	2.022	4.186	79.096	52.432	.663
68.713	13.898	.719	2.022	4.230	82.611	54.815	.664
72.022	13.885	.746	2.022	4.277	85.875	58.106	.677
75.185	14.456	.746	2.022	4.320	89.642	60.729	.677
78.279	15.129	.746	2.022	4.360	93.408	63.150	.676
81.474	15.701	.746	2.022	4.400	97.175	65.773	.677
84.895	16.297	.746	2.022	4.441	101.192	68.598	.678
88.664	16.295	.774	2.015	4.485	104.959	72.369	.689
92.233	16.994	.774	2.015	4.524	109.228	75.239	.689
95.677	17.568	.774	2.015	4.561	113.245	78.109	.690
99.247	18.267	.774	2.015	4.598	117.514	80.980	.689
102.919	18.864	.774	2.015	4.634	121.782	84.055	.690
106.613	19.689	.774	2.015	4.669	126.302	86.925	.688
110.919	19.652	.803	2.020	4.709	130.571	91.267	.699

Table A8 continued

114.867	20.475	.803	2.020	4.744	135.342	94.393	.697
118.690	21.172	.803	2.020	4.777	139.861	97.518	.697
122.513	21.869	.803	2.020	4.808	144.381	100.644	.697
126.461	22.691	.803	2.020	4.840	149.152	103.769	.696
130.409	23.514	.803	2.020	4.871	153.923	106.895	.694
134.232	24.211	.803	2.020	4.900	158.443	110.021	.694
139.354	24.110	.833	2.015	4.937	163.465	115.244	.705
143.328	24.907	.833	2.015	4.965	168.235	118.421	.704
147.303	25.704	.833	2.015	4.992	173.006	121.599	.703
151.403	26.626	.833	2.015	5.020	178.028	124.777	.701
155.165	27.634	.833	2.015	5.044	182.799	127.531	.698
158.908	28.411	.833	2.015	5.068	187.319	130.497	.697
162.757	29.082	.833	2.015	5.092	191.839	133.674	.697
166.268	29.839	.833	2.015	5.114	196.107	136.428	.696
170.011	30.616	.833	2.015	5.136	200.627	139.394	.695
175.085	30.312	.864	1.864	5.165	205.398	144.773	.705
178.728	30.939	.864	1.864	5.186	209.666	147.789	.705
182.496	31.691	.864	1.864	5.207	214.186	150.805	.704
186.389	32.568	.864	1.864	5.228	218.957	153.821	.703
190.032	33.194	.864	1.864	5.247	223.226	156.837	.703
193.925	34.072	.864	1.864	5.267	227.997	159.853	.701
197.693	34.824	.864	1.864	5.287	232.516	162.869	.700
201.461	35.575	.864	1.864	5.306	237.036	165.886	.700
205.462	36.345	.864	1.864	5.325	241.807	169.117	.699
209.230	37.097	.864	1.864	5.343	246.327	172.133	.699
212.998	37.849	.864	1.864	5.361	250.847	175.149	.698
216.640	38.475	.864	1.864	5.378	255.115	178.165	.698
219.806	36.816	.897	1.833	5.393	256.622	182.990	.713
218.435	37.685	.864	1.864	5.386	256.120	180.751	.706
218.274	37.092	.864	1.864	5.386	255.366	181.182	.709
219.694	35.170	.897	1.833	5.392	254.864	184.524	.724
219.192	34.668	.897	1.833	5.390	253.860	184.524	.727
217.019	35.837	.864	1.864	5.380	252.855	181.182	.717
216.409	35.442	.864	1.864	5.377	251.851	180.966	.719
216.400	33.191	.897	1.833	5.377	249.591	183.210	.734

Table A8 continued

214.707	32.374	.897	1.833	5.369	247.080	182.333	.738
211.242	33.076	.864	1.864	5.353	244.318	178.165	.729
207.420	31.625	.864	1.864	5.335	239.045	175.796	.735
202.666	30.102	.864	1.864	5.312	232.767	172.564	.741
197.929	28.812	.864	1.864	5.288	226.741	169.117	.746
191.434	27.272	.864	1.864	5.255	218.706	164.162	.751
184.706	25.714	.864	1.864	5.219	210.420	158.992	.756
178.103	24.282	.864	1.864	5.182	202.385	153.821	.760
169.975	22.617	.864	1.864	5.136	192.592	147.358	.765
160.799	22.252	.833	2.015	5.080	183.050	138.547	.757
152.850	20.659	.833	2.015	5.029	173.509	132.191	.762
143.493	18.716	.833	2.015	4.966	162.209	124.777	.769
132.506	17.901	.803	2.020	4.887	150.408	114.605	.762
123.127	16.232	.803	2.020	4.813	139.359	106.895	.767
113.748	14.563	.803	2.020	4.734	128.311	99.185	.773
102.719	13.539	.774	2.015	4.632	116.258	89.180	.767
93.095	12.115	.774	2.015	4.534	105.210	80.980	.770
84.155	10.760	.774	2.015	4.433	94.915	73.394	.773
74.340	9.778	.746	2.022	4.309	84.118	64.562	.768
65.460	8.363	.746	2.022	4.181	73.823	57.097	.773
57.510	7.273	.746	2.022	4.052	64.783	50.238	.775
49.222	6.522	.719	2.022	3.896	55.744	42.700	.766
41.775	5.431	.719	2.022	3.732	47.206	36.345	.770
34.894	4.779	.692	2.054	3.552	39.673	30.115	.759
28.613	3.778	.692	2.054	3.354	32.391	24.835	.767
22.975	3.139	.667	2.086	3.134	26.114	19.836	.760
18.191	2.399	.667	2.086	2.901	20.590	15.792	.767
14.201	1.869	.642	2.117	2.653	16.070	12.331	.767
10.895	1.409	.642	2.117	2.388	12.304	9.486	.771
8.509	1.032	.618	2.149	2.141	9.542	7.477	.784
6.588	.694	.594	2.180	1.885	7.282	5.895	.810
5.157	.618	.571	2.212	1.640	5.775	4.539	.786
4.050	.470	.549	2.244	1.399	4.520	3.580	.792
3.064	.200	.549	2.244	1.120	3.264	2.864	.878
2.277	-.018	.528	2.275	.823	2.260	2.295	1.016

Table A8 continued

1.836	-.079	.507	2.307	.608	1.758	1.915	1.090
1.275	-.271	.486	2.338	.243	1.004	1.546	1.539
1.054	-.301	.467	2.370	.053	.753	1.356	1.800
.719	-.468	.467	2.370	-.330	.251	1.186	4.727

APPENDIX 3

CONTENTS OF APPENDIX 3

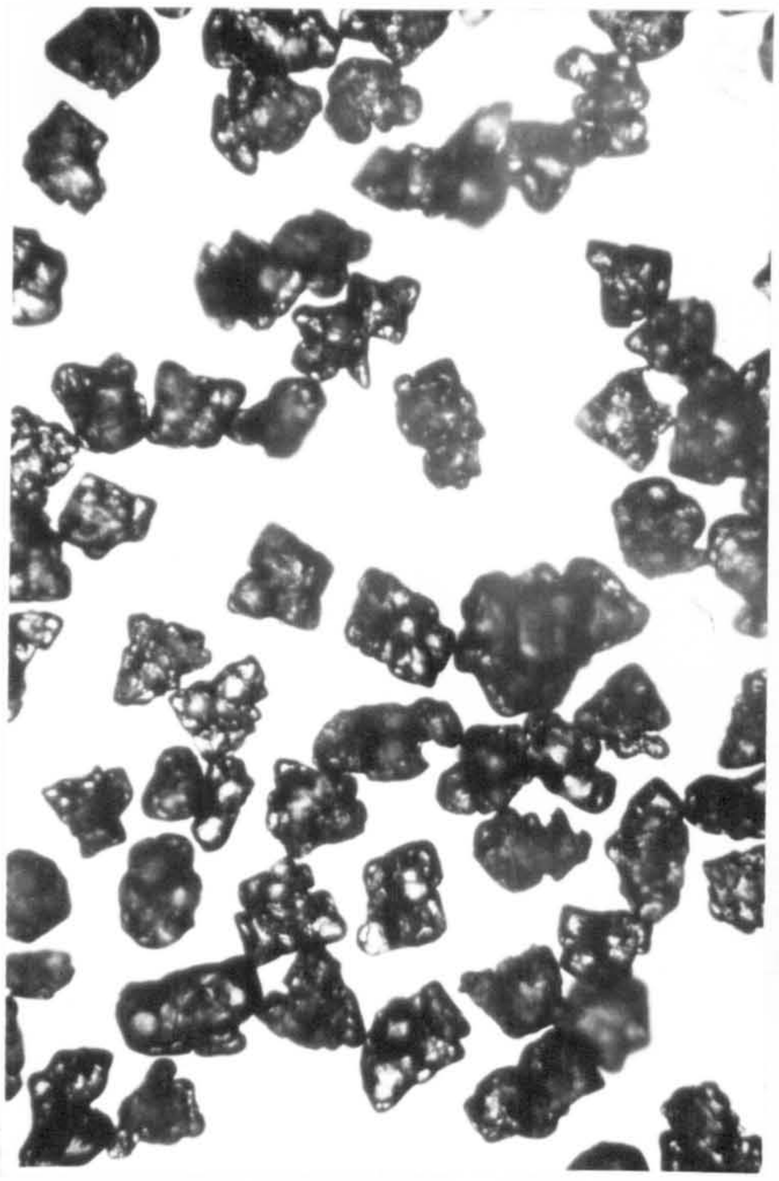

(A) 106 - 125μm

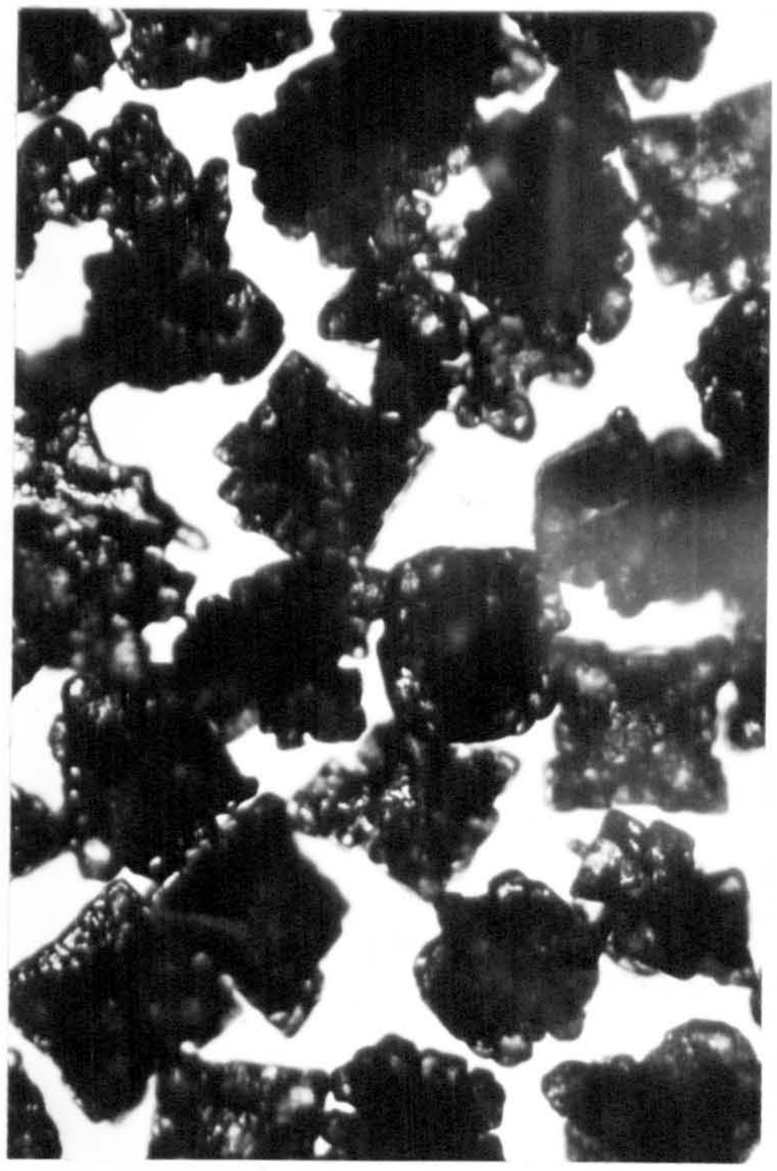

(B) 250 - 300μm

Figure A1 D- Sodium Chloride

(A) 106 - 125μm

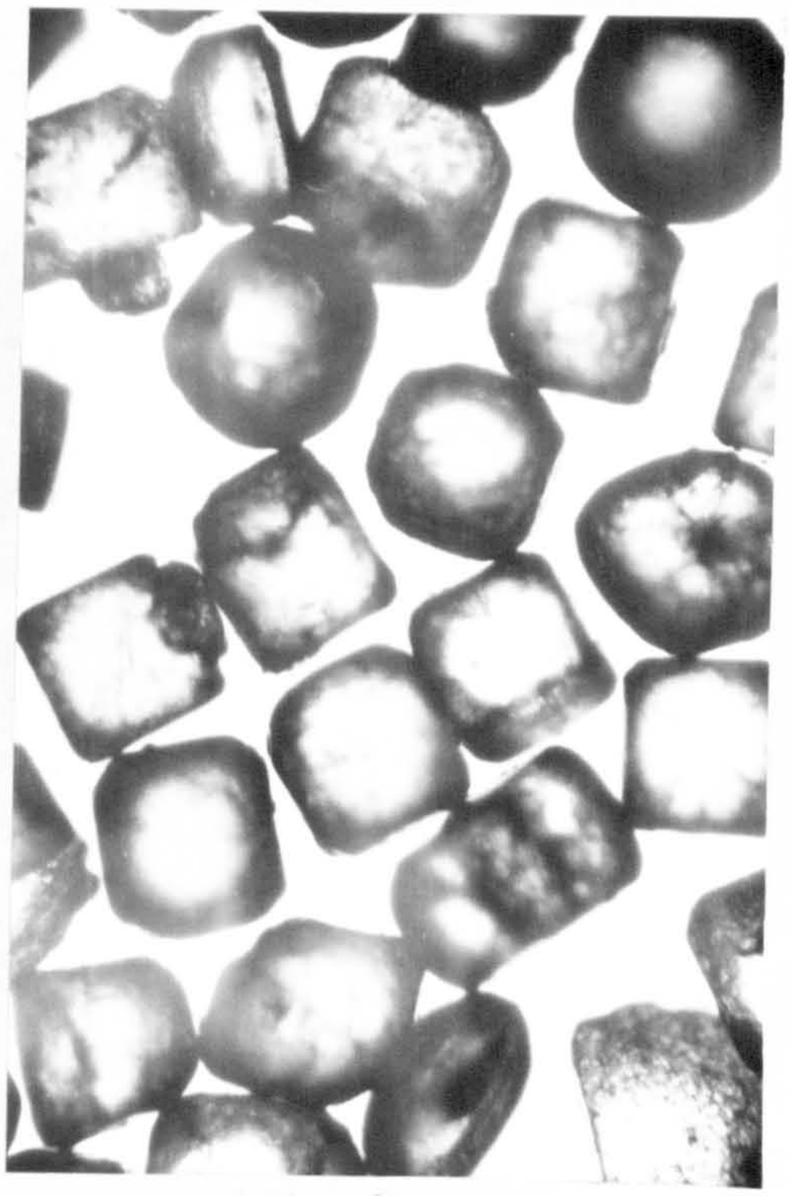

(B) 250 - 300μm

Figure A2 C- Sodium Chloride

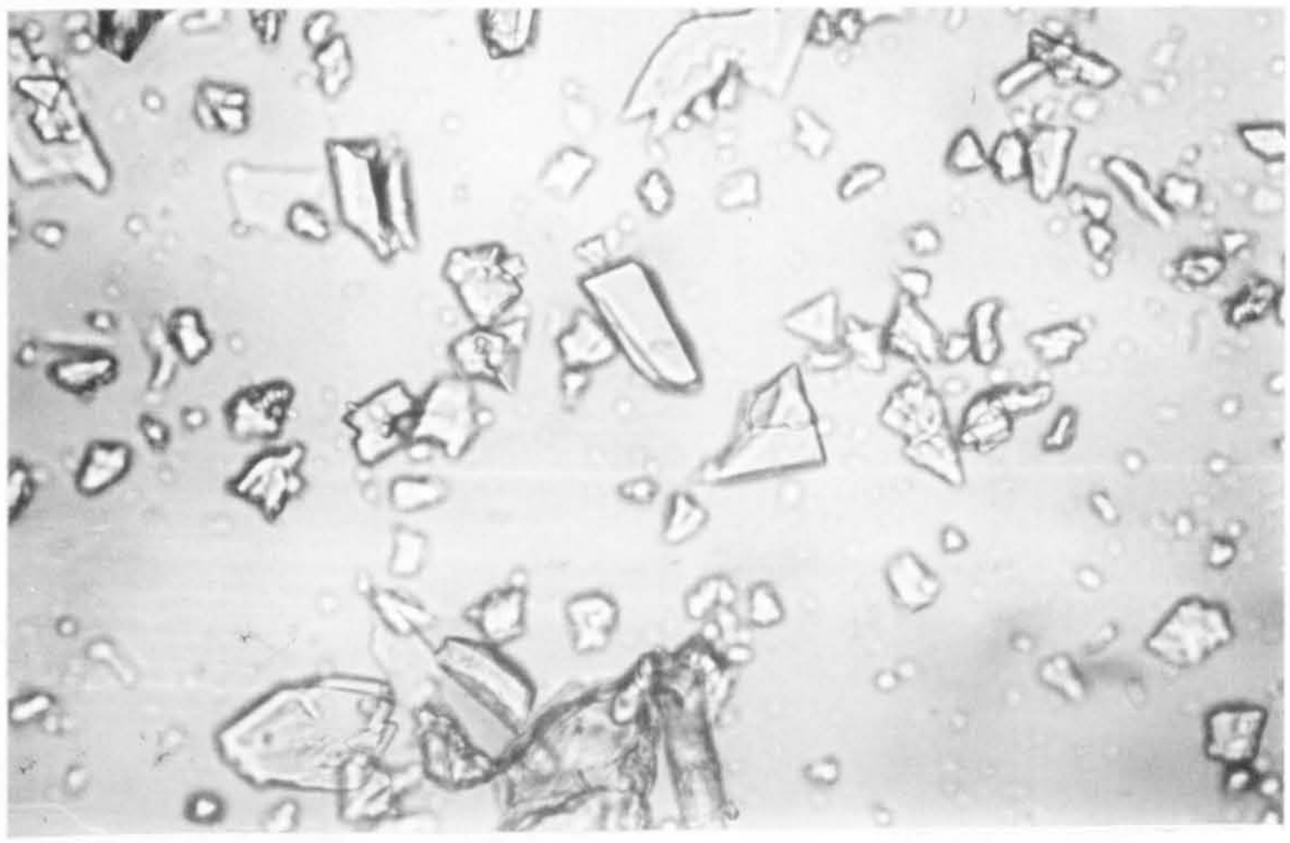

Figure A3 Dicalcium Phosphate

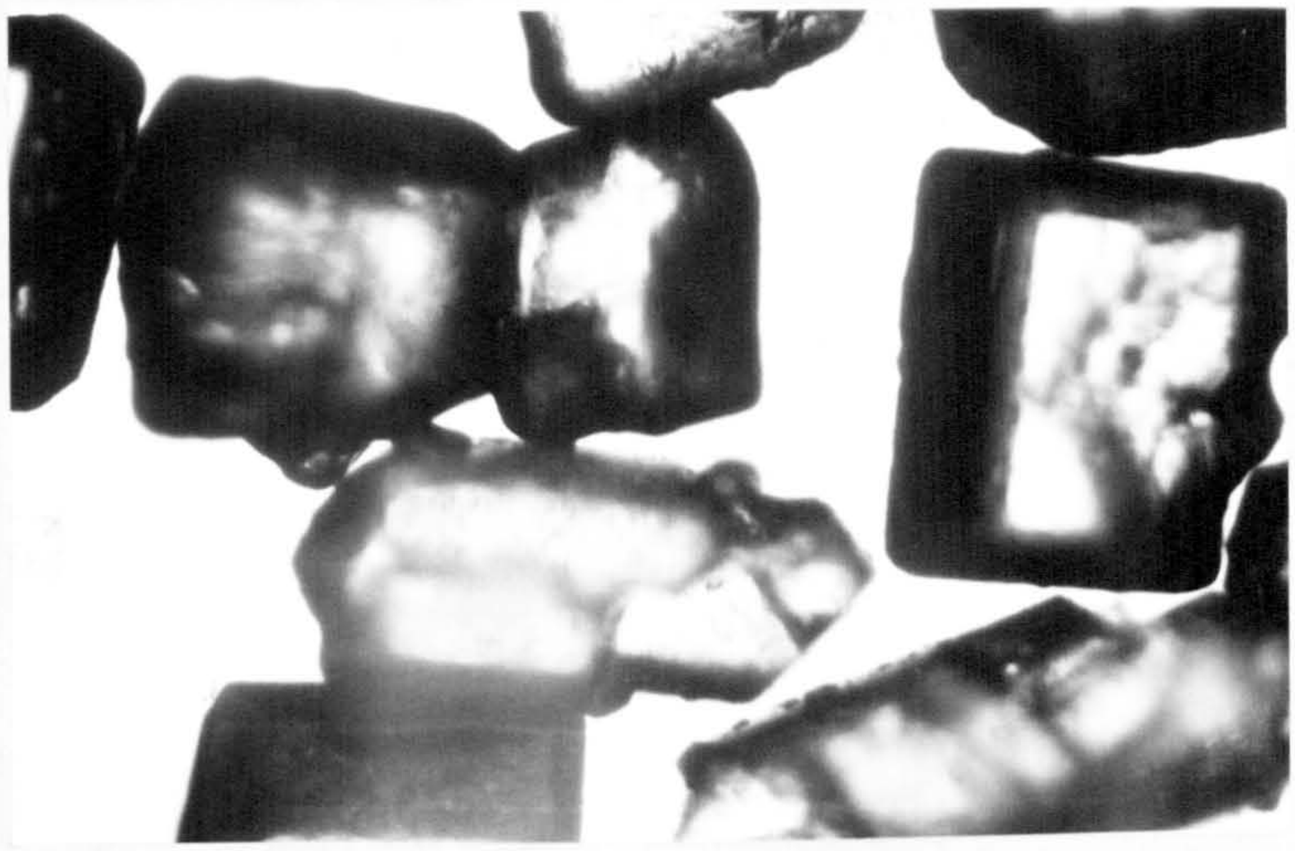

Figure A4 Sugar

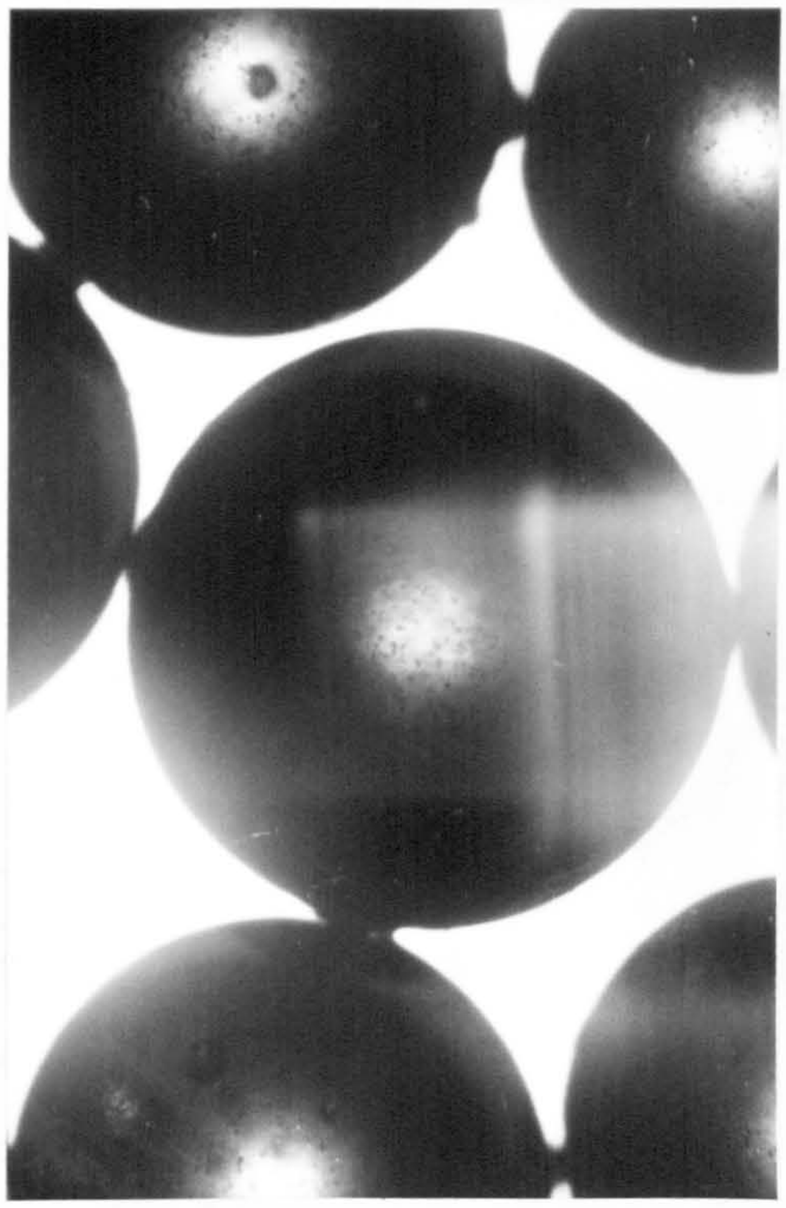

(A)

0 (MPA)

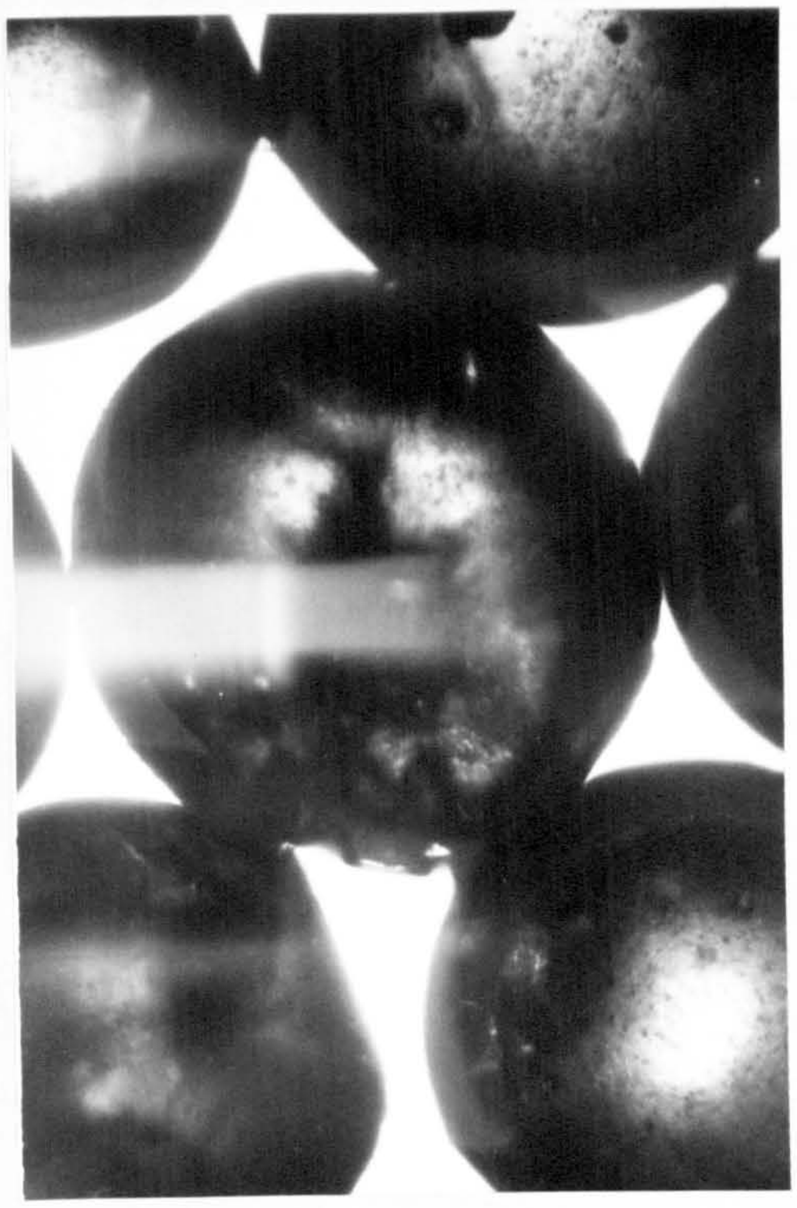

(B)

62 (MPA)

(C)

248 (MPA)

(D)

300 (MPA)

Figure A5 Styrocell

Table A9

Adsorption measurements for dicalcium phosphate powder

P2 TORR	V ADS MLS STP/GM	REL	BET	HUTTIG
30.5	.4348	.0401	C.00000	0.00000
34.0	.4421	.0447	0.00000	0.00000
41.0	.4570	.0539	.12479	.12443
44.2	.4621	.0582	.13362	.13317
75.2	.5058	.0989	.21712	.21499
85.2	.5156	.1121	.24476	.24169
96.4	.5325	.1295	.27928	.27460
105.8	.5393	.1392	.29989	.29406
115.0	.5488	.1513	.32490	.31746
185.5	.6253	.2441	.51640	.48564
209.7	.6528	.2759	.58371	.53927
242.4	.6929	.3189	.67586	.60710
260.3	.7110	.3425	.73267	.64672
282.2	.7373	.3713	0.00000	.69062
350.4	.8235	.4611	0.00000	.81801
394.7	.8838	.5193	0.00000	.89277
452.4	.9781	.5953	0.00000	.97082
482.4	1.0272	.6347	0.00000	1.01019
518.1	1.0957	.6817	0.00000	1.04628
609.4	1.3517	.8018	0.00000	0.00000
661.7	1.6776	.8707	0.00000	0.00000
678.3	1.8719	.8925	0.00000	0.00000
693.9	2.1085	.9130	0.00000	0.00000

SURFACE AREA IS 2.09 M SQRD PER GM

FROM HUTTIGS EQUATION:
SURFACE AREA IS 2.09 M SQRD PER GM

Table A10

Adsorption measurements for dicalcium phosphate compacts produced at 15 MPa

P2 TORR	V ADS MLS STP/GM	REL	BET	HUTTIG
30.7	.4155	.0404	0.00000	0.00000
55.5	.4567	.0730	.17248	.17156
60.7	.4632	.0799	.18740	.18621
66.6	.4767	.0876	.20149	.19994
74.2	.4822	.0976	.22436	.22222
97.2	.5065	.1279	.28954	.28460
117.7	.5333	.1549	.34358	.33534
131.2	.5427	.1726	.38448	.37302

SURFACE AREA IS 2.05 M SQRD PER GM

FROM HUTTIGS EQUATION:
SURFACE AREA IS 2.05 M SQRD PER GM

Table All

Adsorption mesurements for dicalcium phosphate compacts produced at 32 MPa

P2 TORR	V ADS MLS STP/GM	REL	BET	HUTTIG
26.7	.4232	.0351	0.00000	0.00000
28.9	.4292	.0380	0.00000	0.00000
31.7	.4361	.0417	0.00000	0.00000
33.2	.4384	.0437	0.00000	0.00000
35.1	.4405	.0462	0.00000	0.00000
57.6	.4849	.0758	.16912	.16814
63.5	.4876	.0836	.18699	.18568
70.2	.4984	.0924	.20420	.20246
73.8	.5014	.0971	.21449	.21246
77.9	.5070	.1025	.22528	.22291
115.5	.5159	.1520	.34740	.33938
126.7	.5268	.1667	.37974	.36919
140.9	.5418	.1854	.42007	.40563
148.0	.5489	.1947	.44060	.42389
156.4	.5587	.2058	.46377	.44413
207.0	.6178	.2724	.60591	.56096
226.5	.6426	.2980	.66070	.60202
251.3	.6739	.3307	.73301	.65287
263.8	.6878	.3471	.77298	.67985
278.7	.7058	.3667	0.00000	.71007
329.2	.7727	.4332	0.00000	.80340
359.7	.8167	.4733	0.00000	.85380
397.9	.8759	.5236	0.00000	.91071
416.8	.9045	.5484	0.00000	.93888
439.7	.9375	.5786	0.00000	.97419
483.4	1.0187	.6361	0.00000	1.02152
526.7	1.0966	.6930	0.00000	1.07000
578.4	1.2167	.7611	0.00000	0.00000
602.3	1.2851	.7925	0.00000	0.00000
656.2	1.4620	.8634	0.00000	0.00000
701.2	1.6906	.9226	0.00000	0.00000
740.9	2.0811	.9749	0.00000	0.00000

SURFACE AREA IS 1.97 M SQRD PER GM

FROM HUTTIGS EQUATION:
SURFACE AREA IS 1.97 M SQRD PER GM

Table. A12

Adsorption measurements for dicalcium phosphate compacts produced at 47 MPa

P2 TORR	V ADS MLS STP/GM	REL	BET	HUTTIG
29.6	.4181	.0389	0.00000	0.00000
32.0	.4247	.0421	0.00000	0.00000
35.3	.4305	.0464	0.00000	0.00000
36.8	.4342	.0484	0.00000	0.00000
38.9	.4365	.0512	.12358	.12325
55.6	.4693	.0732	.16819	.16729
61.1	.4737	.0804	.18456	.18337
67.6	.4833	.0889	.20200	.20040
70.9	.4874	.0933	.21109	.20925
75.1	.4909	.0988	.22336	.22118
105.6	.5318	.1389	.30346	.29760
115.6	.5437	.1521	.32994	.32231
128.5	.5576	.1691	.36492	.35449
143.0	.5705	.1882	.40624	.39186
165.2	.6224	.2437	.51765	.46691
202.7	.6437	.2667	.56506	.52487
224.7	.6725	.2957	.62418	.56961
249.5	.6986	.3283	.69957	.62418
284.9	.7462	.3749	0.00000	.69072
311.2	.7839	.4095	0.00000	.73625
343.9	.8359	.4525	0.00000	.78629
360.7	.8832	.5009	0.00000	.85124
492.1	1.0767	.6475	0.00000	.99080
539.6	1.1892	.7100	0.00000	0.00000
563.1	1.2412	.7409	0.00000	0.00000
590.1	1.3096	.7764	0.00000	0.00000
651.2	1.5276	.8568	0.00000	0.00000
695.7	1.6087	.9154	0.00000	0.00000
712.3	1.9689	.9372	0.00000	0.00000
727.2	2.1781	.9568	0.00000	0.00000

SURFACE AREA IS 2.11 M SQRD PER GM

FROM HUTTIGS EQUATION:
SURFACE AREA IS 2.11 M SQRD PER GM

Table A13

Adsorption measurements for dicalcium phosphate compacts produced at 77 MPa

P2 TORR	V ADS MLS STP/GM	REL	BET	HUTTIG
37.4	.4556	.0492	0.00000	0.00000
40.9	.4655	.0538	.12217	.12182
43.0	.4674	.0566	.12830	.12789
45.7	.4687	.0601	.13651	.13601
68.6	.5076	.0903	.19546	.19387
75.1	.5157	.0988	.21261	.21053
83.2	.5274	.1095	.23311	.23031
92.8	.5348	.1221	.26005	.25618
130.4	.5797	.1716	.35728	.34677
142.7	.5956	.1878	.38810	.37442
158.6	.6139	.2087	.42955	.41085
176.4	.6315	.2321	.47866	.45287
229.9	.6963	.3025	.62283	.56584
252.1	.7201	.3317	.68926	.61342
279.4	.7583	.3676	0.00000	.66304
309.7	.7961	.4075	0.00000	.72043
369.5	.8858	.4862	0.00000	.81573
403.7	.9364	.5312	0.00000	.86856
446.6	1.0036	.5876	0.00000	.92963
467.8	1.0363	.6155	0.00000	.95960
492.9	1.0780	.6466	0.00000	.99183
546.2	1.1815	.7187	0.00000	0.00000
600.3	1.3015	.7899	0.00000	0.00000
625.8	1.3664	.8234	0.00000	0.00000
654.9	1.4515	.8617	0.00000	0.00000
723.8	1.7574	.9524	0.00000	0.00000
745.8	1.8967	.9813	0.00000	0.00000

SURFACE AREA IS 2.16 M SQRD PER GM

FROM HUTTIGS EQUATION:
SURFACE AREA IS 2.16 M SQRD PER GM

Table - A14

Adsorption measurements for dicalcium phosphate compacts produced at 120 MPa

P2 TORR	V ADS MLS STP/GM	REL	BET	HUTTIG
31.1	.4387	.0409	0.00000	0.00000
36.7	.4551	.0483	0.00000	0.00000
40.9	.4585	.0538	.12406	.12370
72.3	.5131	.0951	.20489	.20303
79.1	.5219	.1041	.22261	.22019
87.6	.5340	.1153	.24396	.24072
97.4	.5435	.1282	.27048	.26604
134.5	.5912	.1770	.36372	.35233
147.5	.6044	.1941	.39841	.38340
163.8	.6237	.2155	.44051	.42005
182.1	.6415	.2396	.49118	.46296
233.4	.7021	.3071	.63130	.57176
255.4	.7299	.3361	.69348	.61516
282.6	.7709	.3718	0.00000	.66167
313.4	.8069	.4124	0.00000	.72178
365.7	.8618	.4812	0.00000	.80826
399.4	.9319	.5255	0.00000	.86028
441.5	.9995	.5809	0.00000	.91889
486.9	1.0739	.6407	0.00000	.97874
541.7	1.1823	.7128	0.00000	0.00000
588.4	1.2840	.7742	0.00000	0.00000
643.9	1.4329	.8472	0.00000	0.00000
669.1	1.5174	.8804	0.00000	0.00000
697.4	1.6270	.9176	0.00000	0.00000
725.4	1.7863	.9545	0.00000	0.00000
761.4	2.2156	1.0018	0.00000	0.00000

SURFACE AREA IS 2.17 M SQRD PER GM

FROM HUTTIGS EQUATION:
SURFACE AREA IS 2.17 M SQRD PER GM

Table A15

Adsorption measurements for dicalcium phosphate compacts produced at 155MPa

P2 TORR	V ADS MLS STP/GM	REL	BET	HUTTIG
30.7	.4517	.0404	0.00000	0.00000
36.4	.4665	.0479	0.00000	0.00000
40.2	.4722	.0529	.11826	.11793
74.4	.5297	.0979	.20487	.20290
81.3	.5395	.1070	.22203	.21949
90.3	.5500	.1188	.24514	.24166
100.3	.5605	.1320	.27124	.26652
143.3	.6123	.1686	.37949	.36600
157.1	.6269	.2067	.41563	.39787
174.4	.6479	.2295	.45963	.43543
183.3	.6560	.2412	.48449	.45631
193.8	.6676	.2550	.51268	.47935
252.1	.7365	.3317	.67397	.59981
276.2	.7637	.3634	0.00000	.64862
305.9	.8059	.4025	0.00000	.70043
338.9	.8472	.4459	0.00000	.76102
399.7	.9412	.5259	0.00000	.85268
436.5	.9962	.5743	0.00000	.90770
481.4	1.0781	.6334	0.00000	.95972
503.8	1.1156	.6629	0.00000	.98606
530.2	1.1637	.6976	0.00000	1.01771
584.7	1.2846	.7693	0.00000	0.00000
633.5	1.4072	.8336	0.00000	0.00000
688.0	1.6054	.9053	0.00000	0.00000
712.3	1.7133	.9372	0.00000	0.00000
737.4	1.6619	.9703	0.00000	0.00000

SURFACE AREA IS 2.20 M SQRD PER GM

FROM HUTTIGS EQUATION:
SURFACE AREA IS 2.20 M SQRD PER GM

Table A16

Adsorption measurements for dicalcium phosphate compacts produced at 248 MPa

P2 TORR	V ADS MLS STP/GM	REL	BET	HUTTIG
32.4	.4467	.0426	0.00000	0.00000
35.2	.4526	.0463	0.00000	0.00000
38.6	.4606	.0508	.11611	.11561
42.7	.4664	.0562	.12763	.12722
78.5	.5248	.1033	.21950	.21716
86.0	.5332	.1132	.23929	.23623
95.4	.5452	.1255	.26330	.25915
100.3	.5494	.1320	.27676	.27194
106.1	.5553	.1396	.29220	.28650
161.7	.6242	.2128	.43296	.41336
177.4	.6396	.2334	.47610	.45016
196.7	.6649	.2588	.52520	.49002
207.0	.6721	.2724	.55693	.51562
218.8	.6855	.2879	.58977	.54089
300.7	.7899	.3957	0.00000	.69905
328.7	.8284	.4325	0.00000	.74786
364.2	.8773	.4792	0.00000	.80602
381.8	.9010	.5024	0.00000	.83772
402.9	.9300	.5301	0.00000	.87223
485.3	1.0662	.6386	0.00000	.98131
580.9	1.2581	.7643	0.00000	0.00000
606.1	1.3160	.7975	0.00000	0.00000
636.1	1.3850	.8370	0.00000	0.00000
659.5	1.4549	.8678	0.00000	0.00000
710.1	1.6295	.9343	0.00000	0.00000
758.9	1.9414	.9986	0.00000	0.00000

SURFACE AREA IS 2.19 M SQRD PER GM

FROM HUTTIGS EQUATION:

SURFACE AREA IS 2.19 M SQRD PER GM

Table A17 Krypton adsorption measurements for dentritic sodium chloride compacts produced at 32 MPa

Experiment	Kr Pressure Torr	$V_{ads./gr}$ $X10^{-3}$	Relative Pressure X	BET function $\left(\frac{1}{1-X}\right)\frac{1}{Va}$
I	0.113	4.677	0.045	10.075
	0.143	5.073	0.057	11.9151
	0.389	7.337	0.155	25.001
	0.580	9.947	0.231	30.199
	0.850	12.22	0.34	42.156

Experiment	Kr Pressure Torr	$V_{ads./gr}$ $X10^{-3}$	Relative Pressure X	BET function $\left(\frac{1}{1-X}\right)\frac{1}{Va}$
II	0.20	6.1022	0.08	14.25
	0.439	8.838	0.175	24.001
	0.540	9.695	0.215	28.25
	0.766	11.703	0.305	37.499

Specific surface area I = 0.0464 m^2/g

II = 0.0477 m^2/g

Table A18 — Krypton adsorption measurements for dentritic sodium chloride compacts produced at 77 MPa

Experiment	Kr Pressure Torr	$V_{ads/gr}$ $\times 10^{-3}$	Relative Pressure X	BET function $\left(\frac{1}{1-X}\right)\frac{1}{Va}$
I	0.163	4.56	0.065	15.245
	0.24	5.26	0.095	19.957
	0.414	6.86	0.165	28.810
	0.51	7.47	0.203	34.520
	0.663	8.54	0.264	42.002
	0.916	10.08	0.365	

Experiment	Kr Pressure Torr	$V_{ads/gr}$ $\times 10^{-3}$	Relative Pressure X	BET function $\left(\frac{1}{1-X}\right)\frac{1}{Va}$
II	0.188	6.01	0.075	13.491
	0.231	6.75	0.092	15.011
	0.459	8.70	0.183	25.746
	0.703	10.482	0.28	37.101
	0.823	11.525	0.33	42.6994

Experiment	Kr Pressure Torr	$V_{ads/gr}$ $\times 10^{-3}$	Relative Pressure X	BET function $\left(\frac{1}{1-X}\right)\frac{1}{Va}$
III	0.326	7.12	0.13	20.987
	0.527	9.17	0.21	28.9883
	0.735	10.76	0.293	38.5155
	0.873	11.914	0.348	44.7996

Graphic surface area

I = 0.0374

II = 0.0439

III = 0.0441

Table A19 Krypton adsorption measurements for dentritic sodium chloride compacts produced at 155 MPa

Experiment	Kr Pressure Torr	$V_{ads/gr}$ $\times 10^{-3}$	Relative Pressure X	BET function $\left(\frac{1}{1-X}\right)\frac{1}{Va}$
I	0.161	2.71	0.064	25.231
	0.314	4.20	0.125	34.0136
	0.464	5.37	0.185	42.3707
	0.615	6.48	0.245	50.0777
	0.678	6.94	0.27	53.2944
	0.979	9.33	0.39	

Experiment	Kr Pressure Torr	$V_{ads/gr}$ $\times 10^{-3}$	Relative Pressure X	BET function $\frac{1}{1-X}\quad\frac{1}{Va}$
II	0.088	1.909	0.035	
	0.201	3.34	0.08	26.035
	0.364	4.46	0.145	38.025
	0.444	4.89	0.177	43.981
	0.489	5.02	0.195	48.254
	0.59	5.59	0.235	54.953
	0.778	6.56	0.31	68.487

Specific Surface Area I = 0.034 m^2/g

II = 0.027 m^2/g

Table A20 Krypton adsorption measurements for dentritic sodium chloride compacts produced at 246 MPa

Experiment	Kr Pressure Torr	$V_{ads/gr} \times 10^{-3}$	Relative Pressure X	BET function $\left(\frac{1}{1-X}\right)\frac{1}{Va}$
I	0.208	0.293	0.083	70.0
	0.377	1.503	0.150	117.4904
	0.527	1.688	0.21	157.478
	0.615	1.854	0.245	175.029
	0.708	1.9159	0.282	204.999
	0.791	1.8924	0.315	243.00
	0.868	2.1794	0.346	242.7512

Experiment	Kr Pressure Torr	$V_{ads/gr} \times 10^{3}$	Relative Pressure X	BET function $\left(\frac{1}{1-X}\right)\frac{1}{Va}$
II	0.113	0.9424	0.045	
	0.301	1.218	0.12	111.957
	0.477	1.3404	0.19	174.9984
	0.55	1.3759	0.22	204.994
	0.778	1.5492	0.31	290.005
	0.853	1.5850	0.34	325.017

Experiment	Kr Pressure Torr	$V_{ads/gr} \times 10^{-3}$	Relative Pressure X	BET function $\left(\frac{1}{1-X}\right)\frac{1}{Va}$
III	0.075	0.4548	0.03	
	0.276	1.0747	0.11	115.00
	0.39	1.265	0.155	145.006
	0.515	1.4326	0.205	179.996
	0.665	1.5676	0.265	230.00
	0.816	1.852	0.325	259.98

Specific surface area I = 0.00785 m^2/gr

II = 0.00565 m^2/gr

III = 0.00735 m^2/gr

Figures A6 -A13 :Adsorption isotherms of dicalcium phosphate powder and compacts

Table A6 Dicalcium phosphate powder

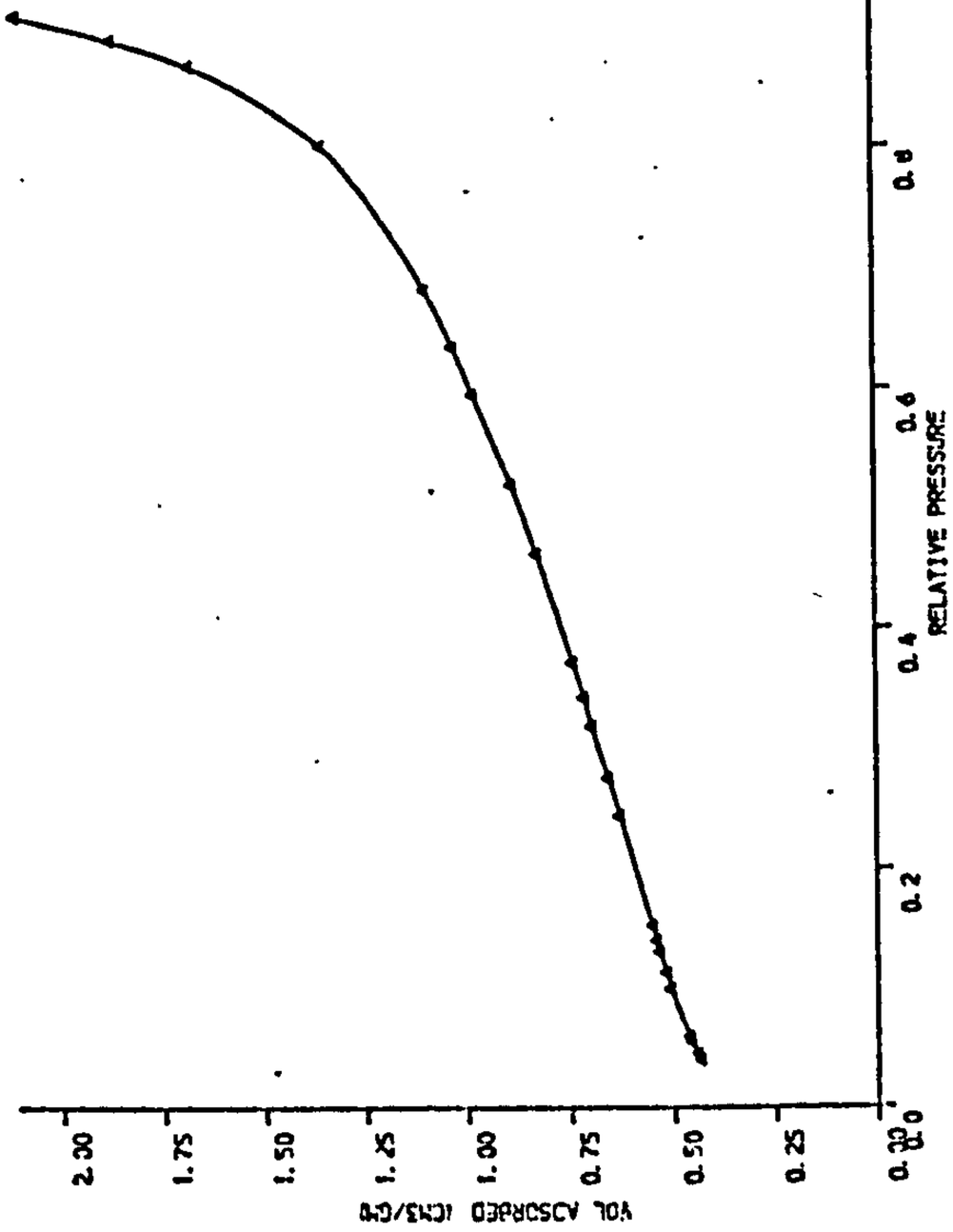

Table A7 Compacts prepared at 15 MPa

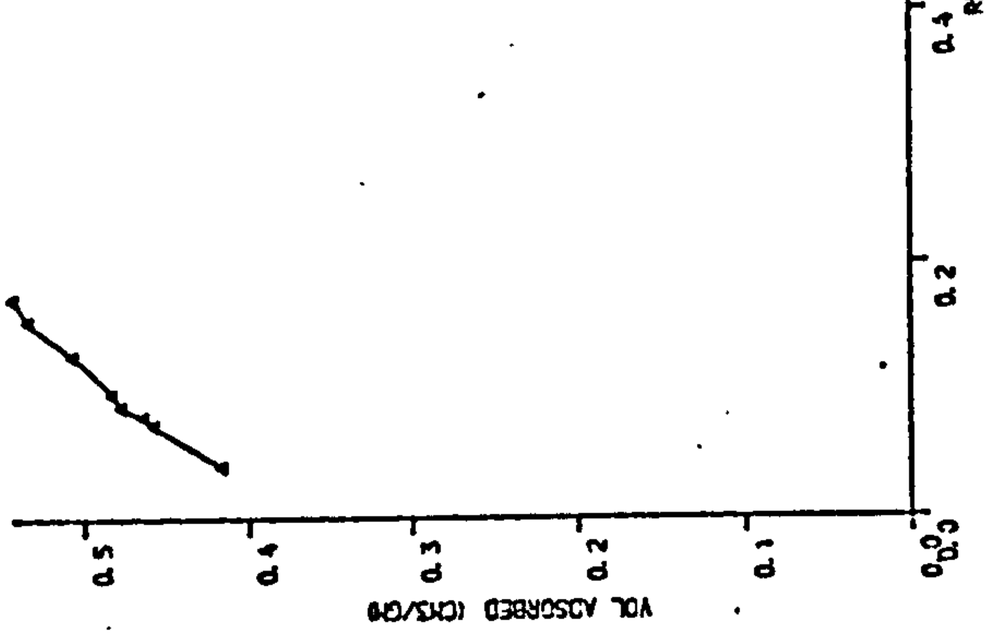

Table A8 Compacts prepared at 30 MPa

Table A9 Compacts prepared at 45 MPa

Table A10 Compacts prepared at 60 MPa

Table A11 Compacts prepared at 75 MPa

Table A12 Compacts prepared at 90 MPa

Table A13 Compacts prepared at 105 MPa

Figure A8 Compacts prepared at 32 MPa

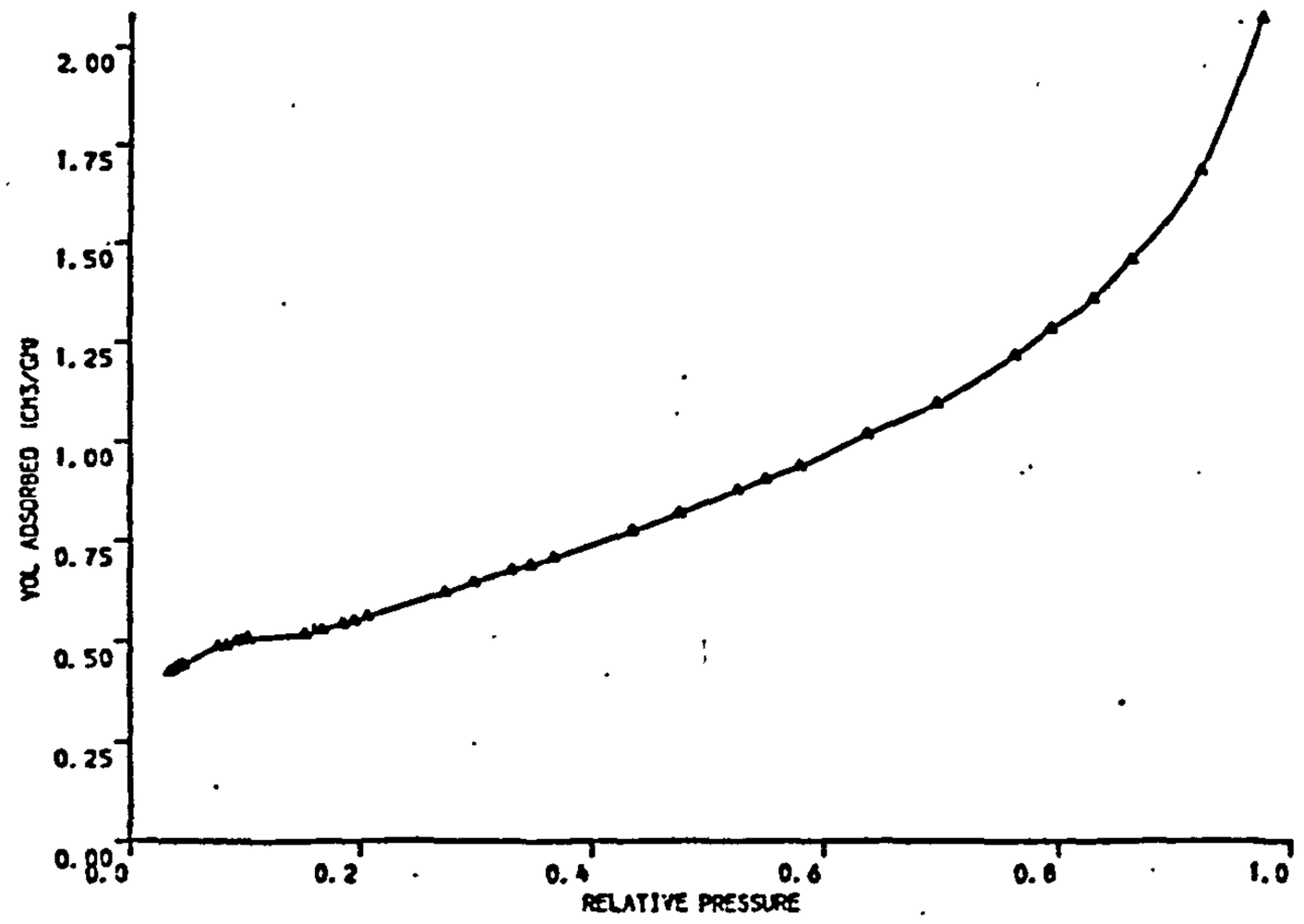

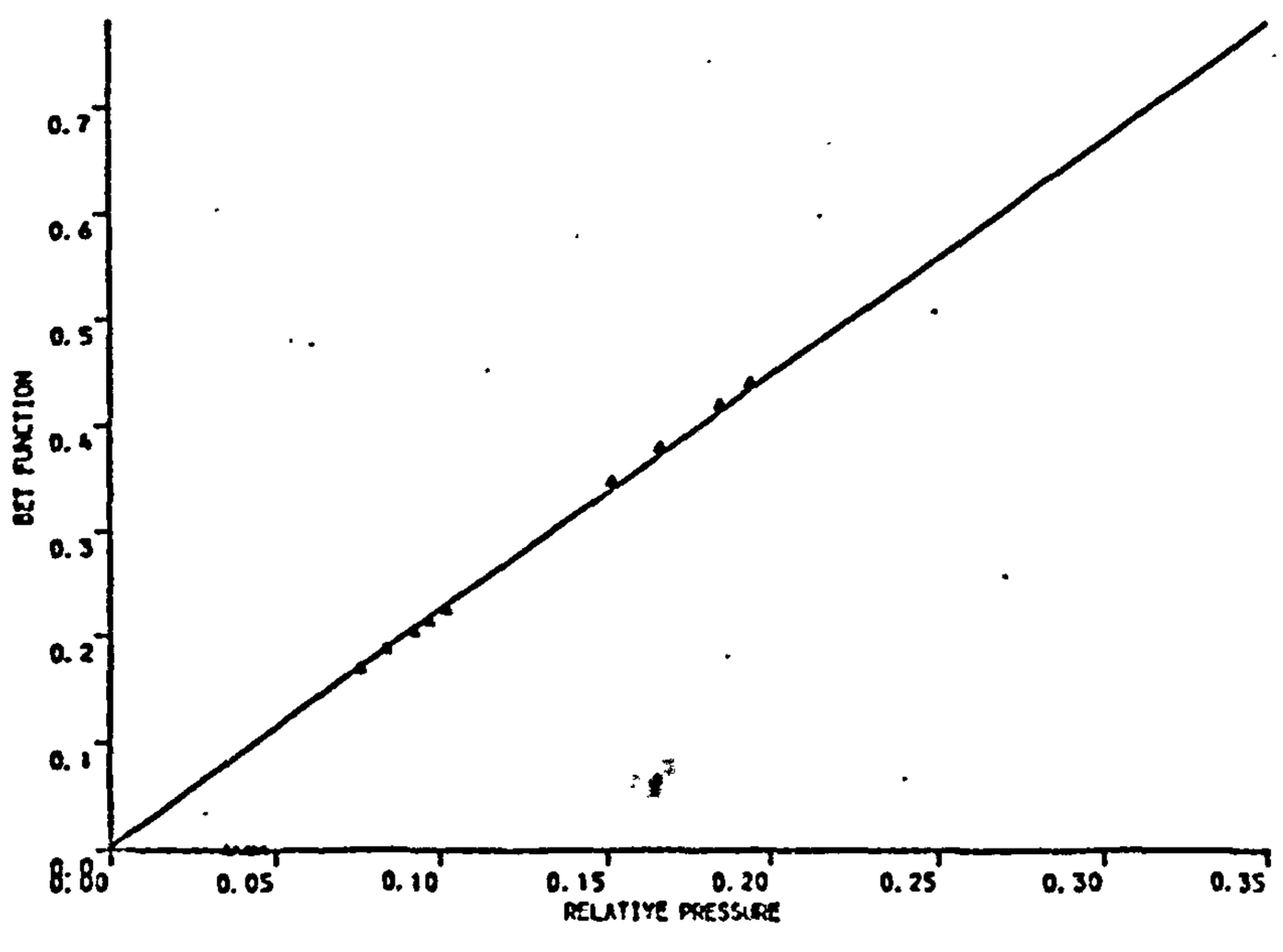

Figure A9 Compacts prepared at 47 MPa

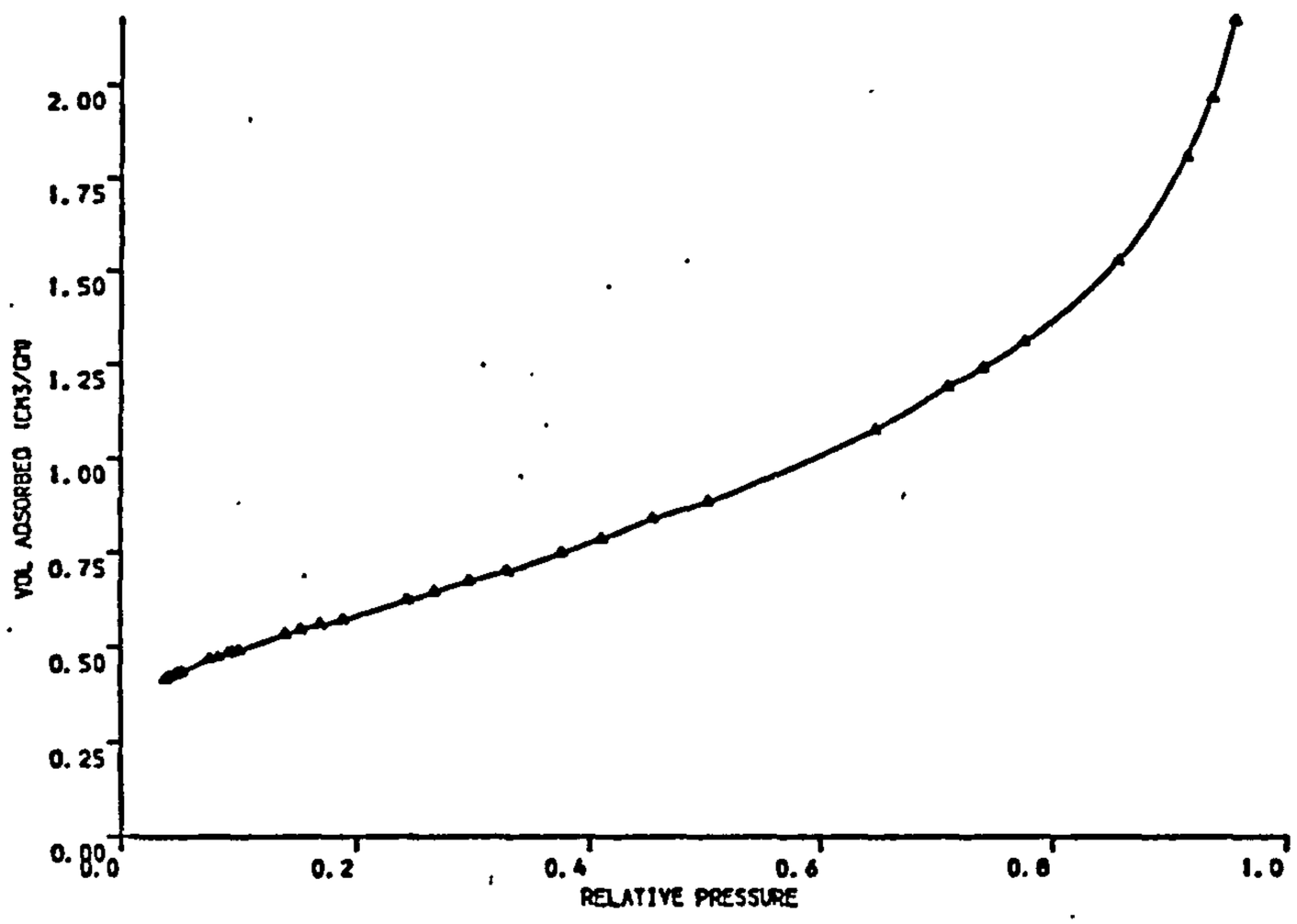

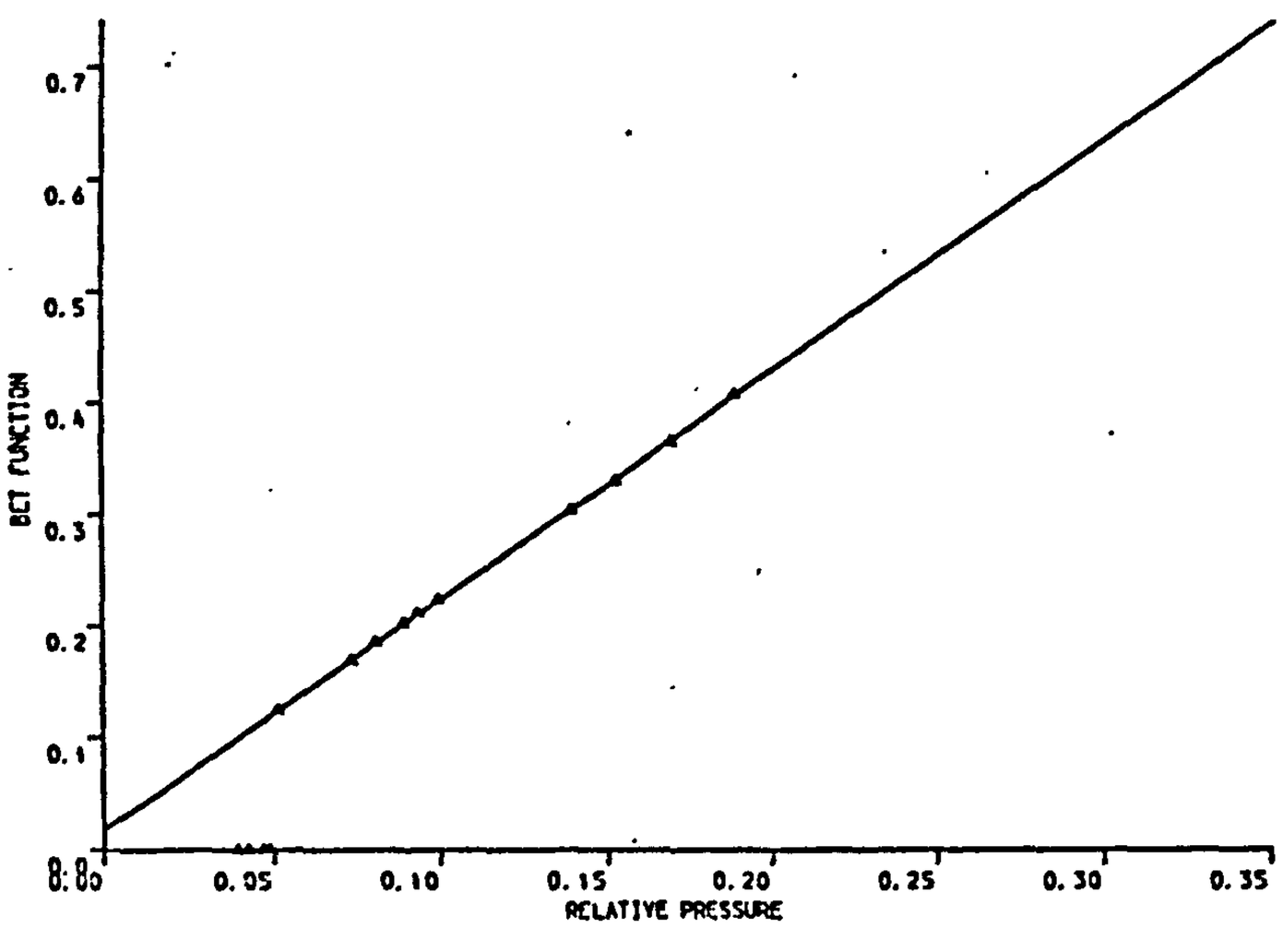

Figure A10 Compacts prepared at 77 MPa

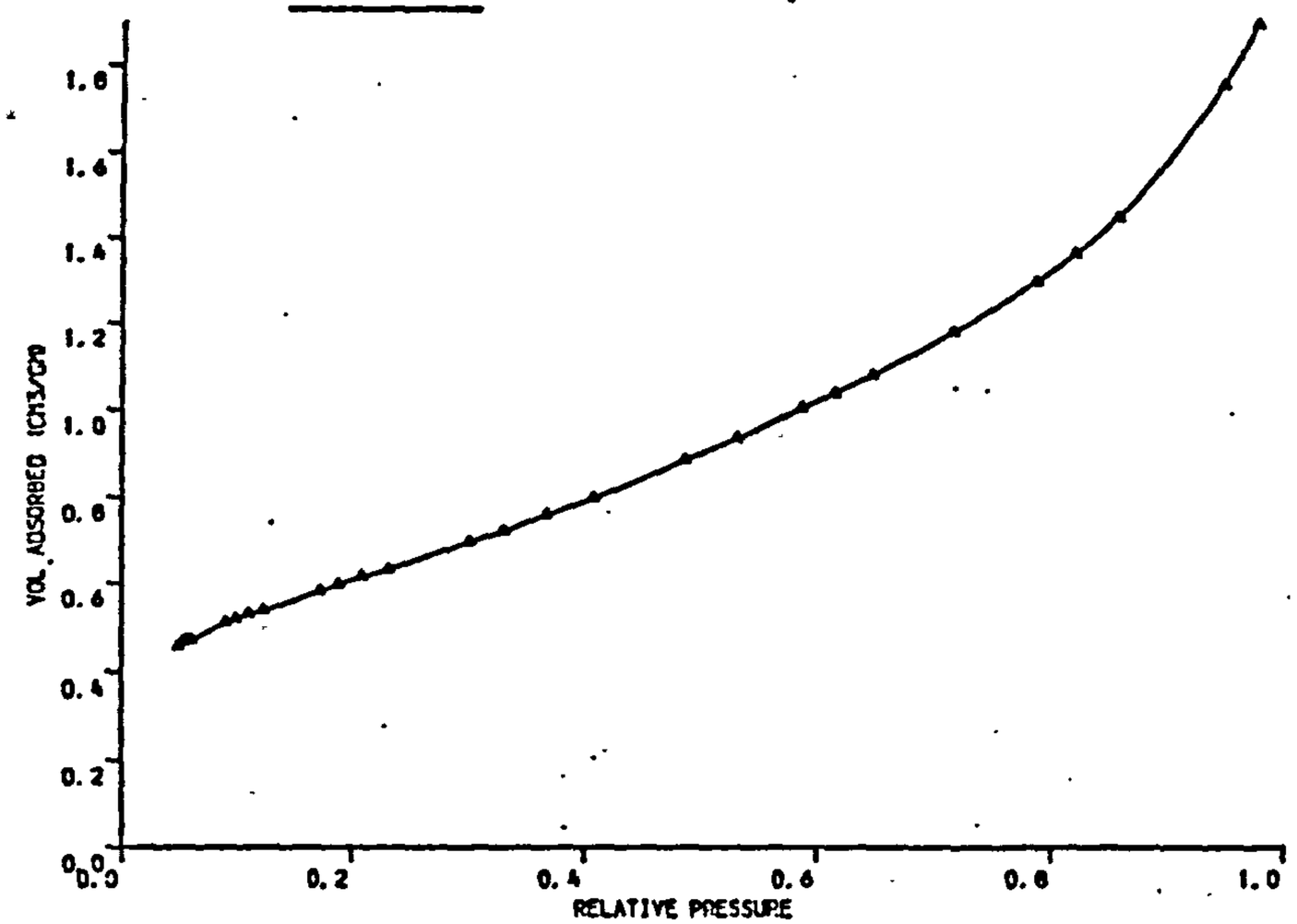

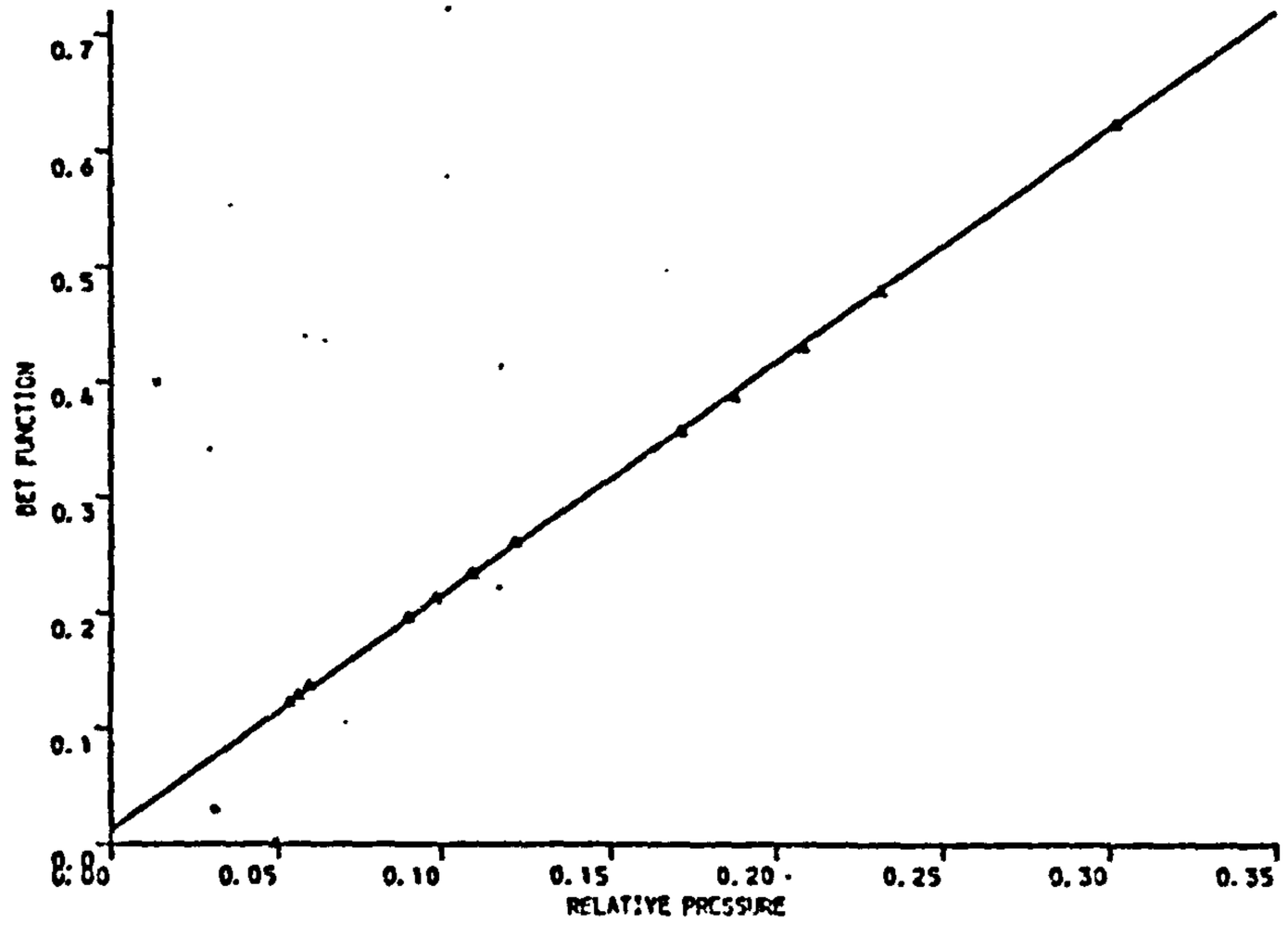

Figure A11 Compacts prepared at 120 MPa

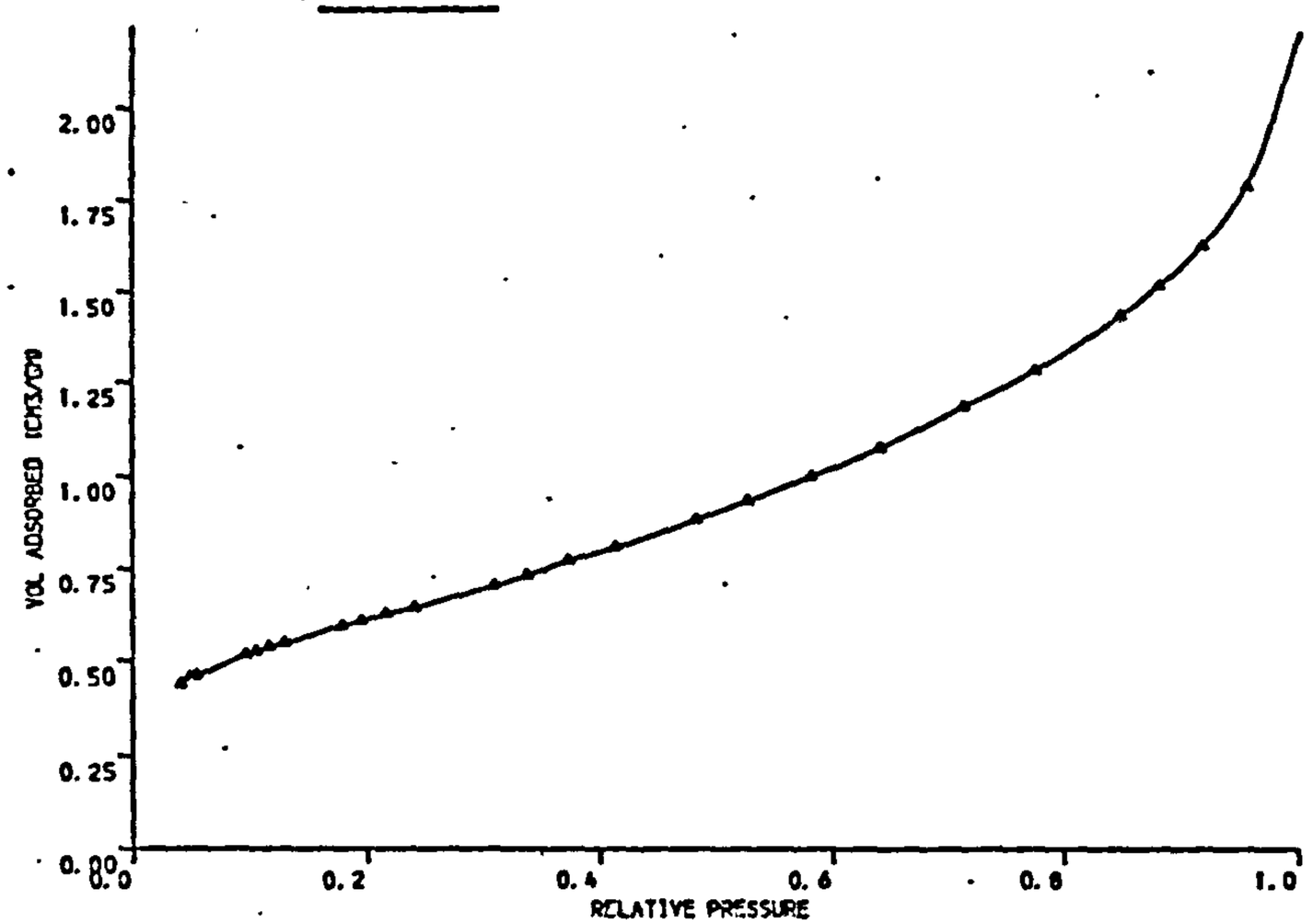

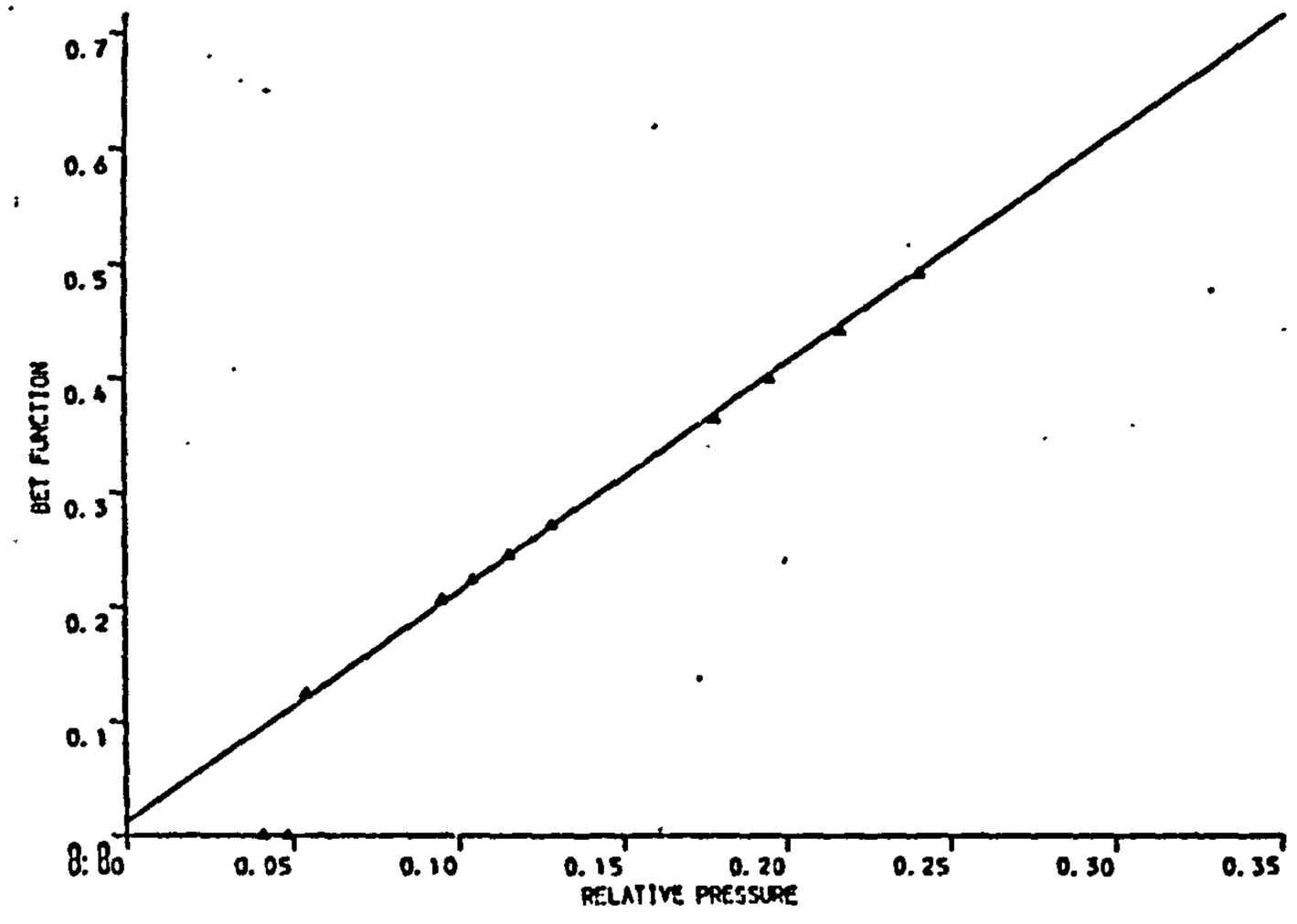

Figure A12 Compacts prepared at 155 MPa

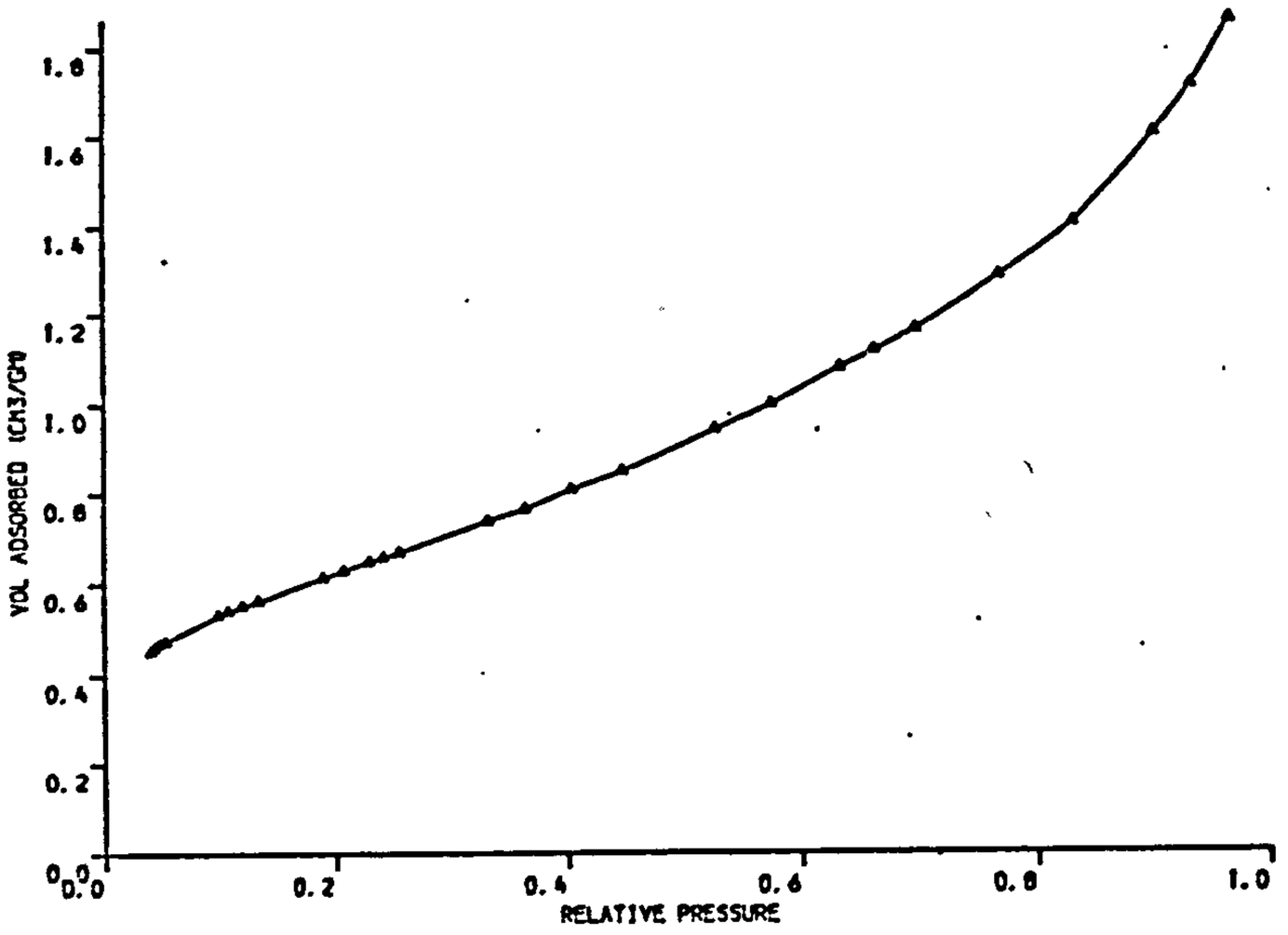

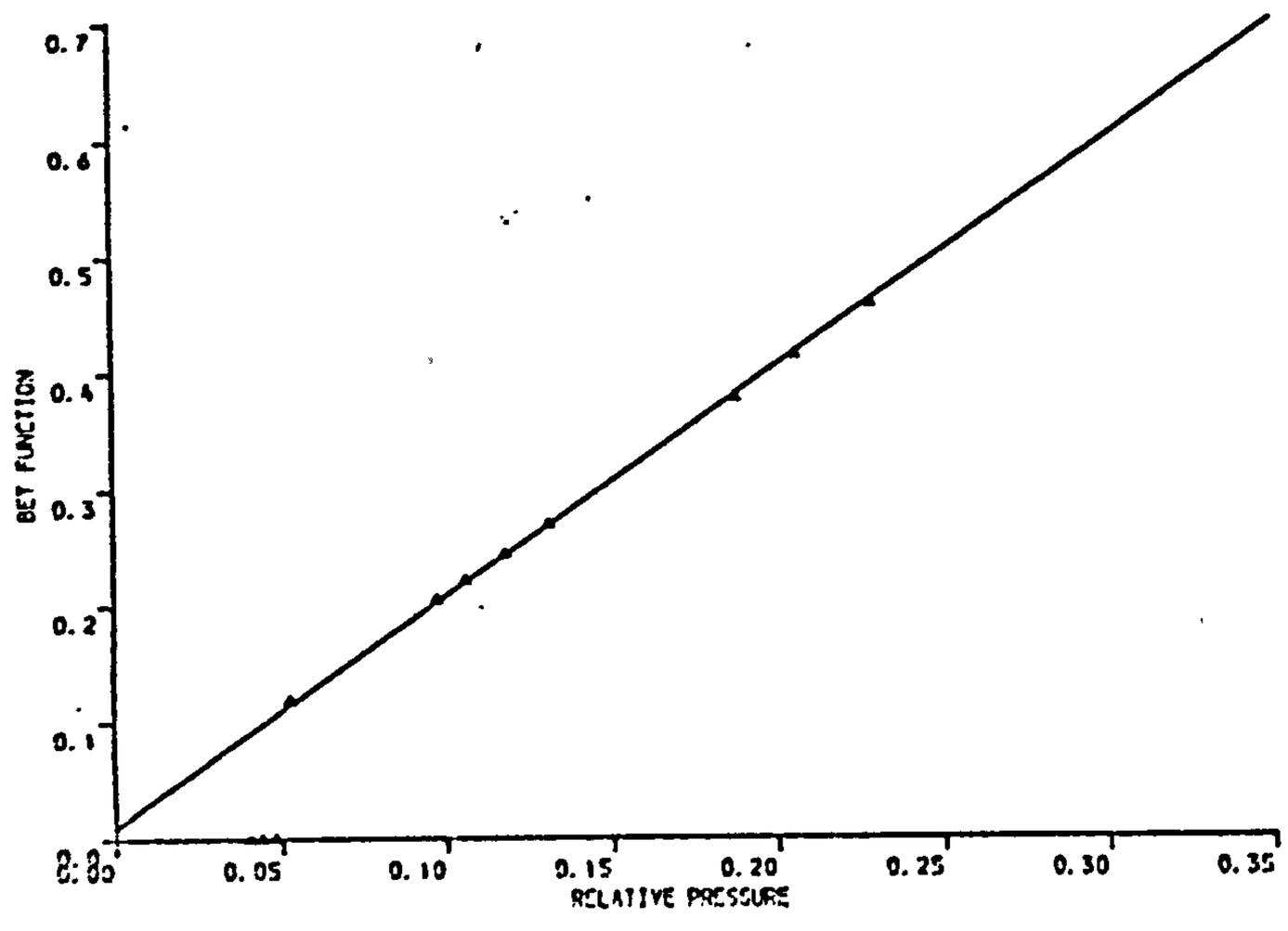

Figure A13 Compacts prepared at 248 MPa

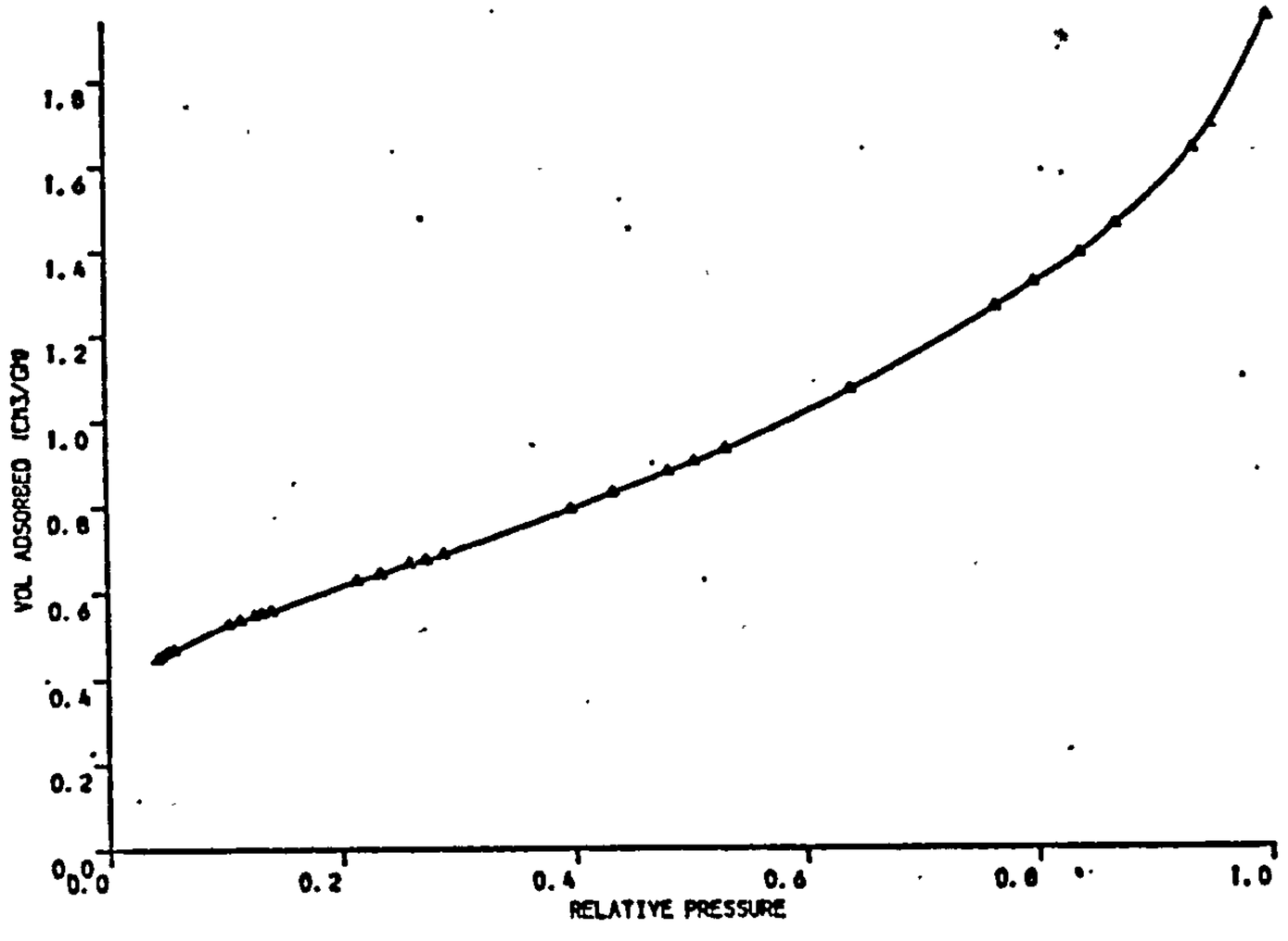

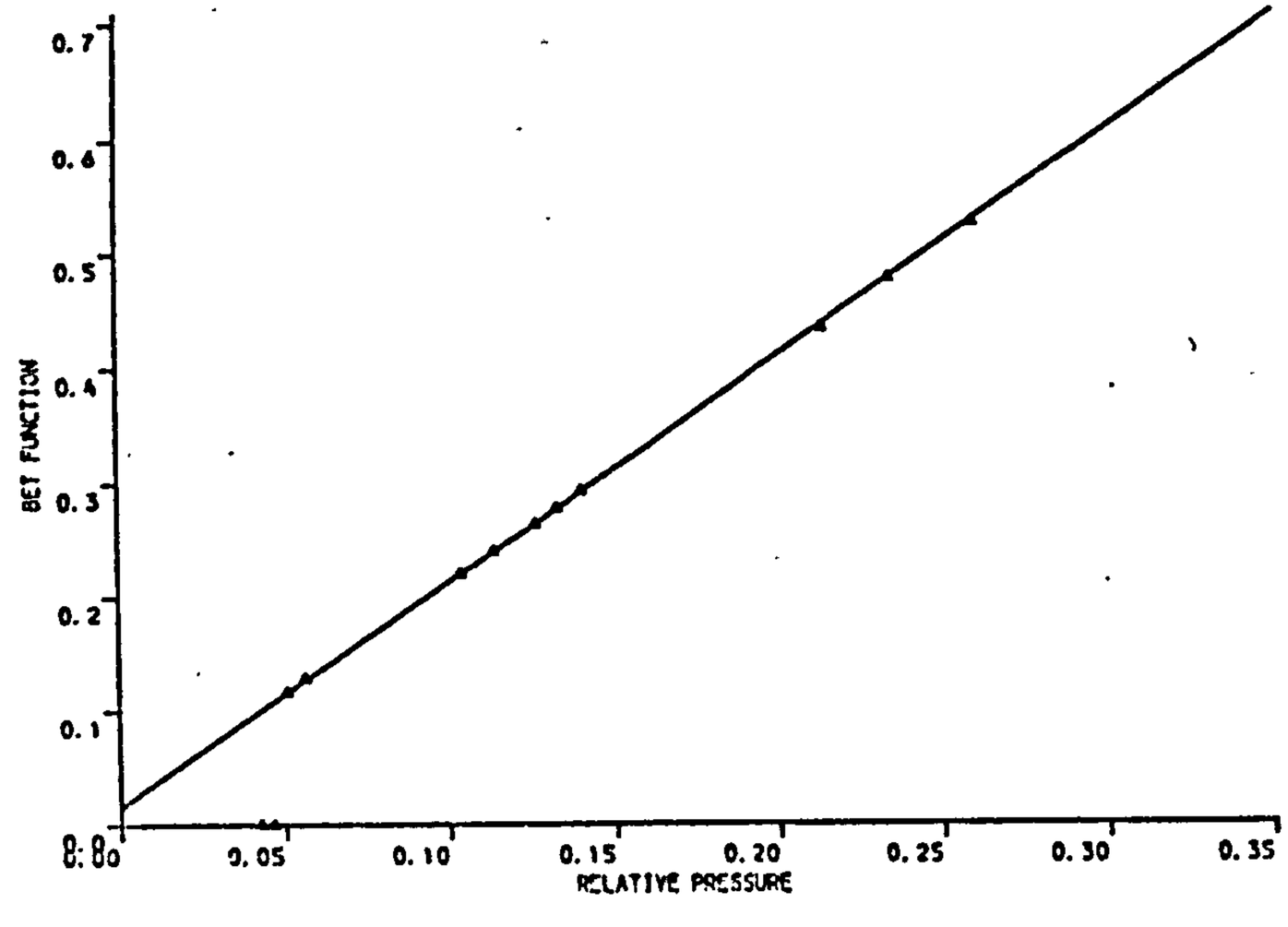

Figure - A14 BET plots for D-sodium chloride compacted at 32 MPa

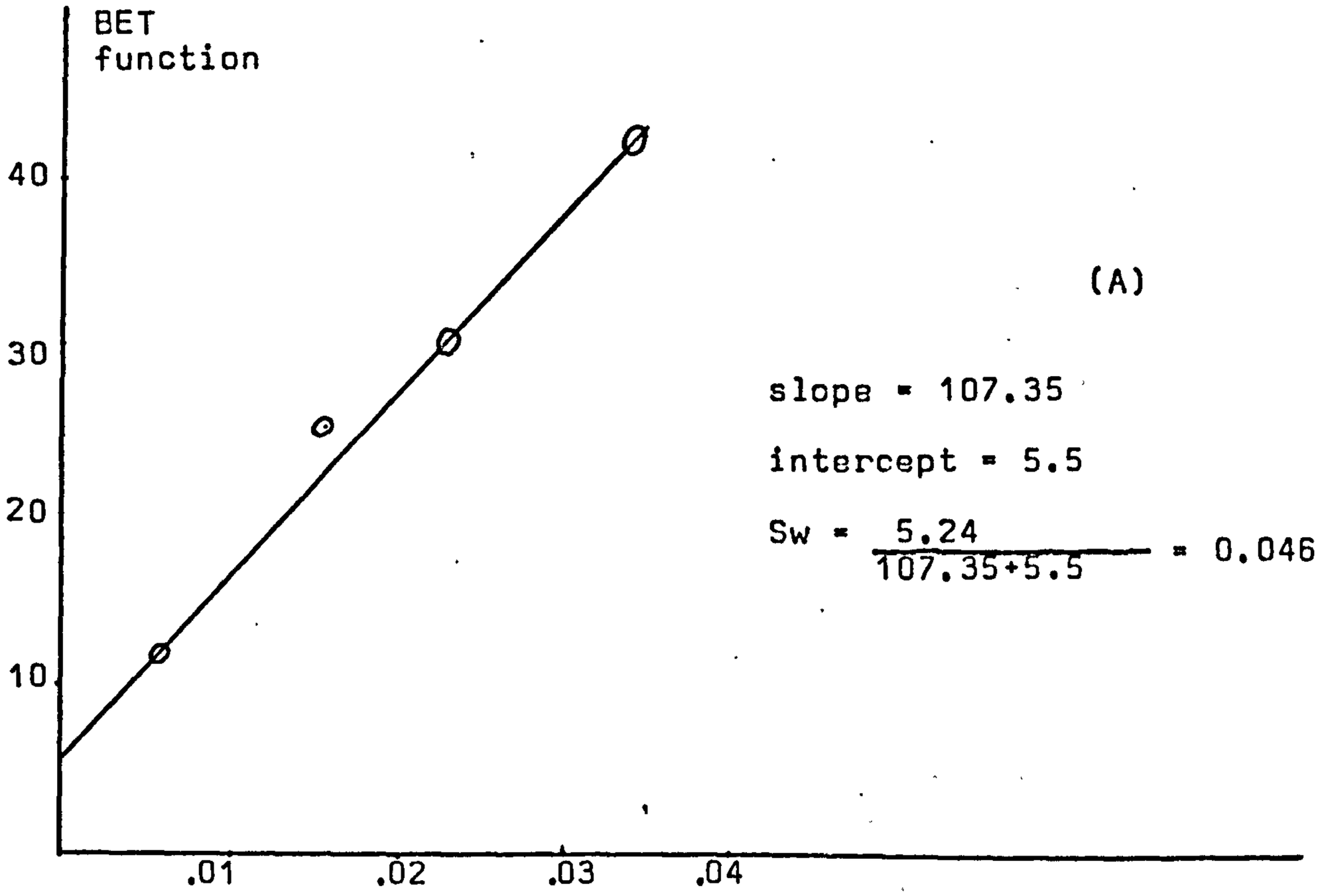

(A)

slope = 107.35

intercept = 5.5

$Sw = \frac{5.24}{107.35+5.5} = 0.0464 m^2/g$

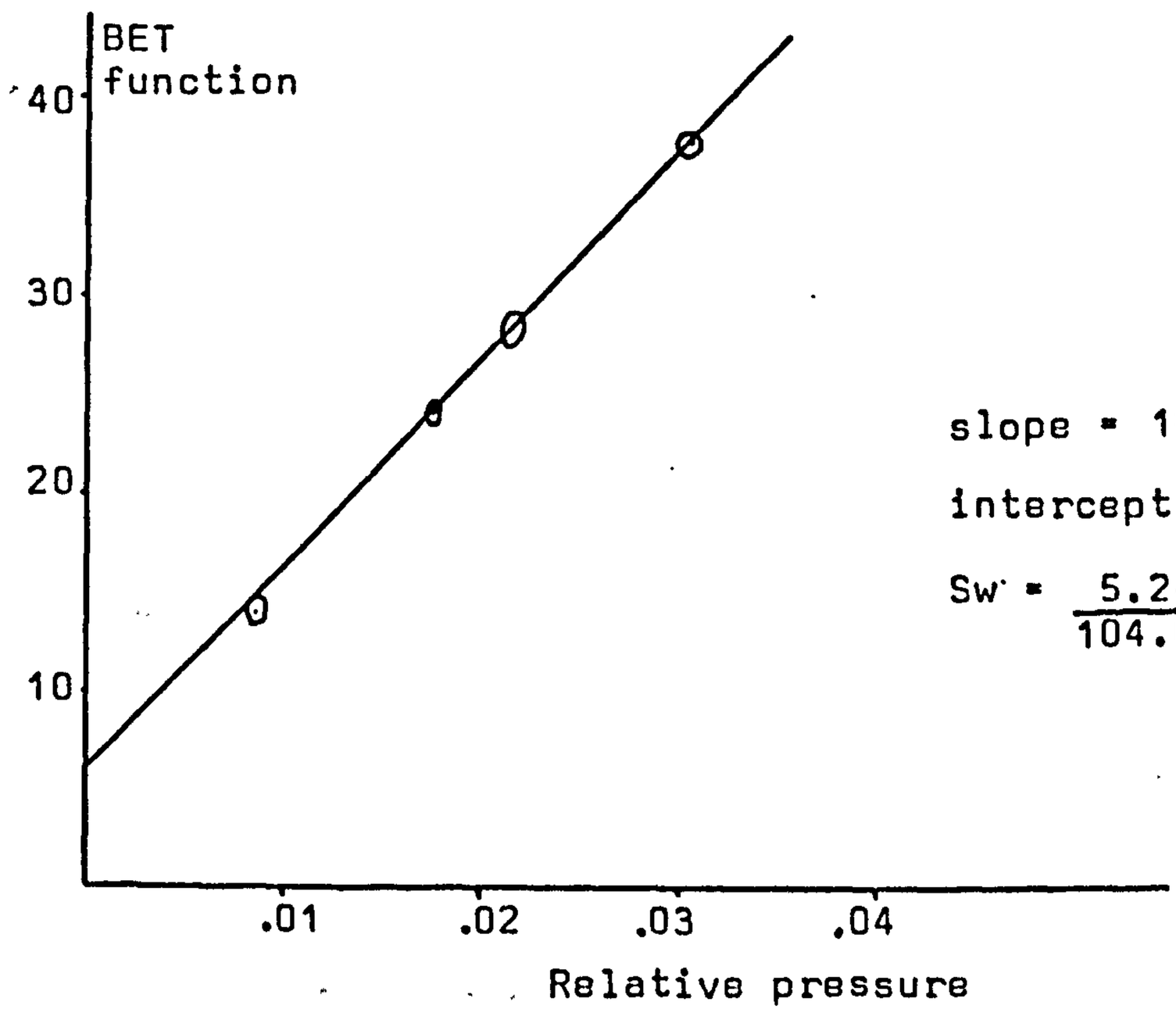

(B)

slope = 104.098

intercept = 5.75

$Sw = \frac{5.24}{104.098+5.75} = 0.0477$

Figure A 15 BET plot for D-sodium chloride compacted at 77 MPa

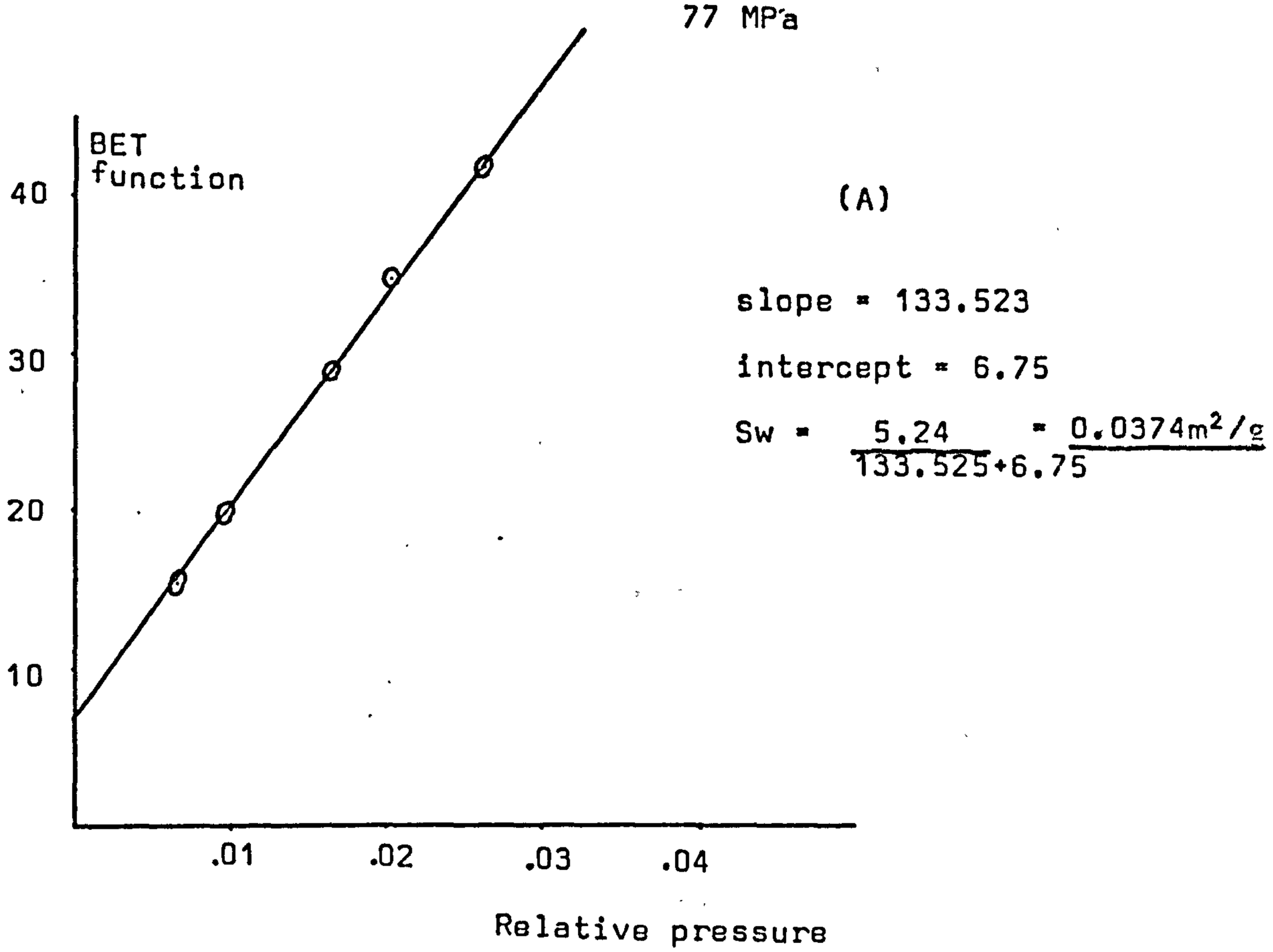

Figure A16 BET plots for D-Sodium chloride compacted at 155 MPa

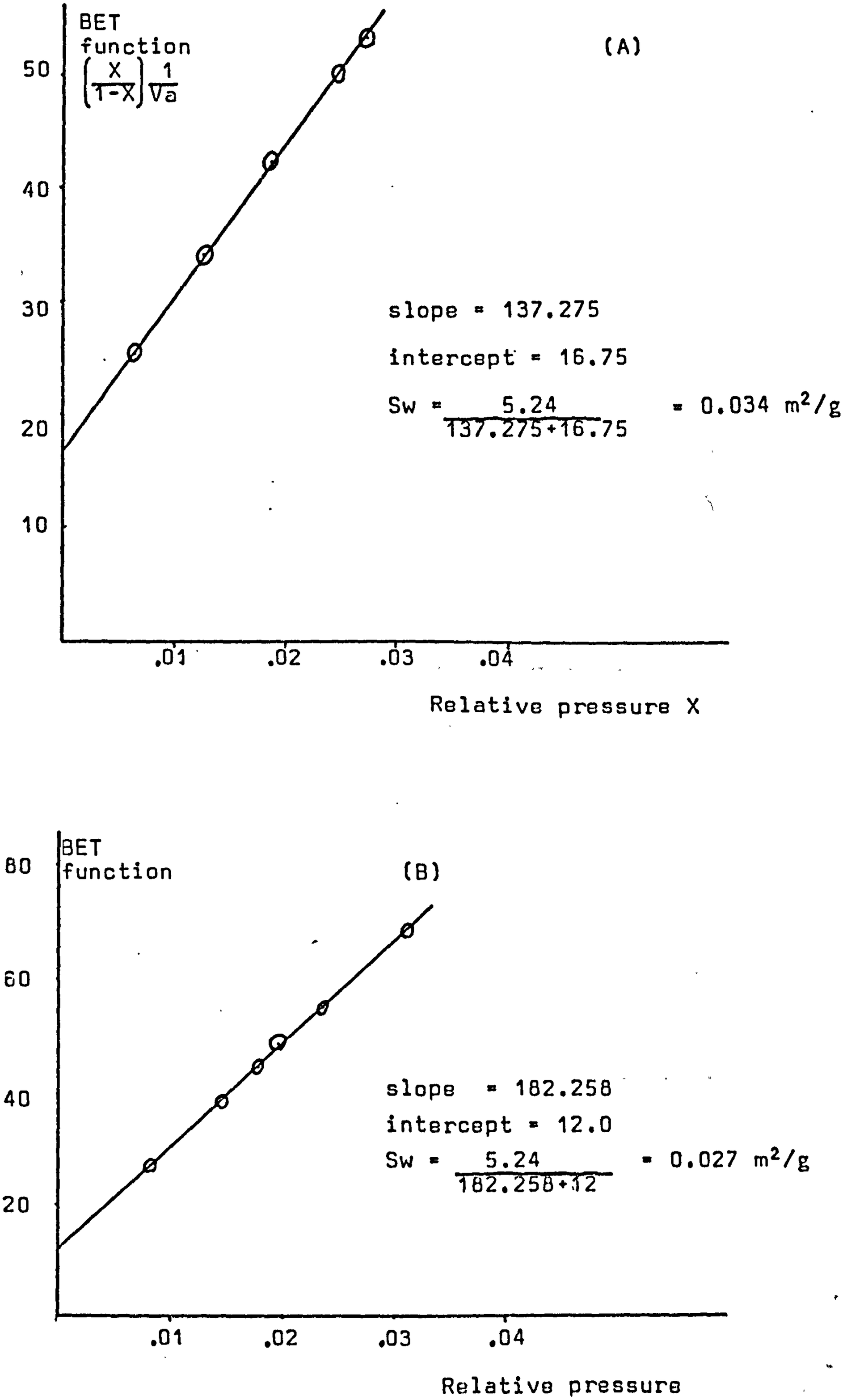

Figure A17 BET plots for D- sodium chloride compacted at 246 MPa

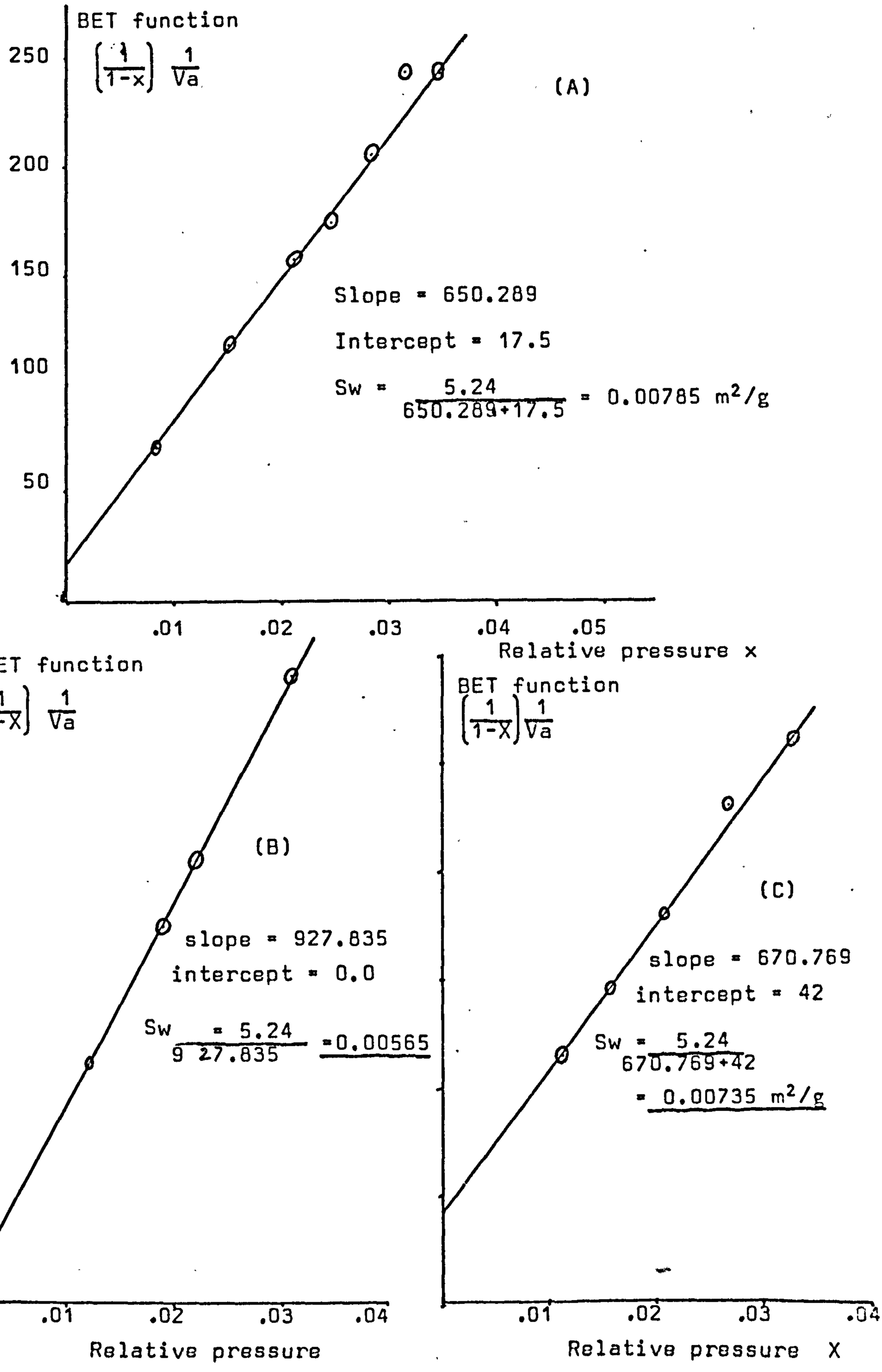

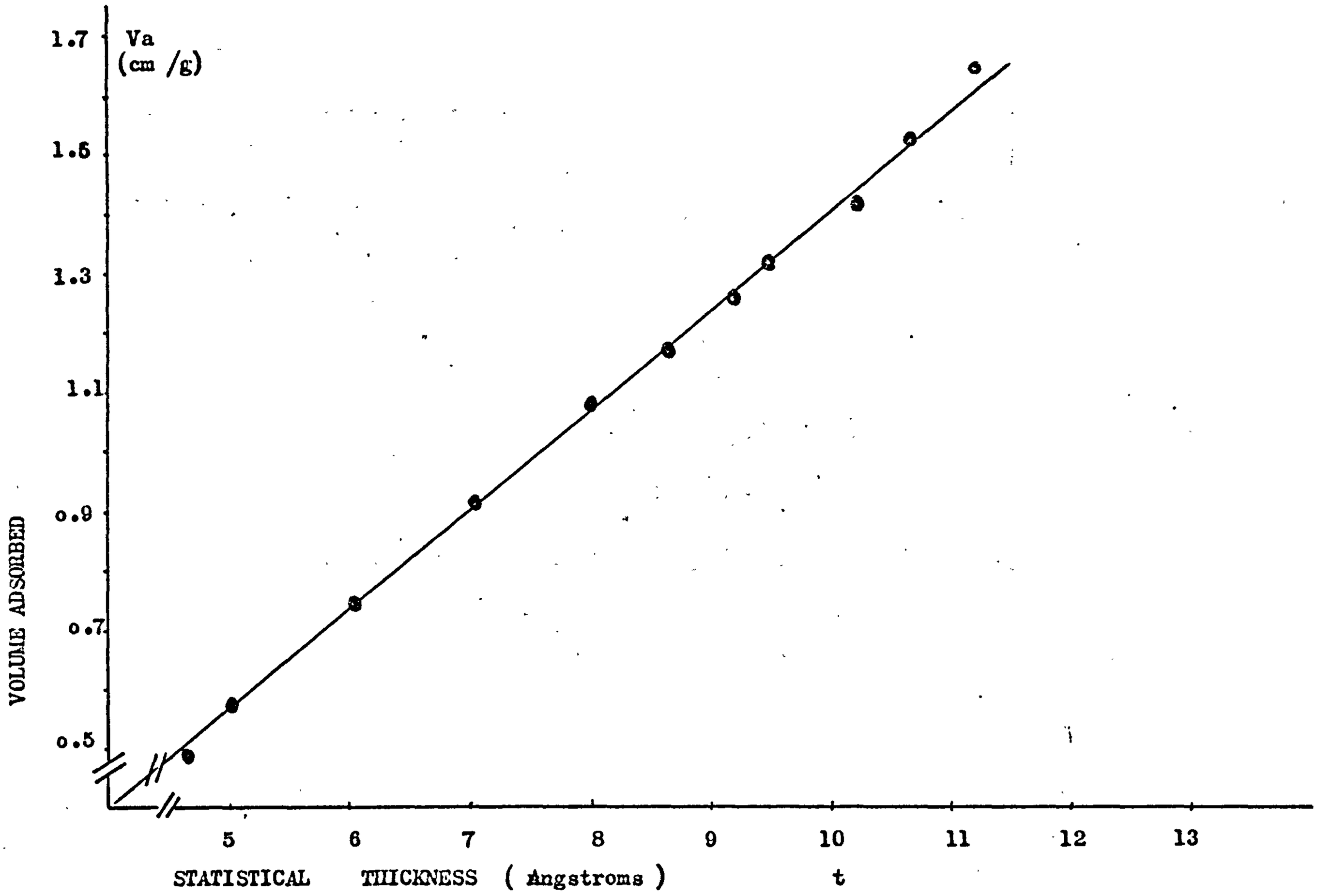

Figure A18 Va - t curve of dicalcium phosphate powder

Table A21 : PORE MODEL OF BARRETT, JOYNER AND HALENDA
DICALCIUM PHOSPHATE POWDER

RELATIVE PRESSURE	VOLUME ADSORBED	CYLINDRICAL PORES KELVIN STAT. RADIUS	LAYER	PORE RADIUS	VOL. PORE GROUP	AREA PORE GROUP	CUM. AREA	PORE VOL. PER GROUP OF PORES
	3 CMS/GM	A	A	A	3 CMS/GM	2 M/GM	2 M/GM	3 CMS/GM/A
.8600	1.649	61.84	11.23	73.1				
.8400	1.528	53.50	10.70	64.2	.0003	.1	.08	.000
.8200	1.415	47.00	10.25	57.2	.0003	.1	.16	.000
.8000	1.364	41.80	9.86	51.7	.0001	.0	.20	.000
.7800	1.362	37.54	9.51	47.1	.0001	.1	.26	.000
.7600	1.262	33.99	9.20	43.2	.0001	.0	.30	.000
.7400	1.209	30.98	8.92	39.9	.0001	.1	.36	.000
.7200	1.172	28.39	8.67	37.1	.0001	.0	.40	.000
.7000	1.132	26.15	8.43	34.6	.0001	.1	.45	.000
.6800	1.098	24.16	8.22	32.4	.0001	.0	.50	.000
.6600	1.083	22.45	8.01	30.5	.0000	.0	.52	.000
.6400	1.043	20.90	7.83	28.7	.0001	.1	.59	.000
.6200	1.017	19.51	7.65	27.2	.0001	.0	.63	.000
.6000	.989	18.26	7.48	25.7	.0001	.1	.69	.000
.5800	.964	17.12	7.32	24.4	.0001	.1	.74	.000
.5600	.936	16.09	7.17	23.3	.0001	.1	.80	.000
.5400	.913	15.14	7.03	22.2	.0001	.1	.85	.000
.5200	.879	14.26	6.89	21.2	.0001	.1	.94	.000
.5000	.868	13.46	6.76	20.2	.0000	.0	.95	.000
.4800	.849	12.71	6.63	19.3	.0000	.0	1.00	.000
.4600	.823	12.01	6.51	18.5	.0001	.1	1.08	.000
.4400	.806	11.36	6.39	17.7	.0000	.0	1.12	.000
.4200	.785	10.75	6.27	17.0	.0001	.1	1.19	.000
.4000	.766	10.18	6.16	16.3	.0001	.1	1.25	.000
.3800	.745	9.64	6.05	15.7	.0001	.1	1.33	.000
.3600	.728	9.13	5.94	15.1	.0000	.1	1.38	.000
.3400	.706	8.65	5.83	14.5	.0001	.1	1.47	.000
.3200	.694	8.19	5.73	13.9	.0000	.0	1.51	.000
.3000	.679	7.75	5.62	13.4	.0000	.1	1.56	.000
.2800	.643	7.33	5.52	12.8	.0001	.2	1.77	.000
.2600	.634	6.92	5.42	12.3	.0000	.0	1.77	.000
.2400	.617	6.54	5.31	11.8	.0000	.1	1.85	.000
.2200	.602	6.16	5.21	11.4	.0000	.1	1.91	.000
.2000	.592	5.80	5.11	10.9	.0000	.0	1.93	.000
.1800	.575	5.44	5.00	10.4	.0000	.1	2.01	.000
.1600	.553	5.09	4.89	10.0	.0001	.1	2.15	.000
.1400	.538	4.74	4.78	9.5	.0000	.1	2.21	.000
.1200	.520	4.40	4.66	9.1	.0000	.0	2.24	.000
.1000	.506	4.05	4.53	8.6	.0000	.1	2.35	.000
.0800	.489	3.69	4.39	8.1	.0000	.1	2.42	.000

					.0028			

TABLE A22 :POROSIMETRY CALCULATIONS PORE AREA DISTRIBUTION/
DICALCIUM PHOSPHATE COMPACTS PREPARED AT 32 MPA

P PSIA	SDV CC	D MICRONS	SDV CC/G	SA M2/G	R BAR MICRONS	DV/DR
.50	0.0000	360.0000	0.0000	0.00000	115.0000	0.00000
.70	.0224	257.1429	.0152	.00021	154.2857	.00045
.90	.0332	200.0000	.0220	.00133	114.2857	.00036
1.15	.0419	156.5217	.0278	.00046	89.1304	.00040
1.35	.0474	133.3333	.0315	.00056	72.4638	.00048
1.50	.0514	120.0000	.0341	.00065	63.3333	.00059
1.75	.0545	102.8571	.0362	.00072	55.7143	.00037
2.20	.0577	81.8182	.0383	.00082	46.1688	.00030
2.65	.0640	67.9245	.0425	.00105	37.4357	.00091
3.40	.0656	52.9412	.0435	.00112	30.2164	.00021
4.50	.0672	40.0000	.0446	.00121	23.2353	.00024
7.80	.0695	23.0769	.0461	.00143	15.7692	.00028
14.30	.0719	12.5874	.0477	.00182	8.9161	.00045
50.00	.0758	3.6000	.0503	.00372	4.0469	.00088
110.00	.0774	1.6364	.0514	.00560	1.3091	.00161
200.00	.2323	.9000	.1541	.36396	.6341	.42055
220.00	.2599	.8182	.1725	.45066	.4295	.67589
265.00	.3010	.6792	.1997	.59440	.3744	.59135
280.00	.3105	.6429	.2060	.63797	.3305	.52105
300.00	.3207	.6000	.2128	.68244	.3107	.47927
340.00	.3429	.5294	.2275	.78613	.2824	.62673
360.00	.3492	.5000	.2317	.82116	.2574	.42976
415.00	.3689	.4337	.2448	.93543	.2334	.59609
445.00	.3737	.4045	.2480	.96587	.2096	.32421
460.00	.3768	.3913	.2501	.98722	.1989	.47915
485.00	.3800	.3711	.2522	1.00951	.1906	.31333
525.00	.3895	.3429	.2585	1.08099	.1785	.67051
555.00	.3926	.3243	.2606	1.10647	.1668	.34102
605.00	.3997	.2975	.2653	1.16604	.1555	.53052
690.00	.4084	.2609	.2710	1.25206	.1396	.47420
750.00	.4124	.2400	.2737	1.29452	.1252	.37854
810.00	.4171	.2222	.2766	1.34973	.1156	.53325
890.00	.4203	.2022	.2789	1.38983	.1061	.31639
1000.00	.4298	.1800	.2852	1.52360	.0956	.85224
1200.00	.4361	.1500	.2894	1.62740	.0829	.42133
1500.00	.4432	.1200	.2941	1.77072	.0675	.47400
2000.00	.4503	.0900	.2986	1.95650	.0525	.47400
2400.00	.4535	.0750	.3009	2.06030	.0413	.42133
3000.00	.4582	.0600	.3041	2.25139	.0336	.63200
4000.00	.4637	.0450	.3077	2.54039	.0263	.73733
5000.00	.4681	.0300	.3093	2.69963	.0203	.52667
6000.00	.4677	.0300	.3104	2.82939	.0165	.52667
7000.00	.4685	.0257	.3109	2.90606	.0139	.36667
8400.00	.4693	.0214	.3114	2.99689	.0118	.36667
10300.00	.4693	.0175	.3114	2.99828	.0097	.00500
13400.00	.4716	.0134	.3130	3.41585	.0077	1.10748
14000.00	.4724	.0129	.3135	3.57745	.0066	2.74452
25400.00	.4724	.0071	.3135	3.57745	.0050	0.00000
37000.00	.4724	.0049	.3135	3.57745	.0030	0.00000
45000.00	.4724	.0040	.3135	3.57745	.0022	0.00000
50000.00	.4724	.0036	.3135	3.57745	.0019	0.00000

TABLE A23 : POROSIMETRY CALCULATIONS PORE AREA DISTRIBUTION/
DICALCIUM PHOSPHATE COMPACTS PREPARED AT 47 MPA

P PSIA	SDV CC	D MICRONS	SDV CC/G	SA M2/G	R BAR MICRONS	DV/DR
.50	0.0000	360.0000	0.0000	0.00000	115.0000	0.00000
2.30	.0040	78.2609	.0038	.00012	109.5652	.00003
55.00	.0063	3.2727	.0060	.00158	20.3834	.00006
160.00	.0079	1.1250	.0075	.00522	1.0994	.00147
190.00	.0095	.9474	.0090	.01116	.5181	.01779
220.00	.0284	.8182	.0271	.04461	.4414	.29353
230.00	.0593	.7826	.0565	.24344	.4002	1.73221
240.00	.0751	.7500	.0716	.32315	.3832	.96907
250.00	.0821	.7200	.0783	.36024	.3675	.47000
260.00	.0924	.6923	.0882	.41879	.3531	.74606
275.00	.0988	.6545	.0942	.45309	.3367	.33473
300.00	.1146	.6000	.1093	.55061	.3130	.57933
325.00	.1240	.5538	.1183	.61422	.2885	.41080
350.00	.1335	.5143	.1274	.68291	.2670	.47927
365.00	.1390	.4932	.1327	.72535	.2519	.52330
375.00	.1430	.4800	.1364	.75673	.2433	.60073
410.00	.1517	.4390	.1447	.82996	.2298	.42415
435.00	.1572	.4138	.1500	.88012	.2132	.43834
470.00	.1620	.3830	.1545	.92617	.1992	.30765
485.00	.1643	.3711	.1568	.95047	.1885	.40018
510.00	.1683	.3529	.1606	.99266	.1810	.43424
525.00	.1699	.3429	.1621	1.01021	.1739	.21337
545.00	.1730	.3303	.1651	1.04651	.1683	.50231
565.00	.1754	.3186	.1673	1.07475	.1622	.40543
585.00	.1770	.3077	.1689	1.09425	.1566	.29013
605.00	.1785	.2975	.1704	1.11443	.1513	.31067
630.00	.1825	.2857	.1741	1.16660	.1458	.66913
670.00	.1841	.2687	.1756	1.18685	.1386	.18526
720.00	.1888	.2500	.1802	1.25958	.1297	.50813
780.00	.1928	.2308	.1839	1.32318	.1202	.41050
2000.00	.2188	.0900	.2088	2.10118	.0802	.37039
2200.00	.2236	.0818	.2133	2.31488	.0730	1.15867
2800.00	.2267	.0643	.2163	2.48449	.0585	.36047
3400.00	.2291	.0529	.2186	2.64223	.0293	.41782
4000.00	.2315	.0450	.2209	2.83049	.0245	.59689
5000.00	.2331	.0360	.2224	2.98314	.0203	.35111
6200.00	.2338	.0290	.2231	3.07079	.0163	.20925
7300.00	.2372	.0247	.2263	3.56047	.0134	1.54478
8300.00	.2340	.0217	.2280	3.86475	.0110	1.22324
19700.00	.2390	.0091	.2280	3.86475	.0077	0.00000
32600.00	.2390	.0055	.2280	3.86475	.0047	0.00000
50000.00	.2390	.0036	.2280	3.86475	.0023	0.00000

TABLE A24 :POROSIMETRY CALCULATIONS PORE AREA DISTRIBUTION/
DICALCIUM PHOSPHATE COMPACTS PREPARED AT 77 MPA

P PSIA	SDV CC	D MICRONS	SDV CC/G	SA M2/G	R BAR MICRONS	DV/DR
.50	0.0000	360.0000	0.0000	0.00000	115.0000	0.00000
1.05	.0047	171.4286	.0026	.00005	132.3571	.00005
7.00	.0087	25.7143	.0048	.00024	49.2857	.00005
14.35	.0119	12.5436	.0066	.00067	9.5645	.00048
50.00	.0120	3.6000	.0066	.00071	4.0359	.00002
240.00	.0158	.7500	.0088	.00769	1.0875	.00270
255.00	.0371	.7059	.0206	.07369	.3640	.96696
270.00	.0758	.6667	.0421	.20072	.3431	1.97421
285.00	.1074	.6316	.0597	.31036	.3246	1.60120
300.00	.1288	.6000	.0716	.38836	.3079	1.35090
340.00	.1612	.5294	.0895	.51794	.2824	.91772
350.00	.1659	.5143	.0922	.53836	.2509	.62673
375.00	.1738	.4800	.0966	.57419	.2486	.46083
405.00	.1999	.4444	.1111	.70130	.2311	1.46644
425.00	.2086	.4138	.1159	.74693	.2146	.56702
450.00	.2141	.4000	.1190	.77752	.2034	.60165
470.00	.2204	.3830	.1225	.81387	.1957	.74260
485.00	.2236	.3711	.1242	.83273	.1865	.53357
500.00	.2291	.3600	.1273	.86078	.1828	.99335
525.00	.2354	.3429	.1308	.90728	.1757	.73733
550.00	.2402	.3273	.1334	.93913	.1675	.60830
565.00	.2433	.3186	.1352	.96115	.1615	.72736
600.00	.2465	.3000	.1370	.98417	.1546	.34006
800.00	.2765	.2250	.1536	1.24668	.1313	.80053
1200.00	.2970	.1500	.1650	1.50368	.0938	.54773
1300.00	.3042	.1385	.1690	1.61479	.0721	1.23240
1600.00	.3144	.1125	.1747	1.80090	.0627	.79117
1800.00	.3192	.1000	.1773	1.90171	.0531	.75840
2000.00	.3239	.0900	.1800	2.01430	.0475	.94800
2300.00	.3286	.0783	.1826	2.14171	.0421	.80750
2700.00	.3326	.0667	.1848	2.26517	.0362	.68130
3000.00	.3365	.0600	.1870	2.40591	.0317	1.18500
3500.00	.3397	.0514	.1888	2.53430	.0279	.73735
4000.00	.3413	.0450	.1896	2.60838	.0241	.49150
4600.00	.3444	.0391	.1914	2.77826	.0210	1.07670
5200.00	.3460	.0346	.1923	2.87505	.0184	.69980
5800.00	.3476	.0310	.1931	2.96369	.0164	.86240
6500.00	.3492	.0277	.1940	3.10518	.0147	.94540
7000.00	.3508	.0257	.1949	3.23851	.0134	1.59750
7600.00	.3516	.0237	.1953	3.31061	.0123	.77630
9800.00	.3539	.0164	.1967	3.56239	.0105	.89150
14400.00	.3547	.0125	.1971	3.68790	.0077	.26920
29600.00	.3547	.0061	.1971	3.68790	.0046	0.00000
40800.00	.3547	.0044	.1971	3.68790	.0026	0.00000
50000.00	.3547	.0036	.1971	3.68790	.0020	0.00000

TABLE A25 : POROSIMETRY CALCULATIONS PORE AREA DISTRIBUTION/
DICALCIUM PHOSPHATE COMPACTS PREPARED AT 155 MPA

P PSIA	SDV CC	D MICRONS	SDV CC/G	SA M2/G	R BAR MICRONS	DV/DR
.50	0.0000	360.0000	0.0000	0.00000	115.0000	0.00000
1.00	.0245	180.0000	.0141	.00024	135.0000	.00027
1.30	.0284	138.4615	.0164	.00030	79.6154	.00019
1.50	.0316	120.0000	.0182	.00035	64.0154	.00034
2.00	.0332	90.0000	.0191	.00039	52.5000	.00011
3.00	.0363	60.0000	.0209	.00049	37.5000	.00021
4.85	.0395	37.1134	.0228	.00065	24.2784	.00028
7.15	.0395	25.1748	.0228	.00065	15.5721	0.00000
11.00	.0395	16.3636	.0228	.00065	10.3846	0.00000
14.30	.0427	12.5874	.0246	.00117	7.2378	.00167
20.00	.0435	9.0000	.0250	.00135	5.3969	.00044
60.50	.0435	2.9752	.0250	.00135	2.9938	0.00000
130.00	.0435	1.3846	.0250	.00135	1.0900	0.00000
155.00	.0450	1.1613	.0259	.00427	.0365	.01415
275.00	.0450	.6545	.0259	.00427	.4540	0.00000
365.00	.0474	.4932	.0273	.01409	.2869	.02937
410.00	.0498	.4390	.0287	.02600	.2330	.06757
450.00	.0608	.4000	.0350	.06764	.2098	.56682
475.00	.0901	.3789	.0519	.26265	.1947	2.77665
515.00	.1232	.3495	.0710	.47572	.1821	2.25463
570.00	.1406	.3158	.0810	.59793	.1663	1.03069
595.00	.1469	.3025	.0846	.64564	.1546	.95263
620.00	.1548	.2903	.0892	.70784	.1482	1.29525
635.00	.1580	.2835	.0910	.73354	.1434	.92155
660.00	.1651	.2727	.0951	.79321	.1390	1.32436
700.00	.1722	.2571	.0992	.85587	.1325	.91245
725.00	.1770	.2483	.1019	.89964	.1264	1.06913
775.00	.1849	.2323	.1065	.97644	.1201	.98640
835.00	.1928	.2156	.1110	1.05886	.1120	.94672
880.00	.1991	.2045	.1147	1.12910	.1050	1.14665
1000.00	.2244	.1800	.1292	1.43709	.0961	2.05965
1200.00	.2354	.1500	.1356	1.59477	.0825	.73733
1800.00	.2552	.1000	.1470	1.97874	.0625	.79000
2050.00	.2599	.0878	.1497	2.09700	.0470	.77736
2300.00	.2631	.0783	.1515	2.18608	.0415	.66220
2800.00	.2710	.0643	.1561	2.44718	.0356	1.13036
3600.00	.2773	.0500	.1597	2.70930	.0286	.68460
4400.00	.2797	.0409	.1611	2.83216	.0227	.52140
5500.00	.2836	.0327	.1634	3.06558	.0184	.96556
6400.00	.2860	.0281	.1647	3.20835	.0152	1.02993
7600.00	.2868	.0237	.1652	3.34002	.0130	.35579
8000.00	.2876	.0225	.1657	3.42090	.0115	1.35111
9300.00	.2891	.0194	.1666	3.54691	.0105	.99836
11400.00	.2899	.0158	.1670	3.70289	.0088	.44315
14000.00	.2899	.0129	.1670	3.70289	.0072	0.00000
24600.00	.2899	.0073	.1670	3.70289	.0050	0.00000
34000.00	.2899	.0053	.1670	3.70289	.0032	0.00000
50000.00	.2899	.0036	.1670	3.70289	.0022	0.00000

1

TABLE A26 :POROSIMETRY CALCULATIONS PORE AREA DISTRIBUTION/
DICALCIUM PHOSPHATE COMPACTS PREPARED AT 248 MPA

P PSIA	SDV CC	D MICRONS	SDV CC/G	SA M2/G	R BAR MICRONS	DV/DR
.50	0.0000	360.0000	0.0000	0.00000	115.0000	0.00000
1.00	.0032	171.4286	.0018	.00003	132.8571	.00003
3.00	.0071	60.0000	.0040	.00013	57.8571	.00007
5.00	.0071	36.0000	.0040	.00013	24.0000	0.00000
7.00	.0071	25.7143	.0040	.00013	15.4286	0.00000
14.20	.0095	12.5874	.0053	.00045	9.5754	.00036
20.00	.0095	9.0000	.0053	.00045	5.3969	0.00000
50.00	.0095	3.6000	.0053	.00045	3.1500	0.00000
75.00	.0095	2.4000	.0053	.00045	1.5000	0.00000
120.00	.0095	1.5000	.0053	.00045	.9750	0.00000
215.00	.0095	.8372	.0053	.00045	.5843	0.00000
400.00	.0198	.4500	.0110	.03998	.3218	.05305
600.00	.0419	.3000	.0233	.17844	.1875	.29493
700.00	.0608	.2571	.0338	.33272	.1393	.86480
730.00	.0711	.2466	.0396	.42465	.1259	1.94369
775.00	.0837	.2323	.0466	.54372	.1197	1.70570
800.00	.0893	.2250	.0497	.59824	.1143	1.52362
850.00	.0940	.2118	.0523	.64719	.1092	.71627
875.00	.0995	.2057	.0554	.70690	.1044	1.82797
900.00	.1035	.2000	.0576	.75079	.1014	1.38250
925.00	.1067	.1946	.0593	.78689	.0986	1.16920
1025.00	.1367	.1756	.0760	1.15330	.0926	3.16252
1200.00	.1469	.1500	.0818	1.29634	.0814	.80204
1600.00	.1541	.1125	.0857	1.42095	.0656	.37920
1800.00	.1572	.1000	.0875	1.48820	.0531	.50560
2000.00	.1659	.0900	.0923	1.69490	.0475	1.73800
2200.00	.1699	.0818	.0945	1.79874	.0430	.96556
2600.00	.1778	.0692	.0989	2.03610	.0376	1.25522
3000.00	.1825	.0600	.1015	2.20225	.0323	1.02700
3900.00	.1912	.0462	.1064	2.57756	.0265	1.25522
4800.00	.1959	.0375	.1090	2.83569	.0209	1.09547
5800.00	.1991	.0310	.1108	3.04535	.0171	.97749
7000.00	.2007	.0257	.1116	3.17194	.0142	.59396
8000.00	.2022	.0225	.1125	3.32029	.0121	.96311
9600.00	.2030	.0188	.1130	3.40732	.0103	.42133
10700.00	.2050	.0166	.1141	3.65826	.0089	2.04921
12300.00	.2054	.0146	.1143	3.71514	.0079	.36101
14000.00	.2054	.0129	.1143	3.71514	.0069	0.00000
16050.00	.2054	.0112	.1143	3.71514	.0060	0.00000
18300.00	.2054	.0098	.1143	3.71514	.0053	0.00000
26300.00	.2054	.0064	.1143	3.71514	.0040	0.00000
35200.00	.2054	.0051	.1143	3.71514	.0029	0.00000
41800.00	.2054	.0043	.1143	3.71514	.0024	0.00000
49300.00	.2054	.0037	.1143	3.71514	.0020	0.00000
50000.00	.2054	.0036	.1143	3.71514	.0018	0.00000

TABLE 427 : POROSIMETRY CALCULATIONS PORE AREA DISTRIBUTION/ DENTRITIC SODIUM CHLORIDE COMPACTED AT 32 MPA

P PSIA	SDV CC	D MICRONS	SDV CC/G	SA M2/G	R BAR MICRONS	DV/DR
.50	0.0000	360.0000	0.0000	0.00000	115.0000	0.00000
1.00	.1841	180.0000	.2457	.00415	135.0000	.00205
1.45	.2078	124.1379	.2773	.00502	76.0345	.00085
1.65	.2125	109.0909	.2836	.00524	58.3072	.00063
2.15	.2220	83.7209	.2963	.00578	48.2030	.00075
2.70	.2283	66.6667	.3047	.00624	37.5969	.00074
4.20	.2338	42.8571	.3121	.00681	27.3810	.00064
5.60	.2354	32.1429	.3142	.00705	18.7500	.00029
6.10	.2394	29.5082	.3195	.00774	15.4128	.00300
6.65	.2441	27.0677	.3258	.00865	14.1440	.00386
7.05	.2504	25.5319	.3343	.00995	13.1499	.00823
7.85	.2820	22.9299	.3764	.01702	12.1155	.02429
8.25	.2978	21.8182	.3975	.02084	11.1870	.02642
8.75	.3097	20.5714	.4133	.02386	10.5974	.01901
9.10	.3168	19.7802	.4228	.02577	10.0879	.01797
10.35	.3302	17.3913	.4408	.02969	9.2929	.01124
11.00	.3342	16.3636	.4460	.03096	8.4367	.00769
11.65	.3405	15.4506	.4545	.03311	7.9536	.01354
12.25	.3437	14.6939	.4587	.03424	7.5361	.00835
12.75	.3476	14.1176	.4640	.03572	7.2029	.01371
13.60	.3516	13.2353	.4692	.03729	6.8382	.00895
14.30	.3547	12.5874	.4735	.03861	6.4557	.00975
20.00	.3768	9.0000	.5030	.05000	5.3969	.01233
32.00	.3855	5.6250	.5146	.05679	3.6563	.00515
45.00	.3871	4.0000	.5167	.05861	2.4063	.00194
105.00	.3903	1.7143	.5209	.06573	1.4286	.00276
315.00	.3918	.5714	.5230	.07570	.5714	.00277
700.00	.3934	.2571	.5251	.09976	.2071	.01005
1000.00	.3942	.1800	.5262	.11994	.1093	.02048
1300.00	.3958	.1385	.5283	.17451	.0796	.07607
3400.00	.3990	.0529	.5325	.39753	.0479	.07390
6000.00	.4013	.0300	.5357	.73206	.0207	.20662
50000.00	.4021	.0036	.5367	1.39637	.0064	.05965

TABLE A28 : POROSIMETRY CALCULATIONS PORE AREA DISTRIBUTION/ DENTRITIC SODIUM CHLORIDE COMPACTS PRODUCED AT 62 MPA

P PSIA	SDV CC	D MICRONS	SDV CC/G	SA M2/G	R BAR MICRONS	DV/DR
.50	0.0000	360.0000	0.0000	0.00000	115.0000	0.00000
1.00	.0169	160.0000	.0216	.00037	135.0000	.00021
3.00	.0226	60.0000	.0260	.00056	60.0000	.00064
8.60	.0264	20.9302	.0303	.00112	20.2326	.00019
11.65	.0294	15.4506	.0337	.00191	9.0952	.00110
12.45	.0332	14.4578	.0381	.00309	7.4771	.00755
13.35	.0377	13.4631	.0433	.00459	6.9852	.00928
14.25	.0550	12.6316	.0632	.01077	6.5287	.04073
20.00	.1123	9.0000	.1289	.03611	5.4079	.03156
29.00	.1199	6.2069	.1376	.04089	3.8017	.00540
55.00	.1252	3.2727	.1437	.04661	2.3699	.00360
80.00	.1282	2.2500	.1471	.05187	1.3807	.00590
175.00	.1304	1.0286	.1497	.05931	.8196	.00370
1000.00	.1335	.1800	.1532	.10507	.3021	.00711
2800.00	.1350	.0643	.1549	.17906	.0611	.02606
3600.00	.1360	.0500	.1564	.42629	.0286	.42224
4600.00	.1395	.0391	.1601	.58795	.0223	.27747
5600.00	.1410	.0321	.1618	.78655	.0178	.43162
7300.00	.1427	.0247	.1637	1.06284	.0142	.44321
8700.00	.1433	.0207	.1644	1.18746	.0113	.30404
50000.00	.1444	.0036	.1657	2.04467	.0061	.13236

TABLE A29 : POROSIMETRY CALCULATIONS PORE AREA DISTRIBUTION/ DENTRITIC SODIUM CHLORIDE COMPACTS PRODUCED AT 124 MPA

P PSIA	SDV CC	D MICRONS	SDV CC/G	SA M2/G	R BAR MICRONS	DV/DR
.50	0.0000	360.0000	0.0000	0.00000	115.0000	0.00000
25.00	.0030	7.2000	.0041	.00119	91.8000	.00002
35.00	.0106	5.1429	.0145	.00619	3.0857	.00733
50.00	.0126	3.6000	.0176	.01117	2.1857	.00293
60.00	.0234	3.0000	.0322	.02914	1.0500	.03519
67.00	.0287	2.6866	.0394	.03952	1.4216	.03366
85.00	.0302	2.1176	.0415	.04307	1.2011	.00530
112.00	.0324	1.6071	.0446	.04996	.9312	.00666
150.00	.0339	1.2000	.0467	.05606	.7016	.00741
225.00	.0362	.8000	.0498	.06921	.5000	.01131
520.00	.0389	.3462	.0536	.07786	.2865	.00331
1400.00	.0392	.1286	.0539	.14520	.1187	.02083
1800.00	.0415	.1000	.0571	.25724	.0971	.15834
3000.00	.0424	.0600	.0581	.31320	.0400	.03770
3400.00	.0437	.0529	.0602	.46265	.0282	.42727
3700.00	.0445	.0486	.0612	.54552	.0254	.32131
4200.00	.0452	.0429	.0622	.63772	.0229	.20038
5400.00	.0463	.0333	.0664	1.06559	.0190	.03294
6400.00	.0505	.0281	.0695	1.49911	.0154	.00936
8000.00	.0513	.0225	.0705	1.06717	.0127	.26609
50000.00	.0520	.0036	.0710	2.34409	.0065	.07979

TABLE A30 :POROSIMETRY CALCULATIONS PORE AREA DISTRIBUTION/ DENTRITIC SODIUM CHLORIDE COMPACTS PRODUCED AT 155 MPA

P PSIA	SDV CC	D MICRONS	SDV CC/G	SA M2/G	R BAR MICRONS	DV/DR
.50	0.0000	360.0000	0.0000	0.00000	115.0000	0.00000
1.15	.0032	156.5217	.0019	.00003	129.1304	.00003
2.60	.0055	69.2308	.0033	.00009	56.4381	.00005
14.15	.0067	12.7208	.0052	.00045	20.4879	.00011
105.00	.0126	1.7143	.0075	.00359	3.6088	.00072
140.00	.0158	1.2857	.0094	.00676	.7500	.01475
160.00	.0213	1.1250	.0127	.01964	.6027	.00682
175.00	.0284	1.0286	.0169	.03574	.5364	.14747
215.00	.0363	.8372	.0216	.05632	.4664	.08257
250.00	.0371	.7200	.0220	.05677	.3893	.01346
320.00	.0403	.5625	.0239	.07080	.3206	.04013
2800.00	.0456	.0643	.0272	.18601	.1567	.02220
7200.00	.0462	.0250	.0274	.21239	.0223	.02011
8600.00	.0478	.0209	.0284	.37409	.0115	.77646
11000.00	.0482	.0164	.0286	.43079	.0093	.17300
17800.00	.0529	.0101	.0314	1.34239	.0066	1.51649
30800.00	.0529	.0058	.0314	1.34239	.0040	0.00000

TABLE A31 :POROSIMETRY CALCULATIONS PORE AREA DISTRIBUTION/ DENTRITIC SODIUM CHLORIDE COMPACTS PRODUCED AT 248 MPA

P PSIA	SDV CC	D MICRONS	SDV CC/G	SA M2/G	R BAR MICRONS	DV/DR
.50	0.0000	360.0000	0.0000	0.00000	115.0000	0.00000
1.50	.0032	120.0000	.0014	.00003	120.0000	.00003
5.00	.0035	36.0000	.0024	.00011	39.0000	.00006
50.00	.0035	3.6000	.0024	.00011	5.9000	0.00000
80.00	.0071	2.2500	.0031	.00110	1.4625	.00234
400.00	.0071	.4500	.0031	.00110	.6750	0.00000
850.00	.0095	.2118	.0041	.01545	.1654	.01990
1000.00	.0111	.1800	.0048	.02961	.0979	.09948
1600.00	.0119	.1125	.0051	.03956	.0731	.02341
2200.00	.0142	.0818	.0061	.08319	.0486	.15449
3000.00	.0166	.0600	.0071	.14290	.0355	.21725
4400.00	.0190	.0409	.0082	.22766	.0252	.24829
6800.00	.0213	.0265	.0092	.35645	.0166	.32829
7800.00	.0219	.0231	.0094	.39925	.0124	.35655
9850.00	.0221	.0183	.0095	.41507	.0103	.07764
11200.00	.0237	.0161	.0102	.57619	.0086	1.43461
25600.00	.0237	.0070	.0102	.57619	.0056	0.00000
32000.00	.0249	.0056	.0107	.90201	.0032	1.75329
46000.00	.0253	.0039	.0109	1.05727	.0024	.46141
48500.00	.0308	.0037	.0133	3.58695	.0019	54.63302

APPENDIX 4

Shear-Normal Stress Relationship for the Compaction of Particulate Solids.

A. Mohr-Coulomb equation

$$\tau = \sigma_n \tan \emptyset + C$$

B. Su .h

$$\left[(\bar{\sigma}_h + K)^2 + {}^2/3\ \tau_{max}\right]^{\frac{1}{2}} - q\left[\cos \frac{\pi}{2} \cdot \frac{\theta}{\emptyset}\right]^n = 0$$

where $\bar{\sigma}_h$ = mean hydrostatic stress

τ_{max} = maximum shear stress

$\tan \theta = {}^2/3\ \tau_{max}\ (\bar{\sigma}_h + K)$

$\emptyset$ = angle of internal friction

K, q, n = positive constants related to material properties

C. Abdelkarim

1. Dentritic sodium chloride

$\tau = 0.6208\sigma - 0.0010501\sigma^2 + 0.3393$ (Fig. A19)

2. Cubic sodium chloride

$\tau = 0.6877\sigma - 0.0017038\sigma^2 + 0.2917$ (Fig. A20)

3. Dicalcium phosphate

$\tau = 0.814\sigma + 0.4738$ (Fig. A21)

4. Sugar

$\tau = 0.7287\sigma - 0.00069591\sigma^2 - 0.9564$ (Fig. A23)

5. Styrocell

$\tau = 0.52\sigma - 0.00010397\sigma^2 + 0.6235$ (Fig. A24)

6. Homopolymer

$$\tau = 0.306\sigma - 0.0004013\sigma^2 + 0.6394 \quad \text{(Fig. A25)}$$

7. Copolymer

$$\tau = 0.1938\sigma - 0.00012165\sigma^2 + 0.8033 \quad \text{(Fig. A26)}$$

In figures A19 -A26

X axis = mean compaction stress (σ) MPa

Yaxis = mean deviatoric stress (τ) MPa

Figure A19

CURFIT GRAPH OF USER FUNCTION

$$Y = C + AX - BX^2$$

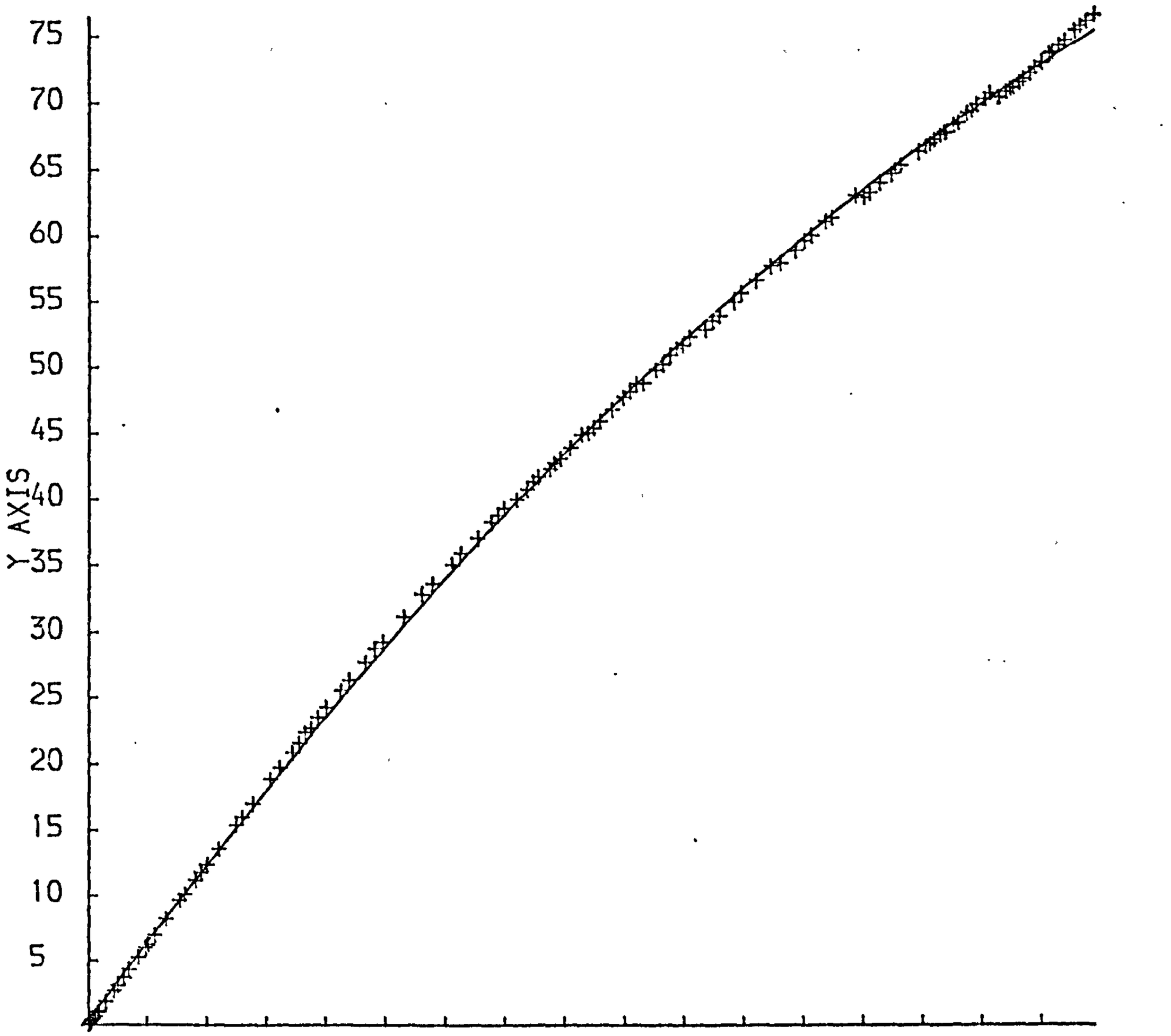

B - sodium chloride

USER FUNCTION MINIMISED ON ABSOLUTE SUM OF SQUARES
PARAMETER VALUES
AFTER FIT C=.3393 A=.6208 B=1.0501E-03

Figure A20

CURFIT GRAPH OF USER FUNCTION

$$Y = C + AX - BX^2$$

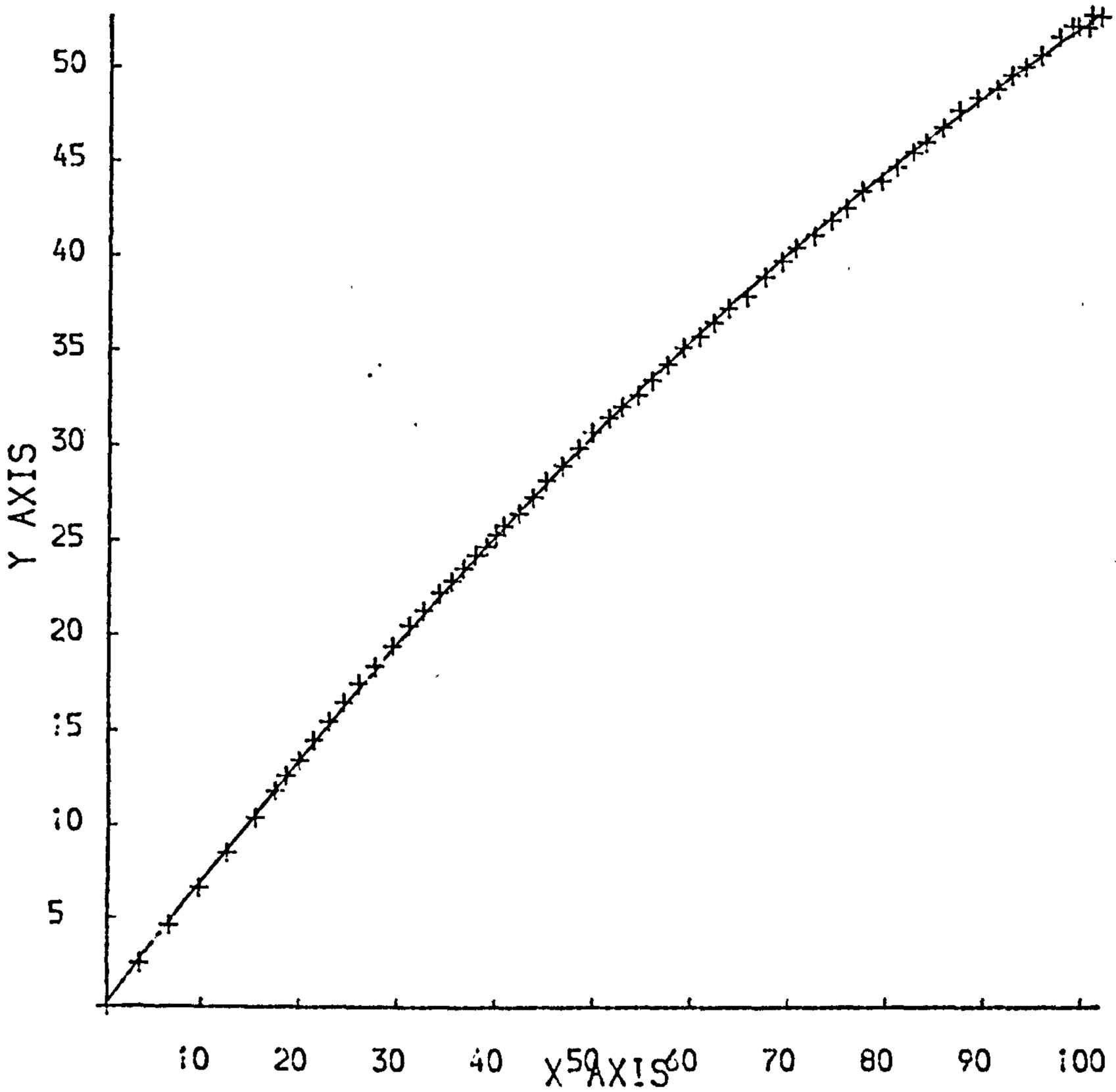

RELATIONSHIP BETWEEN SHEAR & COMPACTION STRESSES C - sodium chloride

USER FUNCTION MINIMISED ON ABSOLUTE SUM OF SQUARES
PARAMETER VALUES
AFTER FIT C=.2917 A=.6877 B=1.7038E-03

Figure A21

CURFIT GRAPH OF USER FUNCTION

$$Y = C + AX$$

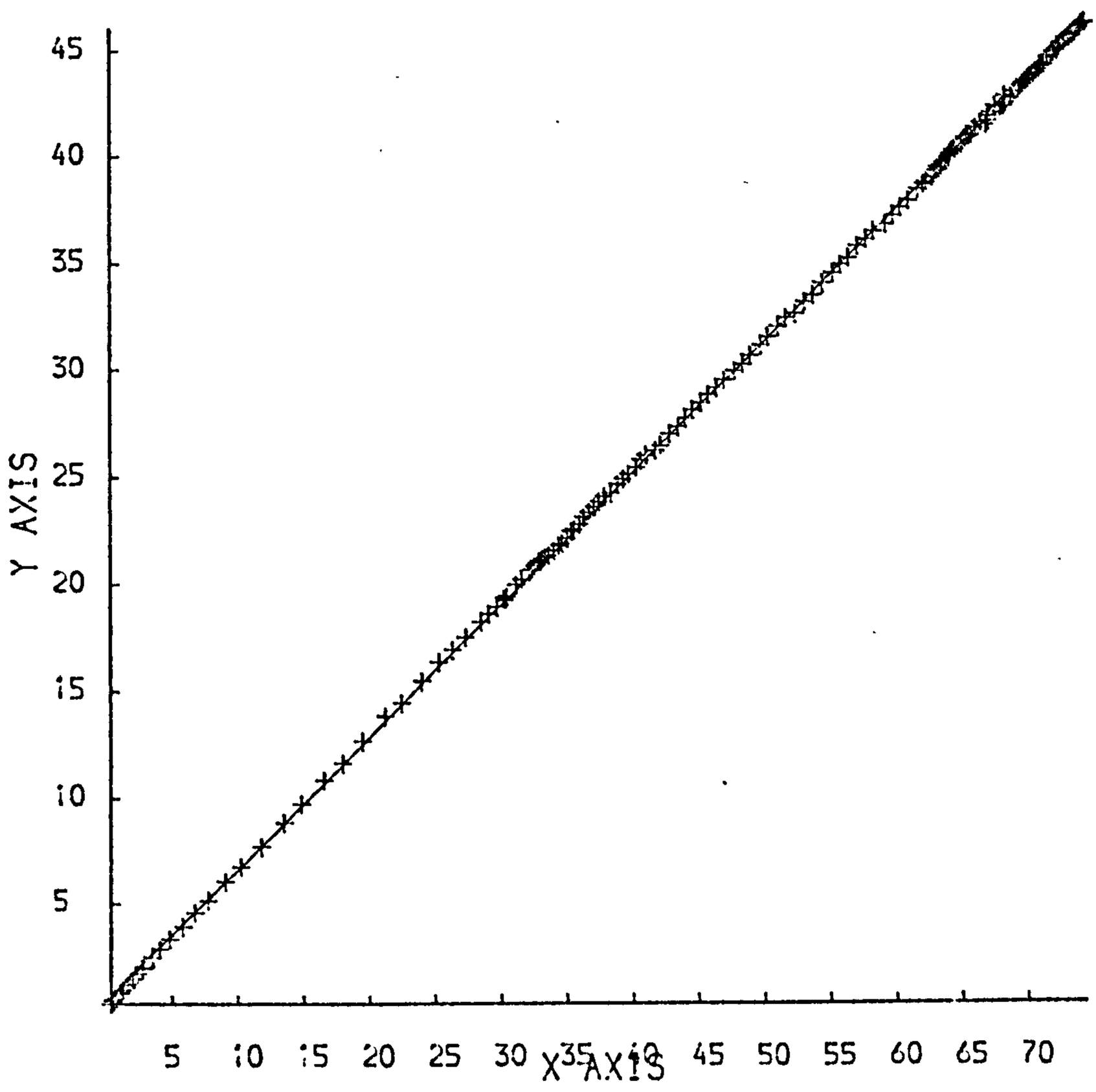

RELATIONSHIP BETWEEN SHEAR & COMPACTION STRESS OF (DCP)

USER FUNCTION MINIMISED ON ABSOLUTE SUM OF SQUARES
PARAMETER VALUES
AFTER FIT C=.4738 A=.6140

Figure A22

CURFIT GRAPH OF USER FUNCTION

$$Y = C + AX$$

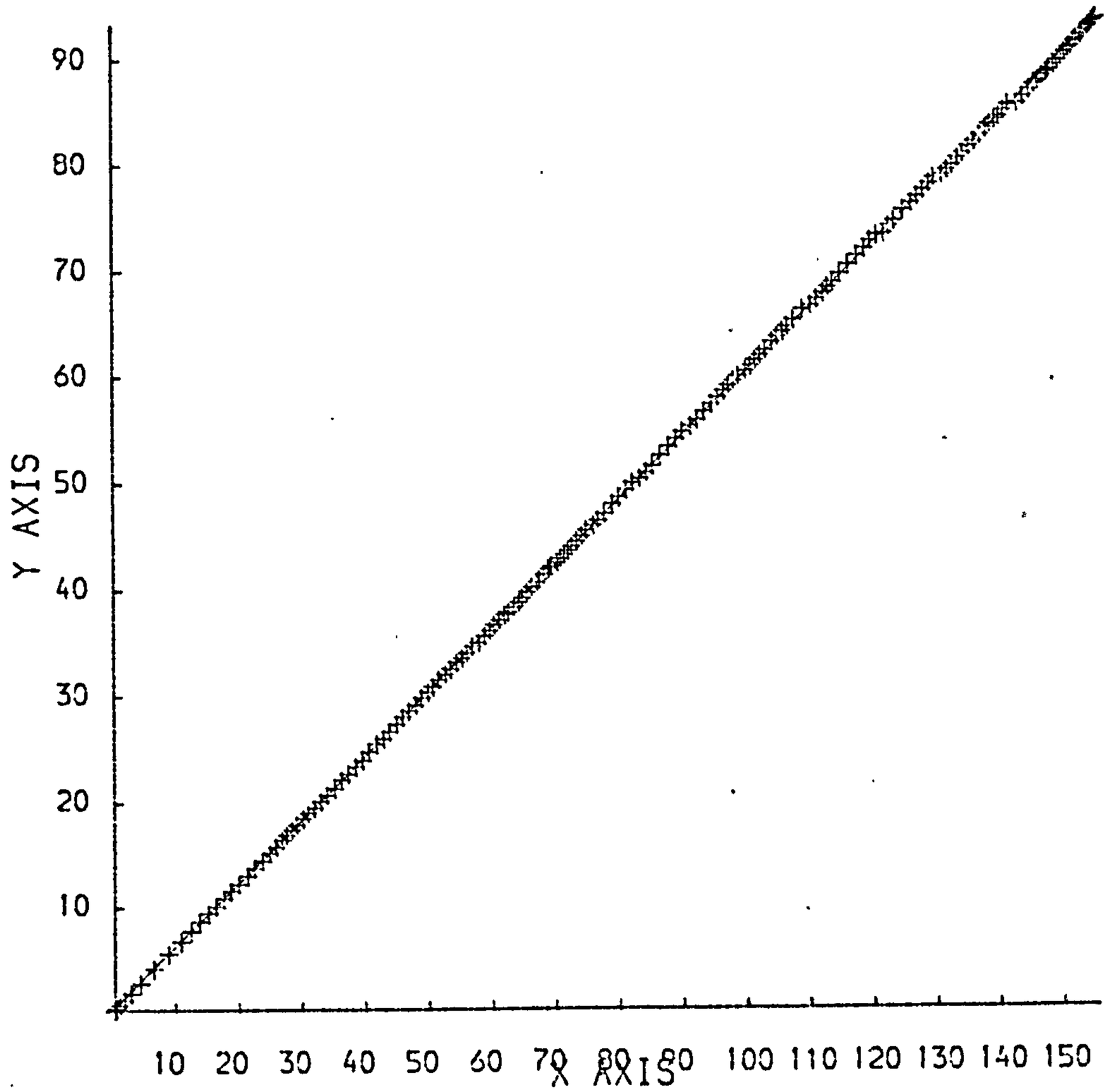

SHEAR-COMPACTION STRESS RELATIONSHIP (DCP248)

USER FUNCTION MINIMISED ON ABSOLUTE SUM OF SQUARES
PARAMETER VALUES
AFTER FIT C=.5720 A=.5982

Figure A23

CURFIT GRAPH OF USER FUNCTION

$$Y = C + AX - BX^2$$

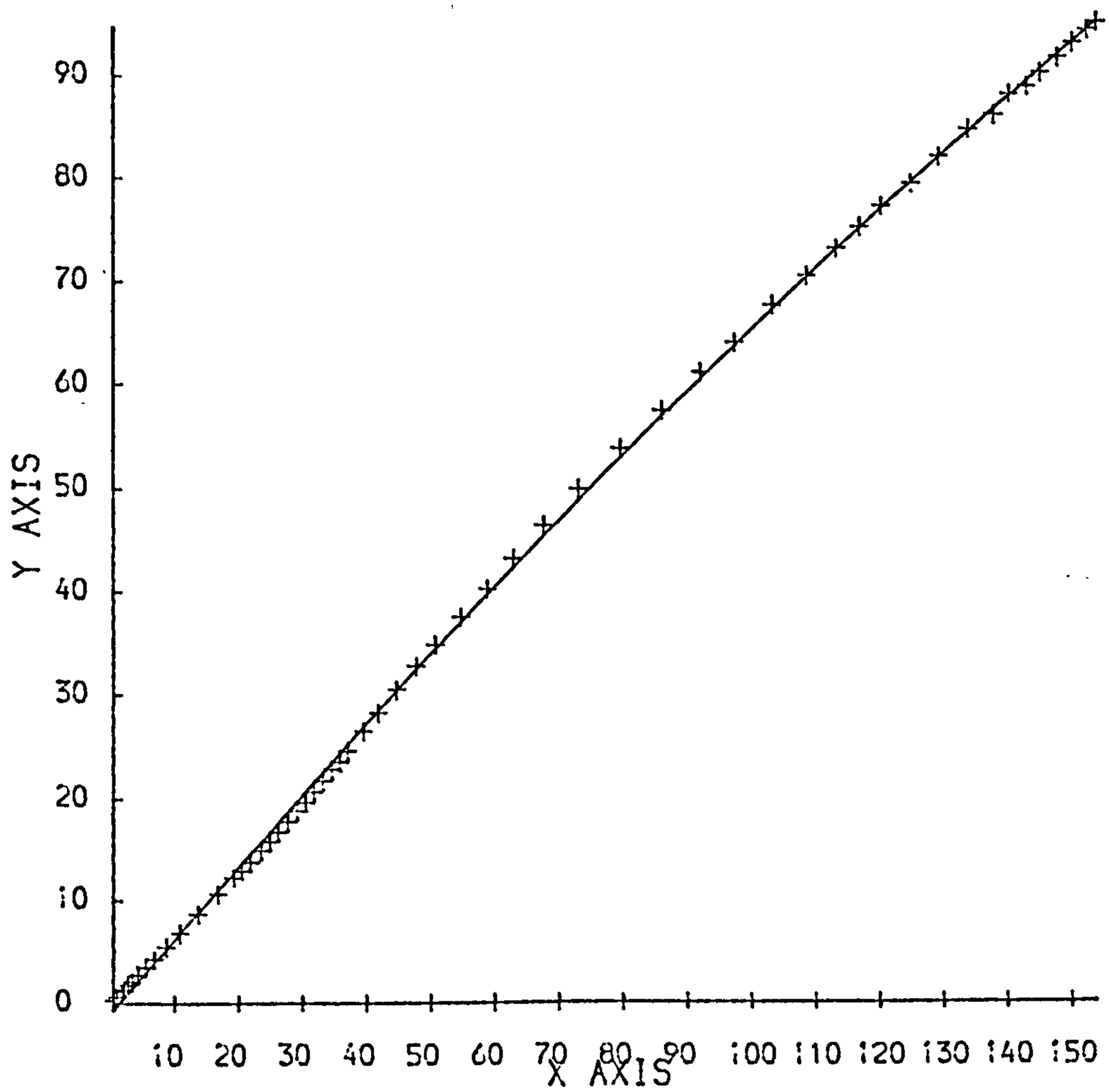

RELATIONSHIP BETWEEN SHEAR & COMPACTION STRESSES (SUGAR)

USER FUNCTION MINIMISED ON ABSOLUTE SUM OF SQUARES
PARAMETER VALUES
AFTER FIT C= -.9564 A = .7287 B= 6.9591E-04

Figure A24

CURFIT GRAPH OF USER FUNCTION

$$Y = C + AX - BX^2$$

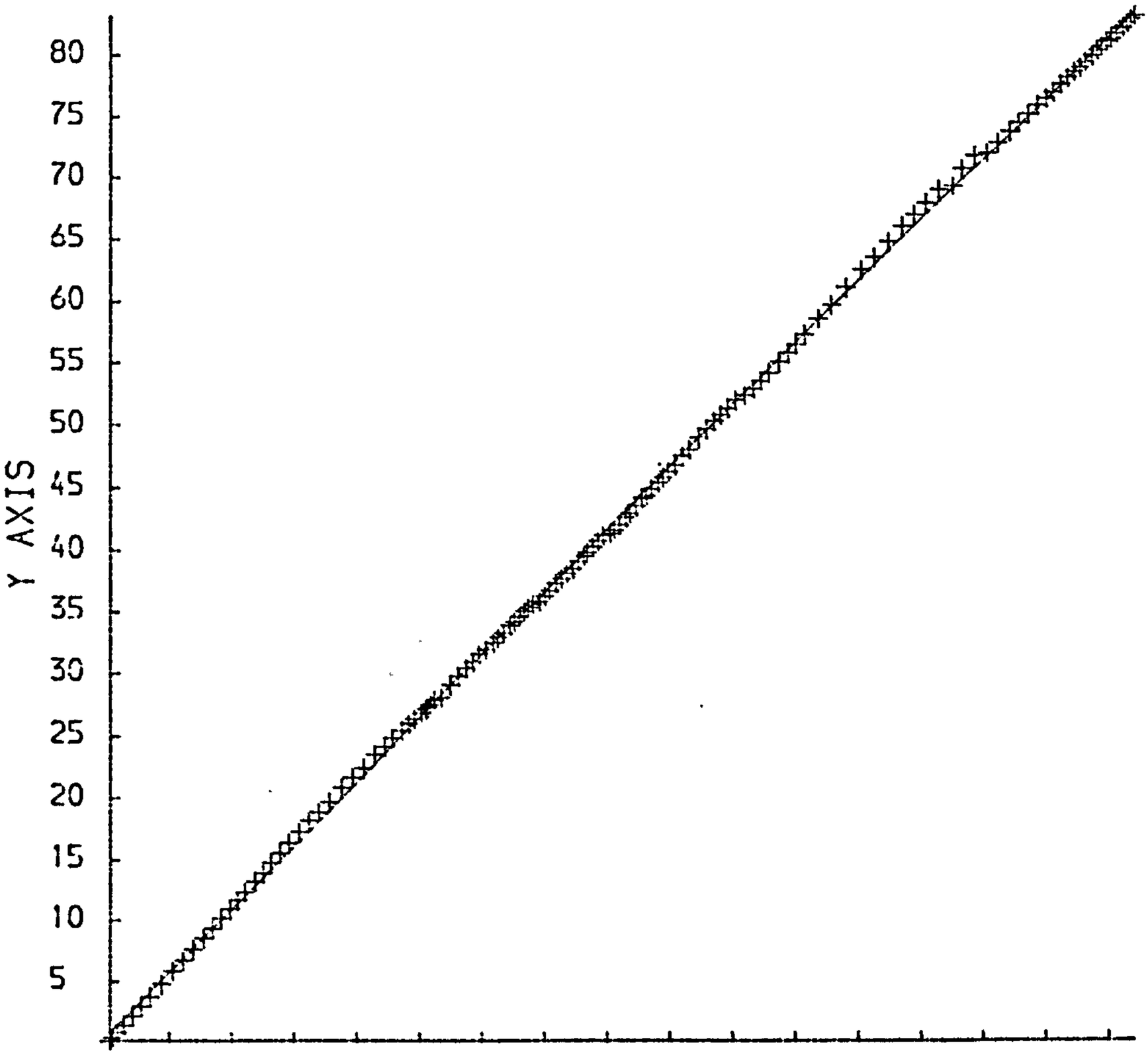

RELATIONSHIP BETWEEN SHEAR & COMPACTION STRESSES (ST.)

USER FUNCTION MINIMISED ON ABSOLUTE SUM OF SQUARES
PARAMETER VALUES
AFTER FIT C = .6235 A = .5200 B = 1.0397E-04

Figure A25

CURFIT GRAPH OF USER FUNCTION

$$Y = C + AX - BX^2$$

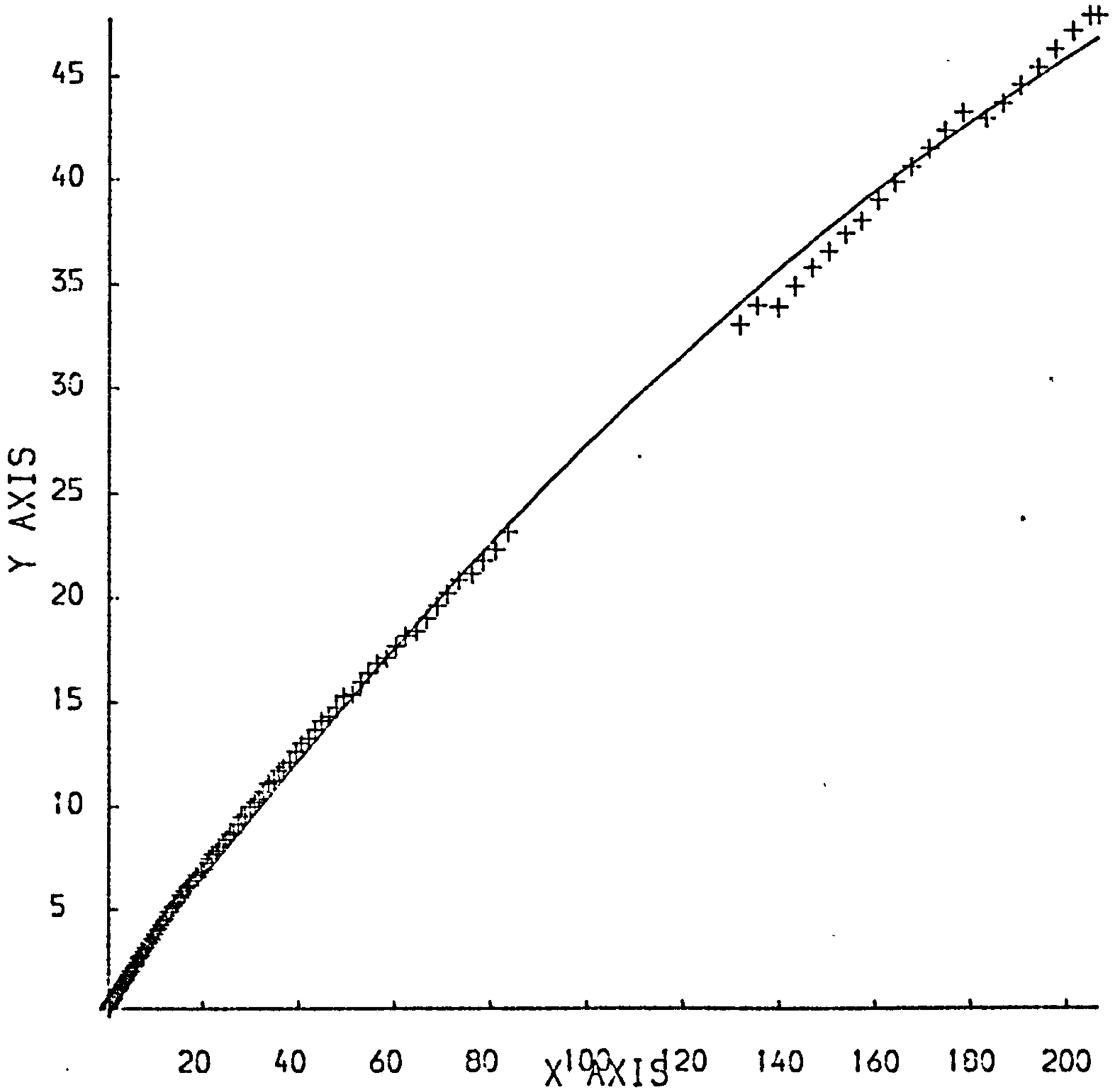

RELATIONSHIP BETWEEN SHEAR & COMPACTION STRESS (HOMOP.)

USER FUNCTION MINIMISED ON ABSOLUTE SUM OF SQUARES
PARAMETER VALUES
AFTER FIT C=.6394 A=.3060 B=4.0130E-04

Figure A26

CURFIT GRAPH OF USER FUNCTION

$$Y = C + AX - BX^2$$

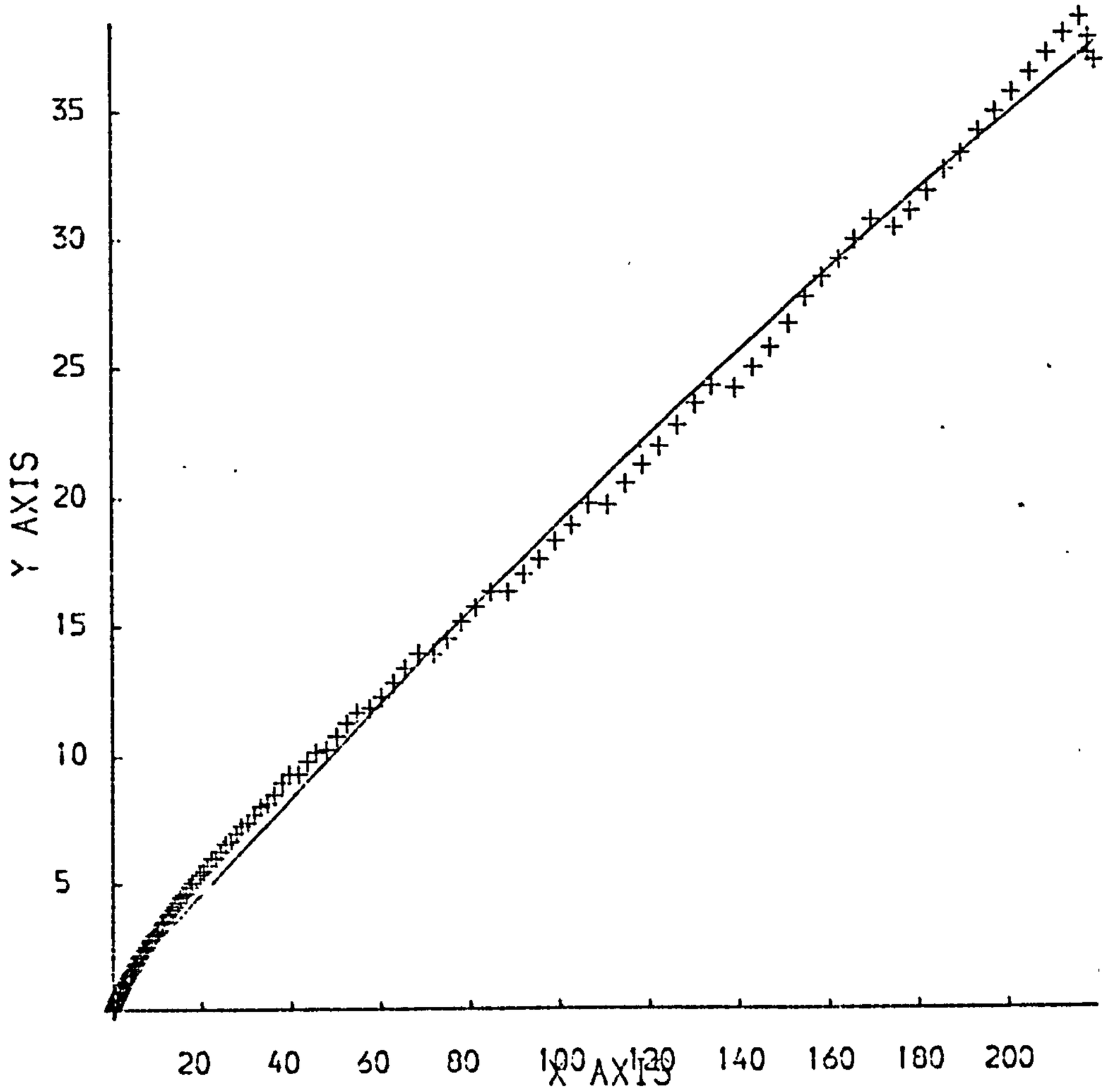

RELATIONSHIP BETWEEN SHEAR & COMPACTION STRESSES (COPOL.)

USER FUNCTION MINIMISED ON ABSOLUTE SUM OF SQUARES
PARAMETER VALUES
AFTER FIT C = .8033 A=.1938 B=1.2165E-04

APPENDIX 5

Computer Programs

TABLE A32 : (PROG 02)

```
      PROGRAM FRED
      EXTERNAL F
C PROGRAM WITH FULL SET OF DATA CHANNELS
C SMALL GRAPHS
      DIMENSION XAFA(2),XFADR(2),XHU(2)
      DIMENSION XFA(2),XFR(2),XDU(2),XLRHOR(2)
      DIMENSION VAR(3),FA(2000),FR(2000),HU(2000)
      DIMENSION ICND(2000),VA(2000),VR(2000),VU(2000)
      INTEGER VA,VL,VR,VD,VU
      COMMON RINTE,GRAD
      DATA XFA/0.0,60.0/
      DATA YFR/0.0,70.0/
      DATA XAFA/-3.0,4.5/
      DATA XDU/0.0,0.015/
      DATA XFADR/0.0,2.5/
      DATA XHU/0.006,0.020/
      DATA XLRHOR/0.0,10.0/

       IS=0
99    READ(1,FMT=*) CA,C2A,CL,C2L,CR,C2R,CD,C2D,CU,
     1C2U,W,A,RHOI
999   K=1
      IFMAX=1
      J=0
      IM=0
C  LOOP TO READ DATA AND CALCULATE OTHER VARIABLES
      DO 8899 I=1,2000
7654  READ(1,FMT=111,END=7777)ICND(I),VA(I),VL,VR(I),VD,VU(I)
  111 FORMAT(1X,I3,5I5)
      IF(ICND(I))7778,2000,2000
 2000 IF(VA(I).LT.2)GOTO 7654
      IF(VU(I).EQ.0)GOTO 7654
8899  J=J+1
7778  IM=ICND(I)
7777  CONTINUE
      IF(J.LT.10)GOTO 767
      JJ=0
      DO 1 I=1,J
      FA(I)=(VA(I)-C2A)/CA
      FL=(VL+C2L)/CL
      FD=(VD+C2L)/CD
      FR(I)=(VR(I)-C2R)/CR
      IF(I.EQ.J-1)GOTO 667
      IF(I.EQ.J.OR.I.EQ.1)GOTO 669
```

Table A32 : Continued

```
      VUR=(VU(I)+VU(I+1)+VU(I+2))/3.0
      GOTO 668
667   VUR=(VU(I)+VU(I+1))/2.0
      GOTO 668
669   VUR=VU(I)
668   HU(I)=CU*VUR+C2U
      DU=HU(1)-HU(I)
      RHOR=K/(HU(I)*A)/RHOI
      FACR=0.0
      IF(FR(I).EQ.0.0)GOTO 9992
      FACR=FA(I)/FR(I)
9992  AFA=ALOG(FA(I))
      JJ=JJ+1
      IF(RHOR.GT.1.0)GOTO 89
      IF(JJ.NE.K+1)GOTO 888
      K=K+1
888   LRHOR=ALOG(1.0/(1.0-RHOR))
89    IF(FA(I).GT.FA(IFMAX))IFMAX=I
      WRITE(2,101)FA(I),FR(I),HU(I)
1      CONTINUE
101   FORMAT(3(2X,F9.4))
777   IF(IM.EQ.0)STOP
      IF(IM.EQ.-1)GOTO99
      GOTO 999
767   IS=IS-1
      GOTO 777
      END
```

TABLE A33 : (GRAPH4)

GRAPH4 WAS USED TO PLOT THE STRESS PATHWAYS PRESENTED IN CHAPTER 6. THE INPUT DATA WAS THE EIGHT PARAMETERS CALCULATED FROM PROGRAM KARIM (CHAPTER 4)

```
      PROGRAM PLOT
      REAL DATA1,COL1,COL2,COL3,COL4,COL5,COL6,XLEN,YLEN
      INTEGER NPOINTS,IXCAPL,IYCAPL
      CHARACTER*70 T1,T2,T3,T4,T5,T6,T7,T8,T9,T10,XCAP,YCAP
      DIMENSION DATA1(500,8),AY1(2)
      DIMENSION COL1(500),COL2(500),COL3(500),COL4(500),
     1          COL5(500),COL6(500),COL7(500),COL8(500)
      EQUIVALENCE  (COL1,DATA1(1,1)),
     1             (COL2,DATA1(1,2)),
     2             (COL3,DATA1(1,3)),
     3             (COL4,DATA1(1,4)),
     4             (COL5,DATA1(1,5)),
     5             (COL6,DATA1(1,6)),
     6               (COL7,DATA1(1,7)),
     7              (COL8,DATA1(1,8))
      DATA (AY1(I),I=1,2) /2.0,5.5/
C
C OPEN FILES
C              CHANNEL 1 :- PARAMETERS
C              CHANNEL 2 :- INPUT DATA
      OPEN(1,FILE='INPUT')
      OPEN(2,FILE='PLOTDTA')
C
C READ IN NUMBER OF DATA SETS
C
      READ(1,FMT=*) NSETS
       READ(1,FMT=*) XPACK,YPACK
      DO 500,I=1,NSETS
C
C
C READ IN NUMBER OF POINTS IN THIS SET
C
      READ(1,FMT=*) NPOINTS
C IF NUMBER POINTS > 500 ONLY READ 500
C
      IF(NPOINTS.GT.500) NPOINTS=500
      DO 100,K=1,NPOINTS
      READ(2,FMT=*) (DATA1(K,J),J=1,8)
  100 CONTINUE
C
C NOW READ IN TITLES ETC FOR GRAPH 1
C
  READ(1,FMT='(A)') XCAP
```

Table A33 : Continued

```
      READ(1,FMT='(A)') T1
      READ(1,FMT='(A)') XCAP
      READ(1,FMT='(A)') YCAP
      READ(1,FMT=*) XLEN
      READ(1,FMT=*) YLEN
      READ(1,FMT=*) IXCAPL
      READ(1,FMT=*) IYCAPL
C
C NOW PLOT GRAPH 1
       CALL PAGE (21.0,29.7)
       CALL PACKIN (XPACK,YPACK)
C
       CALL JBAXES(COL1,NPOINTS,XLEN,XCAP,IXCAPL,
     1             COL2,NPOINTS,YLEN,YCAP,IYCAPL)
       CALL DRAWCV(COL1,COL2,NPOINTS)
       CALL TITLE('B','C',T1,50)
C
C NOW READ IN TITLES ETC FOR GRAPH 2
      READ(1,FMT='(A)') T2,T3,T4,T5
C
      READ(1,FMT='(A)') XCAP
      READ(1,FMT='(A)') YCAP
      READ(1,FMT=*) XLEN
      READ(1,FMT=*) YLEN
      READ(1,FMT=*) IXCAPL
      READ(1,FMT=*) IYCAPL
C
C NOW PLOT GRAPH 2
C
       CALL JBAXES(COL3,NPOINTS,XLEN,XCAP,IXCAPL,
     1             COL1,NPOINTS,YLEN,YCAP,IYCAPL)
       CALL DRAWCV(COL3,COL1,NPOINTS)
       CALL TITLE('R','C',T2,50)
       CALL TITLE('L','C',T3,70)
       CALL TITLE('L','C',T4,70)
       CALL TITLE('L','C',T5,70)
C
C NOW READ IN TITLES ETC FOR GRAPH 3
C
      READ(1,FMT='(A)') T6
      READ(1,FMT='(A)') XCAP
      READ(1,FMT='(A)') YCAP
      READ(1,FMT=*) XLEN
      READ(1,FMT=*) YLEN
      READ(1,FMT=*) IXCAPL
      READ(1,FMT=*) IYCAPL
C
C NOW PLOT GRAPH 3
       CALL PAGE (21.0,29.7)
       CALL PACKIN (XPACK,YPACK)
C
       CALL JBAXES(COL1,NPOINTS,XLEN,XCAP,IXCAPL,
     1             AY1,2,YLEN,YCAP,IYCAPL)
       CALL DRAWCV(COL1,COL4,NPOINTS)
       CALL TITLE('B','C',T6,50)
C
C NOW READ IN TITLES ETC FOR GRAPH 4
C
      READ(1,FMT='(A)') T7,T8,T9,T10
```

Table A33 : Continued

```
      READ(1,FMT='(A)') YCAP
      READ(1,FMT=*) XLEN
      READ(1,FMT=*) YLEN
      READ(1,FMT=*) IXCAPL
      READ(1,FMT=*) IYCAPL
C NOW PLOT GRAPH 4
C
      CALL JBAXES(COL5,NPOINTS,XLEN,XCAP,IXCAPL,
     1            AY1,2,YLEN,YCAP,IYCAPL)
      CALL DRAWCV(COL5,COL4,NPOINTS)
      CALL TITLE('B','C',T7,50)
      CALL TITLE('L','C',T8,70)
      CALL TITLE('L','C',T9,70)
      CALL TITLE('L','C',T10,70)
500 CONTINUE

      CALL END PLT
      STOP
      END
      SUBROUTINE TITLE(IV,IH,LCAP,NCAP)
      CHARACTER*(*)LCAP
      CHARACTER IV,IH
      COMMON/JBJUL/K,MISS,XL,A(3),YL,B(3),F,S,MS(2),GAP,IPOL,E(2)
      COMMON/JBPCH/IND,XM,YM,SS,XLO,YMNEXT,XY(2),FAC,XP,YP
      COMMON/JBRIM/H(2),G(4),V(4),IN,Y,YLIM,FP
      COMMON/JBSYS/KS,KR,CH,CM,PAG(2),INCP,PMAX,MPAG,PIC(2),MPIC,KPIC
      IF(MISS.EQ.C.AND.IND.LE.C)RETURN
      CALL JBVERT(IV,I,LOC)
      CS=SHS
      IF(LOC.GT.0)CS=SS+SS
      IF(CW.NE.0.0)CS=CW
      CC=CS*1.67
      IF(LOC)10,60,30
   10 IF(MISS.EQ.0) GOTO 80
      X=E(1)+0.1*CM
      CMAX=ABS(XL)-0.2*CM
      YLIM=0.0
      IF(I.EQ.2)GO TO 20
      Y=E(2)+ABS(YL)+0.25*CM-CC
      GO TO 60
   20 Y=-0.15*ABS(YL)
      IF(Y.LT.-1.65*CM)Y=-1.65*CM
      Y=Y+E(2)
      GO TO 60
   30 IF(H(1).EQ.0.0) GOTO 80
      X=G(1)-0.7*CM
      CMAX=XP+0.7*CM
      IF(I.EQ.4)GO TO 40
      IF(YLIM.GT.0.0)GO TO 99
      Y=H(2)-G(4)*0.4-SS
      YLIM=YP+0.25*CM+SS
      GO TO 99
   40 IF(YLIM.LT.0.0) GOTO 99
      Y=G(2)-CC
      YLIM=CC-G(2)
   99 IF(Y-G(2).LT.YLIM) GOTO 80
   60 CL=CS*FLOAT(NCAP)
      IF(CL.GT.CMAX)CL=CMAX
      IF(CW.EQ.0.0)CS=CL/FLOAT(NCAP)
```

Table A33 : Continued

```
      NCHAR=INT(CL/CS+0.5)
      IF(JRCOMP(IH,'L',1).EQ.1)GO TO 70
      DIF=(CMAX-CL)*0.5
      X=X+DIF
      IF(JRCOMP(IH,'R',3).EQ.3)X=X+DIF
   70 CALL JBTEXT(X,Y,CS,LCAP,0.0,NCHAR)
      Y=Y-CC
      K=1
      RETURN
   80 CALL JBOMIT(LCC)
      RETURN
      END
```

Table A34 : (NITROPLCT)

```
      PROGRAM VOLUME
      REAL BULB(6),T,DATUM(6),PDI,PDT,DSFT,SAT,PE,
     1VADM,VADS(40),WEIGHT,DSF(6),REL(40),BET(40),HUTTIG
     1(40),A,B,C,D,VM,SW,RUNST,INTCEPT,TRYCK(40)
      READ*,SAT,T,WEIGHT
      READ*,N,NA,GRAPH
      BULB(1)=0.0031*(273.2/T)
      BULB(2)=0.0093*(273.2/T)
      BULB(3)=0.0150*(273.2/T)
      BULB(4)=0.0284*(273.2/T)
      BULB(5)=0.0412*(273.2/T)
      BULB(6)=0.0668*(273.2/T)
      DATUM(1)=139.1
      DATUM(2)=105.2
      DATUM(3)=68.6
      DATUM(4)=25.6
      DATUM(5)=-17.2
      DATUM(6)=-77.2
      WRITE(2,26)
      WRITE(2,27)
      DSFT=0
      DO 2 I=1,N
      READ*,NR,PDI,PDT
      DSF(I)=(PDI-PDT)/(PDT-DATUM(NR))
      DSF(I)=DSF(I)*BULB(NR)
      WRITE(2,21)NR,DSF(I)
      DSFT=(DSFT+DSF(I))
    2 CONTINUE
      DSFT=DSFT/N
      WRITE(2,22)DSFT
      WRITE(2,11)
      WRITE(2,12)
      K=0
      PE=0
      VADM=0
      DO 7 I=1,NA
      READ*,NRA,PA,NE
      PA=PA-DATUM(NRA)
      IF(I.GT.1)GO TO 20
      VADM=VADM+(PA*BULB(NRA))
      GO TO 1
   20 VADM=VADM+(PA*BULB(NRA)-PE*BULB(NRE))
    1 WRITE(2,14)PA,VADM
      DO 6 J=1,NE
      K=K+1
      READ*,NRE,PE
      PE=PE-DATUM(NRE)
      VADS(K)=(VADM-(PE*BULB(NRE)+PE*DSFT))/WEIGHT
      REL(K)=PE/SAT
      IF(REL(K).LT.0.05)GO TO 3
```

Table A34 : Continued

```
      IF(REL(K).GT.0.70)GO TO 3
      HUTTIG(K)=REL(K)*(1+REL(K))/VADS(K)
      IF(REL(K).GT.0.35)GO TO 4
      BET(K)=PE/((SAT-PE)*VADS(K))
      GO TO 5
    3 HUTTIG(K)=0
    4 BET(K)=0
    5 WRITE(2,16)PE,VADS(K),REL(K),BET(K),HUTTIG(K)
      TRYCK(K)=REL(K)
    6 CONTINUE
    7 CONTINUE
      DO 23 I=1,40
      IF(I.LE.K)GOTO 23
      BET(I)=0
      HUTTIG(I)=0
   23 CONTINUE
       A=SLOPE(REL,BET)
      B=INTCEPT(REL,BET,A)
      VM=1/(A+B)
      SW=4.3E*VM
      IF(B.NE.0)GOTO 24
      B=1E-6
   24 KONST=1+A/B
      WRITE(2,17)A,B,VM,KONST,SW
      WRITE(2,18)SW
      IF(GRAPH.EQ.0)GOTO 26
      GRASIZE=GRAPH
      GRASIZE=ABS(GRASIZE)
      CALL MAGNIF(GRASIZE)
      CALL PLOT(BET,TRYCK,A,B,VADS,K,GRAPH)
   26 STOP
   11 FORMAT( /77H     P1          V ADM          P2          V ADS          REL
     1          BET          HUTTIG)
   12 FORMAT(44H    TORR          MLS STP          TORR    MLS STP/GM )
   14 FORMAT( /2X,F6.1,4X,F6.4)
   16 FORMAT( /2X,F6.1,4X,F8.4,5X,F6.4,4X,F7.5,2X,F7.5)
   17 FORMAT(21H    FROM BET EQUATION:/12H SLOPE      ,F8.4/12H INTCEPT
     1  ,F8.5/12H MONOLAYER   ,F6.2,9H  MLS STP/12H ADS KONST   ,F5.1///16
     1H SURFACE AREA IS,3X,F6.2,15H  M SQRD PER GM//)
   18 FORMAT(23H FROM HUTTIGS EQUATION:/16H SURFACE AREA IS,3X,F6.2,
     1 15H M SQRD PER GM)
   21 FORMAT(20H1DEAD SPACE FACTOR   ,I1,3X,F7.5)
   22 FORMAT(25H DEAD SPACE FACTOR MEAN   ,F7.5,//)
   26 FORMAT(////7H SAMPLE,30X,5H DATE,20X,9H OPERATOR)
   27 FORMAT(/21H DEGASSING CONDITIONS,8X,4H HRS,8X,6H DEG C///)
      END
      REAL FUNCTION INTCEPT (X,Y,P)
      REAL X(40),Y(40),MEANX,MEANY,P,Q,R,N
      N=0
      DO 1 I=1,40
      IF(Y(I).GT.0)N=N+1.0
      IF(Y(I).EQ.0)X(I)=0
    1 CONTINUE
      Q=SUM(X)
      R=SUM(Y)
      MEANX=Q/N
      MEANY=R/N
      INTCEPT=MEANY-P*MEANX
      RETURN

          END
```

Table A34 : Continued

```
      REAL FUNCTION SLOPE(X,Y)
      REAL X(40),Y(40),PROD(40),KVAD(40),Q,R,S,T,N
      N=0
      DO 1 I=1,40
      IF(Y(I).GT.0)N=N+1.0
      IF(Y(I).EQ.0)X(I)=0
      PROD(I)=X(I)*Y(I)
      KVAD(I)=X(I)**2
    1 CONTINUE
      Q=SUM(X)
      R=SUM(Y)
      S=SUM(PROD)
      T=SUM(KVAD)
      SLOPE=(S-(Q*R/N))/(T-(Q**2/N))
      RETURN
      END
      REAL FUNCTION SUM(VEC)
      REAL VEC(40)
      SUM=0
      DO 1 I=1,40
      SUM=SUM+VEC(I)
    1 CONTINUE
      RETURN
      END
      SUBROUTINE PLOT(ET,RYCK,AB,BA,ADS,KA,GRAPH)
      REAL ET(40),RYCK(40),ADS(40),SIZX(2),SIZY(2),LINE(2),AB,BA
      INTEGER KA,L
      L=0
      DO 100 I=1,40
      IF(ET(I).EQ.0)GOTO 100
      L=L+1
  100 CONTINUE
      SIZX(1)=0
      SIZY(1)=0
      SIZX(2)=0.35
      LINE(1)=AB*SIZX(1)+BA
      LINE(2)=AB*SIZX(2)+BA
      SIZY(2)=LINE(2)
      CALL JRAXES(SIZX,2,14.0,'RELATIVE PRESSURE',17,SIZY,2,10.0,
     1'RET FUNCTION',12)
      DO 110 I=1,L
  110   CALL MARKPT(RYCK(I),ET(I),2)
      DO 120 I=1,2
  120 CALL JOINPT(SIZX(I),LINE(1))
      IF(GRAPH)135,125,125
  125 SIZX(2)=1.00
      SIZY(2)=ADS(KA)
      CALL JRAXES(SIZX,2,14.0,'RELATIVE PRESSURE',17,SIZY,2,10.0,
     1'VOL ADSORBED (CM3/GM)',24)
      DO 130 I=1,KA
  130 CALL MARKPT(RYCK(I),ADS(I),2)
      CALL DRAWCV(RYCK,ADS,KA)
  135 CALL ENDPLT
      RETURN
      END
```

Table A35 : (BJHPORE)

```
      PROGRAM REST
      DIMENSION V(40),RK(40),T(40),XRP(40),RP(40)
      DIMENSION FILEHI(40)
      READ*,(FILEHI(I),I=1,40)
      READ*,(V(I),I=1,40)
      READ*,N,GRAPH
      WRITE(2,1)
    1 FORMAT(///7H SAMPLE,30X,5H DATE/9H OPERATOR,30X,3H NB)
      DO 30 I=1,N
      RP(I)=FILEHI(I)
      RK(I)=4.05/ALOG(1./RP(I))*2.303
      T(I)=3.5*(5./ALOG(1./RP(I)))**.333
   30 XRP(I)=RK(I)+T(I)
      CALL BAJOHA(V,RK,T,S,U,W,XRP,N,RP,GRAPH)
      STOP
      END
      SUBROUTINE BAJOHA(V,RK,T,S,U,W,XRP,NK,RP,GRAPH)
      DIMENSION RP(40),V(40),T(40),XRP(40),AP(40),RK(40),ADVP(40)
      COMMON AP
      WRITE(2,331)
  331 FORMAT(1H1,26X,'PORE MODEL OF BARRETT,JOYNER AND HALENDA')
      WRITE(2,332)
  332 FORMAT(1HO,36X,'CYLINDRICAL PORES')
      WRITE(2,333)
  333 FORMAT(15X,8HRELATIVE,1X,6HVOLUME,3X,6HKELVIN,1X,5HSTAT.,2X,
     14HPORE,3X,4HVOL.,3X,4HAREA,4X,4HCUM.,2X,9HPORE VOL.)
      WRITE(2,334)
  334 FORMAT(15X,8HPRESSURE,1X,8HADSORBED,1X,6HRADIUS,1X,5HLAYER,2X,
     16HRADIUS,1X,4HPORE,3X,4HPORE,4X,4HAREA,2X,9HPER GROUP)
      WRITE(2,335)
  335 FORMAT(15X,39X,5HGROUP,2X,5HGROUP,8X,8HOF PORES)
      WRITE(2,336)
  336 FORMAT(15X,12X,1H3,27X,1H3,6X,1H2,7X,1H2,7X,1H3)
      WRITE(2,337)
  337 FORMAT(15X,9X,6HCMS/GM,5X,1HA,6X,1HA,6X,1HA,3X,6HCMS/GM,2X,
     14HM/GM,4X,4HM/GM,2X,8HCMS/GM/A)
      WRITE(2,338)RP(1),V(1),RK(1),T(1),XRP(1)
      SDSP=0.0
      SUM=0.0
      SDVP=0.0
      AP(1)=0.0
      ADVP(1)=0.0
      DO 4 I=2,NK
      RPM=(XRP(I)+XRP(I-1))*.5
      RKM=(RK(I)+RK(I-1))*.5
```

Table A35 : Continued

```
      DT=T(I-1)-T(I)
      DV=(V(I-1)-V(I))*1.584E-3
      C=(RPM-(T(I-1)+T(I))*.5)/RPM
      SUM=SUM+C*AP(I-1)
      R=(RPM/(RKM+D1))**2
      R=R*DT*SUM*1E-4
      DVP=R*DV-R
      SDVP=DVP+SDVP
      AP(I)=2.*DVP/RPM*1E4
      SDSP=SDSP+AP(I)
      DVDR=DVP/(XRP(I-1)-XRP(I))
      ADVP(I)=DVP
    4 WRITE(2,336)RP(I),V(I),PK(I),T(I),XRP(I),DVP,AP(I),SDSP,DVDR
  338 FORMAT(15X,F6.4,3X,F7.3,1X,F7.2,1X,F5.2,2X,F6.1,,F6.4,1X,F6.1,
     11X,F7.2,2X,F5.3)
      WRITE(2,339)
  339 FORMAT(55X,6H------)
      WRITE(2,340)SDVP
  340 FORMAT(53X,F7.4)
      WRITE(2,339)
      IF(GRAPH.EQ.0)GOTO350
      GRASIZE=GRAPH
      GRASIZE=ABS(GRASIZE)
      CALL MAGNIF(GRASIZE)
      CALL PLOT(XRP,ADVP,NK,GRAPH)
  350 RETURN
      END
      SUBROUTINE PLOT(PXRP,PADVP,PNK,GRAPH)
      REAL PXRP(50),PADVP(50),SIZX(2),SIZY(2)
      INTEGER PNK
      IF(GRAPH)60,60,60
   60 SIZX(1)=0.
      SIZX(2)=PXRP(2)
      SIZY(1)=0.
      SIZY(2)=STORST(PADVP,PNK)
      CALL JBAXES(SIZX,2,14.0,'PORE RADIUS (A)',15,SIZY,2,10.0,
     1'PORE VOLUME (CM3/GM)',20)
      CALL JOINMK(PXRP,PADVP,PNK)
      CALL CUM(PADVP,PNK)
      SIZY(2)=100.
      SIZY(1)=0.
      CALL JBAXES(SIZX,2,14.0,'PORE RADIUS (A)',15,SIZY,2,10.0,
     1'CUM PORE VOLUME (%)',19)
      CALL JOINMK(PXRP,PADVP,PNK)
      GO TO 200
   80 DO 90 I=2,PNK
   90 PXRP(I)=ALOG10(PXRP(I))
      SIZX(1)=0.
      SIZX(2)=PXRP(2)
      SIZY(1)=0.
      SIZY(2)=STORST(PADVP,PNK)
      CALL JBAXES(SIZX,2,14.0,'LOG PORE RADIUS (A)',19,SIZY,2,10.0,
     1'PORE VOLUME (CM3/GM)',20)
      CALL JOINMK(PXRP,PADVP,PNK)
      CALL CUM(PADVP,PNK)
      SIZY(1)=0.
      SIZY(2)=100.
      SIZY(2)=STORST(PADVP,PNK)
      CALL JBAXES(SIZX,2,14.0,'LOG PORE RADIUS (A)',19,SIZY,2,10.0,
     1'CUM. PORE VOLUME (%)',20)
```

Table A35 : Continued

```
      CALL JOINNK (PXRP,PADVP,PNK)
200   CALL END PLT
      RETURN
      END
      SUBROUTINE CUM (PADVP,PNK)
      DIMENSION PADVP(50),SUM(50)
      INTEGER PNK
      SUM(40)=0.0
      DO 10 I=2,PNK
      J=(PNK+1)-I
      SUM(J)=PADVP(J)+SUM(J+1)
10    CONTINUE
      DO 20 I=2,PNK
      PADVP(I)=(SUM(I)/SUM(1))*100.
20    CONTINUE
1     FORMAT(F7.5,3X,I2,3X,4H CUM)
      RETURN
      END
      SUBROUTINE JOINNK(PXRP,PADVP,PNK)
      DIMENSION PXRP(50),PADVP(50)
      INTEGER PNK
      DO 10 I=2,PNK
      CALL JOINPT(PXRP(I),PADVP(I))
10    CALL MARKPT(PXRP(I),PADVP(I),2)
      RETURN
      END
      FUNCTION STORST(PVP,PN)
      REAL STORST,PVP(50)
      INTEGER PN
      STORST=PVP(1)
      DO 200 I=2,PN
      IF(PVP(I).LE.STORST)GOTO 200
      STORST=PVP(I)
200   CONTINUE
      RETURN
      END
```

Table A36 :Continued

```
      IF(N1-5)52,2,2
11    WRITE(2,1)
      WRITE(2,8)TITLE
      WRITE(2,12)
12    FORMAT("PORE DIAMETER",3X,6HVOLUME,5X,4HAREA/4X,7HMICRONS,6X,
     1 7HPERCENT,3X,7HPERCENT)
      D(J)=D(J-1)
      SD(J)=SD(J-1)
      S(J)=S(J-1)
      JA=J-1
      JB=1
      JC=1
      JD=0
      JE=0
      VPA=0
13    IF(PR(JC)-D(JB))14,20,21
14    IF(PR(JC)-D(JB+1))15,16,19
15    JB=JB+1
      IF(JB-JA)13,23,23
23    IF(VP-100.)24,25,25
24    IF(JD)25,29,25
29    VP=100.
      AP=100
      WRITE(2,18)PR(JC),VP,AP
25    TVSA=4.*SD(JA)/S(JA)
      WRITE(2,35)PD,SD(JA),TVSA,S(JA)
35    FORMAT(////16X,"SUMMARY TABLE"/"1. MEDIAN PORE DIAMETER...",
     1 8X,F7.4,4X,7HMICRONS/"2. TOTAL PORE VOLUME...",9X,F9.4,
     2 4X,4HCC/G/"3. AVERAGE PORE DIAMETER (4V/A)...",F7.4,3X,
     *"MICRONS"/"4. TOTAL PORE AREA...",11X,F8.3,5X,4HM2/G)
      IF(P2(N1).LT.-10..OR.SV2(N1).LT.-10.)GOTO 6
      GOTO 7
16    VP=100.*(SD(JB+1)/SD(JA))
      AP=100.*(S(JB+1)/S(JA))
17    IF(VP-100.)26,26,24
26    IF(JD)25,27,25
27    JD=1
28    IF(VP-50.)30,31,32
31    PD=PR(JC)
      GO TO 34
32    IF(JE)30,33,30
33    PD=PR(JC-1)-(PR(JC-1)-PR(JC))*(50.-VPA)/(VP-VPA)
34    JE=1
30    WRITE(2,18)PR(JC),VP,AP
18    FORMAT(F11.4,5X,F7.2,3X,F7.2)
      JC=JC+1
      VPA=VP
      GO TO 13
19    FR=(D(JB)-PR(JC))/(D(JB)-D(JB+1))
      VP=100.*((SD(JB)+FR*(SD(JB+1)-SD(JB)))/SD(JA))
      AP=100.*((S(JB)+FR*(S(JB+1)-S(JB)))/S(JA))
      GO TO 17
20    VP=100.*(SD(JB)/SD(JA))
      AP=100.*(S(JB)/S(JA))
      GO TO 17
21    WRITE(2,22)
22    FORMAT(4H ERROR)
      GO TO 7
6     STOP
      END
```

Table A36 : (HGPORES)

```
      PROGRAM VOID
C
C     PORE VOLUME  AREA DISTRIBUTION CALCULATION PROGRAMME
C     FROM MERCURY POROSIMETER DATA
C
      DIMENSION D(100),PR(100),SD(100),S(100),P2(5),SV2(5)
      CHARACTER*80 TITLE
      READ*,N,(PR(I),I=1,10)
      IF(N-10)7,7,50
50    READ*,(PR(I),I=11,N)
 7    AK=0.0225
      SPBDV=0.
      P1=0.
      D1=100.
      SV1=0.
      S(1)=0.
      D(1)=D1
      SD(1)=0.
      J=2
      READ*,W
      WOK=AK/W
      READ(*,8) TITLE
8     FORMAT(A)
      WRITE(2,1)
1     FORMAT(1H1,"POROSIMETRY CALCULATIONS PORE AREA DISTRIBUTION/")
      WRITE(2,8)TITLE
      WRITE(2,9)W
9     FORMAT(1H ,
     1"INITIAL P=0.",2X,"INITIAL SUM V=0.",2X,"INITIAL D=100.",
     22X,3H W=,F7.4 ,2X,9H K=0.0225/8X,1HP,6X,3HSDV,6X,1HD,8X,3HSDV,6X,
     32HSA,7X,5HP BAR,5X,5HDV/DR/6X,4HPSIA,6X,2HCC,6X,7HMICRONS,4X,
     44HCC/G,6X,4HM2/G,5X,7HMICRONS)
2     READ*,(P2(N1),SV2(N1),N1=1,4)
      N1=1
 52   IF(P2(N1).LT.0..OR.SV2(N1).LT.0.)GOTO 11
4     PBAR=(P2(N1)+P1)/2.
      DV=SV2(N1)-SV1
      SPBDV=SPBDV+PBAR*DV
      SA=WOK*SPBDV
      D2=180./P2(N1)
      DR=(D1-D2)/2.
      RB=(D1+D2)/4.
      SDV=SV2(N1)/W
      DVSDR=DV/DR
      D(J)=D2
      SD(J)=SDV
      S(J)=SA
      WRITE(2,5)P2(N1),SV2(N1),D2,SDV,SA,RB,DVSDR
5     FORMAT(F10.2,3F10.4,F10.5,F10.4,F11.5)
      P1=P2(N1)

      SV1=SV2(N1)
      D1=D2
      J=J1
      N1=N1+1
```